POLYMER FRACTIONATION BY CONTINUOUS CHROMATOGRAPHY

A thesis submitted by Frederick John Ellison, B.Sc., to the Faculty of Engineering, University of Aston in Birmingham, for the degree of Doctor of Philosophy.

Department of Chemical Engineering,
University of Aston in Birmingham.

April, 1976

ACKNOWLEDGEMENTS

The Author is indebted to the following:

Professor G. V. Jeffreys and the Department of Chemical Engineering for making available the facilities for research.

Professor P. E. Barker and Dr. B. W. Hatt, who supervised the work, for their help and guidance throughout this project.

Mr. A. N. Williams and other research students in the Separation and Purification Group for many invaluable discussions.

Mr. N. Roberts and other members of the departmental technical staff for help with the construction of the sequential unit.

Financial support from Fisons Ltd., and the provision of a scholarship by the Science Research Council, is also gratefully acknowledged.

SUMMARY

A review is given of general chromatographic theory, the factors affecting the performance of chromatographic columns, and aspects of scale-up of the chromatographic process. The theory of gel permeation chromatography (g.p.c.) is reviewed, and the results of an experimental study to optimize the performance of an analytical g.p.c. system are reported.

The design and construction of a novel sequential continuous chromatographic refining unit (SCCR3), for continuous liquid-liquid chromatography applications, is described. Counter-current operation is simulated by sequencing a system of inlet and outlet port functions around a connected series of fixed, 5.1 cm internal diameter x 70 cm long, glass columns. The number of columns may be varied, and, during this research, a series of either twenty or ten columns was used.

Operation of the unit for continuous fractionation of a dextran polymer (M.W. $\simeq$ 30,000) by g.p.c. is reported, using 200-400 μm diameter porous silica beads (Spherosil XOB075) as packing, and distilled water for the mobile phase. The effects of feed concentration, feed flowrate, and mobile and stationary phase flowrates have been investigated, by means of both product, and on-column, concentrations and molecular weight distributions. The ability to operate the unit successfully at on-column concentrations as high as 20% w/v dextran has been demonstrated, and removal of both high and low molecular weight ends of a polymer feed distribution, to produce products meeting commercial specifications, has been achieved. Equivalent throughputs have been as high as 2.8 tonnes per annum for ten columns, based on continuous operation for 8000 hours per annum.

A concentration dependence of the equilibrium distribution coefficient, K_D, observed during continuous fractionation studies, is related to evidence in the literature and experimental results obtained on a small-scale batch column.

Theoretical treatments of the counter-current chromatographic process are outlined, and a preliminary computer simulation of the SCCR3 unit is presented.

CONTENTS

Contents (Continued) Page

Contents (Continued)

Contents (Continued) Page

Contents (Continued)

Contents (Continued) Page

Contents (Continued)

Contents (Continued)

CHAPTER 1

Introduction

For many years dextran polymers have been used, in the field of medicine, for blood plasma volume expanders, and for the production of iron dextran which is used in the treatment of anaemia. Conventionally, the manufacturing process involves fermentation of sucrose, to produce dextrans which range from oligomers to polymers with molecular weights of several hundred millions. This is followed by controlled hydrolysis to produce dextrans of lower molecular weight, and subsequent separation of the hydrolysate into fractions having narrow molecular weight distributions. The separation stage usually involves fractional precipitation of the hydrolysate using aqueous ethanol, which is both expensive to recover and a fire hazard. Other separation methods which overcome these problems, and which may offer improved dextran fractionation, therefore merit investigation.

Many of the usual separation techniques available to the chemical engineer, such as distillation and solvent extraction, are unsuitable due to the non-volatile nature and chemical similarity of dextran molecules. Recently, with the growth of chromatography as a separation process, as well as the more usual analytical use, the possibility of using chromatography, in particular gel permeation chromatography (1), for production-scale fractionation of dextrans has become realistic.

Chromatography stems from the original work of Tsvet (2,3) and has developed in two main forms: liquid chromatography and gas chromatography. Although liquid chromatography was discovered more than one hundred and seventy years ago, little progress was made until relatively modern times. Gas chromatography originates from the work of Martin and Synge in 1941 (4), and enjoyed a rapid growth following later work by James and Martin (5). At the present time it is recognized as a powerful means of resolving chemical species, and is accepted as a standard, rapid, analytical technique. Much of the work

on the development of gas chromatography equipment and techniques has led to the re-emergence of liquid chromatography for the resolution of materials such as proteins, enzymes and polysaccharides. At the present time rapid advances are being made in high speed liquid chromatography due to the availability of new packing materials, making fast sample analyses possible and thus overcoming the previous major drawback of the process.

Gel permeation chromatography (g.p.c.), which is the newest type of chromatography, is a form of liquid chromatography wherein molecules are separated by virtue of their size. The first commercial gel, a cross-linked dextran, Sephadex, was introduced by Porath and Flodin (6) and was suitable for use with aqueous solutions. Later work by Moore (1), who developed cross-linked polystyrene gels suitable for use with organic solvents, led to wide use of the technique, especially in the field of polymer chemistry, where the unique ability of g.p.c. to resolve molecules, by virtue of their size, has been particularly useful for the characterization of polymer molecular weight distributions.

The potential of elution chromatography as a separation technique, as well as the more usual analytical use, was quickly realized with the growth of gas chromatography in the 1950's. Examples of the use of chromatography in this area, on an industrial scale, are available in the literature (7,8). To date, the major theoretical and experimental studies on preparative and production-scale chromatography have been concerned with gas chromatography, although much of the theory and practice is general to all forms of chromatography. Operation of batch columns in a co-current mode, using repeated sample injection, has formed a part of the work in this area, although the batch nature of operation tends to limit column utilization.

Many attempts have been made to develop process schemes based on continuous cross-current or counter-current operation of the chromatographic process. Cross-current process schemes promise the advantage of affording complete, and continuous, separation of a multi-component feed mixture, but to date the practical problems involved have limited their use on a large scale. Considerable effort has been directed towards the development of chromatographic schemes based on a counter-current operating mode. In these, the mobile phase fluid, and stationary phase fluid, are moved counter-currently, and the feed mixture usually introduced at the mid-point of the separating section. The feed material with least affinity for the stationary phase travels with the eluting solvent, to emerge from one end of the separating section, while the material with greatest affinity for the stationary phase travels preferentially with the stationary phase fluid, and emerges from the other end of the separating section. The disadvantage of this mode of operation is the fact that only two products are readily obtained. However, advantages of counter-current operation are that all of the column length can be effectively utilized, and, within a major part of the separating section, only partial resolution of components is necessary to obtain pure products at the column outlets, which enables severe overloading, by conventional batch standards, to be tolerated.

Barker and co-workers (9-31) have been prominent in the development of the counter-current chromatographic process, particularly in the field of gas-liquid chromatography (g.l.c.). The most recent experimental unit is that reported by Barker and Deeble (26-30), based on simulating the relative phase movement by sequencing a system of inlet and outlet port functions around a closed loop of twelve, 7.6 cm-diameter columns. Successful separations of equivolume mixtures

of 1,1,2-trifluoro-1,2,2-trichloroethane and 1,1,1-trichloroethane have been obtained at typical product purities in excess of 99.7% and feed throughputs up to 700 cm^3 hr^{-1}.

Although the majority of studies by Barker and co-workers have been concerned with g.l.c., Barker, Barker, Hatt and Somers (24) have demonstrated the possibility of continuous fractionation of carbohydrates on a small scale, by g.p.c., using distilled water as the eluting solvent, and porous silica beads (Porasil) as packing. The design of the equipment in the present study was based on a scale-up of cross-sectional area by a factor of approximately 40 compared to the equipment used by these workers, while incorporating the principle of simulation of the counter-current mode of operation developed by Barker and Deeble (28). The present experimental studies were directed towards investigation of the fractionation of an industrial dextran polymer, manufactured by Fisons Ltd. (Pharmaceutical Division), Holmes Chapel. In particular, maximization of throughput was of prime importance as a preliminary test of the feasibility of using g.p.c. for production-scale dextran fractionations.

CHAPTER 2

Literature Survey Part 1

Theory of the Chromatographic Process and

Factors Affecting Scale-up

2.1 SCOPE

Since the original work of Tsvet in 1903 (2) chromatography has developed into an accepted analytical and preparative technique. Because of the enormous growth of publications on the subject, it is necessary to be restrictive in the summary of relevant literature. This survey is concerned firstly with the development of theoretical models of the column chromatographic process. An introduction to the basic separation mechanicms of chromatography is given, followed by the theoretical background for sources of imperfection in the process leading to broad component peaks, and methods of minimizing these effects.

Scale-up of the chromatographic process is next reviewed, in two sections: batch chromatography, and continuous chromatography. The author is aware that disagreement exists as to the nature of true continuous operation in chromatography, but a convenient division is obtained if continuous operation is defined as the introduction of a continuous feed stream into a process, and the removal of continuous product streams. All operations which do not satisfy these criteria will be classified as batch processes.

Scale-up of the batch process to the preparative or production level has usually taken the form of sample injection into columns of diameters larger than those employed for conventional chromatographic analysis. Factors affecting the performance of such columns are reviewed, and, as detailed theory for scale-up specifically related to liquid chromatography has been very limited in the literature, it has been necessary to utilize theory originally developed for gas chromatography.

The desire to obtain maximum column utilization by continuous operation has produced a variety of novel process schemes, and the development of the practice of continuous operation is followed. Barker and co-workers (9-31) have figured prominently throughout, and development of the latest unit (28), which has particular relevance to this research programme, is traced from earlier models. Where possible, treatment of the chromatographic process has been restricted to the general case, and a more detailed review of the particular type of chromatography used for this research programme, gel permeation chromatography (g.p.c.), is given in CHAPTER 3.

2.2 GENERAL THEORY OF CHROMATOGRAPHY

2.2.1 Basic Terminology

Separation of a sample into its constituents by chromatography is achieved by the differences in equilibrium distribution of the constituents between two phases. One phase is called the stationary phase and the other, which flows past the stationary phase, is called the mobile phase. Chromatography may be performed in an open bed in certain cases, e.g. thin layer chromatography (TLC), or in a packed column (elution chromatography) where the packing usually acts as a support for the stationary phase. For convenience discussion of terminology in this instance is restricted to zone elution chromatography.

Zone elution chromatography usually involves loading a narrow sample band at the start of a column, followed by elution of that sample from the column by the mobile phase. A typical arrangement of equipment is shown in FIG. 2.1, and FIG. 2.2 shows a typical chart recorder trace, which would be obtained by analysis of the mobile phase, emerging from the end of the column, using a suitable detector.

A component only travels through the column when it is in the mobile phase, and its relative migration rate, R, is therefore given by the fraction of time it spends in this phase. The velocity of a solute zone is thus a fraction, R, of the mobile phase velocity. R may be further defined as:

(i) The probability that a solute molecule is in the mobile phase.

(ii) The fraction of solute molecules in the mobile phase at equilibrium.

Figure 2.1 Arrangement of a Typical Chromatographic System

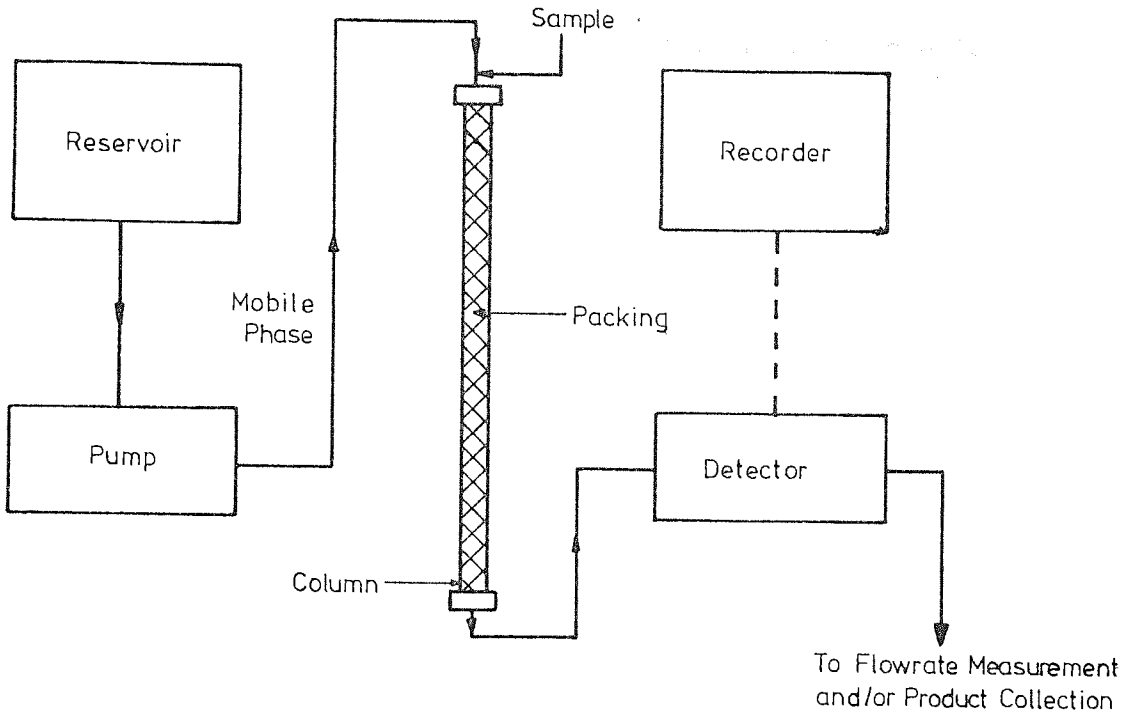

Figure 2.2 Typical Analytical Chromatogram

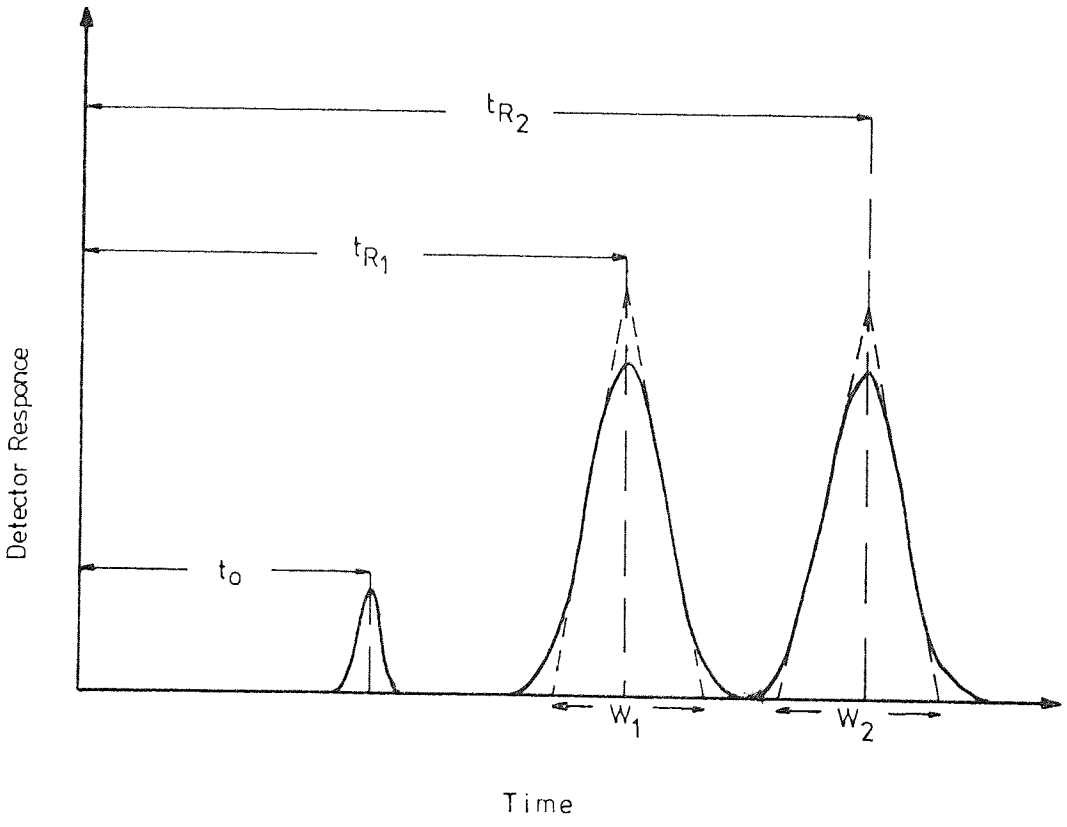

R is governed by the equilibrium distribution of the component between the two phases, components favouring the mobile phase being eluted from the column first, and those favouring the stationary phase being eluted later. The precise value of R only applies at the centre of a solute band travelling through a column, as this is the only point where equilibrium is attained (SECTION 2.2.4.3). Thus we must refer to the centre of the solute zone when relating equilibrium distribution of solute molecules to migration. FIG. 2.2 illustrates complete separation of a two-component mixture, and a non-retained component. A measure of the degree of separation of the two peaks is given by the resolution, R_s, defined as:

$$R_s = \frac{(t_{R_2} - t_{R_1})}{\frac{1}{2}(W_1 + W_2)} \qquad (2.1)$$

t_{R_1} = Elution time, or retention time, for Component 1

t_{R_2} = Elution time, or retention time, for Component 2

W_1 = base width of peak 1

W_2 = base width of peak 2

t_{R_1}, t_{R_2}, W_1 and W_2 may also be defined in volume units, t_R becoming the retention volume or elution volume, V_R, by multiplying by the mobile phase flowrate, and as R_S is a ratio it will not be numerically affected.

N.B. If the peaks are Gaussian $W = 4\sigma$, where σ is the standard deviation of each peak.

To maximize column resolution it is necessary to keep W, which is a function of column dynamics, and extra-column effects, to a minimum. The column factors contributing to W are outlined in

SECTION 2.2.4, and extra-column contributions are discussed in SECTION 4.3.2.2.

The elution volume of an unretarded component is $t_o F_m$, if F_m is the mobile phase flowrate, and this equals the volume of the mobile phase present in the column (V_M) or column 'dead' volume. The fundamental retention equation for a chromatographic system may thus be written:

$$V_R = V_M + KV_s \qquad (2.2)$$

V_R = Retention (or elution) volume of component

V_M = Column mobile phase volume

V_s = Column stationary phase volume

K = Equilibrium partition coefficient

$$= \frac{\text{Concentration of Solute in Stationary phase}}{\text{Concentration of Solute in Mobile phase}}$$

$$= \frac{1-R}{R}$$

The ratio of the K values of two components is often used as a measure of the difficulty of a separation and is known as the separation factor, α:

$$\alpha = \frac{K_2}{K_1} \qquad (2.3)$$

This has a minimum value of 1 where separation is impossible for the system employed, and larger values indicate easier separations.

2.2.2 Types of Chromatography

The names assigned to the various column elution chromatography techniques depend on the nature of the phases used. The mobile phase is usually named first, i.e. gas chromatography (GC) or liquid chromatography (LC), followed by the stationary phase, e.g. gas-liquid chromatography (GLC), liquid-solid chromatography (LSC), liquid-liquid chromatography (LLC).

Another method of characterizing the various techniques is the more important classification of retention mechanisms. For example, liquid chromatography may be divided into four categories:

(i) Partition chromatography

(ii) Adsorption chromatography

(iii) Ion-exchange chromatography

(iv) Exclusion chromatography

Partition chromatography is based on the absorption of solute by a liquid stationary phase, usually held in place by an inert solid support, whereas adsorption chromatography depends on the retention of solute by solid surface adsorption. Ion-exchange chromatography relies on the reversible exchange of ions between the stationary ion-exchange phase and the mobile phase, separation being achieved by a difference in the affinity of solute ions for the ion-exchange stationary phase. These mechanisms are well known, and only the mechanism of exclusion chromatography, which results in a separation by virtue of molecular size, is undecided. The exclusion mechanisms which form the basis of gel permeation chromatography, g.p.c., will be discussed in detail in SECTION 3.2.

2.2.3 Reynolds Numbers in Chromatographic Columns

One representation of flow dynamics in a chromatographic column is given by the Ergun equation (32) which is a summation of the Blake-Konzeny equation and the Burke-Plummer equation. The Ergun equation is illustrated graphically in FIG. 2.3. The regions of the graph may be divided approximately according to the Reynolds Number, $Re = (d_p u\rho/\mu)(\frac{\varepsilon}{1-\varepsilon})$, where d_p = packing particle diameter, u = mobile phase velocity, ρ = mobile phase density, μ = mobile phase viscosity, and ε = fractional column voidage.

$Re < 10$ Laminar flow (Blake-Konzeny)

$10 < Re < 1000$ Transition region

$Re > 1000$ Turbulent flow (Burke-Plummer)

Giddings (33) indicates that, for gas flow in a chromatographic column, a velocity of the order of 10 cm sec^{-1} could produce a moderate departure from laminar flow, while for liquids this value might be an order of magnitude higher. Hamilton et al. (34) noted Re values ranging from 0.003 to 0.2 for a liquid velocity of 0.18 cm sec^{-1}. Although high liquid velocities are used in modern liquid chromatography, values up to 100 cm sec^{-1} could be required before a departure from laminar flow is obtained.

Although Giddings (33) points out that turbulent flow could have significant advantages in chromatography, due to increased mass transfer rates, and a more uniform velocity profile, and he and co-workers (35) have observed a drop in measured Height Equivalent to a Theoretical Plate (H.E.T.P.) values with the onset of turbulence in gas chromatography, the majority of chromatographic operations are carried out in the laminar regime, and further discussion will be limited to this case.

Figure 2.3 Graphical Representation of the Ergun Equation on a log-log plot

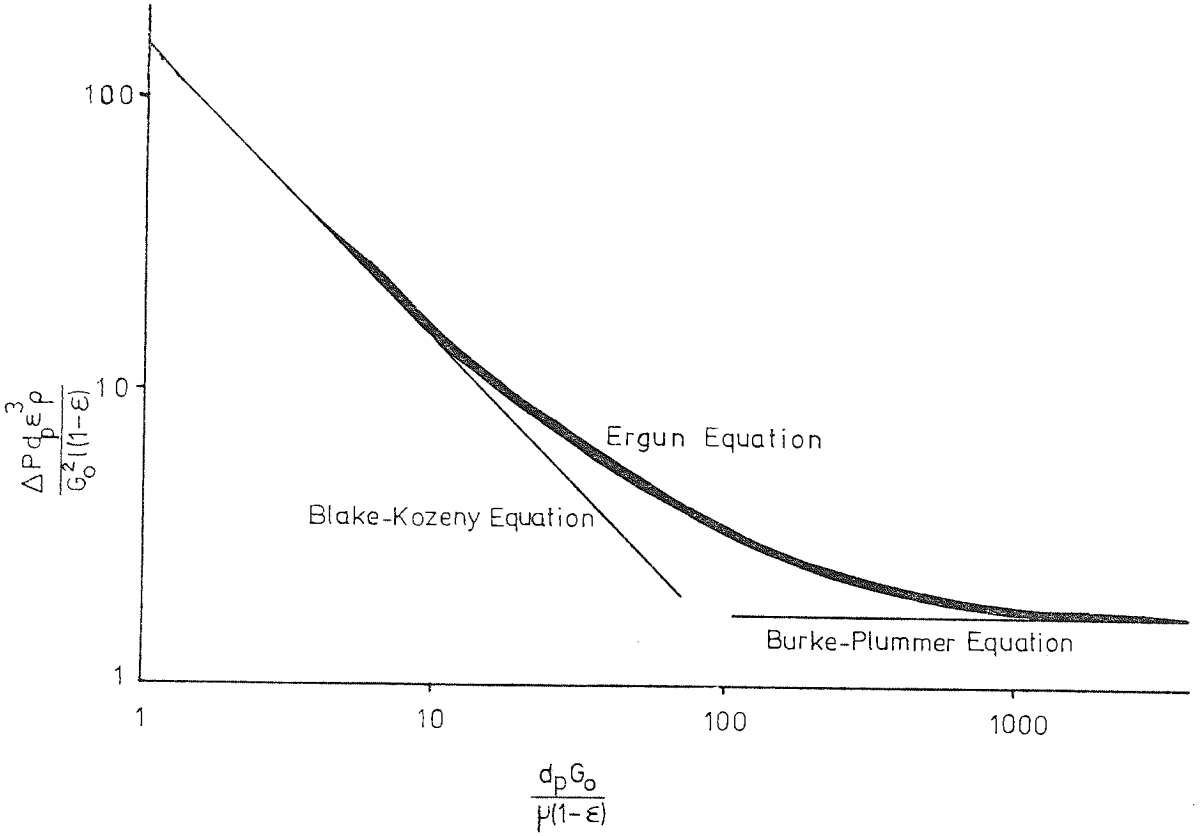

2.2.4 Solute Zone Broadening Theories

2.2.4.1 Introduction

Separation in chromatography is achieved through differences of relative migration rates of solutes, which is governed by thermodynamic equilibrium. However, the effectiveness of any separation if also dependent on the degree of overlap of the solute zones, which is governed by column dynamics. It is obviously desirable to keep zone dispersion to a minimum, as narrower solute zones lead to the achievement of better separations. Chromatographic theories are concerned with the factors that contribute to zone dispersion, and their development is reviewed in the following sections.

2.2.4.2 The Plate Model

A mass transfer process may be considered in the form of a series of equilibrium stages. This method is commonly employed for the treatment of distillation processes, and was first developed for chromatography by Martin and co-workers (4,5), who used it to describe gas-liquid chromatography. Their early work was later expanded by Mayer and Tompkins (36) and Glueckauf (37).

It is necessary to make a number of simplifying assumptions when the plate model is used, which may be listed as follows:-

(i) The chromatographic column is divided into a number of theoretical plates, N.T.P. or N, such that the solution leaving a plate is in equilibrium with the mean solute concentration in the stationary phase throughout that plate.

(ii) The solute exchange process is thermodynamically reversible. This implies instantaneous equilibrium.

(iii) The partition coefficient is constant throughout the column and independent of concentration, i.e. 'linear' chromatography.

(iv) Longitudinal diffusion may be substantially neglected.

(v) Mobile phase flow is discontinuous. The flow is usually achieved by stepwise additions of volumes of mobile phase equal to the mobile phase volume per plate.

Glueckauf (37) in his development reduced the plate volume to an infinitessimally small value, and obtained a continuous model. The elution curve exhibited a Poisson distribution which approximated to a Gaussian distribution for N > 100. The standard deviation (σ) of this Gaussian distribution function is given by:

$$\sigma = \sqrt{HL_M} \qquad (2.4)$$

where L_M is the distance migrated, and H is the height equivalent to a theoretical plate (H.E.T.P.). It can be seen that the standard deviation, which is a measure of peak width, varies as the square root of the distance migrated. However, the peak maxima separation ($t_{R_2} - t_{R_1}$ in FIG. 2.2) varies in direct proportion to the migration distance. Thus the solute bands separate faster than they broaden, so a longer column will give a better separation, a basic fact of the chromatographic process. EQUATION 2.4 shows that H varies directly as σ^2, the variance or second moment of the distribution, and an important

statistical property of σ^2 is that independent contributions to it are additive,

$$\text{i.e.} \quad H = \frac{\Sigma \sigma^2_i}{L_M} \tag{2.5}$$

Thus contributions to the plate height may be determined independently and summed to give an overall H value. This procedure will be apparent throughout the theoretical treatments of SECTION 2.2.4.3.

Although plate height is an empirical quantity, and plate theory does not deal with the mechanisms which determine it, such as partition phenomena, molecular diffusion and flow patterns through packed beds, it has considerable value for comparison of the efficiency of chromatographic columns, and has gained almost universal acceptance in this area. In practice, H is used to describe the summation of all the contributions to peak dispersion (σ^2), which are generally caused by:-

(i) Finite mass transfer rates.

(ii) Longitudinal molecular diffusion.

(iii) Eddy diffusion caused by the heterogeneous nature of the packing.

The following section will deal with the various rate theories advanced to evaluate these effects.

2.2.4.3 Zone Broadening Rate Theories

Lapidus and Amundson (38) developed a mathematical model which included a general mass transfer coefficient, and a longitudinal diffusion coefficient. This theory was extended by Van Deemter, Zuiderweg, and Klinkenberg (39) to form their well known treatment of linear non-ideal chromatography. They included contributions to non-ideality caused by axial molecular diffusion, axial eddy diffusion, and the finite nature of the mass transfer coefficient. A mass balance approach yielded the following equation:-

$$H = 2\lambda d_p + 2\gamma' \frac{D_m}{u} + \frac{8}{\pi^2} \frac{K F_M' u d^2}{(1 + K \frac{F_M'}{F_S'})^2 D_S F_S'} \qquad (2.6)$$

λ = packing characterization factor for eddy diffusivity such that eddy diffusivity, E, = $\lambda u d_p$

d_p = packing particle diameter

γ' = labyrinth factor to allow for tortuous flow path

D_m = mobile phase molecular diffusivity

D_S = stationary phase molecular diffusivity

F_M' = fractional volume of mobile phase

F_S' = fractional volume of stationary phase

K = partition coefficient = $\frac{\text{Equilibrium mobile phase concentration}}{\text{Equilibrium stationary phase concentration}}$

d = effective stationary phase liquid film thickness

u = interstitial mobile phase velocity

The equation may be written in shortened form:

$$H = A + B/u + C_S u \qquad (2.7)$$

A, B and C_s are the eddy diffusion, axial diffusion, and mass transfer resistance terms respectively, stationary phase mass transfer being assumed the controlling factor. Van Deemter (40) later added a term to allow for resistance to mass transfer in the mobile phase (C_m). EQUATION 2.6 has been applied extensively to the field of gas chromatography and was responsible for the significant improvements obtained in column performance therein. It is shown graphically in FIG. 2.4.

The minimum value of the curve is a well-established experimental fact for gas chromatography, showing how the gas phase longitudinal diffusion term becomes significant at low gas velocities. At higher gas velocities the dependence of H on B/u disappears and the stationary phase resistance to mass transfer term ($C_s u$) becomes controlling. The curve obtained for conventional liquid chromatography is usually somewhat different and a minimum value for H.E.T.P. is seldom measured (FIG. 2.5 and SECTION 3.3.1). N.B. The curves are separated for convenience, but their relative position depends on the operating conditions in the columns. The major reason for the difference is that diffusion coefficients in liquids are $\sim 10^5$ times smaller than in gases. As B is proportional to D_m, the mobile phase diffusion coefficient, in most cases of liquid chromatography B becomes insignificant for practical purposes.

More recently the mass balance approach has been extended by Kucera (41), Grubner (42), and Grushka (43). Grushka develops the equation:

$$H = \frac{2D_m}{u} + \frac{2k'd^2u}{3(1+k')^2D_s} + \frac{k'V_s u}{(1+k')^2 V_M k_f} \qquad (2.8)$$

Figure 2.4 Graphical Representation of the Van Deemter Equation (39)

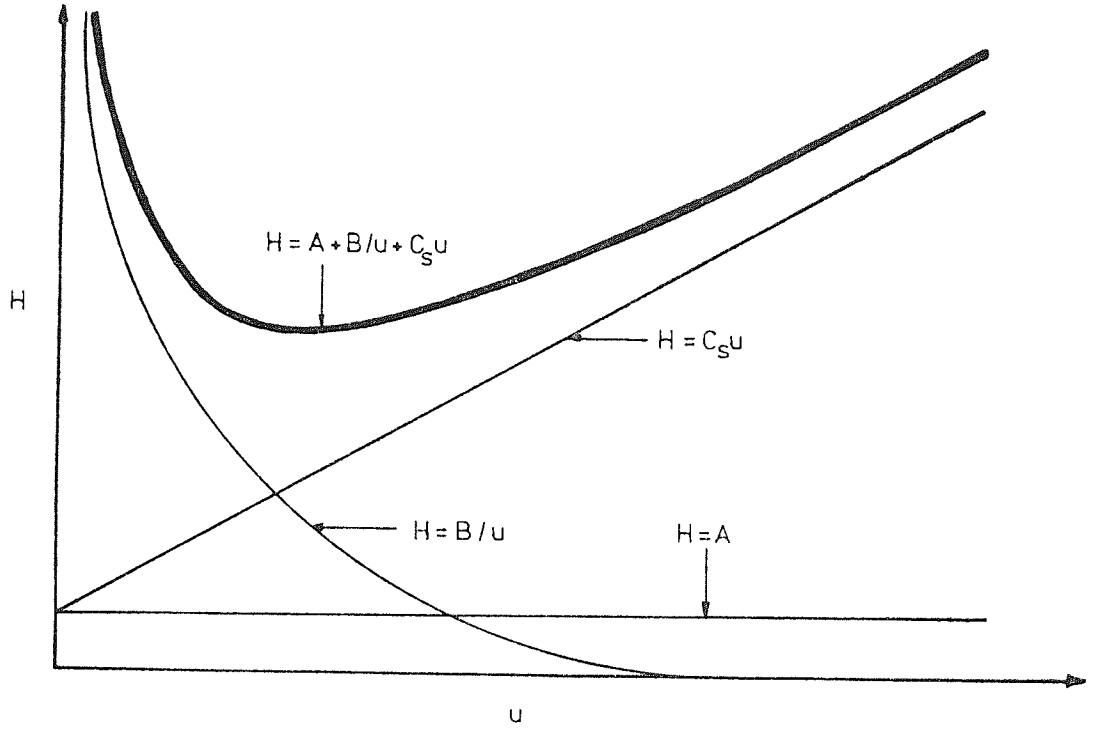

Figure 2.5 Comparison of the Chromatographic Plate Height vs. Mobile Phase Velocity Curves for Gas Chromatography and Liquid Chromatography

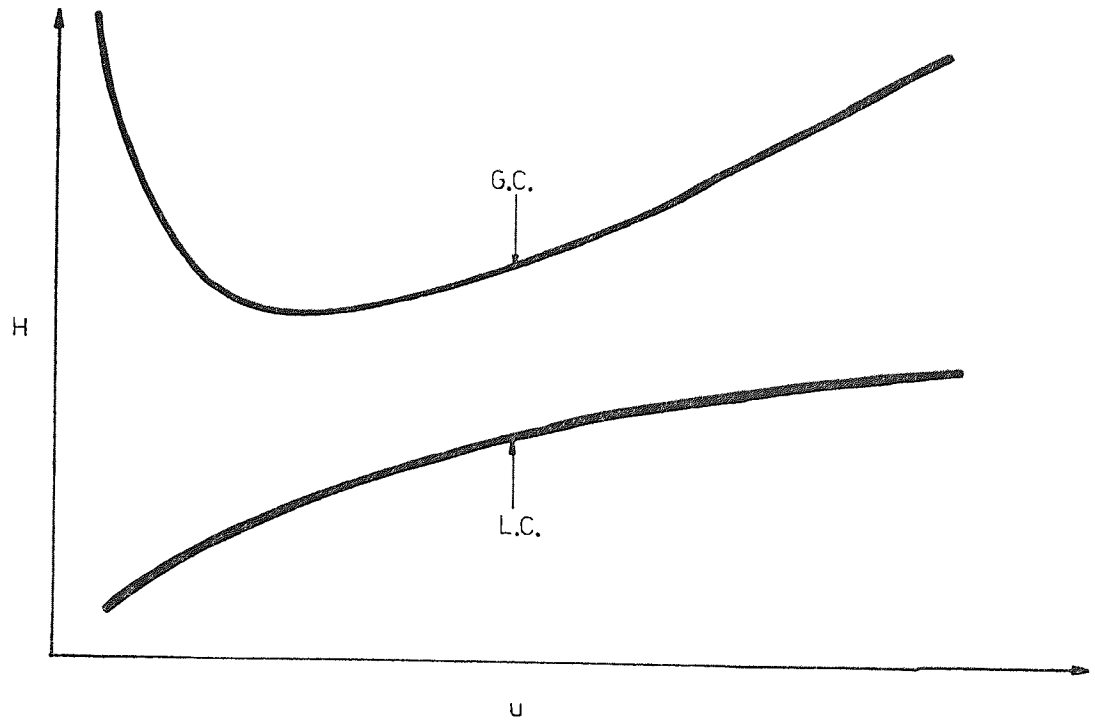

k' = capacity ratio = $K \frac{F_S'}{F_M'}$

k_f = rate of exchange of solute between the two phases

It will be seen that the first two terms are similar to those derived by other models. The last term consists of a contribution due to the finite mass transfer rate between the phases. Disadvantages of the model include the assumption of a flat mobile phase velocity profile, and lack of a term accounting for mobile phase resistance to mass transfer.

Considerable work has been carried out by Giddings on the mechanisms of zone broadening, details of which are given in his well known text (33). His random walk approach (33,44) gives an insight into individual molecular processes occurring in a chromatographic column. A fore-runner of this random walk approach was the more rigorous stochastic theory first developed by Giddings and Eyring (45), which has been applied to multi-site adsorption processes (46). The random walk model is simpler, although also less exact. The molecular movements of the solute, although random, have an equal chance of being forward or backward. It is convenient to define an average (root mean square) step length (ℓ'), although actual molecular displacements differ widely in length. This random molecular movement results in a statistical spread of the molecules in the form of a Gaussian curve. The variance, σ^2, is equal to $\ell'^2 n'$, where n' is the number of steps taken. Each process occurring in the column has its own value of ℓ' and n' which may be summed to give a total variance:-

$$\sigma^2_{TOTAL} = \Sigma\sigma^2_i = \Sigma\, \ell_i'^2\, n_i' = H \qquad (2.9)$$

Giddings (33) uses the variance due to a molecular diffusion process, given by Einstein (47) as:

$$\sigma^2 = 2Dt_d \qquad (2.10)$$

t_d = Diffusion time

D = Diffusion coefficient

to determine the contribution to the plate height from longitudinal mobile phase diffusion:

$$H = \frac{2\gamma' D_m}{u} \qquad (2.11)$$

Longitudinal stationary phase diffusion may be calculated in a similar way, but is usually negligible. Giddings (33) evaluated absorption-desorption kinetics as:

$$H = 2R(1-R)\frac{d^2u}{D_s} \qquad (2.12)$$

d = thickness of stationary phase film

Diffusion processes occurring in the mobile phase are significantly more complex than those in the stationary phase. This is because of the complex nature of the flow channels, and the velocity inequalities, both transcolumn and longitudinal occurring in the mobile phase itself. Giddings (33) defines five mechanisms by which mobile phase velocity inequalities originate:

(i) Transchannel effects caused by a higher velocity in the centre of a channel than at the wall.

(ii) Transparticle effects caused by the stagnant mobile phase in the pores of the support particles.

(iii) Short-range interchannel effects.

(iv) Long-range interchannel effects.

(v) Transcolumn effects between central and outer regions of the column.

A step to a slower streamline is considered a backward step and a step to a faster streamline a forward step. The resulting mobile phase mass transfer term is:

$$H = w d_p^2 u / D_m \tag{2.13}$$

$$w = \Sigma w_i \text{ (five values)} = w_\alpha^2 w_\beta^2 / 2 \tag{2.14}$$

w_α = (distance between velocity extremes)/d_p

w_β = (difference between extreme and average velocity)/u

The eddy diffusion contribution was determined by using the classical theory of solute molecules being locked in fixed stream paths, again considering the five mechanisms, giving:

$$H = 2\lambda d_p \tag{2.15}$$

$\lambda = \Sigma \lambda_i$

$\lambda_i = w_\beta^2 w_\lambda / 2$

w_λ = a structural parameter

Giddings (33) lists approximate values of w_i and λ_i. Summing all the plate height contributions we have:

$$H = 2\lambda d_p + 2\gamma' \frac{D_m}{u} + 2R(1-R) \frac{d^2u}{D_s} + \frac{wd_p^2u}{D_m} \qquad (2.16)$$

$$\text{or } H = A + {}^{B}/_{u} + C_s u + C_m u \qquad (2.17)$$

This is of the same general form as EQUATION 2.7 except for the inclusion of a mobile phase resistance to mass transfer term ($C_m u$).

However, Giddings maintains in his text (33) that the mobile phase mass transfer and eddy diffusion terms are not independent, and consequently their variances not additive. He proposes a coupling theory of eddy diffusion, for which EQUATION 2.17 becomes, in the general case:

$$H = {}^{B}/_{u} + C_s u + \left(\frac{1}{A} + \frac{1}{C_m u} \right)^{-1} \qquad (2.18)$$

The value of the contribution to H of the coupled term is always less than that obtained from either of the component parts (FIG. 2.6). The applicability of this coupled equation has been demonstrated by many workers in the general field of chromatography (e.g. 48). Its relevance to gel permeation chromatography is discussed in SECTION 3.3.1.

Giddings (33) further develops the more powerful generalized non-equilibrium theory of zone broadening, which unlike the microscopic random walk theory considers bulk properties of the chromatographic system. He introduces the theory with a physical picture of non-equilibrium illustrated in FIG. 2.7.

Figure 2.6 Comparison Between Classical and Coupled Equations for Plate Height (33)

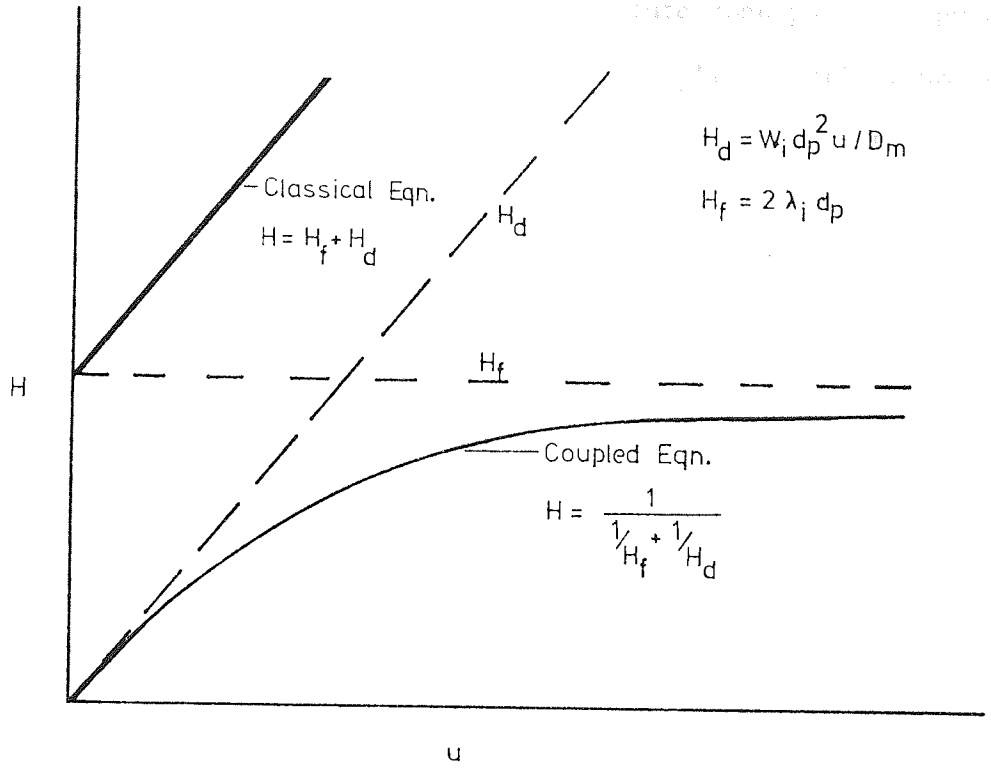

Figure 2.7 Comparison Between Actual and Equilibrium Component Zone Concentration Profiles for Normal Elution Chromatography (33)

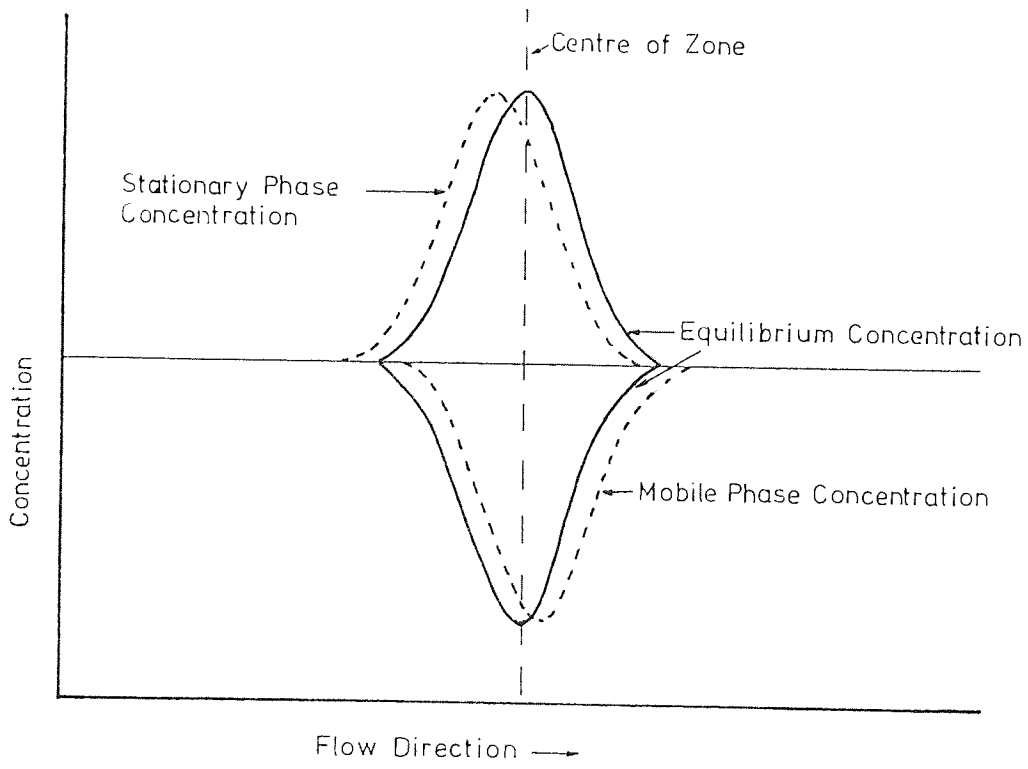

He argues that as the front of a solute zone passes a point in the column devoid of solute, attempts to establish equilibrium occur by solute molecules transferring from the mobile phase into the stationary phase. As the point of maximum concentration of the band is in the centre, and thus the concentration passing the point is continually increasing, equilibrium is not established until the centre point of the zone is reached. After the peak maximum has passed, the solute-rich stationary phase transfers solute into the mobile phase to retain equilibrium, but as the concentration is now gradually decreasing it can never achieve this, the stationary phase concentration changes lagging behind those in the mobile phase. Thus during passage of a solute band through a column, true equilibrium is only achieved at the centre point of the band.

The generalized non-equilibrium theory is only used to calculate the C terms of EQUATION 2.17 (33), which for practical chromatography, using high mobile phase velocities, are the most significant non-equilibrium contributions (FIG. 2.4). The stationary phase contribution may be represented in the following way for most stationary phases:

$$H = q'R(1-R)d^2u/D_s \qquad (2.19)$$

This is a more precise version of EQUATION 2.12 derived from random walk theory. q' is a configuration factor dependent on the shape of the stationary phase layer.

Again derivation of the mobile phase contribution is difficult, especially in its coupled form. However, if simplifying

assumptions concerning packing geometries are made, EQUATION 2.12, obtained by random walk theory, is again produced. However the advantage of the non-equilibrium model lies in its ability to include various packing geometries, so a balance has to be made between the assumptions made and complexity of mathematics thereby involved. The question of the mobile phase term is still an open subject, although Giddings gives some useful examples in his text (33).

The degree of non-equilibrium of a chromatographic process, which determines the extent of solute zone broadening is obviously of extreme importance. This degree is dependent on the migration rate of the solute zone, and solute mass transfer rate. The non-equilibrium may be negligible if the zone velocity is low and the mass transfer rate fast thus preventing large concentration changes. However, many modern analytical methods utilize fast flowrates to decrease analysis time, and in these cases it is critical that mass transfer rates be rapid. Rapid mass transfer rates have been achieved in high performance liquid chromatography (HPLC) using specially designed porous layer particles, the diffusion times being reduced by the much lower liquid film thickness.

For any column optimization procedure it is necessary to decide the significance of the various non-equilibrium contributions. As liquid chromatography is of particular interest in this research programme EQUATION 2.18 will be discussed in this context. It may be written:

$$H = \frac{2\gamma' D_m}{u} + q'R(1-R)\frac{d^2u}{D_s} + \left(\frac{1}{2\lambda d_p} + \frac{D_m}{w d_p^2 u}\right)^{-1} \qquad (2.20)$$

The first term is usually negligible in LC because D_m is $\sim 10^5$ times smaller in liquids than in gases. The second term indicates that for

a greater liquid loading (larger d), the greater is the departure from equilibrium, i.e. the slower is the mass transfer rate. The dependence of H on u indicates less time available to attain equilibrium at a higher flowrate. H also varies directly as R(1-R) which has a maximum at R=0.5, i.e. when 50% of the solute is in the mobile phase. This value of R(1-R) decreases towards the extremes of 0 and 100% solute in the mobile phase. The term also shows the desirability of choosing liquids within which the solute diffusion coefficient is large. Last is the coupled eddy diffusion term. A dependence of H on particle diameter is indicated between $H \propto d_p$ and $H \propto d_p^2$, showing d_p should be as small as possible. At high velocities the term converges to the classical eddy diffusion version of $2\lambda d_p$. Further discussion of the relevance of these terms for gel permeation chromatography is given in SECTION 3.3.1.

The models outlined in the preceding text have provided a firm theoretical background for the molecular processes occurring in chromatographic columns. It will be noticed, however, that as knowledge has developed, the models have necessarily become more complex. Recently several semi-empirical equations have been introduced to provide simple column optimization procedures. One such equation (49,50) which fits most high speed liquid chromatography applications (d_p = 10 → 100 μm, u = 0.5 → 10 cm sec^{-1}) is:

$$H = D' u^b \qquad (2.21)$$

where D' and b are constants for a given column. The equation

$$H = A_u^{0.33} + C_u \qquad (2.22)$$

is proposed by Kennedy and Knox (51) to cover a wider range of velocities. Both these equations, however, fail at reduced velocity (ν) values <30, and neither predicts a minimum value of h for a plot of h vs ν ($= \frac{ud_p}{D_m}$) in this region. Another semi-empirical equation is the Huber Equation (52):

$$H = \frac{a_1 D_m}{u} + \frac{a_2 d_p}{1+a_3(D_m/ud_p)^{1/2}} + a_4 \left(\frac{k'}{1+k'}\right)^2 \left(\frac{d_p}{D_m}\right)^{2/3} u^{1/2} + a_5 \frac{k' d_p^2 u}{(1+k')^2 D_s} \qquad (2.23)$$

where a_1-a_5 are constants to allow for packing geometry. This equation has the advantage of allowing experimental conditions to be related to more fundamental parameters than the two previous equations, although in so doing loses the advantage of simplicity.

Additional contributions to the plate height encountered in large diameter columns are reviewed in SECTION 2.3.2.

2.3 SCALE-UP OF THE BATCH CHROMATOGRAPHIC PROCESS

2.3.1 The Relationship Between Sample Size and Operating Mode

2.3.1.1 Increased Sample Volume

The variation in operating modes of elution chromatography is centred on the feed band concentration profile, which has dimensions of height (concentration of solute) and width (length of column occupied by feed band). The normal situation in elution chromatography, on which discussion has been restricted in SECTION 2.2, is for a narrow feed inlet band to be eluted from a column. This produces a Gaussian outlet profile, the width of which is independent of the inlet band width. The limit for this in practice is found to be that proposed by Van Deemter et al. (39) and Glueckauf (37). This may be stated as the ratio of the widths of the feed inlet and product outlet bands, measured at the points of inflection, being less than $^1/_4$,

$$\text{i.e.} \quad \frac{\sigma_f}{\sigma_p} < \frac{1}{4} \qquad (2.24)$$

σ_f = standard deviation of feed inlet profile

σ_p = standard deviation of product outlet profile

However, it should be noted that this criterion merely defines the limit for the outlet band to be Gaussian, which is not a limiting factor for production scale chromatography. Certain advantages are obtained by operation with larger feed band widths. For narrow feed bands where their width is usually much less than the width of the column outlet bands, it is obvious that a certain fraction of the column is not occupied by solute at a given time, and thus not being used for separation. This fraction is reduced when the feed band width is

increased, and the widths of the inlet and outlet bands are more nearly equal.

If the ratio $\frac{\sigma_f}{\sigma_p}$ is increased, eventually a point will be reached where the product outlet profile will have a flat top, of height equal to that of the feed band, and the suggested name for this mode of operation is eluto-frontal (53). Further increase of the feed band width will eventually lead to a continuous feed input, producing a single or multi-stepped front boundary, followed by a plateau region in which no separation of the feed occurs, and which has a height equal to the feed input. This mode of operation is called frontal analysis.

The criteria for naming the operating mode have been discussed in detail by Conder and Purnell (53,54) who suggested:

$\theta < \frac{1}{2}$	ELUTION	$(\equiv \frac{\sigma_f}{\sigma_p} < \frac{1}{4})$
$\frac{1}{2} < \theta < 6$	OVERLOAD ELUTION	
$\theta > 6$	ELUTO-FRONTAL	

where $\theta = \frac{N_f}{\sqrt{N}}$

N_f = No. of plates occupied by feed inlet band.

N = Total number of plates in column.

For the overload elution mode, the outlet band is intermediate between Gaussian and flat-topped, and its dimensions are dependent on those of the feed inlet band.

Figure 2.8 Illustration of the Operating Modes of Chromatography

(a) Normal Elution

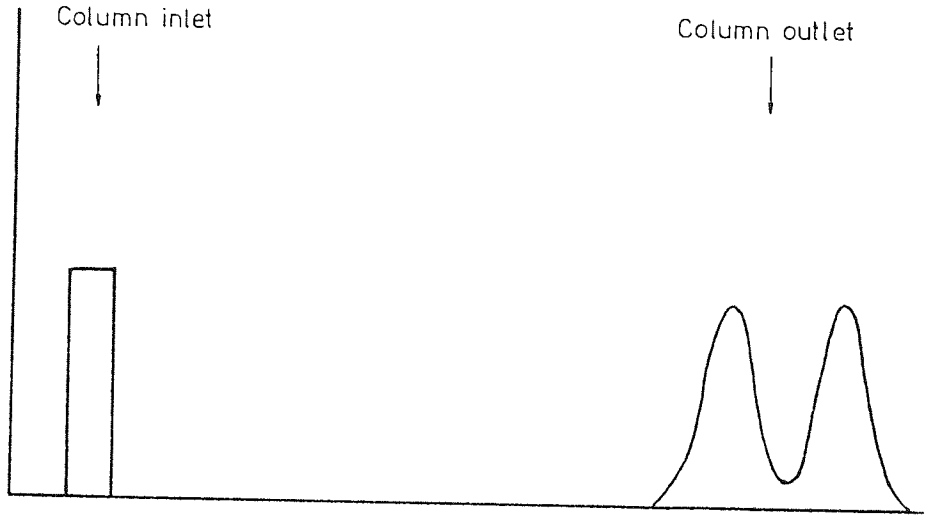

(b) Eluto-Frontal

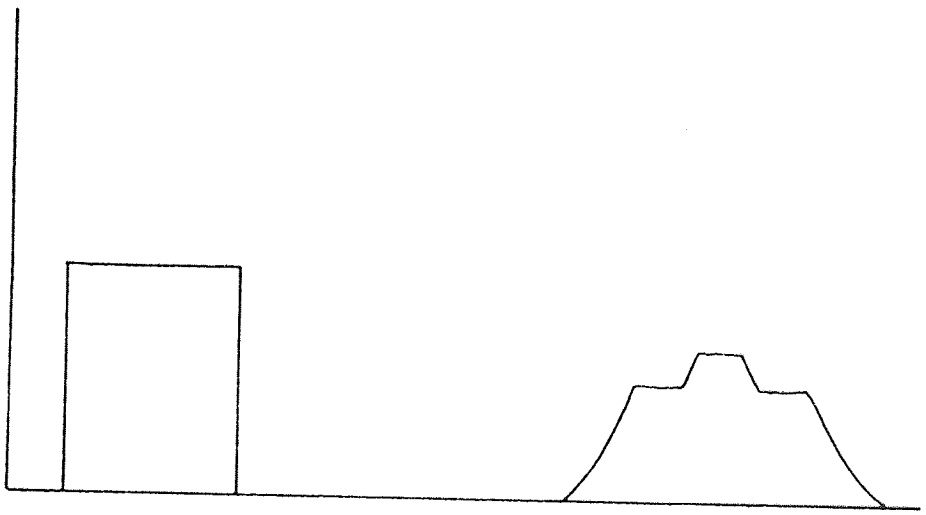

(c) Frontal

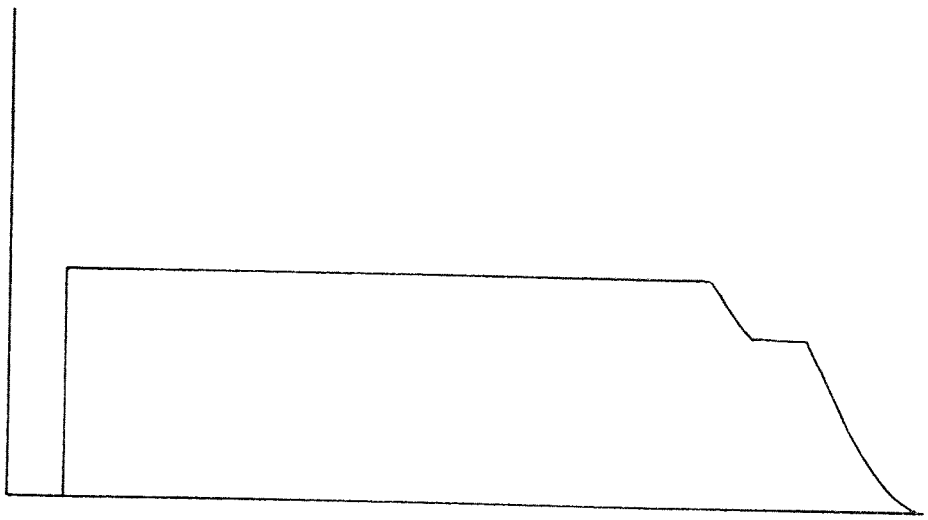

These relationships assume linear chromatography at low concentrations, and consequently show that the mode of operation is dependent only on the width of the feed inlet band and column length. For example, a feed band width which resulted in eluto-frontal operation for one column could, on a longer column, result in overload elution or normal elution operation.

Conder and Purnell (54) indicate how the required number of plates for a given separation may be calculated, and they develop an expression for feed throughput, Q , for the three modes of operation:

$$Q = \frac{n_f}{n} \left\{ \frac{a}{6} \cdot \frac{M_f P_f}{R'T} \cdot \pi r^2 \varepsilon \bar{u} \right\} \qquad (2.25)$$

n = reduced value of $N = \dfrac{N}{36/a^2}$

$$a = 2 \left(\frac{\alpha-1}{\alpha+1} \right) \left(\frac{k}{1+k} \right)$$

$$\alpha = \frac{V_{R_2} - V_M}{V_{R_1} - V_M}$$

V_R = retention volume of component

V_M = mobile phase volume of column

$$k = \frac{1/2 (V_{R_1} + V_{R_2}) - V_M}{V_M}$$

n_f = reduced value of $N_f = \dfrac{N_f}{6/a} = \theta\sqrt{n}$

M_f = (average or component) M.W. of feed

P_f = (total or component) partial pressure of feed input before column inlet

R' = gas constant

T = column temperature

r = internal radius of column

ε = porosity of packing

$\bar{u}$ = compressibility corrected mobile phase velocity

They calculate from this equation that the eluto-frontal mode offers at least a six-fold increase in throughput compared to the elution mode, offset by a three-fold increase in column length. They indicate further that the most economical mode of operation is likely to lie in the overload elution region if expensive packing and column pressure drop make important contributions to cost.

Pretorius and de Clerk (55) have reviewed the extensive results of Krige et al. on preparative frontal analysis, and Gordon et al. on preparative elution chromatography given in the literature (56-61). They conclude that the functional similarity of the respective efficiency equations indicate identical optimum operating conditions for both methods. However they also conclude that repetitive injection of plug samples gives a higher preparative efficiency than frontal analysis under dilute conditions. The decreased sensitivity of frontal analysis to high feed concentrations (non-linear chromatography) compared to elution chromatography, is suggested by the authors as having possible applications in production chromatography.

One obvious drawback to frontal-elution chromatography is that only the component with least affinity for the stationary phase can be recovered directly from the column effluent (2.8(c)). The eluto-frontal method, however, offers direct recovery of the least retarded component from the front of the outlet band, and the most

retarded from the rear of the band (FIG. 2.8(b)). Work in this area has been carried out by Reilly et al. (62), but the preparative efficiency of his schemes have not been clarified.

In conclusion, practical scale-up of co-current batch operation is theoretically most promising in the elution or overload elution modes, and the majority of production scale batch units have been designed around this method, utilizing repeated sample injection into large diameter columns.

2.3.1.2 Finite Concentration Effects

Feed concentration and feed band-width are closely-linked variables, and an increase in either generally results in a broader peak at the column outlet. Consequently, an increased sample size leads to a reduction in column efficiency in terms of the number of theoretical plates. Discussion in SECTION 2.3.1.1 refers to the case of a linear absorption isotherm, i.e. the solute partitioning between mobile and stationary phases is independent of solute concentration. In this case the elution volume of a component from a column is given by EQUATION 2.2. However, the ratio of solute partitioning may vary with solute concentration, and in this case the isotherm is non-linear, the elution volume being given by (63):

$$V_R = V_M + V_S \left(\frac{\partial q}{\partial c} \right)_c \qquad (2.26)$$

q = solute concentration in stationary phase

c = solute concentration in mobile phase

Operation under non-linear conditions produces peak distortion because of the different values of the partition coefficient (K), obtained in

different parts of the solute zone. The variation of $K = \frac{q}{c}$, with concentration is illustrated by FIG. 2.9, which shows the two commonest forms of non-linear isotherms, and the resulting solute boundary shape (64). For the Langmuir isotherm (FIG. 2.9(b)) K decreases with increasing concentration, resulting in a lower elution volume. The eluted band has a characteristic sharpened leading edge and tailed trailing edge. For the anti-Langmuir isotherm (FIG. 2.9(c)) K increases with increasing concentration resulting in a higher elution volume. This produces a diffuse front and sharpened trailing edge. The linear isotherm produces a Gaussian peak as discussed previously (SECTION 2.2.4).

Operation in the non-linear region results in greater product impurity, and hence a longer column is necessary to obtain the same degree of separation. In practice a balance between this and the gain in throughput obtained must be made. Pretorius and de Clerk (55) suggest that a fair amount of skewing may be tolerated in view of the gain in mass throughput. They conclude that such a procedure may considerably enhance the efficiency of preparative operations.

In general it is advantageous to operate at the maximum possible concentration for production chromatography, as concentration is directly proportional to throughput, the particular value of concentration depending on the desired mode of operation. Discussion of concentration effects pertinent to g.p.c. is given in SECTION 3.4.

2.3.2 Scale-up of Column Diameter

2.3.2.1 Solute Velocity Profiles in Large Diameter Columns

The random walk approach of Giddings, outlined in SECTION 2.2.4.3, indicates that solute zone broadening occurs where velocity inequalities

Figure 2.9 The Relationship between the Solute Zone Boundary Concentration Profile and the Type of Partition Isotherm (64)

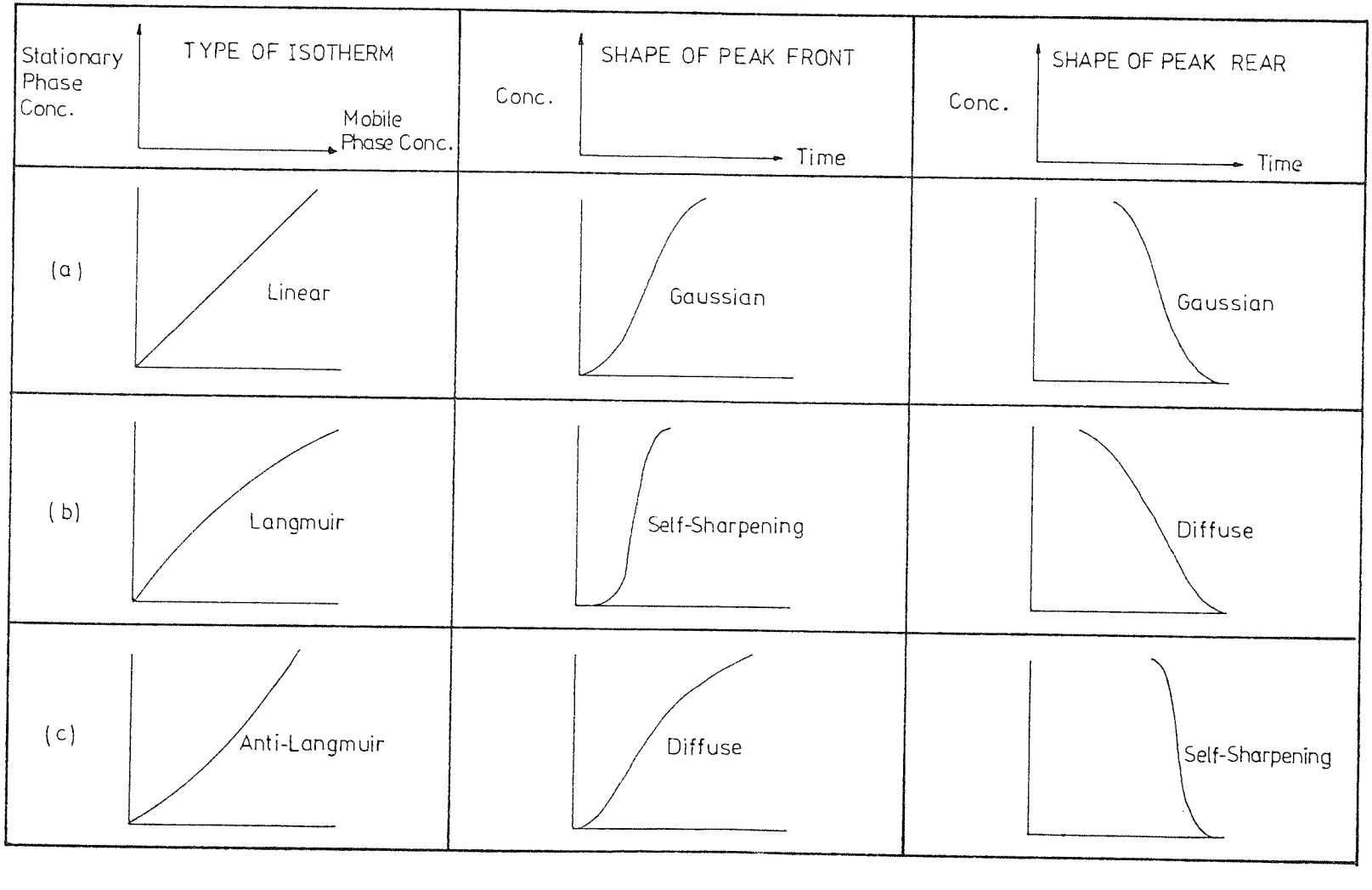

exist next to each other, with solute molecules exchanging between them. A step to a faster streamline is regarded as a forward step, and one to a slower streamline as a backward step. Five suggested ways in which velocity inequalities might occur were outlined in SECTION 2.2.4.3. Of these the transcolumn term is of particular importance for production chromatography when large diameter columns are employed. This is because substantial velocity differences often occur between the central and outer regions of large diameter columns due to affects associated with the column wall.

The frictional drag exerted by the wall on a fluid flowing through a tube, produces lower velocities near the wall. Under laminar flow conditions the velocity profile is as shown in FIG. 2.10(a) with a maximum velocity at the tube axis. A further effect is associated with the lower packed density obtained at the wall for chromatographic columns due to the misfit of the packing particles in this region. Opinion on the effect of these factors on the velocity profile in chromatographic columns differs.

Giddings (65) considers that the effect of the lower resistance to flow near the walls is increased by the fact that larger particles tend to accumulate near the walls during packing. He proposes a velocity profile convex to the direction of flow (FIG. 2.10(b)). Huyten, Van Beersum, and Rijinders (66) observed a profile of this shape for a 7.5 cm diameter column, and a similar observation was made by Friscone(67). However Hupe et al. (68) point out that the increase in packed density at the centre of the column could result in faster mass transfer rates, and they observed a maximum zone velocity at the centre of a 10 cm diameter column. Volkov (69) also observed maximum values of band velocity at the column centre.

Figure 2.10 Flow Profiles in Large Diameter Columns

(a) Laminar Flow in an Open Circular Column

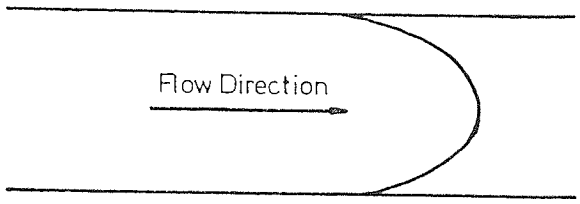

(b) Flow in Packed Columns Postulated by Giddings (65)

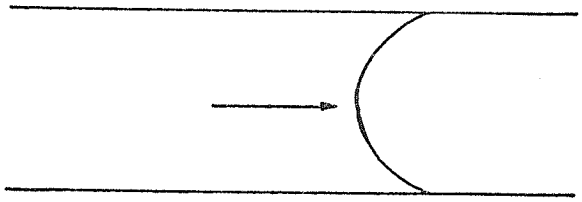

(c) Flow in Packed Columns Postulated by Pretorius and De Clerk (55)

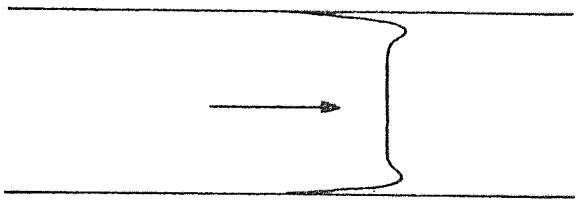

(d) Dependence of the Wall Effect in Packed Columns on Particle/Column Diameter Ratio (55)

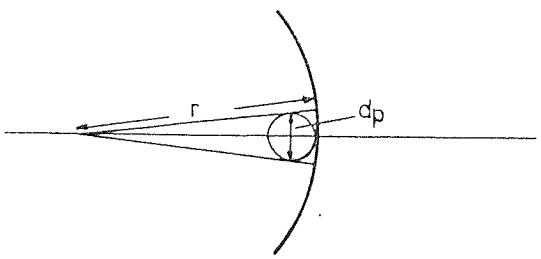

Pretorius and de Clerk (55) reason that the misfit of particles near the wall results in a larger area for flow in this region, and the size of this area is dependent on the ratio of particle to column diameter ($\frac{d_p}{d_c}$). This is illustrated in FIG. 2.10(d). Their expected flow profile also takes into account frictional drag at the wall and is illustrated in FIG. 2.10(c).

Although disagreement exists as to the precise shape of the velocity profile in large diameter columns, non-uniformity may be expected to exist. This non-uniformity contributes to solute band broadening and hence to a loss in efficiency. The following section deals with quantitative treatment of the efficiency loss.

2.3.2.2 The Variation of Column Efficiency with Diameter

Treatment of the effect of non-uniformity of the velocity profile on column efficiency has led to the addition of an extra term, H_c, being included in the standard expressions for plate height (SECTION 2.2.4.3). Thus the Van Deemter Equation would become:-

$$H = [A + \frac{B}{u} + C_m u + C_s u] + H_c \qquad (2.27)$$

Giddings (70) used his non-equilibrium theory to evaluate a plate height contribution, based on a quadratic velocity profile, and found good agreement with data obtained on 0.6 cm and 5.1 cm diameter columns (71). The contribution may be expressed as:

$$H_c = G_2 \left(\frac{r^2 u}{96\gamma' D_m}\right) \qquad (2.28)$$

G_2 = a constant

Higgins and Smith (72), Huyten et al. (66), and Rijinders (73) obtained expressions of a similar form, but in contrast Bayer et al. (74) obtained good experimental agreement for columns between 1.3 cm and 10.2 cm diameter for

$$H_c = 2.83 \frac{r^{0.58}}{u^{1.886}} \qquad (2.29)$$

All of these expressions, however, predict a fall-off in efficiency with increased diameter, differing only in degree.

The relaxing of band spreading by lateral diffusion was discussed by Littlewood (75) and Sie and Rijinders (76). Lateral diffusion was considered as being composed of molecular diffusion (γD_m) and "convective" diffusion ($\alpha' d_p u$) arising from repeated mixing and separation of mobile phase stream. They produced an expression:

$$H_c = \frac{0.5K' d_c^2 u}{\gamma D_m + \alpha' d_p u} \qquad (2.30)$$

α' = constant for packing geometry

K' = dimensionless flow profile factor, proportional to

$$\frac{\text{amplitude of cross-sectional velocity variations}}{u}$$

Pretorius and de Clerk (55) report the use of the model illustrated in FIGS. 2.10(c) and (d) to obtain a semi-empirical expression for the contribution to the reduced plate height. This may be expressed in terms of H_c, as

$$H_c = \frac{m' d_c^2 u}{2D_r d_p} \qquad (2.31)$$

where $m' = \left(\frac{1}{100}\right) \exp\left(-\frac{d_c}{10d_p}\right)$

This indicates that the plate height increases with d_c at constant $\frac{d_p}{d_c}$, reaches a maximum at $\frac{d_p}{d_c} \sim 0.05$, and then decreases with increasing d_c. Support for this theory is given by Spencer and Kucharski (77) and Knox (78).

Charm, Matteo and Carlson (79) suggest that maintaining a constant value of ℓ/d_c and Reynolds number ($Re = \frac{d_c u \rho}{\mu}$) results in dynamic similarity and similar velocity profiles dispersion characteristics irrespective of column diameter. They conclude from their experimental results for g.p.c. analysis of proteins on columns of 3.7 cm to 14.2 cm diameter packed with Sephadex G-100 that resolution is maintained if these ratios remain constant. However, it is difficult to compare these results with those of other workers as no H.E.T.P. values are recorded. They measure the degree of separation by summing the maximum values of the last two peaks of a mixture of proteins, and dividing this by the minimum value between them.

Some interesting results were observed by Bayer et al.(74) and Spencer and Kucharski (77) concerning the effect of column diameter on efficiency. The former recorded that the rate of increase in H.E.T.P. with column diameter fell off for increasing diameter from 1 cm to 50 cm. The latter also observed this trend, with a fall in H.E.T.P. above the 6.4 cm diameter level. This effect could be due to the fact that if the column diameter is so large that radial equilibrium is not achieved, the plate height becomes independent of diameter (65, 71). This 'infinite-diameter' effect was discussed by Knox and Parcher (80), who considered that adverse wall-effects could be overcome by choosing a

column of sufficient diameter that the sample was eluted before solute had time to diffuse to the wall. Alternatively they suggested a 'centre-cutting' technique to remove only the unaffected central portion of a solute band from the column effluent.

De Stefano and Beachell (81) suggested that the improved efficiency they observed for liquid chromatography columns, of 7.94 mm diameter and 10.9 mm diameter, compared with columns of 1.6 to 4.76 mm diameter packed with the same packing (<37μm Controlled Surface Porosity - CSP support), could be due to this effect. Using a rearrangement of the Knox-Parcher equation (80), which defines the limit for the infinite diameter effect to be applicable,

$$d_c = (2.4\ d_p \ell)^{1/2} \qquad (2.32)$$

they calculate that 6 mm is the minimum diameter necessary to achieve the effect for 30 μm particles packed in a 50 cm long column. Consequently column diameters greater than this value produce higher efficiencies than those of lower diameter. They consider the fact that the 7.94 mm and 10.9 mm columns showed very similar H.E.T.P. values supports this argument, as there is no obvious advantage in increasing column diameter once wall effects have been overcome. Recovering the central portion showed no gain in efficiency, further supporting the theory. Typical H.E.T.P. values of 0.01 to 0.04 cm were obtained for mobile phase velocities up to 4 cm sec^{-1}.

This theory would seem to be a possible explanation for observed improved efficiencies with increasing column diameter, but the contrasting results of Wolf (82) should be noted. He ensured that the sample was loaded in a plug across the whole column cross-section and still observed a continual increase in column efficiency as column diameter was increased

from 0.21 cm to 2.36 cm diameter. He used 50 cm long liquid chromatography columns packed with Permaphase ODS (10-40 μm) at 1.4 cm sec^{-1} mobile phase velocity. His data was found to fit the relationship:

$$N = 500\ (d_c)^{1/2} - 107 \qquad (2.33)$$

This indicates a linear increase in the number of theoretical plates with the square root of the column diameter. A maximum efficiency was obtained for the 2.36 cm diameter column, and the H.E.T.P. value was 0.2 mm.

To summarize, differences in opinion exist to the exact nature of the effect of column diameter on operating efficiency. The weight of opinion would seem to indicate a loss of efficiency when columns are scaled to the production level, although this can be substantially offset by better packing techniques and the use of flow distributors to improve radial mixing.

2.3.2.3 Practical Methods of Improving Column Efficiency

2.3.2.3.1 Column Packing Techniques

Practical values of efficiency obtained for gas chromatography in large diameter columns have been reviewed by Deeble (29). It is evident that improvements up to an order of magnitude can be obtained by careful packing. Dry-packing is the conventional method in gas chromatography, and although disagreement exists concerning the best method, such as "mountain packing", fluidization, "bulk packing", typical values of H.E.T.P. between 1 and 3 mm have been obtained (66,67,68,72,74).

Studies of dry-packing techniques for use with liquid chromatography have been carried out using adsorbents (83,84) and CSP supports (85-88) for packing small particles in small diameter columns. The packing technique used for the SCCR3 unit is discussed in SECTION 6.1.4. Summarizing, it is apparent from the literature that a considerable gain in efficiency can be obtained by careful packing of chromatographic columns, although opinion differs on the best method.

2.3.2.3.2 The Use of Flow Distributors

Because of the low radial diffusion associated with large diameter columns, devices to improve radial mixing have been introduced, both at the column inlet and within the column itself. A non-uniform inlet profile is unlikely to be corrected during passage through a column, and various methods to obtain a uniform profile at the column inlet have been proposed.

Musser and Sparks (89) carried out a study of inlet distributor designs to obtain a uniform velocity distribution and low axial dispersion. They studied open cones, cones filled with multiple screens, and partially packed cones (FIG. 2.11). Theoretical treatment of flow through open cones showed that larger cone divergence angles improved performance by reducing dispersion. A continual reduction in dispersion was obtained for 10.2 cm diameter cones containing 0.24 cm diameter lead shot, as the amount of packing was increased. The minimum dispersion was obtained for 60° cones packed to 80% of their total volume beginning from the larger end (FIG. 2.11(b)). Above 80% no significant reduction in dispersion was obtained. Huyten et al. (66) observed a similar trend, and recorded an improvement in H.E.T.P. up to

Figure 2.11 The Design of Inlet Distributors for Large Diameter Chromatographic Columns (89)

(a) Open Cones

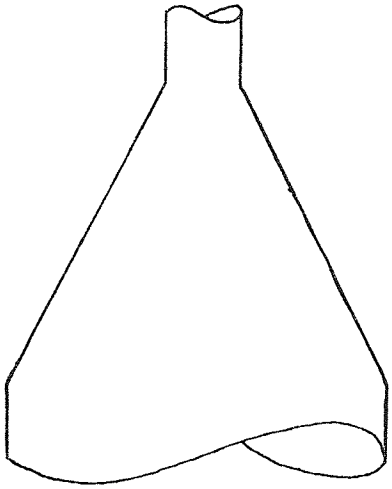

(b) Packed Cones

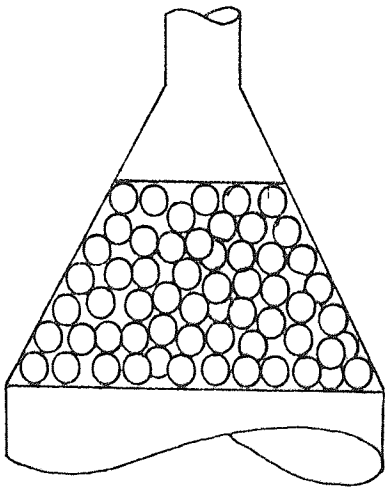

(c) Cones with Screens

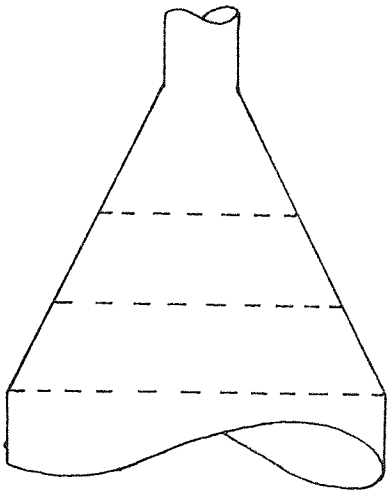

80% packed volume using chromatographic packing. However, when the inlet cone was completely filled with packing, a marked deterioration in H.E.T.P. was recorded. The authors suggested that this was probably due to overloading the packing, making the use of an inert packing material desirable. The best efficiency was obtained when the exit cone was completely filled with chromatographic packing, giving an H.E.T.P. value of 2.2 mm for a 7.6 cm diameter column.

Musser and Sparks (89) further recorded the velocity profiles obtained with 30° and 60° partially packed cones at gas velocities from 1 to 12 cm sec^{-1}. They concluded that the variance of the velocity profile was approximately equal for different packing depths, and showed an order of magnitude increase over the velocity range. The velocity variance for the 60° cone was found to be higher than that for the 30° cone, and was attributed to the increased effect of the wall packing structure for the larger divergence angle. Further work was carried out for 30° and 60° cones using multiple screens (FIG. 2.11(c)). For both cones the use of screens produced a more uniform velocity distribution, and the use of two or three screens reduced the variance of the velocity distribution to ~1%, a factor of ten better than the packed cones. The dispersion obtained with screens was found to decrease as the cone angle increased, but the effect of the screens was found to decrease with increasing cone angle. Thus no significant decrease in dispersion for a 90° cone fitted with screens was observed compared to an open cone of the same angle, but an improvement of a factor of six was found for a 30° cone. For a 60° cone fitted with screens the overall dispersion was an order of magnitude higher than the 60° cone packed to 80% of its volume. Albrecht and Verzele (90) also found an improvement of efficiency by packing the inlet cone of a 7.5 cm diameter column with glass spheres.

In conclusion, the use of multiple screens in inlet cones produces a uniform velocity profile for large diameter columns, while packing with inert spheres reduces axial dispersion by an order of magnitude. Also larger cone angles generally give improved performance.

Several designs of mixing devices for incorporation within large diameter columns have been proposed. These have taken the form of washers and baffles (67,74,91,92) or mixing chambers (93,94). Friscone (67) successfully used washers coated with liquid stationary phase to retard the normally advanced solute profile near the column wall. Improved efficiencies were obtained by Bayer et al. (74) also using washers, placed at 10 cm intervals in the column. The use of baffles is reported (91,92) by workers associated with Abcor Inc., Massachusetts. Efficiencies of 10 cm diameter columns are reported as greatly improved by the use of mixing baffle 'sandwiches' placed at 30.5 cm intervals in the column. H.E.T.P. values of $\leq$ 1 cm are reported (91) as being comparable to those of a 0.64 cm diameter analytical column ($\leq$ 0.7 cm) at equivalent gas velocities ($\leq$ 4-5 cm sec^{-1}).

The mixing chambers employed by Carel et al. (93,94) are based on porous discs. The column is divided into packed sections each supplied with a porous disc at each end and connected by narrow diameter tubing. These authors obtain maximum separable injection volumes, proportional to the cross-sectional area, for scale-up of column diameters from 0.6 cm to 30.0 cm.

Golay (95) suggested that the spacing of mixing devices is critical, and too many may actually contribute to zone broadening.

Giddings (65) proposed that the connecting tubing between column sections should be less than 0.01 times the volume of the column section. Mir (96) has equated the gain in efficiency in terms of H.E.T.P. for n_1 mixing devices as:

$$\frac{H_{CN}' - H'}{H_C' - H'} = \frac{1}{n_1} \qquad (2.34)$$

H' = Intrinsic plate height for packing (without excess caused by large diameter). This would be as obtained for a small diameter analytical column.

H_C' = Plate height obtained for large diameter column without mixing devices.

H_{CN}' = Plate height obtained for the same large diameter column with mixing devices.

This equation indicates that the law of diminishing returns applies to the number of mixing sections employed.

The introduction of baffling in production-scale columns plus the provision of a uniform inlet profile have resulted in efficiencies comparable to analytical columns, although theoretical predictions are difficult. The cost analysis of Conder (97) indicated that production cost is greatly reduced for initial increases in column diameter, although the effect is less marked for column diameter changes on a larger scale.

In conclusion, it is interesting to note that injection of large samples into large diameter columns has become an accepted unit operation in gel permeation chromatography (98). The examples of throughput given by Ek (99) are based on standard, commercially available columns, ranging from 40 cm diameter to 180 cm diameter, packed with coarse Sephadex G-25 (a cross-linked dextran gel). For a feed mixture of a high M.W. substance (>5,000 M.W.) and a low M.W. substance (<ca. 200 M.W.) having a viscosity 1.7 times that of the mobile phase fluid, he calculates feed throughputs up to 625 litres per cycle, or 1490 litres hr^{-1}, for columns up to 180 cm diameter, 100 cm long at a flow rate of 5 cm^3 min^{-1} cm^{-2}. He estimates a 95% yield of the high M.W. fraction having 90% purity in this case as an example, but stresses other results within wide ranges can easily be achieved by choosing alternative process conditions. Other large scale applications of g.p.c. have been reported for materials including proteins (100) and antibiotics (101).

2.3.3 Other Factors Affecting Scale-up

2.3.3.1 Mobile Phase Velocity

An increase in mobile phase velocity allows samples to be eluted in a shorter time and hence greater feed throughput to be attained (EQUATION 2.25). However, increasing the mobile phase velocity increases the value of H.E.T.P. (FIG. 2.5), and hence reduces column efficiency. As these two effects are opposed, an optimum flow velocity exists for batch chromatography in the elution mode, which increases proportionally to column length and exceeds that for the corresponding analytical case (55). Conder (97) indicates for operation outside the elution mode that the maximum possible velocity should be used notwithstanding the resulting need for a long column.

2.3.3.2 Column Length

Separation of peak centres is proportional to column length (ℓ), while peak width is proportional to $\sqrt{\ell}$ in conventional elution chromatography. Thus an increase in column length will produce improved separation of a mixture. However, economic reasons associated with expensive packing and costs incurred for operation at higher pressure drop could make long columns undesirable . Recycle operation reduces the column length required for a given separation by passing the components through the column several times, the effluent from one operation becoming the feed for the next. However improved resolution is obviously obtained at the expense of throughput, which could make this mode of operation undesirable.

The number of plates required to exactly separate two peak centres by 6σ, in the elution mode, was given by Purnell (102) as:

$$N_{REQ.} = 36 \left(\frac{\alpha}{\alpha-1}\right)^2 \left(\frac{1+k'}{k'}\right)^2 \qquad (2.35)$$

or in terms of resolution ($R_S = 1.5$) as:

$$R_S = \frac{1}{4} \left(\frac{\alpha-1}{\alpha}\right) \left(\frac{k'}{1+k'}\right) \left(N_{REQ.}\right)^{1/2} \qquad (2.36)$$

k' refers to the slowest moving component.

Equation 2.35 indicates that for a given separation the required number of plates, and hence column length, is only dependent on the thermodynamics of the system. In gas chromatography k' is usually much greater than unity, making $\left(\frac{1+k'}{k'}\right)$ unity, and so it is the separation factor (α) that governs the number of plates and column length. However, in liquid chromatography k' is often small and has

to be considered. The elution time may be written in terms of k' as:

$$t_R = t_o (1+k') \tag{2.37}$$

This equation shows that for high-speed operation it is desirable to keep k' as small as possible, but high k' values are required for better resolution (EQUATION 2.36), making a compromise necessary. In general, the required separating length, or number of plates, increases with the difficulty of separation.

The effective number of plates in a column may be written:

$$N_{EFF.} = \left(\frac{k'}{1+k'}\right)^2 N \tag{2.38}$$

This equates more universally the separating capability of a column, as k' may be so small as to make a very large number of plates necessary for a separation. EQUATION 2.36 may be written:

$$R_s = \frac{1}{4}\left(\frac{\alpha-1}{\alpha}\right)(N_{EFF.})^{1/2} \tag{2.39}$$

For a given resolution the number of effective plates required increases as α decreases towards unity. Small changes in α near unity produce large changes in $N_{EFF.}$ required. A decrease in α from 1.10 to 1.01 would produce an increase in the required number of effective theoretical plates of two orders of magnitude for example.

The required number of plates for operation outside the normal elution mode has been discussed by Conder and Purnell (53). They suggest

that EQUATION 2.35 is valid for overload elution, except that N_{REQ} must be replaced by N^*_{REQ}, the apparent number of plates required, which is a function of feed input width. They illustrate the relationship between N and N^* derived by Glueckauf (103) as a graph of N/N^* vs. y_i/y_o where y_i and y_o are the widths of the input and output bands at the points of inflection. An expression for N_{REQ} is obtained for the eluto-frontal mode of operation as:

$$N_{REQ} = \frac{36}{\left[\left(\frac{\alpha-1}{\alpha}\right)\left(\frac{k'}{1+k'}\right) - \frac{N_f}{N_{REQ}}\right]^2} \qquad (2.40)$$

where N_f is the number of plates occupied by the feed band. EQUATION 2.40 reduces to EQUATION 2.35 as $N_f \rightarrow 0$. The throughput optimization of Conder and Purnell (54) indicated that the three-fold increase in column length necessary to retain separation for operation in the eluto-frontal mode was likely to be the optimum value for batch operation.

2.3.3.3 The Use of Repeated Sample Injections

Practical scale-up of the co-current batch process has mainly consisted of repeated injection of samples into columns of diameter larger than the usual analytical columns. If each injection is made after the peaks from the previous injection emerge from the column, then the column is being used exclusively for a single separation at any given time. To increase column utilization, it is usual to introduce subsequent injections before the previous injection has emerged from the column. In this way several samples are being separated by the column at a given time. In practice a limit must be made to the rate of injection if

excessive overlap of successive samples is to be avoided, and considerable work has been carried out in this area.

Timmins et al. (92) suggest an equation for throughput in linear liquid chromatography, for the case when the front-running peak of a given injection just begins to catch the late running peak of the previous injection, as:

$$Q = 0.4[(A'\phi u\rho x)/R_s][1-(\ell_{MIN}/\ell)]^{1/2} \qquad (2.41)$$

Q = production rate

A' = column area

ϕ = column porosity

ρ = mobile phase density

x = concentration of feed in mobile phase during injection

R_s = resolution

ℓ_{MIN} = minimum column length that will still achieve separation

$= N_{MIN}.H$

H = plate height obtained from an experimental equation of the Van Deemter form (SECTION 2.2.4.3)

$$N_{MIN} = 16(R_s)^2 \left(\frac{\alpha}{\alpha-1}\right)^2 \left(\frac{k+1}{k}\right)^2$$

This equation illustrates the straightforward dependence of throughput on the parameters in the first bracket, and indicates that increasing column length will permit an increase in throughput. Re-arrangement of EQUATION 2.41 into a mobile phase utilization efficiency, η_L, defined as the ratio of feedrate to carrier rate, and also into a column utilization efficiency, ε_L, defined as the ratio of

feedrate to column volume, produced the following two equations:

$$\eta_L = 0.4 \left(\frac{x}{R_s} \right) \left[1 - (\ell_{MIN}/\ell) \right]^{1/2} \qquad (2.42)$$

$$\varepsilon_L = 0.4 \left(\frac{x}{R_s} \right) \left[(\rho u \phi)/\ell_{MIN} \right] \left(\frac{\ell_{MIN}}{\ell} \right) \left[1 - \left(\frac{\ell_{MIN}}{\ell} \right) \right]^{1/2} \qquad (2.43)$$

The authors conclude from EQUATION 2.42 that the required amount of carrier is reduced by a factor of 2.1 for an increase in column length of a factor of four. From EQUATION 2.43 they calculate a substantial increase in ε_L up to $\left(\frac{\ell}{\ell_{MIN}} \right) = 1.5$, after which ε_L decreases, in contrast to the continual increase in η_L. The suggestion is made that the best economic conditions prevail when a compromise between maximum η_L and ε_L is obtained. Generally they conclude that operation will be carried out at relatively high flowrates, with the maximum feed concentration possible without obtaining peak-spreading due to non-linearity, and at (ℓ/ℓ_{MIN}) in the range 1.5 to 3. This latter result is of the same order as the optimum value predicted by Conder and Purnell (54), discussed in SECTION 2.3.1.1.

Pretorius and de Clerk (55) suggest a production rate for the case where two cuts are made per binary sample, one between the component peaks, and one after the second peak, before the next sample (Y and Z FIG. 2.12), as:

$$E_p = \frac{(m-\Delta_m)u}{w_{to}(1+K_1)} \qquad (2.44)$$

E_p = Production rate of a given component

m = Total mass of component in sample

Δ_m = Mass of component discarded during fraction cutting

Figure 2.12 Illustration of Repetitive Injection Technique for Two-Component System

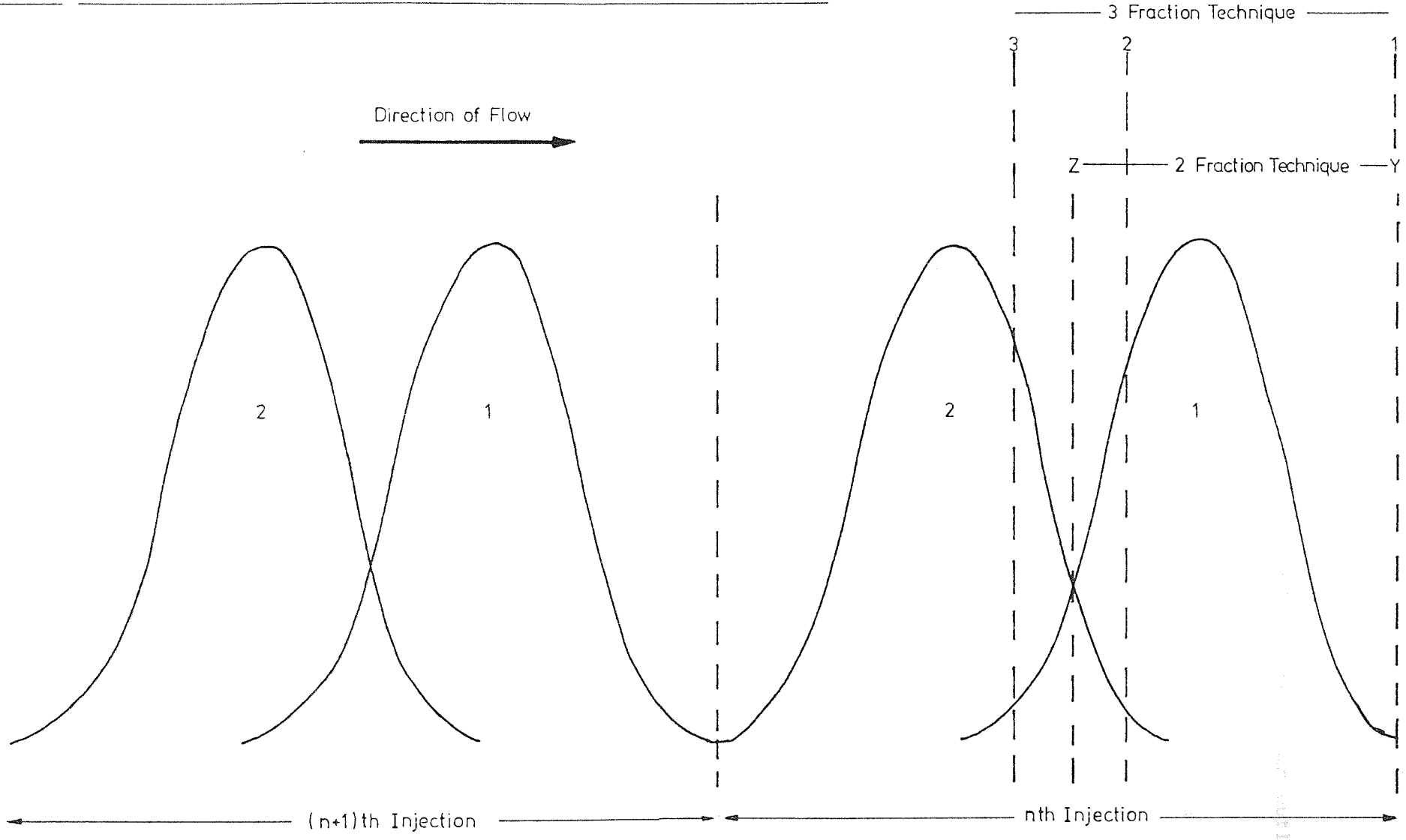

u = Mobile phase velocity

w_{to} = Total chromatogram width per sample at the column outlet

For the case where the outlet peaks are approximately Gaussian the authors conclude that a peak separation of four standard deviations produces about 2% product contamination, while for six standard deviations this figure is 0.15%. When w_{to} is fixed so that successive samples do not overlap, a value of $w_{to} = 12\ R_s\ \sigma_{to}$ is obtained.

The authors concluded from their study of repetitive injection under the above conditions that the plate height, H, plays only a secondary role in preparative chromatography as opposed to its dominant role in the analytical case. Further conclusions concerning feed band concentration and width, mobile phase velocity, and column length, have been discussed previously in this chapter. A technique for maintaining product purity at an increased feed volume is outlined by these authors. This is the three-fraction technique wherein the centre, impure portion, of the sample is removed by making a total of three cuts per sample (FIG. 2.12). They review the work of Gordon et al. (57-61) on this method, which indicates substantial gains in throughput where high purification is required, but shows only small gains at lower purities. Whether or not this method is used they conclude depends on the economics of increased equipment and operating costs against any gain in throughput.

Conder (97) concluded that for a 'heart-cutting' technique the optimum recovery of product per injected sample is 60%, the impure 40% being recycled, and generally that columns should be operated at maximum carrier velocity and feed band width.

In conclusion, general factors emerging from the previous sections may be summarized (55):

(i) If increased production is effected by an increase in one or more of the parameters: column diameter, flow velocity, and sample inlet volume, an increase in column length is required.

(ii) An optimum in throughput exists, represented by a simultaneous increase in sample volume, and increase in mobile phase velocity above the value producing minimum H.E.T.P.

(iii) Increase in column length and flow velocity leads to an increase in pressure drop, and a compromise should be made.

(iv) Radial mixing devices effectively minimize disadvantages associated with large diameter columns, and optimum diameters will probably be determined as a balance between capital and operating costs.

(v) Optimisation of production should include maximization of profits.

(vi) Generally H.E.T.P. plays a secondary role in production chromatography.

Other conclusions are:

(vii) Repeated sample injection improves column utilization and hence throughput.

(viii) Feed sample concentration should be the maximum possible.

2.3.3.4 The Use of Different Column Geometries

A different approach to maintaining column efficiency during scale-up is to use a system of small diameter parallel columns, producing a large effective column diameter . The problems associated with this type of arrangement are the need to maintain geometric similarity and obtain equal stationary phase loading of the columns. The first is

necessary to ensure a similar mobile phase flow in each column, and the second to ensure similar solute velocities to prevent peak overlap at the outlet. Although some success has been obtained on the preparative scale (104), the difficulty of matching a large number of columns make it less attractive for production operation.

Giddings (65) has suggested radial velocity variations might be overcome by the use of annular columns if uniform packing could be achieved. The use of finned columns has been evaluated (105), and while an improvement in H.E.T.P. was noted for a 7.6 cm diameter column fitted with fins, this did not compare favourably with a 4.4 cm diameter column without fins, suggesting the use of fins is not sufficient to counteract the loss of efficiency with increasing column diameter. Several of the designs mentioned here have been incorporated into devices providing continuous operation, and are reviewed in the SECTION 2.4.

2.4 CONTINUOUS CHROMATOGRAPHY

2.4.1 Introduction

Relative movement of the stationary and mobile phases in a continuous cross-current or counter-current manner allows the components of a continuous feed mixture, which exhibit different affinities for the two phases, to be separated into two continuous streams of pure products. The increased utilization of the chromatographic column over normal batch operation is illustrated in FIG. 2.13. Although repeated sample injection (SECTION 2.3.3.3) and optimization of the sample size (2.3.1) have improved batch column utilization, it is evident that continuous operation has the advantage of allowing the whole of the column to be used for separation for all of the time. This should allow a significant gain in throughput to be obtained by continuous operation, and, as continuous mass transfer separation processes are generally more economical than batch processes, cheaper products.

These goals have led many workers to design process schemes capable of operation in a continuous manner. A review of both conceptual and operational systems is given, which for reasons of convenience have been grouped into static bed, moving bed, and simulated moving bed classes.

2.4.2 Fixed-Bed Systems

Tiley and co-workers (106) investigated the performance of a single stationary column of 2.5 cm diameter, in which counter-current operation was achieved by allowing the liquid stationary phase to flow over the column packing in a downward direction, against the carrier gas

Figure 2.13 Chromatographic Concentration Profiles obtained for Separation of Two Components

(a) Repeated Batch Co-current Operation

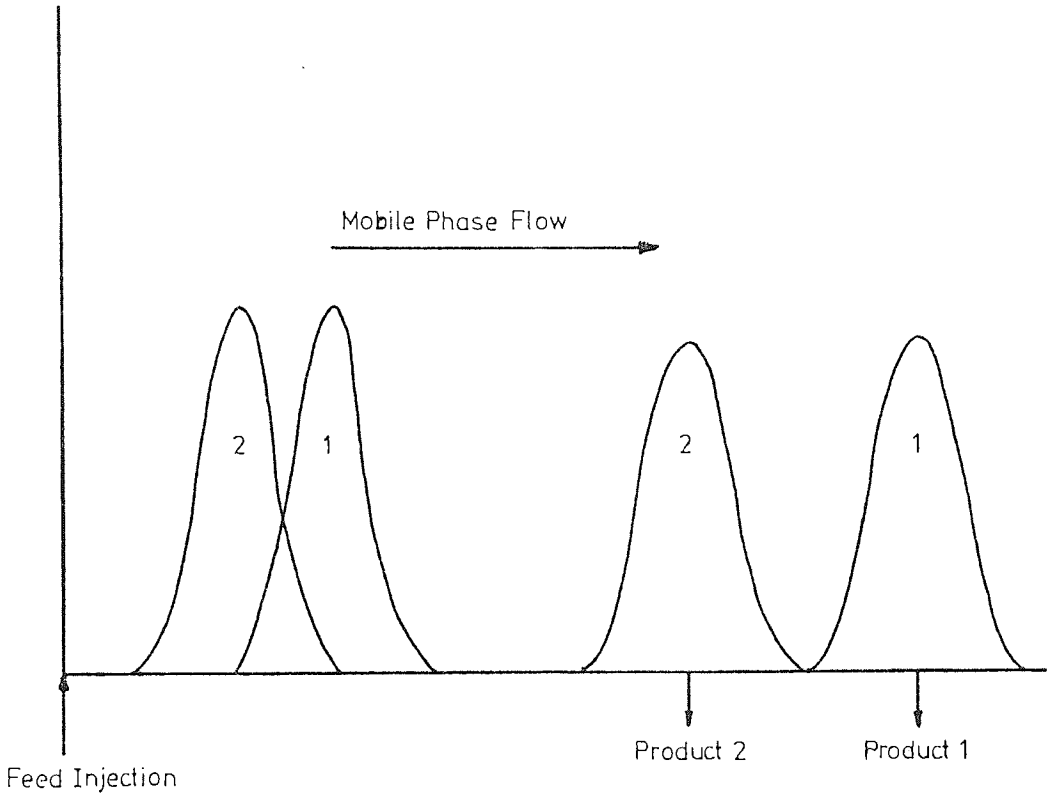

(b) Continuous Counter-current Operation

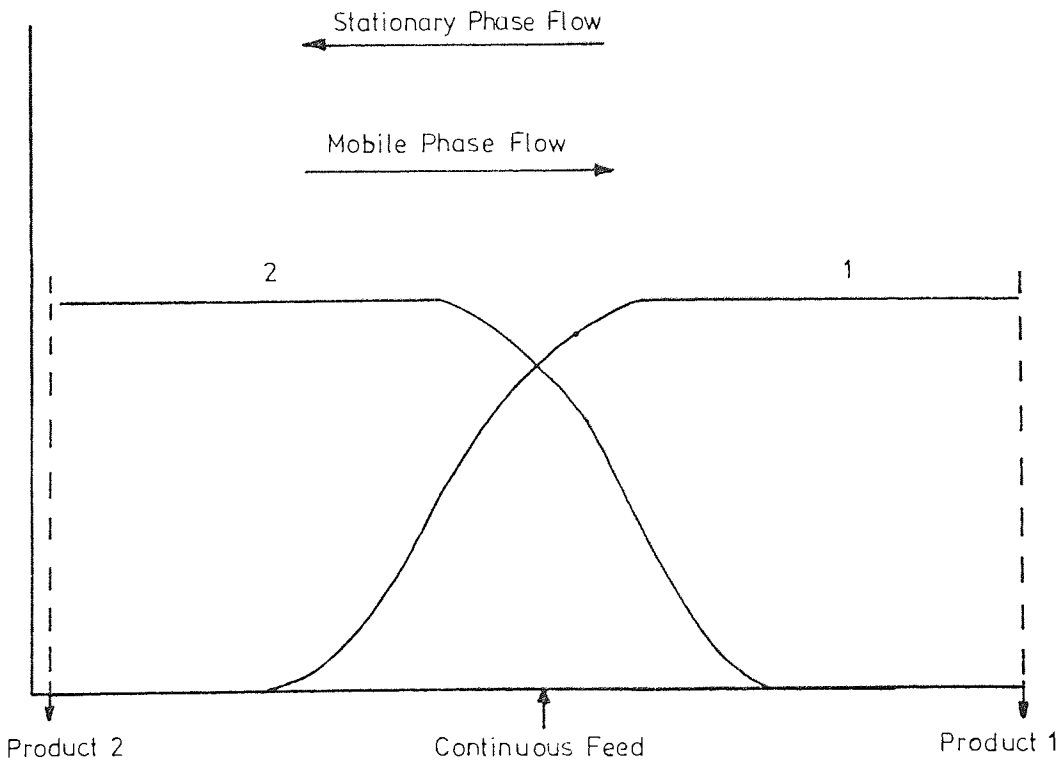

flow. Purities in excess of 99.9% were obtained for up to 5 cm^3 hr^{-1} of a 1:1 feed mixture of diethyl ether and dichloromethane, with dinonyl phthalate as the stationary phase. However, efficiencies were much less than those obtained for columns in which the packing was flowing (107,108) mainly due to the slow solute diffusion rates caused by the relatively thick liquid film obtained for the former case.

A flowing liquid stationary phase was also used by Kuhn et al. (109,110) in a counter-current operation which included the use of a temperature gradient along the column. The temperature gradient improves separation as the ratio of the partition coefficients of the components is temperature dependent. In this case individual components of a multi-component feed mixture collected in different sections of the column, and could be withdrawn continually. Purities of 95% were achieved during separation of the ternary mixture n-valeric acid/n-butyric acid/propionic acid, using paraffin oil containing 10% stearic acid as the stationary phase.

Although the methods mentioned above are both counter-current there have been other attempts at continuous operation of a column, in which the packing remains stationary, which may be classed as co-current or cross-current. Thompson (111, 112) used a single column to obtain semi-continuous co-current GLC separations of ethane and propane. The inlet stream to the column was varied sinusoidally from 100% feed mixture to 100% carrier gas. By adjustment of the frequency of the inlet waves and carrier gas flowrate the individual component waves left the column out of phase by virtue of their different affinities for the stationary phase. Individual components were collected by

switching valves, positioned at the column outlet, which operated at the same frequency as the inlet waves. Product purities of 70% (ethane) and 74% (propane) were obtained for 82 $cm^3 min^{-1}$ of a 1:1 feed mixture and a frequency of 40 c.p.m. with carbon dioxide and benzyl ether as the mobile and stationary phases respectively.

Another form of co-current cyclic operation was demonstrated by Wilhelm et al. (113,114,115) which incorporated mobile phase flow and column temperature cycling within a solid adsorption bed. Mobile phase flow alternated between the upward and downward direction, and the packing was heated during the downward flow to utilize the temperature dependence of the partition coefficient mentioned earlier. Although good separations had been achieved under batch operating conditions, the effectiveness of the process was greatly reduced when continuous feed input and continuous product removal were employed.

Temperature cycling was also employed by Pigford et al. (116,117) for a constant mobile phase flow through a fixed bed of solid adsorbent. They employed a continuous feed mixture which was alternately heated and cooled to produce temperature cycling within the column. The preferentially-adsorbed component showed a greater affinity for the stationary phase relative to the other component, and this difference in affinities was increased with temperature. Thus the product outlet stream concentration cycled between being rich or poor in the preferentially-adsorbed component. Improvement in the separation obtained for a single column can be obtained if several additional columns are used, alternatively heating and cooling a column. These cyclic separation techniques are sometimes referred to as parametric pumping, and have been reviewed by Wankat (118). Wankat has also studied the applications of the technique to the separation of multicomponent mixtures (119).

A cross-current system has been used by Turina et al. (120) in which carrier gas and liquid stationary phase flow at right angles through an inert support. The apparatus consisted of two parallel glass plates 1 mm apart containing the packing. The carrier gas enters one vertical edge and flows horizontally through the packing, existing through a series of outlet ports in the opposite edge. Stationary phase enters through the top horizontal edge, travels through the packed bed, and leaves from the opposite (bottom) edge. Feed enters continuously into the corner of the bed between the two fluid inlets, and the individual components travel at different angles through the bed, due to their different relative affinities for the stationary phase, emerging from different mobile phase outlet ports. This is illustrated in FIG. 2.14(a). The main advantage of this type of system is its potential for the separation of multi-component mixtures into individual components in a single operation. A logical final step for improvement of the stationary bed would be to continue the idea of Turina et al. for cross-flow through a 'slab' of packing with parametric pumping. Such a system has been proposed by Tuthill (121), and is illustrated in FIG. 2.14(b). Feed mixture is introduced continuously into one corner of the slab, and entry of the mobile phase alternates between the two sides of the slab forming the corner. When the mobile phase flow alternates between the two sides of the slab, the temperature of the whole system is also alternated, in phase, between two values. This change of temperature results in a change in the ratio of the component velocities through the slab, and, by selection of the appropriate flowrate and temperature conditions, the individual components can be made to move preferentially in the horizontal or vertical direction, and

Figure 2.14 Slab Chromatographs for Continuous Chromatography

(a) Scheme of Turina et al. (120)

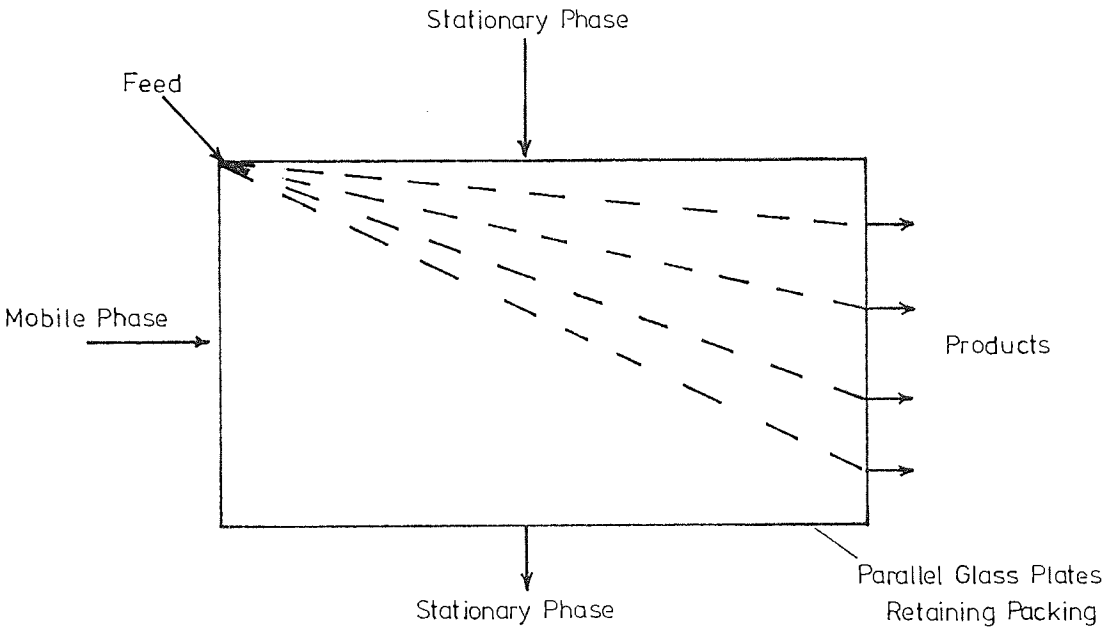

(b) Scheme of Tuthill (121)

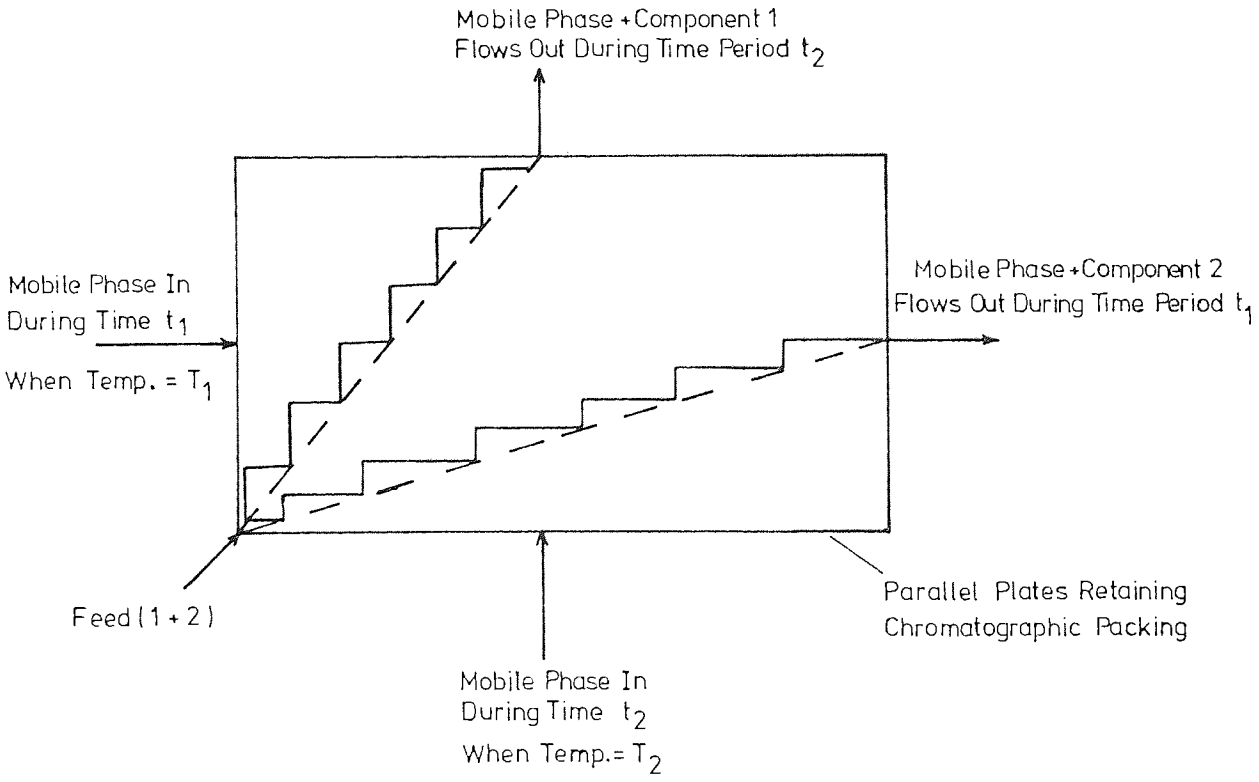

thus emerge from different sides of the slab. No experimental results have been reported for the unit to date.

A final method in this section is provided by Electro-chromatography (122,123) which combines chromatography with electrophoresis. The method relies on an electric field traversing the mobile phase flow path, which causes different components of the feed to be deflected by various degrees giving a series of curved flow paths. The feed components thus appear in the column effluent in different positions in a similar manner to the previous two methods described. A difference in electrophoretic mobilities of the feed components is necessary for this method.

2.4.3 Moving Bed Systems

2.4.3.1 Cross-Current Flow

Development of moving bed systems operating under cross-current flow conditions has taken two main forms. In one case development has been concerned with helical flow through annular columns, or tube bundles arranged in annular shape, and in the second case with radial flow across annular columns or between parallel discs.

2.4.3.1.1 Helical Flow

This type of flow scheme was first proposed by Martin (124) and is illustrated in FIG. 2.15(a). The feed and mobile phase fluid enter the top of the annular column and, as the column rotates, the components of the feed follow helical flow paths. Separation occurs in the column and the components of the feed thus leave the column at various points around the circumference of the base. Giddings (125) carried out a

Figure 2.15 Helical Flow Schemes for Continuous Chromatography

(a) Principle

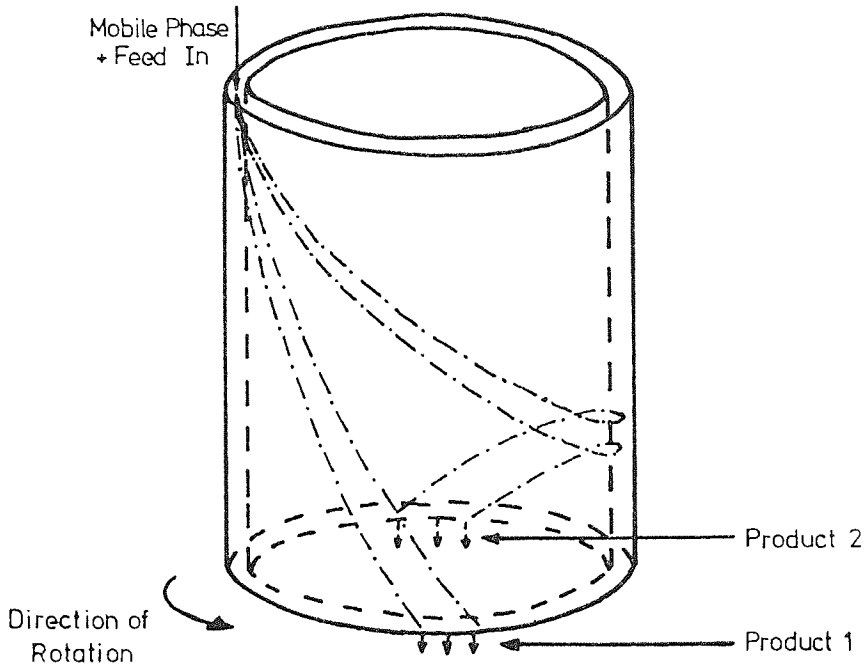

(b) Scheme of Fox et al. (126)
for Liquid Chromatography

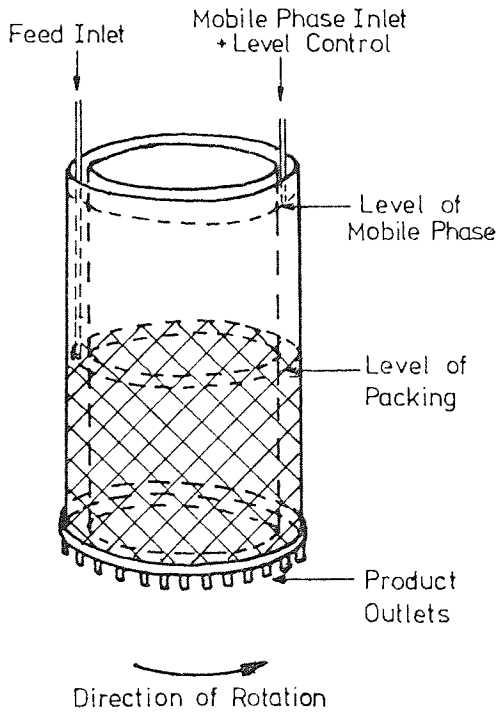

(c) Scheme of Taramasso et al. (131)
for Gas Chromatography

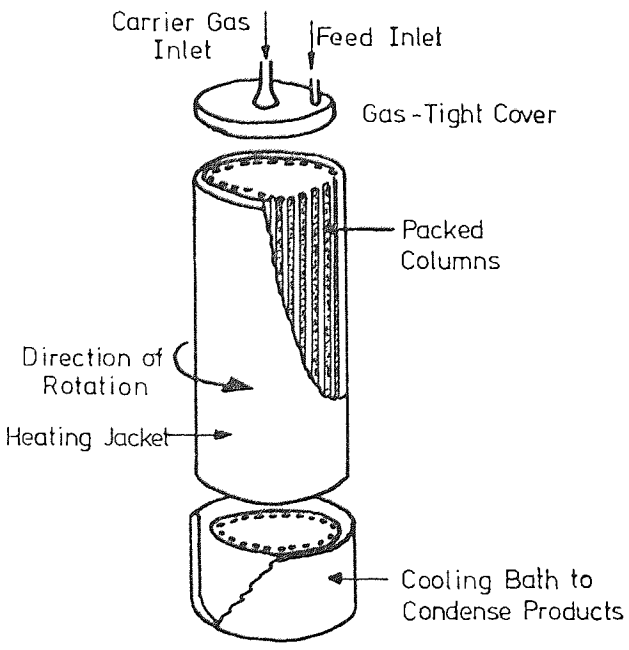

theoretical study of this type of flow system and concluded that improved resolution and throughput could be obtained when compared with a conventional chromatographic column of similar geometry.

In a series of articles Fox et al. cover the construction (126), operation (127) and applications (128) of a continuous chromatographic apparatus operating on this helical flow principle (FIG. 2.15(b)). The annular column had an inner diameter of 27.3 cm, an outer diameter of 29.2 cm, and was 30.5 cm high. Separation of proteins was performed on Sephadex (a cross-linked dextran gel) by gel permeation chromatography, using 0.02M Tris-HCl buffer (pH 8) as eluting solvent. Feed inputs of up to 22 $cm^3\ hr^{-1}$ of 5% total protein concentration were achieved using a solvent flowrate of 1000-1500 $cm^3 hr^{-1}$, giving typical purities of 97%. It should be noted here that this form of operation is merely a form of multi-batch column chromatography, and similar results would be obtained if samples are injected around a series of stationary batch columns, and a fraction collector is switched around the column outlets.

One of the first descriptions of an apparatus incorporating a series of vertical tubes arranged in the form of an annulus, rather than an annular column, was given by Svensson and co-workers (129,130) for continuous separation of feed mixtures by liquid chromatography. Taramasso et al. (131,132) also utilized the concept of a tube bundle in the construction of a 100, 0.6 cm x 1.2 cm column unit which rotated at speeds of 1-50 revolutions per hour past a fixed feed inlet port and product receivers (FIG. 2.15(c)). For a g.l.c. separation of cyclohexane-benzene on tricresyl phosphate at 80°C a maximum throughput of 200 $cm^3 hr^{-1}$ was obtained for 99.9% purity. A larger unit has been used for separation of isomers and close-boiling mixtures (133,134,135).

2.4.3.1.2 Radial Flow

An annular packed column has been patented by Mosier (136) wherein component paths are radial (FIG. 2.16(a)). The feed enters at the centre of the annulus and travels towards the circumference where products are removed from the base of the unit. The unit requires rotation of the packed section, relative to the feed input and product collection systems, to produce a separation, and is illustrated in FIG. 2.16(b). Sussman (137) has reduced the packed annulus to an annular channel between two flat discs, the stationary phase being coated to the adjacent faces of the discs. Typical dimensions employed are channel widths of 0.01 cm, and 30.5 cm diameter discs. The arrangement is illustrated in FIG. 2.16(c) for separation of a binary feed mixture. It has been used for g.l.c. separations of hydrocarbon mixtures and experimental and theoretical results are compared (138,139). Scale-up of this unit may prove difficult because of the high degree of precision engineering needed for the discs.

2.4.3.2 Counter-Current Flow

2.4.3.2.1 Moving Packing

The counter-current movement of packing and mobile phase is perhaps the most obvious method of obtaining continuous operation of a chromatographic column. Barker and co-workers (9-14) have studied this method extensively, and have developed and operated the apparatus illustrated in FIG. 2.17, which has particular use in gas chromatography applications. The column used was 2.5 cm in diameter and 2.74 m long, packing coated with stationary phase entering at the top, and allowed to flow downwards under gravity. The outlet rate was controlled by a variable orifice at the bottom of the column, and packing

Figure 2.16 Radial Flow Schemes for Continuous Chromatography

(a) Principle

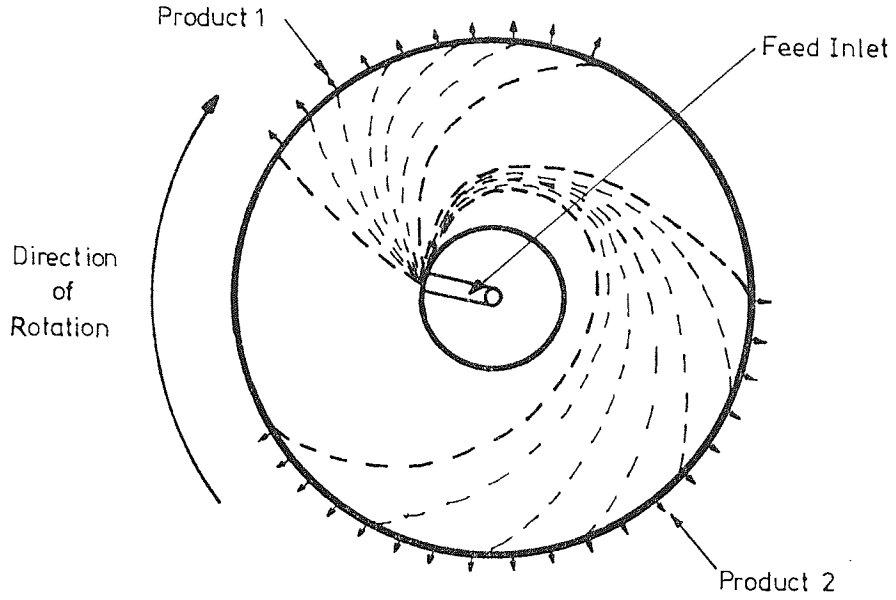

(b) Scheme of Mosier (136)

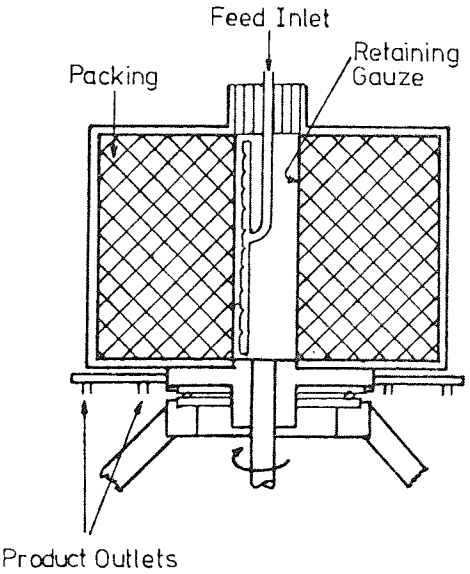

(c) Scheme of Sussman (137)

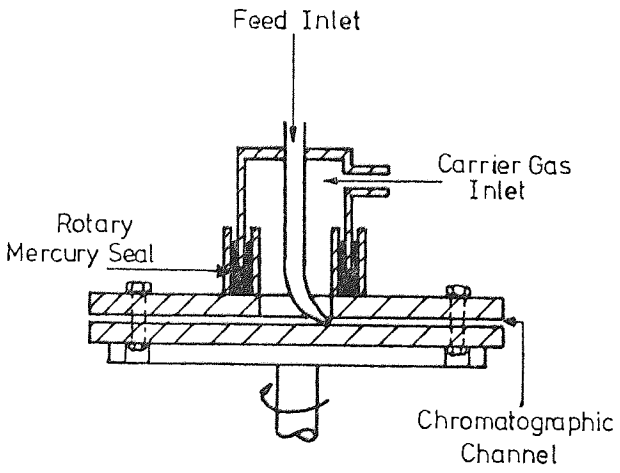

was removed by a rotating table and recycled to the top of the column. The column was vibrated to ensure a steady flow of packing.

The least strongly absorbed component was carried with the mobile phase and eluted at the product 1 port. The more strongly absorbed was carried with the packing and removed in the stripping section at the bottom of the column, leaving at the product 2 port, before the packing left the column for recycle. The unit has been used for binary hydrocarbon mixtures, and was later modified (13) for use with ternary hydrocarbon mixtures by introduction of a side-arm between the bottom product offtake and feed inlet (FIG. 2.17). For separation of an equivolume mixture of cyclohexane, methylcyclohexane and benzene at 12.6 cm^3 hr^{-1}, product purities of 99.5% were obtained for the top and bottom products (cyclohexane and benzene) and 78.6% for the sidestream, methylcyclohexane (14,16).

Scott (140), Schultz (141), and Tiley et al. (107,108) have also reported successful operation of small diameter units operating in a similar moving packing principle.

Industrially this technique has been developed by the Union Oil Company, California, U.S.A., (142) where activated carbon adsorbent flows continuously down through a stream of hydrocarbon gases. Reactivation of the carbon adsorbent by steam was carried out in the lower, stripping, section of the column, and packing re-circulation achieved by a gas lift. A unit having a capacity of 16 million cubic feet per day was built by the Dow Chemical Company, Michigan, U.S.A., but is no longer in operation as it proved to be uneconomical compared to distillation. The Phillips Petroleum Co. (143) constructed a 15 cm dia., 2.5 m long column, and used it to separate up to 225 cm^3 min^{-1} of a 30% cyclohexane/70% benzene mixture. However, applications of this

Figure 2.17 Counter-Current G.L.C. Apparatus with Circulating Packing (12)

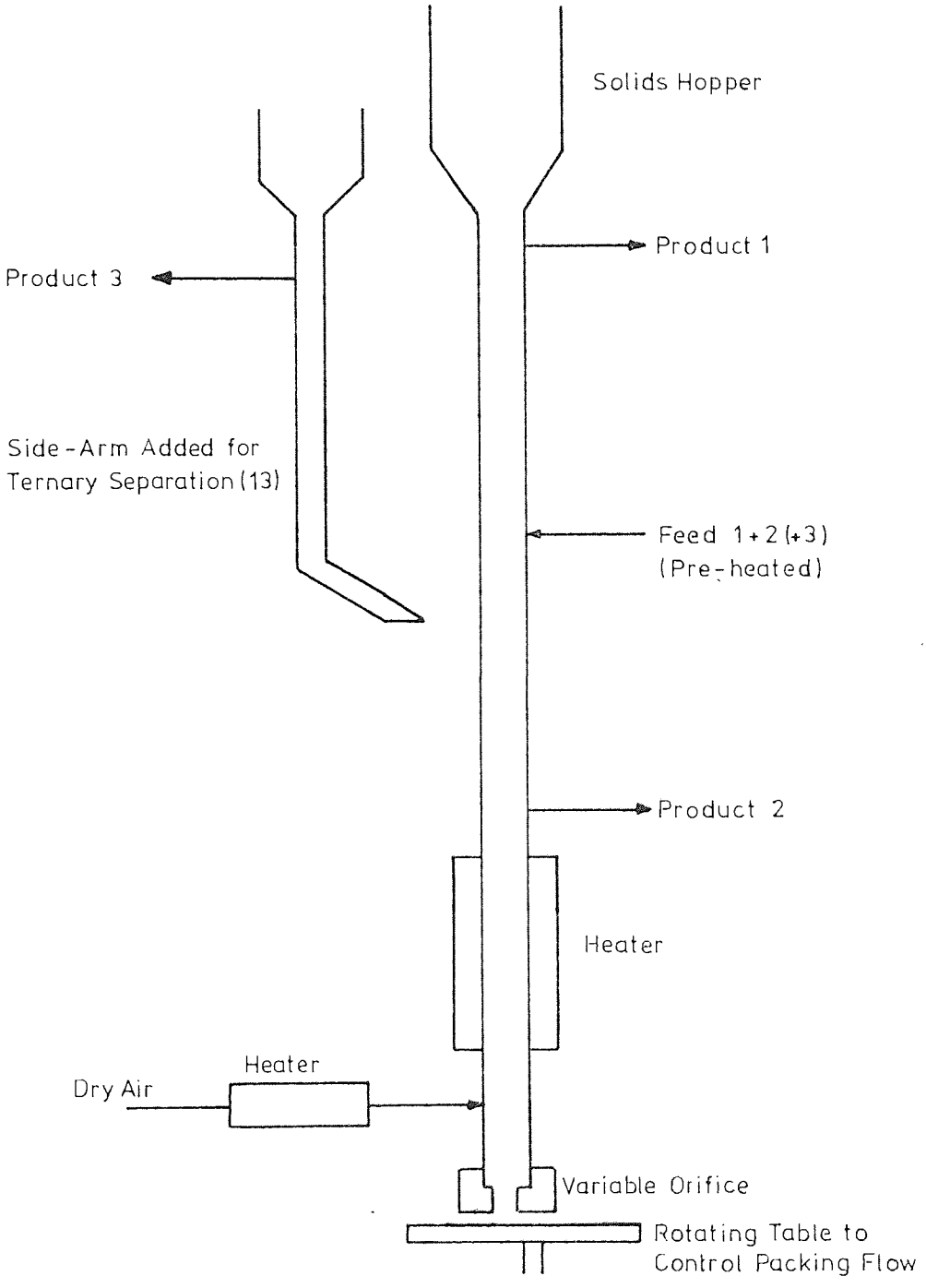

type of system have largely been abandoned because of the problems associated with movement and control of large quantities of solids, and the resulting attrition which necessitates re-sieving and re-plenishing of expensive packing.

2.4.3.2.2 Moving Columns

Several workers overcame the problem of packing attrition, while maintaining continuous counter-current operation, by rotating a circular column past fixed inlet and outlet ports and against the direction of mobile phase flow in the separating region (FIG. 2.18(a)-(d)). The designs of Pichler and Schultz (144), Gulf Research and Development Corporation (145), Luft (146) and Glasser (147) all controlled the direction of mobile phase flow by balancing pressure drops within the system. Barker (18) removed this necessity by introducing a cam-operated lock between the mobile phase inlet and product 1 offtake. This had the added advantage of increasing the effective separating length, which may be regarded as the distance between the mobile phase inlet and product 1 offtake, or between both product offtakes, whichever is the shorter.

Barker and Huntington (15,16,17) constructed the unit illustrated schematically in FIG. 2.19(a) which was based on this system. It took the form of a 1.5 m diameter wheel, incorporating a 3.8 cm square cross-section column around the outer part of the wheel, which rotated at speeds between 1 and 10 revolutions per hour. 180 gas passages in and out of the column were each opened or closed by self-operating valves, and sealing between the ports and rotating toroid was obtained by 'O' rings set in the toroid face. High purity products were obtained with this unit for a wide range of feed mixtures,

Figure 2.18 Moving Column Schemes for Continuous Chromatography

(a) Scheme of Pichler and Schultz (144) and Gulf Research and Development (145)

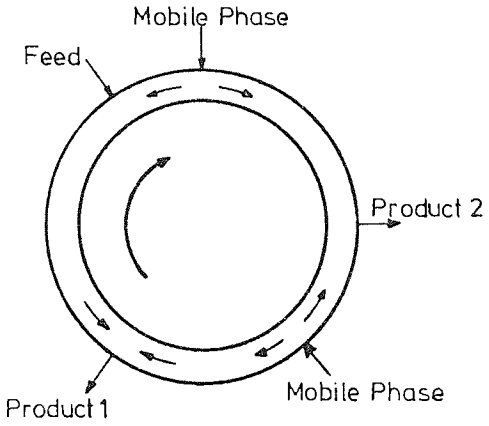

(b) Scheme of Luft (146)

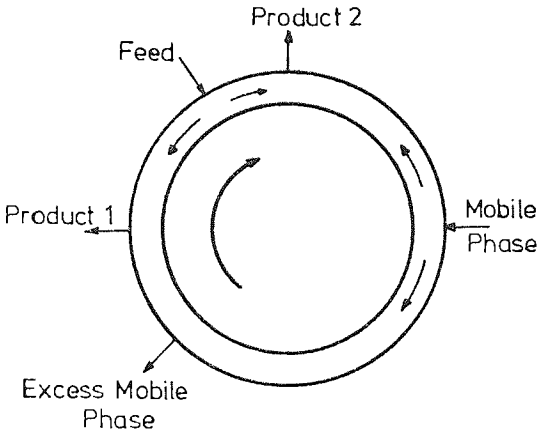

(c) Scheme of Glasser (147)

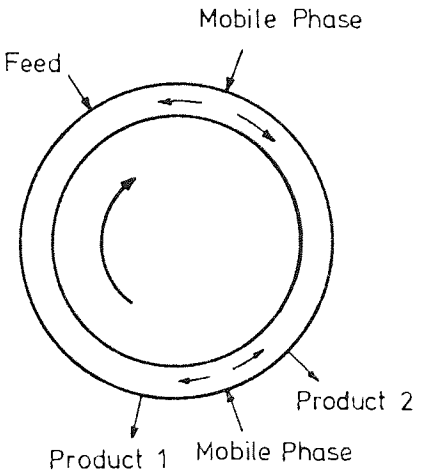

(d) Scheme of Barker (18)

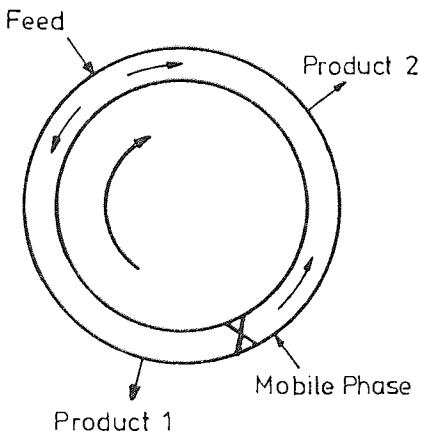

including anzeotropic and close-boiling systems, at typical feed flowrates of 100-400 $cm^3\ hr^{-1}$ (15,16,21). Hatt (23) describes conversion of the machine for use with liquids, and although stable operating conditions were difficult to achieve, due to leakage from the inlet ports and valves, he separated mixtures of glucose and soluble starch, at feed rates up to 120 $cm^3\ hr^{-1}$ of a 4% w/v solution.

The main drawbacks to scale-up of this machine are the general difficulties associated with large moving seals, and mechanical movement of a large unit. Barker and the Universal Fisher Group Ltd. (18) overcame the problem of size by replacing the large toroid with a more compact unit consisting of a tube bundle arranged in a similar circular form to systems described earlier (SECTION 2.4.3.1). The machine had 44, 2.5 cm diameter, 22.8 cm long tubes linked in series, alternatively top and bottom, to give a closed loop, in contrast to the parallel operation of the similarly shaped units. Speeds of rotation between 0.2 and 2 revolutions per hour were possible, and transfer of fluid between tubes was automatically controlled during rotation by cam-operated "poppet" valves. Spring-loaded "graphlon" (P.T.F.E.-CARBON composite) face seals were employed at the inlet and outlet ports to prevent leakage from the unit when the valves were open, replacing the 'O' ring seals of the 1.5 m dia. machine. Data published for a wide range of separations with this unit demonstrate greater separating power than for the 1.5 m dia. machine, and typical throughputs of 150 $cm^3\ hr^{-1}$ have been obtained with high purity products (19-22).

The main disadvantages of this unit were the sometimes unreliable nature of the poppet valves and face seals during operation. A prototype machine was built (24) to overcome the first of these problems by replacement of the inlet and outlet valves with a "graphlon" seal

Figure 2.19 Moving Column Equipment for Continuous Chromatography

(a) Toroidal Design (18)

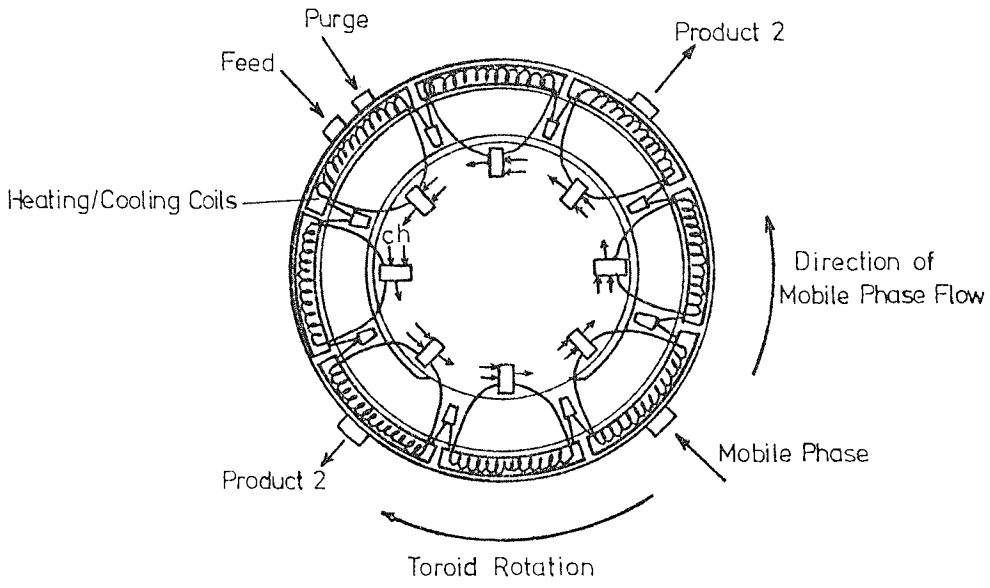

(b) Tube Bundle Design (18)

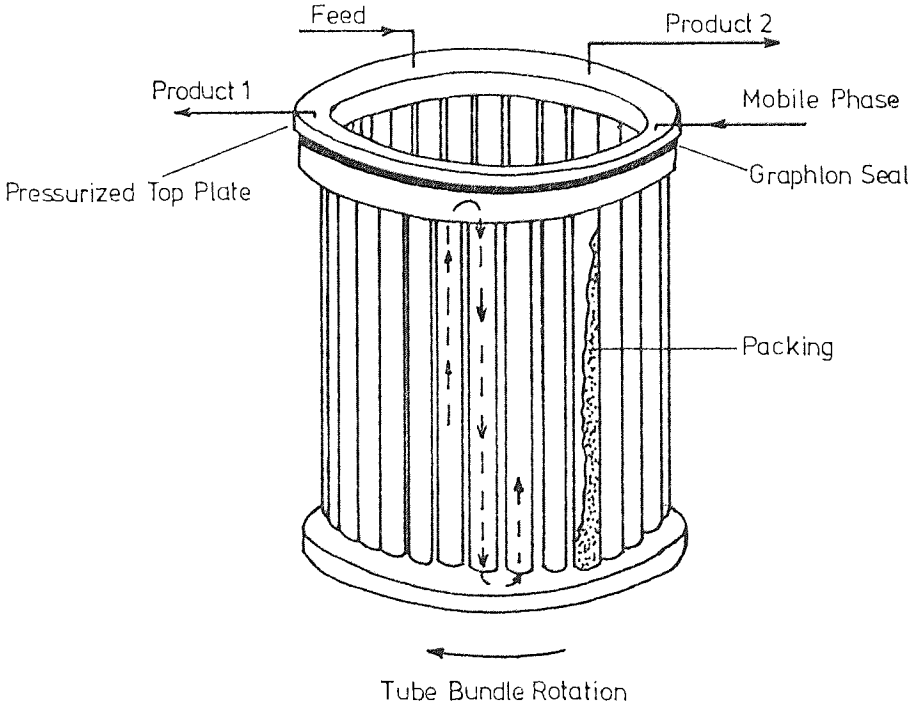

(FIG. 2.19(b)). Slots were machined in the disc which matched slots in the face of the tube bundle during rotation to provide inlet and outlet fluid flow. The prototype consisted of 44 tubes each 0.95 cm diameter, 30.5 cm long, again arranged in a circular form. Hatt and co-workers (23,24) carried out separations of carbohydrates on this machine, operating in the liquid phase. Of particular interest was the fractionation of a dextran polymer (Dextran T-110, Pharmacia Ltd., Uppsala, Sweden) having a molecular weight of 96,000. This was carried out on Porasil D (porous silica beads) using water as mobile fluid, by gel permeation chromatography. Fractionation of the polymer into two samples of narrower M.W. distribution was achieved at 1.9 $cm^3\ hr^{-1}$ of 10% w/v feed solution. Further increase in throughput was not limited by the separating power of the machine, but by mechanical weaknesses associated with the bundle structure and face seal. Operation of an improved version of similar dimensions is described by Williams (31).

It is interesting to note a commercial machine that uses a graphlon seal between two faces moving relative to each other. This is the small-scale Unidev sequential separator (148), marketed by Unidev Ltd., Crawley, England, for preparative gas and liquid chromatography applications. The relative movement of the column bundle and inlet and outlet ports is obtained by indexing the columns at a predetermined time interval. Operation of a machine of this type is reported (149).

2.4.4 Simulated Moving Bed Counter-Current Systems

Scale-up of moving column units is limited by the mechanical difficulties and expense of rotating large tube bundles, and the degree of precision engineering, and hence expense, necessary for the

manufacture of moving face seals, which becomes more acute as the seals become larger.

The first of these problems has been overcome by Szepesy et al. (150) who utilize a switching valve which contains a rotary P.T.F.E. disc. Rotation of the valve moves the inlet and outlet ports relative to a series of stationary columns. In this manner simulation of column movement is obtained, avoiding the need for mechanical movement. The authors suggest that the switching valve they employed would be suitable for use with column diameters up to 3 cm, as it can handle flowrates up to about 330 $cm^3\ min^{-1}$. A schematic of the process is given in FIG. 2.20(a), (150).

A rotary valve has been employed industrially by Universal Oil Products (7,8), and applied to separation of paraffins from other hydrocarbons on molecular sieves (Molex process), for separating olefines from paraffins (Olex process), and for recovering p-xylene from mixtures with other C_8 hydrocarbons (Parex process). They employ a single column in the process scheme and simulate movement of the column packing, by indexing the column inlet and outlet ports, to obtain counter-current operation. The flow scheme used for adsorptive separation of normal paraffins from other hydrocarbons using five angstrom molecular sieves is given in FIG. 2.20(b), (7). Flow schemes for the other processes are similar in principle. In operation the various zones in the column, adsorption, desorption, and rectification, are stepped along the column to simulate the counter-current operating mode. Pilot plant studies (8) produced p-xylene purities of 99.5% for a feed mixture containing 14.3% w/w p-xylene in a mixture of C_8 aromatic isomers, and 99.6% for a feed mixture of a C_8 cut of a catalytic reformate containing 18.9% p-xylene.

Figure 2.20 Equipment for Continuous Chromatography using a Rotary Valve

(a) Scheme of Szepesey et al (150)

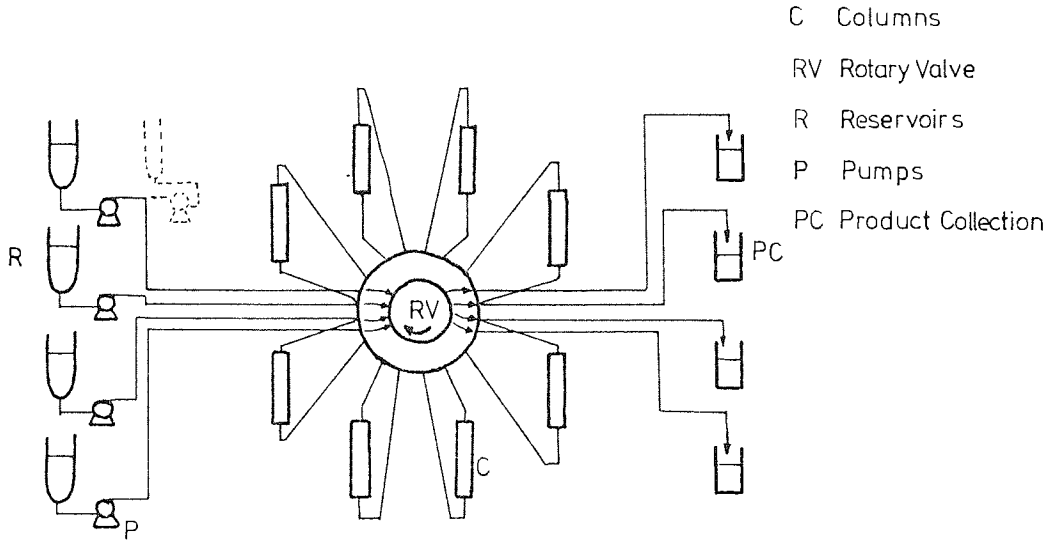

(b) U.O.P. Process Scheme (7, 8)

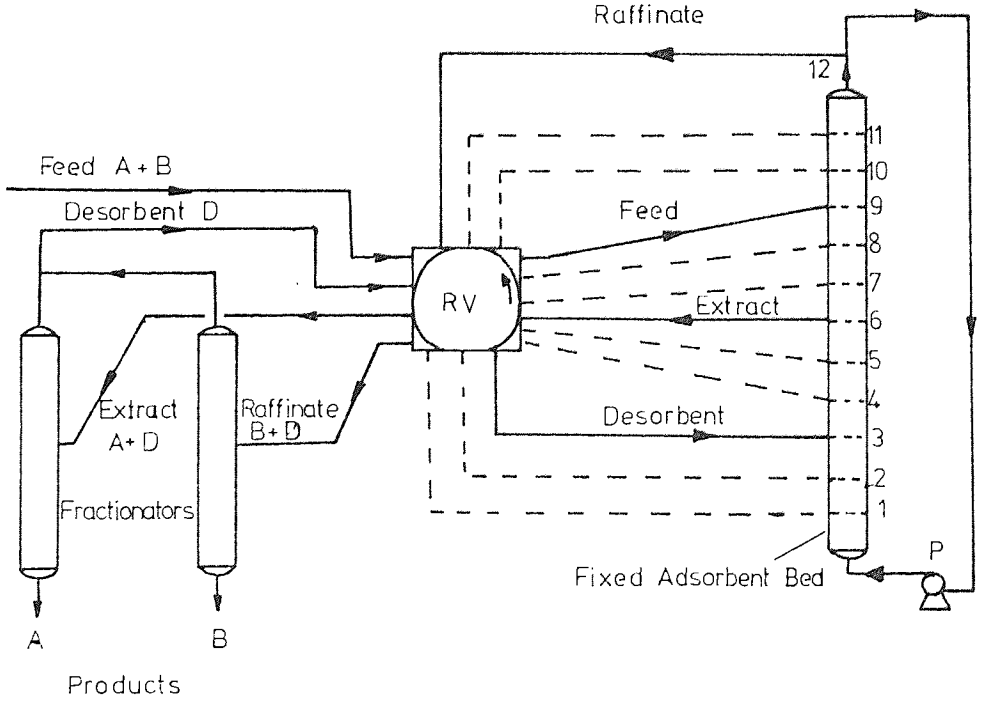

Experience gained on the unreliability of moving seals (23,25) under arduous operating conditions, led Barker and co-workers to investigate alternative means of scale-up of the continuous counter-current process. Barker and Deeble (26-30) designed a process scheme wherein all moving parts are eliminated save for the operation of valves of proven reliability. The scheme involves simulation of the movement of a series of columns by movement of the inlet and outlet ports around the column series. The movement is obtained by using solenoid valves, placed at the inlet and outlet ports of the columns, and switching them in a programmed sequence. 12, 7.6 cm diameter, 61 cm long columns are arranged vertically in a circular form, and each column requires six solenoid valves to control the inlet and outlet of fluids to the system. The unit was designed for operation by gas-liquid chromatography, and has been operated successfully for separation of binary hydrocarbon mixtures. A further machine for separations requiring temperatures up to ~200°C has been built, also for gas-liquid chromatography applications. The development of a machine having a similar operating principle, but suitable for liquid chromatography applications, is presented in CHAPTER 5.

CHAPTER 3

Literature Survey Part 2

Gel Permeation Chromatography

3.1 INTRODUCTION

3.1.1 The Basic Process

Many names for the process of fractionating molecules by virtue of their size have been proposed, including "gel filtration" (6), "molecular-sieve chromatography" (151), "exclusion chromatography" (152), "restricted-diffusion chromatography" (153), "hydrodynamic fractionation" (154), "separation by flow" (155), "gel chromatography" (156) and "gel permeation chromatography" (1).

The first two terms indicate a separation mechanism which produces a similar result to a sieving or filtration process, where the larger material is retained. However the opposite effect occurs in the separation process as larger molecules are retained for the shortest time. The next four terms all imply different mechanisms for the separation process. However, as the mechanism of separation is in dispute (SECTION 3.2), if indeed one mechanism alone can define the process, it would seem that a more neutral term is required. "Gel chromatography" suffers from the disadvantage of having the same initials as gas chromatography which may lead to confusion, and also the fact that all packings are not strictly gels (SECTION 3.1.2.1). Although "gel permeation chromatography" (g.p.c.) also suffers from the latter disadvantage, it has gained wide acceptance by workers in the field, and will be used in this thesis.

G.p.c. is a form of liquid chromatography wherein solute molecules are retarded as a result of their permeation into solvent-filled pores in the column packing material. The separation is usually carried out in columns tightly-packed with a gel or some other porous material, and both the interstitial space and intra-particle space is filled with

the solvent employed. The same solvent is used to dissolve the sample before introducing it into the column, and also as the mobile phase. The mobile phase flows through the interstitial regions, and solute molecules only travel through the column when they are in these regions. Solute molecules in the pores are thus retarded, and the more time molecules spend in the pores the more they are retarded. Large molecules which are completely excluded from the pores are thus eluted first, and small molecules which can penetrate the pores freely are eluted last. A species is eluted at a volume equal to the volume available to it in the column, which in the case of completely excluded molecules is V_o, the column interstitial volume, and for completely included molecules is $V_o + V_i$, where V_i is the internal (pore) volume. For intermediate molecules the elution volume is dependent on the pore volume accessible to the species ($V_{i_{ACC}}$) and is given by:

$$V_R = V_o + K_D V_i \tag{3.1}$$

K_D = Distribution coefficient = $V_{i_{ACC}}/V_i$

Alternatively, EQUATION 3.1 may be written:

$$V_R = V_o + K_{AV}(V_t - V_o) \tag{3.2}$$

$(V_t - V_o)$ is the total volume of the gel phase, including the solid structure. EQUATIONS 3.1 and 3.2 differ only by a constant factor for a given solute. EQUATION 3.1 is illustrated schematically in FIG. 3.1.

Figure 3.1 Illustration of the G.P.C. Fractionation Process

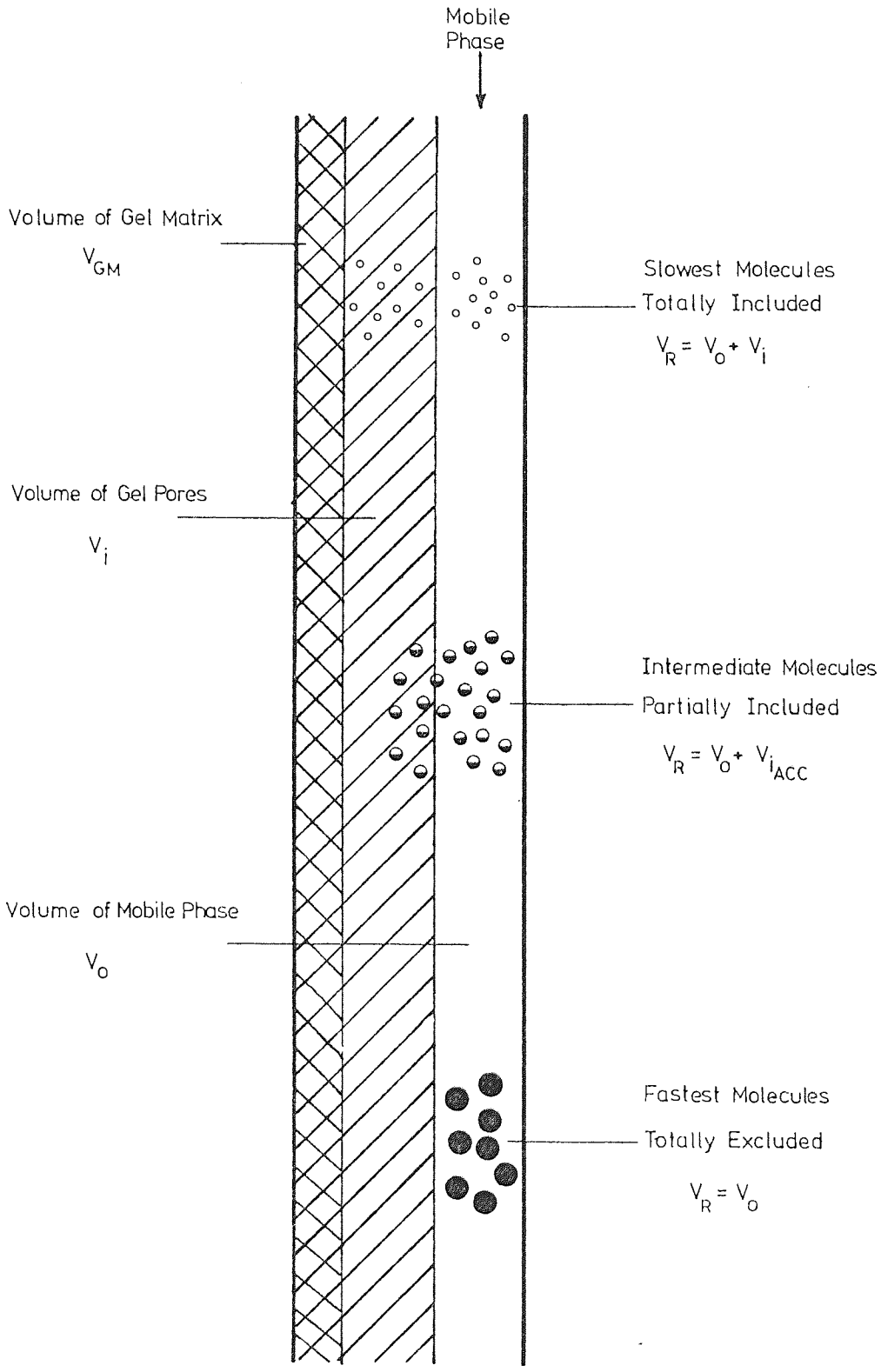

The similarity of EQUATION 3.1 and EQUATION 2.2 in SECTION 2.2.1 ($V_R = V_M + KV_S$) will be noted. However, it should also be noted that V_M in conventional liquid chromatography usually includes a contribution from the 'stagnant mobile phase' within the pores of the packing, whereas in g.p.c. this volume is in fact the stationary phase (V_i). It is also apparent from EQUATION 3.1 that K_D is restricted to values between 0 and 1, all molecules being eluted within a volume equal to the total liquid volume of the column, whereas in conventional liquid chromatography the partition coefficient may take very large values >> 1, and molecules may take many column volumes of mobile phase to emerge. Thus g.p.c. may be thought of as a special case of partition chromatography, wherein partition occurs between like solvents in different locations.

3.1.2 Practical Aspects of G.P.C.

3.1.2.1 Column Packings

It is possible to divide commercial g.p.c. packings into three classes:

(i) Xerogels. These are soft gels consisting of a cross-linked structure of polymer chains in the form of a three-dimensional network, the spaces within the network being filled with solvent. Soft gels are capable of taking up large quantities of solvent and swell to many times their dry volume, and are only suitable for use with solvents in which the individual polymer chains are soluble. The main disadvantage of this type of gel is its soft nature. Because of this the gel deforms in a chromatographic column, under high flowrate

conditions, causing high pressure drop and 'plugging' of the column, and the gel may even extrude through screens in the column end fittings. The advantages, at low flow velocities, are the high efficiency and capacity that they offer, the value $\frac{V_i}{V_o}$ often being greater than 2.

(ii) Aerogels. These are rigid materials, and not strictly gels at all, but consist of a rigid porous structure, usually porous glass or silica. The advantages of this type of material lie in the rigid structure which does not deform under flow and the suitability for use with a wide range of solvents. Disadvantages lie in the lower value of $\frac{V_i}{V_o}$, usually about 1, and the adsorption properties, and partial dissolution, in certain solvents, sometimes associated with this type of material.

(iii) Xerogel-Aerogel Hybrids. These are semi-rigid gels which swell to about 1-2 times their dry volume, and exhibit properties of both the previous cases. They exhibit $\frac{V_i}{V_o}$ values ~1 and do not deform under high flow, although are often more suitable for use with organic rather than aqueous solvents.

A summary of commercial g.p.c. packings is given in FIG. 3.2. Methods of introducing the packing materials into g.p.c. columns, relevant to this research, are given in SECTIONS 4.2.2.1 and 6.1.4.

3.1.2.2 Sample Detectors

Sample detection in g.p.c. is usually carried out in one of two ways. The first involves collection of fractions from the column outlet stream, followed by analysis of the fractions by one, or several, techniques. The second method is to monitor the column outlet stream

Figure 3.2 G.P.C Packings

Nature	Chemical Structure	Commercial Name	Maximum M.W. Fractionated	Suitable Solvents
Soft	Cross-Linked Dextran	Sephadex (9 Grades)	200 000 (Dextrans/Aqueous)	Aqueous
"	Cross-Linked Polyacrylamide	Bio-Gel P(10 Grades)	400 000 (Proteins/Aqueous)	"
"	Cross-Linked Polystyrene	Bio-Beads S (7 Grades)	14 000 (Polystyrenes/THF)	Organic
"	Cross-Linked Polyacrylomorpholine	Enzacryl K (2 Grades)	100 000 (Polyethylene Glycols/Aqueous)	Aqueous and Polar Organic
Semi-Rigid	Agarose	Bio-Gel A (6 Grades) Sepharose B(3 Grades) SAG (5 Grades)	15 000 000 (Dextrans/Aqueous) 40 000 000 (Proteins/Aqueous) 150 000 000 (Proteins/Aqueous)	Aqueous
"	Polyacrylamide/Agarose	Ultrogel (4 Grades)	1 000 000 (Proteins/Aqueous)	"
"	Cross-Linked Polystyrene	Styragel (12 Grades) Aquapak (1 Grade)	400 000 000 (Polystyrenes) 100 000 (Polystyrenes)	Non-Polar Organic Aqueous
"	Cross-Linked PVA	Merck-O-Gel OR (6 Grades)	1 000 000 (Polystyrenes)	Polar-Organic
"	Cross-Linked Hydroxy-Alkyl Methacrylate	Spheron P (7 Grades)	1 000 000 (Dextrans/Aqueous)	Aqueous
"	Unknown Aerogel-Xerogel	Hydrogel (3 Grades)	250 000 (Dextrans/Aqueous)	"
Rigid	Porous Glass	Bio-Glass (5 Grades) CPG 10 (8 Grades)	9 000 000 (Polystyrenes/Toluene) 1 200 000 (Dextrans/Aqueous)	Aqueous and Organic
"	Porous Silica	Porasil or Spherosil (6 Grades) Merck-O-Gel Si (3 Grades)	20 000 000 (Dextrans/Aqueous) 1 000 000 (Polystyrenes)	"

which allows a chromatogram to be produced simultaneously.

A list of some common detectors for the latter case is given below:

(i) Refractive Index. A differential refractometer continuously monitors the difference in refractive index between the mobile phase and column eluate. This method is suitable for a wide range of samples, but suffers from the disadvantages of being extremely sensitive to temperature, and sensitive to a lesser degree to flow changes in the system.

(ii) Ultraviolet Absorption. An ultraviolet absorption detector monitors the absorbance of the solute at the test wavelength. This method is relatively insensitive to flow and temperature, but obviously requires that the compound has some absorbance in the UV region. Absorbance may also be measured at other wavelengths by spectrophotometry.

(iii) Colorimetric analysis. This method measures the concentration of a solute by virtue of the optical density of the eluate. Non-coloured substances may be dyed, or reacted chemically to produce a colour, which may then be detected.

(iv) Fluorimetry. This type of detector measures the fluorescent emission from a solute that has been excited by electromagnetic radiation of a suitable wavelength.

(v) Heat of adsorption. This method relies on measurement of the changes in temperature that accompany adsorption or desorption of a solute at a solid surface.

(vi) Flame ionization. The flame ionization detector is commonly used in gas chromatography. In liquid chromatography the solvent is first evaporated by passing a wire, coated with some of the sample, continuously through an oven, followed by detection using flame ionization. However sealing problems and the relative

insensitivity for many liquid chromatography systems are some of the disadvantages with this type of detector.

Other less common detectors measure such parameters as radioactivity, electrical conductivity, and capacitance.

General requirements of detectors are low noise and drift, high sensitivity with respect to the measured parameter, low sensitivity to changes in operating parameters, low 'dead' volume, and a linear relationship between the detector output and solute concentration.

3.1.2.3 Other Equipment

The other parts of a typical g.p.c. arrangement are the column itself, a sample injection device, and a flow measuring device. Columns employed in analytical g.p.c. are typically 0.8 cm in diameter, up to several metres long, and constructed of glass or stainless steel. Sample injection is usually carried out manually or by means of an automatic sample loop, wherein the solvent stream is diverted through the loop to push the sample out, before entering the column. Flowrate measurement is either carried out manually by weighing a sample collected in a given time interval, or automatically by a siphon arrangement that discharges when full, each discharge sending a signal to the chart recorder producing a blip on the chromatogram.

3.1.3 Analysis of Polymer Molecular Weight Distributions by G.P.C.

The unique ability of g.p.c. to separate molecules by virtue of their size makes it particularly useful for polymer fractionation.

G.p.c. has been used widely on the laboratory scale for analysis of polymer molecular weight distributions (M.W.D.'s), and, on a preparative scale, for obtaining narrow M.W.D. polymers. The fractionation of polymers is of particular interest to this research project, both on an analytical and preparative, or production, scale. The following sections cover polymer M.W.D.'s, and their determination by g.p.c. Preparative g.p.c. studies carried out in this research project are covered in CHAPTER 7.

3.1.3.1 Methods of Characterizing Polymer M.W. Distributions

With very few exceptions, polymer samples consist of a mixture of various molecular-chain lengths and therefore a distribution of molecular weights. This may be represented in the form of a histogram (FIG. 3.3a), which truly represents the discreteness of the distribution. However, the polymer usually contains a very large number of discrete molecular weights, and it is convenient to treat the distribution as continuous. The ordinate may be the weight fraction or cumulative weight fraction, and the abscissa is molecular weight (FIG. 3.3(b)). The shaded area represents the weight fraction of material between M.W.1 and M.W.2.

Since no single number can adequately characterise the molecular weight of such a material various averages are used. These are:

$$\text{Number Average M.W.} = \bar{M}_n = \frac{\Sigma N_i W_i}{\Sigma N_i}$$

$$\text{Weight Average M.W.} = \bar{M}_w = \frac{\Sigma N_i W_i^2}{\Sigma N_i W_i}$$

Figure 3.3 Representation of Polymer Molecular Weight Distributions

(a) Histogram

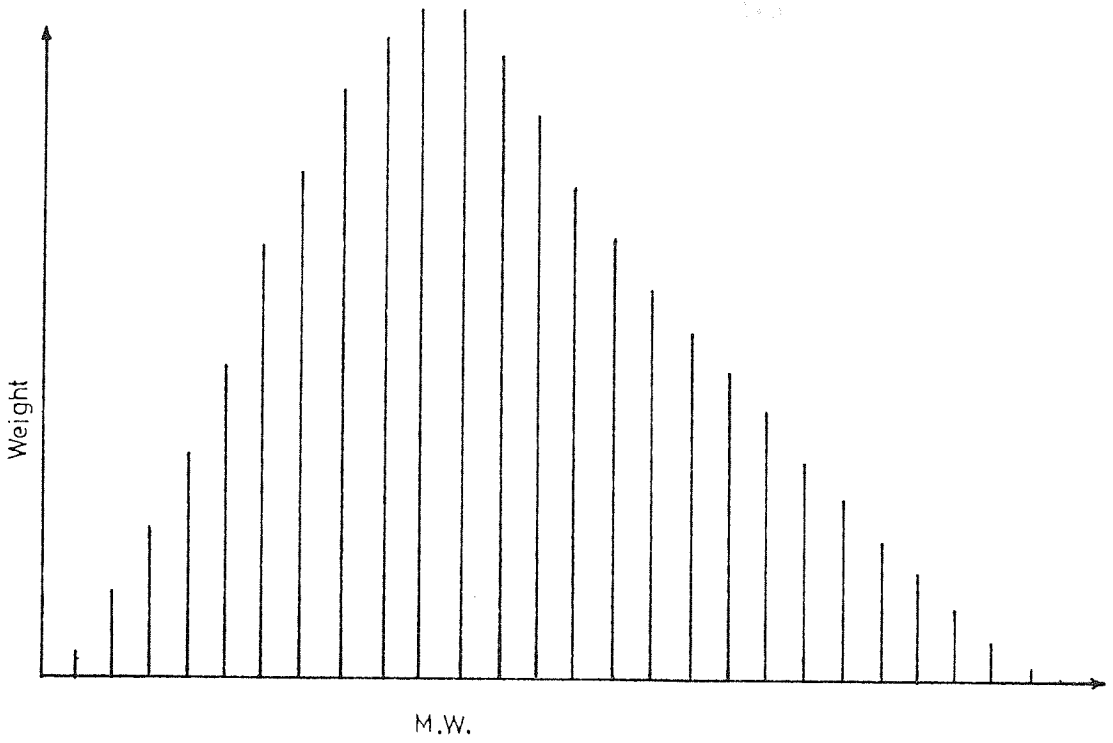

(b) Continuous Distribution

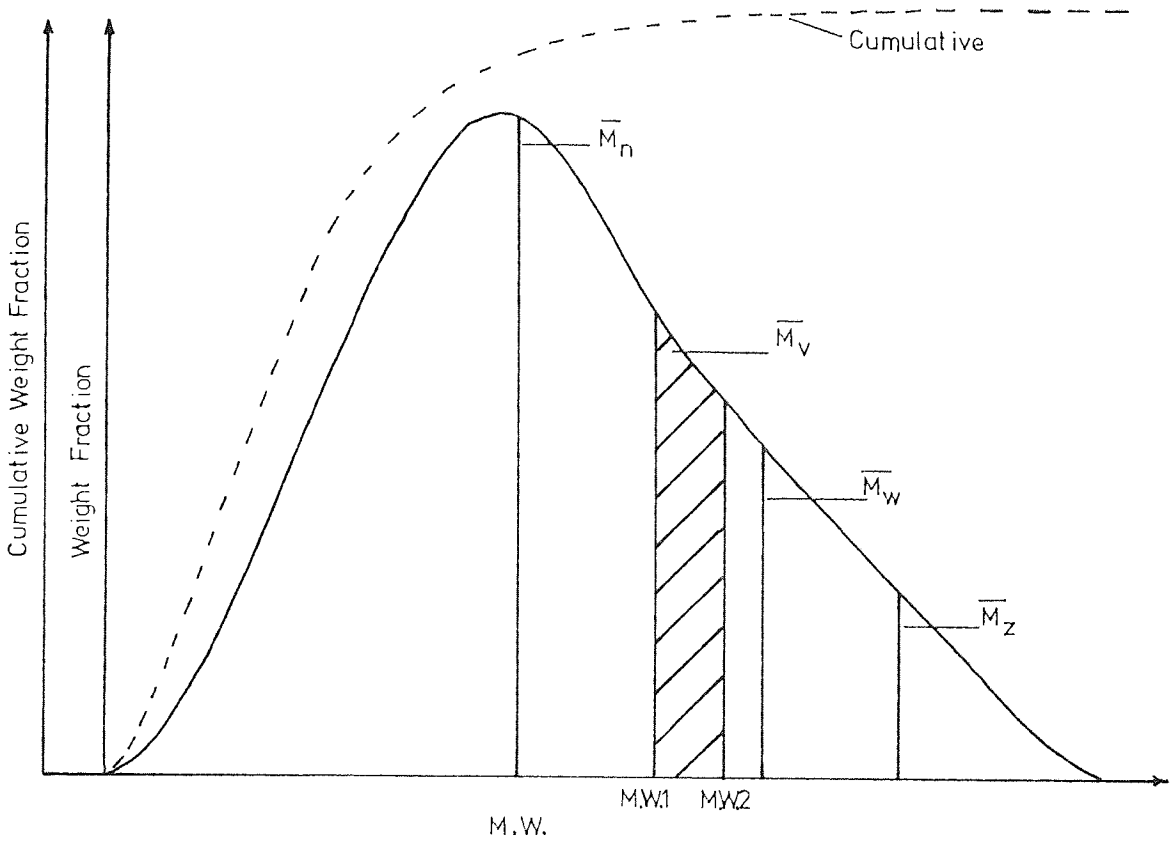

$$\text{Z Average M.W.} = \bar{M}_z = \frac{\Sigma N_i W_i^3}{\Sigma N_i W_i^2}$$

$$\text{Viscosity Average M.W.} = \bar{M}_v = \left[\frac{\Sigma N_i M_i^{1+b}}{\Sigma N_i M_i} \right]^{1/b}$$

where

$k_1 (M.W)^b$ = intrinsic viscosity

k_1 and b are constant for a particular system

b ranges from 0.5 to about 0.8 for random-coil molecules

N_i = Number of chains of ith length

W_i = Molecular weight of the ith chain length

The choice of one of these averages depends on the intended use of the data, and typical values of their relative positions are shown in FIG. 3.3(b). Combination of $\bar{M}_w$ and $\bar{M}_n$ is often used, to describe the 'sharpness' of a polymer distribution, by means of the "polydispersity ratio" $\bar{M}_w/\bar{M}_n$. Values of this ratio are usually in the range 1 to 2, the lowest number indicating the narrowest distribution.

3.1.3.2 Data Treatment

A typical chromatogram obtained, by monitoring the column outlet stream, when a sample of a polymer in solution is injected on to a g.p.c. column, and eluted by the mobile phase, is shown in FIG. 3.4(a). The ordinate represents the variable being measured by the detector, but, as this is usually proportional to concentration, concentration will be used for convenience. The abscissa is the elution volume, or elution time, the area under the curve represents the weight of sample loaded on the column and the shaded area represents

Figure 3.4 G.P.C. Chromatograms

(a) Typical Polymer Chromatogram

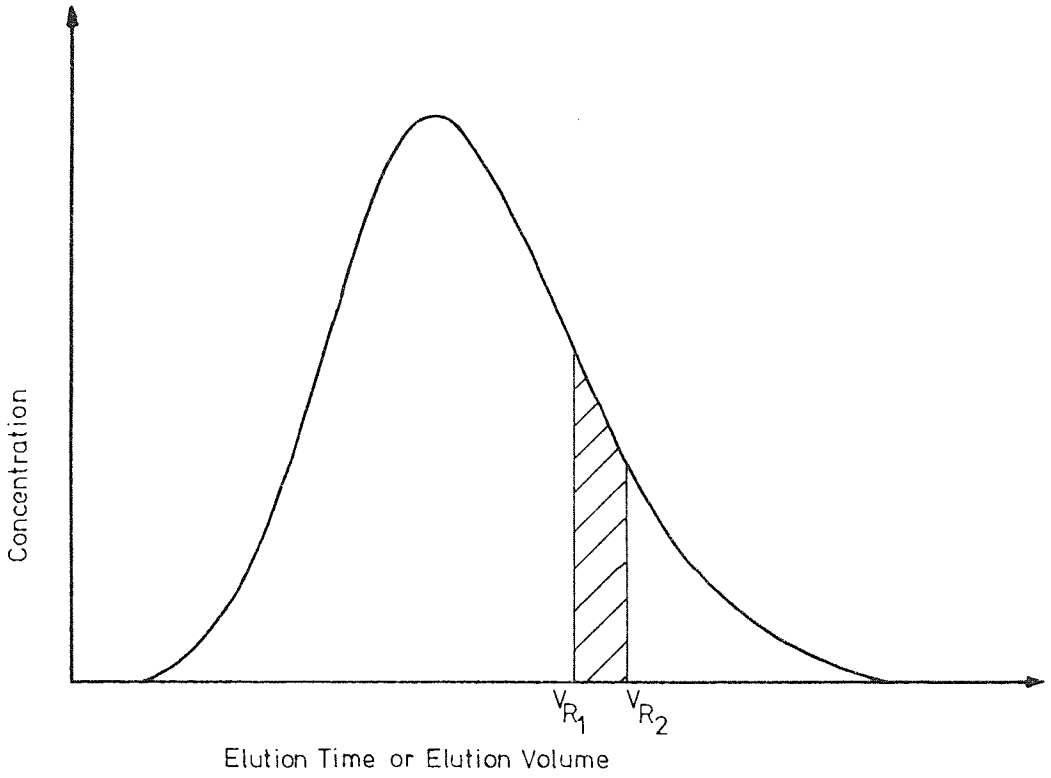

(b) Contribution to Chromatogram from Individual Molecular Sizes in Polymer

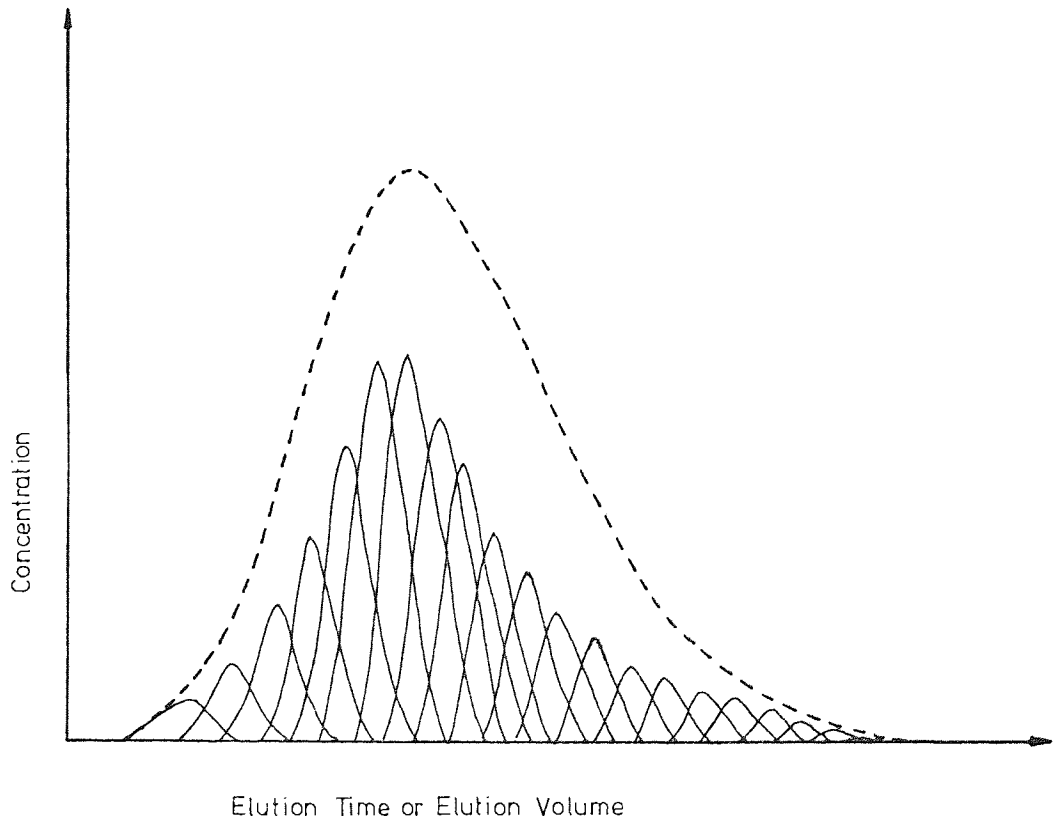

the weight between V_{R_1} and V_{R_2}. The chromatogram represents the summation of the individual contributions from discrete molecular sizes present in the polymer (FIG. 3.4(b)), which are Gaussian in shape due to zone broadening processes occurring in the column (SECTION 3.3).

Representation of molecular size in terms of its elution volume from a column is sometimes sufficient. For example a comparison of the relative narrowness of two distributions may be obtained from comparison of their chromatograms obtained directly by g.p.c. analysis. However, it is sometimes necessary to obtain the distribution in terms of molecular weight. This is done by collecting fractions of the column outlet stream, and analysing them individually for molecular weight using an apparatus such as a light scattering photometer. In this way the distribution of molecular weight is built up.

Another method for relating elution volume to molecular weight is by calibration of the column with standards of known M.W. values. The molecular weight distribution of a sample of the same species may then be estimated from the calibration plot. In practice, as high molecular weight monomers of the chemical species under study often do not exist, it is necessary to calibrate the column with narrow polymer fractions, of known M.W. distribution, of the same material, differing only in chain length. If the elution volumes of these standards are plotted against the logarithm of the corresponding molecular weight, a typical calibration curve is obtained (FIG. 3.5). This relationship, $\text{Log } M = A_1' - B_1' V_R$, was first suggested by Moore (1). The dotted line represents the idealized case, and the continuous line is that obtained in practice. The reason for the difference is that, in practice, the range of sizes of the gel pores is not linear (see

Figure 3.5 Typical G.P.C. Column Calibration

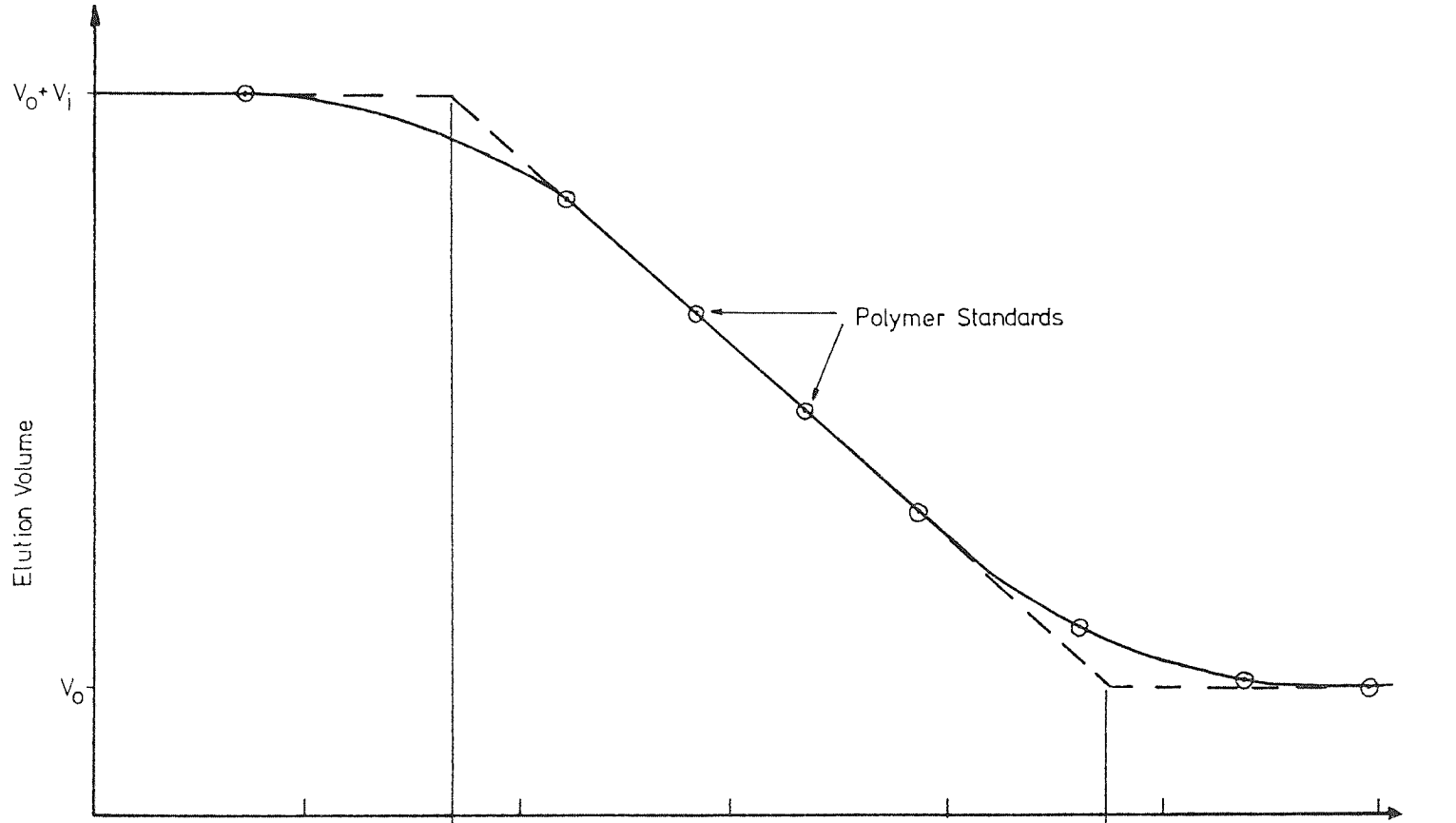

FIG. 6.6(a) SECTION 6.1.2) and the polymer chains can assume a variety of configurations. The calibration is thus a statistical average of molecular size and pore size distribution. If the curve is steep, this means that the packing will produce large differences in the relative elution positions of solutes, but a limited fractionating range (X-Y). If the curve is shallow, the packing will fractionate solutes over a wider molecular weight range, at the expense of less relative separation of each solute.

The particular value of elution volume plotted for a calibration sample depends on the characteristic molecular weight chosen. This is apparent from FIG. 3.3(b). If samples are sufficiently narrow, $\overline{M}_w/\overline{M}_n \sim 1$, the peak elution volume (p.e.v.) is often plotted against $\overline{M}_w$ or $\overline{M}_n$. However, if samples do not have narrow distributions, the elution volume corresponding to the particular M.W. average used must be calculated. For calibrations in this research, the M.W. distributions of the dextran standards were fairly broad, and the M.W., $M_{0.5}$, corresponding to the 50% weight fraction point on the sample cumulative distribution, supplied by the manufacturers (Pharmacia Ltd.), was plotted against the elution volume corresponding to the half-area point of the distribution, as this was the most readily-determined standard point. The method is discussed in SECTION 4.2.2.4.

A great deal of work has been carried out on g.p.c. analysis to find a universal 'size' parameter, to relate different chemical species, and thus obtain a 'universal' column calibration. Some examples of these have been the use of the extended chain length (157), the Stokes radius (158), and the hydrodynamic radius (159). However, for the purposes of this thesis, it has only been necessary to consider one polymer species, dextrans, and in this case the increase in size accompanying an increase in polymer chain length also results in a

proportional increase in molecular weight. It should be noted here that the effective size of a molecule in solution may be altered by changes of solvent type, temperature, and molecular concentration. Thus a molecule may exhibit a different 'apparent' molecular weight if account is not taken of these factors.

Evaluation of molecular weight of a polymer distribution by analysis of a g.p.c. recorder trace suffers from the disadvantage of not accounting for dispersion of the peak during progress through the column and associated equipment. Dispersion in the column can be minimized in the manner indicated in SECTIONS 2.2.4 and 3.3. Dispersion during passage of the sample through flow lines, and detectors, should also be minimized, by reducing their volumes to a minimum.

If sample dispersion is still significant, with these factors minimized, it may be necessary to correct the chromatogram by mathematical techniques. Many techniques to achieve this have been proposed (e.g. 160-163), and compared (164). These methods often suffer from artificial oscillations in the corrected chromatogram, often do not account for sample 'skew', and are mathematically complex, although recent methods (e.g. 165) claim improvements.

3.2 THEORY OF G.P.C. RETENTION MECHANISMS

3.2.1 Introduction

The relationship of the chromatographic process to a true equilibrium situation was discussed in SECTION 2.2.4. Although true equilibrium only exists at the centre of a solute band during migration through a chromatographic column, the process is generally very close to equilibrium, and the assumption that equilibrium exists is at the centre of chromatographic theory. The evidence that most chromatographic migration is an "equilibrium" process is summarised by Giddings et al. (166) as:

(i) K values obtained by chromatographic measurements usually agree with those obtained by static methods.

(ii) Peak elution volume is usually flow independent.

(iii) A large departure from equilibrium is totally incompatible with the narrow peaks obtained in good chromatographic processes.

Models for the g.p.c. separation mechanism, based on equilibrium partitioning of solute molecules between the interstitial volume and pore volume of a gel, have taken two forms:

(i) Steric exclusion theories.

(ii) Thermodynamic theories.

However, factors occur in g.p.c. operations, such as low solute diffusion rates and the relative inaccessibility of deep micro-pores in the packing, which may result in a significant departure from the equilibrium partitioning situation. Models based on factors other than equilibrium partitioning have been based on:

(iii) Restricted diffusion.

(iv) Separation by flow.

3.2.2 Steric Exclusion

Steric exclusion may be thought of as exclusion of the solute from a certain part of the gel volume due to the steric configuration of the gel matrix.

One of the earliest attempts to describe the g.p.c. separation process, based on steric exclusion, was given by Porath (167) who related the distribution coefficient, K_D, to the Stokes radius, a_r, of a solute molecule. He described the available pore volume by means of a model consisting of an equivalent spherical molecule and conical pores, and obtained the expression:

$$K_D = p\left(1 - \frac{a_r}{r_p}\right)^3 \qquad (3.3)$$

p = a constant

r_p = radius of an average conical pore

He used the equation $a_r = (M.W.)^{1/2}$ for flexible macromolecules by which a linear relationship between $K_D^{1/3}$ and $M.W.^{1/2}$ should be obtained for EQUATION 3.3. This was confirmed by experimental data obtained for elution of dextran samples on Sephadex. However, this relationship, derived for flexible macromolecules, was also found to hold for spherical protein molecules by several authors (e.g. 168) which it should not do theoretically. In contrast Squire (169) claims experimental agreement between $(V_R/V_o)^{1/3}$ and $M.W.^{1/3}$, i.e. $K_D^{1/3} \propto M.W.^{1/3}$, for globular proteins, for which his model was derived, and dextran fractions, which his model should theoretically not fit. Squire considered steric exclusion from cones, cylinders, and 'crevices', and obtained an expression:

$$V_R/V_o = [1 + g(1 - a_r/r_p)]^3 \qquad (3.4)$$

where g is a constant

This conflicting evidence suggests that the models are not very sensitive to molecular shape, and therefore of limited use.

Laurent and Killander (170) developed a model originally introduced by Ogston (171), and considered the volume fraction available to a spherical solute molecule in a network of random infinitely long straight rods. They obtained an equation:

$$K_{AV} = e^{-[\pi L''(a_r+r')^2]} \qquad (3.5)$$

$$K_{AV} = K_D\,[V_i/(V_i + V_{GM})]$$

V_{GM} = volume of gel matrix

L'' = concentration of rods as cm. rod cm^{-3}

r' = radius of rods

The authors found good agreement between EQUATION 3.5 and data obtained by g.p.c. on Sephadex for a large number of proteins and dextrans, taken both from the literature and their own experiments.

Support for EQUATION 3.5 is given by Fawcett and Morris (172) and Partridge (173). Also, Fischer (174) has pointed out that this treatment can be adapted for non-spherical molecules. He considers any molecule with a positively curved surface and obtains, for $a_r >> r'$:

$$K_{AV} = \exp\left(-\frac{L''A_1}{4}\right) \qquad (3.6)$$

A_1 = surface area of molecule

3.2.3 Thermodynamic Theories

A more rigorous treatment than the models discussed in the previous section has been given by Casassa (175) and Casassa and Tagami (176) for linear and branched polymer chains in various simple pores. They consider that molecular configuration can be described more satisfactorily then pore geometry, and consequently a comparison between different molecules in simple pore structures is undertaken, the assumption being that similar behavioural differences will exist in more complex pore geometries. Expressions for K are obtained in terms of pore geometry for cavities of three shapes - a sphere, an infinite cylinder, and the space between two parallel infinite planes. The unexpected result was found (175) that the parallel infinite planes, or 'slab', model fitted the data of Moore and Arrington (177) obtained by elution of linear polystyrene polymers of narrow molecular weight distribution on porous glass, using a binary θ solvent. It is concluded that the result is coincidental, as pores in the glass are not likely to be 'slab'-shaped. An error in measurement of the dimensions of non-uniform pores by mercury penetration in the data (177) is suggested by Casassa as an explanation, as a wide pore with a narrow entrance may be recorded as having the radius of the opening using this method.

Casassa concludes from the theoretical treatment that the equilibrium distribution of a solute's molecules between the mobile and stationary phases should determine its elution volume under a broad range of conditions, and that the hydrodynamic radius is the determining parameter for this distribution.

Giddings et al. (166) have evaluated the loss of statistical or configurational entropy in pores of simple shape, a distribution of simple pores, and random porous networks. They calculate that characterization of the partitioning can generally be represented by the mean external length of a molecule ($\bar{L}$), and the pore surface per unit free volume, for rigid molecules. They conclude that $\bar{L}$ better characterizes partitioning in the examined systems than parameters such as molecular weight, radius of gyration (167), or equivalent hydrodynamic radius (159).

Van Kreveld and Van den Hoed (178) developed a model based on the structure of Porasil (porous silica) beads. Each bead was considered to be built up from a large number of randomly overlapping microspheres of solid silica, the pore space being formed by the remaining space between the microspheres. The solute molecules were considered as fluctuating random coils, of effective radius $\bar{r}$, which is related to the pore volume by:

$$\ln \psi'(\bar{r}) = \left(\frac{Rs' + \bar{r}}{Rs'} \right)^3 \ln \varepsilon \qquad (3.7)$$

$\psi'(\bar{r})$ = void fraction of packing available to molecule of radius $\bar{r}$

Rs' = radius of solid microspheres

For linear macromolecules near a surface $\bar{r}$ is derived as:

$$\bar{r} = 0.886\ r_g$$

r_g = radius of gyration

EQUATION 3.7 is used to determine the theoretical distribution coefficient, $\psi'(\bar{r})/\varepsilon$ as a function of $\bar{r}$ and hence molecular weight. Excellent agreement is obtained between predicted values of the distribution coefficient, and experimental values obtained by g.p.c. of polystyrene fractions on Porasil C and D using tetrahydrofuran as the mobile phase at 1.5 $cm^3 min^{-1}$ on an 0.8 cm diameter column. This leads the authors to conclude that exclusion on the basis of geometry alone, fully describes the processes in the case considered. They also suggest that the "steric exclusion" model and the "loss of configurational entropy" approach lead to similar results.

3.2.4 Restricted Diffusion

Colton et al. (179) describe two independent phenomena which may result in a reduced solute diffusion rate, both as a result of the proximity of the pore wall. The first is due to the fact that a solute molecule is excluded from part of the pore volume due to a 'wall effect'. This leads to a solute partitioning wherein the solute concentration inside the pore is less than the bulk concentration outside the pore. Secondly, the additional hydrodynamic resistance, above that in free solution, hinders the movement of solute molecules through the pore. The authors conclude that solute partitioning and/or restricted diffusion can determine solute mass transfer rates in g.p.c.

A direct test of whether or not a significant departure from equilibrium partitioning occurs in g.p.c. is to compare values of K_D obtained from static, equilibrium, measurements to those obtained from elution data on a g.p.c. column. Another test is to observe if the elution volume of a solute shows any dependence on the operating flowrate. Yau et al. (180,181) compared static and elution experiments and found them to be in agreement for ordinary operating conditions for g.p.c. columns.

However for polystyrene standards of higher molecular weight a dependence of the elution volume on flowrate was noted for elution from columns of cross-linked polystyrene gels. Yau and Malone (180) formulate an equation based on separation being attributed to lateral diffusion in the column:

$$V_R = V_o + V_{i_{ACC}} \left[\frac{p}{(\pi u \ M^b)^{1/2}} (1-e^{-u M^b/p^2}) + \text{erfc} \left\{ \frac{(uM^b)^{1/2}}{p} \right\} \right] \quad (3.8)$$

p = constant

M = molecular weight

b = M.W. coefficient $\sim 1/2 - 2/3$

The predicted effect of flowrate on elution volume of EQUATION 3.8 was found to be in the same direction (180) as the experimental observations, the elution volume decreasing with increasing flowrate, but the quantitative prediction was poor. The authors suggest that an additional exclusion term would be necessary to describe the mechanism satisfactorily.

Van Kreveld and Van den Hoed (178) consider that the variation of peak elution volume with flowrate observed by Yau and Malone (180) was due to an incorrect criterion for establishing the elution volume. The first moment of the distribution is suggested as a more accurate measurement of V_R, and when they applied this to the data of Yau and Malone, no effect of flowrate on elution volume was observed.

Although there is considerable evidence in the literature that elution volume is independent of flowrate (1,23,170,180,182,183,184,

185), several other authors have recorded a flow dependence (186,187, 188,189,190,191,192). Yau, Suchan and Malone (193) consider that some of the inconsistency may be due to mobile phase evaporation, and faults in syphon systems, causing errors in mobile phase flowrate measurements. Little et al. (183) also show a need to correct for solvent evaporation. From the variation in the findings outlined below, it may be that experimental errors such as these contribute the major part of the observed effects, and no definite conclusions can be drawn on the experimental evidence available to date.

The change in elution volume of low M.W. solutes (186,187, 188,189) has usually taken the form of a decrease in elution volume at slow flowrates. Beau et al. (191) observed a reduction in elution volume for a low M.W. solute, benzene, and high M.W. polystyrene standards, 90,000 - 1,800,000 M.W., for flows velocities up to 0.6 cm sec^{-1} using a mixture of Porasil D and E. However, the opposite effect has been obtained by Gudzinowicz and Alden (190), who observed an increase in elution volume with flowrate for a polystyrene standard of 1,800,000 M.W.

Ackers (158) compared static and g.p.c. values of K_D for proteins and viruses on Sephadex, and obtained good agreement for tightly cross-linked gels (G-75 and G-100), but large differences for the loosely cross-linked G-200. He considered that the latter was due to a process other than simple molecular exclusion governing solute retention, and formulated an expression based on a mechanism of steric and frictional hindrance to molecular diffusion within the gel matrix as:

$$K_{GPC} = (1 - \frac{a_r}{r_p})^2 \left[1 - 2.104 \left(\frac{a_r}{r_p}\right) + 2.09 \left(\frac{a_r}{r_p}\right)^3 - 0.95 \left(\frac{a_r}{r_p}\right)^5\right] \quad (3.9)$$

a_r = Stokes radius

r_p = effective pore radius

A disadvantage of this result is pointed out by Casassa (194) in that there is no flow-rate dependence and hence no way for K_{GPC} to approach the equilibrium value, $K_D = (1 - \frac{a_r}{r_p})^2$, at the limit of slow flow. Perhaps it should be noted that Ackers (158) indicated several mechanisms by which flow-rate insensitivity could be encountered under a diffusion-controlled mechanism. One of these concerned the fact that the thickness of the stagnant layer around a gel particle varies inversely with the flowrate, diffusion distances being thus reduced with flowrate and making solute flux across the stagnant layer insensitive to the velocity of the surrounding fluid. Altgelt (195), however, suggests that such a layer while reducing the flowrate dependence of elution volume, would also enhance tailing, which is rarely observed.

Theoretical treatment of diffusion in gel pores has been carried out by Kubín (196). He considers K_{GPC} as being composed of both steric exclusion and restricted diffusion as suggested by Yau (197), and derives an expression.

$$K_{GPC} = K_D [1 - (Q')^3] \qquad (3.10)$$

Q' = a packing geometry factor.

Kubín indicates qualitatively that a dependence of Q' on flowrate would be an increasing function which would support the results of Yau et al. (181). Hermans (198) also considers the theory of g.p.c. diffusion. The gel particles are considered to be homogeneous spheres into which diffusion takes place, and the mobile phase concentration is

assumed to be uniform across the column. Hermans' results indicate that when diffusion into the gel particles plays an appreciable role in the separation process, long tails should be observed in the elution peaks, and these tails would become more pronounced at lower diffusion rates, or higher molecular weights. Further, at low flow rates, when diffusion is unimportant, the separation is due only to the equilibrium partition coefficient, K_D.

3.2.5 Separation by Flow

Pedersen (152) has discussed the phenomenon of enhanced migration of large solute molecules with respect to small solute molecules in capillaries. Because of wall effects, the larger molecules tend to travel nearer the axis of the capillary, where the liquid velocity is greatest, and their migration is thus enhanced relative to smaller molecules. The enhanced migration of red blood cells over plasma molecules in blood capillaries has been observed (199), and Pederson (152) recorded a similar effect with large and small protein molecules on columns packed with solid glass spheres of 20-35 μm diameter, which led him to propose that size separation in g.p.c. may be related to capillary action.

A comprehensive discussion of this phenomenon under the heading "separation by flow" has been given by Dimarzio and Guttman (155,200-202). They consider a solution of polymer molecules undergoing laminar flow in a uniform cylindrical tube. For a spherical molecule of effective radius $\bar{r}$ they obtain:

$$\frac{\langle u_p \rangle}{\langle u \rangle} = 2 - \left(1 - \frac{\bar{r}}{r_c}\right)^2 - 2\gamma \left(\frac{\bar{r}}{r_c}\right)^2 \qquad (3.11)$$

$\langle u_p \rangle$ = mean particle velocity

$\langle u \rangle$ = mean solvent velocity

r_c = radius of cylinder

γ = coefficient dependent on the polymer distribution

= ~0.1

To adapt this model to g.p.c., a column is modelled as a series of sections, consisting of bundles of parallel tubes, and separated by mixing chambers. The tube bundles consist of equal numbers of both large and small tubes, the volume of the large tubes (V_L') representing the interstitial volume, and the volume of the small tubes (V_s') the intra-particle volume. The separation by flow effect occurs in the smaller size, and the particular tube that a molecule enters is characterized by a probability function. This leads to:

$$\bar{V}_R = Q_f n_t \ell_t \left[\frac{p_L}{\langle u_p \rangle_L} + \frac{p_s}{\langle u_p \rangle_s} \right] \qquad (3.12)$$

$\bar{V}_R$ = Average elution volume

Q_f = Total carrier flowrate

n_t = Number of tube sections

ℓ_t = Length of a tube section

p_L = Probability that a molecule will travel through a large tube

p_s = Probability that a molecule will travel through a small tube

EQUATION 3.12 is developed for the cases where the concentrations of particles in a column cross-section are locally in equilibrium, and the corresponding non-equilibrium case. The equations developed have the

same functional form as EQUATION 3.1:

$$\overline{V}_R = V_L' + KV_s' \qquad (3.13)$$

K has been evaluated for the equilibrium case and the flow case, to give:

$$\overline{V}_{R_E} = V_L' + V_s' \left[1 - \frac{\overline{r}}{r_c}\right]^2 \qquad (3.14)$$

$$\overline{V}_{R_F} = V_L' + V_s' \left[2 - (1 - \frac{\overline{r}}{r_c})^2 - 2\gamma \left(\frac{\overline{r}}{r_c}\right)^2\right]^{-1} \qquad (3.15)$$

Casassa (194) shows how this model leads to the equilibrium case when the velocity of a molecule through a small tube is much less than its velocity through a large tube, which he suggests is a necessary criterion for the model to be at all representative of a g.p.c. column.

Verhoff and Sylvester (154) propose a theory based on flow through the gel pores as well as in the interstitial regions, and suggest the term 'Hydrodynamic Fractionation' for the mechanism. It may be summarized as molecules being separated by the flow patterns which they follow through the bed, small molecules which flow through the pores being delayed relative to large molecules which do not. Their model of the g.p.c. column is essentially similar to that of Dimarzio and Guttman, and they obtain an expression which, if the velocity in the small pores is much less than that in the large pores, reduces to (194):

$$\overline{V}_R \simeq V_L' + V_s' (1 - \frac{\overline{r}}{r_c})^2 \left[1 + \frac{2\overline{r}}{r_c} - \left(\frac{\overline{r}}{r_c}\right)^2\right] \qquad (3.16)$$

This equation is reduced, for small pores where Brownian motion would predominate, to a form previously derived, EQUATION 3.14.

Casassa (194) suggests that $(1 - \frac{\bar{r}}{r_c})^2$ is merely the equilibrium constant for partitioning of rigid spheres between cylindrical pores and a macroscopic solution phase, and EQUATION 3.16 thus reduces to the equilibrium case. He also considers that the assumption $\langle u_p \rangle = \langle u \rangle$, used by Verhoff and Sylvester for the small cylinders of the model, ignores the flow effect discussed by Dimarzio and Guttman. Further, that by use of a derivation by Ferry (203), the flow effect is assumed operative, resulting in an inconsistency. Casassa rectifies this inconsistency and obtains the same result as that of Dimarzio and Guttman. From his treatment of the theories of Verhoff and Sylvester, and Dimarzio and Guttman, he concludes that, when the flow velocity through the pores, $\langle u \rangle_S$, is small compared to that in the mobile phase, $\langle u \rangle_L$, as in practical cases of g.p.c., their results become indistinguishable from an equilibrium model.

Casassa also interprets the model of Ackers (158), by assuming mobile phase flow through the pores, and suggests that this model, properly considered, also leads to the equilibrium relation at low flow rates. Support for Casassa's considerations is given by Anderson and Stoddart (204), who noted the similarity between Ackers' restricted diffusion mechanism and Pedersen's flow model.

Summarizing, the equilibrium partition coefficient of a molecular species determines its elution position in g.p.c. under ordinary conditions. Various models for characterizing the partition coefficient in terms of molecular and pore dimensions are proposed. Non-equilibrium separation models essentially reduce to the equilibrium case at slow flowrates. Whether or not the departure from equilibrium partitioning is significant under certain conditions is not clear from the experimental evidence available at this time.

3.3 THEORY OF G.P.C. ZONE BROADENING

3.3.1 Theoretical Equations for G.P.C. Column Efficiency and the Effects of Basic Chromatographic Parameters

The complement of retention theory in any chromatographic process is solute zone broadening theory (SECTION 2.2.4). EQUATION 2.20, developed by Giddings (33) describes the contribution to plate height from longitudinal molecular diffusion, mass transfer or non-equilibrium effects in the stationary phase, and mass transfer (non-equilibrium) and eddy diffusion effects in the mobile phase, in a chromatographic column. Giddings and Mallik (205) develop the individual contributions of EQUATION 2.20 for g.p.c., and obtain an expression:

$$H = \frac{4D_m}{3Ru} + \frac{1}{20} R(1-R) \frac{d_p^2 u}{D_m} + \left[2\lambda d_p + \frac{D_m}{w d_p^2 u} \right]^{-1} \qquad (3.17)$$

EQUATION 3.17 expressed in reduced parameters is:

$$h = \frac{4}{3R\nu} + \frac{1}{20} R(1-R)\nu + \left[2\lambda + w\nu\right]^{-1} \qquad (3.18)$$

$$h = H/d_p$$

$$\nu = d_p u/D_m$$

The shape of the curve described by EQUATION 3.18 is shown in FIG. 3.6(a). For typical g.p.c. applications the curve approaches a minimum at $\nu = 1$, and for values of ν below this minimum a steep increase in h is obtained. However, operation of g.p.c. columns is usually at flowrates about $\nu = 1$, and the minimum is rarely encountered.

D_s of EQUATION 2.20 is replaced by D_m in EQUATION 3.17 by Giddings and Mallik, who assume the relationship $D_s/D_m = 2/3$, obtained

Figure 3.6 Sample Dispersion in G.P.C

(a) Reduced Plate Height as a Function of Reduced Velocity

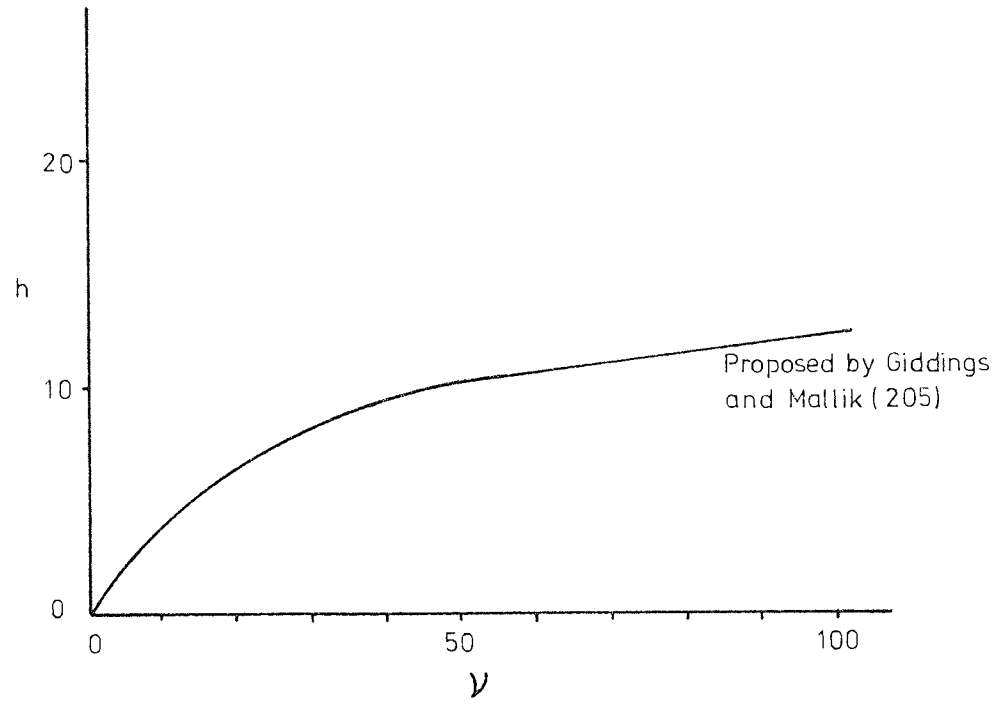

(b) Comparison of Dispersion for Porous and Non-Porous Packings (211)

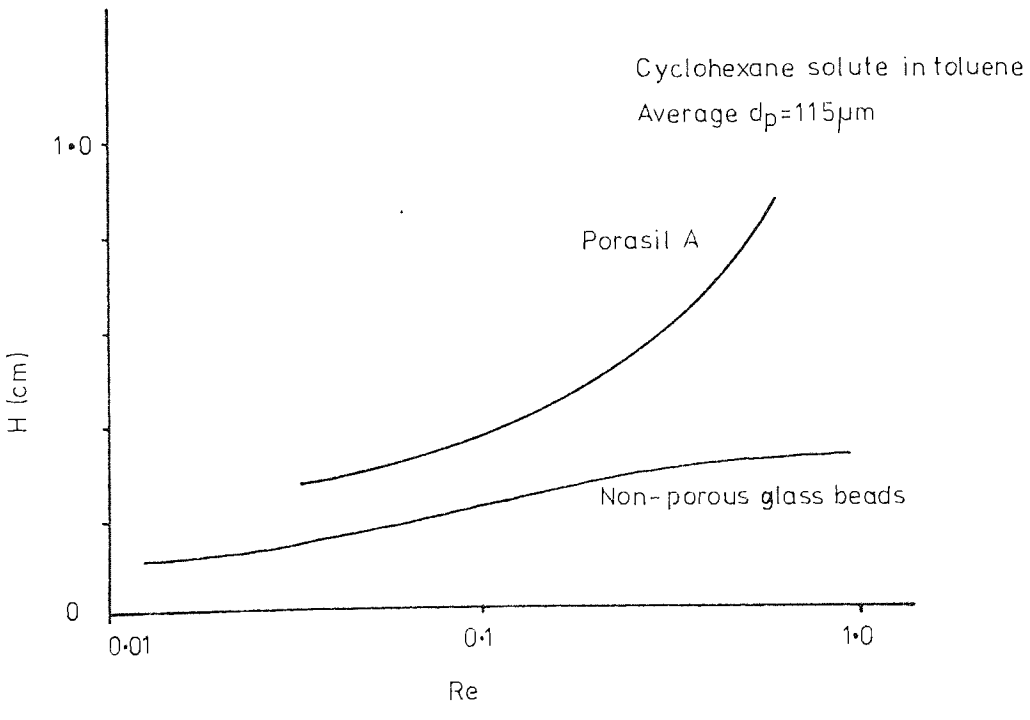

by Horowitz and Fenichel (206) for diffusion in swollen dextran gels. However D_s/D_m may change substantially in rigid gels with variations in molecular radius and pore size, as indicated by Ackers (158). EQUATION 3.17 is also based on an assumption of trans-column equilibrium, and hence does not include an additional term of the type outlined in SECTION 2.3.2.2. A criterion for trans-column equilibrium is given by Giddings (65) as the "transition length", L_d, defined by:

$$L_d = \frac{d_c^2 u}{8D_m} \qquad (3.19)$$

If values of L_d are less than the column length, then lateral equilibrium may be assumed. Giddings and Mallik (205) calculate L_d for typical g.p.c. operating conditions given in the literature, and obtain values $\sim 10^4$ cm, indicating trans-column equilibrium is not established by the criterion of EQUATION 3.19. This is re-iterated by Altgelt (195) who quotes typical g.p.c. values of d_c = 0.8 cm, u = 6 cm min^{-1}, $D_m = 10^{-6}$ cm^2 sec^{-1}, $L_d = 10^4$ cm. Altgelt also suggests that EQUATION 3.17 does not account for any viscosity effects which may occur when polymers of high intrinsic viscosity are being used as samples. He summarizes that EQUATION 3.17 is not strictly applicable to g.p.c. but it is useful for obtaining qualitative information about column performance.

Giddings and Mallik (205) consider that the reduced plate height, h, not only transforms a wide variety of experimental measurements to a common basis, but provides a 'criterion of excellence' for a chromatographic system. An inherently efficient column should produce h values from 10 → 2 at reduced velocity values of 0.2 → 10. They also calculate that the stationary phase term of

EQUATION 3.18 makes no significant contribution to h until $\nu >> 100$, and consider that the contribution would be < ~5% for most points, which suggests that the stationary phase diffusion is rarely a rate-controlling step in liquid chromatography if $D_s = \sim D_m$. This indicates that high relative velocities, greatly exceeding those at the minimum plate height ($\nu = 1$), can be used in g.p.c. (205), without producing tailing of the sample.

Support for the shape of the curve illustrated in FIG. 3.6(a) is given by the results of Smith and Kollmansberger (186). Further support is given by Altgelt (195) who compares the data of Heitz and Čoupek (207), for elution of oligophenylenes with tetrahydrofuran on cross-linked PVA gels, with the theoretical curve of Giddings and Mallik, and obtains good agreement. The data of Le Page, Beau and de Vries (208) also produces the same concave-downward curve for the h vs. ν plot using various particle sizes of Porasil E. Experimental data obtained with 0.8 cm diameter columns using benzene as solute for 100-125 μm, 125-150 μm, 160-200 μm, and 200-250 μm diameter packings all lie closely to a plot of EQUATION 3.18. However these must be contrasted with the higher h values, than those predicted from EQUATION 3.18, with 60-80 μm, and 80-100 μm diameter particles.

Conversely Billmeyer, Johnson and Kelley (209) expect that EQUATION 3.17 would not describe g.p.c. adequately because the g.p.c. retention mechanism is different from those of other forms of chromatography, and that its chief value may lie in studying why it does not describe g.p.c. adequately. In a major study (209-211) they approach the problem by considering the causes of zone broadening for small molecules in g.p.c. as being composed of two independent contributions. These are free-stream dispersion, outside the gel, and

the permeation process itself:

$$H = \frac{2D}{u} + C_p u \qquad (3.20)$$

Mobile phase effects — Permeation effects

A diffusion model is developed based on an effective dispersion coefficient, which includes velocity profile effects not included in EQUATION 3.17, and produces the equation:

$$H = \left[2\gamma' \frac{D_m}{u} + 2\lambda d_p + \frac{2h'R^2}{(\gamma' D_m/u + \lambda d_p)} \right] + C_p u \qquad (3.21)$$

γ' = tortuosity factor = $^2/_3$

λ = eddy diffusion proportionality constant = $^1/_{11}$

h' = velocity profile constant

C_p = permeation constant, depending on solute and column packing

The first three terms of EQUATION 3.21, inside the bracket, produce curves similar in form to those obtained by Giddings' coupling theory (FIG. 3.6(a)), the relative position of the minimum depending on the size of D_m. The authors calculate that, for typical Reynolds numbers in g.p.c., 0.01 → 1.0, a lower molecular diffusivity produces a higher H.E.T.P. value, and this dependence disappears at higher Re values. Also, at a given Re value and column diameter, larger values of d_p (lower aspect ratio) should produce greater dispersion.

Experimentally, the two contributions to dispersion were evaluated independently. This was done by considering firstly the mobile phase effects alone (210) and measuring H.E.T.P. values for columns packed with solid glass spheres of varying diameter. As no

permeation occurred, the recorded H.E.T.P. values represented only the mobile phase contributions. The same size columns were then packed with Porasil (d_p = 100-125 μm), each with one of six different grades, A-F (211). Determination of H.E.T.P. values in this case is a measure of mobile phase dispersion plus permeation dispersion. Thus the contribution of the permeation process alone can be evaluated by subtraction.

The mobile phase contributions were measured for a range of narrow polystyrene standards, M.W. = 2000-160,000, and hexane, cyclohexane, and n - $C_{36}H_{74}$; using toluene as mobile phase on 0.775 cm diameter columns. For high M.W. materials such as 160,000 M.W. polystyrene the mobile phase dispersion was found to be independent of flowrate up to Re = 2, the maximum studied. This finding is supported by the work of Dawkins and Taylor (212) who found the mobile phase dispersion for a 111,000 M.W., non-permeating, polystyrene standard to be unaffected by flowrate up to 4 cm^3 min^{-1}. The study was carried out on 0.3 cm diameter columns packed with Porasil A.

Continuing with Kelley and Billmeyer's study; for low M.W. solutes such as hexane, H.E.T.P. drops with decreasing Re, and H.E.T.P. values for low M.W. solutes were less than those for high M.W. solutes at the same Re values.

The authors consider (210) that the data follows the shape of the theoretical curves, except that the absolute values obtained experimentally, are greater than the predicted values. However, this was explained as being due to the fact that the particle diameters in practice were greater than the size used for the theoretical calculations, and had a range of particle diameters, both factors being expected to add to dispersion. The experimental results also showed that smaller

aspect ratios (d_c/d_p) gave larger H.E.T.P. values for a given column diameter. This result was obtained from comparison of packings of approximate sizes 100-125 μm, 125-150 μm, and 150-175 μm glass beads. Further, the range of particle size distribution was not found to increase the resulting peak broadening significantly. This was determined by comparison of 100-175 μm and 125-175 μm particles. The authors quote the work of Horne, Knox and McLaren (213), who found only a slight increase in broadening for a wider size range, to support the latter finding. However this is contradicted in a study by de Vries et al. (214), and also in an investigation by Dawkins and Taylor (212), both discussed later in this section.

The contribution to H.E.T.P. from the permeation process was found by Kelley and Billmeyer to increase linearly with increasing Reynolds number, as formulated in EQUATION 3.21. Support for this finding is given by Beau, Le Page and de Vries (191) who obtain a linear increase of the stationary phase contribution to h with increasing ν. Theoretical values of the mobile phase dispersion were calculated from Giddings' coupled equation and subtracted from the total experimental dispersion obtained with Porasil to obtain values of the stationary phase dispersion. The slopes of the $H_{PERMEATION}$ vs. Re plots in the study of Kelley and Billmeyer were found to be greatly affected by the solute diffusivity, but the plots tended towards similar small intercepts at low Re values. The overall H.E.T.P. values were measured for cyclohexane, and hexatriacontane, with toluene as mobile phase, and the general shape of the H.E.T.P. vs. log (Re) plot is shown in FIG. 3.6(b). Kelley and Billmeyer suggest this shape differs from the concave-downward curve shape obtained with Styragel packings because the deep, accessible pore structure of Porasil allows a small molecule to diffuse more freely towards the centre of the bead

than in the case of Styragel, resulting in an increase in the observed dispersion. However, the Porasil particles were larger than the Styragel particles, making comparison difficult. A later paper by Kelley and Billmeyer (215) plots the Porasil data as h vs. ν and the more usual concave-downward curve (FIG. 3.6(b)) is obtained, illustrating how an apparent contradiction may occur depending on the plotting technique. Le Page, Beau and de Vries (208) also obtain a concave -downward h vs. ν plot, for Porasil.

An earlier paper by de Vries et al. (214), however, using benzene as solute on 0.8 cm diameter columns, but this time with Porasil C, disagrees with some of Kelley and Billmeyers' findings. De Vries et al. (214) found that a wider particle size range gave a higher H.E.T.P. value. For a 40-100 μm particle range, an H.E.T.P. of 0.20 cm was obtained, while for a 60-80 μm particle range (having the same average particle size as the wider range) the value obtained was more than halved at 0.09 cm. To attempt to relate the studies of de Vries et al. and Kelley and Billmeyer, Cooper and Kiss (216) carried out H.E.T.P. determinations using Bioglass porous glass in particle size ranges of 44-53 μm, 53-62 μm, 62-74 μm and 74-149 μm. Using a 0.775 cm diameter column and solutes of o-dichlorobenzene and n-hexane in toluene and tetrahydrofuran solvents respectively, the minimum H.E.T.P. values were obtained for the 62-74 μm particle range, and the maximum for the 74-149 μm range. Although this study does not decide the issue of particle size range, it indicates that smaller particles do not produce the increased performance characteristic of conventional liquid chromatography, generally supporting the findings of de Vries and co-workers.

The study by Dawkins and Taylor (212) supports the findings of de Vries et al. concerning particle size range. H.E.T.P. values

were approximately halved for 37-50 μm Porasil A, compared with 37-75 μm Porasil A, using 0.3 cm diameter columns and toluene, tetraphenylethylene, and a 111,000 M.W. polystyrene standard as solutes. H.E.T.P. values were also found to increase approximately linearly with flowrate.

The study of de Vries et al. (214), recently discussed, also compares H.E.T.P., h, and ν values for 40-60 μm, 40-100 μm, 60-80 μm, 100-125 μm, and 200-250 μm diameter Porasil C particles at a constant flowrate of 0.56 cm^3 min^{-1}. The smallest reduced plate height was obtained for the largest particle diameter (200-250 μm), and a value of 4.8 was calculated, which the authors suggested met the Giddings and Mallik 'criterion of excellence' discussed earlier in this section. They conclude from this that the highest inherent efficiency is obtained with columns packed with particles at least 100 μm in diameter. However, this statement is misleading, and it is the value of H.E.T.P., not h, that gives an absolute measure of column efficiency. The reduced plate height, and corresponding reduced velocity, is used to give a more meaningful comparison of chromatographic systems, which may cover a wide variety of column geometries and operating conditions, and also to describe how closely a system approaches its optimum efficiency. However, the optimum efficiency of a column is related to the operating variables as indicated by, say, EQUATION 3.17. An experimental h value indicates how close operation of the chromtographic system is to this optimum.

Chromatographic dispersion theory (SECTION 2.2.4) shows that larger particle diameters generally lead to less efficient columns. Thus a column containing large diameter particles would be expected to be less efficient than a similar column containing smaller particles, and if a smaller h value was obtained with the larger diameter particles, this would merely show that this column was operating closer to its own

optimum efficiency, not that it was more efficient in absolute terms. In terms of H.E.T.P., the most efficient columns (214) were those containing 60-80 μm, and 100-125 μm packing, giving values of 0.09 cm and 0.08 cm respectively. Larger or smaller particles than these all give poorer efficiencies. Cooper and Kiss (216) indicate that the 60-80 μm and 100-125 μm packings used in the work of de Vries et al. (214) give the highest efficiencies, and also back-calculate H.E.T.P. values at 0.56 cm^3 min^{-1} from the later graph (208) of these workers, which was plotted in reduced co-ordinates. These results then also show the lowest H.E.T.P. value (0.08 cm) for 100-125 μm diameter Porasil E, compared with 60-80 μm, 80-100μm, 125-150 μm, 160-200 μm, 200-250 μm Porasil E packings. H.E.T.P. values increased for the larger particle diameters, up to 0.15 cm for the 200-250 μm packing. A slight increase in H.E.T.P. was also obtained for the smaller packings, both grades giving a value of 0.09 cm.

The effect of particle diameter has also been considered by Little et al. (183,184). For 10-15 μm, 25-37 μm, and 37-42 μm diameter Styragel particles, solute diffusion coefficients from 10^{-5} to 10^{-7} cm^2 sec^{-1}, and flowrates from 0.1-35 cm^3 min^{-1} on 0.775 cm diameter columns, the data was scattered for plots of h vs. ν, and H vs. ν. However, the data produced a straight line for a plot of log(H) vs. log (ud_p/D_m^2), using Acetonitrile, and polystyrene standards (19,850 and 411,000 M.W.) as test solutes.

Summarizing, qualitative agreement exists concerning zone broadening in g.p.c., but data concerning the quantitative effect of changes in both column and operating conditions on values of H.E.T.P. and h, in the literature, is varied. Another factor to be considered is that H.E.T.P. or h may not be the most suitable parameter for

expressing efficiency of g.p.c. columns. Smith and Feldman (160) consider that the plate count, based as it is on a single component, can never alone describe the separation efficiency of a column for a mixture. They develop a resolution index, R.I., for g.p.c. columns defined by:

$$\log(R.I.) = S'W \tag{3.22}$$

S' = slope of the calibration curve of log M.W. vs. peak elution volume for narrow polymer fractions

W = width of the g.p.c. curves for narrow fractions.

The resolution index may thus be thought to be the ratio of molecular weights corresponding to a displacement, w, in peak positions (160). It may be written, for two monodisperse polymers:

$$R.I. = (M.W.1/M.W.2)^{\overline{W}_{12}(P'_1-P'_2)} \tag{3.23}$$

$\overline{W}_{12}$ = Average peak width of samples 1 and 2

P' = Peak elution position

An interesting result was recorded by these authors in that R.I. was found to improve with increased flowrate, from 1 $cm^3\ min^{-1}$ to 2 $cm^3\ min^{-1}$, and decrease slightly at 6 $cm^3\ min^{-1}$.

Cooper and Kiss (216) discuss the use of resolution index, resolution, number of theoretical plates, and $\overline{M}_w/\overline{M}_n$ to characterize the efficiency of polymer fractionations. The calculated order of efficiency for various columns, using both resolution and resolution index,

agreed with the order obtained using the number of theoretical plates. The values of $\overline{M}_w/\overline{M}_n$ gave a similar order of efficiency to the other methods except in one instance. The use of parameters such as these to express column efficiency, however, has yet to gain wide acceptance with workers in the field of g.p.c.

3.3.2 Other Factors

3.3.2.1 Solute Molecular Weight

A major difference between g.p.c. and other forms of liquid chromatography is shown experimentally, using triglycerides, by Bombaugh et al. (217), in that peak width of a single component is approximately independent of K_D for g.p.c. This is considered (218) as being caused by two compensating interactions. As molecular size increases, the solute diffusion coefficient decreases, and the band spreading resulting from slowed diffusion is exactly compensated by the reduced solute retention time. The number of plates therefore increases, at constant peak width, as the square of the retention time. Bombaugh and Levangie (219) have also shown that at constant molecular size, a lower diffusion coefficient produces a wider peak, and hence lower efficiency. Le Page et al. (208) also suggest a strong dependence of H on the diffusion coefficient, and further support is given by the data of Little et al. (184). In contrast, from results with polystyrene standards on Corning porous glass, Cooper et al. (220) observed that peak widths, corrected for the sample distribution, decreased with increasing M.W., which they suggest indicates little dependence of efficiency on the diffusion coefficient.

Generally, however, the number of plates decreases as the M.W. increases, although disagreement exists as to the exact nature of the effect. Examples of lower N values obtained with higher M.W. solutes are available in the literature (e.g. 184,216,220).

3.3.2.2 Temperature

Use of elevated temperature in g.p.c. may be necessary to dissolve materials not soluble at room temperature. However, the use of higher temperatures has another attraction, in that the reduction of operating viscosity and increase of the solute diffusion coefficient generally give improved resolution, or allow faster separations at the same resolution. Little et al. (184) obtained narrower peaks and better resolution at higher temperature (80°C), which they attributed to the factors mentioned above. They also observed lower elution volumes at higher temperature, and suggested that this might be due to the polystyrene molecules relaxing, or uncoiling, and thus having a larger effective size. Support for both of these findings is given by Hatt (23) who observed a narrower peak and ~5% reduction in elution volume, from 25°C-75°C, using a dextran 80,000 M.W. fraction.

3.4 G.P.C. AT FINITE CONCENTRATION

3.4.1 Concentration Effects Causing Poorer Separations

Altgelt and Moore (221) consider that the amount of sample loaded on a g.p.c. column affects the resolution of its components in three inter-related ways:

(i) The sample volume is added arithmetically to the volume of the elution peak the column is capable of producing for each component.

(ii) The concentration of each component affects its own peak width. This effect is proportional to molecular size, and secondarily affects molecules in proportion to the time spent in the overloaded zone.

(iii) "Viscous fingering" may occur, resulting in unstable sample zone boundaries. This effect is greater for larger solution/solvent viscosity changes.

Cantow, Porter and Johnson (222) showed a distinct dependence of elution volume on concentration, which increased with increasing M.W., for elution of polystyrene standards on cross-linked polystyrene gels. This was observed for broad M.W. distributions, and only a small effect was observed for narrow distributions, up to a 2 cm^3 injection of a 0.6% w/v solution. The work of Rodriguez et al. (223) is quoted to support these findings. Further support is given by Boni et al. (189) who found a linear increase in the concentration dependence of elution volume, with increasing M.W., for polystyrene, polybutadiene, and polyethylene samples.

Gudzinowicz and Alden (190) studied sample concentrations of polystyrene standards from 0.025-1.0% w/v with Corning porous glass. They found that a 10% increase in retention time was obtained, for a

standard of 160,000 M.W., in the concentration range studied, together with skewing of the sample peak. Laurent and Granath (224) noted a strong concentration dependence of the elution volume of a Dextran T-40 fraction, V_R increasing with increased concentration. Goetze, Porter and Johnson (225) summarize observed concentration effects and consider, in general, elution volume increases with increasing sample size for narrow distribution samples, and the rate of change increases with M.W. Broad distributions show changes in peak elution volume and shape with concentration. These authors consider that it is difficult to decide if the effects have been caused by viscosity effects alone, as these have usually been accompanied by changes in polymer concentration and M.W. In their experimental study (225) changes in the sample/mobile phase viscosity ratio were made at constant polymer concentration, by varying the sample solvent viscosity. In this case a slight increase in elution volume (~4%) was obtained with increased relative viscosity, up to 37, for 411,000 and 1,800,000 M.W. polystyrene standards on cross-linked polystyrene gels. For the same increases in relative viscosity, obtained this time by an increase in sample concentration, the increase in V_R was substantially larger (~15%), at relative viscosities up to ~15. They conclude from this study that viscosity effects are only partly responsible for changes in elution volume.

Altgelt (195) has also discussed the problems associated with the use of polymers of high intrinsic viscosity in g.p.c. He considers that the viscosity difference between sample and solvent would be expected to contribute to zone broadening, and hence less efficient operation. The effect is explained (195) in terms of the Hagen-Poisseuille law for flow of a viscous fluid through capillaries, represented by the

column intersticies, where flowrate is proportional to solution viscosity. Eddy diffusion effects would therefore be expected to affect the solution more than the solvent, because of the greater viscosity of the former, resulting in broadening of the solute zone.

Goetze et al. (225) show the drop in column efficiency, with relative viscosity increasing from 1-3, to be ~60%, thereafter the efficiency remaining relatively constant up to relative viscosities of 37. The difference in measured column efficiencies, obtained for the two methods of increasing viscosity outlined earlier, were slight for polystyrene standards of 411,000, 860,000, and 1,800,000 M.W. Polymer samples of 2 cm^3 with concentrations up to 13% w/w were used in the study. The work of Flodin, who also obtained increased sample dispersion at sample viscosities above 0.004 Ns m^{-2}, using haemoglobin and salt as solutes in the presence of high M.W. dextrans, is reported (221). Berger (226) also observed broadened, assymetric peaks when he used sample solutions different in viscosity to the mobile phase.

3.4.2 Concentration Effects Producing Improved Separations

A concentration effect which may be opposite to the effects discussed above, and beneficial to separation, is apparent from the literature. This is an effect commonly referred to as 'secondary exclusion' (195). When operation of a g.p.c. column is being carried out at higher polymer concentrations, large molecules have less pore volume available to them because the smaller molecules, which penetrate the pores more rapidly, effectively reduce the pore volume by their presence. Thus large molecules are eluted earlier than they would be under dilute conditions, and the effect has been called 'secondary exclusion'.

Another aspect of elution under concentrated conditions in g.p.c., is that molecules present in the mobile phase at high concentrations may act as extensions of the gel phase. Laurent (227,228) showed that solutions of high M.W. polymers, such as dextran, have molecular exclusion properties similar to solid-phase molecular sieves. This has been confirmed by Hellsing (229). Hellsing has also shown that human serum albumin is eluted later from columns of Sephadex G-200 when the mobile phase contained polymers, including dextrans. The fractional available volume for the serum albumin in the mobile phase, $(K_{AV})_M$, was determined for polymer concentrations up to 4% w/v using polymers including Dextran T-500, T-150, T-40, and T-10, having $\overline{M}_w$ values 420,000, 153,000, 35,000 and 9,400 respectively. The values of $(K_{AV})_M$ are listed in FIG. 3.7(a). A plot of $-\log(K_{AV})_M$ vs. the mobile phase polymer concentration showed $-\log (K_{AV})_M$ to increase linearly with increasing polymer concentration for Dextran 500 (229). It is also interesting to note from FIG. 3.7(a) that Dextran 150 and Dextran 35 also exclude the serum albumin from the mobile phase to approximately the same extent as the Dextran 500, although the data is rather limited. The net effect of the presence of dextran polymers in the mobile phase was that serum albumin was eluted later as the dextran concentration was increased, and this was ascribed to an activity increase of the protein in the mobile polymer phase (229).

It is apparent from these two exclusion effects, that fractionation of a polymer under concentrated conditions by g.p.c. may give an improved fractionation than would be expected if the disadvantages of concentration, outlined in SECTION 3.4.1, are considered. The first exclusion effect mentioned as 'secondary exclusion' would tend to accelerate large molecules present in the column, while the second effect

Figure 3.7 Secondary Exclusion in G.P.C

(a) Data of Hellsing for Elution of Human Serum Albumin on Sephadex(229)

Polymer in Mobile Phase	Concentration (% w/v)	$K_{AV} = \frac{(K_{AV})_G}{(K_{AV})_M}$	$(K_{AV})_M$
Dextran T-500	0	0·39	1·0
"	1	0·47	0·81
"	2	0·54	0·67
"	3	0·62	0·53
"	4	0·73	0·42
Dextran T-150	0	0·41	1·0
"	1	0·51	0·81
"	2	0·57	0·68
Dextran T-40	0	0·41	1·0
"	1	0·46	0·83
"	2	0·50	0·66
Dextran T-10	0	0·35	1·0
"	4	0·40	0·46

(b) Data of Barker, Hatt, and Somers for Elution of Dextrans on Porasil(230)

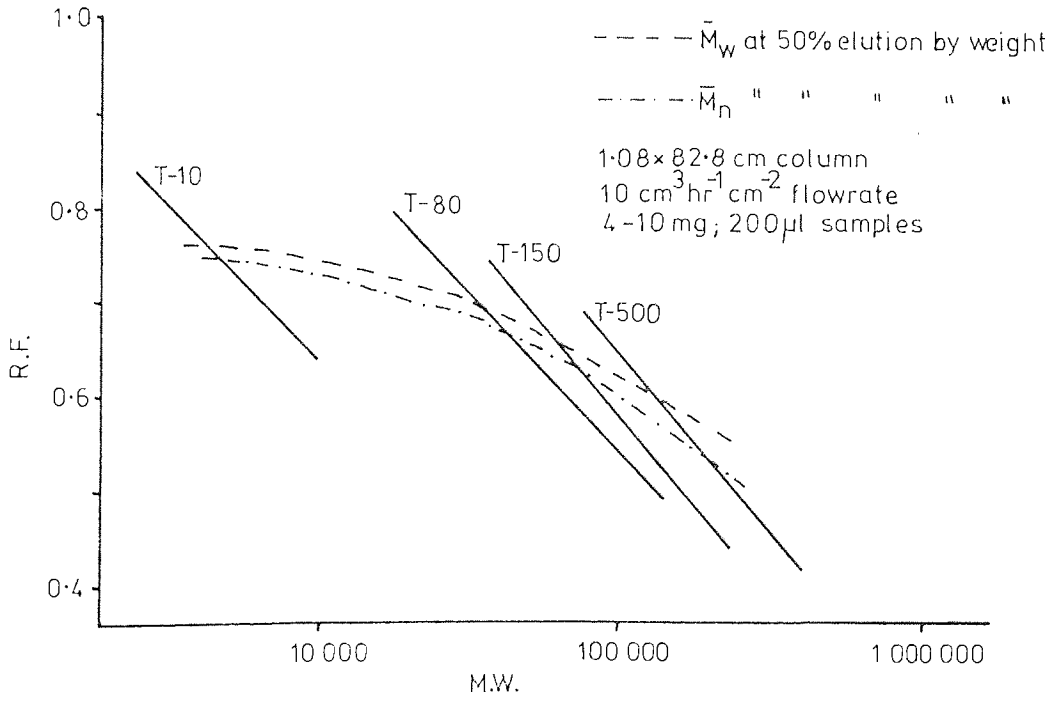

would tend to retard small molecules in the column, both effects improving separation of large and small molecules. This concept has been discussed by Hatt (23) and later by Barker, Hatt and Somers (230), for elution of a polymer species under concentrated conditions. They consider that a species of a certain molecular weight will be affected both by molecules of greater and lesser molecular weight. Lower molecular weight material excludes the species from the stationary phase to a greater extent, while higher molecular weight material causes it to be included in the stationary phase to a greater extent. These opposing effects would cancel each other out in the middle of the distribution, where the concentrations of lower and higher molecular weights are approximately equal. However, at the low M.W. end of the distribution the greater concentration of larger molecules would retard the small species, while at the high M.W. end the greater concentration of smaller molecules would tend to accelerate the large species. The sum effect would be to increase the separation of large and small species. The authors (230) expect as a result of these processes that the characteristic calibration curve (FIG. 3.5 would exhibit an increased gradient for operation in concentrated conditions.

Experimentally (230) fractionation of Dextran T-10, T-80, T-150 and T-500 was carried out by loading samples of 0.2 cm^3 at concentrations from 2-5% w/v, and eluting at 0.17 $cm^3\ min^{-1}\ cm^{-2}$ from a 1.08 cm diameter column packed with Porasil-D. Simultaneous analysis of the column effluent for weight and number of molecules was carried out using a cysteine-sulphuric acid assay and a reducing end-group assay. By superimposing the two recorder traces, the weight and number of molecules of a species, corresponding to a particular elution volume, enabled the M.W. of that species to be calculated. Plots of elution volume vs. M.W. for the dextran fractions all exhibited increased gradients, compared to

the calibration line under dilute conditions, and these curves were crossed by the calibration line at points corresponding to 50% elution by weight of the samples (FIG. 3.7(b)). These findings support the effects discussed in this section, i.e. the use of high concentration may be beneficial to polymer fractionation. Further discussion of the relevance of these phenomena to the research programme reported in this thesis is given in SECTION 4.4.

CHAPTER 4

Analytical G.P.C. Experimental Work

4.1 INTRODUCTION

The basic method of analysis used throughout this research project was column gel permeation chromatography. Use was made of this method in three main areas:

(i) Calibration of packing materials.

(ii) Analysis of dextran samples from the SCCR3 machine.

(iii) Investigation of the effects of concentration on the migration of dextran molecules through chromatographic columns.

This chapter deals firstly with general techniques associated with the use of g.p.c. as an analytical tool, and secondly with the results of an experimental study of the factors affecting efficient operation of batch g.p.c. equipment. This study was carried out primarily to obtain the best analytical system which would enable accurate analyses of dextran samples, obtained from the SCCR3 machine, to be performed.

During operation of the SCCR3 machine concentration effects were observed which caused departure from theoretical predictions based on dilute conditions (SECTION 7.3.4). The final section of this chapter deals with investigation of these concentration effects on an analytical, batch scale.

4.2 GENERAL CONSIDERATIONS

4.2.1 Analytical Equipment

The general arrangement of the column chromatography equipment used for analysis of carbohydrate samples is shown in FIG. 4.1. The heart of the unit is the analytical column (FIG. 4.2). Columns used in this research period were typically 0.4 or 0.8 cm internal diameter, 80-120 cm long, made from glass, and surrounded by a constant temperature water jacket usually operating at 25°C. The columns were tapered to a narrow outlet at the bottom, which held a small plug of glass wool to retain the column packing. The 0.4 cm diameter columns were also flared to 0.8 cm diameter immediately above the level of packing, which allowed micro-pipettes, greater than 0.4 cm diameter, to be positioned immediately above the packing during sample loading. The top of the column was sealed with a rubber bung fitted with a 5 cm length of 0.1 cm I.D. stainless steel tube, connected to the PVC mobile phase inlet line.

The bottom of the column was fitted with a glass T-piece. One arm of the T-piece contained a stainless steel sampling needle and the other arm carried excess mobile phase to waste. One end of the sampling needle was positioned as close to the bottom of the packing as possible, to minimize column 'dead volume', while the other end was connected to the sample pumping line which transported the sample to the detector.

The main detection system used was a Technicon AutoAnalyser unit. The unit is based on the chemical reaction of a continuous sample stream with metered quantities of reagents, designed to produce a chromophore, the optical density (O.D.) of the chromophore being proportional to the sample concentration. The particular assay (FIG. 4.1) used in this research was an automated version (230) of the cysteine hydrochloride/sulphuric acid assay (231) which produces a yellow

Figure 4.1 Arrangement of Equipment for L-Cysteine/H_2SO_4 Assay

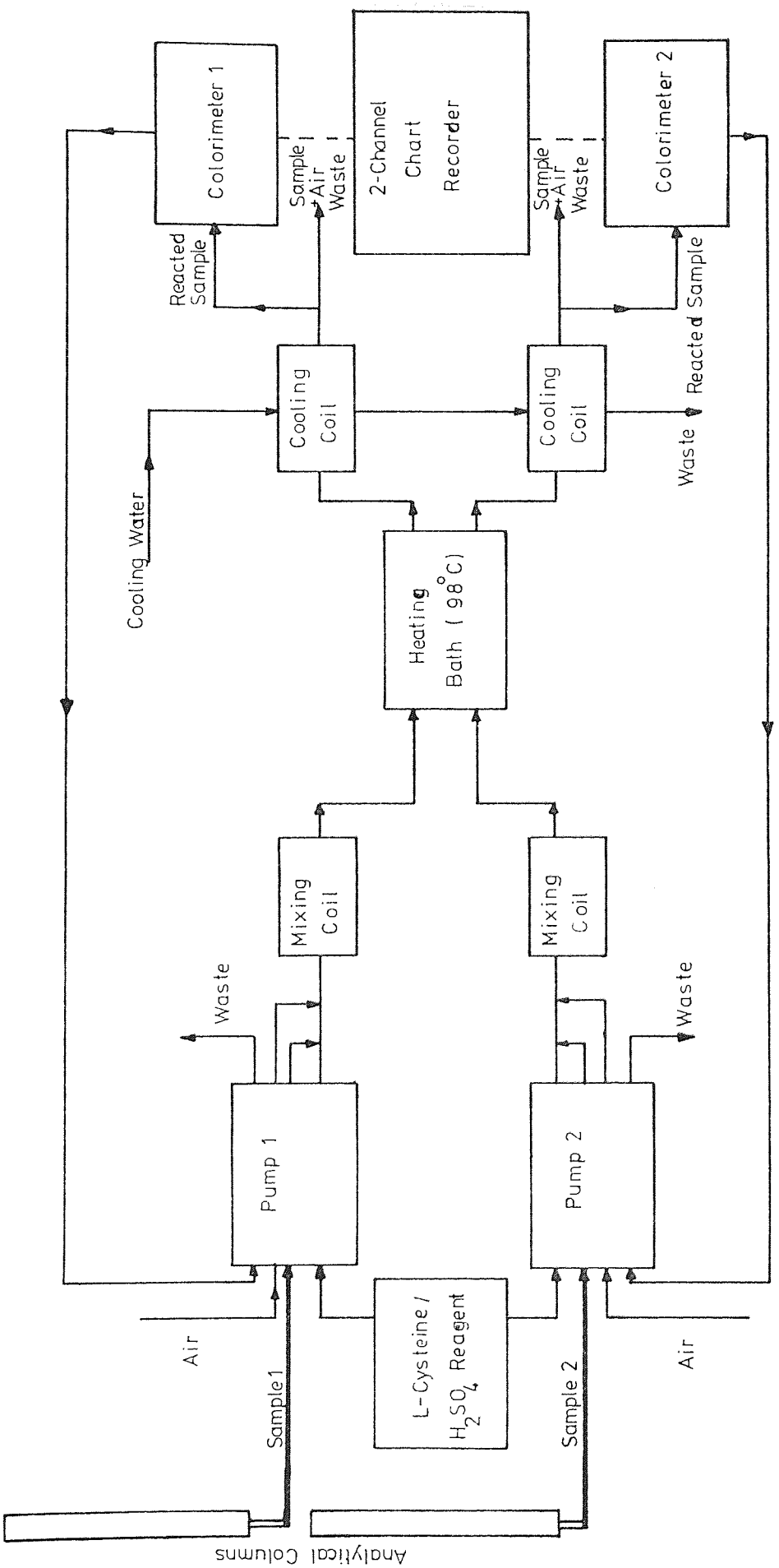

Figure 4.2 Typical Analytical Chromatographic Column

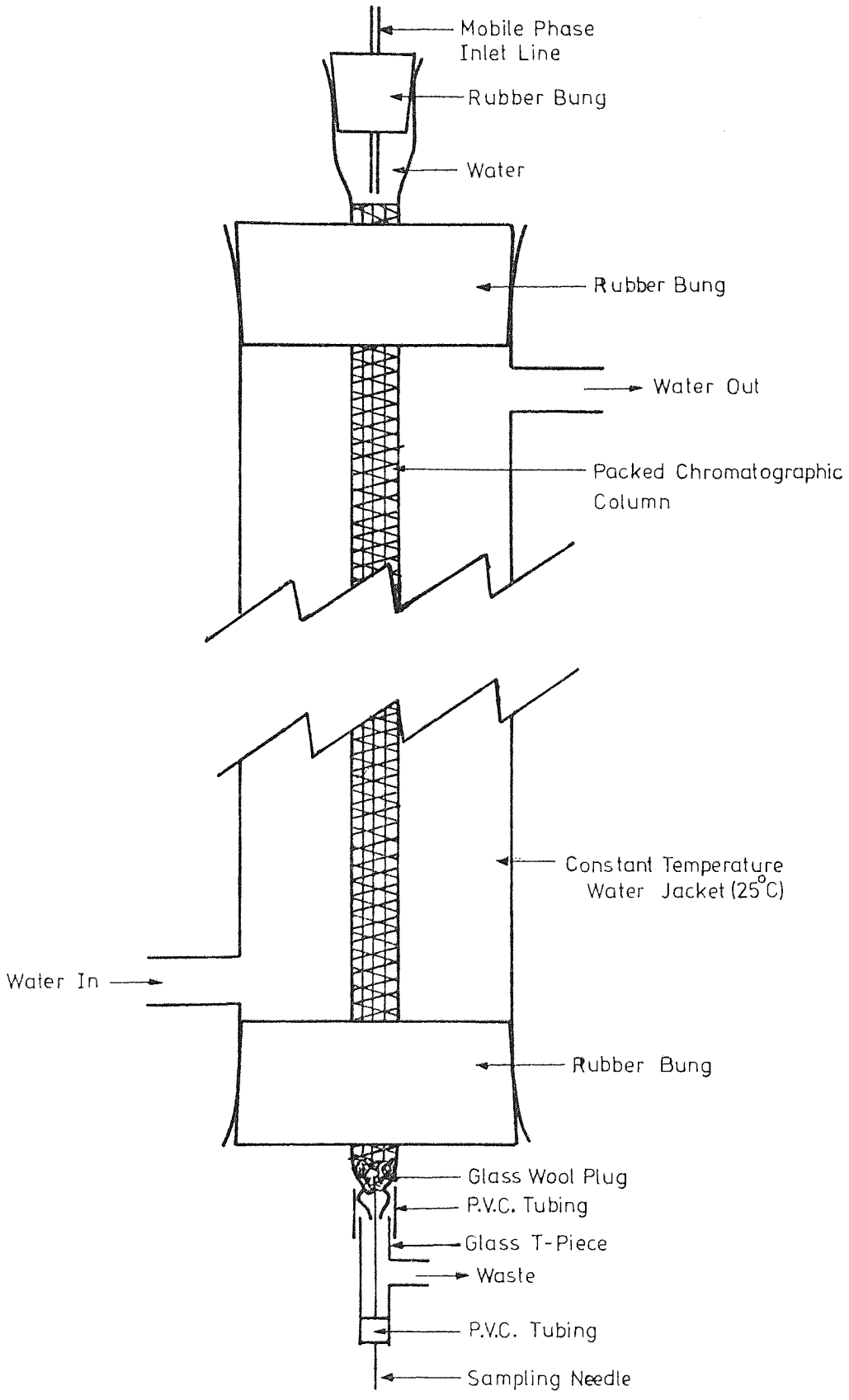

chromophore of optical density (O.D.) proportional to the concentration of carbohydrate present in the sample. The O.D. of the chromophore was measured at a wavelength of 420 nm by means of a colorimeter, incorporating a continuous flow cell (1.5 cm path length), and a reference beam to give a continuous zero balance.

Metering of mobile phase, sample, and reagent streams was carried out by a multi-channel proportionating pump which allowed flowrates between 0.015 and 3.90 cm^3 min^{-1} of liquid to be obtained. The pump worked on a peristaltic principle, and flowrates were altered by changing the pumping tubes, which were PVC, or Acidflex, of very accurate bore, and had a life of approximately 200 hours.

Sample and reagent streams were mixed by firstly merging the streams in a glass T-piece, followed by passage of the combined streams through a horizontal helical glass mixing coil, surrounded by a water jacket. The stream was next heated at 98°C, for ~5 minutes, by passage through a glass coil immersed in a thermostatically-controlled oil bath. After emerging from the oil bath the stream was passed through a glass cooling coil surrounded by a water jacket, and then to the colorimeter for analysis. Heating, cooling, and mixing times were adjusted if necessary, within the limits of the assay, by changing the length of the flow lines or altering the operating flowrates. Longitudinal back-mixing in the flow lines of the AutoAnalyser unit was minimized by introducing air to form slugs in the sample stream, separated by air bubbles.

Other detectors used in this study were an LKB Uvicord ultra-violet absorption detector, and a Pye-Unicam SP1800 Spectrophotometer.

4.2.2 Analytical Techniques

4.2.2.1 Column Packing Procedure

Packing of all analytical columns was carried out by a

slurry-filling technique. The column was fixed vertically and a small amount of glass wool packed into the bottom of the column, which was then filled with distilled water and the outlet plugged.

The packing was first sieved to the desired size range according to B.S. 1796 (1952). Next it was covered with distilled water, placed in a buchner flask, and deaerated under vacuum. The packing slurry was introduced into the top of the column using a glass funnel, and the column was then vibrated manually until the packed section reached a constant volume. Before initiating any experiments the columns were flushed with concentrated nitric acid, to remove any contaminating matter, and then thoroughly flushed with deaerated water.

4.2.2.2 Sample Loading

The rubber bung and mobile phase inlet tube were first removed from the top of the column. A screw slamp, used to seal the column outlet, was opened to allow the liquid level in the column to fall until it reached the top of the packing, and then closed again. The sample solution was then injected on to the centre of the packing, using a micro-pipette. The liquid level was again allowed to fall until it reached the top of the packing. A volume of distilled water, approximately equal to the sample volume, was next injected on to the top of the packing, and the liquid level once more allowed to fall to the top of the packing. The column outlet was sealed after each of these operations. The column, above the packed section, was next filled with distilled water, and the rubber bung replaced. This ejected excess distilled water from the column through the stainless steel tube fitted in the bung. Finally the mobile phase inlet line was connected to the stainless steel tube, and at the same time the

column outlet was opened and the chart recorder started. Care was taken, during all of these operations, to ensure that the packing was not disturbed.

To obtain reproducible analyses the loading technique was standardized. For the 0.4 cm diameter column used for analysis of SCCR3 samples 50 µl of ~2-4 mg cm^{-3} was loaded and eluted at a flowrate from 0.07-0.22 cm^3 min^{-1}. For 0.8 cm diameter columns, used in other studies, ~200 µl of ~2-4 mg cm^{-3} was loaded.

4.2.2.3 General Measurements

The mobile phase flowrate was measured at least twice per day for each flowrate used. Measurement was carried out by weighing the amount of water leaving the column outlet in a measured time interval, usually ~5 minutes. The delay time of the detection system, that is the time interval between the sample leaving the column and the chart recorder responding to the sample, was measured twice per day. This was achieved by placing the sample needle in a beaker of glucose solution and, at the same time, starting the chart recorder. The delay time was then measured from the chart, and subtracted from the measured total sample elution time, to give the elution time of the sample from the column alone. Recorded delay times were usually 10-15 minutes. Elution volumes were calculated by multiplying the corrected elution time by the mobile phase flowrate. For convenience the retention factor, R.F., which is the elution volume divided by the total bed volume, was sometimes used.

The automated cysteine/H_2SO_4 assay was used to determine dextran sample concentrations. This was achieved by placing the sample needle in the solution of unknown concentration, and allowing the chart recorder response to reach a plateau value. This value was

then compared with the response of a sample of glucose of known concentration, usually ~0.04 mg cm^{-3}, to obtain the concentration of the unknown solution, c:

$$c(\text{mg cm}^{-3}) = \begin{bmatrix}\text{RESPONSE OF SAMPLE (O.D. units)}\end{bmatrix} \times \frac{\begin{bmatrix}\text{CONCENTRATION OF GLUCOSE SOLUTION (mg cm}^{-3}\text{)}\end{bmatrix}}{\begin{bmatrix}\text{RESPONSE OF GLUCOSE SOLUTION (O.D. units)}\end{bmatrix}} \times \frac{162}{180} \quad (4.1)$$

The factor of 162/180 in EQUATION 4.1 is the ratio of the molecular weight of one dextran unit to the molecular weight of glucose. This factor is necessary to allow for the greater response produced by a dextran solution compared to a glucose solution of the same concentration. Optical density (O.D.) was read directly from the charts, by means of a logarithmic scale on the chart paper:

$$\text{Absorbance, or O.D.} = -\log_{10} {}^{1}/I_o = -\log_{10} T' \quad (4.2)$$

I_o = Intensity of radiation incident upon a sample

I = Intensity of radiation emerging from the sample

T' = Transmittance

Care was taken when using the AutoAnalyser unit to maintain sample concentrations below 0.06 mg cm^{-3} (within the linear operating range - FIG. A.1.1. in APPENDIX 1).

Readings from the Uvicord unit were obtained as % Transmittance and converted to O.D. using EQUATION 4.2, where required.

4.2.2.4 Column Calibration

Calibration of an analytical column was carried out using

glucose, as a single M.W. totally included species, and a range of Dextran T fractions (Pharmacia Ltd., Uppsala, Sweden), ranging from ~10,000 M.W. to ~2,000,000 M.W. (details are given in APPENDIX 2). The mobile phase flowrate was maintained at a constant value for elution of each sample. Elution volumes corresponding to the 50% area (weight) point of the peaks were recorded, which correspond to the 50% points on the cumulative weight vs. M.W. distributions supplied by Pharmacia. In this way elution volume was related to M.W. Elution volume was converted to Retention Factor, (elution volume)/(total bed volume), or K_D, to allow comparison of results obtained for columns of different bed volumes. Calibration graphs were plotted as R.F., or K_D, vs. log (M.W.). The total bed volume was measured, prior to packing a column, by weighing the volume of water required to fill the column to the height of the packed section.

4.3 OPTIMIZATION OF ANALYTICAL SYSTEM

4.3.1 Introduction

A detailed experimental study of the variation of analytical column efficiency with both column and operating parameters is beyond the scope of this research. The aim of the experimental work was simply to obtain an analytical system capable of reproducible sample analyses, in the shortest time, and with the best accuracy obtainable with available equipment.

The effect of column length is well established in chromatography, and did not necessitate investigation. For practical convenience columns ~100 cm long were used. Next a choice of packing type was made, followed by the choice of grade most suitable for analysis of feed material used with the SCCR3 machine. The type and grade used were the same as those used in the SCCR3 machine (SECTION 6.1.1), to allow direct comparison of K_D values obtained in analytical and preparative columns. Various sizes of the chosen grade were then compared in terms of H.E.T.P. values, calculated from elution peaks of glucose samples, to allow a choice of the optimum particle size, producing minimum H.E.T.P. This was necessary because data available in the literature was inconclusive (SECTION 3.3.1). Also compared was the performance of a 0.8 cm diameter column, the size usually employed for g.p.c. analysis, against a smaller column diameter (0.4 cm).

The extra-column contributions to sample dispersion were also studied, measured in terms of the second moment, and their effect minimized by improving the detection system. Allowance was made for the extra-column contribution to sample variance in the calculation of H.E.T.P. results. With both column, and extra-column, dispersion minimized, the effect of operating parameters was next studied. Finally, performance of the analytical system was further tested by

Williams (31), who compared the analysis of a dextran T-40 fraction with the data supplied by the manufacturers (Pharmacia Ltd., Uppsala, Sweden).

4.3.2 The Criterion for Efficient Column Operation

The criterion for the best column in this study was the one which produced the lowest H.E.T.P. value for a single M.W. species (glucose). Although it is appreciated (SECTION 3.3.2.1) that, in absolute terms, these H.E.T.P. values do not represent the efficiencies obtained when polymers of higher M.W. are fractionated, they are adequate for a comparative study.

4.3.2.1 Calculation of On-Column Dispersion

Values for the number of theoretical plates (N) were calculated for glucose from the chromatograms obtained. Assuming a Gaussian peak (232):

$$N_1 = 8 \left(\frac{t_R}{w_{h'/e}} \right)^2 \qquad (4.3)$$

t_R = Peak retention time

$w_{h'/e}$ = Width of glucose peak at h'/e

h' = Height of glucose peak

Corresponding H.E.T.P. values were calculated from:

$$H.E.T.P._1 = \ell/N_1 \qquad (4.4)$$

ℓ = Length of packed column section

As a check on the validity of the results, i.e. whether or not the glucose peaks were Gaussian, H.E.T.P. values were also calculated based on the computed time-based variance, σ_t^2, of the chromatograms, and mean (50% area point) retention time:

$$N_2 = \frac{t_R^2}{\sigma_t^2} \qquad (4.5)$$

and again $$H.E.T.P._2 = \ell/N_2 \qquad (4.6)$$

It should be noted here that the computed variance, σ_t^2, is the observed total variance of the chromatogram, which may receive contributions from outside the column, and hence not be the true variance of the peak as it leaves the column. The computer program written for calculation of these H.E.T.P. values is listed in APPENDIX 5.

4.3.2.2 Calculation of Extra-Column Dispersion

With peak dispersion associated with the chromatographic process minimized, and hence column efficiency optimized, it is still possible to have excessive sample dispersion in the chromatographic system as a whole. This is because the sample injection system, detector, and flow lines may all contribute to increased sample dispersion. Sternberg (233) has carried out an extensive study of extra-column contributions to band broadening. The contributions of independent factors to sample dispersion are additive in their second moments, so that the observed sample variance, calculated from the chromatogram, σ^2_{TOTAL} is given by:

$$\sigma^2_{TOTAL} = \sum_{i=1}^{n} \sigma_i^2 \qquad (4.7)$$

The variance contributions using the analytical system described

in SECTION 4.2.1 can be identified mainly as:

$$\sigma^2_{TOTAL} = \sigma^2_{COLUMN} + \sigma^2_{INJECTION} + \sigma^2_{AUTOANALYSER} \qquad (4.8)$$

The technique of sample injection employed in this study (SECTION 4.2.2.2) is unlikely to contribute significantly to zone broadening, as very small samples are loaded directly into the packed column. Thus σ^2_{COLUMN} can be calculated from:

$$\sigma^2_{COLUMN} = \sigma^2_{TOTAL} - \sigma^2_{AUTOANALYSER} \qquad (4.9)$$

4.3.3 Experimental Studies of Sample Dispersion

4.3.3.1 Extra-Column Effects

$\sigma^2_{AUT.}$ was computed from the observed response of the AutoAnalyser system alone. The sample needle was dipped in a 0.04 mg cm^{-3} glucose solution for 15 minutes, and the injection variance of the 15 minute rectangular step input was subtracted from the recorded variance to produce $\sigma^2_{AUT.}$ from EQUATION 4.8 with σ^2_{COLUMN} equal to zero.

To minimize $\sigma^2_{AUT.}$, the flow lines in the detection system were shortened, and all joints in these lines carefully made to reduce any back-mixing that might occur. The variance of the AutoAnalyser was again measured, after these modifications, from the response of a 15 minute rectangular input. Variance calculations were carried out by dividing the chromatogram into at least 30 sections as this is the minimum number of points for statistical significance (234). The computer program used for calculation of all variances is listed in APPENDIX 5. Values of the extra-column variances before and after the improvements, and a comparison of the respective AutoAnalyser responses is given in FIG. 4.3.

It is apparent that the modifications carried out on channel 1

Figure 4.3 Responce of AutoAnalyser System to a Step Change in Sample Concentration

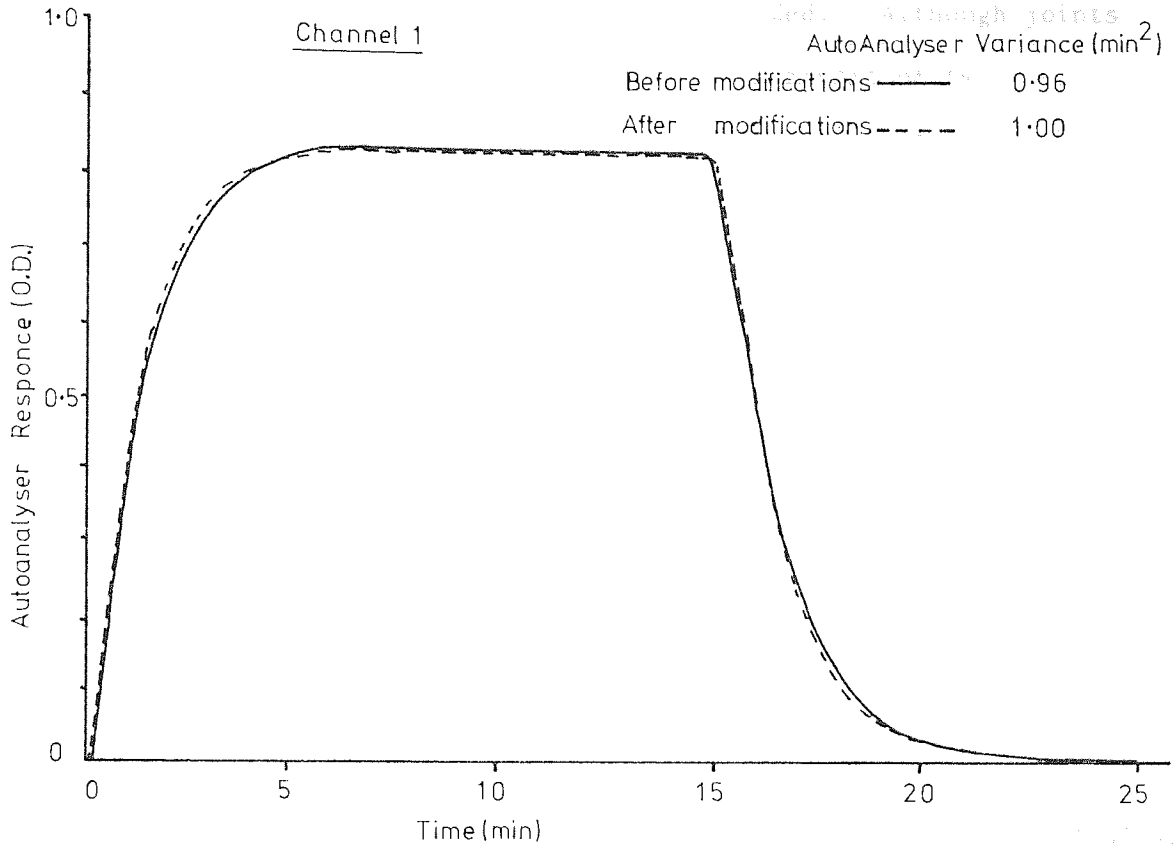

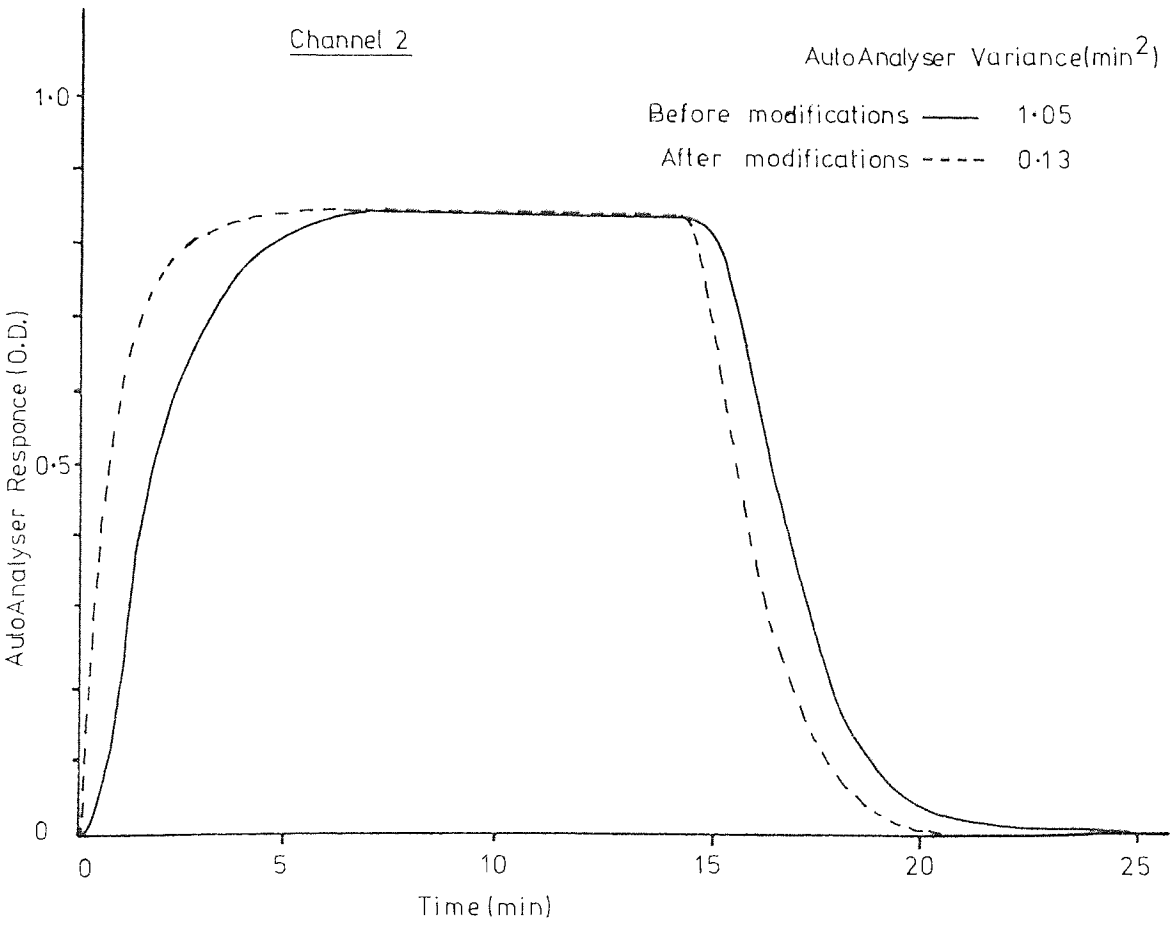

of the AutoAnalyser system did not decrease the variance associated with it, and in fact a slight increase was recorded. Although joints in the lines were checked, it is possible that a misfit of two adjacent lengths of glass tube may have caused significant sample hold up, and resultant back-mixing, adding to dispersion. In contrast, the modifications carried out to channel 2 proved very effective, and the variance associated with this channel was reduced, by almost 90%, to an insignificant amount for most analytical experiments. Where possible accurate analyses of dextran distributions were carried out on channel 2, to obtain minimum extra-column dispersion, although, at slow flow rates, the effect of channel 1 is likely to be minimal, as shown later in this section. The effect of channel 1 dispersion is only important for fast flowrate studies, i.e. certain H.E.T.P. measurements, when sample time-based variance is small and extra-column dispersion has a greater effect. It should be noted here that the contribution of the AutoAnalyser system to sample variance has a constant value, whatever operating conditions occur in the column, because its operating conditions remain essentially constant.

σ^2_{COLUMN} values were calculated from EQUATION 4.9, and used to calculate corrected H.E.T.P. values:

$$N_3 = \frac{t_R^2}{\sigma^2_{COLUMN}} \qquad (4.10)$$

$$\text{and } H.E.T.P._3 = \ell/N_3 \qquad (4.11)$$

These calculations were carried out using the computer programme for H.E.T.P. calculations, listed in APPENDIX 5. This program was also written to provide additional information on the shape of the glucose peaks by inclusion of steps to calculate the third moment

(skew) and fourth moment (kurtosis).

The effect of extra-column dispersion on H.E.T.P. values is apparent from a study of the values of $H.E.T.P._2$ and $H.E.T.P._3$ in FIG. 4.4 (SECTION 4.3.3.2). At flowrates below about 1.5 $cm^3\ min^{-1}\ cm^{-2}$, the contribution of extra-column dispersion to H.E.T.P. is negligible. However, above this flowrate the effect increases with increasing flowrate, until at about 6.0 $cm^3\ min^{-1}\ cm^{-2}$ the contribution may be as high as 30%. The values of H.E.T.P. calculated by assuming a Gaussian peak shape ($H.E.T.P._1$) are also significantly different from either $H.E.T.P._2$ or $H.E.T.P._3$ at high flowrates. This indicates a source of error in the determination of H.E.T.P. values, by assumption of a Gaussian profile, for certain operating conditions. The fact that the peaks differ significantly from the characteristic Gaussian shape is also indicated by the skew and kurtosis readings in FIG. 4.4. For a perfect Gaussian profile both of these should have a value of zero. For low flowrates the skew of the curves is minimal, indicating that the AutoAnalyser variance is negligible and the peaks are symmetrical. The values of kurtosis at low flows are also often small, which, in conjunction with the low values of peak skew, indicate that the curves are of the normal Gaussian shape. However, some values of the kurtosis are negative, indicating flatter peaks than the normal Gaussian shape. This difference is reflected in the differences between $H.E.T.P._1$ and $H.E.T.P._3$ values in these cases.

At high flowrates peak skew increases markedly. This could be due to effects occurring in the column, as well as effects associated with the AutoAnalyser, although the present study does not differentiate between these effects. It is interesting to note that the kurtosis sometimes becomes positive at high flowrates, indicating a sharper peak than the usual Gaussian profile, although this effect must be contrasted

with the inherent high skew at these flows.

Summarizing, the results show that a significant departure from the normal Gaussian elution profile is obtained at high flowrates, and correction must be made for the contribution to peak dispersion of the AutoAnalyser detection system at these flows.

4.3.3.2 Effects of Column Diameter and Packing Size

Glucose samples were eluted from 0.4 cm and 0.8 cm diameter columns containing a series of different packing sizes, all of the same packing type and grade, Spherosil XOB-075 (Porasil 'C'). A range of flowrates, from 0.28-6.13 $cm^3\ min^{-1}\ cm^{-2}$, was studied to determine the effect of flowrate on column efficiency, and establish if the results agreed with the general trends indicated in SECTION 3.3. The results are tabulated in FIG. 4.4. A plot of $H.E.T.P._3$, thought to be the most meaningful value of H.E.T.P., for the reasons discussed in SECTION 4.3.3.1, was made against operating flowrate (FIG. 4.5). The curves obtained for the columns studied have the same general shape as the curves obtained by other workers, for g.p.c. experiments, discussed in SECTION 3.3.1.

Comparison of the H.E.T.P. values of columns 1 and 3 in FIG. 4.5 indicates that, at a constant aspect ratio (d_c/d_p), the combination of lower column diameter and smaller particles produces more efficient operation. This agrees with chromatographic theory in that, assuming particle diameter to be the dominating factor for columns of small diameters, i.e. analytical columns, efficiency improves with the use of smaller diameter particles. H.E.T.P. values are more than halved by reducing particle diameter from 300-350 μm to 150-180 μm, at constant aspect ratio. The reduction of H.E.T.P., with smaller diameter particles, obtained here, agrees with general chromatographic theory, and experimental H.E.T.P. values obtained by g.p.c., discussed in SECTION 3.3.1.

Figure 4·4 The Variation of H.E.T.P. with Column and Operating Parameters for Porasil C

Column Number	Column Diameter	Column Length	Packing Batch	Flowrate / c.s.a	Packing Particle Diameter	H.E.T.P. 1	H.E.T.P. 2	H.E.T.P. 3	Skew	Kurtosis
	cm	cm		$cm^3min^{-1}cm^{-2}$	μm	cm	cm	cm		
1	0·8	90·8	1	0·541	300–500	0·55	0·51	0·51	0·002	−3·00
"	"	"	"	0·800	"	0·60	0·57	0·56	0·002	−2·95
"	"	"	"	1·70	"	1·00	1·00	0·96	0·032	−3·00
"	"	"	"	3·36	"	1·44	1·44	1·30	0·032	−3·00
"	"	"	"	6·05	"	1·78	1·93	1·51	0·109	−2·96
2	0·4	87·5	"	0·280	300–350	0·26	0·26	0·26	0·410	0·30
"	"	"	"	0·610	"	0·43	0·42	0·42	0·275	0·19
"	"	"	"	1·60	"	0·76	0·77	0·73	0·027	0·01
"	"	"	"	3·31	"	1·08	1·14	0·99	0·623	0·53
3	"	88·2	2	0·290	150–180	0·076	0·075	0·074	0·007	0·0
"	"	"	"	1·73	"	0·23	0·26	0·22	0·266	0·17
"	"	"	"	5·34	"	0·77	0·93	0·61	3·06	4·43
4	"	88·6	3	0·290	105–125	0·098	0·093	0·093	0·002	0·0
"	"	"	"	1·71	"	0·27	0·29	0·28	0·0	0·0
"	"	"	"	6·13	"	0·72	0·82	0·57	0·183	0·10
5	"	120·0	"	0·760	95–105	0·088	0·10	0·093	0·006	−2·98
"	"	"	"	2·59	"	0·18	0·25	0·24	0·065	−2·83
"	"	"	"	5·61	"	0·42	0·97	0·65	3·27	4·03

Figure 4.5 The Variation of H.E.T.P. with Column and Operating Parameters for Porasil C

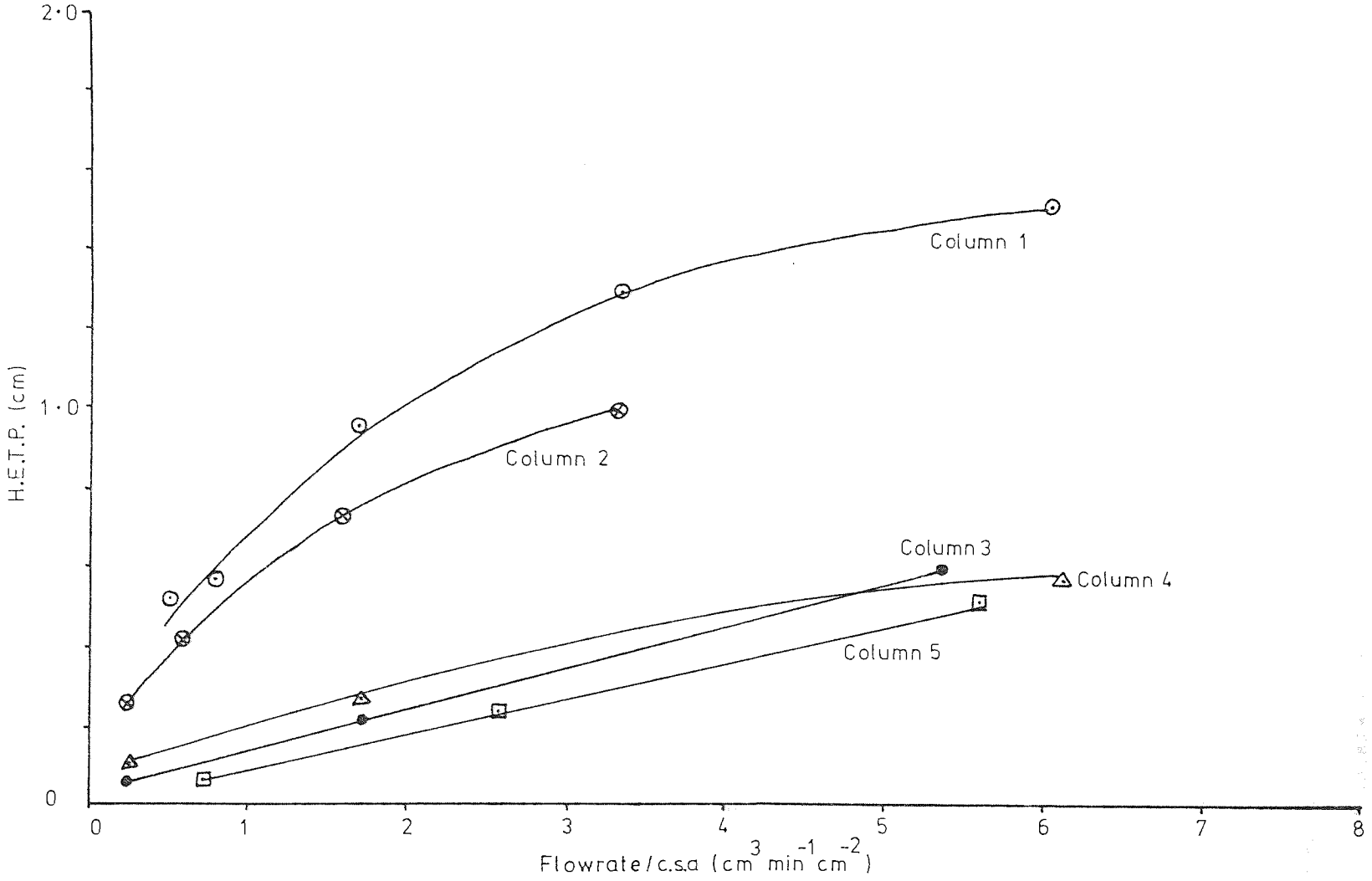

The effect of column diameter for such small columns is observed by comparison of columns 1 and 2. Column 1 shows an increase in H.E.T.P. values of ~25% over column 2, in the range of flowrates studied, which indicates improved operation with smaller diameter columns for this case. Comparison of columns 3, 4 and 5 shows that, at a constant column diameter of 0.4 cm, lowering particle diameter below 150-180 μm does not produce the dramatic improvement in efficiency that was obtained for a change in particle diameter from 300-350 μm to 150-180 μm. The 105-125 μm and 150-180 μm packings show very similar H.E.T.P. values, while only a marginal improvement is obtained for the 95-105 μm range. This is in qualitative agreement with the studies of de Vries et al. (208, 214), and Cooper and Kiss (216), both of which indicated a lower limit of particle diameter, below which there is a limited decrease in H.E.T.P. with decreasing particle diameter.

The most efficient column in this study was column 5, which was used for all analyses of dextran samples obtained from the SCCR3 machine during the research period. The calibration curve for this column is given in FIG. 4.6.

4.3.4 The Choice of Column Operating Conditions

4.3.4.1 Sample Size

The use of column 5 for analysis of dextran samples requires samples of only small volume, 25-100 μl, and low concentration, 1-4 mg cm^{-3}, to obtain a suitable chromatogram with the cysteine/H_2SO_4 detection assay. At these values, overloading effects of the type discussed in SECTION 3.4.1 will not be present. This study of sample size was carried out to establish the reproducibility of sample analyses over the range of sample sizes likely to be encountered in this research project. To this end glucose samples ranging in volume from 25 to 200 μl, having concentrations

Figure 4.6 Calibration of Analytical Column 5 (Porasil C) with Dextran T-Fractions

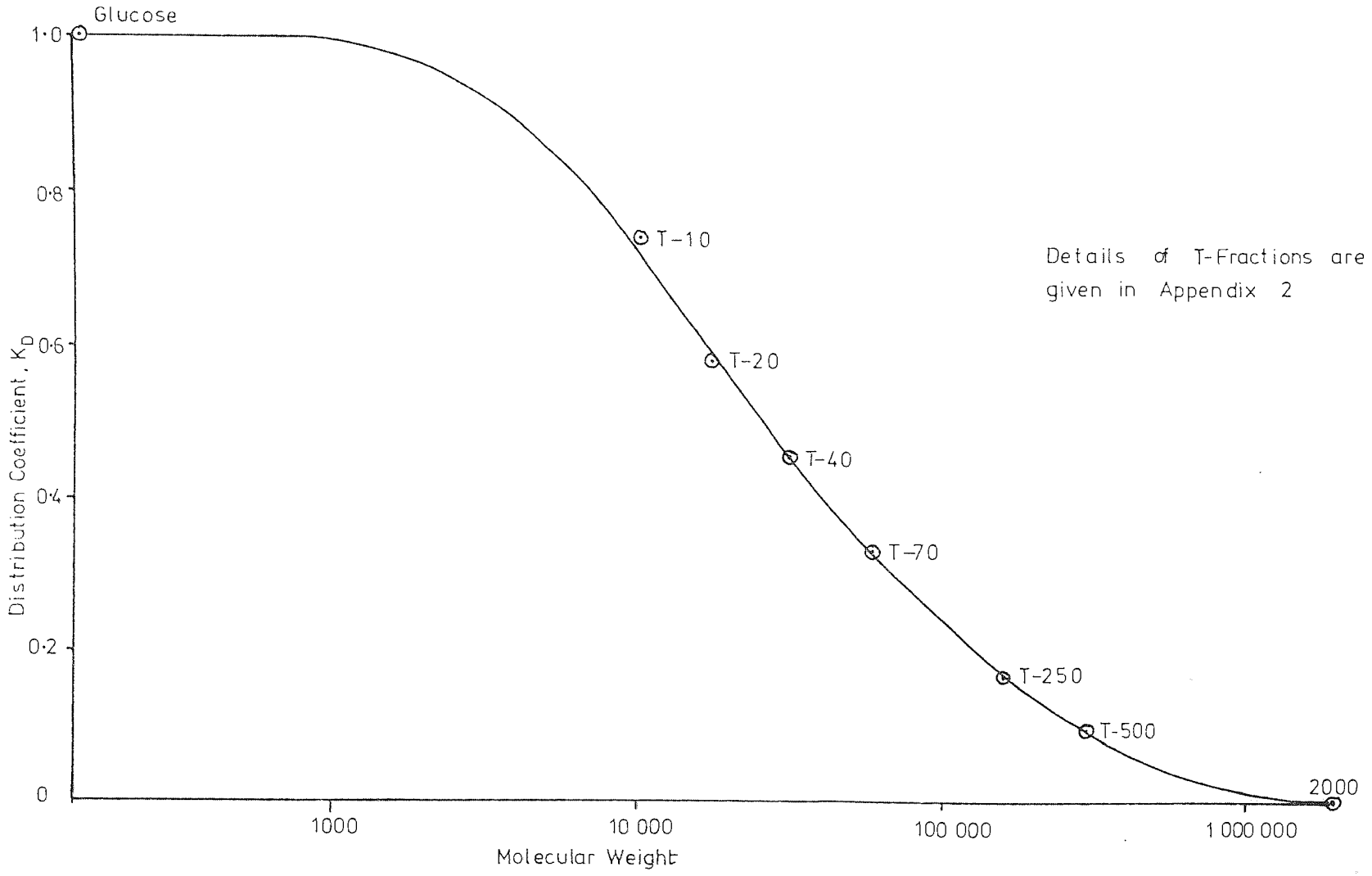

Details of T-Fractions are given in Appendix 2

from 0.5-4 mg cm^{-3}, were eluted from column 4, at a mobile phase flowrate of approximately 0.21 cm^3 min^{-1}. This flowrate was chosen as it was likely to be the highest flow used for analysis of dextran samples, and, as experimental errors were thought likely to increase with increasing flowrate, the maximum experimental errors for this study could be assessed at this flowrate. The results are tabulated in FIG. 4.7. Elution times would be expected to vary, in addition to any variation due to experimental error, because of variation of the mobile phase flowrate in the study (1-2%). The variation in elution volume is ±2% for the whole study. This is due to the two extreme results differing significantly from the remainder. If the 25 µl and 100 µl samples of 2 mg cm^{-3} are ignored, the remaining eight samples show elution volumes with a ±1.3% variation. It will be noticed that the three 50 µl samples show the lowest variation of all the volumes tested, ±0.6%, and produce an average elution volume, 10.20 cm^3, closest to the average for all the samples tested (10.22 cm^3). The loading of 50 µl samples was adopted for all analyses of SCCR3 samples. Experimental errors would be expected to be <1% for 50 µl samples at a mobile phase flowrate of 0.1 cm^3 min^{-1} (SECTION 4.3.4.2) with a standardized sample loading technique (SECTION 4.2.2.2).

4.3.4.2 Mobile Phase Flowrate

The mobile phase flowrate has two main effects on sample analyses:

(i) Increased flowrate produces increased sample dispersion, making the analysis of polymer distributions less accurate. This is apparent from FIG. 4.8, which shows the apparent change of the distribution of a dextran sample, analysed on column 5, with flowrate. If an accurate measure of a sample distribution was required, analysis was carried out at

Figure 4.7 The Variation of Elution Volume Measurements with Sample Size for the Analytical Chromatographic System

Sample Concentration	Sample Volume	Elution Time (Glucose)	Elution Volume (Glucose)
$mg\,cm^{-3}$	μl	min	cm^3
0·5	100	48·2	10·07
0·5	200	49·5	10·35
1·0	25	49·0	10·34
1·0	50	48·2	10·17
1·0	200	48·6	10·16
2·0	25	47·5	10·02
2·0	50	48·8	10·26
2·0	100	50·0	10·45
4·0	25	48·9	10·22
4·0	50	48·6	10·16

Figure 4.8 The Effect of Operating Flowrate on the Accuracy of Polymer Analysis by g.p.c

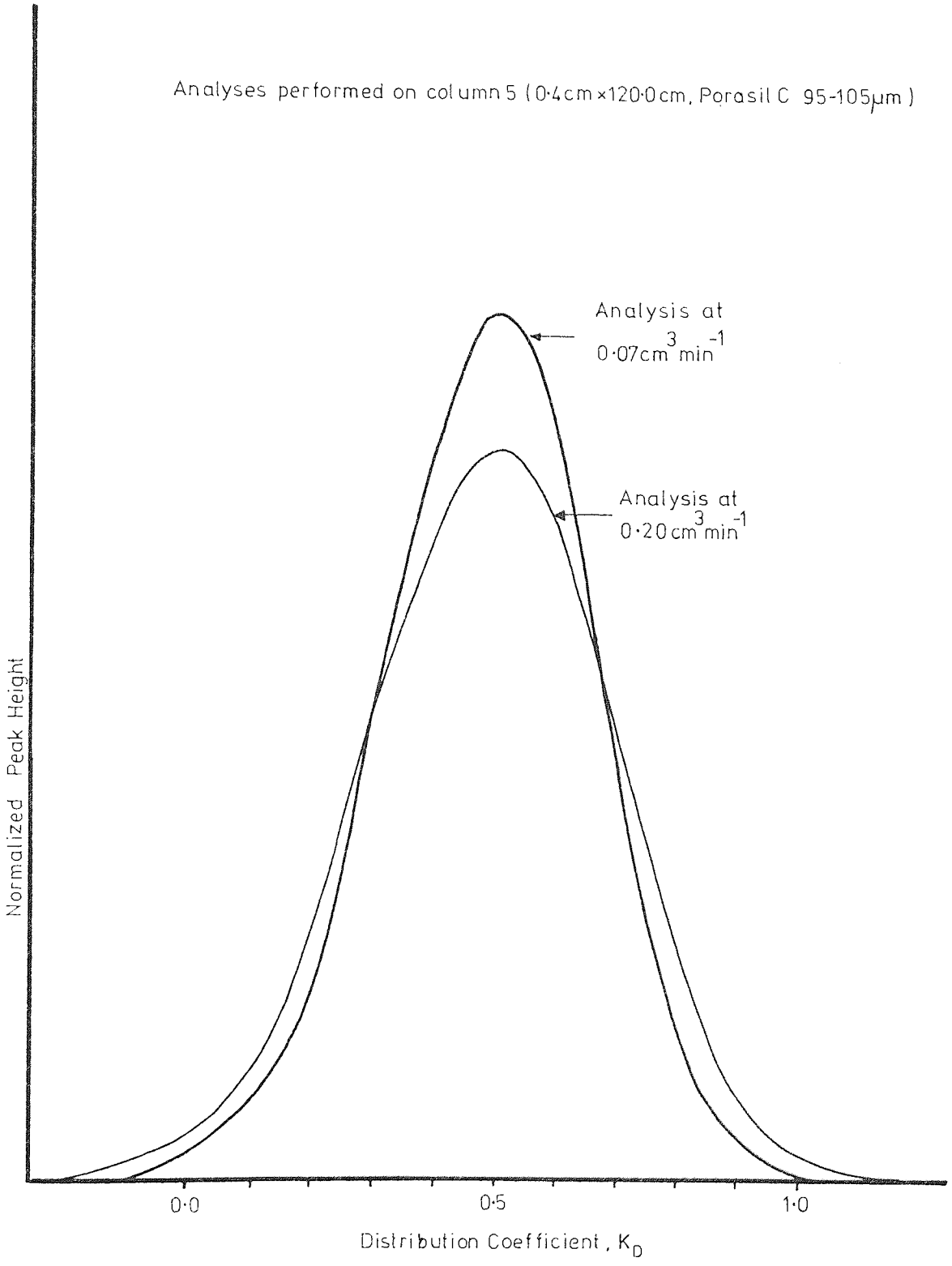

a slow flowrate, <0.1 cm^3 min^{-1} on column 5, the disadvantage of this being the increased time of analysis.

(ii) The elution volume of a species may change with flowrate. This may occur because of two independent causes. Firstly a diffusion-controlled separation mechanism can lead to a change in elution volume with flowrate, although experimental evidence in the literature is not conclusive on this issue (SECTION 3.2.4). Secondly, the measured elution volume of a species may change with flowrate. With the sample loading technique employed in this study (SECTION 4.2.2.2) there is a certain error. When the chart recorder is started the sample has already travelled a certain distance through the column. This error is approximately constant if a constant loading technique is used, at a constant mobile phase flowrate, and is negligible for most purposes, as samples are usually analysed at the same, slow, flowrate, with the same sample loading technique. However, at increased flowrates, a constant error associated with sample loading would have an increased effect, as elution times would be shorter.

With the available equipment it was not possible to differentiate between these two effects. However, Holding (235) using a sample injection system which minimized loading errors observed no change in the elution volume of glucose or dextran T-fractions for flowrates of 0.2-1.2 cm^3 min^{-1}, using a 0.4 cm diameter x 100 cm long column packed with 37-75 μm Porasil C. Thus, it seems likely that the observed increase in elution volume for a flowrate change from < 0.1 cm^3 min^{-1} to >0.2 cm^3 min^{-1} in this study was due to sample loading errors. However, it should be pointed out that the reproducibility of two analyses of the same sample, at the same flowrate, was better than 1%. In practice the majority of analyses were performed at ~ 0.1 cm^3 min^{-1}, below which no change in elution volume with flowrate was recorded. Any analyses that

Figure 4.9 Comparison of the M.W.D. Determined by g.p.c. Analysis on Column 5, and the Pharmacia Data, for Dextran T-40

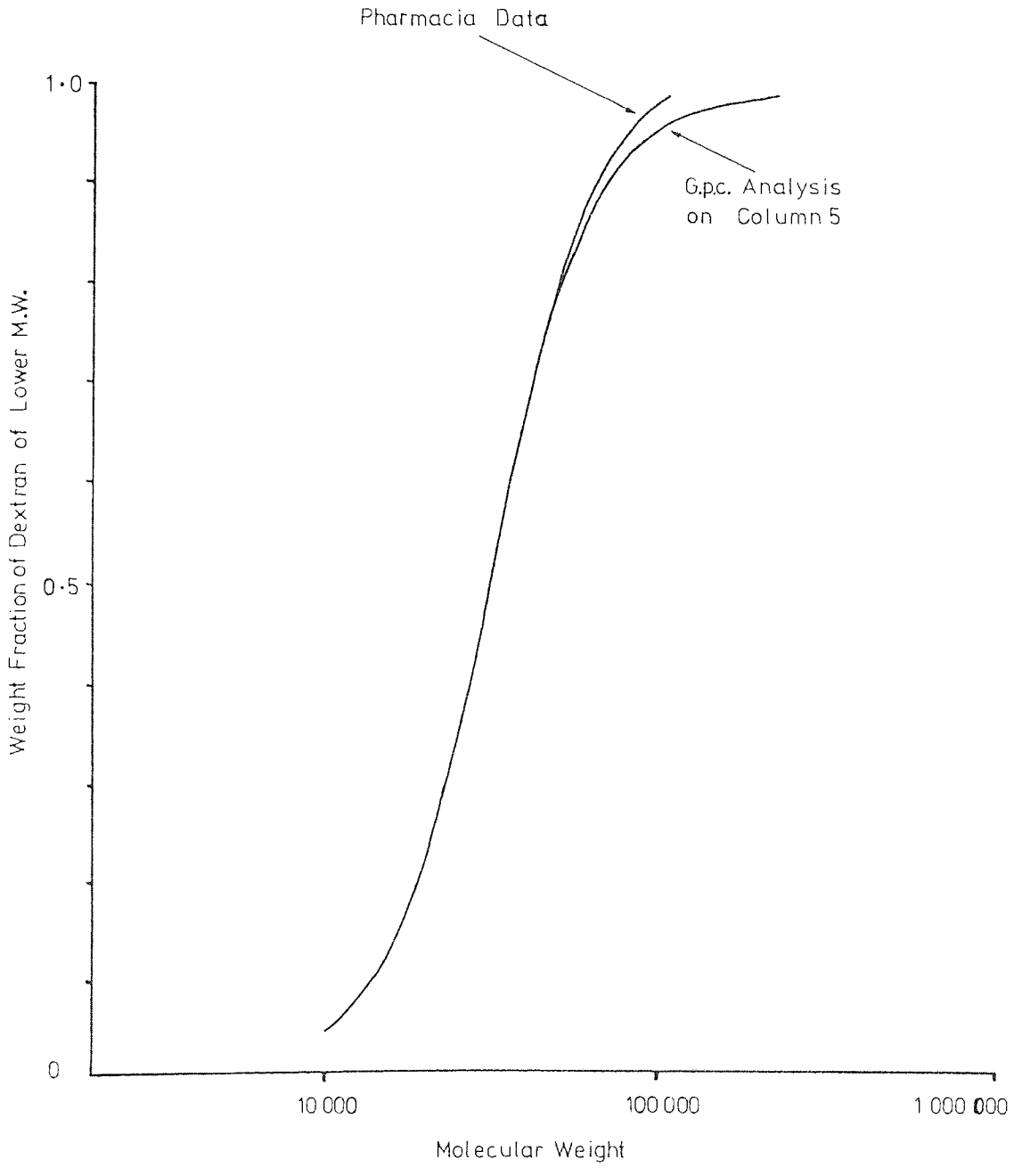

were performed at ~0.2 $cm^3 min^{-1}$ were corrected by displacement of the chromatogram, to the left, by 0.027 R.F. units. FIG. 4.9 (31) compares the cumulative distribution of dextran T-40, supplied by Pharmacia Ltd., with the calculated cumulative distribution based on an analysis of dextran T-40 on column 5 at 0.097 $cm^3 min^{-1}$. The agreement between the two curves is excellent except for the extreme high M.W. end of the distribution. This is probably because T-40 contains material which is of too high M.W. to be properly fractionated using Porasil 'C'. FIG. 4.9 may be regarded as a measure of the degree of accuracy expected with g.p.c. analyses of SCCR3 products, performed during this research.

4.4 EVALUATION OF CONCENTRATION EFFECTS IN G.P.C.

4.4.1 Scope

A complete study of the complex molecular interactions for dextran/water systems in g.p.c. would require a substantial body of theoretical and experimental work. Evidence from the literature, discussed in SECTION 3.4.2, suggests that certain effects of the use of increased polymer concentration may not be disadvantageous and may even produce improved fractionations. A major portion of the continuous dextran fractionations, reported in SECTION 7.4 of this thesis, was carried out with on-column concentrations as high as 20% w/v dextran in parts of the separating section. The scope of the work reported in this section was to demonstrate, on a small scale batch column, the form of concentration dependence of the dextran/water system which had been observed during SCCR3 experimental runs (SECTION 7.4.3). To this end the elution characteristics of a marked dextran 40 fraction were studied, at mobile phase concentrations up to 15% w/v dextran.

4.4.2 Materials and Equipment

Dextran 40 (batch no. BT192), which was the dextran feed for continuous fractionation studies (SECTION 7.4), was used in the mobile phase at concentrations up to 15% w/v, in distilled water containing 0.5% w/v NaCl and 0.02% sodium azide. The marked dextran fraction used was FITC - Dextran 40 (Lot no. 3567), $\overline{M}_w$ = 39,000, $\overline{M}_n$ = 32,000, obtained from Pharmacia Ltd., Uppsala, Sweden, which is a dextran fraction that has been labelled with fluorescein isothiocyanate. The distribution of FITC-Dextran 40 is compared with that of BT192 dextran in FIG. 4.10. This shows that the FITC-Dextran 40 fraction is a slightly lower M.W. fraction then the BT192 dextran, but they may be

Figure 4.10 Comparison of the Elution Positions of FITC-Dextran 40 and Dextran 40 (BT192) on Porasil C

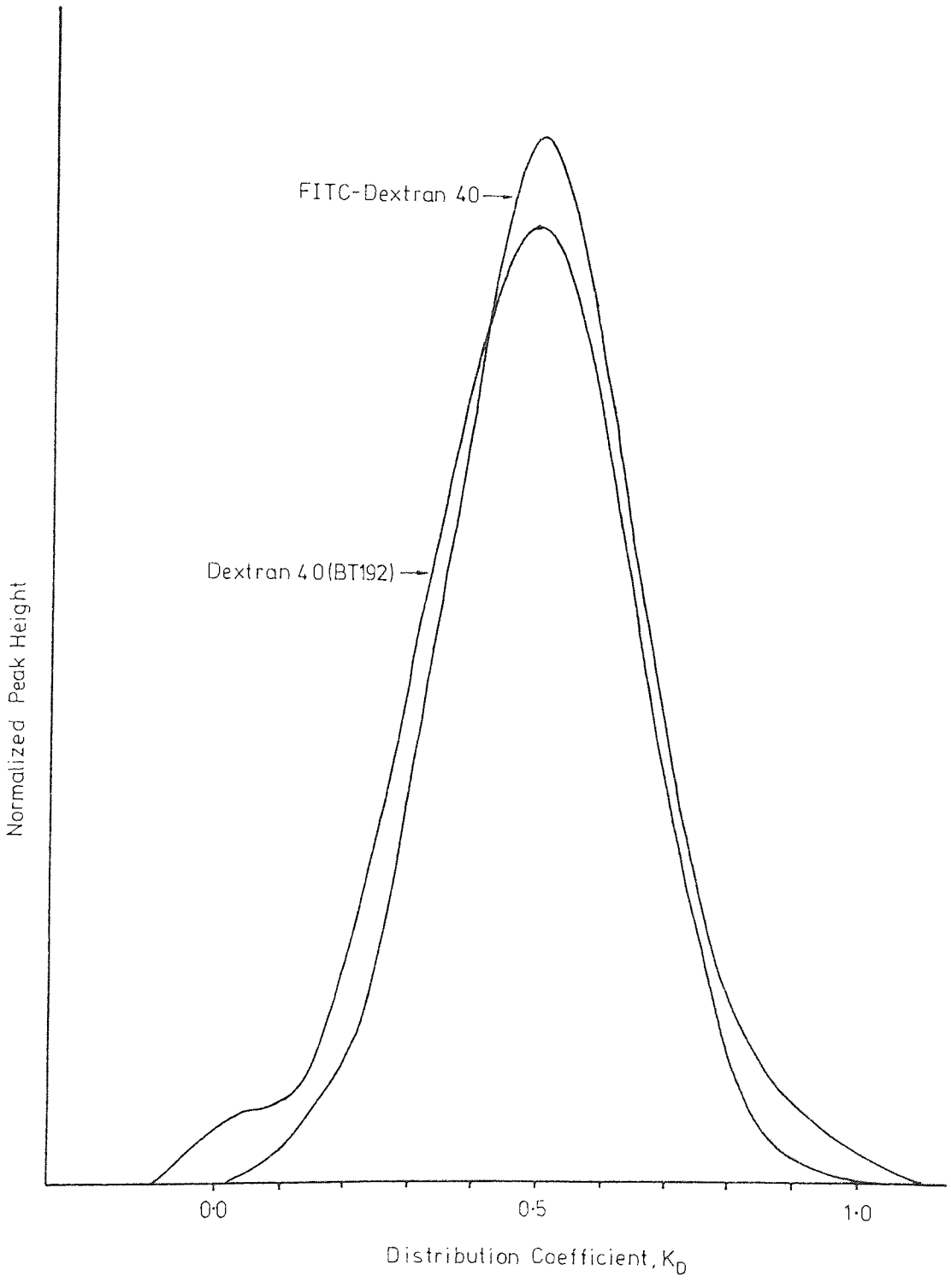

regarded as similar for the purposes of this study. Samples of FITC-Dextran 40 were dissolved to form 2% w/v solutions in distilled water containing 0.5% w/v NaCl, 0.02% sodium azide, and dextran BT192. The amount of BT192 was adjusted to give an overall dextran concentration in the sample equal to the dextran concentration in the mobile phase. The densities of BT192 solutions were calculated from the data given in APPENDIX 2.

Analyses were performed on analytical column 5 (SECTION 4.3.3.2) at a mobile phase flowrate of ~0.1 cm^3 min^{-1}. The detector used was a Pye-Unicam SP1800 Spectrophotometer, incorporating a continuous flow cell, at a monitoring wavelength of 220 nm.

4.4.3 Results

FIG. 4.11 shows the effect of the concentration of NaCl, in a distilled water mobile phase, on the K_D of FITC-Dextran 40.

FIG. 4.12 shows the change of elution characteristics of FITC-Dextran 40 when the concentration of BT192 dextran, in the mobile phase, is increased from 0.0% to 15.0% w/v. All of the chromatograms have been scaled to an equal peak area for purposes of comparison. A summary of the change in the measured K_D of FITC-Dextran 40 with increasing BT192 concentration in the mobile phase is given in graphical form in FIG. 4.13.

To check that fractionation was occurring in the column, the precaution of re-running a fraction collected from each side of the FITC-Dextran 40 peak was taken. This experiment was performed using 7.5% BT192 dextran in the mobile phase, and collecting 5-minute fractions for re-running at 7.5% dextran concentration. Comparison of the re-run fractions with the original sample is given in FIG. 4.14.

Figure 4.11 The Variation of K_D with Mobile Phase NaCl Concentration for FITC-Dextran 40

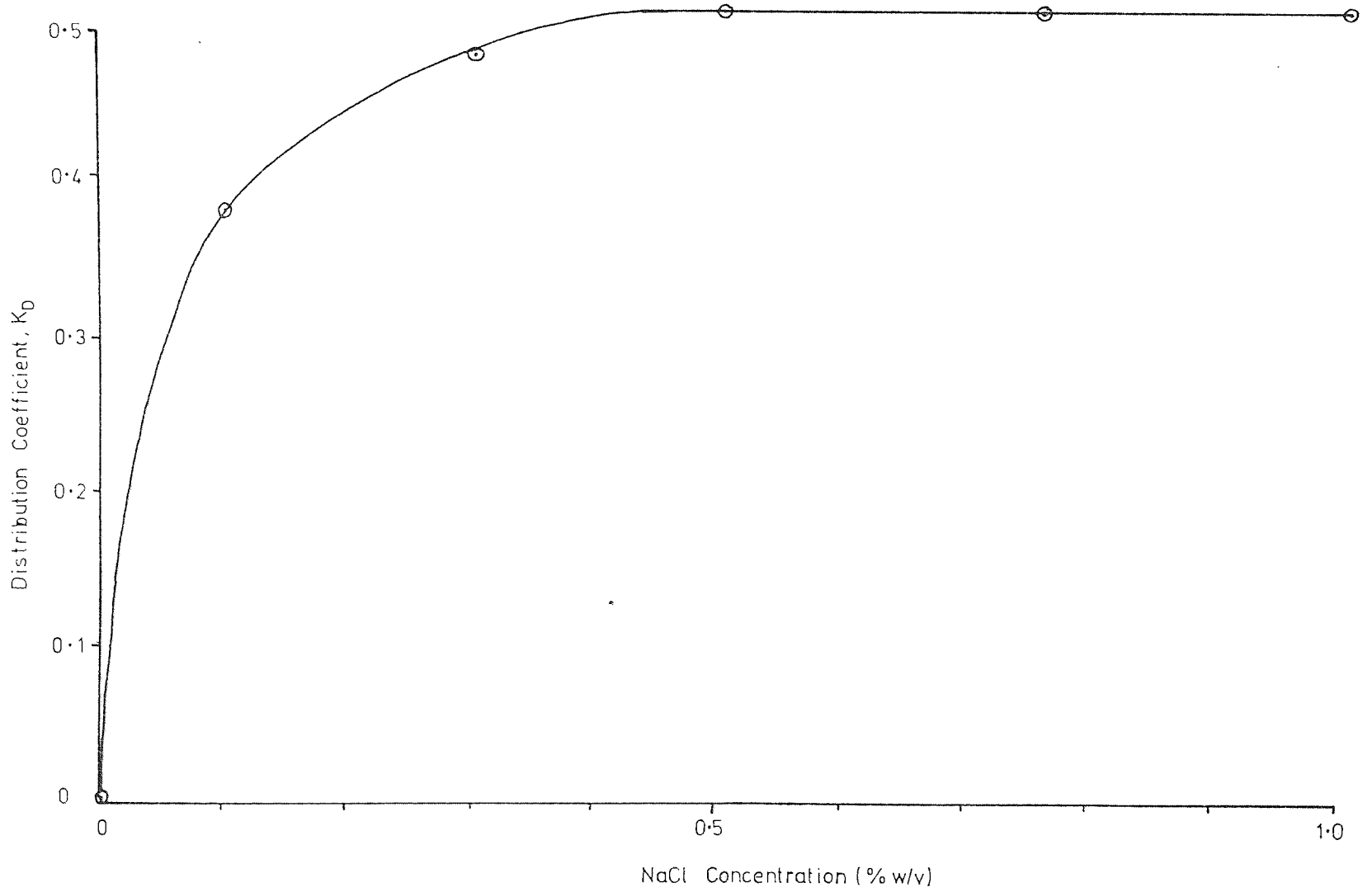

Figure 4.12 The Variation of Elution Position of FITC-Dextran 40 with Mobile Phase Dextran 40 Concentration

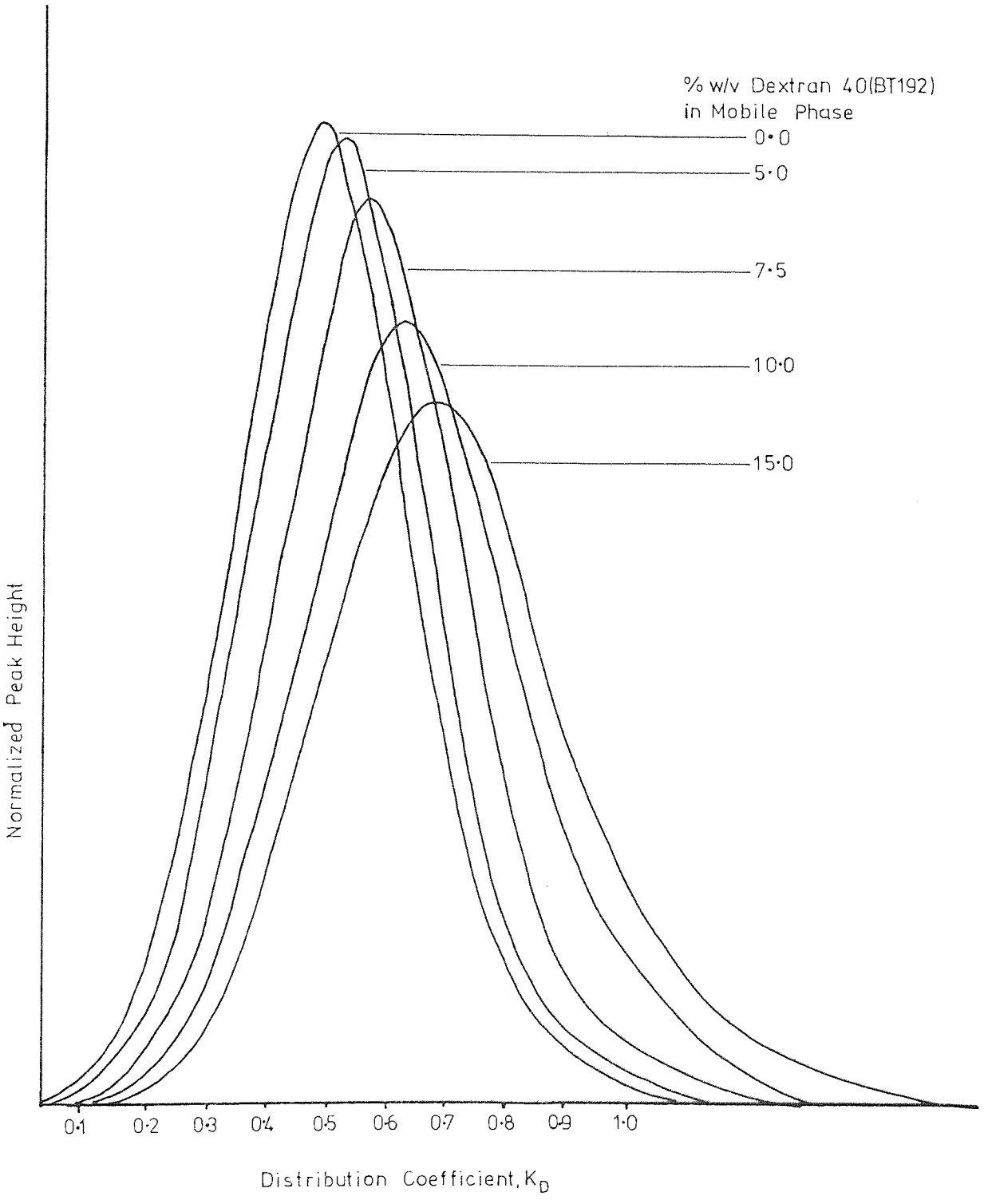

Figure 4.13 The Variation of K_D of FITC-Dextran 40 with Mobile Phase Dextran 40 Concentration

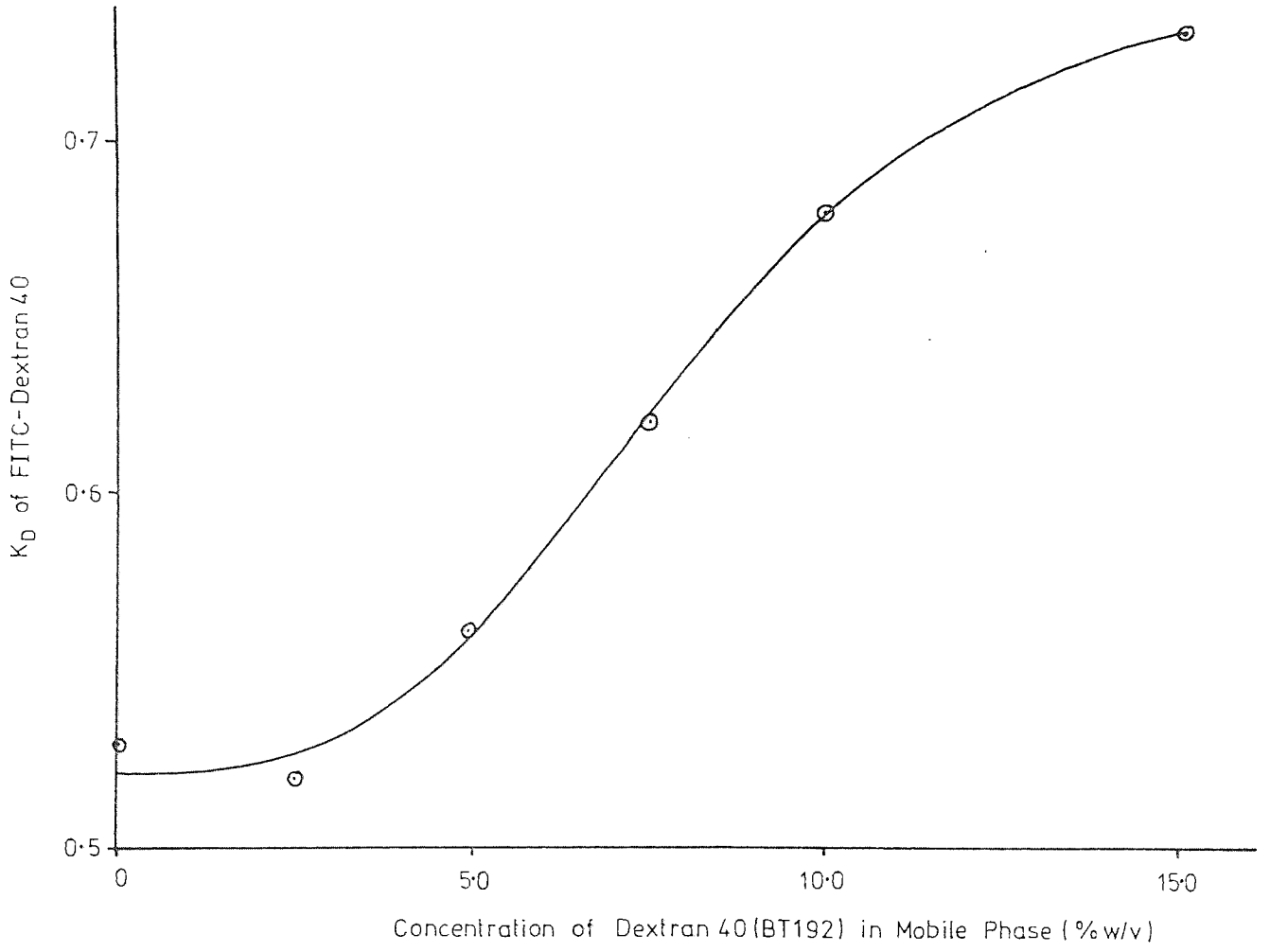

Figure 4.14 Fractionation of FITC-Dextran 40, and Refractionation of Two Portions of the Column Effluent, at a Mobile Phase Dextran 40 Concentration of 7·5% w/v

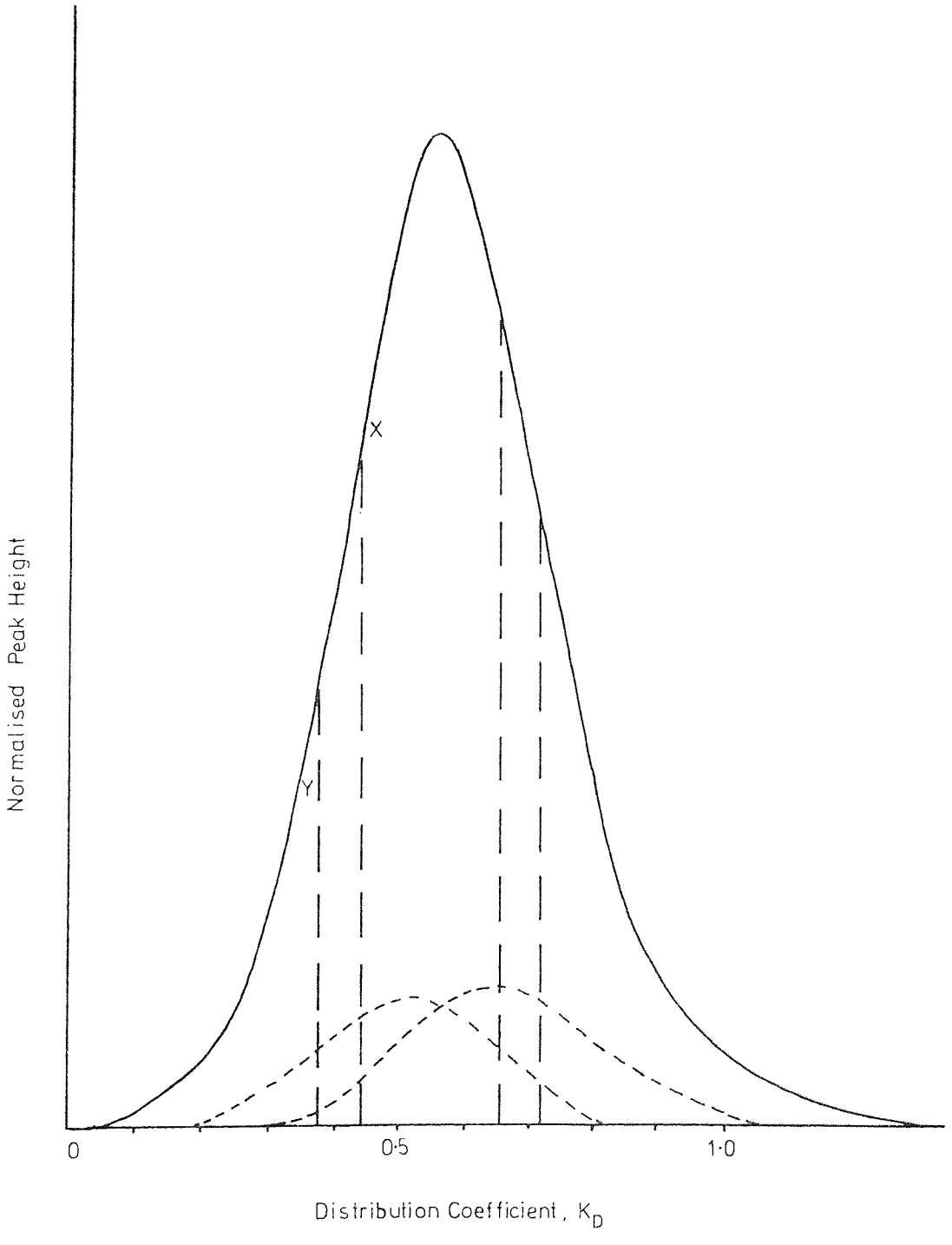

4.4.4 Discussion

FIG. 4.11 demonstrates the necessity of using NaCl in the mobile phase during elution of FITC-Dextran 40 from columns packed with Porasil. If no NaCl is present in the mobile phase, the FITC-Dextran 40 exhibits a K_D value of zero, i.e. it is totally excluded from the pores of the packing. A similar effect was noted when eluting dextran fractions, which had been dyed according to the method of Dudman and Bishop (236), from columns packed with Porasil. The exact method of this exclusion process is uncertain, although a possible explanation is a form of ionic exclusion, whereby ions, present on active sites on the surface of the silica beads, repel dextran molecules which carry ionic groups. This effect may be swamped by an excess of added ions. Holding (235) found that a NaCl concentration greater than 0.6% w/v in the mobile phase was necessary to overcome this effect for elution of dyed dextrans from columns packed with Porasil. Williams (31) found 0.1M Tris Hydroxymethyl aminomethane in the mobile phase overcame this exclusion effect, for elution of dyed proteins from columns packed with Porasil. NaCl was added to the mobile phase in this study, at a concentration of 0.5% w/v, as this was the minimum concentration found necessary to swamp the ionic exclusion effect of Porasil C on FITC-Dextran 40 (FIG. 4.11).

FIG. 4.14 shows that the re-run fractions both appear closer to the peak centre than the positions of their respective collection time intervals on the original peak. This is expected, and occurs even under normal dilute operating conditions (e.g. 23) because a side-fraction of the peak receives, due to zone broadening processes, more material from the higher concentration region near the peak mean (X) than from the lower concentration region near the peak extreme (Y). The re-run fractions appear rather broad, but again it is not clear whether this is

due to increased zone broadening or displacement of molecular position. The re-run experiments show that a separation mechanism, based on molecular size, is still operating in the g.p.c. column under high concentration conditions.

The increase of K_D with increasing polymer concentration in the mobile phase, shown in FIG. 4.13, is accompanied by an increase in the broadening and 'tailing' of the sample peaks (FIG. 4.12), although it is not clear how much of this broadening is due to an actual displacement in the elution position of molecules, and how much is due to increased zone broadening due to departure from a linear distribution isotherm and viscosity effects. The equilibrium distribution coefficient of a solute under concentrated conditions may be written:

$$K_D = \frac{(K_D)_S}{(K_D)_M} \qquad (4.12)$$

$(K_D)_S$ = Fractional pore volume accessible to a solute = $\frac{(Vi_{ACC})_S}{(Vi)_S}$

$(K_D)_M$ = Fractional mobile phase volume accessible to a solute = $(Vi_{ACC})_M/(Vi)_M$

$(Vi_{ACC})_S$ = Volume of stationary phase (pores) accessible to a solute

$(Vi)_S$ = Total volume of stationary phase (pores)

$(Vi_{ACC})_M$ = Volume of mobile phase accessible to a solute

$(Vi)_M$ = Total volume of mobile phase

If a material of molecular weight within the fractionating range of the packing is added to the mobile phase, it would distribute itself between the mobile and stationary phases, and would reduce the fractional volume accessible to molecules of a solute in the mobile phase, $(Vi_{ACC})_M/(Vi)_M$, to a greater degree than the fractional volume accessible to molecules of the solute in the stationary phase, $(Vi_{ACC})_S/(Vi)_S$.

This is because the fractionated material ($0 < K_D < 1$) included in the mobile phase would distribute itself such that, at equilibrium, its concentration in the mobile phase, as a whole, would exceed that in the stationary phase, as a whole,

$$\text{since } K_D = \frac{\text{CONCENTRATION OF SOLUTE IN STATIONARY PHASE}}{\text{CONCENTRATION OF SOLUTE IN MOBILE PHASE}}$$

The net effect is an increase in the K_D of the solute molecule, and the magnitude of the increase would be dependent on the concentration and molecular weight of the material included in the mobile phase. A higher concentration of fractionated material included in the mobile phase would produce a greater increase in K_D for the solute molecule. Also, for a given mobile phase concentration, a fractionated material of higher molecular weight would produce a further increase in the K_D of the solute, because it would reduce the fractional pore volume accessible to the solute, $(K_D)_S$, to a lesser extent than a material of lower molecular weight, as it can penetrate less of the pores. A low molecular weight material for which all of the pore volume is accessible would have no effect on the K_D of a solute molecule. This has been shown experimentally by Hellsing (229).

The increase in K_D observed in the present study is in qualitative agreement with the increase in K_D measured by Hellsing (229) for elution of proteins from Sephadex columns, using Dextran T-fractions at concentrations up to 0.04 g cm^{-3} in the mobile phase. Hellsing's results are summarized in FIG. 3.7(a) in SECTION 3.4.2, and illustrate the effects of the concentration and molecular weight of the material included in the mobile phase, discussed in the previous paragraph. Quantitatively, the increase in K_D for FITC-Dextran 40 on Porasil recorded in the present study was less than the K_D increase recorded by Hellsing

for human serum albumin on Sephadex, for a given mobile phase dextran concentration and molecular weight. However this is expected because FITC-Dextran 40 has a molecular weight ~30,000 while serum albumin has a molecular weight ~70,000.

Summarizing, it has been demonstrated that a dextran fraction (M.W. ~30,000) is eluted later if the concentration of dextran (M.W. ~30,000) in the mobile phase is increased. This is in qualitative agreement with data reported in the literature, and the magnitude of the increase in the elution volume of a dextran solute would be dependent on the concentration and molecular weight of dextran in the mobile phase, and the molecular weight of the dextran solute.

CHAPTER 5

Design and Construction of the Sequential Chromatographic Unit

5.1 INTRODUCTION

5.1.1 Development of SCCR3 Design

The successful scale-up of the continuous Gas-Liquid Chromatographic process by Barker and Deeble (26-30), using experience gained from earlier continuous g.l.c. equipment (9-22), suggested a similar scale-up operation could be undertaken for the continuous Liquid-Liquid Chromatographic process, investigated by Hatt (23), and Barker, Barker, Hatt and Somers (24), on a small scale.

The special features incorporated into the design of the SCCR3 unit were based on experience gained with the earlier machines, and the envisaged experimental programme. These may be summarized:

(i) Use valves operating in a programmed sequence to provide a fixed-bed, moving port system of operation instead of the fixed-port, moving bed system of operation of the CCR1 continuous liquid-liquid chromatograph (23,24). This would remove the necessity for large moving face seals, which previous experience with face seals indicated would be difficult to operate effectively, and mechanical movement of a large series of columns, and had proved successful when incorporated into the design of the SCCR1 continuous Gas-Liquid Chromatograph (26-30).

(ii) Use a separating length of approximately 14 m, compared to the 9 m separating length which had proved satisfactory for small-scale continuous fractionation of carbohydrates (23,24), to allow for any fall off in efficiency with increased column diameter.

(iii) Use materials of construction not only resistant to water and dextran solutions, but also resistant to dilute mineral acids which could be used in future work on the SCCR3 machine.

(iv) Utilize a purging section which is independent of the main mobile phase stream, to purge the slowest moving component(s). This feature had proved successful when used in the SCCR1 model, and introduces an added degree of flexibility.

(v) Base the design on proven reliable components, not exceeding the capital equipment budget of £4,500 supplied by Fisons Ltd. (Pharmaceutical Division) to finance the research programme.

(vi) Design into the machine the greatest degree of flexibility possible within the limits imposed by the envisaged research programme.

5.1.2 Principle of Operation

FIG. 5.1 illustrates operation of the SCCR3 machine for separation of a binary feed mixture. Feed is introduced into the system at port 4 and mobile phase at port 3. Product 1, which has least affinity for the stationary phase, travels with the mobile phase and is eluted at port 1. An independent purge section is provided to strip product 2, which has greater affinity for the stationary phase, and travels with the packing, from the unit. Two valve locks B-B isolate one column from the main mobile phase stream and product 2 is purged from the machine, leaving at port 2, by an independent liquid stream entering at port 5.

The major difference between the principle of operation of the SCCR3 unit and the earlier small-scale CCR1 unit (23,24) lies in the fact that instead of the packed section rotating in a clockwise direction past fixed inlet and outlet ports, (as in the case of the CCR1 machine), the inlet and outlet ports advance in an anti-clockwise direction past fixed columns. This is illustrated if we examine the position after the valve locks and inlet and outlet ports have been advanced one position in a direction co-current to the direction of mobile phase flow. The

Figure 5.1 Illustration of the Operating Principle of the SCCR3 Unit

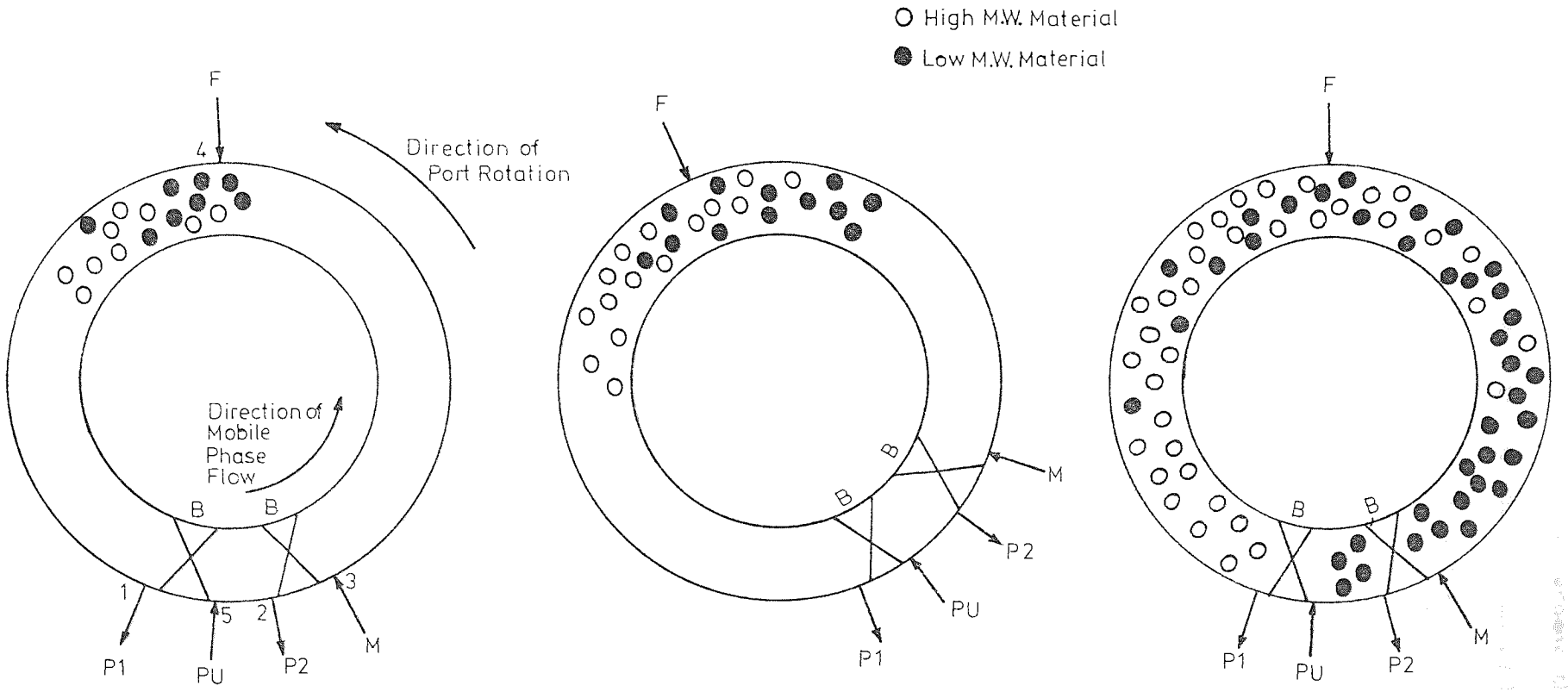

(a) Start-up (b) Start-up +1 Sequencing action (c) Pseudo-Equilibrium Condition

F Feed M Mobile Phase P1 Product 1 P2 Product 2 PU Purge B Transfer Valve Lock

purging section from the previous position now becomes the product 1 outlet section, and all of the ports have been advanced by one column. The final diagram in FIG. 5.1 represents the fully-established operating condition of the unit.

It will be noted that the movement of the purge locks and inlet and outlet ports in a direction co-current to the direction of mobile phase flow produces an 'effective' movement of the packed columns in a direction counter-current to the direction of mobile phase flow. This is the operating principle of the SCCR3 machine, and it should be noted that, in the present form, the machine is capable of producing only two products from any multi-component (or polymer) feed that may be used, in any single operation. Obviously, however, products may be collected and re-run if more than two fractions are required, or the desired product does not lie at one end of a multi-component mixture or polymer distribution.

5.1.3 General Description

An overall view of the SCCR3 unit is shown in photographic form in FIG. 5.2 and schematic form in FIG. 5.3.

The twenty (5.1 cm internal diameter x 70 cm long) glass columns of the central unit are mounted on a metal frame, and connected alternatively at top and bottom to form a closed column loop. Isolation of an individual column is achieved by energizing, to close, two consecutive transfer valves, one transfer valve being situated in each transfer line between each pair of columns.

A solenoid valve is mounted on the feed inlet line to each column, the remaining purge inlet, mobile phase inlet, and products outlet lines being controlled by twenty 4-line solenoid valves (SECTION 5.2.1). Inlet and outlet lines are arranged in a ring main

Figure 5.2

General View of the Sequential Unit

A	Automatic Timing Unit
C	Conduit Containing Electrical Wiring
F	Feed Valve
M	Four-Line Valve
P	Pressure Gauge
PD	Pulsation Dampener
PP1	Pump 1 (Mobile Phase/ Purge)
PP2	Pump 2 (Feed/Mobile Phase)
PRV	Pressure Relief Valve
SP	Septum Sealed Sample Point
T	Transfer Valve

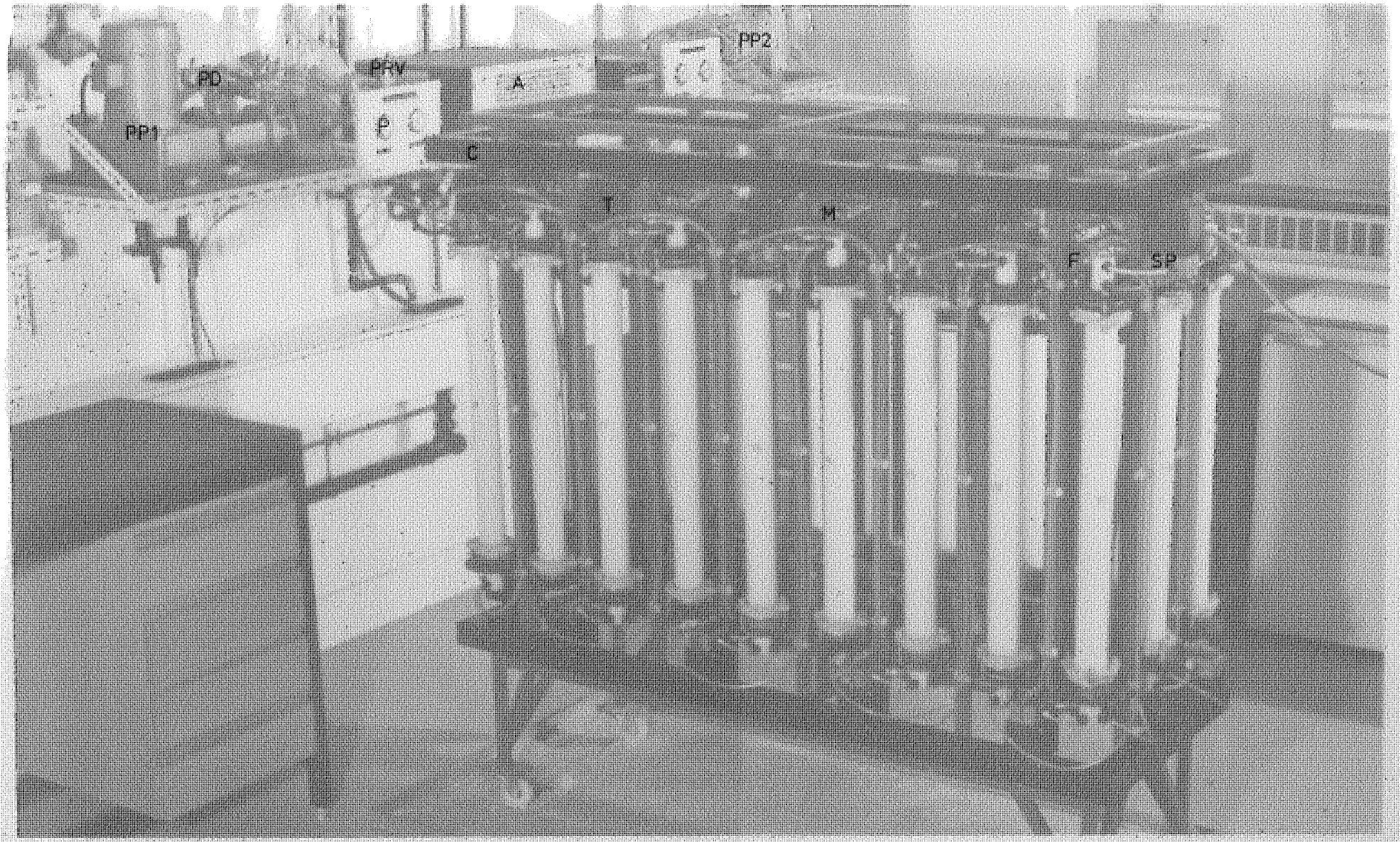
PP2
PD
PRV
A
PP1
P
C
T
M
F
SP

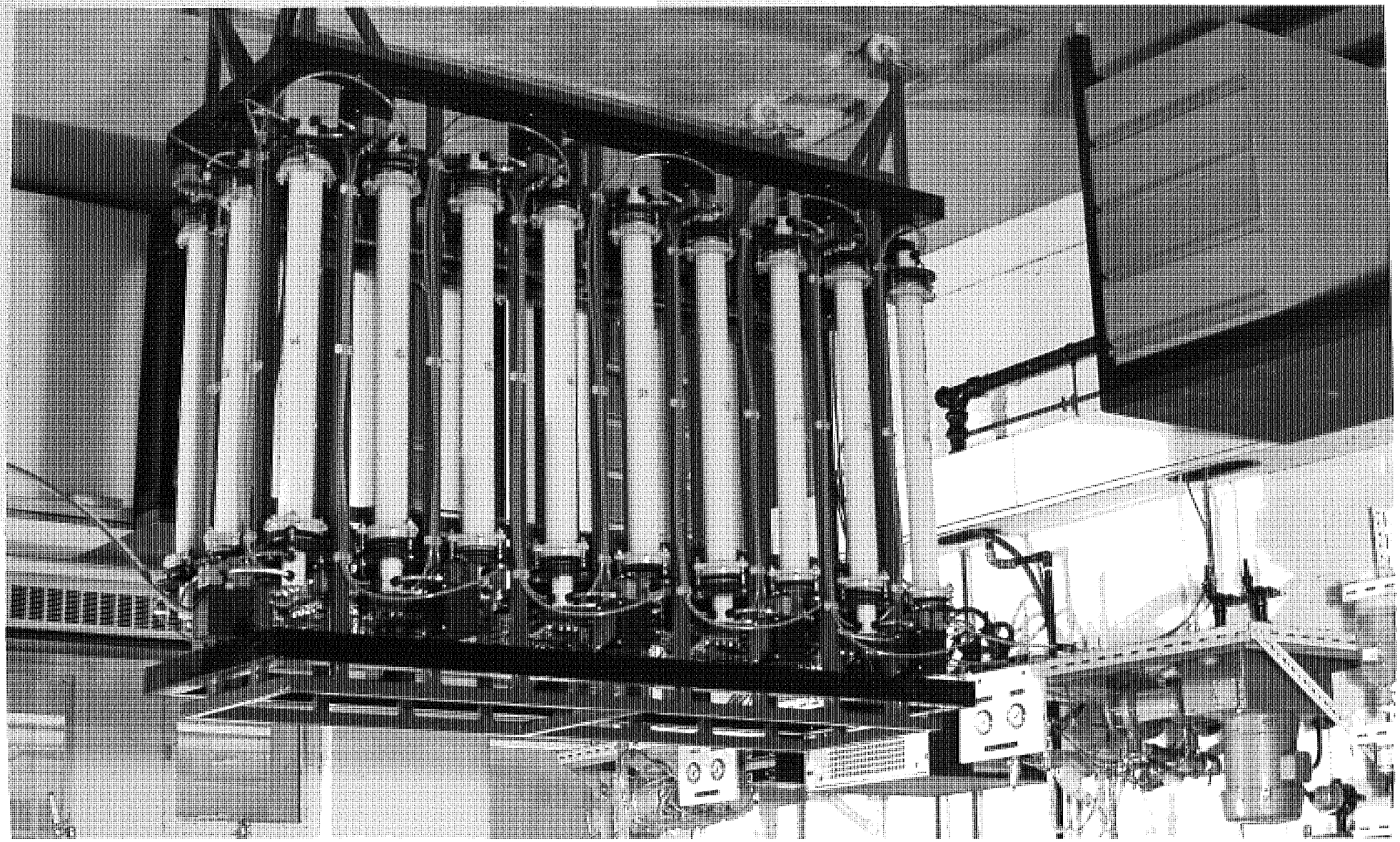

Figure 5.3 Schematic Diagram of the Complete SCCR3 System

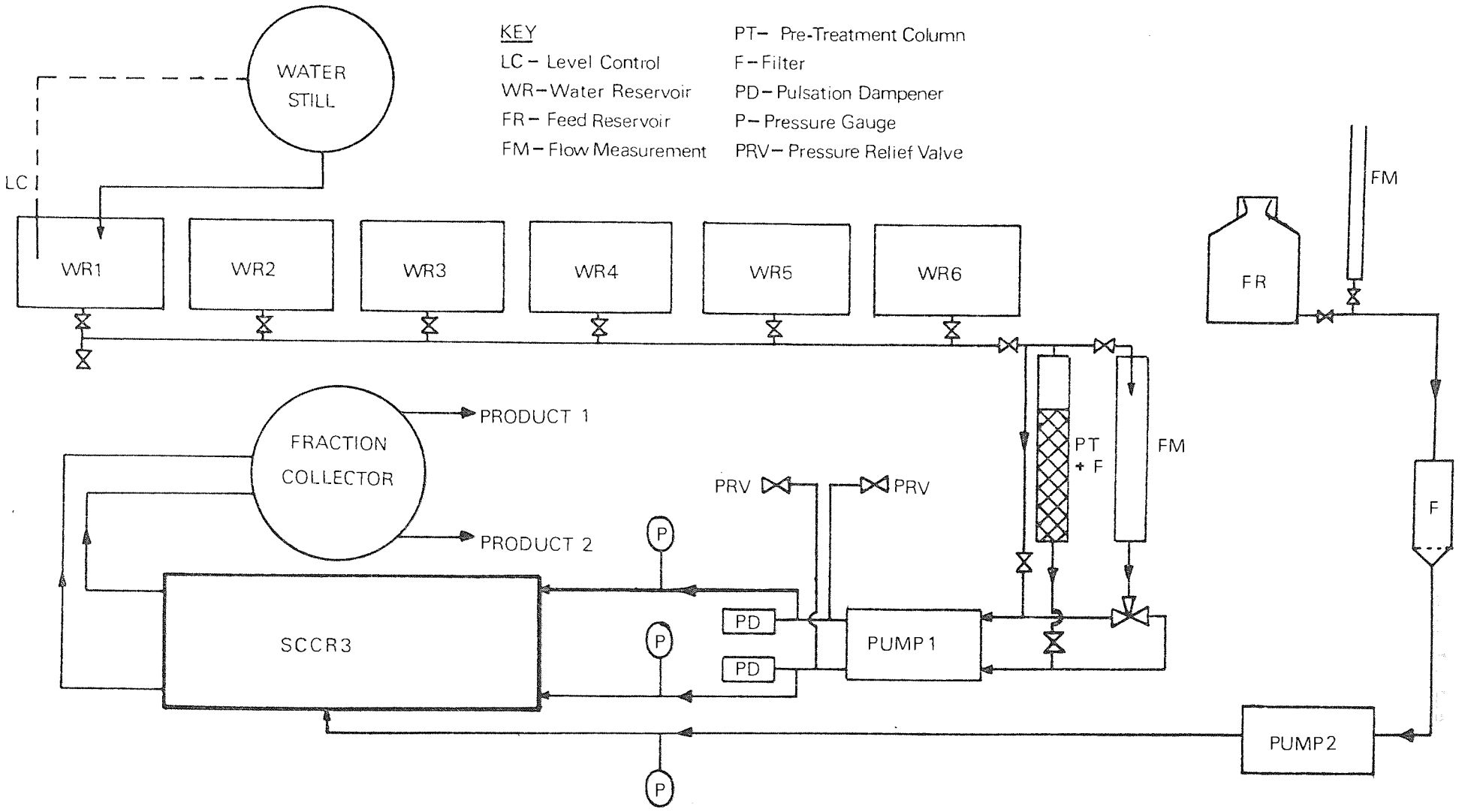

distribution network (SECTION 5.2.3), connected respectively to the metering pumps (SECTION 5.2.4), and product collection device (SECTION 5.3.2) of the system.

The electrically operated solenoid valves are controlled by an automatic timing unit (SECTION 5.2.2), which advances the valves in the required operating sequence at the desired time interval.

The rectangular arrangement of the columns and framework is used to enable future work involving more, or less, than twenty columns to be carried out without complete re-building of the central unit being necessary (as in the case of a circular arrangement with a central distribution system). In fact this facility was used during the research period when the number of columns was reduced from twenty to ten.

Detailed design features of the SCCR3 unit are given in SECTIONS 5.2, 5.3 and 5.4.

5.2 THE FRACTIONATING UNIT

5.2.1 The Valves

5.2.1.1 Introduction

A major part of the preliminary design work for the SCCR3 machine was centred on the development of a novel solenoid valve. In previous SCCR machines, the number of solenoid valves necessary was 6 x number of columns used, in each case 72, and in the case of the SCCR3 machine this would mean 120 conventional valves. The development of a novel solenoid valve for the SCCR3 unit reduced the valves required to 60 and showed a considerable saving in space and capital.

5.2.1.2 Principle of Operation

The valves essentially work on a principle similar to pneumatic 'pinch' valves, wherein the required shut-off is usually obtained by applying pressure to a length of flexible tubing via a diaphragm. The main differences between this type of 'pinch' valve and the SCCR3 valves are that the SCCR3 valves have the following characteristics:

(a) The 'pinching' is done between two lengths of metal rod.

(b) The required force comes via a solenoid.

(c) One valve may close several tubes simultaneously.

(c) is of particular use for the SCCR3 machine, as certain valve operations are required to be carried out simultaneously. This is illustrated in FIG. 5.4, which shows a typical arrangement for one of the SCCR3 valves. If we consider, for example, column 2 being purged, the purge inlet line and low M.W. product outlet line of column 2 are required to be open,

Figure 5.4 Arrangement of SCCR3 Valves and Flow Lines

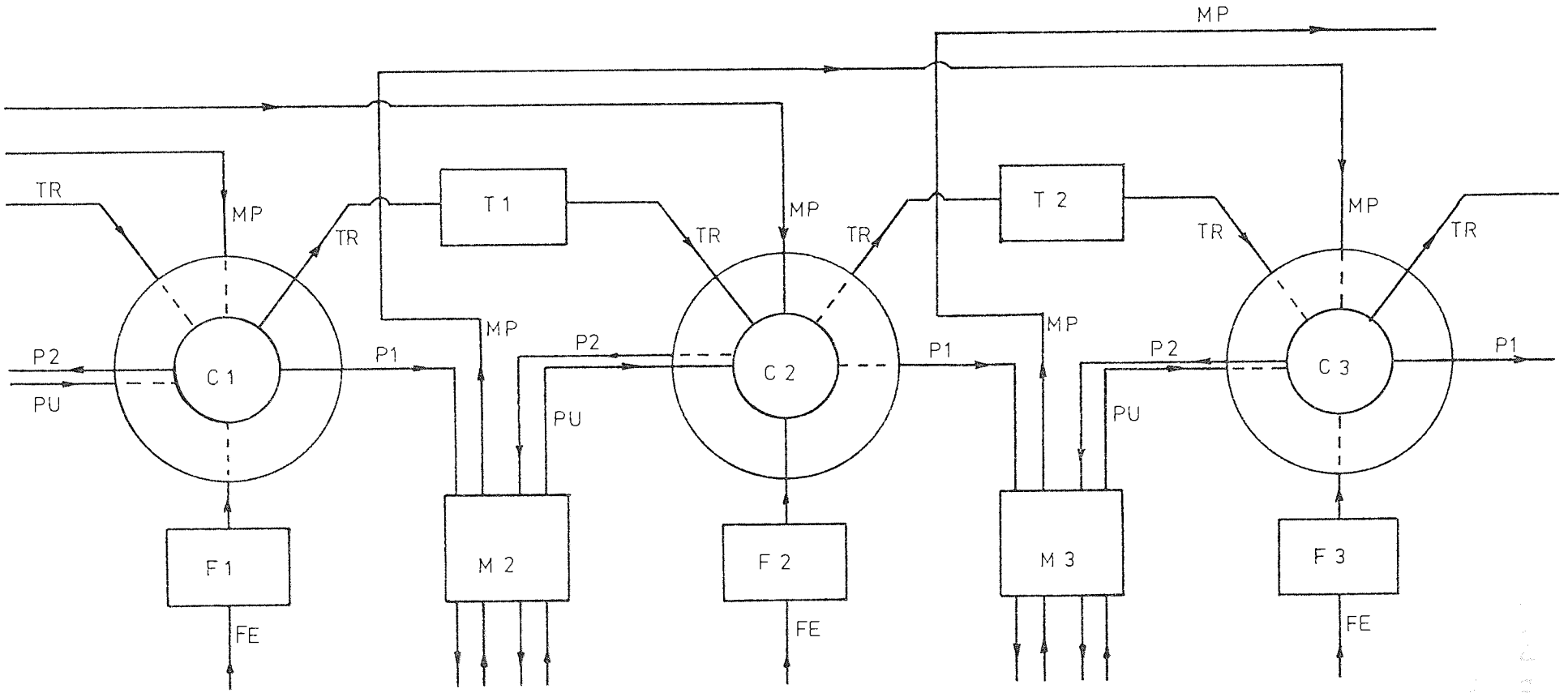

C Column , F Feed Valve , FE Feed Line , M 4-Line Valve , MP Mobile Phase Line , P1 Product 1 Line , P2 Product 2 Line , PU Purge Line , T Transfer Valve , TR Transfer Line .

as is the high M.W. product outlet line from column 1, and the mobile phase inlet to column 3. As these four lines are always required to be either all open, as in the previous example of purging column 2, or all closed, for every other position in the cycle, they are bought together and pass through one SCCR3 valve (No.M2).

This one example is repeated throughout the SCCR3 machine, e.g. valve No.M3 would contain the Purge inlet and low M.W. product outlet lines from column 3, the high M.W. outlet line from column 2 and the mobile phase inlet to column 4. Thus 80 valve functions are performed by 20 4-port SCCR3 valves.

It would be theoretically feasible to include the feed lines in these valves, as the feed is introduced into the machine a fixed number of columns ahead of, say, the purge inlet. However, because the feed inlet position is, in most cases, a large distance from the position of the other four operations, any combination of the feed line into these valves would result in a large 'dead' volume in the feed lines, and would also fix the feed inlet position to the SCCR3 machine.

Thus, as it is desirable to keep the 'dead' volume of any chromatographic unit to a minimum, and fixing the feed inlet position would restrict the flexibility of the machine, the feed inlet lines are opened and closed independently, as are the transfer lines.

The valves used for the feed and transfer operations are single-line solenoid-operated 'pinch' valves, similar in principle to the 4-line versions. 40 such valves are required for the SCCR3 machine, making a total of 60 valves.

5.2.1.3 Preliminary Design and Testing

The design requirements of the SCCR3 valves were as follows:-

(i) Capable of withstanding an internal pressure of 620 kN m^{-2} (75 p.s.i.g.), which was the maximum safe operating pressure of the SCCR3 glass columns.

(ii) To seal against a pressure differential across the valve of 620 kN m^{-2} (maximum pressure differential inherent in SCCR3 machine) over long periods of time.

(iii) All materials in contact with the working fluid to be resistant to dilute hydrochloric acid, to allow the use of HCl as a hydrolysis agent if the SCCR3 unit is ever used as a reactor/separator (23) for dextrans.

(iv) Easy and cheap to construct from materials commercially available.

The first stage in the design procedure was to find a type of tubing that would be resistant to acid attack, withstand high internal pressures, and at the same time be 'soft' enough to be easily pinched. FIG. 5.5 shows the results obtained for the pressure testing of a number of commercial tubing types, and it can be seen that PVC tubing is by far the most resistant to expansion under pressure. As purple-white AutoAnalyser tubing, manufactured by Technicon Instruments Co. Ltd., Basingstoke, had the most convenient dimensions for the SCCR3 machine it was decided to base the valve design on this.

The force required to close a length of this tubing at an internal pressure of 620 kN m^{-2} was calculated based on the assumption that the fluid pressure within the tube acts over an area of $\pi \times D \times d$ where D = diameter of tubing and d = length of cut-off bar circumference over which the seal is affected. For tubing of 0.32 cm diameter, four tubes, and assuming $d \simeq 0.32$ cm, the required force, F, is given by:-

$$\pi \times 0.32 \times 10^{-2} \times 0.32 \times 10^{-2} \times 4 \times 620 = 0.08 \text{ kN}$$

Figure 5.5 Comparison of Tubing Materials for SCCR3 Valves

Material	Dimensions		Test Pressure (kNm^{-2})	Results	Comments
	I.D.(cm)	O.D.(cm)			
Silicone Rubber	0·1	0·5	600	Tubing expanded to twice normal size	Expansion too large at 600 kNm^{-2}
"	0·2	0·4	250	Tubing expanded excessively	"
"	0·25	0·45	"	"	"
"	0·4	0·6	"	"	"
"	0·3	0·7	"	"	"
Butyl Rubber	"	"	"	"	"
Neoprene Rubber	"	"	"	"	"
Natural Rubber	0·25	0·4	"	"	"
P.T.F.E.	0·35	0·5	600	No expansion	Reliable seal could not be obtained when used in valve
P.V.C. (Tygon)	0·15	0·35	1000	Very little expansion	Suitable for use with valve
P.V.C. (Technicon P/O)	0·25	0·45	"	Tubing expanded to 0·6cm o.d.	"
P.V.C. (Technicon P/W)	0·28	0·48	"	Tubing expanded to 0·7cm o.d.	"

Thus a solenoid producing a holding force of 0.30 kN was thought to give a suitable safety margin, as it is usual to over-design solenoids.

An a.c. solenoid was chosen for economic reasons although it is appreciated that d.c. solenoids are generally smaller and quieter in operation. Consequently an E14 240v a.c. solenoid manufactured by Oliver Pell Control Ltd., Crayford, was used for initial studies. This produced a holding force of approximately 0.3 kN and had force-distance characteristics as shown in FIG. 5.6. Initial studies were based on the 4-line valve because of its greater complexity. Testing of solenoid valve designs was carried out under simulated SCCR3 conditions using the equipment illustrated in FIG. 5.7.

The test pressure, usually 620 kN m^{-2}, was maintained by means of an adjustable pressure relief valve, supplied by Clockhouse Engineering and Instrument Co., New Barnet. Water was metered using a Series II Micro-pump, supplied by Metering Pumps Ltd., London, at a flowrate of approximately 50 cm^3 min^{-1} the water being recycled to the inlet reservoir.

Valve switching was performed using a 240 volt/2 contact programmable drum timer, supplied by Electroplan Ltd., Royston, with a cycle time of one hour. The usual operating mode was to perform one ON→OFF→ON, or OFF→ON→OFF, operation over a five-minute period, and retain the valve either on, or off, without a further switch for the remaining 55 minutes.

When the valve was switched to the non-energized, or open, position, a solenoid-operated two-way pneumatic valve, supplied by Schrader Industrial Fluid Power Products, Cannock, was also switched, by the timer, to its closed position, to maintain the test pressure. When the valve under test was switched to its energized, or closed, position, the two-way pneumatic valve would switch to its open position

Figure 5.6 Power Curves for SCCR3 Solenoids

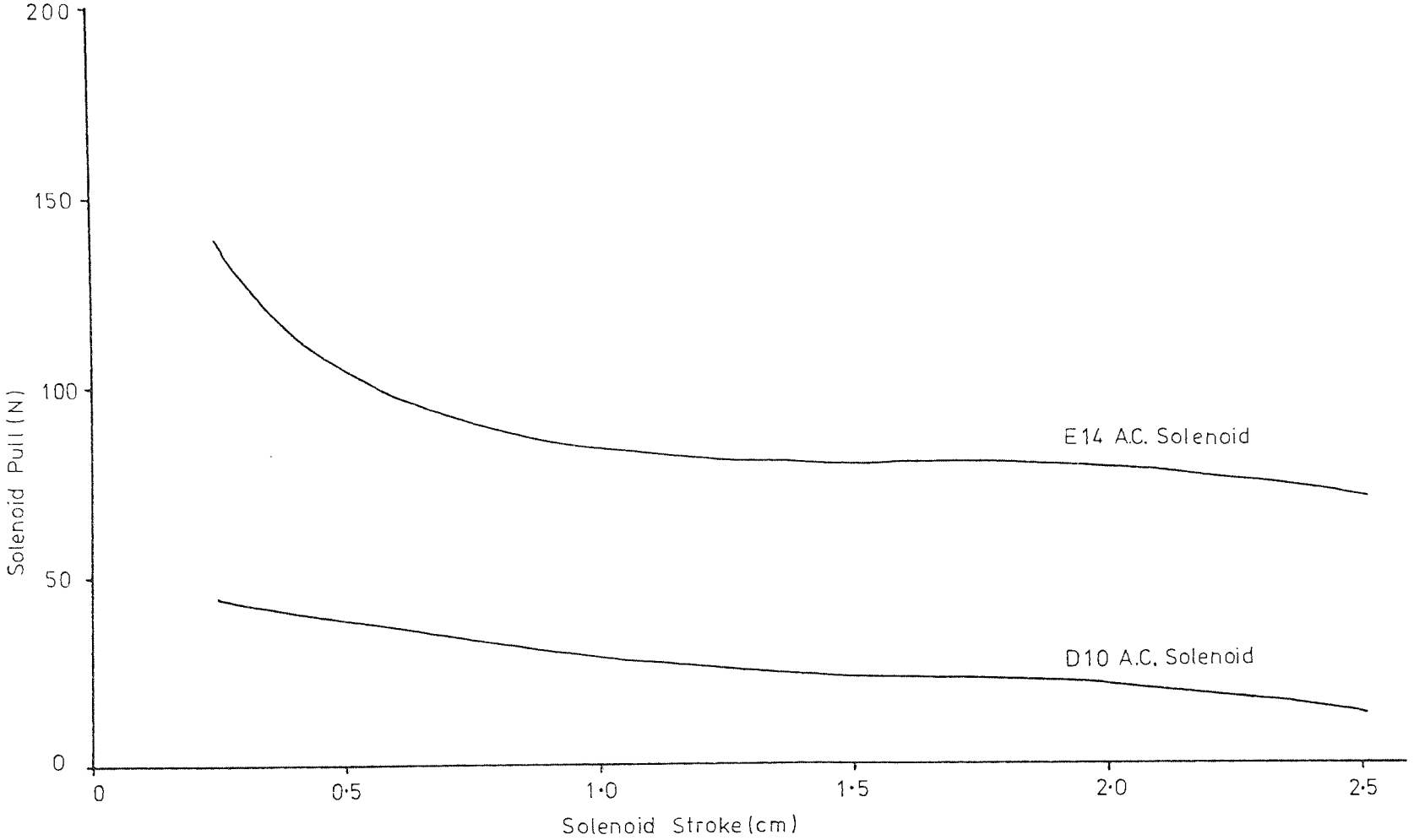

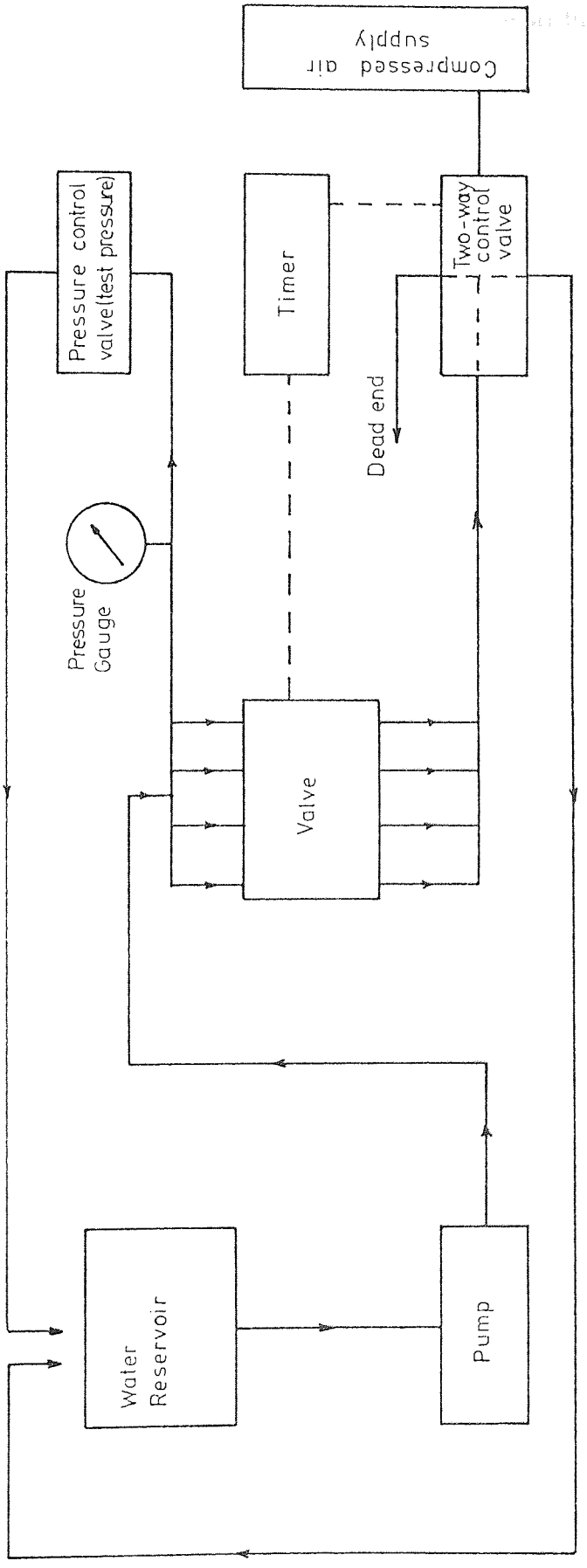

Figure 5.7 Apparatus for Testing Solenoid Valves

to allow passage of any fluid leaking through the test valve.

The test conditions employed were more arduous than the expected operating conditions of the SCCR3 machine. For example, although the valve was maintained at 620 kN m^{-2} continuously when under test, the normal operating pressure of the SCCR3 unit would be lower than this figure, and also the frequency of valve operation would be reduced under actual operating conditions. Therefore, simulation of many hours of actual operation could be performed in a much shorter test time when arduous test conditions were used. The initial valve design is shown in simplified form in FIG. 5.8. During testing at 620 kN m^{-2} the following faults became apparent, and modifications were made as indicated:-

(i) The solenoid rod was inherently weak at the point where the diameter changed, and consequent fracture occurred. It was replaced with a 0.64 cm diameter rod of constant diameter, which was also shorter, so that it could be retained inside the box and thereby give a more compact assembly. The connecting bolts between the solenoid rod and cut-off bar assembly were now passed through the roof of the solenoid box.

(ii) A reliable seal was not easy to achieve without damaging the valve tubes. This was because it was difficult to maintain the cut-off bar edge, and solenoid box, parallel to each other, and this sometimes resulted in overtightening of the cut-off assembly, and consequent cutting of the valve tubing.

It was found that the top of the solenoid box was not of sufficient 'flatness' over its whole length, and therefore a 2.5 cm wide x 10.2 cm long x 0.64 cm thick mild steel strip was welded to the top of the box to provide a flatter surface.

Figure 5.8 Initial Solenoid Valve Design

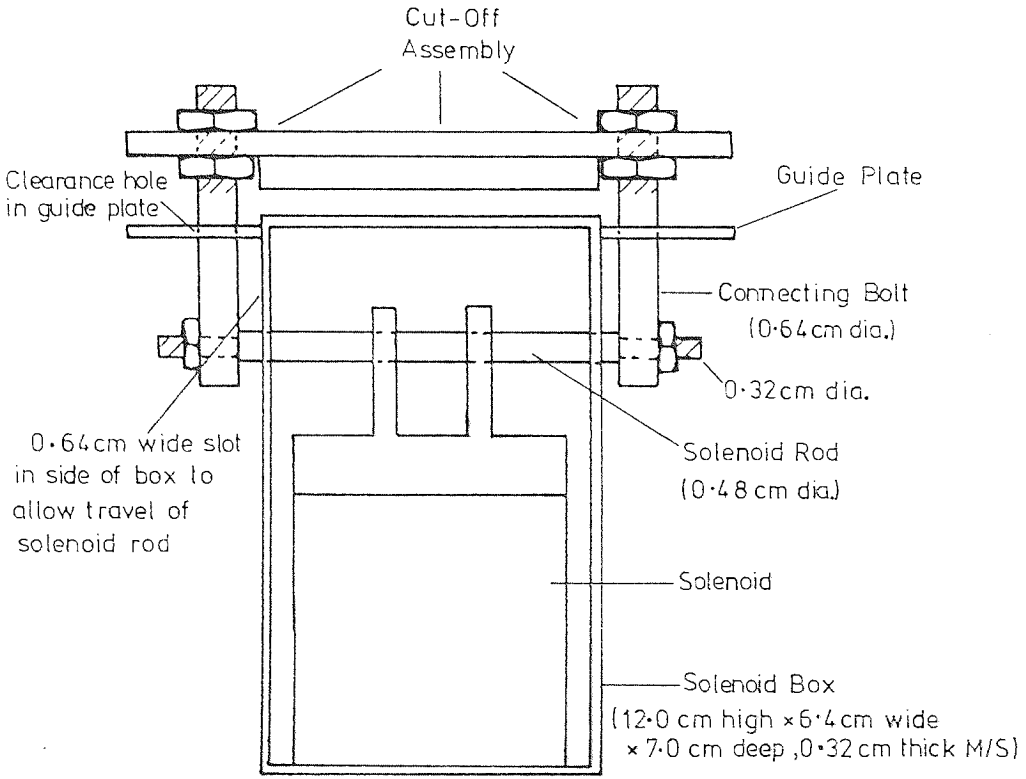

General Assembly

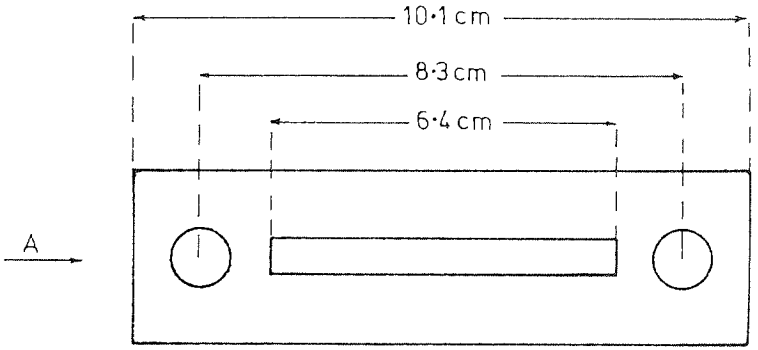

Cut-Off Bar

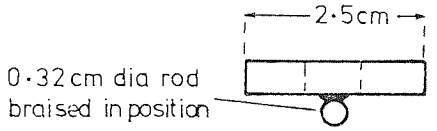

View in direction A

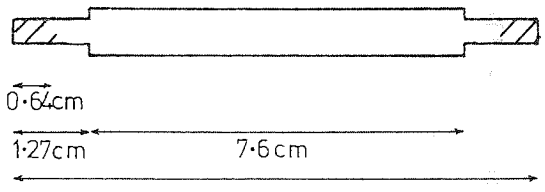

Solenoid Rod

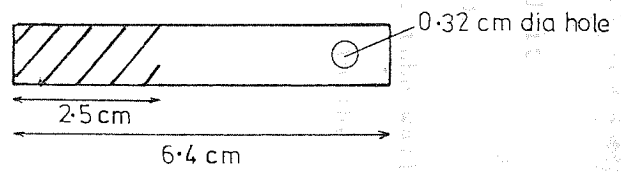

Connecting Bolt

However, although this provided a more reliable seal it was apparent that a true 'pinch' effect was not being obtained. Because one of the surfaces used for the cut-off was flat, one tube wall was being stretched excessively, in the direction of the arrows in the diagram which follows, while the other remained flat. The diagram also

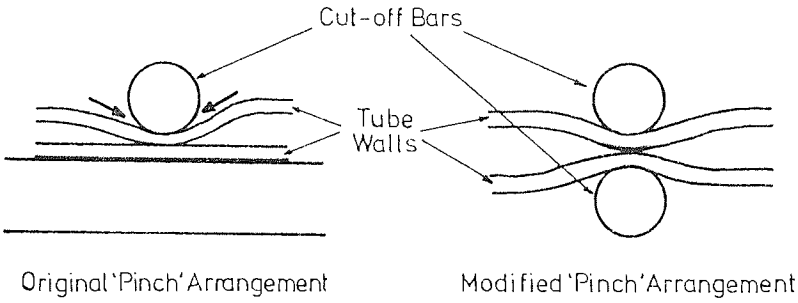

shows how the arrangement was modified to give a better 'pinch', each tube being stretched to a lesser degree, which had the effect of prolonging tube life.

In practice two 0.32 cm diameter parallel rods were found to give the most reliable seal with the least damage to the tubing.

(iii) The PVC valve tubing expanded with time until bursting occurred, usually after approximately 40 hours of continuous operation. Electrical sleeving was placed around the tubes over their entire length to attempt to overcome this problem, but with this arrangement it was found to be impossible to obtain a reliable seal.

The next stage was thus to restrict the sleeving to that part of the tubing not involved in the 'pinch' procedure, i.e. about 1 cm of each tube length, was not sleeved. A good seal was effected

here but tube life only increased marginally as tubes still expanded in the uncovered portions.

The final stage was to incorporate a tube holder into the design to limit the uncovered portion of the tubing to the minimum length possible, which in practice was found to be 0.48 cm. This restricted tube expansion to a minimum, and resulted in a considerable increase in the time that the tubes lasted.

These faults occurred, and modifications were effected, over a period of approximately 1500 hours of valve testing under simulated SCCR3 operating conditions, resulting in the final design given in SECTION 5.2.1.4.

5.2.1.4 Final Design and Commissioning

5.2.1.4.1 The Four-Line Valve

This valve is illustrated in FIG. 5.9 and the details of construction are shown in FIG. 5.10. Essentially, the 'pinch' is achieved between the cut-off bars, and sections of rod in the bottom of the slot in the tube holder. The cut off bars are made from bright steel rod, because this type of rod has a good surface finish, and the remainder of the cut-off assembly is normal mild steel.

The motion required for the 'pinch' is obtained by a 240 volt E14 a.c. solenoid, supplied by Oliver Pell Ltd., Crayford, which, when energized, pulls the cut-off assembly, via the mild steel connecting bolt and solenoid bar, towards the lengths of rod fixed in the bottom of the slot in the tube holder. This continues until the solenoid reaches the end of its travel, i.e. when the solenoid is closed and exerting a maximum holding force of 0.3 kN. Adjustment of the distance between the cut-off bar and rod sections, in the tube holder slot, is carried out by means of the adjusting bolts, which also allow

Figure 5.9

SCCR 3 Solenoid Valves

A	Adjusting Bolt
CA	Cut-Off Assembly
CB	Connecting Bolt
S	Solenoid
SB	Solenoid Bar
SX	Solenoid Box
T	Tube Holes
TH	Tube Holder

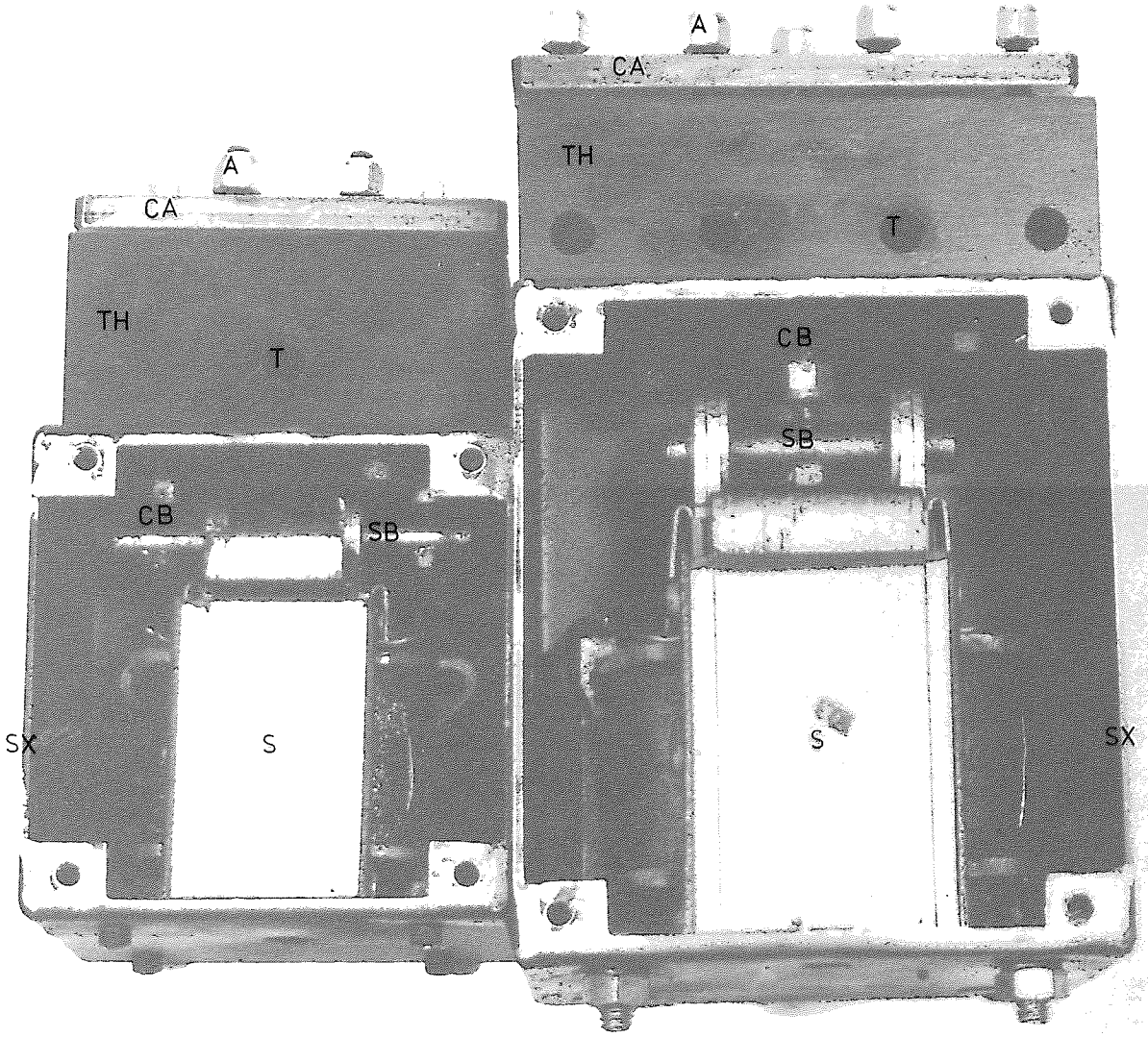
A
CA
TH
T
CB
SB
S
SX
A
CA
TH
T
CB
SB
S
SX

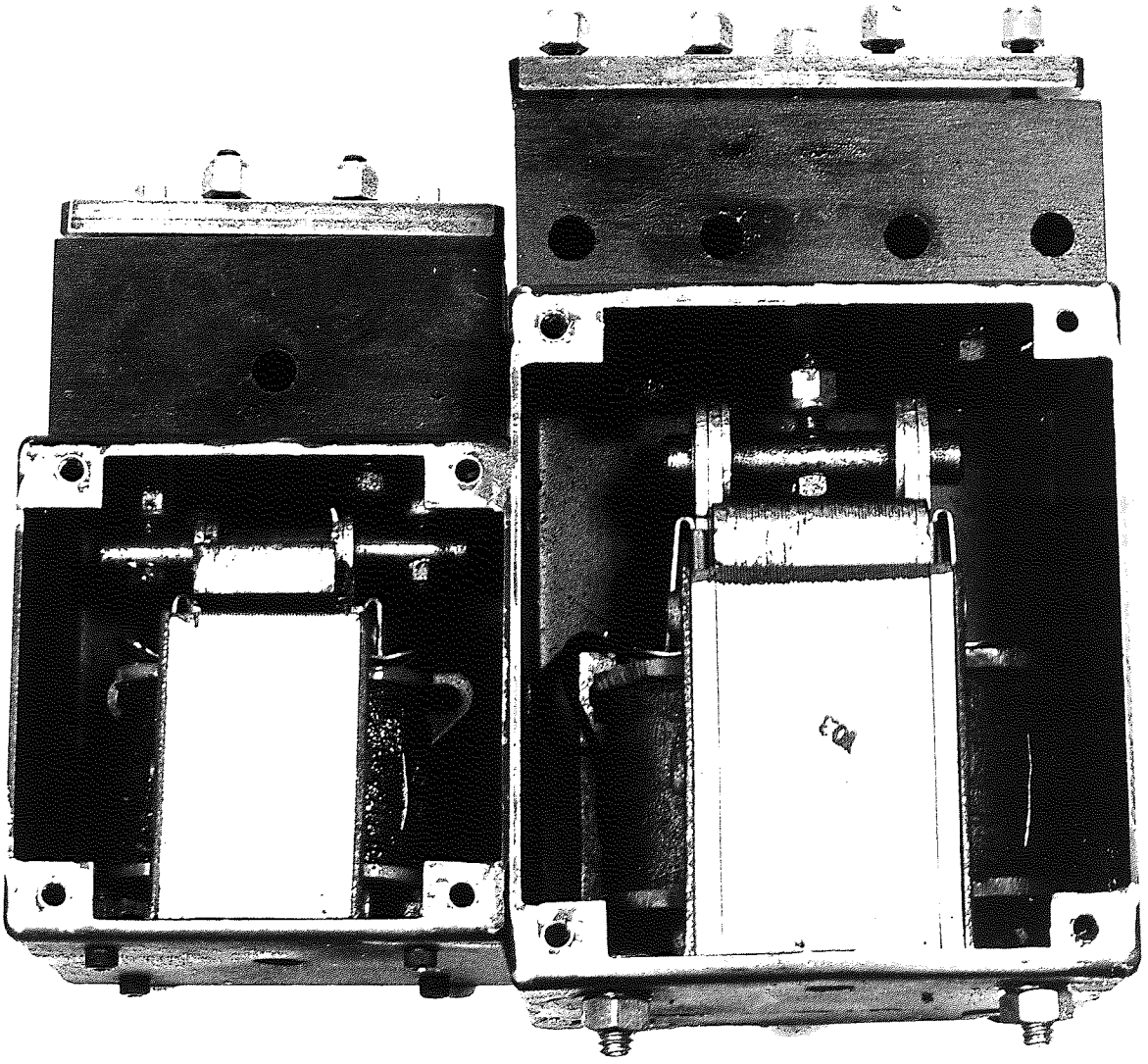

Figure 5.10 Details of SCCR3 Four-Line Valves

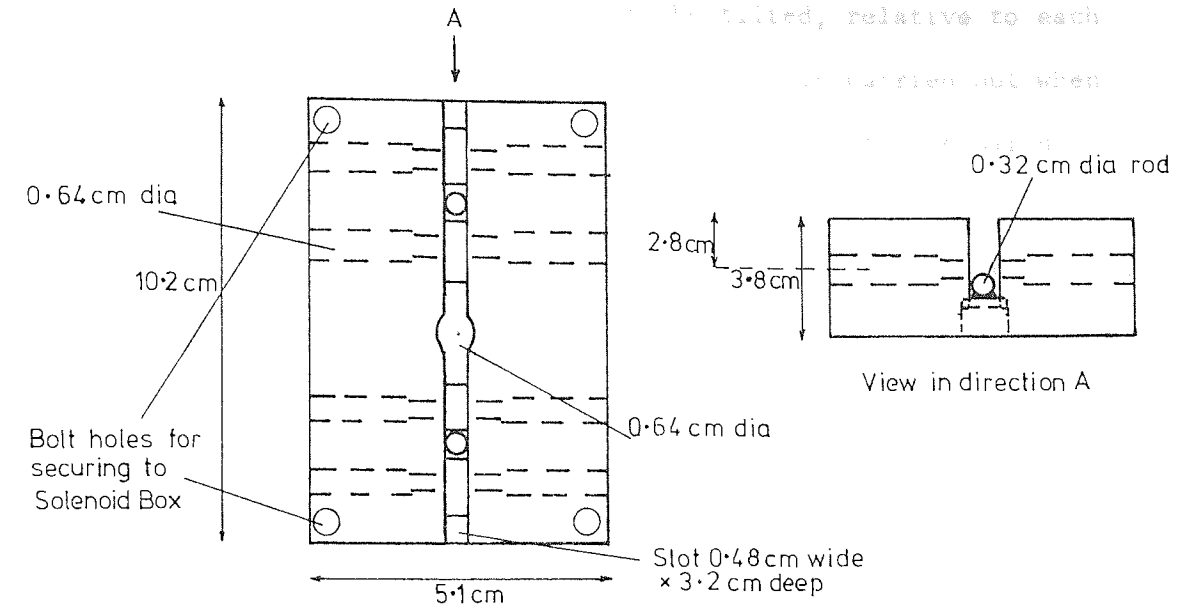

Tube Holder

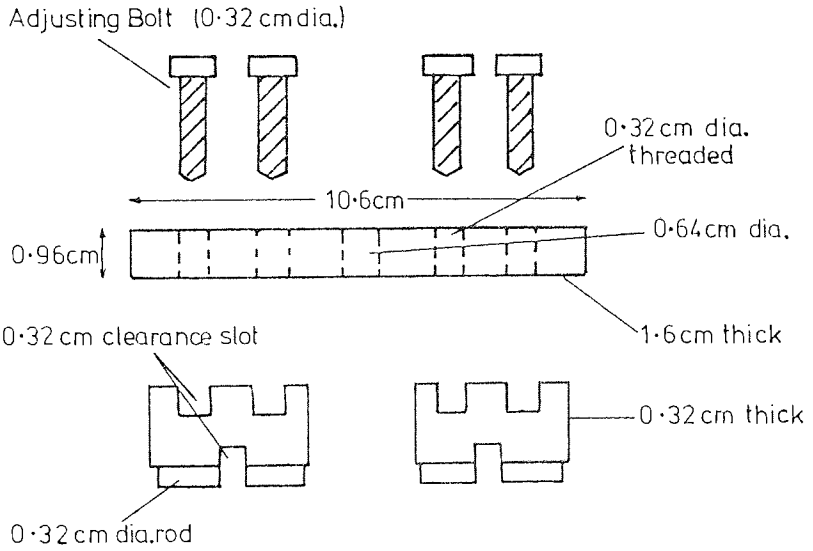

Cut-Off Assembly

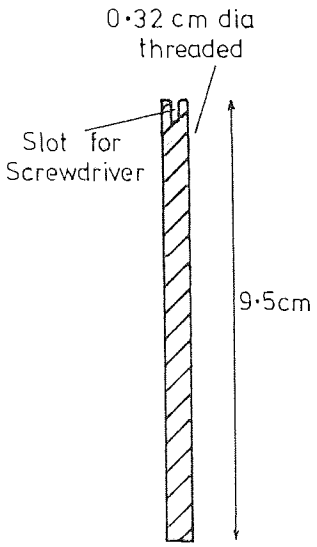

Connecting Bolt

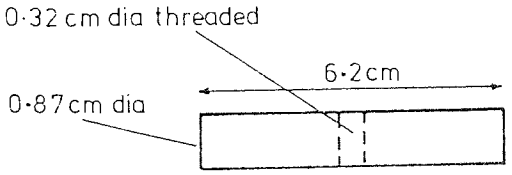

Solenoid Bar

the two bars which produce the cut-off to be tilted, relative to each other, until they are parallel. This adjustment is carried out when the solenoid is energized until a seal is obtained at the required pressure.

The tube holder is machined from Tufnal, chosen because it is tough and yet easy to machine, and bolted to the top of the solenoid box. The tube holder consists of a block of Tufnal 10.2 cm long x 5.1 cm wide x 3.8 cm deep, with a 0.48 cm wide x 3.2 cm deep slot along its length. A 0.64 cm diameter clearance hole, passing through the centre, allows passage of the bolt connecting the solenoid bar and cut-off mechanism, which passes through a hole in the top of the solenoid box.

In the bottom of the slot, which is machined flat, are four lengths of bright steel rod, each 0.32 cm diameter and fixed in place with Araldite adhesive. These match the cut-off bars of the cut-off assembly, and are arranged two on each side of the central hole in the tube holder. One end of a return spring, for each pair of these rod lengths, fits in a 0.32 cm deep hole between the rods, and the other end fits in a slot in the cut-off assembly. These springs ensure that the cut-off assembly is lifted when the solenoid is not energized, which in turn ensures that the flow of liquid through the valve tubes is not restricted. The amount of travel of the cut-off assembly is controlled by the locking nuts on the adjusting bolts, which are adjusted until the valve tubes are open sufficiently to allow normal passage of liquid. Restricting the travel of the assembly to a minimum, in this manner, was found to be important in restricting tube expansion when under pressure, and hence prolonging tube-life.

Four holes pass through the tube-holder, at 90° to the direction of the slot, to hold the PVC valve tubes. The top of the rod lengths in the tube holder slot are 0.24 cm above the bottom of these holes to ensure

that the desired 'pinch' effect, discussed in SECTION 5.2.1.3, is obtained. The holes decrease in diameter, near the centre of the tube holder, to allow passage of the PVC valve tubes, while retaining each length of PVC electrical sleeving in the section of the hole away from the cut-off area, so that they do not interfere with the seal.

The cut-off assembly, especially the cut-off bars and the exterior of the valve tubes, were thoroughly coated with silicone grease before assembly, as this was found to prolong tube 'life' during the test period.

Commissioning of one valve of this type was carried out at 620 kN m^{-2} water pressure, using the test apparatus shown in FIG. 5.7. The valve was tested for approximately 1000 hours at a switching time of 1 hour (normally energized), and tubes lasted between 100 and 500 hours. The time that a tube lasted was the time of the test until the tube was severed by the cut-off mechanism.

Tube expansion was not a problem during commissioning of the valve, although there was slight expansion of the valve tubes and electrical sleeving over long periods of time. Adjustment of the valve, although at first difficult, became easier as experience was gained with operation.

Under SCCR3 operating conditions, internal tube pressures will vary for the four tubes in any four-line valve, which could result in the cut-off bar becoming unbalanced, preventing an effective seal being obtained. To determine if this was likely to have any effect, a 4-line valve was operated by firstly pressurizing all four tubes to 620 kN m^{-2} and setting the valve to seal, followed by releasing the pressure in two of the tubes to see if the seal was affected. The seal was found to be unaffected, indicating that variations in the internal tube pressures is unlikely to have any affect on successful valve operation.

Throughout the commissioning stage the valve was found to operate reliably with no further faults becoming apparent.

5.2.1.4.2 The Single Line Valve

Essentially this valve (FIG. 5.9 and FIG. 5.11) is a simpler version of the four-line valve. Because there is only one tube to seal, and hence a single cut-off mechanism, it is convenient to place both the tube and cut-off mechanism centrally in the tube block.

The size of slot in the tube is the same as that used for the four-line valve, but two connecting bolts are now necessary to connect the solenoid bar and cut-off assembly, and two return springs are also required.

The parts of the cut-off mechanism are of similar dimensions as for the four-line valve, but the connecting bolts, solenoid box etc. are of smaller dimensions, because of the smaller size of the solenoid required for the single-line valve. The solenoid is a 240 volt D10 a.c. solenoid, also supplied by Oliver Pell Controls Limited, Crayford, which has a maximum holding force of approximately 0.09 kN and a force-distance curve as shown in FIG. 5.6. The required force was calculated, in a manner similar to that used for the four-line valve, and found to be approximately 0.02 kN.

One valve of this type was commissioned at an operating pressure of 620 kN m^{-2}, using the test apparatus shown in FIG. 5.7. A one hour switching interval was used, with the valve normally energized, or closed, for five minutes in each hour, and a tube failure did not occur during a 250 hour test period.

The apparent wear on the valve tube at the end of the commissioning run appeared to be less than for a comparable tube from the commissioning of the four-line valve. This was probably due to the

Figure 5.11 Details of SCCR3 Single-Line Valves

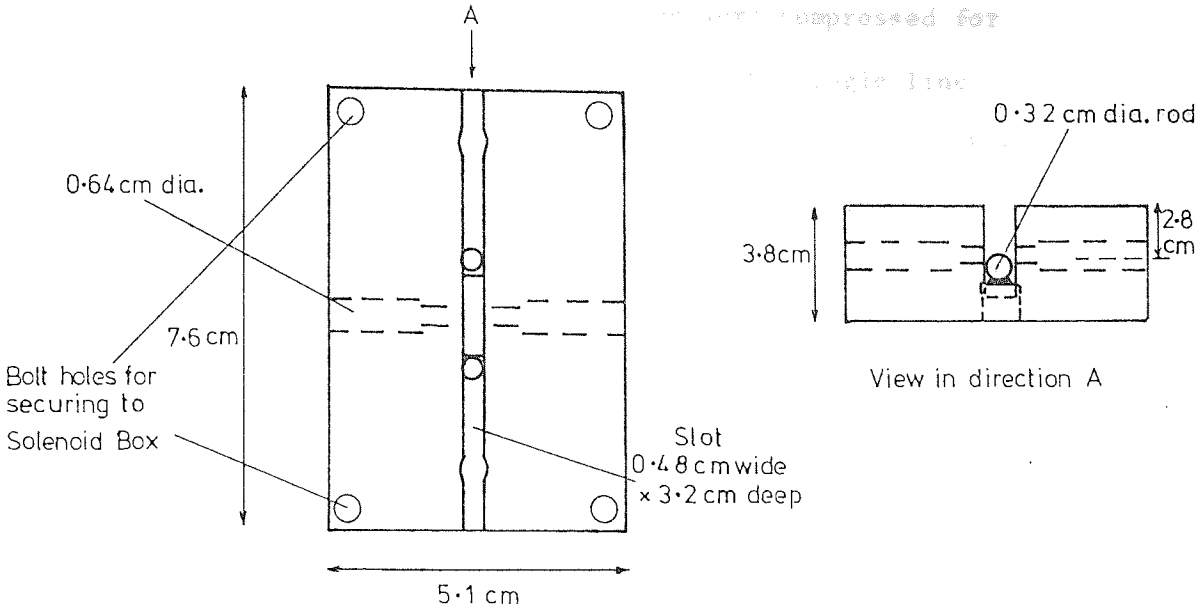

Tube Holder

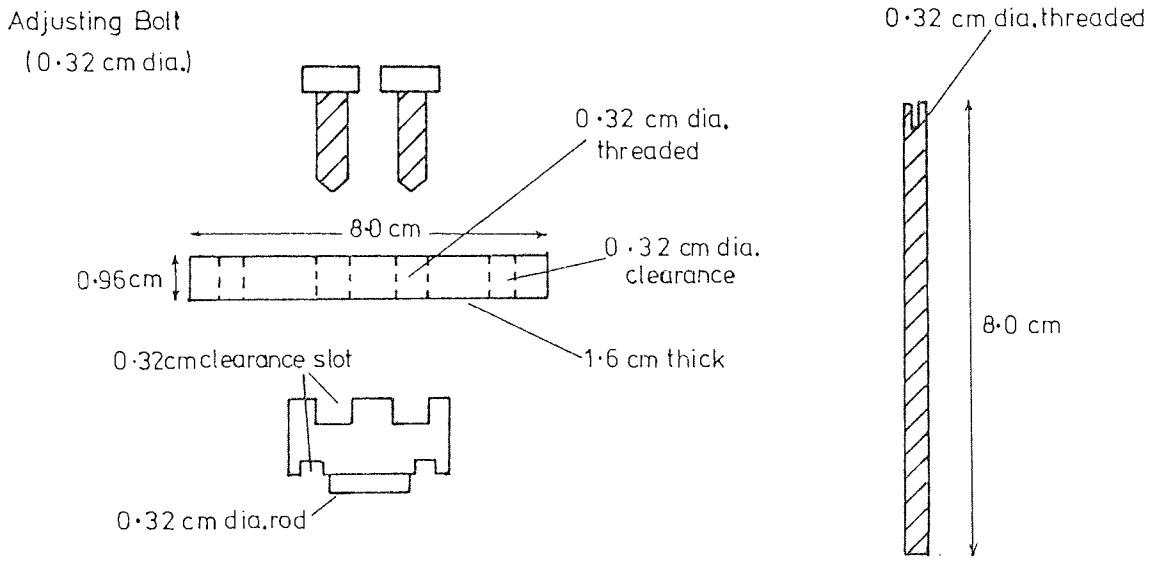

Cut-Off Assembly

Connecting Bolt

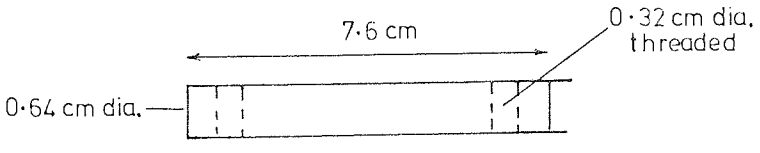

Solenoid Bar

fact that the tubes in the four-line valve were compressed for 55 minutes in every hour, while the tubes in the single-line valves were compressed for only 5 minutes in every hour. This indicates the tubes in transfer valves, which are normally non-energized, or open, will last longer than tubes in the other valves during SCCR3 operation, which was found in practice (SECTION 7.1.3). Adjustment of the cut-off mechanism for the single-line valve required less experience than adjustment of the four-line valve, and again the valve sealed reliably during the commissioning.

5.2.2 The Timing Unit

The design of automatic electronic timing units used with earlier SCCR machines is well documented elsewhere (29) and, as the operating principle of the timer used in this study is similar to earlier models, detailed wiring diagrams are not given. It is proposed to outline the operating principle using a block diagram, and describe the essential differences between the SCCR3 timing unit and earlier models.

The SCCR3 timer was designed and constructed by M. F. Lea, the departmental electronics technician, and it is shown schematically in FIG. 5.12. Operation of the sequencing unit is controlled by the time interval set on the variable timer, which has a range of approximately 16 seconds to 18 minutes. The switching unit has twenty terminals, and automatically re-starts at terminal No. 1 after reaching the last terminal.

The timer terminals are connected to two independent sets of twenty relays, one set transmitting current to the transfer solenoids, and one set transmitting current to the multi-port and feed solenoids.

Figure 5.12 Operating Scheme of SCCR3 Automatic Timing Unit

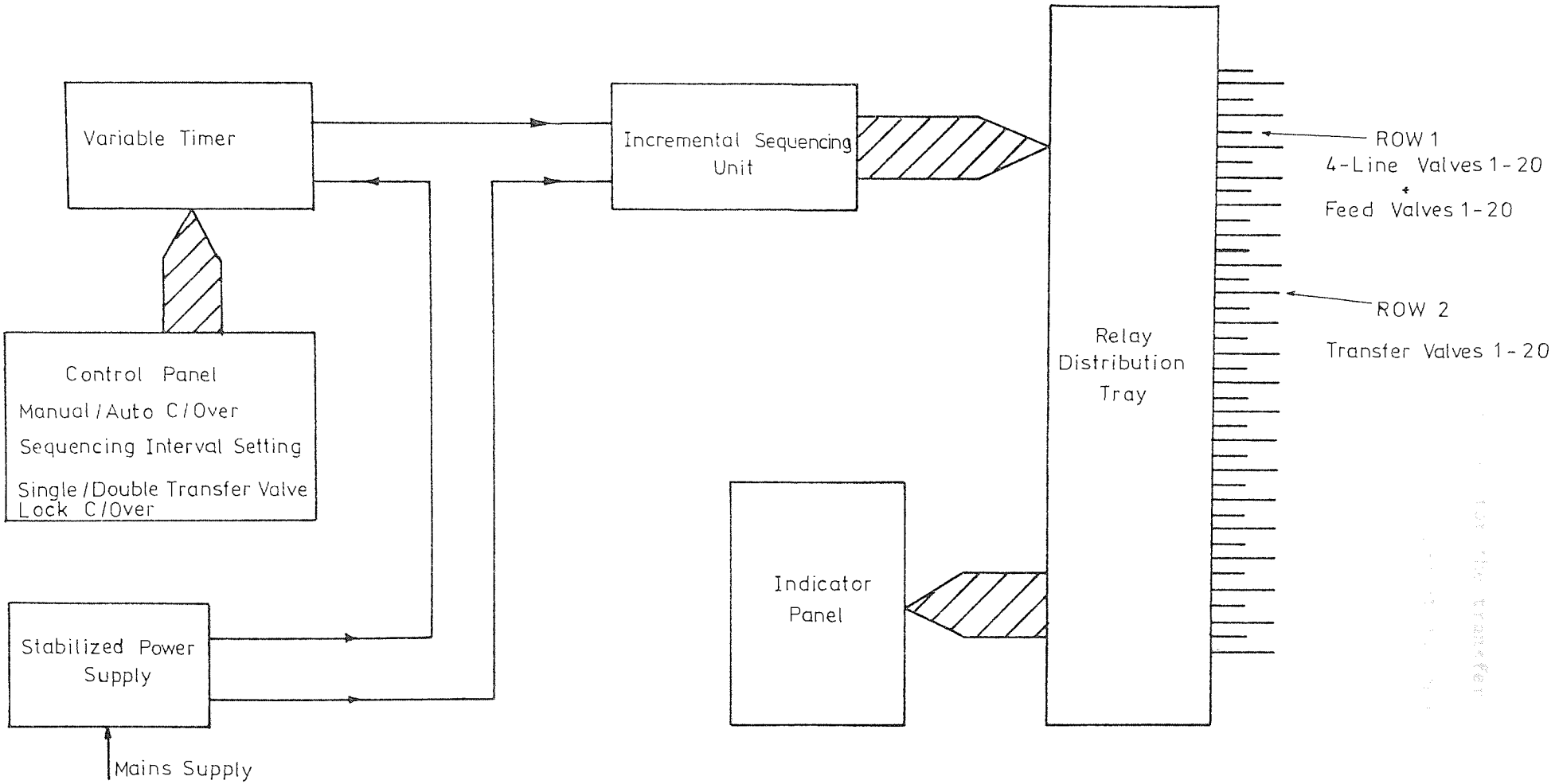

It is necessary to use a separate set of relays for the transfer solenoids because they are advanced with two energized at any one time, whereas the multi-port and feed solenoids are advanced with one non-energized at any one time. This occurs because all the valves used for the SCCR3 machine incorporate solenoids which when non-energized ensure that the valve is open, and are energized to close the valve. As the transfer valves are normally required to be open, and the multi-port valves are normally required to be closed, nineteen multi-port, nineteen feed, and two transfer solenoids are energized at any one time.

The two rows of relays, 2 (Transfer) and 1 (Multi-port and feed), are shown in FIG. 5.13, which indicates the transfer valves that are energised (N.B. T 7 say, indicates the valve between the outlet from column 7 and inlet to column 8), and the Multi-port and Feed valves that are non-energized at the various positions of the switching unit in the cycle. Also given with the multi-port valve number is the column that is receiving purge (PU) and mobile phase (MP) and delivering the two products (P1 and P2). It will be noted that the number given to a multi-port valve corresponds to the column being purged when that valve is open.

The number of the feed valve corresponds to the column that is receiving feed when this valve is open. The feed point was set as the column in the middle of the fractionating section.

A facility for operating the SCCR3 machine in the same operating mode as the CCR1 machine is incorporated into the design of the timing unit. This mode has a single transfer valve closed at any one time instead of the two valves energized in the normal purge mode using an isolated column. A selector switch on the control panel allows a choice to be made between these two modes. This facility

Figure 5.13 Details of Sequencing Pattern of SCCR3 Unit

No. of Isolated Column		1	2	3	4	5	6	7	8	9	10	11	12	13	14	15	16	17	18	19	20
No. of Energized Terminals in ROW 2 = No. of Transfer Valves Energized (Closed) 20 Columns (10 Columns)		20 1 (10,1)	1 2 (1,2)	2 3 (2,3)	3 4 (3,4)	4 5 (4,5)	5 6 (5,6)	6 7 (6,7)	7 8 (7,8)	8 9 (8,9)	9 10 (9,10)	10 11	11 12	12 13	13 14	14 15	15 16	16 17	17 18	18 19	19 20
No. of Non-energized Terminal in ROW 1 = No. of Multi-port valve Non-energized (Open)		1	2	3	4	5	6	7	8	9	10	11	12	13	14	15	16	17	18	19	20
No. of Feed Valve Non-energized (Open) 20 Columns (10 Columns)		11 (6)	12 (7)	13 (8)	14 (9)	15 (10)	16 (1)	17 (2)	18 (3)	19 (4)	20 (5)	1	2	3	4	5	6	7	8	9	10
Column No. Receiving or Issuing Fluid 20 Columns	PU MP PR1 PR2	1 2 20 1	2 3 1 2	3 4 2 3	4 5 3 4	5 6 4 5	6 7 5 6	7 8 6 7	8 9 7 8	9 10 8 9	10 11 9 10	11 12 10 11	12 13 11 12	13 14 12 13	14 15 13 14	15 16 14 15	16 17 15 16	17 18 16 17	18 19 17 18	19 20 18 19	20 1 19 20
Column No. Receiving or Issuing Fluid 10 Columns	PU MP PR1 PR2	1 2 10 1	2 3 1 2	3 4 2 3	4 5 3 4	5 6 4 5	6 7 5 6	7 8 6 7	8 9 7 8	9 10 8 9	10 1 9 10										

was, however, not used during the present research.

A manual re-set button is incorporated to allow the switching unit to be quickly switched to any desired position, and is mounted on the control panel.

An indicator panel, set in the control panel, is fitted with 120 neon lamps, and gives an immediate visual display of:-

(i) The column that is isolated.

(ii) The columns that are receiving, respectively, feed, purge and mobile phase.

(iii) The columns from which the products are issuing.

(iv) The operating mode being employed.

A calibration for the timing unit is given in APPENDIX 1.

5.2.3 Columns and Fittings

The overall column length employed in the SCCR3 machine, 14 m, was based on a 50% increase in the separating length used in the CCR1 unit (23,24) for successful small scale carbohydrate fractionations, to allow for some fall-off of efficiency with increasing column diameter. The length and diameter of the individual columns was based on both economic and theoretical factors. It was thought desirable to reduce the discontinuity imposed by the discrete operating nature of the SCCR3 machine by having the maximum number of columns, within the economic restrictions imposed by the research grant. Twenty columns were therefore utilized, having an internal diameter of 5.1 cm and length of 70 cm.

This diameter of column, having a cross-sectional area of approximately 20 cm^3, gives a scale factor of forty, based on c.s.a., when compared with the CCR1 machine (c.s.a. $\simeq$ 0.5 cm^3). At the same time, column diameter at the 5.1 cm level allows glass to be used as the

column material of construction (at diameters > 5.1 cm standard glass columns cannot be used at an operating pressure of 620 kN m^{-2} for safety reasons).

The original SCCR3 fractionating unit contained 20, 5.1 cm diameter x 70 cm long, PS 2/700 QVF glass pipe sections supplied by Jobling Ltd., Stoke-on-Trent, arranged vertically in the form of a rectangle (FIG. 5.14). The number of columns in the unit was reduced to 10 for the majority of the experimental runs, retaining the pipework in a similar arrangement.

The fluid tubes are 0.64 cm O.D., 0.42 cm I.D., nylon, colour coded for each particular liquid:-

GREEN	MOBILE PHASE AND PURGE INLETS
YELLOW	FEED INLET
RED	HIGH M.W. PRODUCT OUTLET
BLUE	LOW M.W. PRODUCT OUTLET

Liquid inputs and outputs are arranged in a ring-main distribution network (FIG. 5.15), in a vertical plane, to facilitate liquid entry and exit at both the top and bottom of columns.

Connecting lengths of nylon tube together was achieved using jointing pieces, supplied by Delta Copeley Ltd., Loughborough. These are in the form of straight connectors, T-pieces, or Y-pieces, connected to the tubing using metal 'O' clips.

This method is, however, not suitable for connecting the PVC valve tubing because of its non-rigid nature. Connection of the valve tubing was carried out using plastic straps which are tightened around the tubing using a strap gun. Both of these items were obtained from Hopkins and Williams Ltd., Romford.

Figure 5.14

Plan View of the Sequential Unit

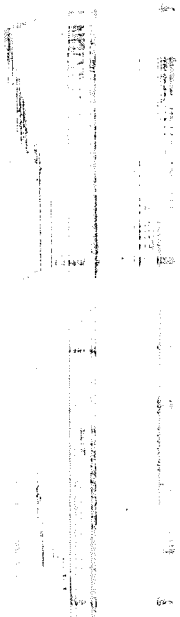

CO	Tube Connection with Metal 'O' Clip
CS	Tube Connection with Plastic Strap
F	Feed Valve
FE	Feed Line
FI	Flow Indicator
L	Main Liquid Inlet and Outlet Lines
M	Four-Line Valve
MP	Mobile Phase Line
P1	Product 1 Line
P2	Product 2 Line
PU	Purge Line
T	Transfer Valve
TR	Transfer Line

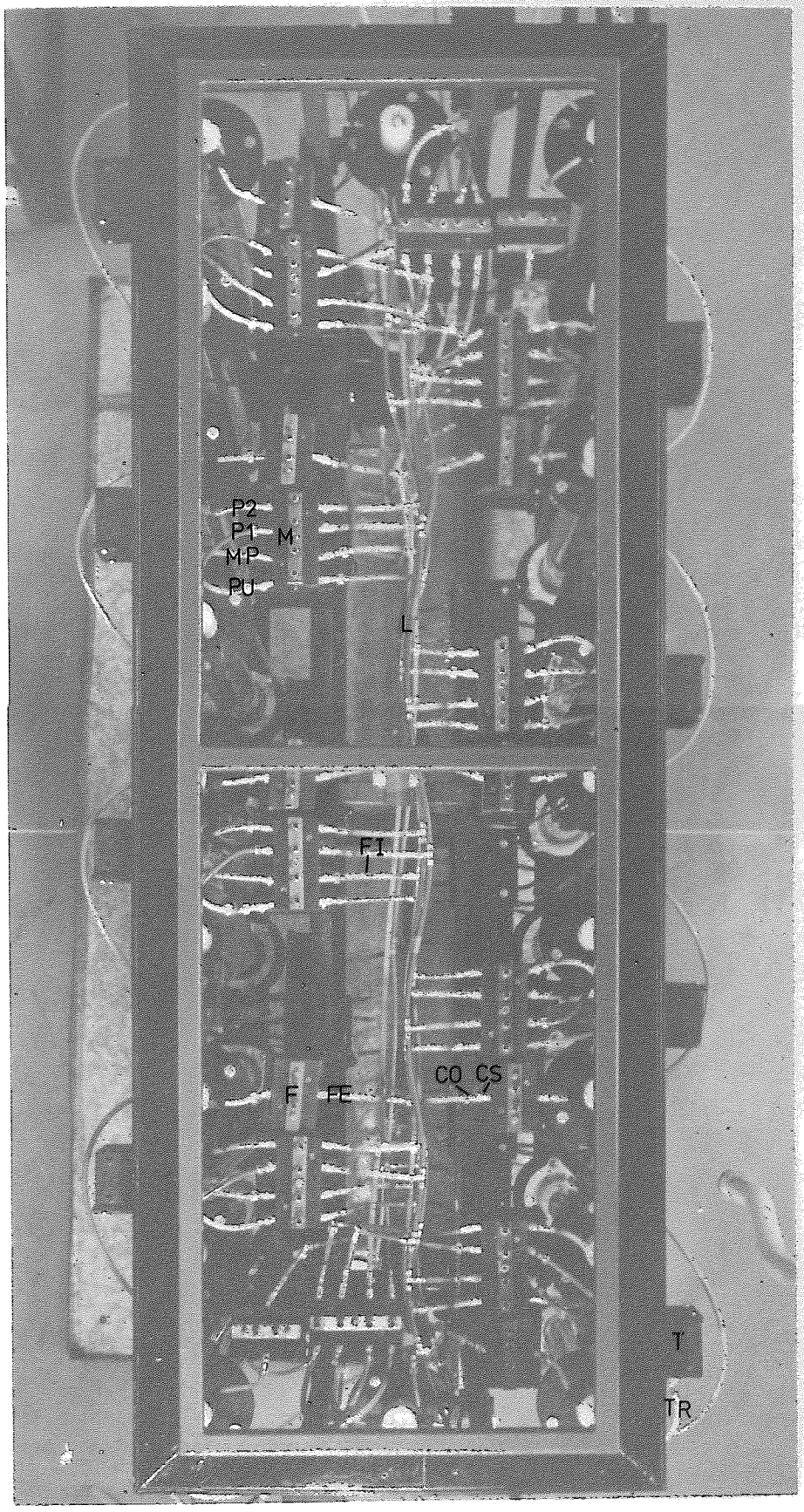
P2
P1
M
M-P
PU
L
FI
CO
CS
F
FE
T
TR

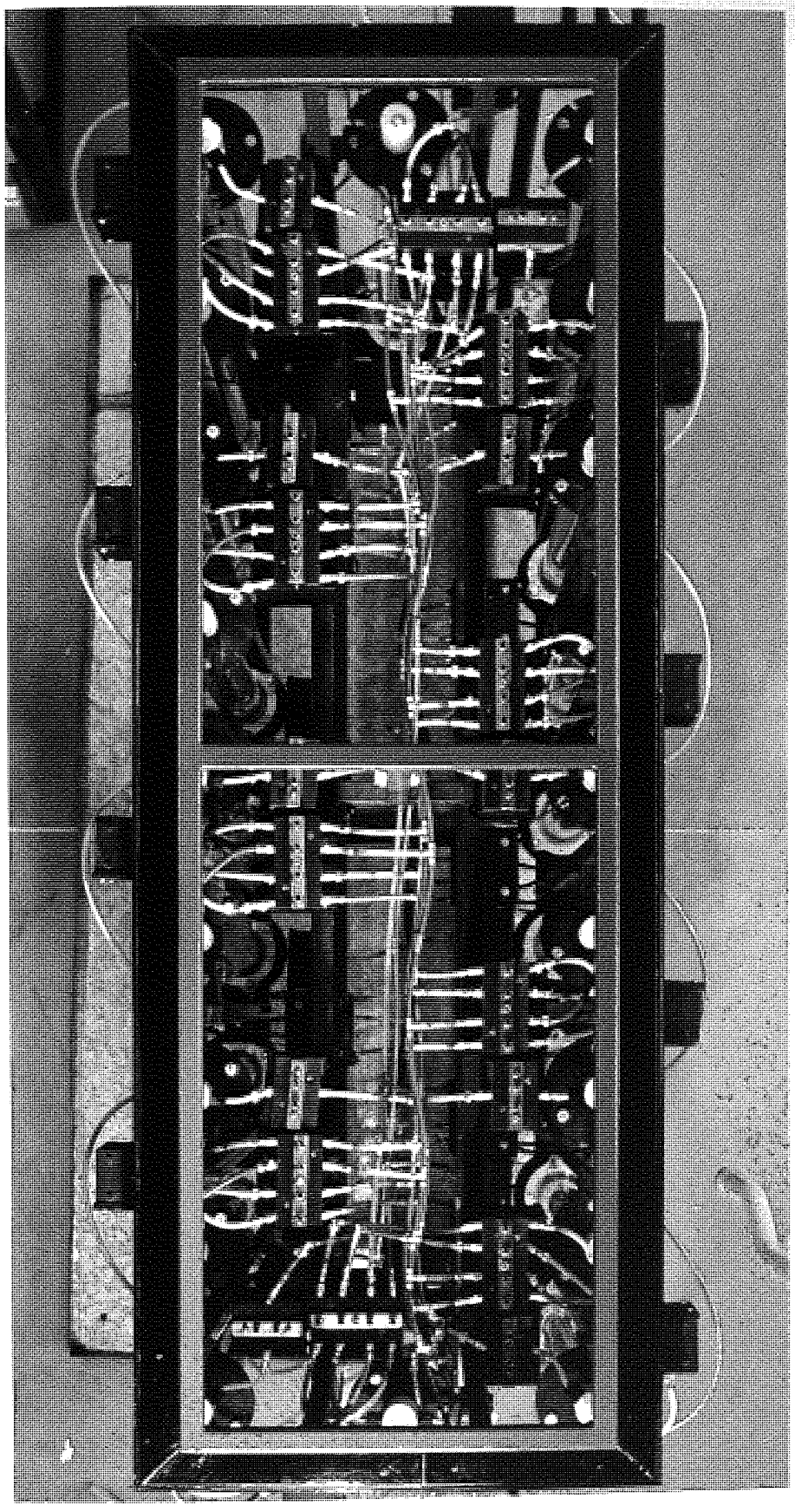

Figure 5.15 Pipework Arrangements for SCCR3 Unit

(a) Feed Inlet and Transfer Lines

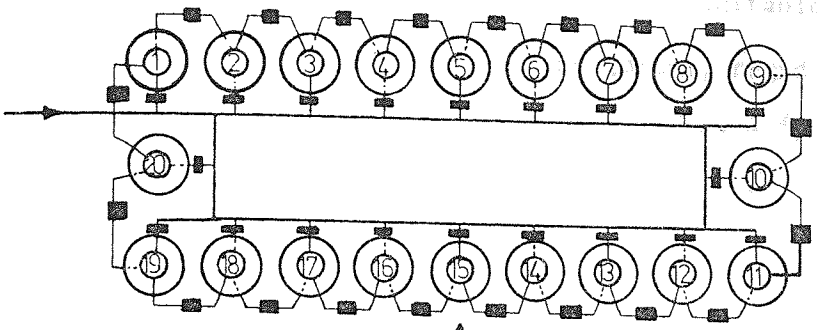

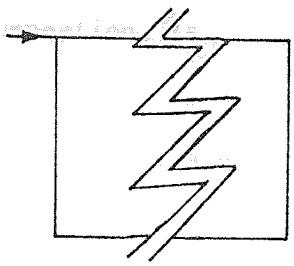

A

Liquid Inlet Line
View in Direction A

(b) Mobile Phase Inlet

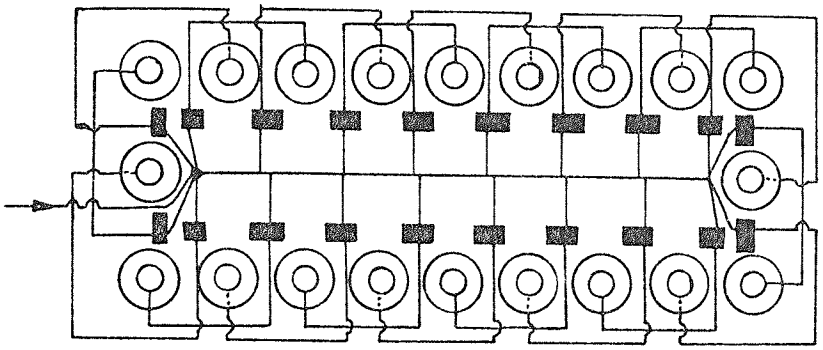

(c) Purge Inlet

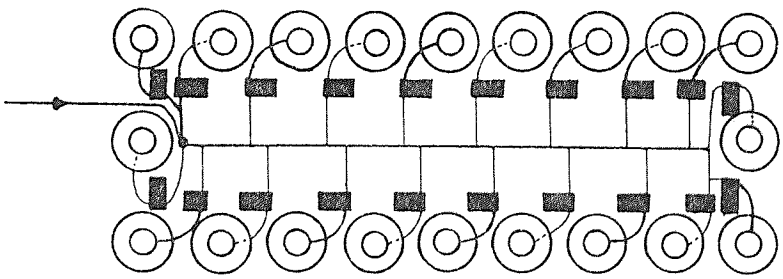

(d) Product 1 Outlet

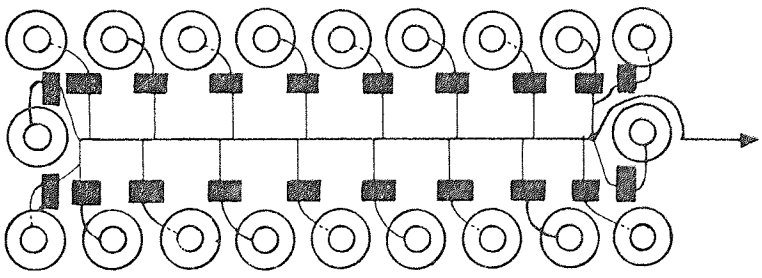

B

(e) Product 2 Outlet

Product Outlet Line
View in Direction B

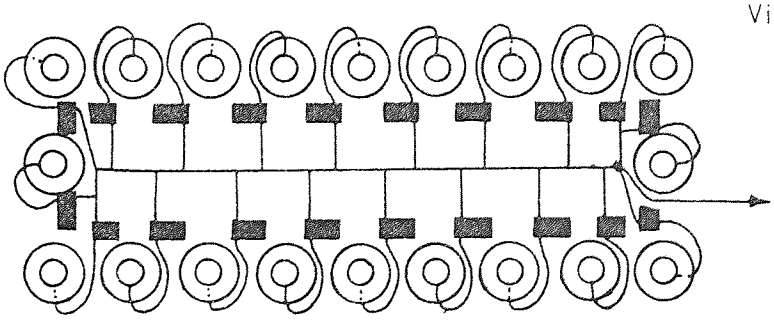

The latter type of connection is suitable for operating at pressures < 600 kN m^{-2}, while the former, rigid connection, is suitable for pressures up to at least 4000 kN m^{-2}.

Incorporated in the liquid lines of the SCCR3 machine are miniature flow indicators, designed for the machine during this research programme, which would indicate fairly small flowrates, ~1 cm^3 min^{-1}. These are necessary because, during adjustment of the solenoid valves, it is important to know which valves are leaking and need adjustment.

The flow indicators consist, essentially, of a length of 0.64 cm O.D., 0.42 cm I.D., semi-transparent nylon tubing containing a nylon ball, 0.32 cm diameter, which has been dyed black. Plastic connectors at each end of the tube retain the ball, and the connector on the outlet side is fitted with a piece of narrow gauge metal wire to stop the ball blocking the connector inlet and preventing flow.

These flow indicators were found to operate very successfully and simplified the task of valve adjustment.

Connections of nylon tubing to the SCCR3 columns was achieved using specially designed column end-fittings. A typical inlet fitting is illustrated in FIG. 5.16, and a typical outlet fitting is illustrated in FIG. 5.17.

The fittings were machined from a length of 6.4 cm diameter polypropylene rod, being essentially cylindrical, 3.8 cm diameter x 6.4 cm high, with a wider base, 6.4 cm diameter x 0.64 cm high, to accommodate a metal backing flange. The inside of the base was machined to form a hole in the shape of a 130° cone. The conical shape was used to ensure good flow patterns at the column entrance, as discussed in SECTION 2.3.2.3.2, and the wide cone angle of 130° minimized the 'dead' volume in the cone. From the top of the cone,

Figure 5.16 SCCR3 Column Inlet Fitting

Full Scale

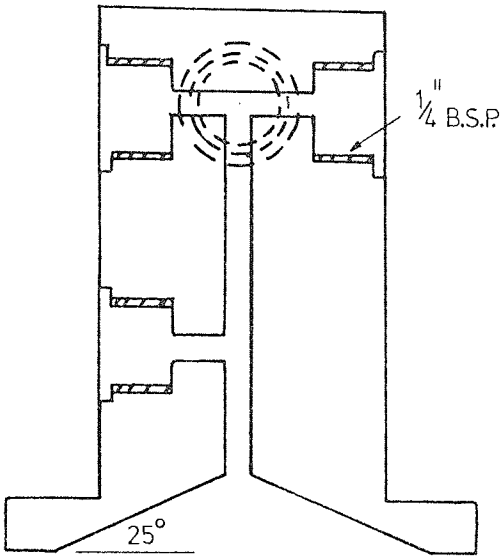

SECTION X-X

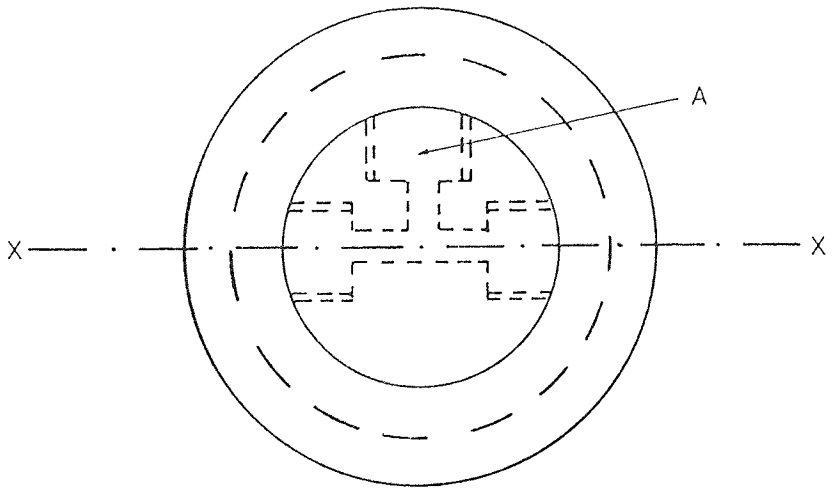

N.B. Half of inlet fittings have port A at 180° to above position

Material - Polypropylene

Figure 5.17 SCCR3 Column Outlet Fitting

Full Scale

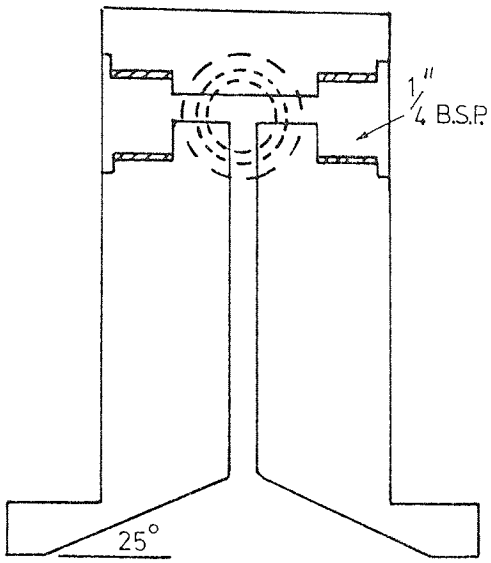

SECTION X-X

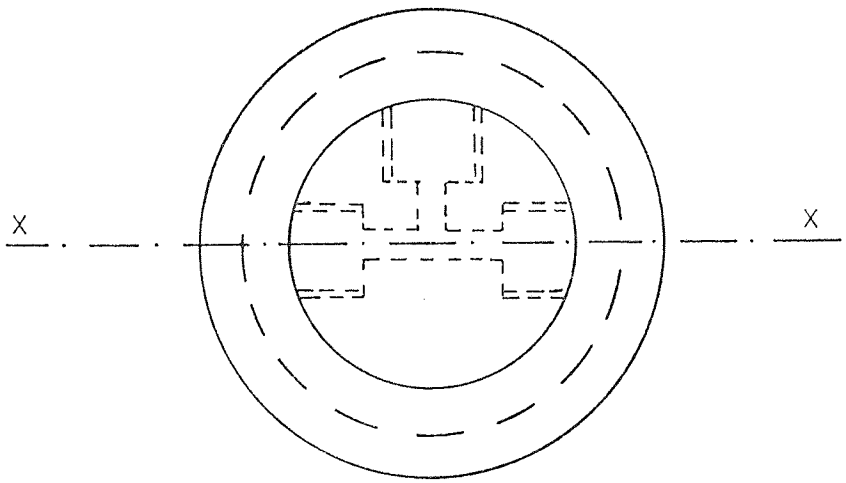

Material - Polypropylene

to within 1.3 cm of the top of the fitting, runs a 0.32 cm diameter hole, and branching out from this at right-angles are further 0.32 cm diameter holes, leading to larger threaded holes, which fit 0.635 cm (¼") B.S.P. parallel plastic compression fittings. These fittings connect to the 0.64 cm O.D. x 0.42 cm I.D. nylon tubing. Between the base of the fitting and the top of the column is a polypropylene mesh 'sandwich' with a rubber gasket on each side to provide an effective seal. The mesh has a dual purpose, firstly to retain the packing in the column, and secondly to produce a uniform distribution of solute across the column (SECTION 2.3.2.3.2). The polypropylene mesh, obtained from Henry Simon Ltd., Stockport, is arranged in two layers, one of 150 μm to retain the packing in the column and one of 1500 μm for support. These meshes were fixed between two 'O' shaped pieces of polypropylene, 6.4 cm O.D. x 5.1 cm I.D. x 0.16 cm thick, using Araldite AY 103 + HY 991 hardener, supplied by Ciba-Geigy (U.K.) Ltd., Duxford. To ensure that the layers remained joined, the polypropylene pieces and mesh were first cleaned with detergent, and then etched with hot chromic acid for approximately thirty minutes, before gluing with Araldite. This was necessary because it was found difficult to glue untreated polypropylene, due to its 'non-stick' nature.

The metal backing flanges which hold the column fittings in place are 0.95 cm thick 'O'-shaped mild steel flanges, 12.7 cm O.D. x 3.8 cm clearance I.D. These fit over the narrow section of the fittings and rest on the wider base. The three holes in each flange allow connecting bolts to join the flange to a 5.1 cm CF2 QVF flange, supplied by Jobling Ltd., Stoke-on-Trent, which fits around the neck of the column. When the bolts are tightened, the whole assembly is pulled together, compressing the rubber gaskets, and forming a seal.

There is one such assembly on each end of each column, the only difference between each one being the arrangement of the inlet and outlet holes in the polypropylene end fittings, which depend on whether the inlet is at the top, or bottom, of the column.

The column assemblies are supported on a metal frame by mild steel angle brackets. These brackets have 1.3 cm long slots in the vertical face to allow the columns to 'hang' fairly loosely from the frame, as a rigid connection could result in excessive stress being applied to one of the glass columns which could result in its cracking.

The frame is constructed from mild steel tube of square cross section, the individual pieces being welded together to form a rectangular box construction, with twenty vertical bars to support the columns.

The box structure rests on four vertical legs, each with two support struts, and these are fixed to castors, supplied by Flexello Castors Ltd., Slough, which are suitable for a maximum standing load of 160 kg each and maximum moving load of 110 kg each. The total weight of the original SCCR3 machine was estimated as approximately 300 kg.

The SCCR3 machine, when completely assembled, was found to move easily on the castors, but was retained stationary, in a metal tray, to collect any water spillage, during the research period.

5.2.4 Pumps

Maintaining reliable and accurate liquid flowrates is important for successful operation of the SCCR3 machine. The degree of accuracy required is dependent on the difficulty of the separation

being attempted, and, for the requirements of the SCCR3 machine, ±1% is thought to be a suitable accuracy.

The pumps chosen are positive displacement metering pumps, supplied by Metering Pumps Ltd., London, which have an accuracy specification of approximately ±1%, between 10% and 100% of the maximum stroke of the pump, and wherein one motor drives several pumpheads.

The mobile phase and purge are pumped by a MPL KV TWIN METRIPUMP fitted with a 1400 r.p.m. motor operating at 72 strokes per minute. The two plastic metering heads are a PG13G, plunger type head, and a D45P, diaphragm type head, for the mobile phase and purge respectively. A diaphragm head was used for the purge because the large flowrate required precluded the use of a plunger type head, and, although this type of head is less accurate than the conventional plunger type of head, very accurate flow was not required for the purge as this does not control the flow in the separating section of the SCCR3 machine.

The K-twin pump was only used for the mobile phase when flows greater than 40 cm^3 min^{-1} were required, as the accuracy was found to decrease below this level. The materials in contact with the fluids being pumped are polypropylene, glass, P.T.F.E., and Viton, so that dilute acids may be used for future work with the SCCR3 unit, if required.

The second pump for use with the SCCR3 machine is a MPL Series 2 positive displacement metering pump fitted with two PC4G plastic pumpheads. Again all parts in contact with the working fluids, polypropylene, ceramic, saphire, and Viton are resistant to acids.

The first plastic pumphead was used for pumping the mobile phase at flowrates <40 cm^3 min^{-1}, as it has an operating range of

approximately 5-45 cm^3 min^{-1}. The second plastic head was used for pumping dextran feed solutions.

It should be noted that, for a positive displacement pump to operate effectively, the back pressure against which it is delivering should be considerably greater than the inlet pressure to the pump. This is necessary to ensure that the non-return valves of the pump seal on the back stroke, and do not allow liquid to syphon through the pump. The back pressures found to be necessary for the SCCR3 pumps were approximately 170 kN m^{-2} for the purge and mobile phase, and 140 kN m^{-2} for the feed, with the inlet water heads provided by the SCCR3 liquid supplies. A nominal calibration of the pumps for the SCCR3 unit is given in APPENDIX 1.

5.3 AUXILLIARY EQUIPMENT

5.3.1 Mobile Phase, Purge and Feed Supply

The liquid inputs to the SCCR3 machine were metered into the fractionating unit from storage tanks, which were fixed at a level higher than the unit to provide a positive inlet pressure for the pumps.

Mobile phase and purge liquid for the research programme was distilled water obtained from an 8000 cm^3 hr^{-1} automatic water still, supplied by Fisons Scientific Apparatus, Loughborough. Distilled water was collected in a bank of eight rigid polythene reservoirs, having a total storage capacity of approximately 500ℓ. In the base of each reservoir is a 1.9 cm diameter hole to allow connection of a threaded polythene tap, fixed in position by a rubber washer and backing nut on the inside of the tank, the whole assembly being sealed with Araldite. A plastic T-piece was joined to each tap, and the series of tanks interconnected, using PVC tubing, to maintain an equal level of water in the tanks.

The distilled water outlet from the still was introduced into the top of tank 1 and the water drawn off for use from the base of tank 8 to provide a circulation of water in the reservoirs. Periodically the liquid level in the reservoirs was decreased, especially after long periods when the distilled water had not been used, to ensure a regular supply of fresh water.

The still is controlled automatically by means of a level control, connected to the inlet of tank 1, which automatically trips a pressure switch in the still control box, to turn off the still, when the distilled water reaches the desired height in the tanks.

Before entering the SCCR3 unit, the mobile phase water passed through a 5.1 cm diameter glass QVF pipe section containing

~1000 cm^3 of porous silica beads of the same type as used in the SCCR3 machine (CHAPTER 6). Essentially, this was intended to saturate the mobile phase with silica and prevent any dissolution of the SCCR3 packing (CHAPTER 6.1.2).

Feed inlet to the SCCR3 machine was supplied as a solution, which was stored in two 20ℓ glass aspirators, the top of each being covered by an inverted beaker to keep out dust and foreign matter.

A general view of the liquid input arrangements is shown in FIG. 5.18.

5.3.2 Product Collection

Lightweight plastic containers of 10, 25 and 80 litres capacity were used for collection of the two product streams from the SCCR3 machine.

Switching of the product streams from one container to the next was achieved using the fraction collector, illustrated in FIG. 5.19, which was designed and constructed during the research period. The operating principle consists of moving the product outlet lines, at the desired, regular, time interval, from delivering to one pair of collection vessels to delivering to the next pair.

Two polypropylene discs 56 cm diameter, 2.5 cm thick, form the basis of the fraction collector, and are arranged in a horizontal plane, one about 10 cm above the other. The lower disc has 24 equally spaced vertical holes, the centres arranged in a circular manner on a 24.1 cm radius. The holes are 2.5 cm diameter in the bottom half of the disc and open out to 6.0 cm diameter in the top half. The bottom of the 6.0 cm diameter sections slope downwards slightly towards the 2.5 cm diameter sections to allow liquid to run down into the lower parts of the holes. The 6.0 cm diameter section collects any liquid

Figure 5.18

Liquid Input Arrangements

for the Sequential Unit

A	Automatic Timing Unit
D	Distilled Water Inlet Line
FE	Feed Line
FM	Flowrate Measurement
FR	Feed Reservoir
MP1	Mobile Phase Line ($< 40\,cm^3\,min^{-1}$)
MP2	Mobile Phase Line ($> 40\,cm^3\,min^{-1}$)
P	Pressure Gauge
PT	Mobile Phase Pre-Treatment Column
PU	Purge Line
WR	Mobile Phase Reservoir

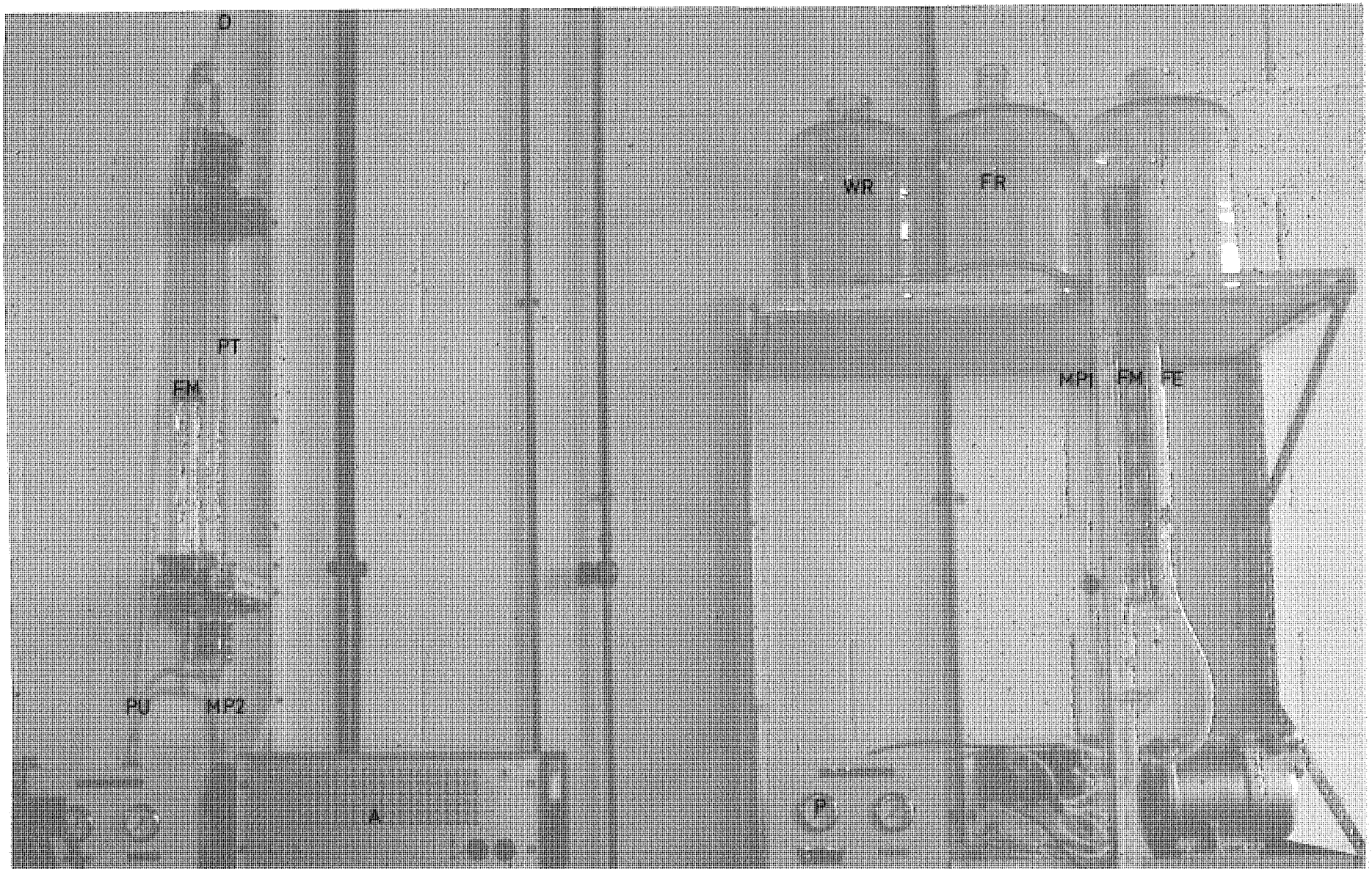
D
WR
FR
PT
FM
MP1
FM
FE
PU
MP2
A
P

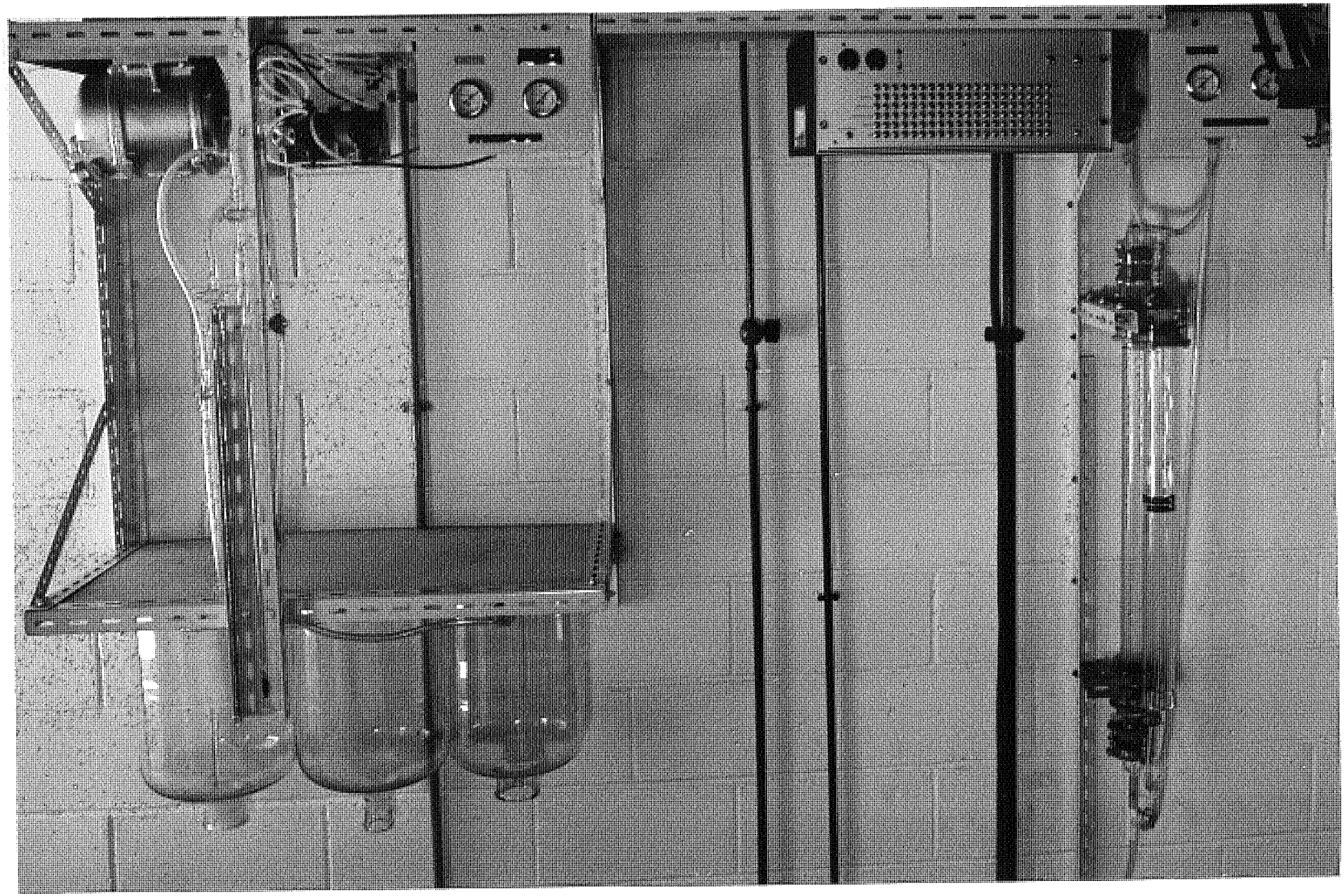

Figure 5.19

Fraction Collector

B	V-Belt
C	Collection Vessels
D	Flexible Drive
L	Electronic Latch
M	Micro-Switch
P1	Product 1 Line
P2	Product 2 Line
S	Electrical Supply
T	Drum Timer
V	Variable Speed Motor

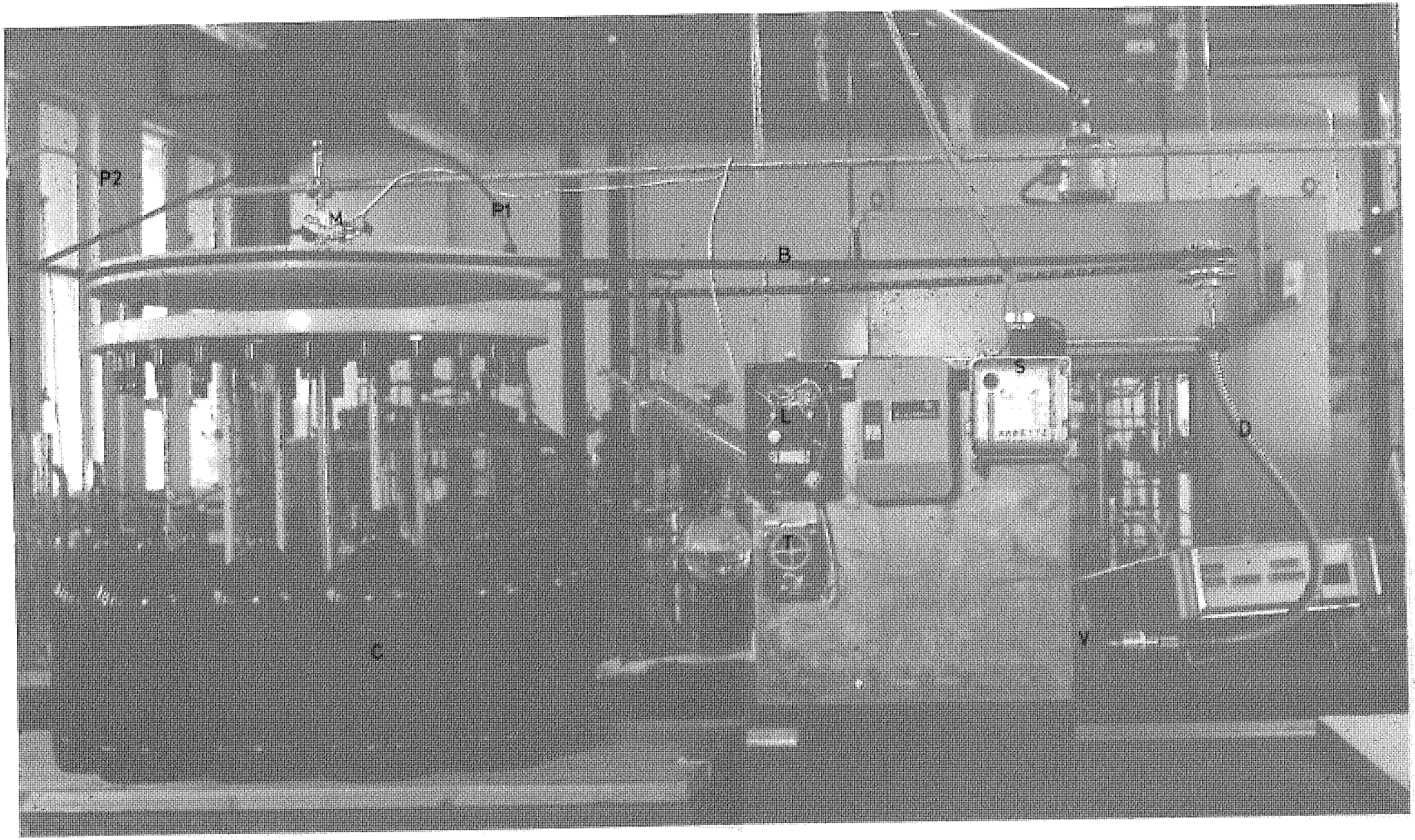
P2
M
P1
B
S
L
T
C
D
V

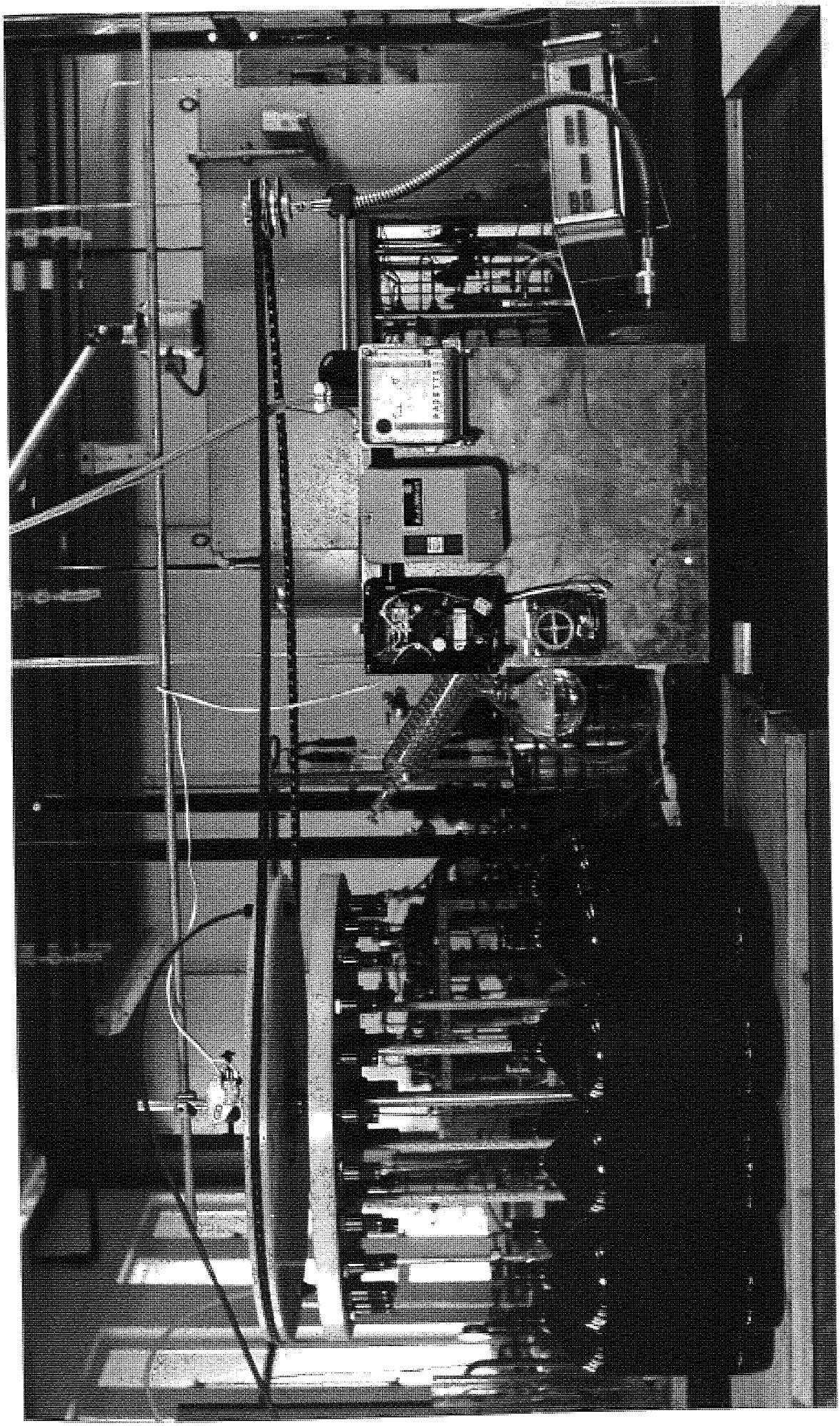

that may splash, from the product outlet lines, during operation of the SCCR3 unit.

The 2.5 cm diameter sections of the holes are threaded and each one fitted with a plastic hose connector. These in turn are connected to lengths of PVC tubing which convey liquid to the various collection vessels. The disc is mounted on four legs of 1.2 cm diameter metal rod, which are bolted to a wooden base to retain the disc in a rigid position.

The upper disc is fixed to a central 1.9 cm diameter rod by means of two bearings which allow it to revolve freely. The central rod passes through the lower disc and is bolted to the wooden base. The upper disc has two 1.3 cm diameter threaded holes drilled vertically, opposite each other, on a 24.1 cm radius. These holes each accommodate two plastic compression couplings, one on each side of the disc. The compression fittings on the top of the disc are connected to the product outlet lines from the SCCR3 machine, while those on the bottom of the disc are connected to short lengths of nylon tubing to direct the liquid into the collection holes in the bottom disc.

The top disc is driven via a V-belt by a variable speed motor, and the V-belt drive is connected to the top disc, around the circumference, resting in a 1.2 cm deep slot machined in the side of the disc.

The motor is started by a 240 volt, 2 contact, 1 revolution per hour programmable drum timer, supplied by Electroplan Ltd., Royston, and when the desired rotation has been obtained is cut out by an adjustable micro-switch attached to the central fixed shaft of the fraction collector. Re-setting the circuit is achieved using an electronic latch designed by the departmental electronics technician, M. F. Lea. The switching time may be further altered by changing the

drum timer for one of slower speed (e.g. 1 revolution per day).

In practice the fraction collector was found to operate reliably, with very little maintenance required. If desired the V-belt was easily removed from the motor and the fraction collector could be operated manually.

It is interesting to note that, since the design of this unit, a commercial model has been introduced, by Pharmacia Ltd., which has basically the same operating principle.

5.3.3 Flowrate and Pressure Measurement

All flowrate measurement associated with the SCCR3 machine was concerned with liquids. Inlet flows were measured using a calibrated glass QVF pipe section of 5.1 cm diameter, or glass burrettes of 50 cm^3 and 100 cm^3 volume.

Measurement of the feed flowrate was carried out using the 50 cm^3 burrette, while the mobile phase flowrate was measured using either the 100 cm^3 burrette, for flows less than 40 $cm^3\ min^{-1}$, or the 5.1cm diameter, 70 cm long QVF pipe section, for flows greater than 40 $cm^3\ min^{-1}$. The purge flowrate was also measured using this QVF pipe section.

Inlet pressures to the SCCR3 machine were continuously monitored by Bourdon gauges. One 100-515 kN m^{-2} (0-60 p.s.i.g.) gauge was positioned in each of the purge and feed inlet lines, and one 100-690 kN m^{-2} (0-100 p.s.i.g.) in the mobile phase inlet line. Pulsing, which damages this type of pressure gauge, was reduced by incorporating stainless steel pulsation dampeners, supplied by Fawcett Engineering Co., Bromborough, and further by partially restricting fluid movement in the branches of the flow lines containing the gauges, by using screw clips to partially close the sections of nylon

tube immediately before the gauges.

Outlet flowrates from the SCCR3 machine were measured by weighing the products, and outlet pressures were equal to atmospheric pressure.

5.4 SAFETY

5.4.1 Electrical Equipment

The possibility of water leaking from one of the connections in the liquid lines, or from one of the column seals, on to any of the solenoid electrical connections, necessitated shielding of the electrical wiring. Two continuous lengths of box section metal conduit are attached to the outside of the SCCR3 frame, one near the top and one near the bottom, around the circumference (FIG. 5.2). The electrical leads from the solenoids mounted at the top of the frame pass through side holes, fitted with rubber grommets, into the top conduit, and those mounted at the bottom of the frame in a similar manner into the bottom conduit. These leads are connected, inside the conduit, to their corresponding leads from the timing unit.

The conduit has holes drilled in the base to allow water to drain out, if leakage of any water into it occurs.

The solenoids are mounted on the metal frame with metal bolts and nuts, and the frame is earthed, and mounted on plastic castors.

The SCCR3 timing unit is protected with a polythene cover in case of any water spillage which might occur from the water storage tanks mounted above the unit.

The still supplying distilled water for the SCCR3 machine has a thermostatic cut out, in case of any water supply failure.

5.4.2 Pressure Equipment

Because the maximum operating pressure envisaged for the SCCR3 machine was 620 kN m^{-2} (75 psig), it was decided to pressure test the glass columns to 1140 kN m^{-2} (150 psig) before assembly of the machine. This was thought to be a suitable safety margin for

glass columns when using water as the working fluid, and all columns tested withstood this pressure.

The columns and fittings were re-tested in situ after the machine was assembled, but for practical reasons the valve tubes and connections could only be tested when the valves had been adjusted at the beginning of a run.

In case of a blockage occurring in one of the flow lines, adjustable pressure relief valves, fitted to the purge and mobile phase inlet lines, were set to relieve pressure at approximately 380 kN m^{-2} (40 psig), and 720 kN m^{-2} (90 psig) respectively. For operation of the SCCR3 machine during the research period the pressure relief valves were not required to operate, although testing was periodically carried out to check that they would function correctly.

Care was taken to ensure that all air was removed from the SCCR3 machine, before commencement of a run, as any air in the machine under pressure is a potential explosion hazard.

5.4.3 General Safety

The SCCR3 machine was not designed to be left unattended during experimental runs for periods longer than the time interval between successive sequencing actions. This is because of the necessity of immediate action in the case of a valve tube failure, which is most likely to occur at the switch over of the solenoid valves, i.e. at the end of a sequencing interval.

A metal tray 1.83m x 0.81m is positioned underneath the SCCR3 machine, fitted with an outlet pipe leading to the drain. This pipe is covered with a layer of 150 μm polypropylene mesh, to prevent solids going down the drain, but allow passage of water should

a substantial leak from the machine occur. In practice it was not necessary to use this drain, however, as only minor leaks occurred during the research period.

CHAPTER 6

Commissioning of the SCCR3 Unit

6.1 SCCR3 COLUMN PACKING

6.1.1 The Choice of Packing

The choice of the type of packing used with the SCCR3 machine in this research was based on the following requirements:

(i) Chemically suitable for use with dextran/water systems.

(ii) Incompressible at high liquid flowrates.

(iii) Commercially available with a pore size suitable for fractionation of approximately 10,000-150,000 M.W. dextrans.

(iv) Commercially available in a particle size range >200 μm, to allow a low resistance to flow.

(v) Available at a cost considerably lower than the normal commercial price for ~100 gm quantities of g.p.c. packings.

A study of FIG. 3.2 in SECTION 3.1.2.1, based on these requirements, led to the choice of Spherosil porous silica beads, manufactured by Rhone Progil, France, and marketed in the U.K. as Porasil by Waters Associates Ltd., Stockport. Previous work with this type of packing for continuous fractionation of carbohydrates (23,24) indicated that separations could be obtained with a total separating length of approximately 9 m.

Selection of the grade of packing was based on the calibration curves for three grades of Porasil (31), B, C and D (FIG. 6.1). Of these, Porasil C (≡ SPHEROSIL XOB075) is most suitable for fractionation of 10,000-150,000 M.W. dextrans, as this range of molecular weights is completely covered by the linear fractionating range (X-Y) of the packing.

The choice of packing size was based on a compromise between the efficiency, measured in terms of H.E.T.P., and pressure drop, consistent with low cost. From the study of the effect of

Figure 6.1 Calibration of Porasil Packings

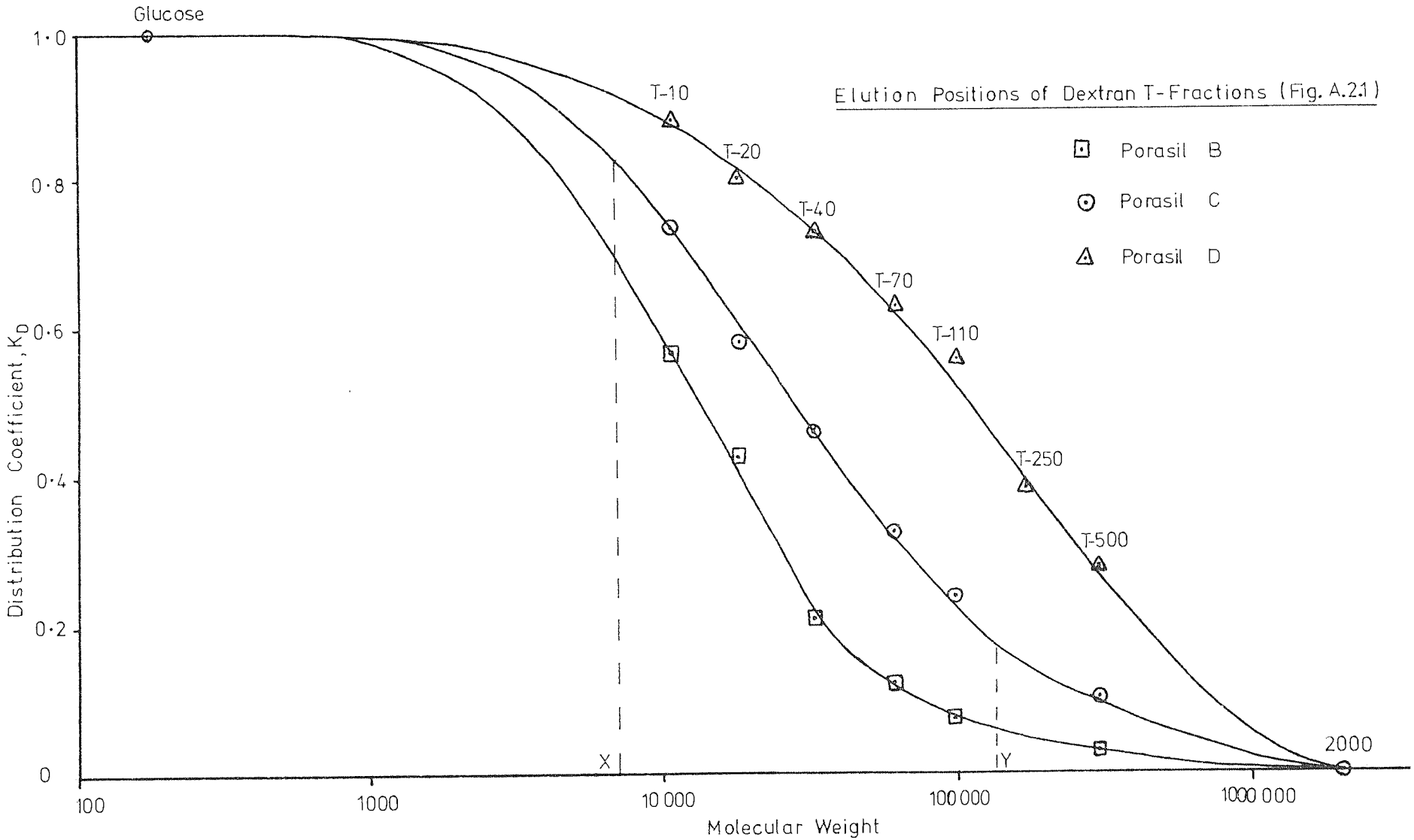

particle diameter on H.E.T.P., discussed in SECTION 4.3.3.2, it was apparent that ~100 μm particles produced the lowest H.E.T.P. for the sizes studied. However, this is gained at the expense of a greatly increased column pressure drop compared with particles of larger diameter. EQUATION 6.2 in SECTION 6.2.1 shows that pressure drop is inversely proportional to (particle diameter)^2. Thus, the pressure drop encountered with 100 μm particles could be reduced by a factor of nine if 300 μm particles were used instead. This was a crucial factor in the choice of packing size for the SCCR3 machine as the allowable pressure drop was limited to ~600 kNm^{-2} because this was the maximum safe operating pressure of the valves and glass columns. H.E.T.P. values for 200-400 μm XOB075 in a 5.1 cm diameter, SCCR3, column are compared to values for 95-105 μm XOB075 in a 0.4 cm diameter, analytical column, at equivalent mobile phase velocities in FIG. 6.2. It can be seen from this that the number of theoretical plates is reduced by, on average, a factor of approximately 3 by the combined use of the larger column and particles, but the resultant pressure drop, for a given mobile phase velocity, would be expected from EQUATION 6.2 to be reduced, by a factor of approximately 9, by the use of the larger diameter particles. Consideration of these factors led to the choice of 200-400 μm XOB075 packing for the SCCR3 machine.

6.1.2 Properties of the SCCR3 Packing

Determination of the particle size range of the packing was carried out by sieve analysis, as indicated in SECTION 6.1.3, using 125, 180, 250, 355, 500 and 710 μm sieves. The data is plotted in cumulative form in FIG. 6.3, and shows 90% of the packing lies between 200 and 400 μm. Pressure drop readings at a series of flowrates were recorded for a typical SCCR3 column by the method described in SECTION 6.2.2.

Figure 6.2 Comparison of H.E.T.P. Values of Analytical and SCCR3 Columns

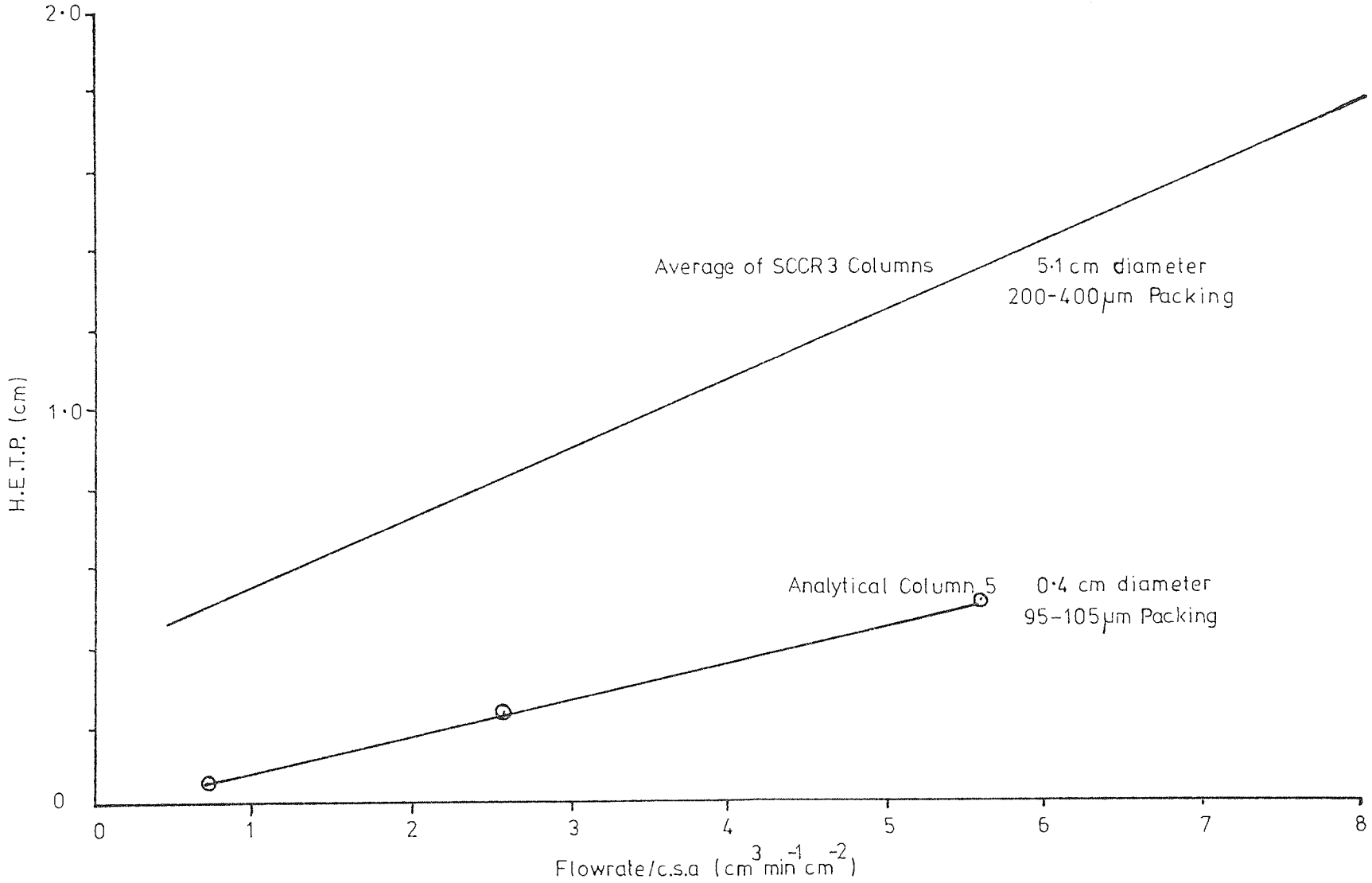

Figure 6.3 Particle Size Distribution of SCCR3 Packing

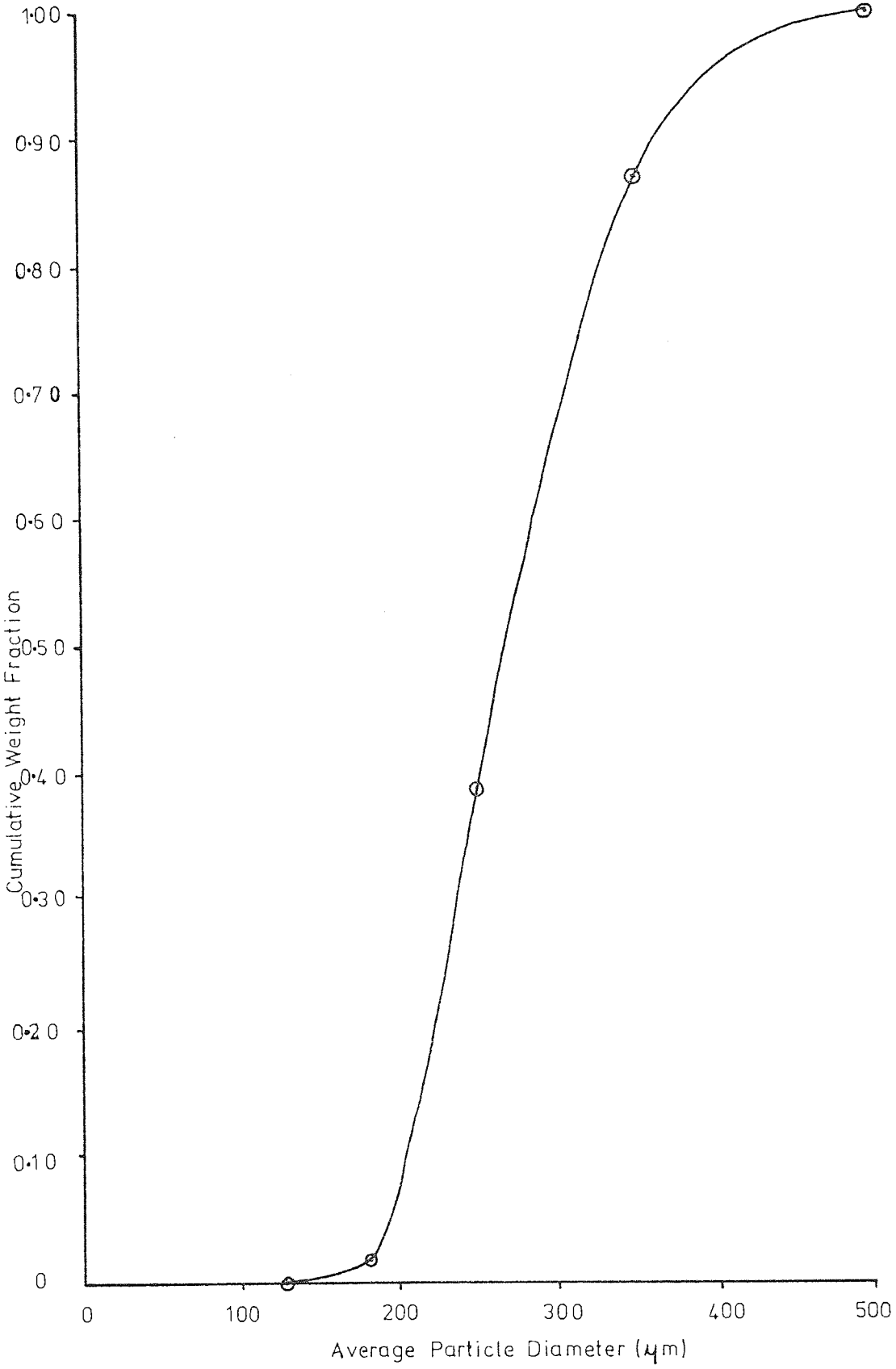

The data is given in FIG. 6.4. FIG. 6.5(a) illustrates the calibration curve of the SCCR3 packing for dextran T-fractions. This was carried out using a 0.8 cm diameter, 65.0 cm long column at a flowrate of 0.27 cm^3 min^{-1} using water as the mobile phase.

To check that dextran molecules exhibit the same K_D values in the SCCR3 columns, and the analytical column used in this research (SECTION 4.3.3.2), the K_D of dextran T-fractions fora typical SCCR3 column and the analytical column were determined experimentally, and plotted against each other. The result is shown in FIG. 6.5(b), which indicates that the K_D of a dextran molecule is approximately the same in both columns, i.e. the packings have similar pore size distributions, which simplifies treatment of results for the SCCR3 machine. The pore size distribution of Porasil C (237) is given in FIG. 6.6(a). Detailed physical properties of Porasils have been reported in the literature (238).

One disadvantage of the use of Porasil is the fact that, under certain conditions, the mobile phase may leach silica from the packing. This would have the effect of altering the calibration of the packing due to silica loss, especially from within the pores where the surface area is large. Packing taken from the SCCR3 mobile phase pre-treatment column (SECTION 5.3.1), which was intended to prevent silica loss from the SCCR3 packing, was removed at the end of the research period and calibrated in terms of the exclusion and inclusion volumes (V_o and V_i). These values were compared with the calibration of some similar packing, which had been unused, under identical conditions. Samples of glucose (completely included, $V_R = V_o + V_i$) and dextran 2000 (completely excluded, $V_R = V_o$) were eluted from a 0.8 cm diameter, 65 cm long column, packed firstly with one packing, and then with the other, at a flowrate of ~0.3 cm^3 min^{-1} cm^{-2}. The results are shown in FIG. 6.6(b), and show that there was no significant silica loss during the research period.

Figure 6.4 Variation of Pressure Drop with Flowrate for a Typical SCCR3 Column

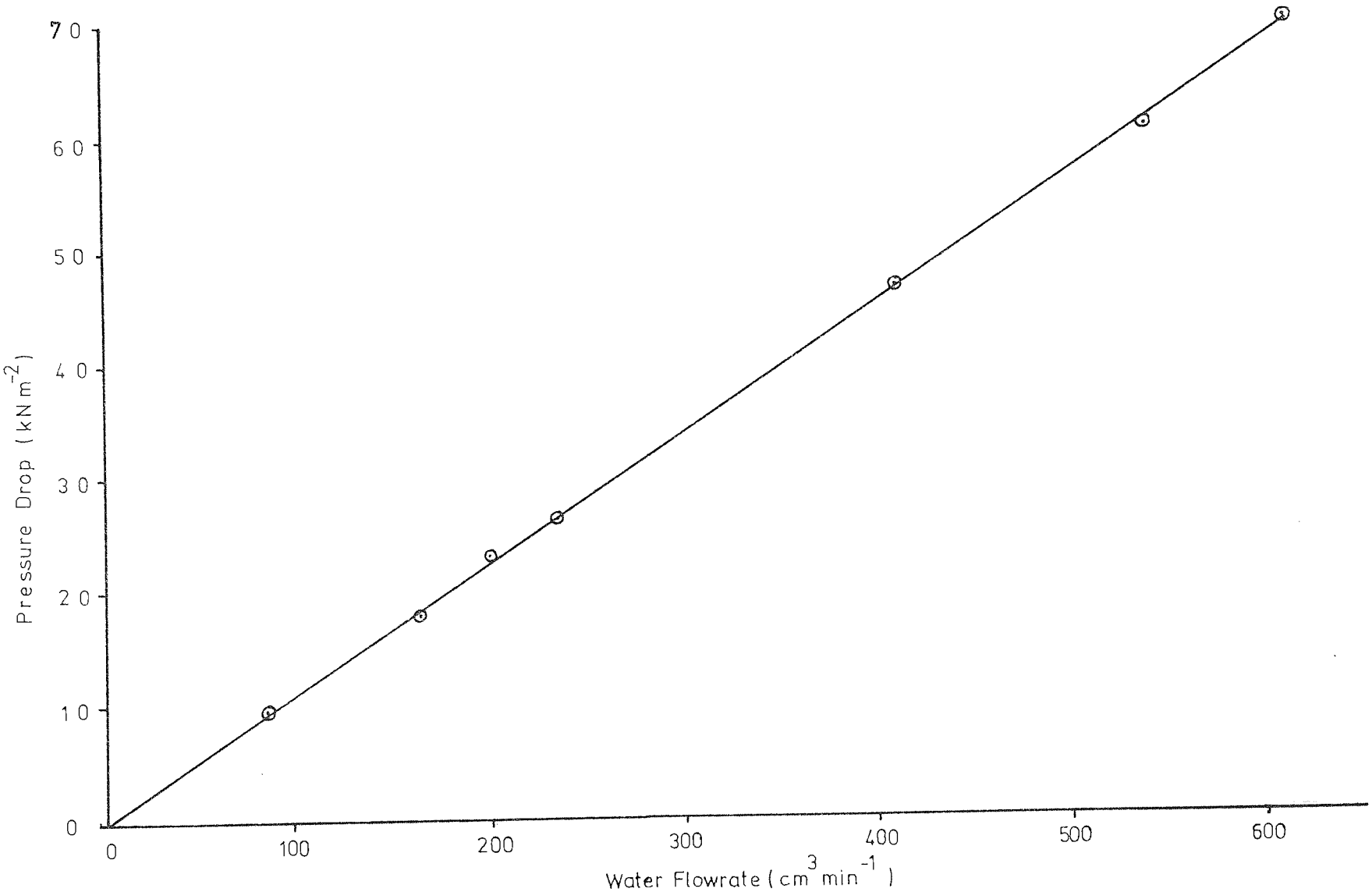

Figure 6.5a Calibration of SCCR3 Packing (Spherosil XOB075) with Dextran T-Fractions

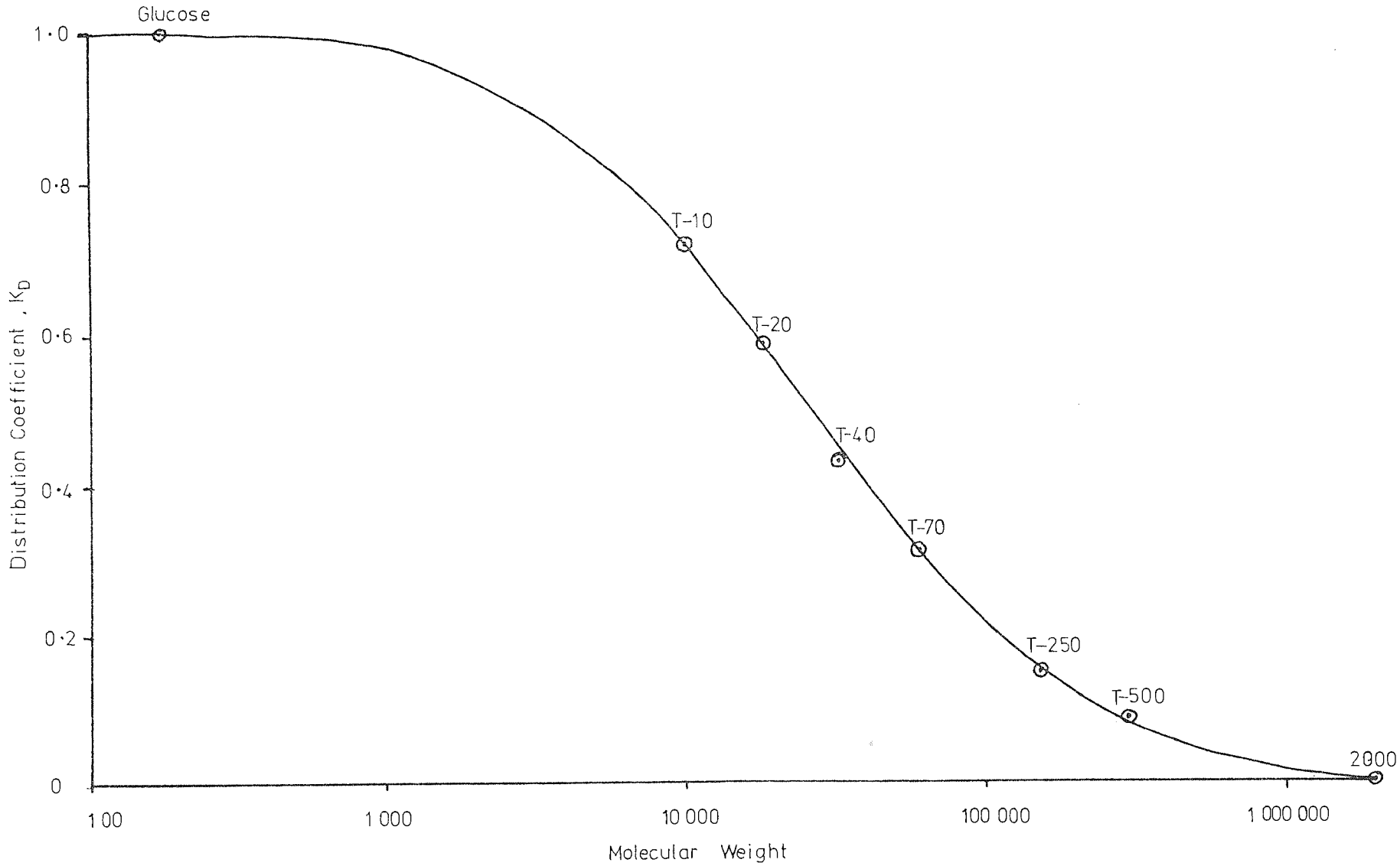

Figure 6.5.b Comparison of the Elution Positions of Dextran T-Fractions on Porasil C (Analytical) and Spherosil XOB075 (SCCR 3)

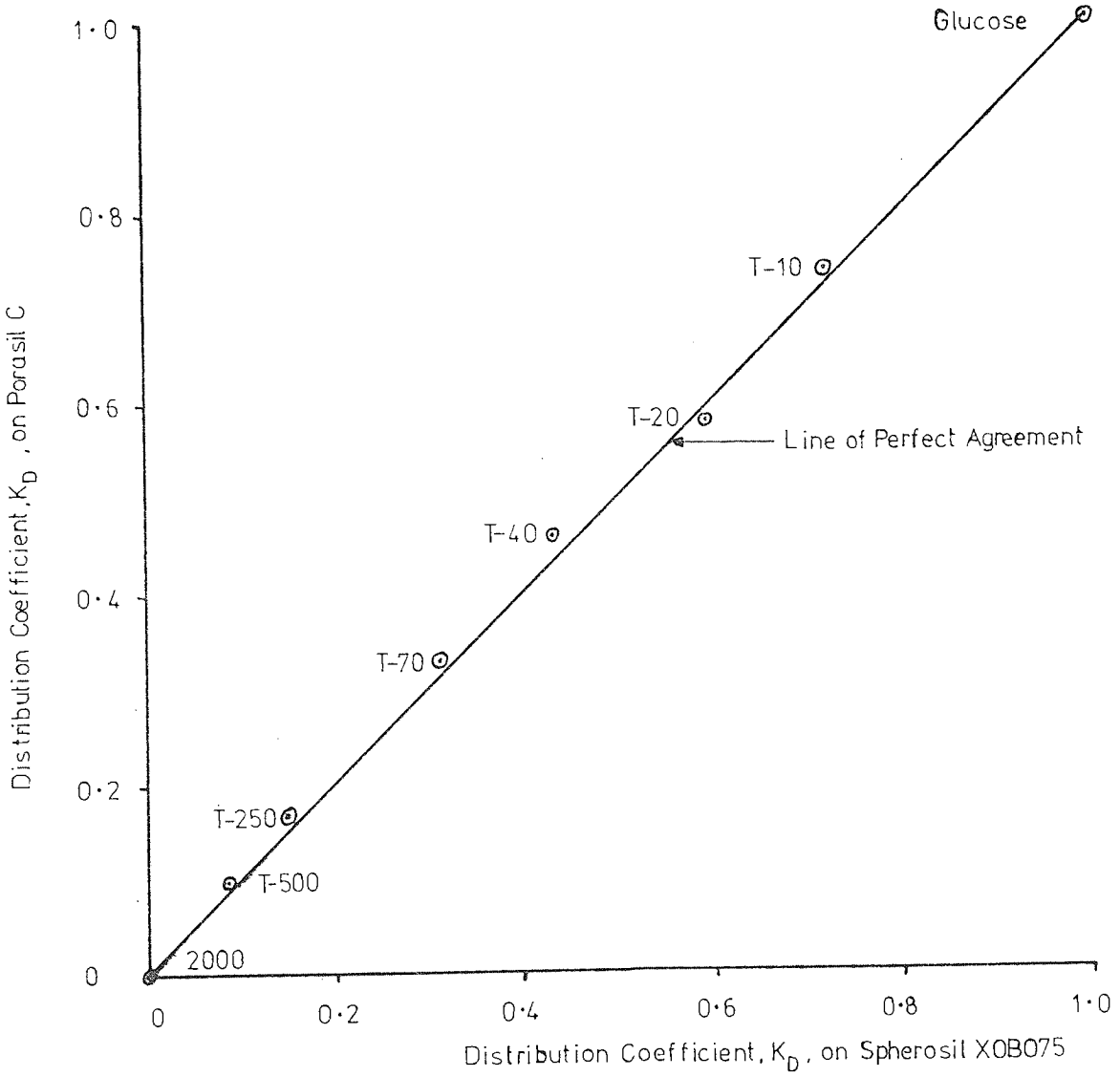

Figure 6.6a Pore Size Distribution of SCCR3 Packing

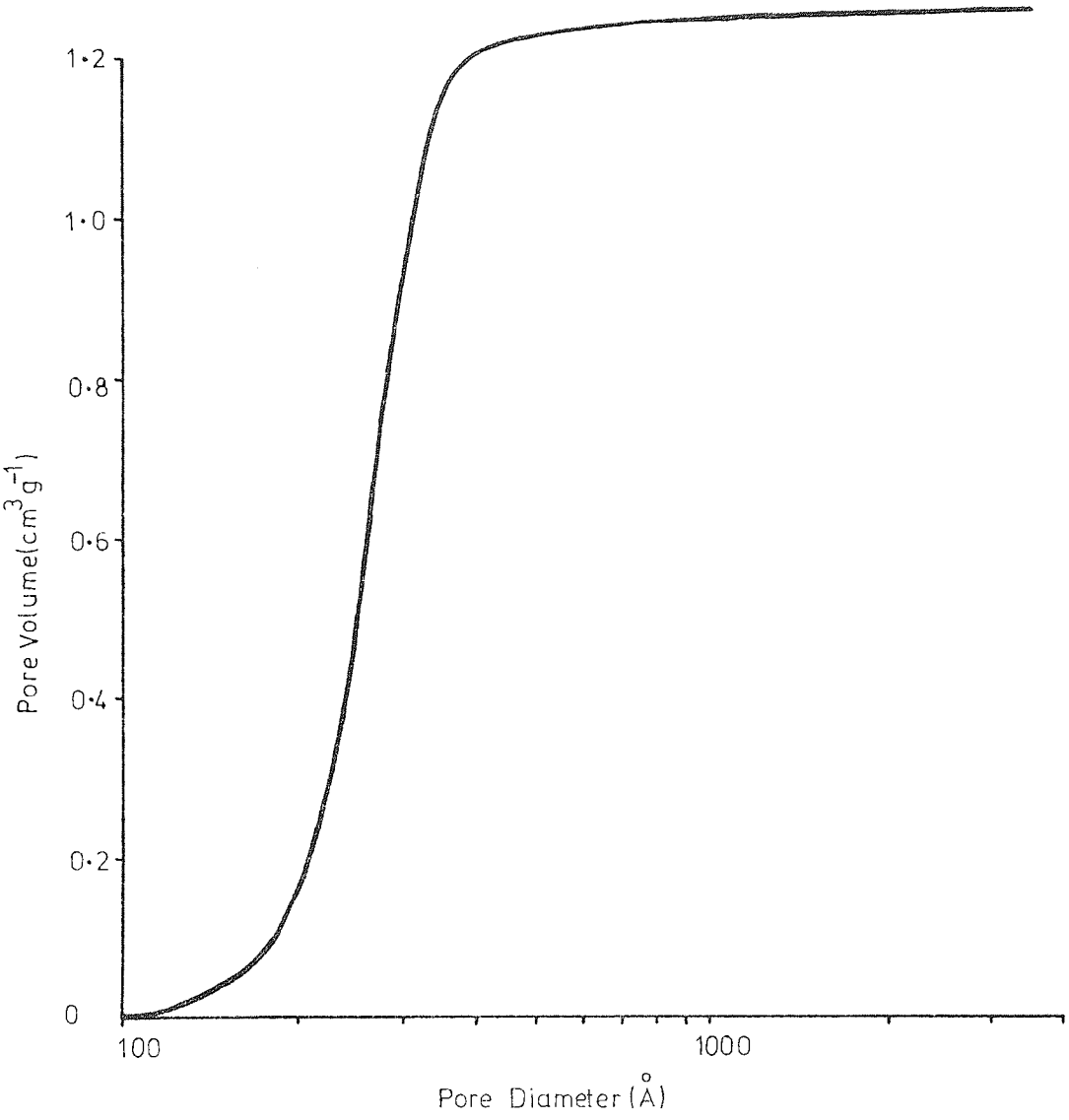

Figure 6.6b Comparison of SCCR3 Packing before and after Experimental Programme

	Pre-SCCR3 Runs	Post-SCCR3 Runs
Fractional Interstitial Volume (V_o / V_t)	0·390	0·394
Fractional Pore Volume (V_i / V_t)	0·403	0·401

It is estimated that approximately 3000 litres of distilled water were pumped through the pre-treatment column over a period of approximately 700 hours during the research period.

6.1.3 Preliminary Treatment of Packing

A preliminary treatment of the SCCR3 packing was carried out to ensure that each column would contain packing of approximately the same particle size distribution. This was achieved using the sample splitter illustrated in FIG. 6.7(a).

The sample splitter was designed to divide a sample of particles having a certain size distribution into two samples, of equal weights, with the same size distribution as the original sample. This was achieved by two rows of channels, set at X° to the vertical, crossing between each other. Each row occupies the same surface area in plan view, to ensure an equal division of the sample between the two rows, and hence to the collection boxes.

The 15 kg sample of Spherosil XOB075 (200-400 μm) was divided into twenty-one batches, each weighing 0.71 kg, by the sample splitter. However, it is not possible to produce twenty-one batches of equal size from one original sample, directly, as one sample produces 2, 4, 8, 16, 32, etc. Therefore thirty-two samples, each weighing ~470g, were obtained conventionally using the sample splitter, and twenty-one of these were put aside. The remaining eleven were divided again to make twenty-two, and one of these added to each of the twenty-one samples from the first series of passes through the sample splitter. The remaining sample was set aside for sieve analysis. This was used to test the accuracy of the sample splitting technique. The sample was divided into eight samples, each of 25-30 g, using the sample splitter, and two of these were compared by sieve analysis. The results are given in

Figure 6.7 Division of SCCR3 Packing into Batches for Individual Columns

(a) Equipment

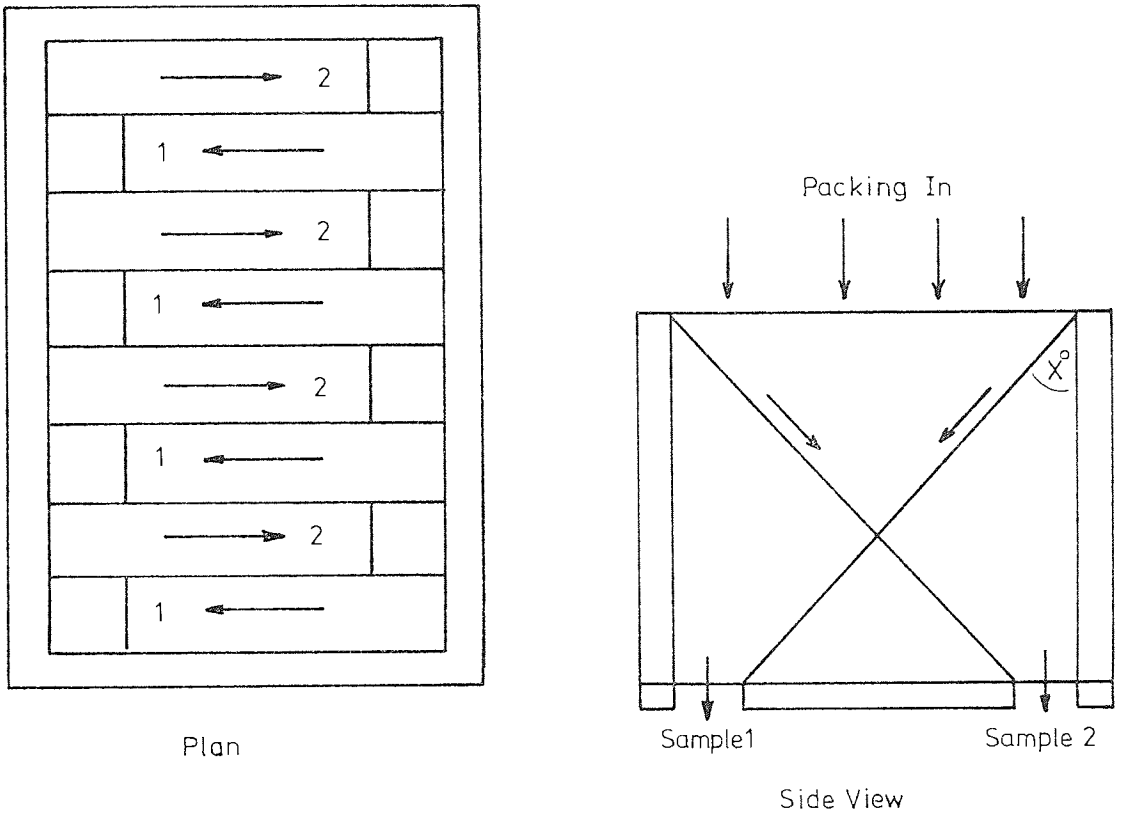

(b) Comparison of Two Batches by Sieve Analysis

Size Range (μm)	Sample 1	Sample 2
	Weight Fraction	Weight Fraction
>710	0·0	0·0
500 - 710	0·004	0·004
355 - 500	0·118	0·127
250 - 355	0·477	0·493
180 - 250	0·383	0·357
125 - 180	0·018	0·019
<125	0·0	0·0
$d_{P_{AV}}$	283 μm	286 μm

FIG. 6.7(b), and show the two samples to be reasonably similar, allowing for some degree of error in the sieve analysis. The average particle diameter for each sample was calculated by:

$$d_{p_{AV}} = \frac{\Sigma x_i d_{p_i}}{\Sigma x_i} \qquad (6.1)$$

x_i = weight fraction of sample retained on a given sieve tray

d_{p_i} = average particle diameter of material retained on the same given tray

Pre-treatment of the SCCR3 packing was continued by removing air from twenty of the samples, particularly from the pores. This was achieved by immersing each sample in distilled water contained in a buchner flask, applying a vacuum, and shaking the flask, until no further air was seen to escape from the packing. The packing was retained under water for introduction into the SCCR3 columns.

6.1.4 Column Packing Technique

The apparatus used for packing the SCCR3 columns consisted of a simple funnel and tube arrangement to introduce the packing into the column, and a line connected to a vacuum pump to remove excess water.

The column was first filled with water, and the funnel and tube placed in position, with the bottom of the tube near the base of the column. As the packing was introduced into the funnel, in the form of a slurry, the funnel was slowly raised to maintain the bottom of the tube level with the top of the packing as it filled the column.

While the column was filling with packing, the water level was being maintained at the top of the column by sucking off excess water

with the vacuum line. Also, while the column was being filled, it was tapped sharply to ensure that the packing settled completely. This tapping was carried out in a random manner to avoid setting up standing waves in the column which might segregate the packing.

This packing procedure was employed until the packing was approximately 5 cm from the top of the column. The remaining 5 cm of packing was introduced gradually, with tapping of the column being continued, until the column was full, i.e. the level of the bed did not fall after several days of intermittent tapping.

This method of packing the columns was thought most likely to give uniform packing over the whole length. It is an improvement over simply introducing a packing slurry into the top of a column, and letting it settle under gravity as this often results in segregation of the particles, because of the variation of settling velocity with particle diameter.

However, dry packing of the column may be a more suitable technique, but in this case the problem of removing air from the internal pores of the packing, once the column was dry-packed, would require a large quantity of de-aerated water, which was not readily available, and it would also be difficult to ensure that all of the air was removed. Throughout the research period the level of packing in every column remained unaltered.

6.2 COMPARISON OF PACKED COLUMNS

6.2.1 Theoretical Basis for Comparison

The general structure of a bed of spherical particles may be partly characterized by its fractional voidage, which is usually ~0.4. In g.p.c. this represents the fractional interstitial volume, V_o/V_{TOTAL}, and the elution volume of a totally excluded species, V_o, is thus a measure of the bed voidage. Comparison of V_o values obtained for columns of similar dimensions thus indicates their relative packed densities. A loosely-packed column would have a higher voidage than a more tightly-packed column, when the same packing and column dimensions are used, and comparison of the voidages of a series of such columns is a measure of the reproducibility of the packing technique employed.

A further comparison of the packed densities of a series of columns may be carried out by recording the pressure drop through each column at the same flowrate. The pressure drop, ΔP, through a packed bed under laminar flow conditions, and assuming no wall effects, may be written (239):

$$\Delta P = \frac{K'' S_p^2 (1-\varepsilon)^2 \mu \ell u}{\varepsilon^3} \qquad (6.2)$$

K'' = Kozeny's constant ($\simeq 5$)

S_p = Specific surface area of packing particles

= $6/d_p$ for spheres

d_p = particle diameter

μ = fluid viscosity

ℓ = bed length

u = average fluid velocity, defined as $\frac{1}{A'} \frac{dV}{dt}$

v = volume of fluid flowing in time, t

A' = total cross-sectional area of bed

For spherical particles, EQUATION 6.2 becomes:

$$\Delta P \simeq \frac{180(1-\varepsilon)^2 \mu \ell u}{\varepsilon^3 d_p^2} \qquad (6.3)$$

Comparison of pressure drop readings for a series of columns using the same fluid and at the same average fluid velocity should provide a comparison of voidage and particle diameter:

$$\Delta P \propto \frac{(1-\varepsilon)^2}{\varepsilon^3 d_p^2} \qquad (6.4)$$

If the columns contain particles of a similar size, pressure drop readings should be proportional to $(1-\varepsilon)^2/\varepsilon^3$.

Values of the interstitial volume, V_o, and pore volume, V_i, should ideally be constant for all columns in a continuous chromatographic machine. This ensures that a component has a constant migration rate through successive columns, under idealized conditions of constant flowrate and concentration. However, variation in V_o and V_i values can be tolerated in the SCCR3 unit because the separating section consists of a series of columns, and variations in V_o and V_i values for individual columns are smoothed out over the total separating section. Thus, although the migration rate

of a component through individual columns may vary, its average migration rate through the whole machine will be essentially constant. The maximum variation in V_o and V_i values for the whole of the separating section is discussed in SECTION 6.2.3.

Comparison of the performance of batch chromatographic columns is usually based on their respective H.E.T.P. values. The significance of the H.E.T.P. concept has been discussed in SECTION 2.2.4. While H.E.T.P. values determined for a low M.W. monomer, such as glucose, give some measure of batch column performance, it is appreciated that the absolute values of H.E.T.P. obtained will not apply to dextran polymers. As such the H.E.T.P. values determined for SCCR3 columns, using glucose as solute, were used merely as an indication of the degree of similarity of column performance. Values of H.E.T.P., skew and kurtosis were computed using PROGRAM 2 in APPENDIX 5.

6.2.2 Experimental Techniques

Values of the interstitial volume, V_o, the pore volume, V_i and H.E.T.P. for the SCCR3 columns were determined by treatment of the elution curves of a totally included substance (glucose, M.W. = 162) and a totally excluded substance (Blue Dextran 2000, M.W. ~2 x 10^6).

The apparatus used for the experiments is shown in FIG. 6.8. Distilled water was pumped into the column, in situ in the SCCR3 unit, through the normal column fitting. A T-piece in the outlet line containing a silicone rubber septum allowed a sampling needle, connected to a Technicon AutoAnalyser pump, to be introduced and a continuous sample stream removed. This sample stream was monitored continuously using either an automated cysteine-sulphuric acid assay, for glucose analysis, or a UV monitor (LKB Uvicord), for Blue Dextran 2000 analysis, outlined in SECTION 4.2.1.

Figure 6.8 Arrangement of Equipment for Comparison of SCCR3 Columns

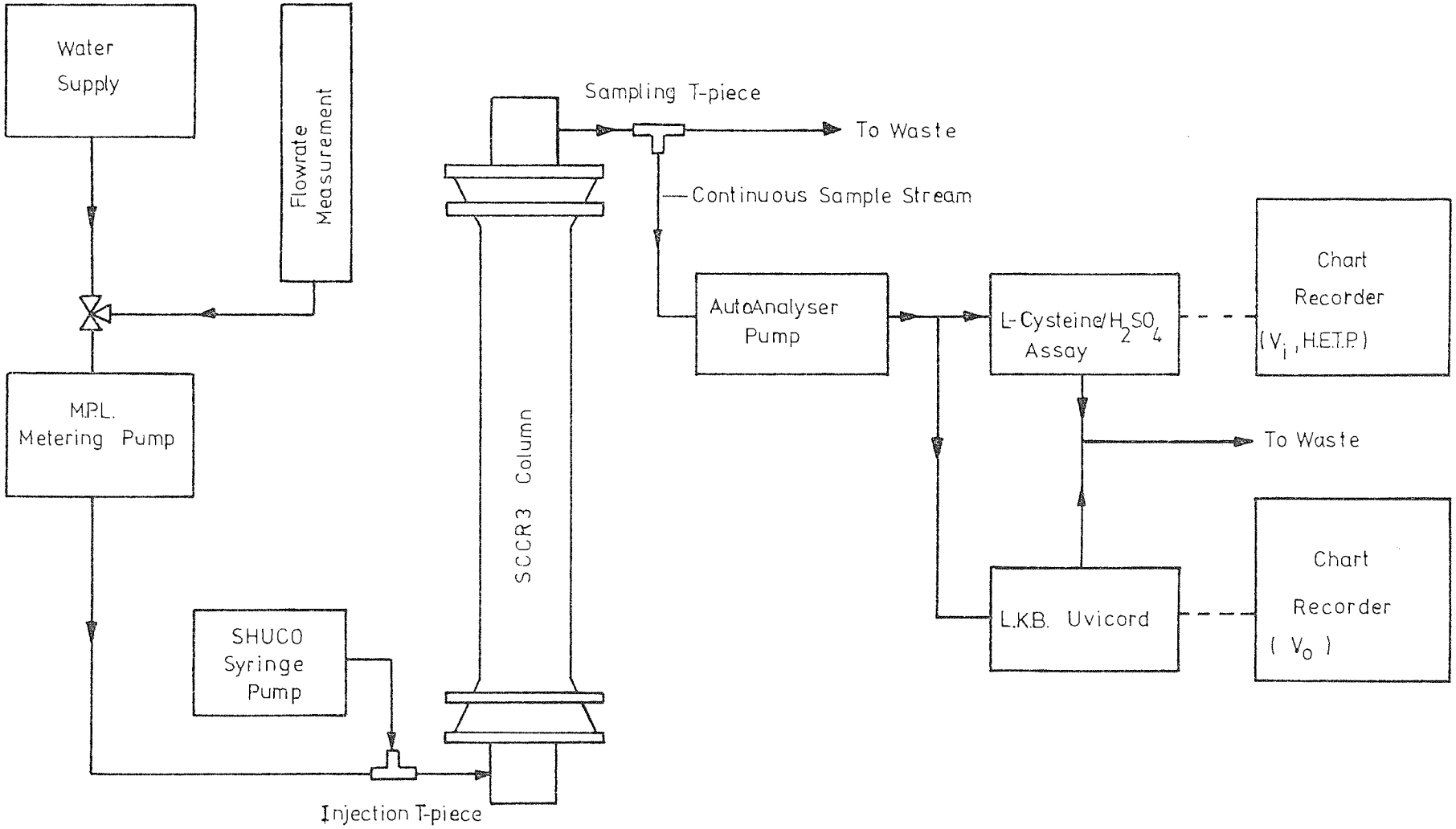

Samples were introduced into the system through another T-piece, also containing a silicone rubber septum, in the mobile phase inlet line to the column. The sample injection was carried out using a SCHUCO 20 r.p.m. syringe pump to obtain a reproducible rate and volume for the sample injection. The pump operates by producing a fixed movement of a flat metal plate in a horizontal direction, the amount of movement being controlled by the time that the pump motor is switched on. The movement of the metal plate depresses a syringe plunger, forcing liquid from the attached needle at a controlled rate. This rate may be altered by varying the size of syringe employed.

The sample injection T-piece and product removal T-piece were positioned as close to the column as practically possible to minimize extra-column contributions to sample variance.

Comparison of the V_o, V_i and H.E.T.P. values for the SCCR3 columns was carried out using a mobile phase flow of approximately 50 cm^3 min^{-1}, which was the approximate mobile phase flowrate employed in SCCR3 runs during the research programme.

For determination of V_o values, 0.5 cm^3 of 10% w/v Blue Dextran solution was injected, and for V_i and H.E.T.P. determinations, 0.5 cm^3 of 2% w/v glucose solution was injected.

The reproducibility of calculated V_o, V_i, and H.E.T.P. values was determined by repeated injection of glucose and Blue Dextran samples under similar conditions.

The effect of sample volume,concentration, and injection time on calculated V_i and H.E.T.P. values was also investigated by injecting samples of 1%, 3% and 5% glucose for 10 secs. (1.0 cm^3), 5 secs. (0.5 cm^3) and 3 secs. (0.3 cm^3) respectively on the same column, using the same size of syringe.

For the variation in V_o values 0.3 cm^3 of 15%, 0.5 cm^3 of 10%, and 1.0 cm^3 of 5% Blue Dextran samples were injected under similar conditions.

To determine the variation of H.E.T.P. with mobile phase flowrate, the SCCR3 column with the highest H.E.T.P. value (column 6) and that with the lowest H.E.T.P. value (column 2) were used in a further experiment.

The H.E.T.P. values of glucose for these two columns were calculated for a range of flowrates from 7.4 → 214.0 $cm^3\ min^{-1}$ adjusting the sample injection size, and concentration to give an initial band concentration of ~2 mg cm^{-3}, and band volume of ~5 cm^3 in all cases, by varying the injection time between 1.5 and 10 seconds.

Using the same apparatus, but replacing the sample injection needle and sample removal needle with connections to a mercury manometer, the pressure drop for each SCCR3 column was recorded at ~200 $cm^3\ min^{-1}$, and the pressure drop for one column recorded at several flowrates.

6.2.3 Results and Discussion

The reproducibility of the experimental techniques for determination of V_o, V_i, and H.E.T.P. values was found to be good. V_o and V_i values varied by <1% and H.E.T.P. values by <3% from comparison of results obtained for one column under the same operating conditions. A slightly larger variation in these values was obtained when the sample volume and concentration were varied at the same flowrate. V_o and V_i values varied by <2%, and H.E.T.P. values by <5%, in this case. The former variations would be expected to apply from the results obtained for comparison of the SCCR3 columns at ~50 $cm^3\ min^{-1}$ as these were obtained using the same sample volume and concentration. However, variations at least as large as the latter

case would be expected to apply for the results of H.E.T.P. variation with flowrate. This is because any errors associated with the use of high flowrates would be additive to the errors associated with changes of sample volume and concentration.

V_o and V_i values (FIG. 6.9) for the SCCR3 columns varied by 8% and 17% respectively, for twenty columns, and by 5.2% and 9.4% for the ten column series used in later work:- 1,6,7,8,12,13,14,15,17,19 . The variation in V_o values is not unreasonable, considering the wide size range of the packing would tend to produce less uniform packing than a narrower size range. The magnitude of the variation in V_i values suggests that the ratio of pore volume to volume of solid silica may not be constant for the packing used, or, more likely, that the amount of packing varies from column to column, due to variations in packing density. Although there is significant variation in V_o and V_i values for individual columns, this is greatly reduced when the separating section (nineteen or nine columns) is considered as a whole. Then the maximum variation in V_o is 0.8% and 1.2% for the nineteen and nine columns respectively. Corresponding V_i values vary by 1.7% and 1.9%.

Pressure drop readings for the columns, recorded at 200 cm^3 min^{-1}, are also given in FIG. 6.9. These show a variation of 32% for the twenty column series and 15% for the ten column series used in this research, which highlights the difficulty of obtaining reproducible packing for a series of columns when the packing has a wide particle size range.

H.E.T.P. values for the SCCR3 columns, recorded at 50 cm^3 min^{-1}, are tabulated in FIG. 6.9. The values were calculated from EQUATION 4.11, which allows for extra-column dispersion in the detection system. The column fittings may cause the slight skewing of the samples, apparent from the results given in FIG. 6.9, although kurtosis values show that the majority of peaks do not differ significantly from the usual Gaussian shape (kurtosis = 0.0).

Figure 6.9 Comparison of Individual SCCR3 Columns

Column Number	Pressure Drop Across the Column $kN\,m^{-2}$	Interstitial Volume (V_o) cm^3	Pore Volume (V_i) cm^3	H.E.T.P cm	Skew	Kurtosis
1 *	28·3	544	622	0·67	0·349	0·006
2	24·1	531	612	0·90	0·319	-0·156
3	21·4	572	565	0·72	0·355	0·492
4	26·2	564	590	0·83	0·433	0·118
5	24·1	526	622	0·78	0·378	0·034
6 *	30·3	531	658	0·60	0·462	0·266
7 *	26·9	556	596	0·70	0·478	0·518
8 *	28·3	551	642	0·66	0·263	-0·099
9	21·4	563	608	0·72	0·418	0·011
10	25·5	533	667	0·75	0·298	-0·043
11	26·9	538	625	0·79	0·424	0·086
12 *	29·0	540	636	0·63	0·385	0·162
13 *	29·0	534	610	0·64	0·490	0·198
14 *	31·7	527	643	0·74	0·526	0·369
15 *	27·6	534	621	0·58	0·460	0·015
16	23·4	542	679	0·75	0·302	-0·144
17 *	28·3	529	635	0·64	0·340	0·115
18	28·3	535	623	0·74	0·346	0·147
19 *	28·3	533	619	0·65	0·382	0·039
20	27·6	534	626	0·93	0·468	0·224
AVERAGE	26·9	541	625	0·72	0·372	0·118
* Denotes Column used in 10 Column Series						

The ten columns having the lowest H.E.T.P. values were used as the ten column series for SCCR3 runs with the exception of RUN 10-500 - 0.5. It is interesting to note that the columns giving lowest H.E.T.P. values on average produced the highest pressure drop readings. The average pressure drop for the ten columns is 28.9 kN m^{-2} compared to an average of 26.9 kN m^{-2} for all the columns. This suggests that a more tightly-packed column gives more efficient chromatographic performance.

Values of H.E.T.P. recorded at various flowrates for columns 6 and 2 are given in FIG. 6.10. In this case the AutoAnalyser contribution to peak variance was often significant, especially when the channel producing the greater sample dispersion was used. FIG. 6.10 shows that the eluted samples are skewed and the skew increases with increasing flowrate. The skew may in part be caused by non-equilibrium effects or extra-column dispersion caused by the column fittings, although a more thorough study would be needed to clarify this point. Readings of kurtosis (FIG. 6.10) indicate that the chromatograms often differ significantly in shape from the usual Gaussian profile.

FIG. 6.11 illustrates the variation of H.E.T.P. with flowrate for the SCCR3 columns graphically. The shaded area represents the range of H.E.T.P. values expected for all of the SCCR3 columns, as columns 2 and 6 are representative of the highest, and lowest, H.E.T.P. values respectively. It is interesting to note that the H.E.T.P. values converge at higher flowrates, indicating that the column to column variation in H.E.T.P. would be slight under these conditions. Also, when the SCCR3 unit is used at high solute concentration (SECTION 7.4) the H.E.T.P. values of individual columns would be expected to increase, and the column to column variation in H.E.T.P. to diminish. This effect has been recorded experimentally by Deeble (29).

Figure 6.10 Variation of H.E.T.P. with Flowrate for SCCR3 Columns

Column No.	Flowrate/c.s.a	H.E.T.P.	Skew	Kurtosis
	$cm^3 min^{-1} cm^{-2}$	cm		
6	0·75	0·39	0·274	0·989
6	2·52	0·60	0·462	0·266
6	6·03	1·42	0·607	0·482
6	10·8	2·12	0·781	0·891
2	2·52	0·90	0·319	−0·156
2	6·03	1·52	0·599	0·501
2	10·6	2·12	0·732	0·652

Figure 6.11 Variation of H.E.T.P with Flowrate for SCCR3 Columns

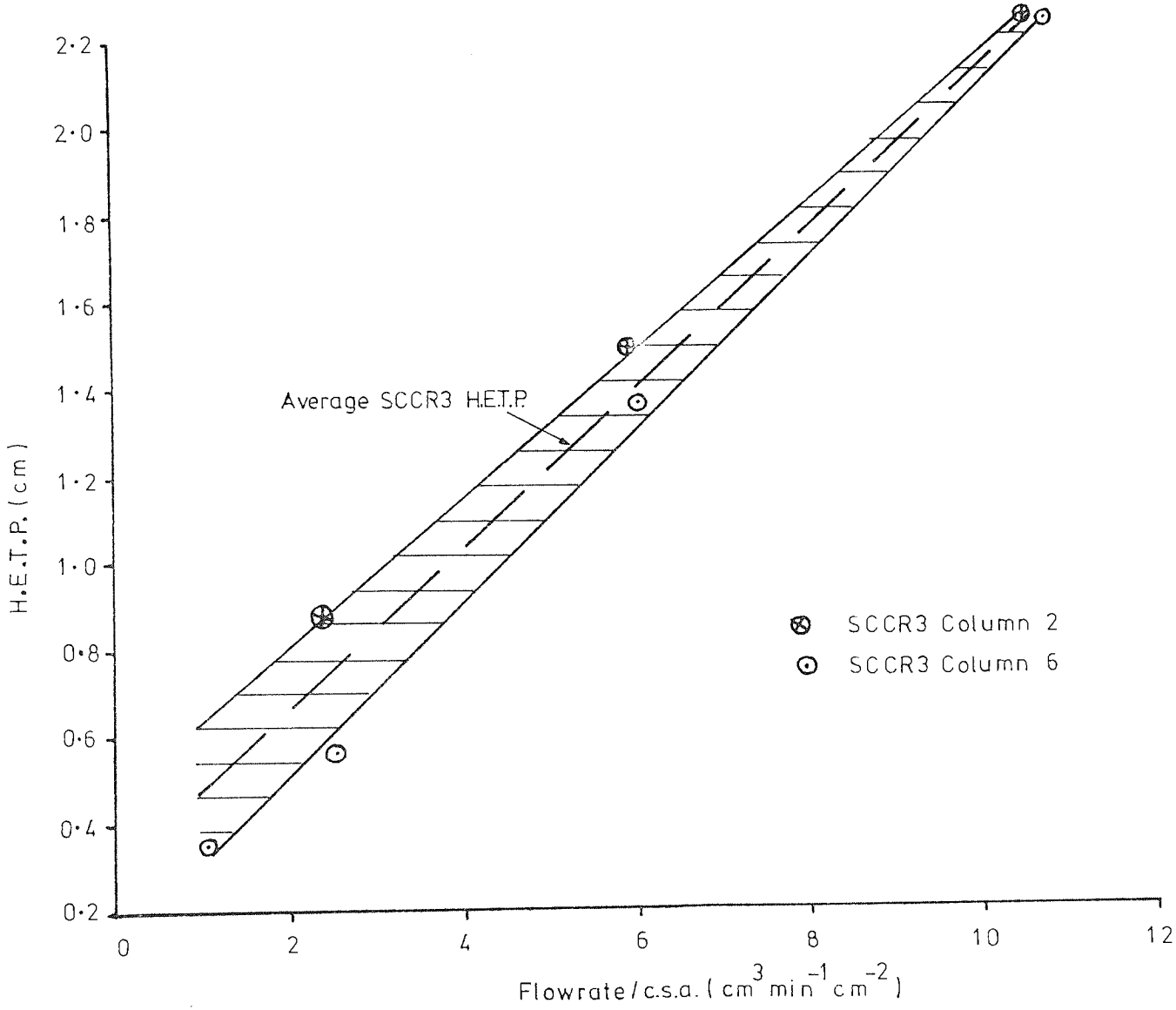

6.3 CALIBRATION OF OTHER SCCR3 EQUIPMENT

The QVF pipe section used to measure the mobile phase/purge inlet flowrates to the SCCR3 machine (SECTION 5.3.3) was fitted with a 50 cm long scale. The weights of water required to fill the column between recorded scale intervals (~5 cm) were measured, over the scale range and checked by weighing the water required to fill the column between the top and bottom of the scale. The difference between the two measurements was 0.6%.

Pressure gauges were calibrated using a dead weight pressure gauge tester, manufactured by Bryans Aeroequipment Ltd., Mitcham Junction, Surrey, and gave readings ±7 kN m^{-2}.

Calibration curves for the SCCR3 metering pumps were supplied by the manufacturers. These were useful for adjusting the pump strokes, approximately, to the desired flowrates, although accurate adjustment was carried out in situ for each run. This was necessary as the metered flow at a fixed setting was found to vary when the pump was switched off for long periods. It was also found that the metered flowrate of the feed pump dropped significantly as the concentration of dextran was increased. With this pump the maximum dextran concentration that could be metered at a constant rate was found to be approximately 20% w/v, probably due to the high viscosity of the feed solution. Nominal throughputs for the SCCR3 pumps, based on readings taken during operation, are given in APPENDIX 1.

Measurement of the flowrates into and out of the SCCR3 machine were checked by means of a liquid mass balance, using water for all input streams at typical flowrates. Measurement of the total liquid flow in the separating section, i.e. mobile phase + feed, was found to differ from the weighed amount leaving the machine from the separating section by <1%, if all flowrates were measured over a suitable time

period (~5 minutes). Measurement of the purge inlet flowrate was found to differ from the weighed liquid output from the purge section by ~2% at a typical flowrate of 200 cm^3 min^{-1}, measurements being carried out over a 5 minute time period.

Calibration of the timing unit was carried out using a stop watch. At the maximum end of the timing range this calibration was found to alter over long periods of time. For example a timer setting which produced a timing interval of 18 minutes at the start of the research period dropped to 17 minutes during the first two months of operation. However, the value remained approximately constant after this. The calibration curve, shown in APPENDIX 1, was used to set the time approximately, and accurate adjustment was carried out in situ at the start of each run. Variation during a run was found to be <1%.

6.4 PRELIMINARY DEXTRAN FRACTIONATIONS

The aims of preliminary runs carried out with the SCCR3 machine may be summarized:

(i) To ensure that liquid inputs to the SCCR3 machine travelled in the correct directions, which necessitated the valves to be functioning correctly. This was tested by means of a liquid balance for the unit.

(ii) To establish if the concentrations and molecular weight distributions of products from the SCCR3 machine reached pseudo-equilibrium values, and the approximate number of cycles of the machine to achieve pseudo-equilibrium operation.

(iii) To determine if the product M.W. distributions were as expected from theoretical predictions of the operating conditions (SECTION 7.3).

(iv) To determine if the total dextran content and molecular weight distributions of the products, when summed, matched their values in the original feed solution.

(v) Generally, to ensure that the equipment was operating satisfactorily by means of frequent checks, e.g. checks for valve leakage, and inconsistency in the pump flowrates.

One disadvantage of the mobile phase/purge metering pump was discovered during the preliminary runs, when the machine was shut down overnight. The mobile phase flowrate before and after the shut-down period differed by up to 10%. This could possibly be due to the pump parts cooling during the shut down period, and was substantially overcome by running the pump in a re-cycle mode, to allow it to 'warm up', before connection to the SCCR3 machine.

Until experience was gained with the SCCR3 unit, accurate adjustment of the solenoid valves was found to be difficult. This was because the complex nature of the SCCR3 flow lines made identification of the particular valve that was leaking difficult, and the preliminary runs were used to test the technique employed. In practice, experience with the SCCR3 machine enabled a maladjusted valve to be identified quickly, and corrected, although with experience the valves seldom required further adjustment after their initial setting. This was usually found to be necessary only if the pressure in the separating section increased substantially during a run to >515 kN m^{-2} (60 psig).

Three preliminary dextran fractionations were carried out, increasing the time of operation of the SCCR3 machine in each case while maintaining the operating conditions essentially constant. The average conditions may be summarized:

MOBILE PHASE FLOWRATE	65 cm^3 min^{-1}
FEED FLOWRATE	9 cm^3 min^{-1}
PURGE FLOWRATE	170-370 cm^3 min^{-1}
SWITCHING INTERVAL	12 min
FEED COMPOSITION	10% w/v DEXTRAN 40 (BATCH No. BT 85)
NO. OF COLUMNS	20
TIME OF RUN	12,16,28 hrs.

Samples of the products were collected during the runs for periods up to one hour, and the concentration of dextran in these samples was found to increase as the run progressed. However, none of the runs was of sufficient length to establish reproducible, successive, cycles, and the overall rate of dextran leaving the machine was less than

the average dextran input rate. The M.W. distributions of the samples also varied considerably, which is reflected in the change of mean K_D values for the products:

PRODUCT 1	$K_D = 0.25 \rightarrow 0.4$
PRODUCT 2	$K_D = 0.5 \rightarrow 0.65$

Some of this variation is due to fluctuations in the operating conditions, due to inaccurate settings of the valves and the variation in mobile phase flowrate discussed earlier in this section. Also samples were taken at widely-different positions in the SCCR3 cycle, and at widely-different time intervals, which may contribute to the variation in observed product distributions. However, the samples showed that a good fractionation of the feed was being obtained in the SCCR3 machine, and that the separation position was in approximately the expected area. However, future experimental runs would need to be longer to attain pseudo-equilibrium operation.

By the end of the preliminary runs operational experience gained with the SCCR3 unit indicated that the valves could be adjusted accurately in situ, and would operate reliably for long periods of time, and that the unit was generally operating satisfactorily.

CHAPTER 7

Operation of the SCCR3 Unit in the Continuous Mode

7.1 EXPERIMENTAL METHODS

7.1.1 Handling of Dextran

The growth of moulds, bacteria, and other micro-organisms in dextran solutions is a common problem, and one recommended preventative procedure is to add sodium azide (NaN_3) to the dextran solution at a concentration of 0.02% w/w (240). However, care must be taken when handling sodium azide because solutions are toxic by skin absorption.

Also the azides of heavy metals can be explosive if subjected to mechanical shock, and solutions of azides liberate poisonous fumes of hydrazoic acid (HN_3) when acidified. Consequently, dissolving sodium azide to form a stock solution was carried out in a fume cupboard, with the usual laboratory precautions, and dilution of the solution carried out as required.

Dextran feed for the SCCR3 machine was made up as a solution of Dextran 40 powder, and sodium azide, in distilled water. A batch of feed was usually made up before each fractionation run, in sufficient quantity for the length of time of the run.

The ease of dissolving the dextran powder varied depending on the particular batch. This was possibly because the dryness of each batch varied. Raised temperatures were found to be necessary for dissolving batch No. BT 192 B/M, but batch No. BT 185 B/M dissolved readily at room temperature. The use of raised temperature was a recommended procedure (241).

The apparatus used when heating was required consisted of a 50ℓ QVF spherical vessel resting in an isomantle and fitted with a stirrer and thermometer. The ingredients for the feed solution were introduced through the large inlet neck, and the final solution run off via an outlet tap attached to the base of the vessel.

A measured amount of water and sodium azide stock solution was placed in the vessel and heated to 90°C, when the heaters were turned off. A weighed amount of dextran powder was added gradually, with stirring until it dissolved, and the solution run off and allowed to cool. The dextran powder was found to dissolve readily up to the maximum concentration used in the research programme (~20% w/v), when this method was employed.

Occasionally a small amount of insoluble matter remained in the solution, and was removed by decantation. Any residual matter was removed by a filter in the feed inlet line to the SCCR3 machine.

All vessels used for handling dextran solutions were first cleaned with detergent solution, and then soaked in a solution of Decon 90 (surface active cleaning agent) overnight, and finally thoroughly rinsed with distilled water before use. No microbiological growth was detected during the research programme after these measures had been employed.

7.1.2 Start-up/Shut-down Procedures

The time of operation of the SCCR3 machine in the fractionating mode varied between 28.4 hours and 94.3 hours per experimental run, during the research programme, although frequently an operational time of approximately 40 hours was used. It was not convenient to operate the machine continuously for such long time periods, and consequently operation was restricted to approximately 8-10 hours every day. When running equipment in this manner, and treating the run as a continuous operation, it is obviously necessary to establish that no substantial change occurs during the period that the equipment is shut down.

This was the first fact that was established before the major experimental programme was started. Both the internal concentrations

and product concentrations for samples taken immediately before shut-down and after start-up indicated that no substantial change had occurred. Also, the product concentrations reached pseudo-equilibrium values, which seemed to be unaffected by shut-downs, for the experimental runs (SECTION 7.4.2.2).

The shut-down procedure employed consisted essentially of switching off the pumps and immediately closing the inlet taps from the reservoirs to stop liquids 'syphoning' through the machine. The timing unit was then switched to manual operation, which effectively stopped the valves switching but retained them in the same operating condition. In this manner, no liquid input to the machine was possible, and the only likely detrimental effect was diffusion of dextran in individual columns, or through the transfer lines between columns. The former could only have a limited affect on the system as a whole, while the latter was not thought likely to have a significant effect, because of the restriction imposed by the narrow liquid transfer lines.

The details of the start-up and shut-down procedures are as follows:

(i) At the end of every experimental run the valves, pumps, and timer were switched off, and the following routine maintenance procedures were carried out. The feed reservoirs and filters were removed and cleaned thoroughly. The latter often needed soaking in chromic acid for several days, and consequently two filters were used, and changed over as required. The feed inlet lines to the SCCR3 columns were flushed out with distilled water, and the septums in the sampling T-pieces were replaced as needed.

(ii) If the valve tubes had been replaced (SECTION 7.1.3) it was necessary to re-set the valves before the next experimental run.

In practice the best method was found to be setting the valves by gradual adjustment of all of them in situ, when pumping mobile phase and purge into the machine. This was carried out, using the flow indicators, until all valves appeared to seal, and was checked, by carrying out a liquid balance for the machine, at the estimated operating pressure.

(iii) All visible air in the lines and columns was removed by purging each column, individually, at high pressure (~350 kN m^{-2}).

(iv) The fraction collector was set to collect products as required.

(v) The switching unit was set approximately to the desired time interval using the calibration chart (FIG. A.1.2 in APPENDIX 1) and finely adjusted using a stop-watch.

(vi) The mobile phase and purge pumps were set to the required flowrate for the fractionation run to be undertaken. This was done, using the flow measurement technique outlined in SECTION 5.3.3, while pumping water into the SCCR3 machine. If the required back pressures, necessary to ensure that the non-return valves in the pumps were seating correctly, were not obtained in this way, they were induced by partially restricting the flow lines with screw clips. The feed pump was set with the outlet line arranged to re-cycle feed back to the reservoirs, as input of feed to the SCCR3 machine was not carried out until the start of the run. Back-pressure was again induced using a screw clip on the flow line.

(vii) The feed inlet lines were filled with feed solution, when isolated from the columns, and then connected to the columns for the run to start. The pumps and timing unit were started simultaneously to begin the run, and the timing unit switched to automatic operation.

7.1.3 Maintenance of Valves

Routine maintenance of the solenoid valves was carried out at regular intervals. This maintenance involved inspection of the valves for metal corrosion and general damage, and inspection of the valve tubes for wear. Any corroded metal parts were dismantled and the rust removed with fine glass paper, the parts being greased before re-assembly. However, metal corrosion was rare, and the major maintenance problem was concerned with renewing the valve tubes.

It is extremely difficult to define an average 'life' for an SCCR3 valve tube, as this is dependent on the following variables:-

(i) the internal tube pressures

(ii) the fraction of time that the valve is energized

(iii) the rate of on/off operations of the valve

(iv) the degree of adjustment of the cut-off assembly

However, during operation of the SCCR3 machine it was found advantageous to change the feed and multi-port valve tubes either after every one, or every two, experimental runs. This ensured that virtually no tubes needed to be changed during a run. The transfer valve tubes were only changed as required because of their long life time, each valve only being energized for less than one-tenth of the time for which the feed and multi-port valves were energized.

Changing a valve tube during a run, when necessary, was carried out after shutting down the system in the manner outlined in SECTION 7.1.2. Liquid loss was usually small, as the leak was sealed immediately after shutting down the system, before the tube was changed. In practice, a tube could usually be changed and the valve reset in less than two minutes. Before re-starting the run, the timing unit was re-set

to the same position in the switching interval, but, as the tube failures usually occurred at the end of a switching interval (i.e. at an on/off operation of the valve), this did not present a problem. Any new tube placed in a valve was first greased with silicone grease, as was the cut-off assembly during routine maintenance.

The valves required little attention during operation, and only rarely was further adjustment required after they had been set at start-up. However, periodic checks of the flow indicators were carried out to establish that the valves were operating correctly. If one of the valves was thought to be leaking, it was also found useful to measure point pressures around the SCCR3 machine, in the area of the suspect valve. This was carried out by inserting a hypodermic needle, connected to a pressure gauge using an adapted Luer fitting.

7.1.4 Sampling Techniques

The maximum product flowrates obtained during the research period were 200 cm^3 min^{-1} and 75 cm^3 min^{-1} for the low M.W. product (purged product), and high M.W. product (mobile phase product), respectively. Bulk samples of both products were collected in plastic containers of 80 litres, and 10 or 25 litres, capacity for the purged product, and mobile phase product, respectively.

The usual procedure was to collect the products from one or two complete cycles of the SCCR3 machine, and then to switch over containers, using the fraction collector (SECTION 5.3.2), to collect products from the next one or two cycles. In this way representative bulk samples were obtained, corresponding to regular operating periods of the machine. These samples were weighed, and, after being thoroughly mixed, small samples were removed for determination of concentration and M.W. distribution.

If a product flowrate was required immediately, however, the usual procedure was to collect the product for a short time interval, and weigh it. Products were usually sufficiently dilute to assume an approximate density of unity for this case. This method was used when checking if a valve was leaking by carrying out a liquid mass balance for the machine, while the former method was used for carrying out an overall liquid mass balance for the run.

Point samples were taken from the SCCR3 machine using a 1 cm^3 plastic syringe, and sampling from the sample T-pieces placed in the transfer lines between each pair of columns. These were analysed for concentration, and allowed a concentration profile around the machine to be plotted at a given time. The SCCR3 machine was maintained in the shut-down position while these samples were taken. 0.5-1.0 cm^3 of sample was usually taken from each sampling T-piece, after first cleaning out the syringe with a preliminary quantity of the sample.

After completion of the operating period for each experimental run, the mobile phase and feed pumps were disconnected from the machine, and one cycle of the timing unit was carried out manually, allowing approximately fifteen minutes in each position. During these fifteen minute periods the solution in each column was purged out at a high purge flowrate (~250 $cm^3\ min^{-1}$), using the usual purge pump. Thus representative samples of material present in each column at the end of a run were obtained. These were weighed, and small samples removed, after thorough mixing, for determination of concentration and M.W. distribution.

Small samples of all products, and samples collected during a run, as well as of the feed solution were taken and stored in a fridge at a temperature below 5°C.

7.1.5 Analysis of Samples

7.1.5.1 Determination of Sample Dextran Concentration

All dextran sample concentrations were determined using the cysteine/sulphuric acid AutoAnalyser assay discussed in SECTION 4.2.1. As the maximum dextran concentration that this unit can measure, within its linear range, is 0.06 mg cm^{-3}, all samples of greater concentration were diluted before analysis. In practice this often required a dilution factor up to 10,000. Dilution was carried out using calibrated micro-pipettes (50 µl-250 µl) and volumetric flasks (10 cm^3-500 cm^3). The pipettes were re-calibrated by measuring the volume of solution that they contained, not the amount which they delivered. This was necessary as the volume delivered was found to vary with dextran concentration, because at higher sample viscosities more liquid was retained, on the walls of the pipette, after delivery of the solution. Each pipette was filled with a glucose solution of known concentration. The contents of the pipette were blown into a volumetric flask, and the pipette washed several times with distilled water. After each washing the liquid in the pipette was also blown into the volumetric flask. This ensured that all of the initial solution in the micro-pipette was transferred to the volumetric flask, which was then filled with distilled water. The concentration of the resulting solution was then determined by comparing its response to that of a glucose standard of known concentration, using the cysteine/sulphuric acid assay. The calculated dilution factor of the original solution thus enabled the micro-pipette volume to be determined. The above procedure for emptying a micro-pipette was used for all determinations of sample concentration. The volumetric flasks were calibrated by weighing the volume of water required to fill each one.

7.1.5.2 Determination of Sample Dextran Molecular Weight Distribution

M.W. distributions were determined by g.p.c., using the

analytical column, and analytical procedures, described in CHAPTER 4. However, this method had the disadvantage of requiring approximately 3-4 hours for each sample analysis at a flowrate of ~0.1 cm^3 min^{-1}. Although operation at this flowrate gave a more accurate measure of sample distribution than operation at a flowrate of ~0.2 cm^3 min^{-1}, it was necessary to analyse some samples at the faster flowrate to shorten the analysis time. One disadvantage of this was the fact that the measured elution volume changed with increasing flowrate (SECTION 4.3.4.2) and it was necessary to subtract a constant factor of 0.027 R.F. units from the observed R.F. values at the faster flowrate. In practice samples of bulk products from the SCCR3 machine were analysed at a flowrate of 0.1 cm^3 min^{-1} to obtain the most accurate measure of their M.W. distributions possible for calculation of a dextran mass balance (SECTION 7.2.2). Analyses of other samples were usually carried out at 0.2 cm^3 min^{-1}, when the mean molecular weight only was required.

The sample distributions were plotted with K_D as the abscissa, which may be related to molecular weight by the calibration curve for the analytical column used (FIG. 4.6). However, even using an efficient column at slow flowrates does not produce a perfect analysis. This is because of band broadening occurring during passage through the column, which spreads the sample zone. This has the effect of spreading the individual components of a distribution, and the effect is most obvious at the extremes of the distribution where molecules appear to have K_D values outside the theoretical range of 0-1. It is obviously not possible to relate molecular weight values to these regions of the distribution, but an estimate of the molecular weight of the mean of the distribution may be made more accurately, as spreading of molecules on both sides of the mean will tend to cancel out. The accuracy of the analysis is further discussed in SECTION 7.2.3.

Sample distributions in this study are plotted as normalized optical density (O.D.) against distribution coefficient (K_D). The normalization of O.D. was carried out in order to scale each sample to the required area, based on its dextran rate from the SCCR3 unit (SECTION 7.2.3).

7.2 DATA RECORDED DURING SCCR3 RUNS

7.2.1 Liquid Flowrates

Frequent measurement of liquid inlet and outlet flowrates to the SCCR3 machine was necessary to ensure that the pumps and the valves were operating correctly. A liquid balance was usually determined twice per cycle of the machine, to ensure that liquids were flowing at a constant rate and in the correct direction. An overall liquid balance was also determined for every cycle, or two cycles, of the machine, by weighing the bulk products collected in this period, and comparing them with the average inlet flowrates during the same time interval.

The feed flowrate was measured at least five times per cycle of the SCCR3 machine, and the average value taken as the flowrate during the cycle. The average mobile phase flowrate for each cycle, or two cycles, of the SCCR3 machine was taken as the total mobile phase flowrate, determined by weighing the bulk product 1 sample collected during this period, minus the average feed flowrate for the same period. These values of mobile phase and feed flowrates were taken as the average flowrates through the separating section of the SCCR3 machine, during the period of collection of product 1 for which they were measured. It was necessary to measure the average mobile phase flowrate in this manner, because it did not remain constant over long periods of operation (SECTION 7.4.2.2).

Average product 2 flowrates were measured by weighing bulk samples collected during one, or two, cycles of the SCCR3 machine.

7.2.2 Dextran Mass Balance

Performance of a material balance is a fundamental requirement if a detailed study of a production operation is to be undertaken. Dextran mass balances were carried out for each complete cycle, or two

cycles, of the SCCR3 machine. These were based on the analysis of bulk samples collected from the machine, and calculation of the average dextran input, based on an average feed flowrate and known feed concentration, during these periods. The dextran mass balance was used as a criterion for the attainment of reproducible conditions during successive cycles, or pairs of cycles, of the SCCR3 machine. This can be seen from FIG. 7.1 which represents the general shape of the variation of dextran input and output, to the SCCR3 unit, with time. Reproducible conditions are indicated by the plateau regions of these curves, when an input/output dextran balance is obtained. The shaded area of FIG. 7.1 represents the dextran hold-up of the SCCR3 machine.

7.2.3 Dextran Molecular Weight Balance

Another criterion for deciding if reproducible operation of the SCCR3 machine had been obtained was provided by a molecular weight balance of material into, and out of, the machine. To carry out this balance it was necessary to scale the feed and product chromatograms to areas corresponding to their respective relative dextran rates (g min^{-1}). For example, if the feed input rate was 10 g min^{-1}, and the high M.W. and low M.W. product outlet rates were 3 g min^{-1} and 7 g min^{-1} respectively, the feed chromatogram would be scaled to an area of 1 R.F.-O.D. unit, and the two product chromatograms to an area of 0.3 and 0.7 R.F.-O.D. units respectively. If the distributions of the two products, added together, equal the feed distribution, then a dextran M.W. distribution balance is obtained. An example is illustrated in FIG. 7.2.

The M.W. distribution balance ignoresthe fact that zone broadening during passage through the analytical column may affect the sum of the product distributions to a greater extent than the feed distribution, because the sum of the product distributions is obtained

Figure 7.1 General Shape of the Variation of Product Dextran Rates with Time for the SCCR3 Unit

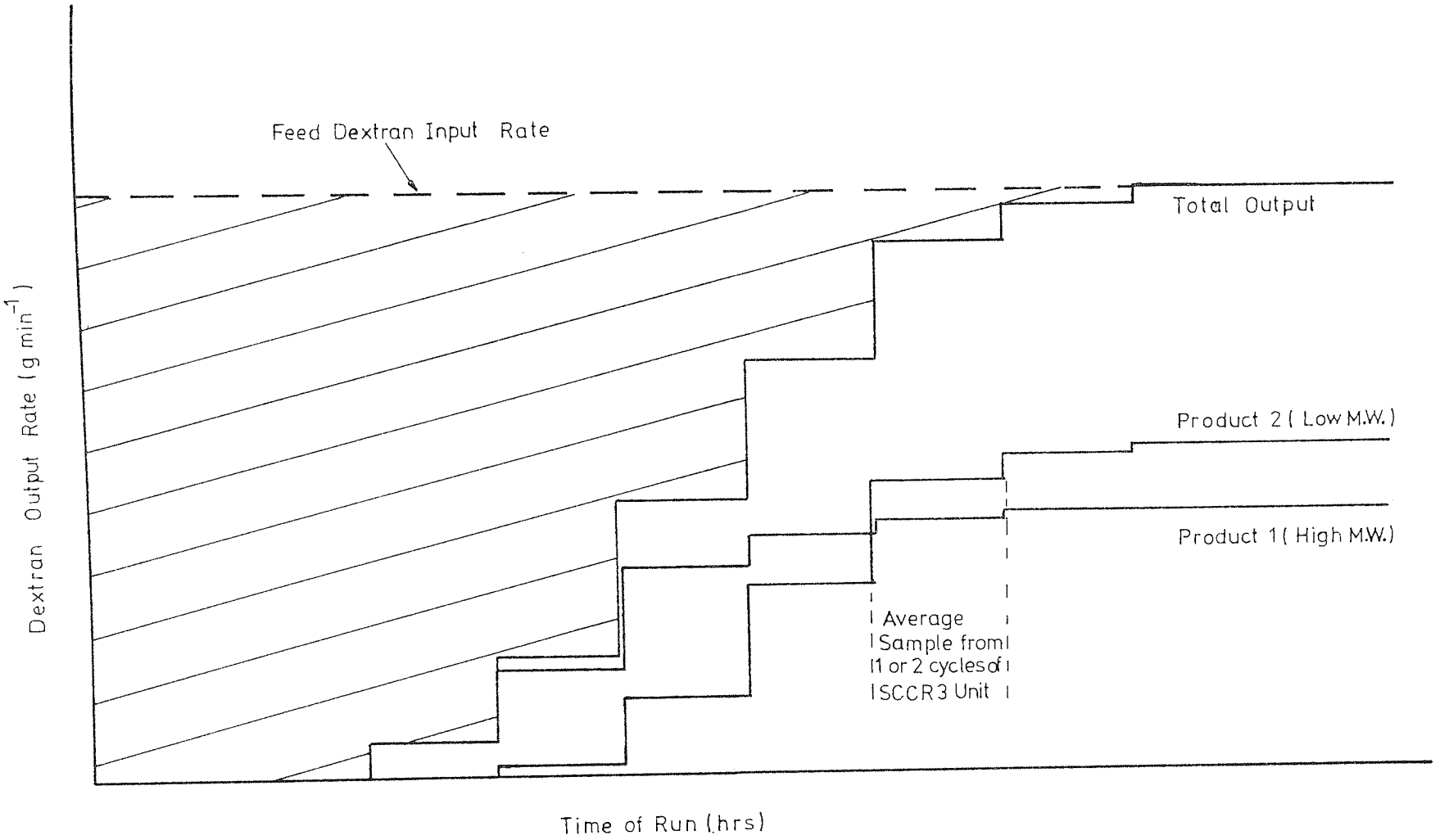

Figure 7.2 An Example of the Comparison of Feed and Product Distributions for the SCCR3 Unit

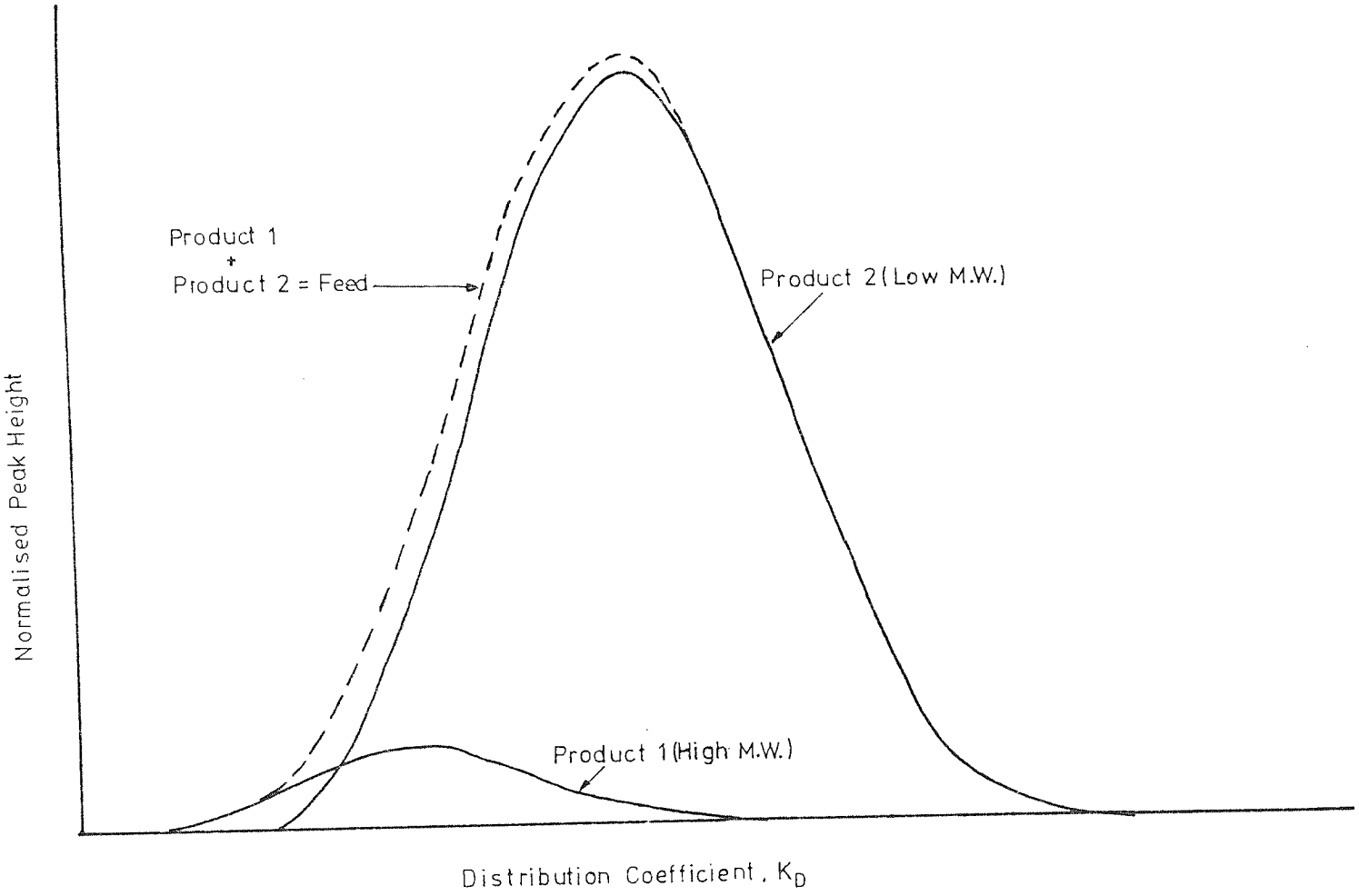

by two passes through the column, one for each product, while analysis of the feed only requires one pass. In practice however, this was not found to have a significant effect for the greater part of the distribution, although slight differences were noted occasionally at the ends. This was probably because, in the bulk of the distribution, spreading effects tend to cancel each other out, and also small variations in one product have an insignificant effect on the summed distribution. When contributions to the ends of the summed product distribution are made by both products, the overlap would be most noticeable, whereas, if the summed distribution received contributions from only one product in these areas, the agreement with the feed should be good. A typical calculation of a chromatogram scaling factor is given in APPENDIX 3.

7.2.4 Dextran Concentration and Molecular Weight Distribution Profiles

Direct analysis of samples taken from the transfer lines between columns (SECTION 7.1.4) proved an unreliable technique, on certain occasions, notably when high feed concentrations, ~ 20% w/v dextran, were used. There are several possible reasons to account for observed oscillations in point sample concentrations. The first is that these oscillations in concentration are actually present throughout the SCCR3 machine. This is possible, as it is expected that the K_D of a molecular species changes with concentration, which would be particularly noticeable at high feed concentrations and may cause localized peaks and troughs in the concentration profile, due to molecular species changing their effective migration rates through the SCCR3 machine with variations in the concentration that they experience. Also, changes in the operating flowrates in the separating section could result in variations in migration rates. However, it is notknown if the size of the fluctuations expected by these mechanisms would account for some of the (large) measured variations.

Another explanation is that these point samples were not representative of material present within the SCCR3 columns. This could be caused by liquid hold-up in the column end fittings and transfer lines, or slight leaking of material into a transfer line from a part of the SCCR3 machine at a higher pressure. Again the first of these mechanisms would not be expected to account for large fluctuations in concentration, but the second could, under certain circumstances, produce very large changes. One such circumstance would be 'surging' of concentrated dextran solution, or water, from the feed or mobile phase input lines, at each valve sequencing action, into the transfer lines, because of the finite time that the valves take to close. Another circumstance could be slight leakage of fluid into the transfer lines in a continuous manner, which, although it might be very small in absolute terms, could have a significant effect on any sample taken in the area where this leakage was occurring.

To establish the cause for concentration fluctuations of this kind would necessitate samples to be taken from a point within a packed column. As this facility had not been built into the SCCR3 machine, because addition of sample points in the columns would weaken the glass and lower the maximum safe operating pressure, it was necessary to obtain a more reliable sampling technique. Point sample analyses were only used for RUNS 10-500-0.5, and 01-600-0.7, using feed concentrations of 10.1% and 1.02% w/v dextran respectively, when oscillations in measured concentrations were not observed.

Data for calculation of the concentration profile around the SCCR3 machine was usually obtained from analysis of samples purged from individual columns at the end of an experimental run. The concentration of dextran in each sample was determined, and multiplied by the measured sample volume, to give the weight of dextran in each

column. The volume available to each sample, before purging from its respective column, was estimated from a knowledge of the mean K_D of the sample, determined by g.p.c. analysis, and the characteristics, V_o and V_i, of the particular column. This enabled the on-column sample concentration, in the SCCR3 machine, to be calculated. A typical calculation is given in APPENDIX 3. Taking the K_D corresponding to the 50% cumulative weight point as representative of the average molecular size of the sample was thought to be a reasonable assumption, as the peaks were approximately symmetrical about this point. FIG. 7.3 represents the form of concentration profile obtained when the majority of the feed input travels with the packing, during fractionation in the SCCR3 machine. An approximate mirror-image of this profile is obtained if operating conditions are set to send the majority of the feed with the mobile phase. The plateau region of the profile represents a region of the SCCR3 machine where little, or no, fractionation is being achieved. This effect is discussed in SECTION 7.4.3.1. The fall of concentration at the low M.W. end of FIG. 7.3 is caused by dilution occurring in the column immediately before the purge column, because the mobile phase enters the machine in this column. The gradual fall of concentration, at the high M.W. end of FIG. 7.3, is caused by dilution in this region, because, after the purge column is purged of low M.W. dextran material, and in the process is filled with water, it 'advances' towards the low M.W. end of the separating section with the sequencing action of the machine. The effect of this column is greatest in the first switch after it is purged, as it is then full of water. After each subsequent switch its effect is lessened because the concentration in this column is gradually increased in the advancing high M.W. dextran material. Any point concentration fluctuations that may occur are smoothed when analysis of a sample taken from a whole column is carried out.

Figure 7.3 An Example of the SCCR3 Concentration and Molecular Weight Distribution Profiles for Fractionation of Dextran 40

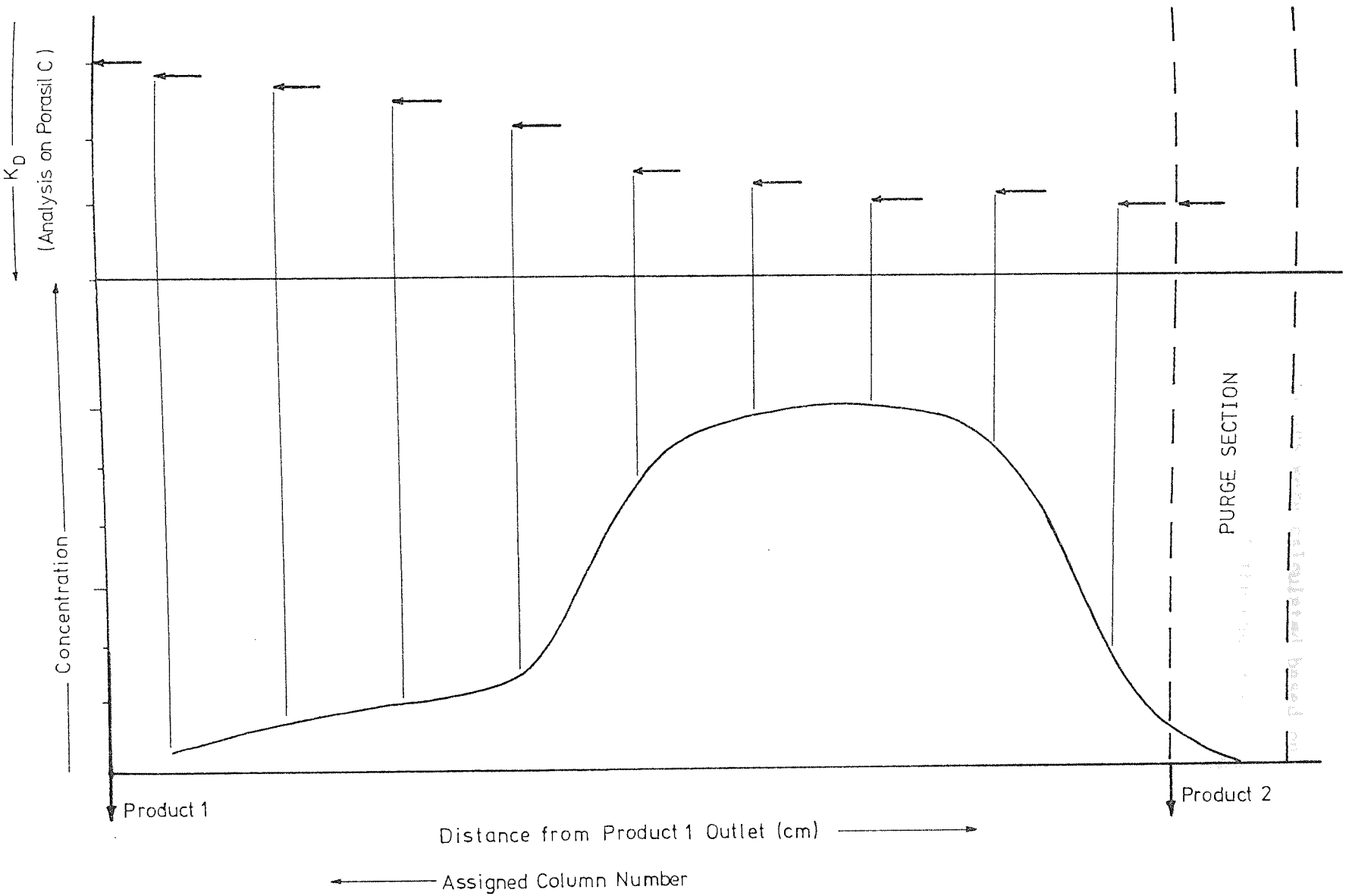

Sample distribution profiles were calculated based on analysis of samples purged from each column at the end of each experimental run. In practice, to reduce analysis time, these samples were usually analysed at ~0.2 cm^3 min^{-1}. This effectively produced'broader' sample chromatograms (7.1.5.2), and therefore a less accurate measure of sample distribution. Thus, when samples were analysed under these conditions, the mean of each sample distribution only was used (FIG. 7.3).

7.3 THE SELECTION OF EXPERIMENTAL OPERATING CONDITIONS

7.3.1 Introduction

The mechanisms of separation in chromatography were discussed fully in CHAPTERS 2 and 3. These mechanisms result in a difference in the relative migration rates of components through a batch chromatographic column. If the packing of the column is moved counter-current to the direction of mobile phase flow, and the rate of packing movement is correctly adjusted, the slowest moving component(s) can be made to travel with the packing, while the faster moving component(s) travel with the mobile phase. In essence this is the operating principle of the SCCR3 machine, although the physical movement of packing is simulated by a valve sequencing action (SECTION 5.1.2). A schematic diagram of the SCCR3 unit, illustrating the operating flowrates, is given in FIG. 7.4. The fastest moving material which has the least affinity for the stationary phase, is preferentially carried with the mobile phase and eluted at the product 1 port. The slowest moving material which has the greatest affinity for the stationary phase, is preferentially carried with the packing and eluted at the product 2 port. The following sections deal with the development of a model for the prediction of theoretical operating conditions for the separation of a multi-component, or polymer, feed into two desired products.

7.3.2 The Idealized Case

7.3.2.1 Two-Component Feed

The rate of movement of a component with the mobile phase, r_{m_i}, is proportional to the fraction of its molecules in the mobile phase at equilibrium. Similarly the rate of movement of a component with the stationary phase, r_{s_i}, is proportional to the fraction of its molecules in the stationary phase at equilibrium:

Figure 7.4 Schematic Diagram of the SCCR3 Unit

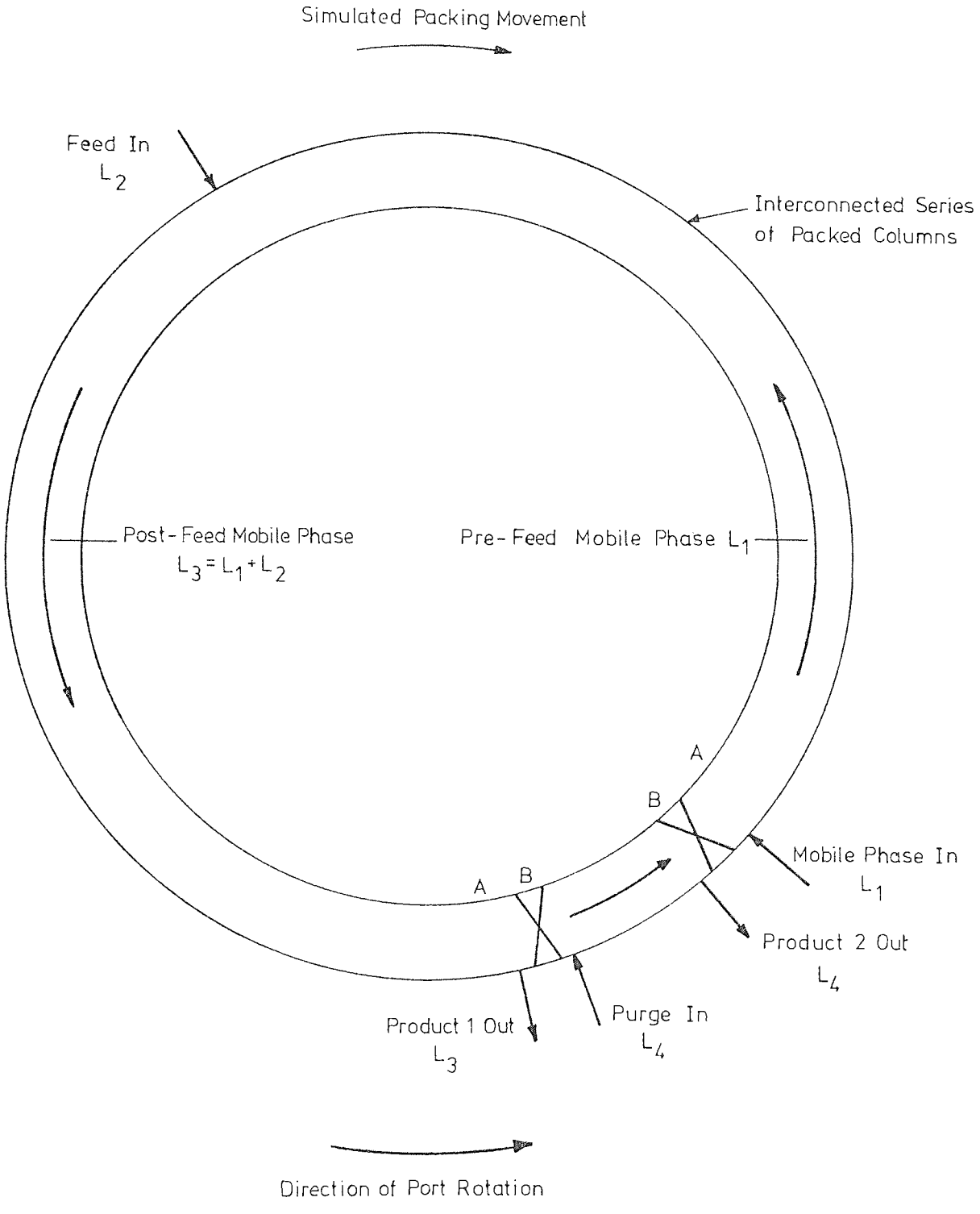

A-A Separating Section

B-B Purge Section

$$r_{m_i} = V_{m_{AV.}} \cdot \frac{A_o}{A_o + A_i K_{D_i}} \qquad (7.1)$$

$$r_{s_i} = V_{s_{AV.}} \cdot \frac{A_i K_{D_i}}{A_o + A_i K_{D_i}} \qquad (7.2)$$

$V_{m_{AV.}}$ = average velocity of mobile phase = L'/A_o

L' = effective mobile phase flowrate

$V_{s_{AV.}}$ = average velocity of stationary phase = P/A_i

P = stationary phase flowrate

A_i = average cross-sectional area of pores in column

A_o = average cross-sectional area of interstices in column

In the SCCR3 machine, movement of the stationary phase is achieved by sequencing each packed column, by one position, at the end of every switching interval. As each column contains mobile phase liquid, in addition to the stationary phase liquid within the pores, each sequencing operation also transfers a quantity of mobile phase liquid, in the direction of stationary phase movement. This reduces the effective mobile phase rate, so that:

$$L' = L_i - \frac{A_o \ell}{s} \qquad (7.3)$$

L' = effective mobile phase flowrate

$L_i = L_1$ or L_3 = recorded mobile phase flowrate

ℓ = length of one SCCR3 column

s = time of one sequencing interval

A molecule will travel preferentially with the mobile phase if $r_{m_i} > r_{s_i}$ or:

$$\frac{L'}{A_o} \cdot \frac{A_o}{A_o + A_i K_{D_i}} > \frac{P}{A_i} \cdot \frac{A_i K_{D_i}}{A_o + A_i K_{D_i}} \tag{7.4}$$

or $$\frac{L'}{P} > K_{D_i}$$

Similarly a molecule will travel preferentially with the stationary phase if:

$$\frac{L'}{P} < K_{D_i} \tag{7.5}$$

For complete separation of two components, 1 and 2:

$$K_{D_1} < \frac{L'}{P} < K_{D_2} \tag{7.6}$$

Also, component 2 is completely purged from the isolated section if:

$$L_4 > \frac{\ell(A_o + A_i K_{D_2})}{s}$$

$$\text{or } \frac{L_4'}{P} > K_{D_2} \tag{7.7}$$

$$\text{where } L_4' = L_4 - \frac{\ell A_o}{s}$$

$$P = \frac{\ell A_i}{s}$$

7.3.2.2 Multi-Component or Polymer Feed

For a multi-component feed mixture, EQUATION 7.6 still represents the condition for complete separation, and K_{D_1} and K_{D_2} now represent the K_D values for the slowest of the faster moving components, and the fastest of the slower moving components, respectively. The case of a polymer feed, such as the dextran 40 polymer used in this research, is similar to the multi-component feed case. The values of K_{D_1} and K_{D_2} refer, for a polymer, to the lowest M.W. unit of the faster-moving, high M.W. material, and the highest M.W. unit of the slower-moving, low M.W. material, respectively. However because K_{D_1} and K_{D_2} for most polymer distributions are extremely close together ($K_{D_2}/K_{D_1} < 1.001$), complete separation is impracticable. In practice a degree of overlap in the product M.W. distributions must therefore be tolerated.

7.3.3 The Practical Case

Factors which cause departures from the idealized case are:

(i) Chromatographic zone broadening.

(ii) Finite column length.

(iii) The sequential nature of operation.

(iv) Finite feed flowrate.

(v) Finite concentration effects.

7.3.3.1 Zone Broadening

Chromatographic zone broadening has been discussed in SECTION 2.2.4 and SECTION 3.3. This has the effect of causing a component with a K_D value K_{D_i} to elute from a chromatographic column over a range of K_D values, from $K_{D_i} - \delta_i$ to $K_{D_i} + \delta_i$, where $2\delta_i$ is the

total baseline peak width, in K_D units. Thus the L'/P ratio must be maintained within narrower limits for a successful separation:

$$K_{D_1} + \delta_1 < \frac{L'}{P} < K_{D_2} - \delta_2 \qquad (7.8)$$

Also, in the isolated section, the purge flowrate must be increased:

$$\frac{L'_4}{P} > K_{D_2} + \delta_2 \qquad (7.9)$$

7.3.3.2 Finite Column Length

Column length in chromatography has been discussed in SECTION 2.3.3.2. The closer together the values of K_{D_1} and K_{D_2} are, the closer they both are to the value of L'/P, and the lesser is the tendency for the components to move apart. Thus a longer column length is required, to achieve the same degree of separation, as K_{D_1} and K_{D_2} approach each other. For a finite column length this has the effect of further reducing the range of the L'/P ratio criterion for complete separation:

$$K_{D_1} + \delta_1 + \delta'_1 < \frac{L'}{P} < K_{D_2} - \delta_2 - \delta'_2 \qquad (7.10)$$

where δ' may be regarded as a function of the number of theoretical plates for the system, and would need to be determined experimentally.

7.3.3.3 The Sequential Nature of the SCCR3 Machine

The counter-current 'movement' of packing in the SCCR3 machine does not occur in a continuous manner, but rather as a step movement of one column length of packing every sequencing interval. Thus, at the

end of each sequencing interval, material is transported, in the direction of the packing movement, in a discontinuous manner, and the degree to which this discontinuity affects the system would increase as the number of columns was decreased. This has the effect of again reducing the range of the L'/P criterion:

$$K_{D_1} + \delta_1 + \delta_1' + \delta_1'' < \frac{L'}{P} < K_{D_2} - \delta_2 - \delta_2' - \delta_2'' \qquad (7.11)$$

δ_1'' and δ_2'' are factors to allow for the reduction in the limits of L'/P attributable to the sequencing action of the SCCR3 machine, which would be dependent on the number of columns in the unit.

7.3.3.4 Finite Feed Flowrate

FIG. 7.4 shows that the mobile phase flowrate has two values within the separating section of the SCCR3 machine, a pre-feed column value, L_1, and a post-feed column value, $L_1 + L_2$, = L_3. This is because the feed has to be introduced into the machine in a finite volume, and, ideally, for maximum separation $L_1 >> L_2$, to minimize the effect of this flow discontinuity. However, it is desirable to maintain L_2 as high as possible, to increase the feed throughput, and in practice a compromise between throughput and product purity is necessary. The limit for complete separation is now defined by:

$$K_{D_1} + \delta_1 + \delta_1' + \delta_1'' < \frac{L_1'}{P} < \frac{L_3'}{P} < K_{D_2} - \delta_2 - \delta_2' - \delta_2'' \qquad (7.12)$$

7.3.3.5 Finite Concentration Effects

Possible concentration effects that may be encountered in g.p.c. were discussed in SECTION 3.4. For a non-linear partition isotherm (SECTION 2.3.1.2), the distribution coefficient, K_D, changes

with solute concentration. Experimental evidence in the literature for g.p.c., discussed in SECTION 3.4, suggests that the K_D of a solute increases, when other molecules are present at significant concentrations, during elution of the solute from a g.p.c. column. The effective K_D of a solute at a finite concentration may thus be expressed in terms of its K_D at infinite dilution, K_{D_∞}, and the change of K_D, ΔK_D, which may be positive or negative, occurring at this concentration:

$$K_D = K_{D_\infty} + \Delta K_D \tag{7.13}$$

For complete separation of components 1 and 2 we now have:

$$K_{D_{\infty 1}} + \Delta K_{D_1} + \delta_1 + \delta_1' + \delta_1'' < \frac{L_1'}{P} < \frac{L_3'}{P} < K_{D_{\infty 2}} + \Delta K_{D_2} - \delta_2 - \delta_2' - \delta_2'' \tag{7.14}$$

where ΔK_{D_1} and ΔK_{D_2} represent the change of K_D of components 1 and 2 at the average on-column concentrations in the high M.W. and low M.W. side of the unit respectively.

In the isolated section, the purge flowrate must be further increased, such that:

$$\frac{L_4'}{P} > K_{D_{\infty 2}} + \Delta K_{D_2} + \delta_2 \tag{7.15}$$

A further effect of concentration is that it would generally be expected to result in an increase in zone broadening, which would mean that δ_1 and δ_2 would have higher values in EQUATIONS 7.14 and 7.15.

7.3.4 Method Used for Selection of SCCR3 Settings

EQUATION 7.14 represents the limits for complete separation of components 1 and 2. However, use of this equation would require detailed knowledge of the parameters involved, which in turn would necessitate an extensive experimental and theoretical study. In practice the operating conditions in the separating section were set so that:

$$\frac{L'_1}{P} = K_{D_{\infty_1}} \tag{7.16}$$

$$\frac{L'_3}{P} = K_{D_{\infty_2}} \tag{7.17}$$

In the isolated section $\frac{L'_4}{P} >> 1.0$ to ensure complete purging of the low molecular weight product. Because of the differences between the practical case, and the idealized case, discussed earlier, it is expected that considerable 'overlapping' of products may occur if the two K_D values are close together. For a polymer feed this would be especially apparent, as neighbouring molecular sizes have very similar K_D values. Thus it would not be practically possible to obtain two product distributions which did not overlap to some extent. The factors discussed in SECTION 7.3.3 would have the effect of increasing this overlap, and the experimental programme undertaken was concerned with investigation of three of these factors, finite feed flowrate, finite concentration, and column length. A summary of the experimental settings used in this research is given in SECTION 7.4.2.1.

7.4 THE CONTINUOUS FRACTIONATION OF DEXTRAN

7.4.1 Scope of the Experimental Programme

Because of the industrial nature of this research project, the experimental programme undertaken was necessarily a compromise between industrial and academic requirements. For example, one possible experimental programme could involve the use of a two-component feed mixture, which would avoid the added complications associated with the use of a polymer, with a molecular weight distribution. However, the industrial interest was centred on the improvement of the molecular weight distributions of dextran polymers and the particular polymer used for this research was a dextran 40 fraction having a molecular weight of approximately 30,000. The relative molecular weights of the two batches of this particular fraction, determined by g.p.c. analysis using a column that had been previously calibrated with dextran T-fractions (SECTION 4.2.2.4), are given in APPENDIX 2. The experimental programme was concerned with fractionation of these dextran 40 materials, and the aims may be listed as follows:

(i) Continuously fractionate a dextran 40 polymer to produce a product of narrower molecular weight distribution. Specifically, to remove a portion of both the high M.W. and low M.W. ends of the polymer distribution, and therefore produce a narrow central fraction as product. As only two products can be produced by a single pass through the SCCR3 machine, removal of both ends of the feed distribution necessitates two operations of the machine.

(ii) Determine the maximum throughput of dextran 40 possible with the SCCR3 machine, within the limits of fractionation performance and pressure drop. In practice this may be achieved by maximizing the concentration and/or volumetric throughput of the dextran 40 feed solution.

Both of these parameters were investigated.

(iii) Investigate the effect of concentration on both fractionation efficiency and theoretical 'cut' position.

(iv) Investigate the effect of the mobile phase/feed flowrate ratio, at a constant overall mobile phase flowrate (L_3) and stationary phase rate (P).

(v) Investigate variation of the L'/P ratio on the observed separation position.

(vi) Investigate the sensitivity of product M.W. distribution to fluctuations in the overall mobile phase flowrate.

(vii) Investigate the effect of the length of the separating section on fractionation efficiency. If possible, to reduce the number of columns in the separating section, within the limits of fractionation performance. This would enable greater liquid throughputs in the separating section, at the same overall pressure drop.

7.4.2 Experimental Operating Conditions

7.4.2.1 Average Experimental Settings

FIG. 7.5 summarizes the average experimental operating conditions for dextran fractionations during this research programme. L_1'/P and L_3'/P represent the theoretical minimum and maximum K_D values, K_{D_1} and K_{D_2} (SECTION 7.3.4), that can be completely separated if factors causing departures from the idealized case (SECTION 7.3.3) are ignored. As such they merely represent an approximate guide for setting the operating conditions for the SCCR3 machine.

At the beginning of this experimental programme, Williams (31) had obtained good fractionations of a dextran 40 hydrolysate, having a broad molecular weight distribution, using the

Figure 7.5 Average Experimental Operating Conditions for SCCR3 Dextran Fractionations

RUN NUMBER	NO. OF COLUMNS	S	P	CONC. OF FEED	FEED FLOW	ELUENT FEED FLOW RATIO	SEPARATING SECTION							PURGE SECTION	
							PRE-FEED SECTION			POST-FEED SECTION			MEAN		
							L_1	L_1'	L_1'/P	L_3	L_3'	L_3'/P	L'/P	L_4	L_4'/P
		min	$cm^3 min^{-1}$	$g\ cm^{-3}$	$cm^3 min^{-1}$		$cm^3 min^{-1}$	$cm^3 min^{-1}$		$cm^3 min^{-1}$	$cm^3 min^{-1}$			$cm^3 min^{-1}$	
10-500-0·5†	20	17·7	35·3	0·101	8·22	5·51	45·3	14·7	0·416	53·5	22·9	0·649	0·533	190	4·5
20-500-0·5†	10	17·6	35·7	0·210	7·90	5·56	43·9	13·3	0·373	51·8	21·2	0·594	0·484	195	4·6
20-1000-0·4†	10	17·3	36·3	0·206	17·1	2·13	36·5	5·4	0·149	53·6	22·5	0·620	0·385	185	4·2
20-1700-0·3††	10	17·1	36·7	0·202	28·8	0·95	27·4	−4·1	−0·112	56·2	24·7	0·673	0·281	185	4·2
20-600-0·7††	10	17·0	36·9	0·220	10·0	5·26	52·6	21·0	0·569	62·6	31·0	0·840	0·705	190	4·3
20-500-0·8††	10	23·0	27·3	0·202	8·17	5·04	41·2	17·8	0·652	49·4	26·0	0·952	0·802	180	5·8
20-400-1·1††	10	30·0	20·9	0·220	7·22	5·23	37·8	19·9	0·951	45·0	27·1	1·297	1·124	160	6·7
01-600-0·7††	10	16·9	36·9	0·0102	10·1	5·12	51·7	20·1	0·544	61·8	30·2	0·818	0·681	190	4·3

† Feed = Dextran 40 (Fisons Ltd. Batch BT 85)

†† Feed = Dextran 40 (Fisons Ltd Batch BT192)

All Runs Carried Out at Ambient Temperature (20 → 25°C)

CCR1 machine, at feed concentrations up to ~10% w/v dextran, and a mobile phase/feed flow ratio of 20/1. Consequently 10% w/v dextran was taken as a starting point for the first experimental run (10-500-0.5), and to increase the dextran throughput, the mobile phase/feed flowrate ratio was reduced to ~5.5/1 by increasing the feed flowrate. The overall mobile phase flowrate was set at ~54 cm^3 min^{-1}, and a nominal switching interval of eighteen minutes was employed to remove a portion of the high M.W. end of the feed distribution. Run 20-500-0.5 was performed at a similar mobile phase/feed flowrate ratio and values of the pre-feed and post-feed L'/P ratios, but at a higher feed concentration (21% w/v dextran), and reduced number of columns. This was done to establish the extent of any loss of fractionation that may occur under these more arduous conditions.

RUNS 20-500-0.5, 20-1000-0.4, and 20-1700-0.3 show the effect of reducing the mobile phase/feed flowrate ratio while maintaining L'_3/P, and feed concentration approximately constant, using the same number of columns. This was done by increasing the feed flowrate, and hence dextran input, to the SCCR3 machine.

RUNS 20-500-0.5, 20-600-0.7, 20-500-0.8, and 20-400-1.1 establish the effect of increasing the average L'/P ratio, while maintaining the mobile phase/feed flowrate ratio, and feed concentration, approximately constant, using the same number of columns.

RUNS 20-600-0.7 and 01-600-0.7 show the effect of changing the feed concentration from 22% to 1% w/v dextran, while maintaining approximately equal values of the L'/P ratios, and mobile phase/feed flow ratio, using the same number of columns.

7.4.2.2 Variation of Operating Conditions During an Experimental Run

FIGS. 7.6 to 7.13 summarize graphically the operating conditions for the experimental runs. More detail is given in tabular

Figure 7.6 Variation of Operating Conditions During Run 10-500-0·5

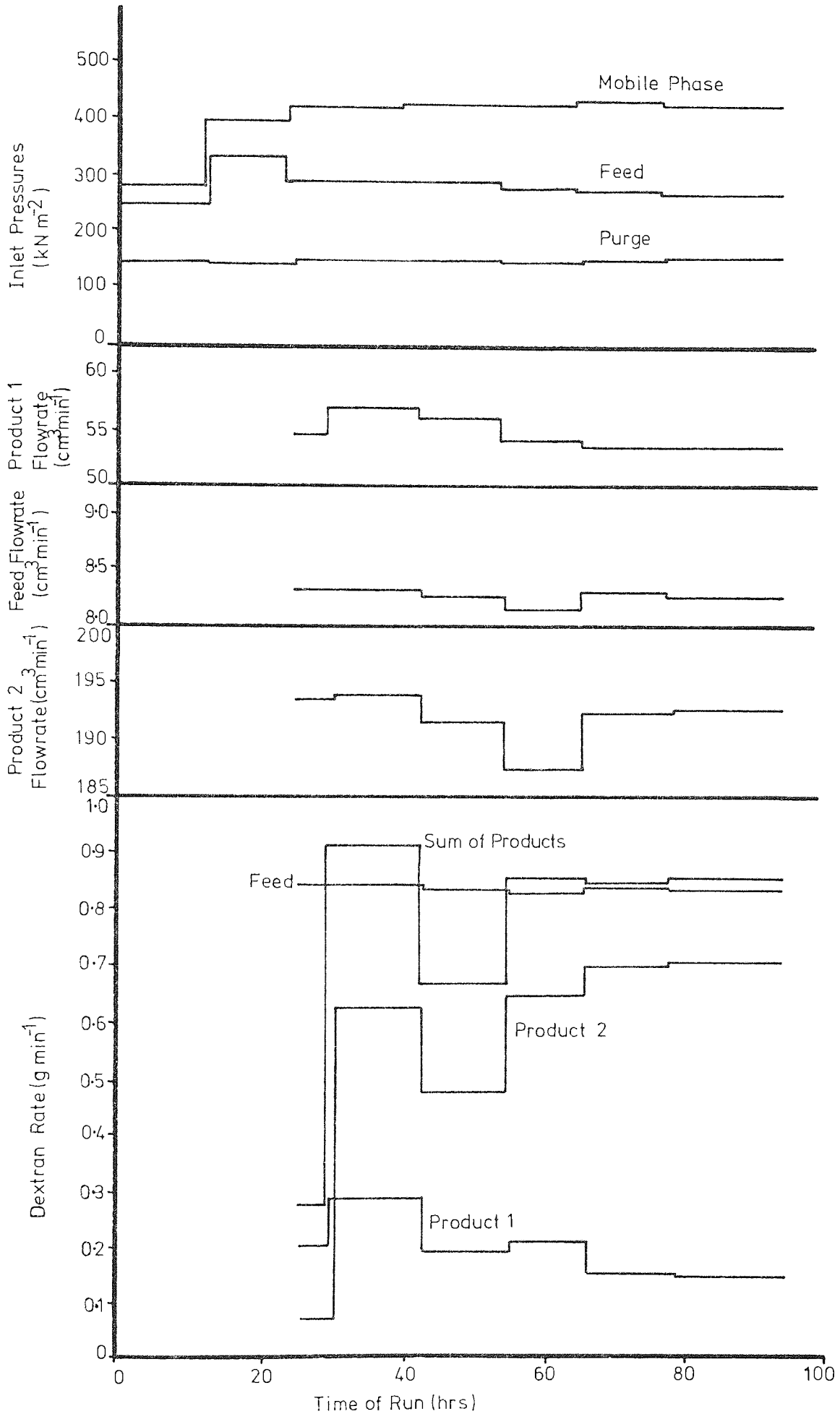

Figure 7.7 Variation of Operating Conditions During Run 20-500-0·5

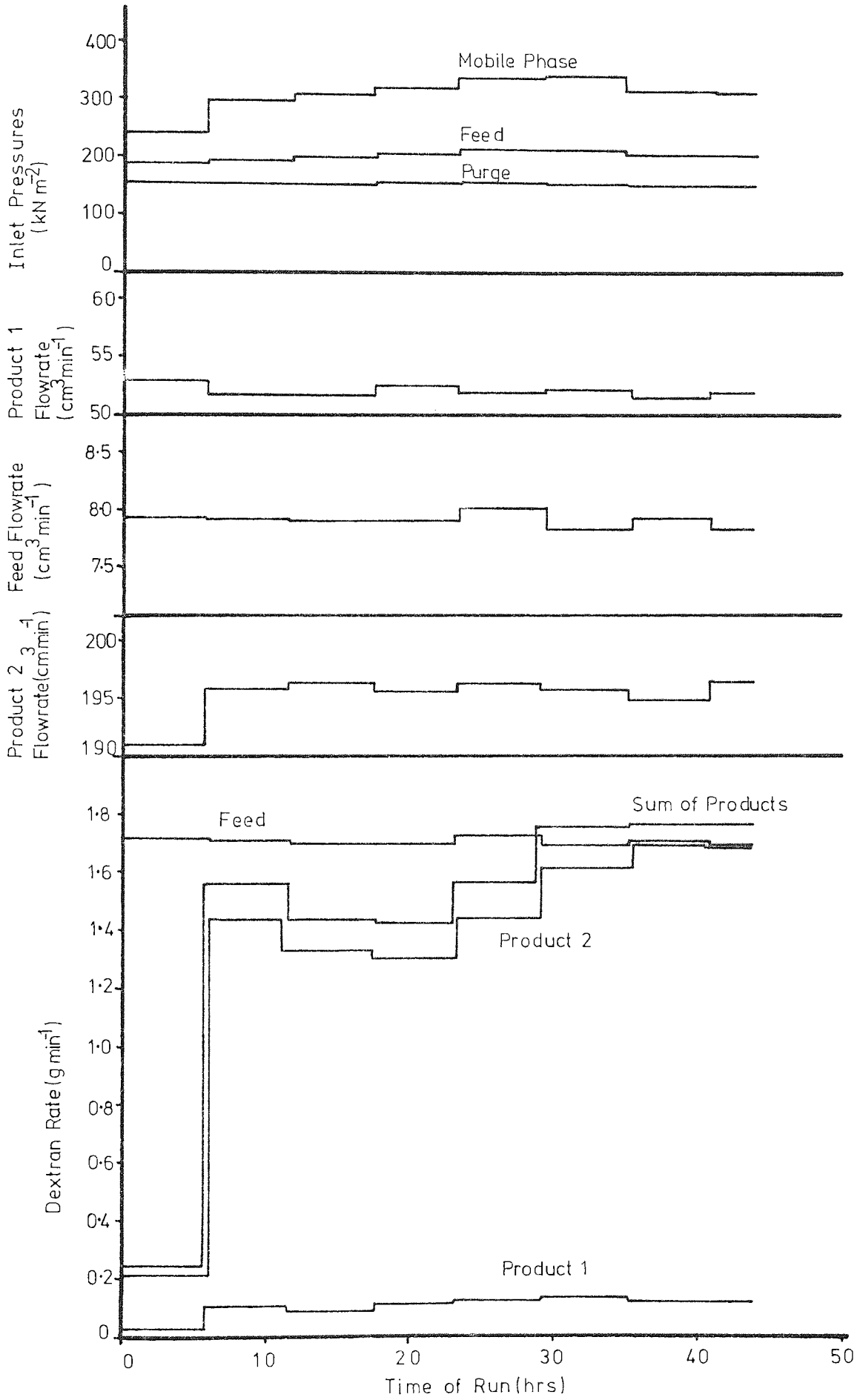

Figure 7.8 Variation of Operating Conditions During Run 20-1000-0·4

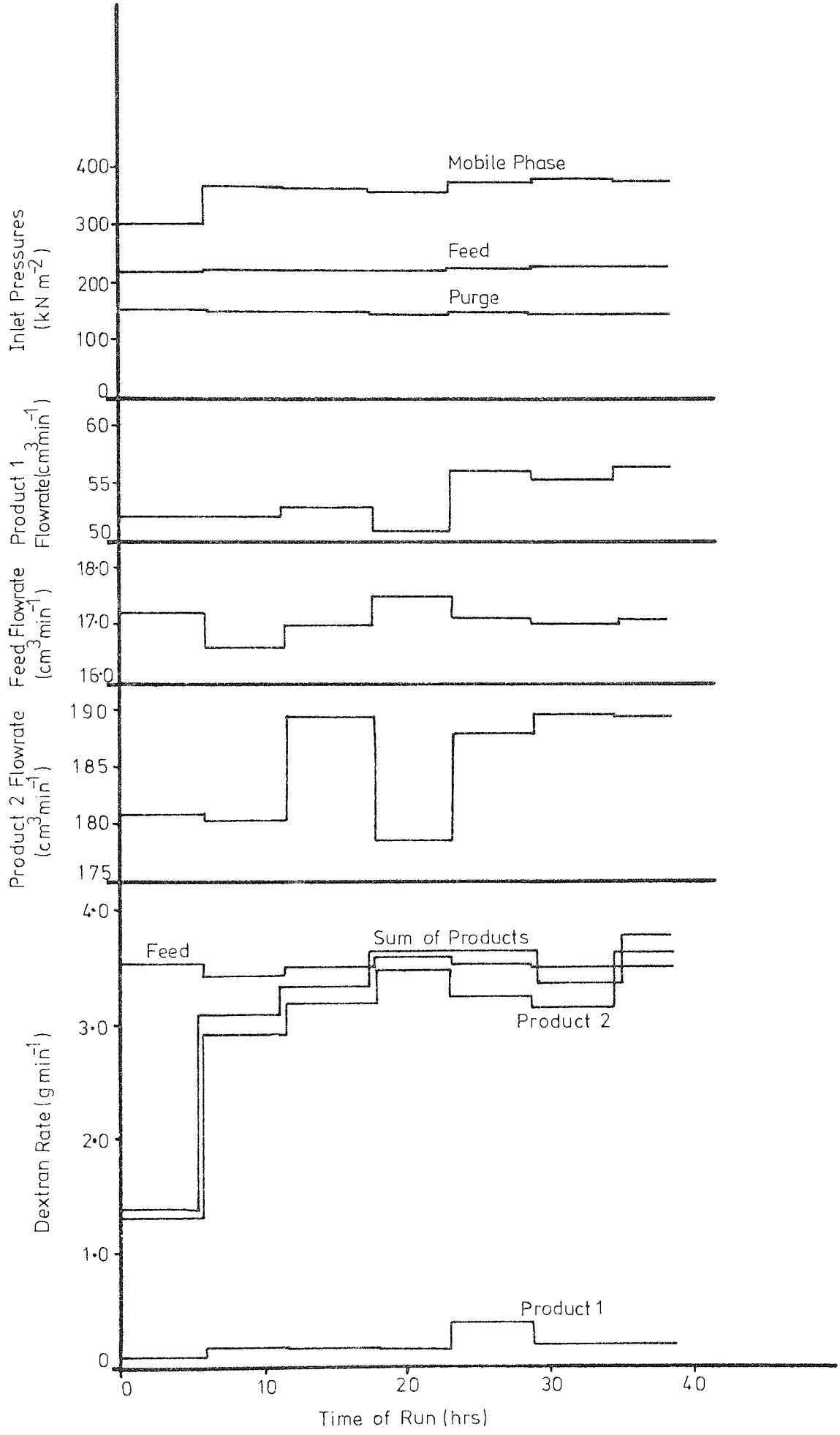

Figure 7.9 Variation of Operating Conditions During Run 20-1700-0·3

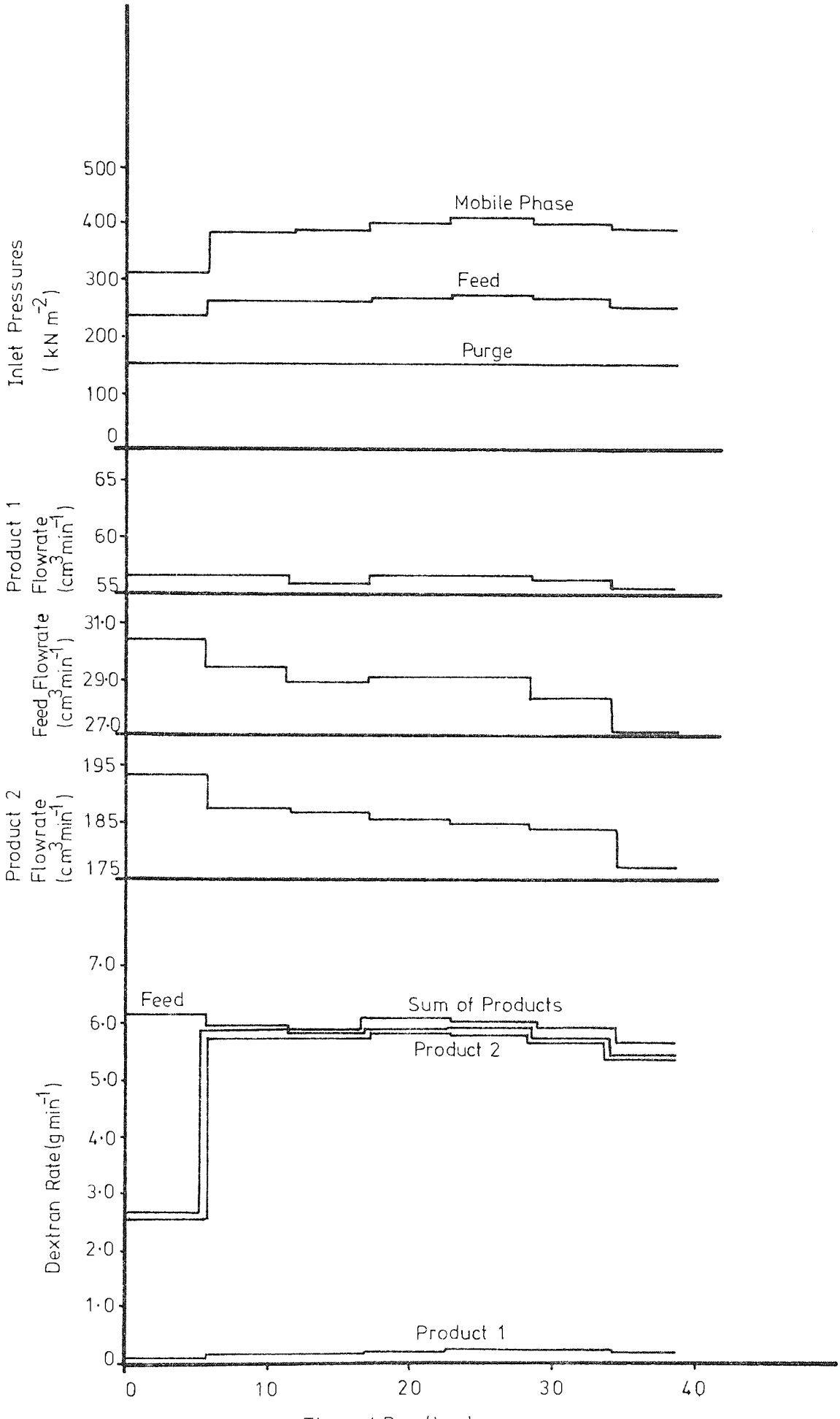

Figure 7.10 Variation of Operating Conditions During Run 20-600-0·7

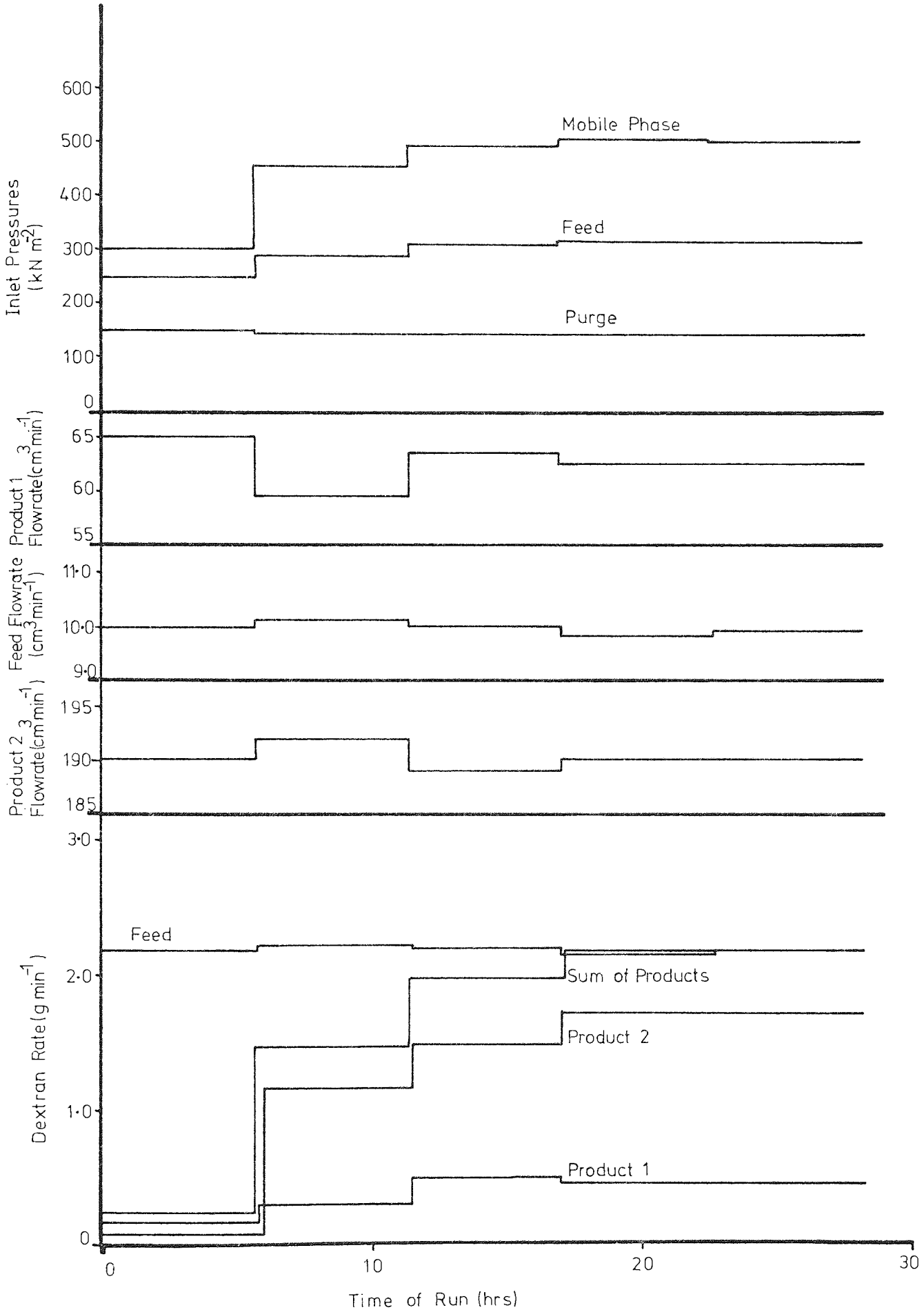

Figure 7.11 Variation of Operating Conditions During Run 20-500-0·8

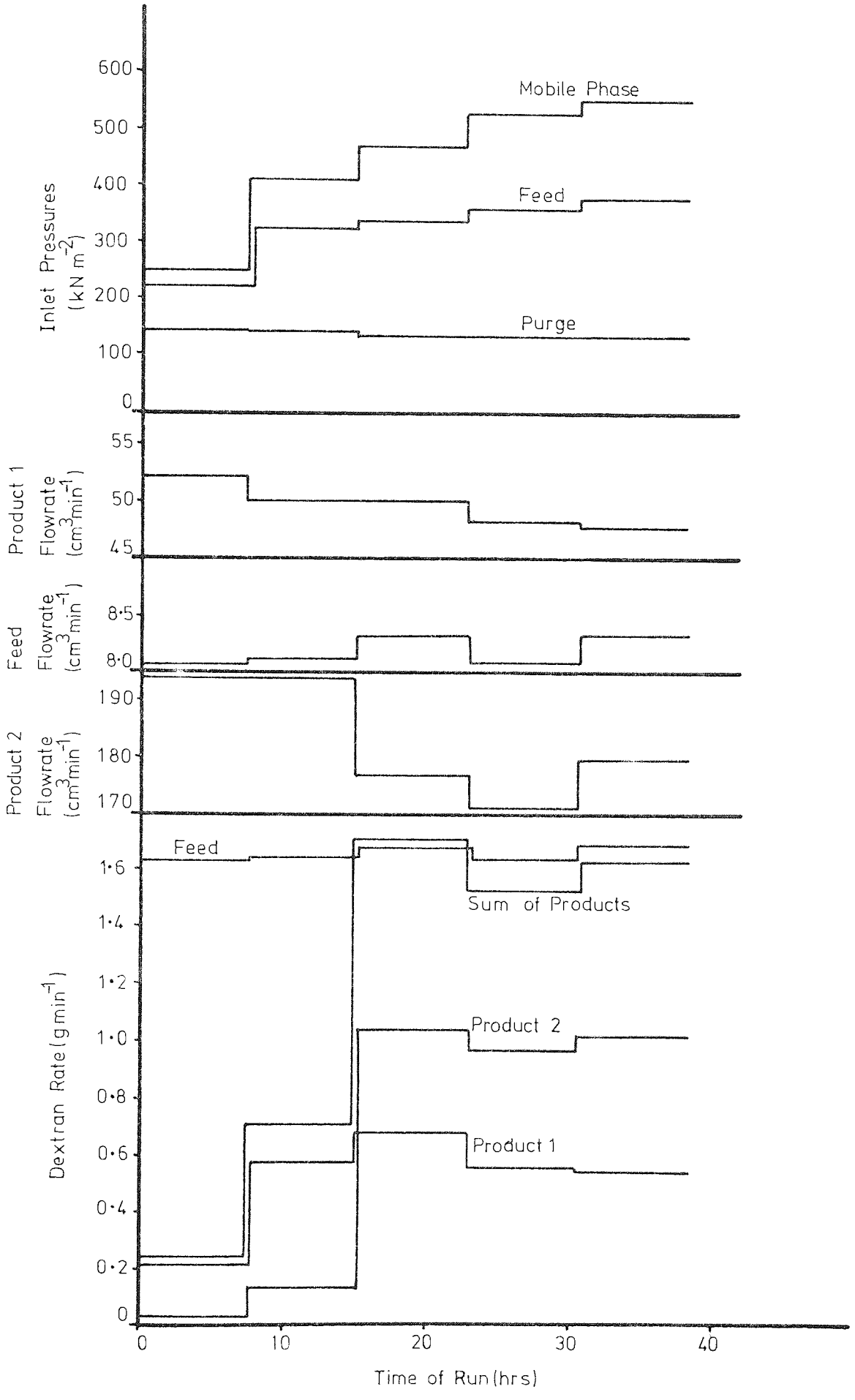

Figure 7.12 Variation of Operating Conditions During Run 20-400-1-1

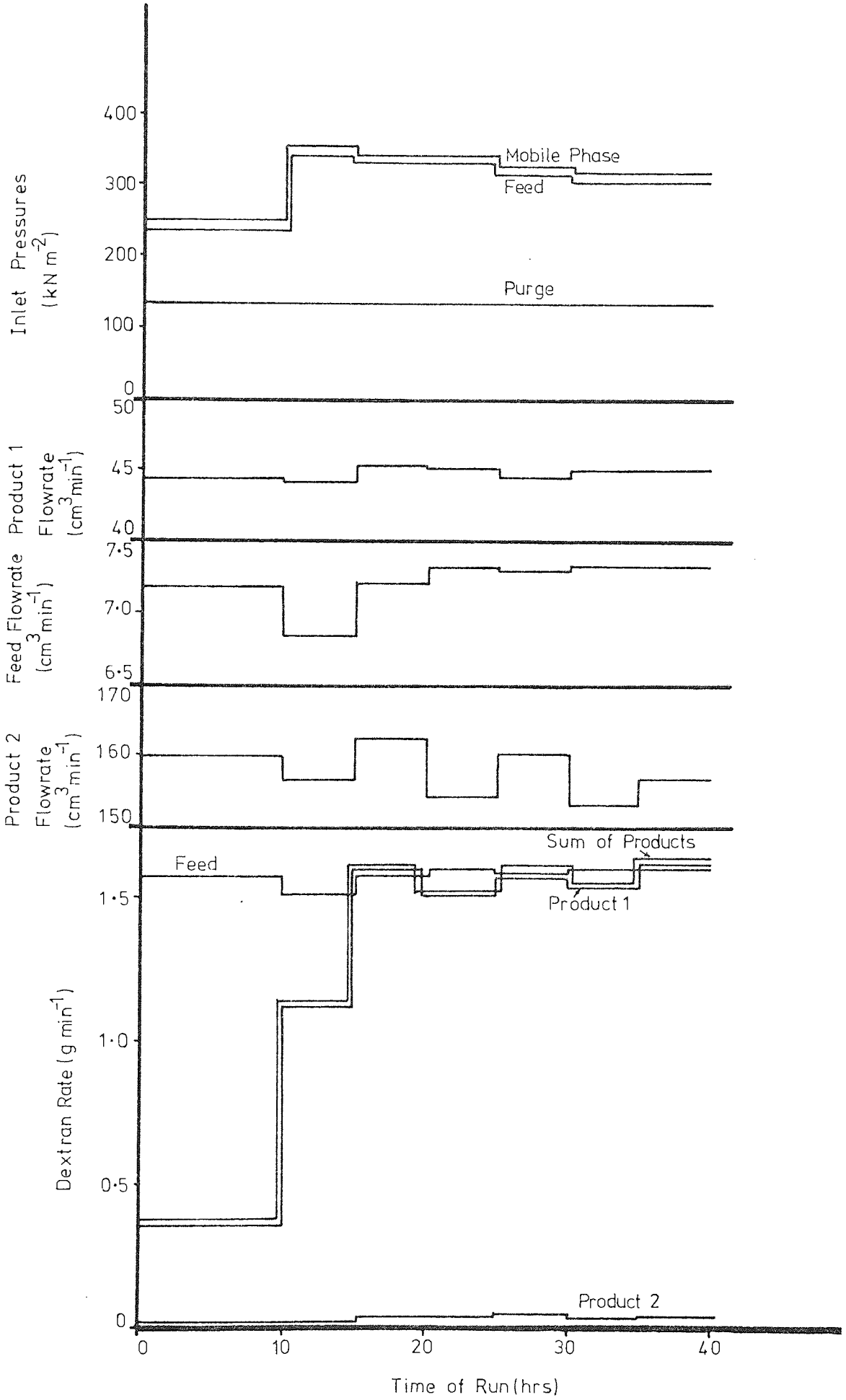

Figure 7.13 Variation of Operating Conditions During Run 01-600-0·7

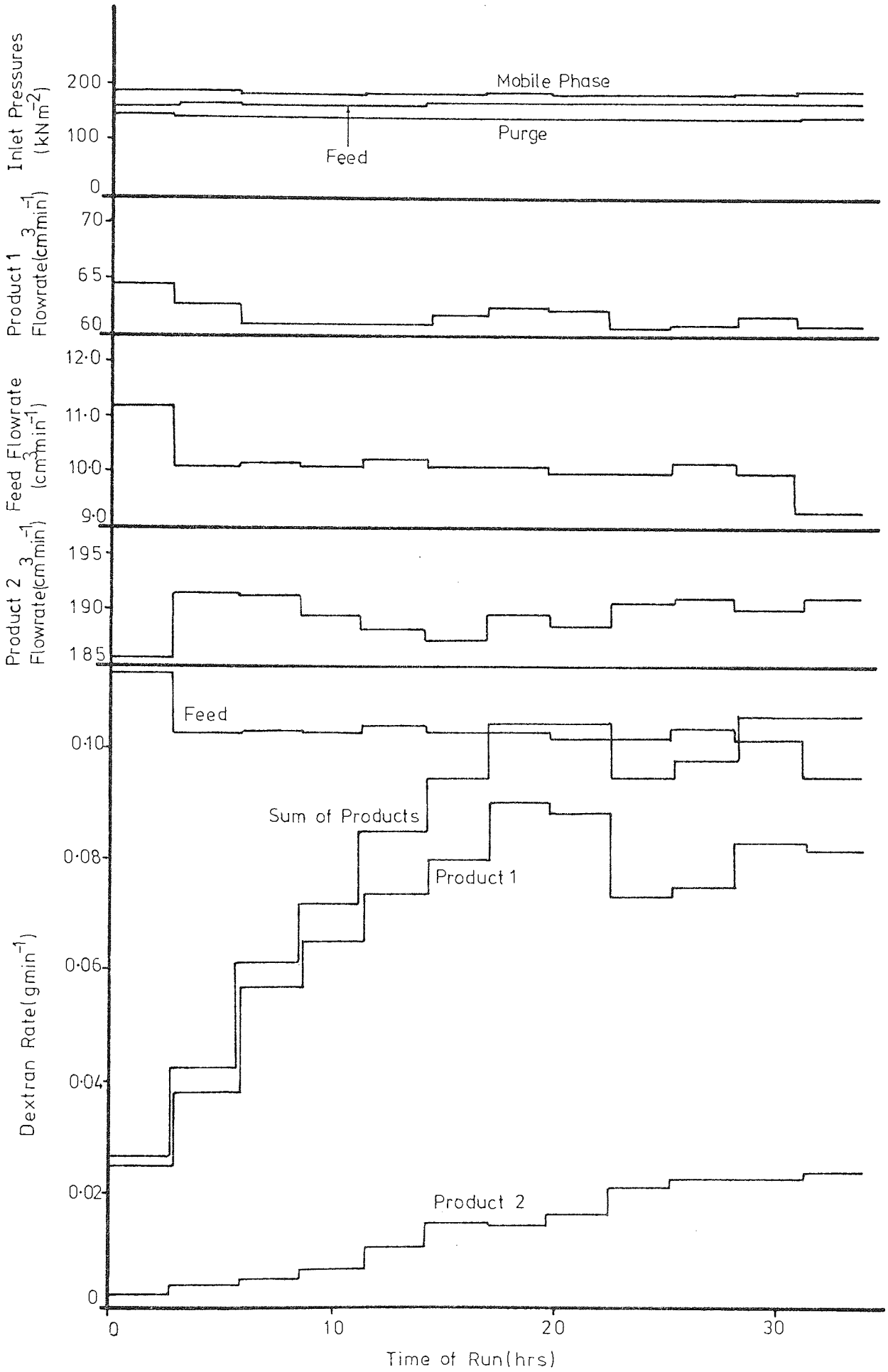

form in APPENDIX 4. The largest fluctuations in the L'/P ratios occurred for RUN 20-1000-0.4 (FIG. 7.8). The average feed flowrates, each determined over two cycles, varied by 5.1%, average product 1 flowrates varied by 10.4%, and the sequencing interval by 1.7%, giving a maximum variation of L_3'/P of 17.2%. Although these fluctuations were significantly greater than for the majority of the other runs, they highlight the difficulty of maintaining steady operating conditions for long periods of time, due mainly to fluctuations in the mobile phase and feed flowrates. The average maximum variations for the remaining runs were 3.7%, 3.6%, and 0.1% for product 1 flowrate, feed flowrate, and sequencing interval respectively. However, significant departures from the average flowrate usually only occurred for short periods of time, and FIGS. 7.6 to 7.13 show that operating conditions were generally more stable than these maximum variations indicate. This is supported by FIG. 7.14 which shows the variation in M.W. distribution of products for RUN 20-500-0.5. Each product was collected for one cycle of the SCCR3 unit, and the total time interval spanned by the products was 29.3 hours. The major difference between samples was the variation of concentration with time, and the product M.W. distributions remained substantially constant. Similar results were obtained by Williams (31) with the smaller CCR1 unit. It should be noted here that this consistency only occurs when a pseudo-equilibrium state is reached, and the M.W. distributions of products emerging from the SCCR3 machine before this stage will vary. This latter phenomenon has been investigated by Williams (31) within the context of the smaller-scale CCR1 unit. Essentially material of lowest M.W. and highest M.W., present in the feed, will elute first from the product 2 and product 1 ports respectively. As the run progresses,

Figure 7.14 Variation of Product Distributions During Run 20-500-0·5

Samples	Time of Run (hrs)	Cycle No.
– – – –	5·9 – 8·8	3
—·—·—·—	14·7–17·6	5
—×—×—×—	20·6–23·5	7
—▲—▲—▲—	26·4–29·3	9
—■—■—■—	32·3–35·2	11

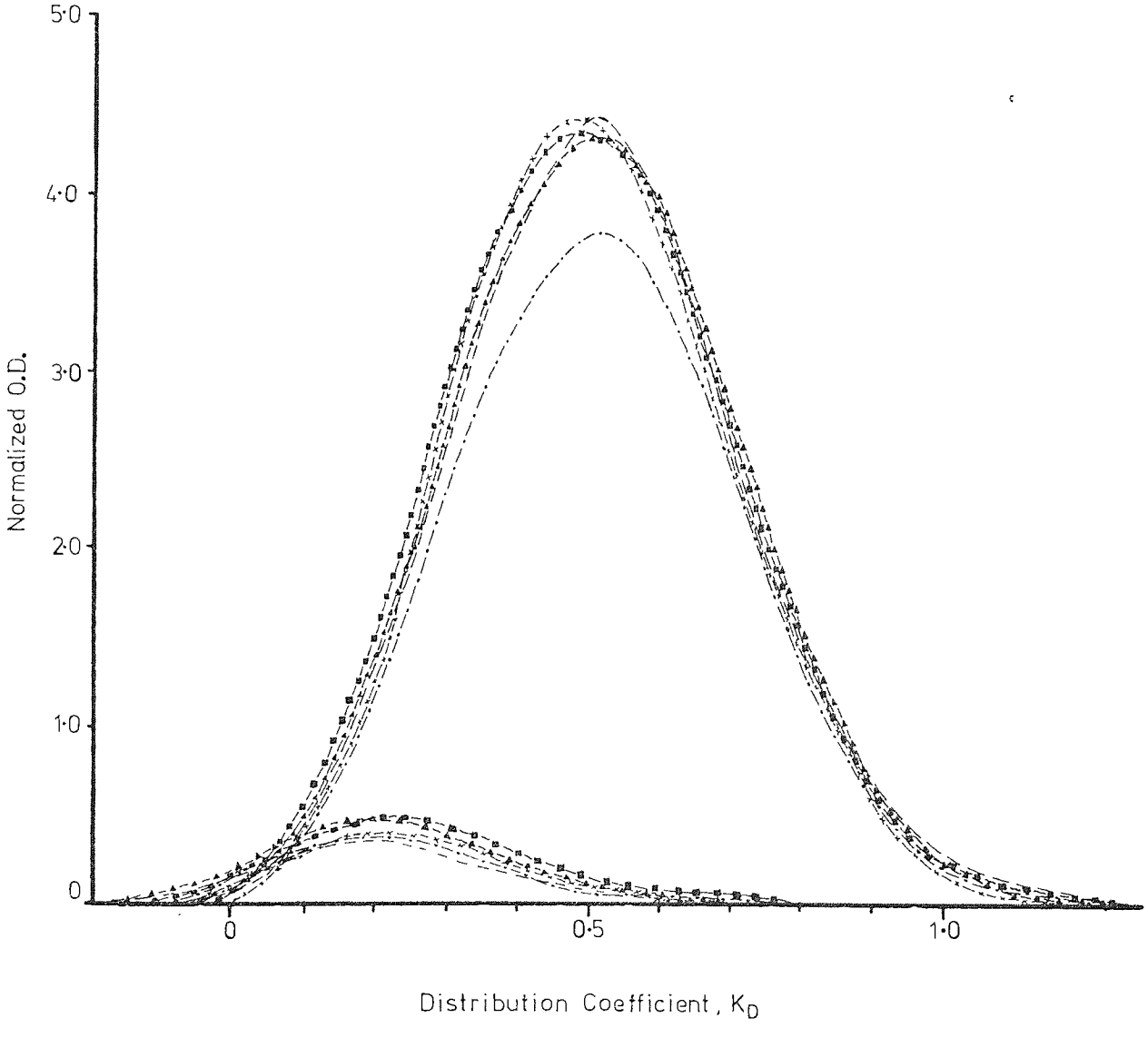

the average molecular weights of the two products will tend towards each other until their pseudo-equilibrium values are reached. At this stage the two product M.W. distributions, when summed, should be equivalent to the original feed distribution.

The general build-up of dextran concentration within the SCCR3 unit, during a run, had the effect of causing a substantial increase in pressure drop across the separating section, because of the high viscosity of concentrated dextran solutions (APPENDIX 2). This is apparent from a study of the variation of the mobile phase and feed inlet pressures with time in FIGS. 7.6 to 7.12. These pressures provided a crude indication of the attainment of maximum concentration within the separating section, when approximately constant pressure levels were reached, allowing for variations in the mobile phase and feed flowrates. All pressures were recorded at the end of each sequencing interval, which represented the maximum mobile phase and feed inlet pressures, as these increased during a sequencing interval, and minimum purge pressure, as this decreased during a sequencing interval. As such, the purge pressure recorded gave a coarse indication of complete purging, i.e. when it reached its minimum, constant, value. FIG. 7.15 illustrates the build-up of dextran concentration with time for RUN 01-600-0.7. The similarity between the profiles after 31.1 and 33.9 hours of operation indicate that maximum concentrations have been reached within the SCCR3 machine between 16.9 and 31.1 hours of operation. FIG. 7.16 compares the point concentration profile after 33.9 hours of operation with the column concentration profile obtained at the end of the run (34.0 hours). The displacement of the profiles in the horizontal direction is due mainly to the fact that they represent different times during the sequencing interval, as indicated on the diagram. For direct comparison, the profile for 33.9 hours, which was

Figure 7.15 Dextran Build-up within the SCCR3 Unit During Run 01-600-0·7

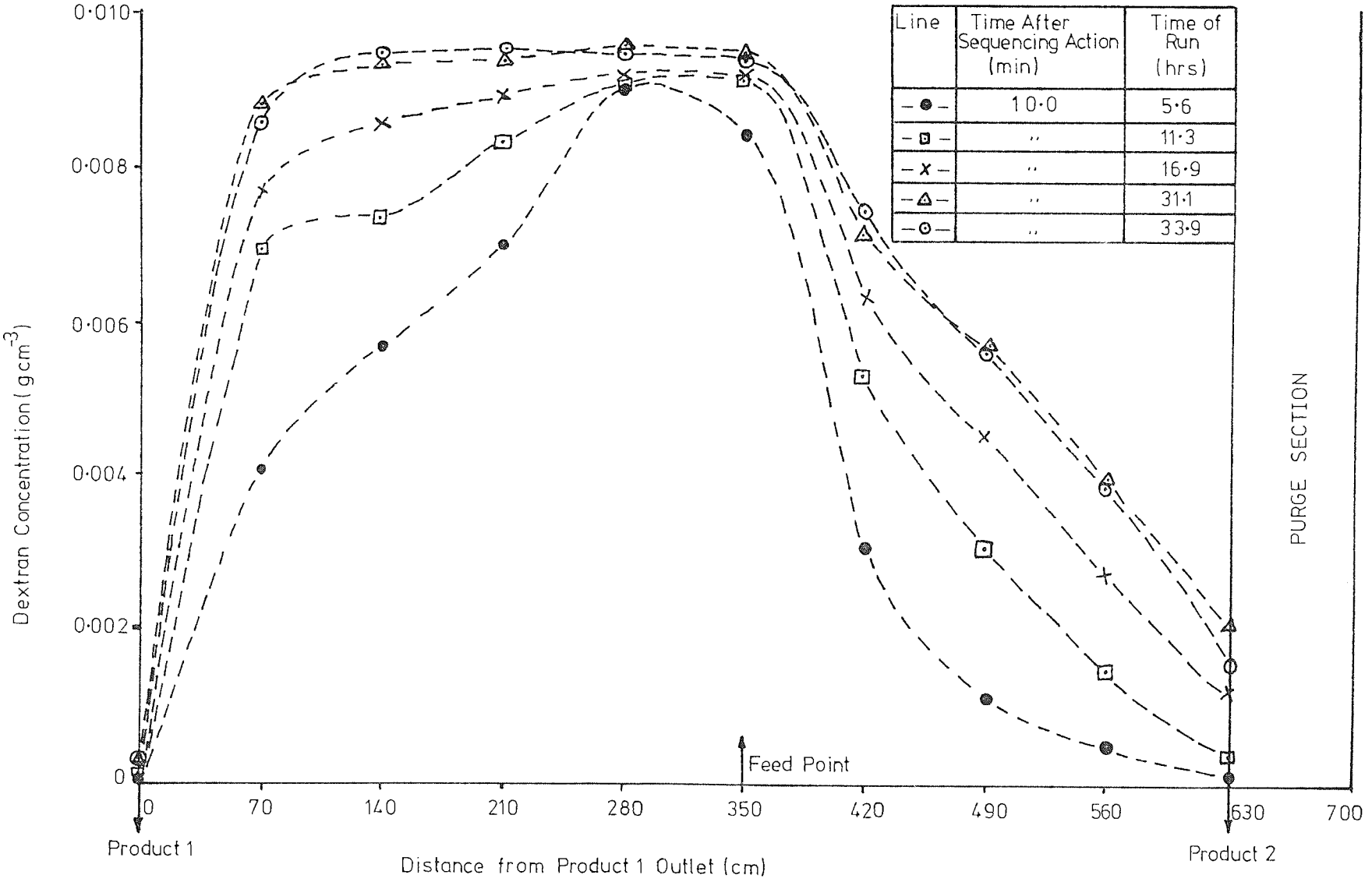

Figure 7.16 Comparison of Final Point Concentration Profile with Standard Concentration Profile (FIG. 7.26) for Run 01-600-0·7

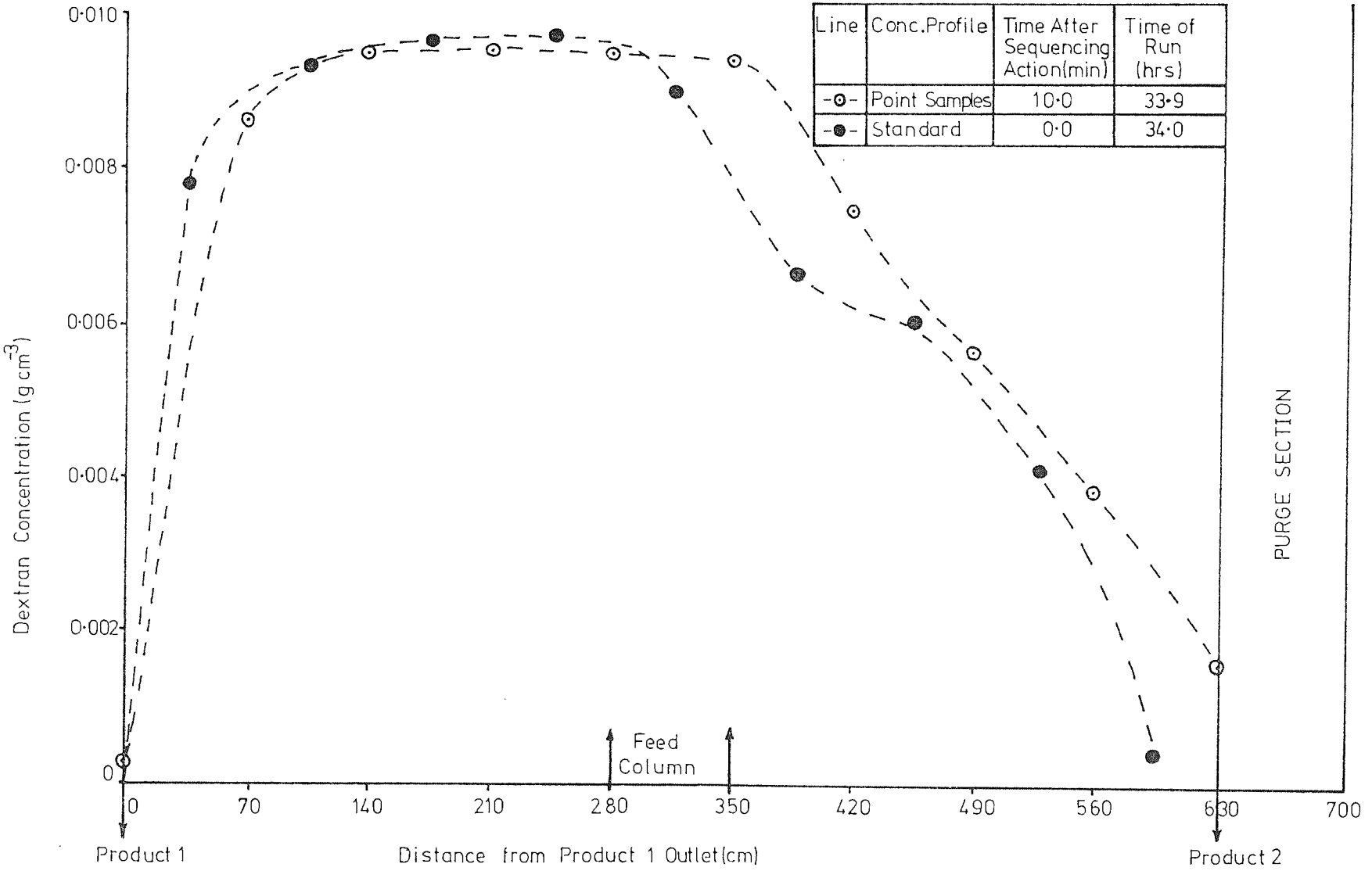

taken approximately half-way through the sequencing interval, should be displaced by approximately half of one column length, or 35 cm, to the left. In this case the agreement is fairly good, indicating that the two techniques for obtaining concentration profiles, discussed earlier in this section, are compatible at moderate feed concentrations. It is therefore thought that the concentration profile for RUN 10-500-0.5, obtained by analysis of point samples, is comparable with concentration profiles obtained for the other runs, obtained by analysis of samples purged from individual columns at the end of each run.

The reproducible nature of point concentrations within the SCCR3 machine, over long periods of time, is shown by FIG. 7.17, which compares the concentration profiles after 63.3 and 83.4 hours of operation for RUN 10-500-0.5. However, for reasons given in SECTION 7.2.4, it was not possible to use this criterion for deciding when pseudo-equilibrium was obtained for the majority of experimental runs. Deciding when pseudo-equilibrium was reached was therefore based on attainment of an approximately constant average pressure drop across the separating section, as a crude guide, and approximately constant average dextran output rates for the products, as a finer guide. The latter was measured by the technique discussed in SECTION 7.2.2 and the results are summarized graphically in FIGS. 7.6 to 7.13, and tabulated, in more detail, in APPENDIX 4. These results show a gradual increase in concentrations of the products, until approximate plateau regions are reached. In practice the experimental runs were continued for a number of cycles after this point to ensure that approximately constant product concentrations were maintained. The amount of fluctuation in the average dextran output rates varied from run to run, depending primarily on the stability of the mobile phase and feed flowrates. Agreement between the measured total dextran output rate, and feed dextran input rate was usually good, once the plateau regions had been

Figure 7.17 Reproducibility of SCCR3 Concentration Profiles after the Attainment of Pseudo-Equilibrium

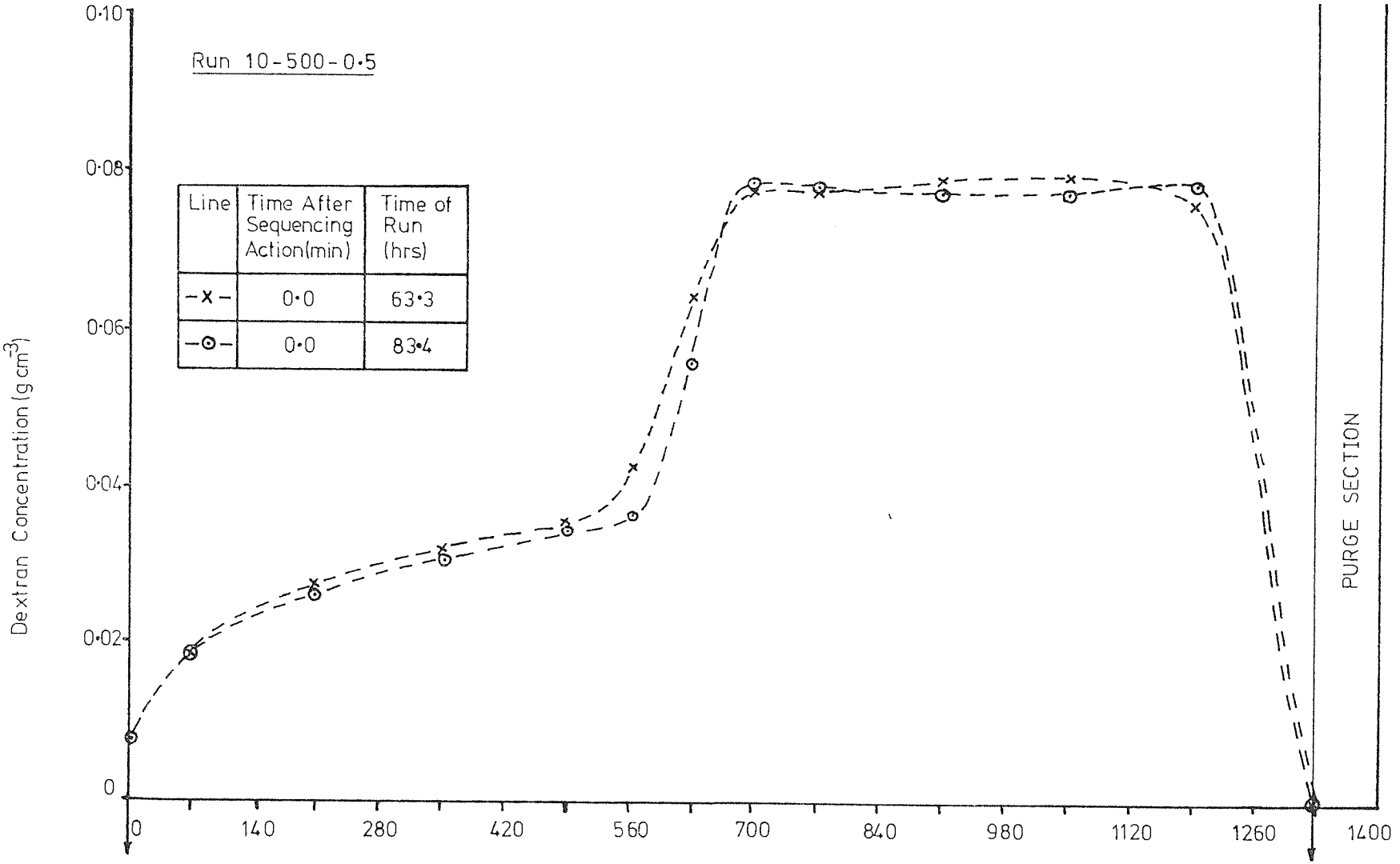

attained.

FIG. 7.18 summarizes the complete dextran balance for each experimental run. Measured total dextran input throughout each run is compared with the sum of the total measured dextran output, with the two products, and total dextran hold-up in the SCCR3 unit. Agreement between the two sets of measurements is generally good, thereby accounting for all dextran used during the experimental runs. The number of cycles of the SCCR3 unit required for the products to reach the plateau regions varied from run to run. Although it is difficult to be precise as to the exact point that the dextran rates reached approximately level values, especially as the operating flowrates tended to fluctuate, lower values of the mobile phase/feed flowrate ratio, at high feed concentrations (~20% w/v dextran), tended to need less cycles to attain the plateau values. This indicates that the use of high, initial, on-column feed concentrations leads to early establishment of a pseudo-equilibrium condition.

7.4.3 Results and Discussion of Dextran Fractionations

7.4.3.1 Concentration and Molecular Weight Distribution Profiles

FIGS. 7.19 to 7.26 illustrate the concentration and M.W. distributions of dextran around the SCCR3 unit at the end of each experimental run. The concentrations are average column concentrations determined as indicated in SECTION 7.2.4, and sample M.W. values are given in terms of the mean K_D values (50% area point) of average samples from each column (SECTION 7.2.4). These results are tabulated, in more detail, in APPENDIX 4.

FIGS. 7.19 - 7.24 show that, for the experimental conditions used, a major part of the feed input travelled with the stationary phase. FIGS. 7.25 and 7.26 show a major part of the feed to be

Figure 7.18 Overall Dextran Balances for SCCR3 Runs

Run No.	Total Dextran Input	Dextran Output with Products	Dextran in SCCR3 Unit at End of Run	% Error
	g	g	g	
10-500-0·5	—	—	—	—
20-500-0·5	4370	3770	541	- 1·3
20-1000-0·4	8093	7320	728	- 0·6
20-1700-0·3	13380	12520	822	- 0·3
20-600-0·7	3730	2740	902	- 2·3
20-500-0·8	3790	2670	1145	+ 0·7
20-400-1·1	3810	3260	684	+ 3·4
01-600-0·7	211	165	52	+ 2·8

Figure 7.19 The Variation of Concentration and K_D around the SCCR3 Unit at the End of Run 10-500-0·5

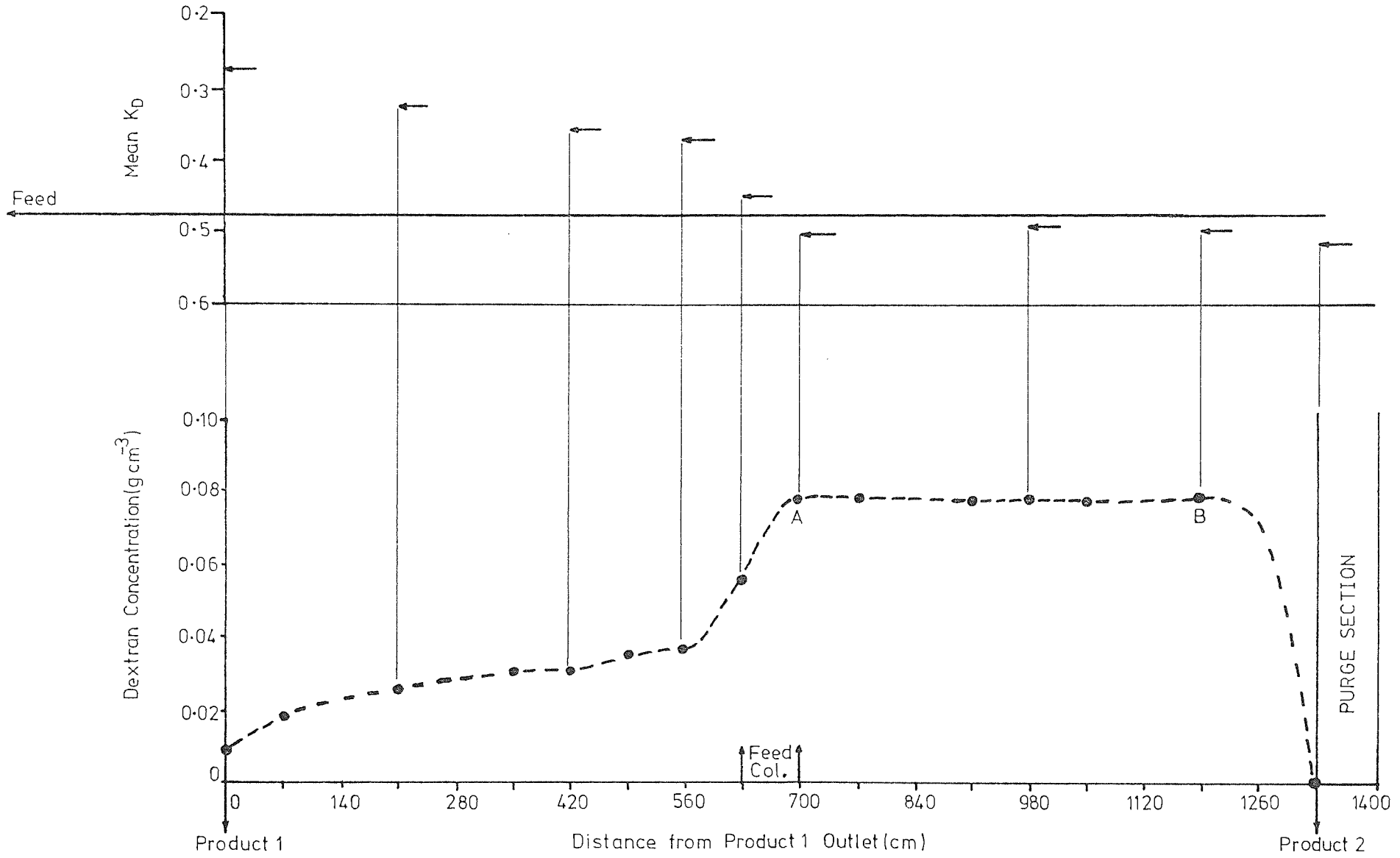

Figure 7.20 The Variation of Concentration and K_D around the SCCR3 Unit at the End of Run 20-500-0·5

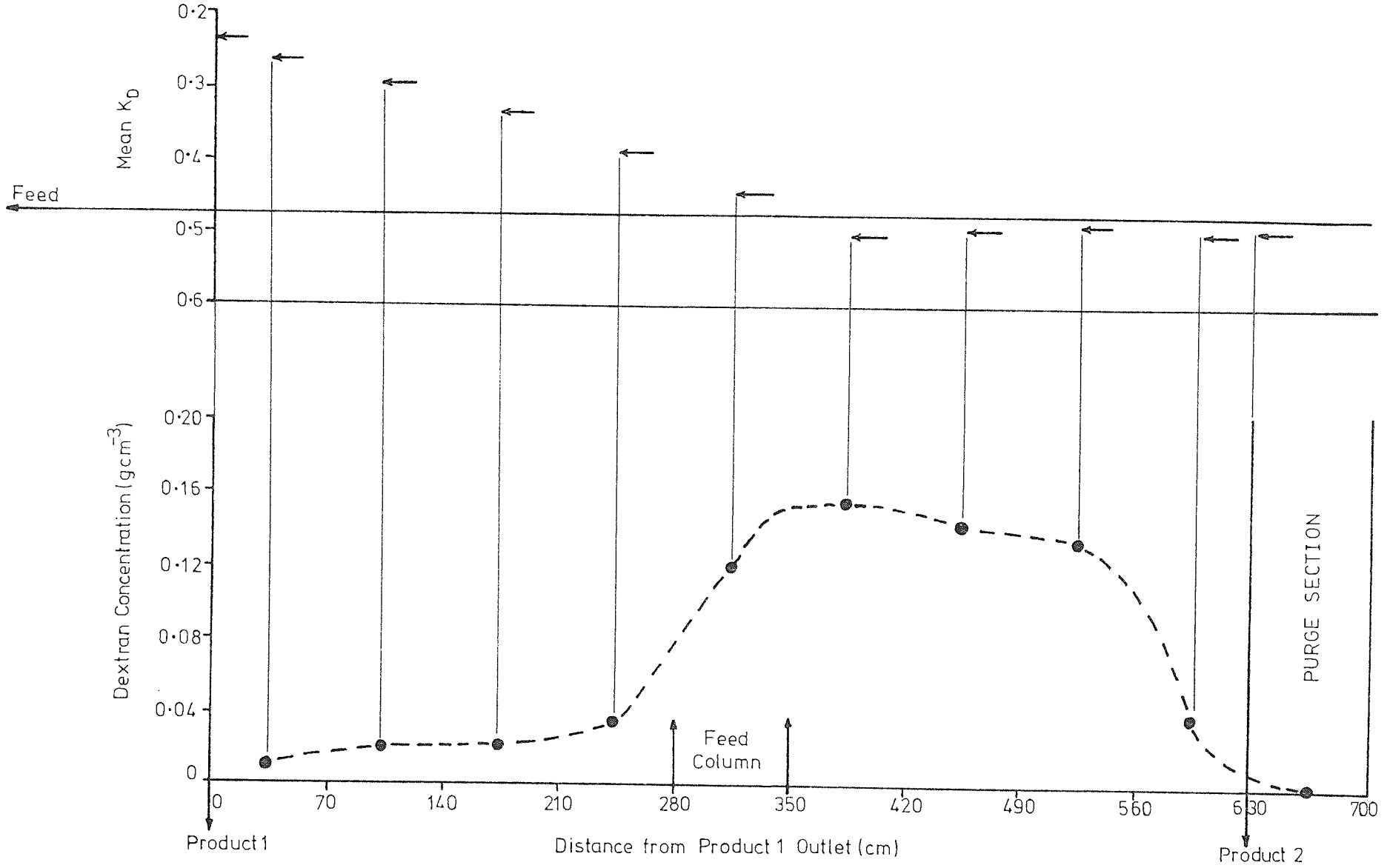

Figure 7.21 The Variation of Concentration and K_D around the SCCR3 Unit at the End of Run 20-1000-0·4

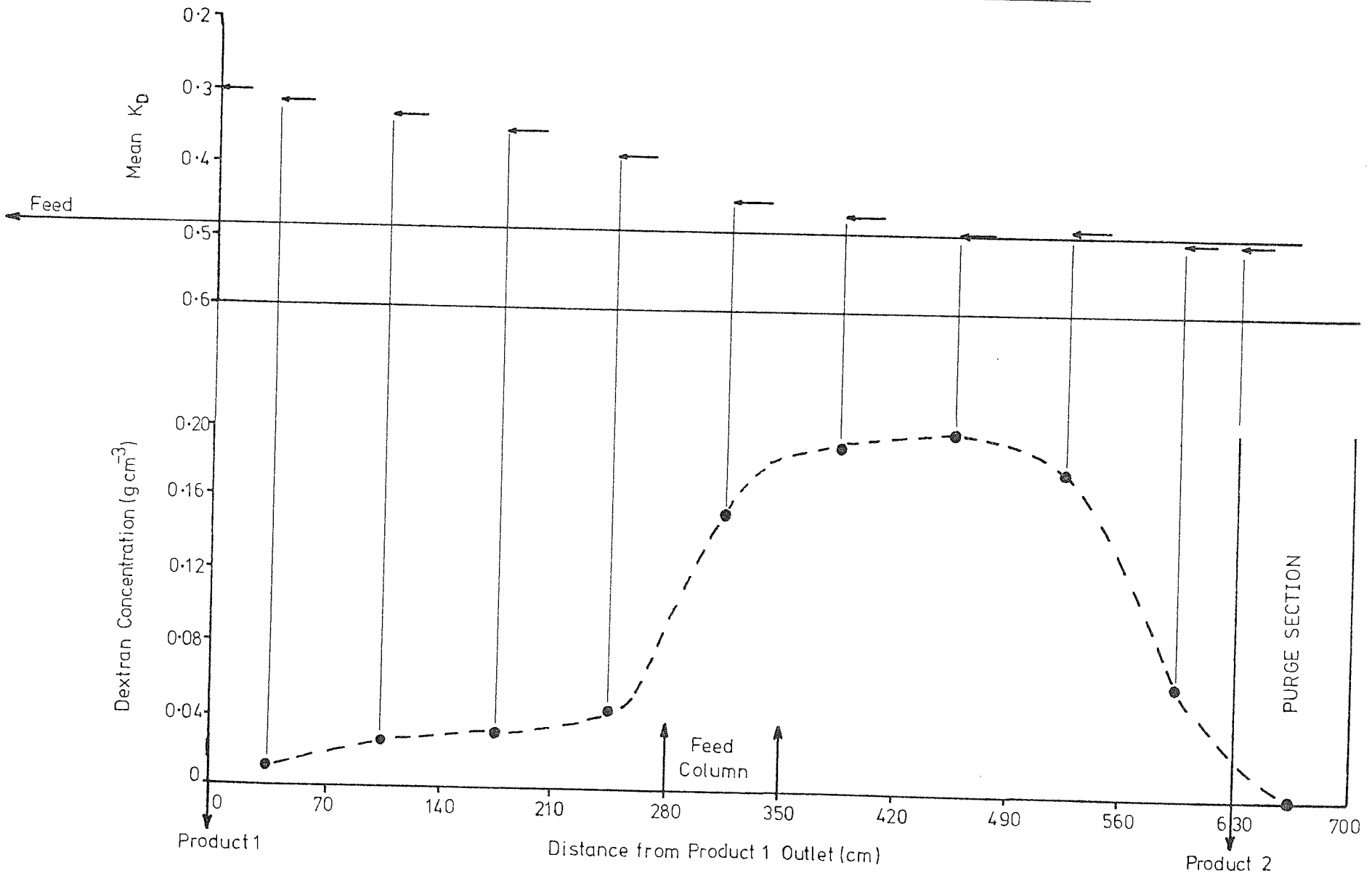

Figure 7.22 The Variation of Concentration and K_D around the SCCR3 Unit at the End of Run 20-1700-0·3

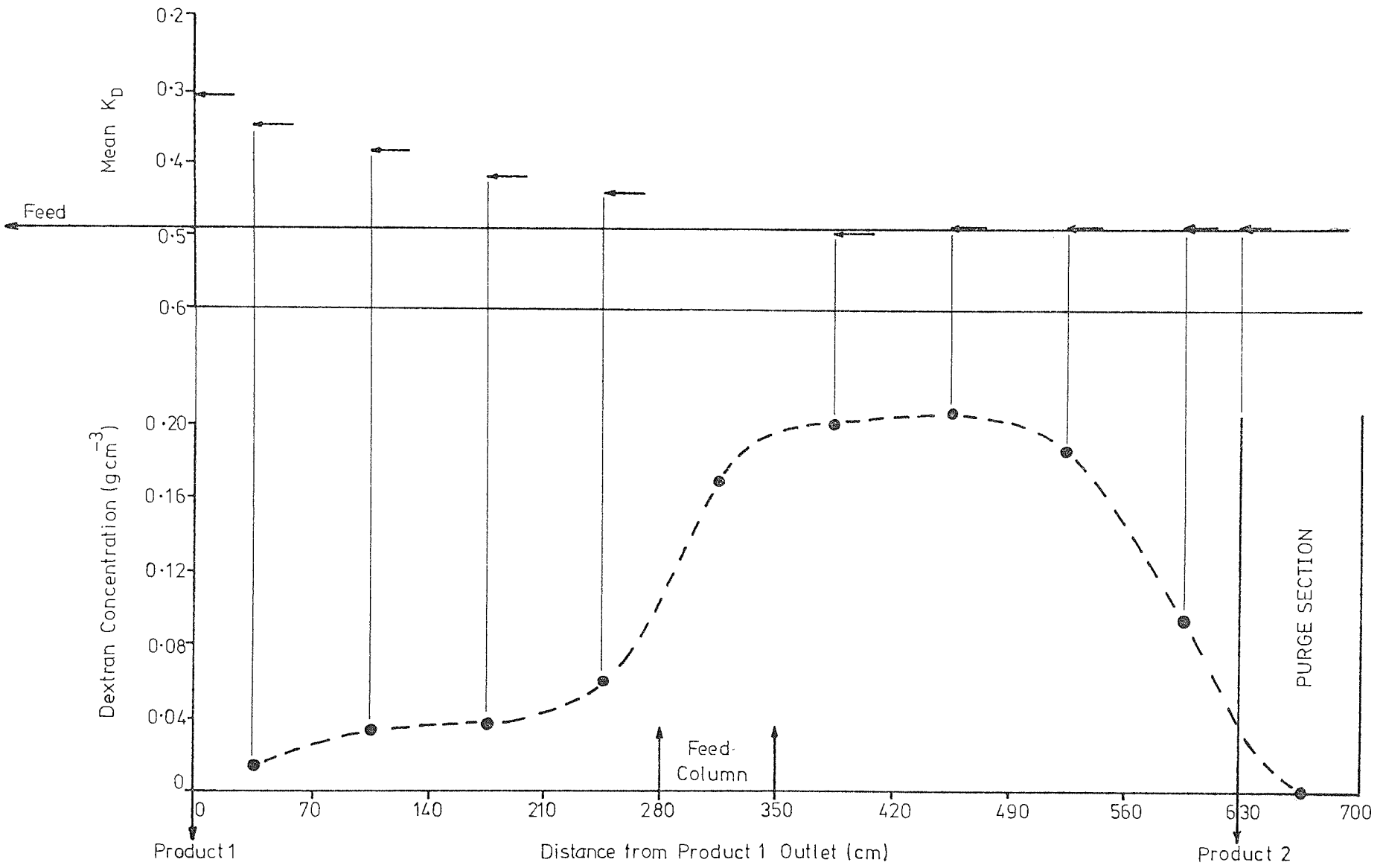

Figure 7.23 The Variation of Concentration and K_D around the SCCR3 Unit at the End of Run 20-600-0·7

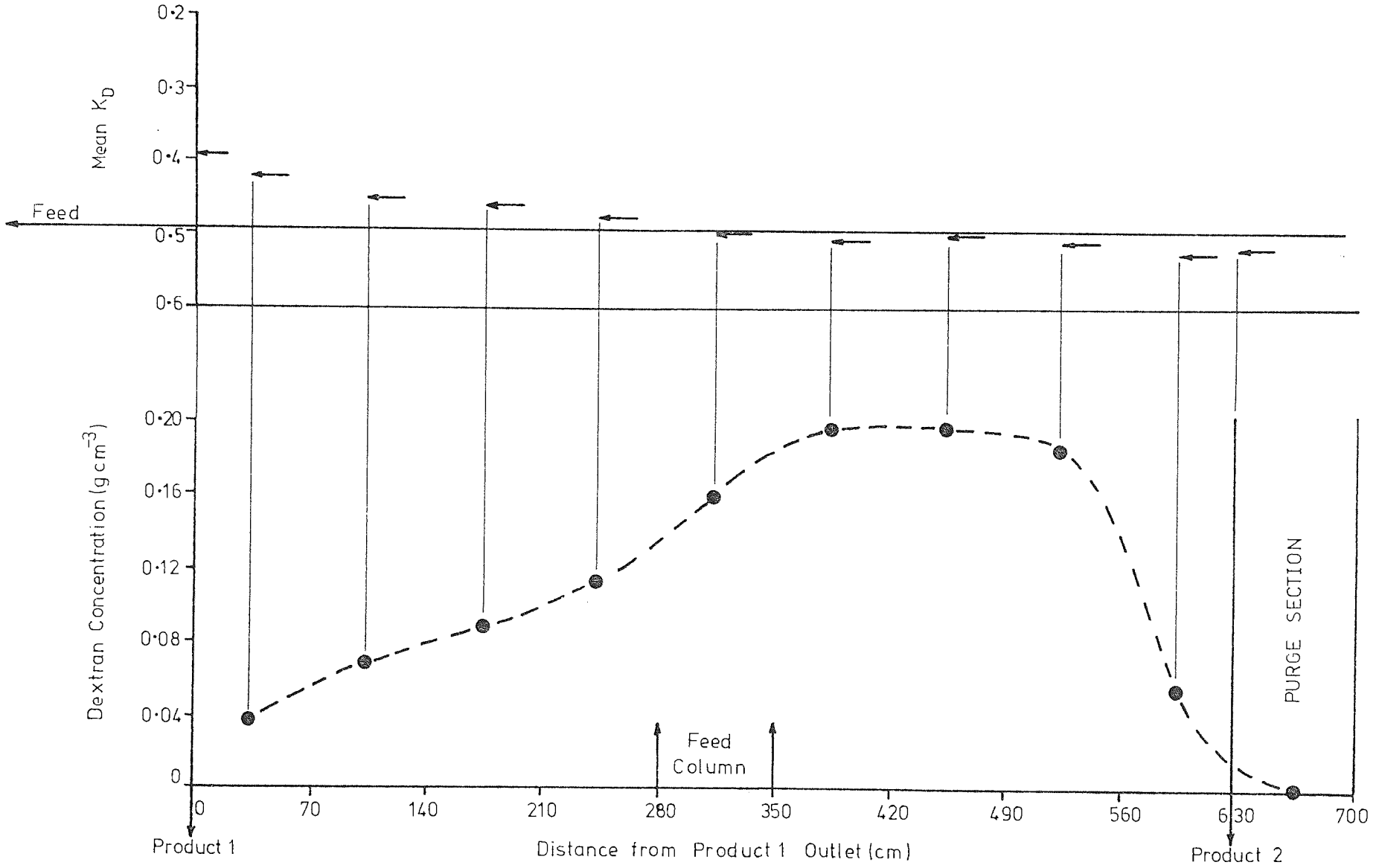

Figure 7.24 The Variation of Concentration and K_D around the SCCR3 Unit at the End of Run 20-500-0·8

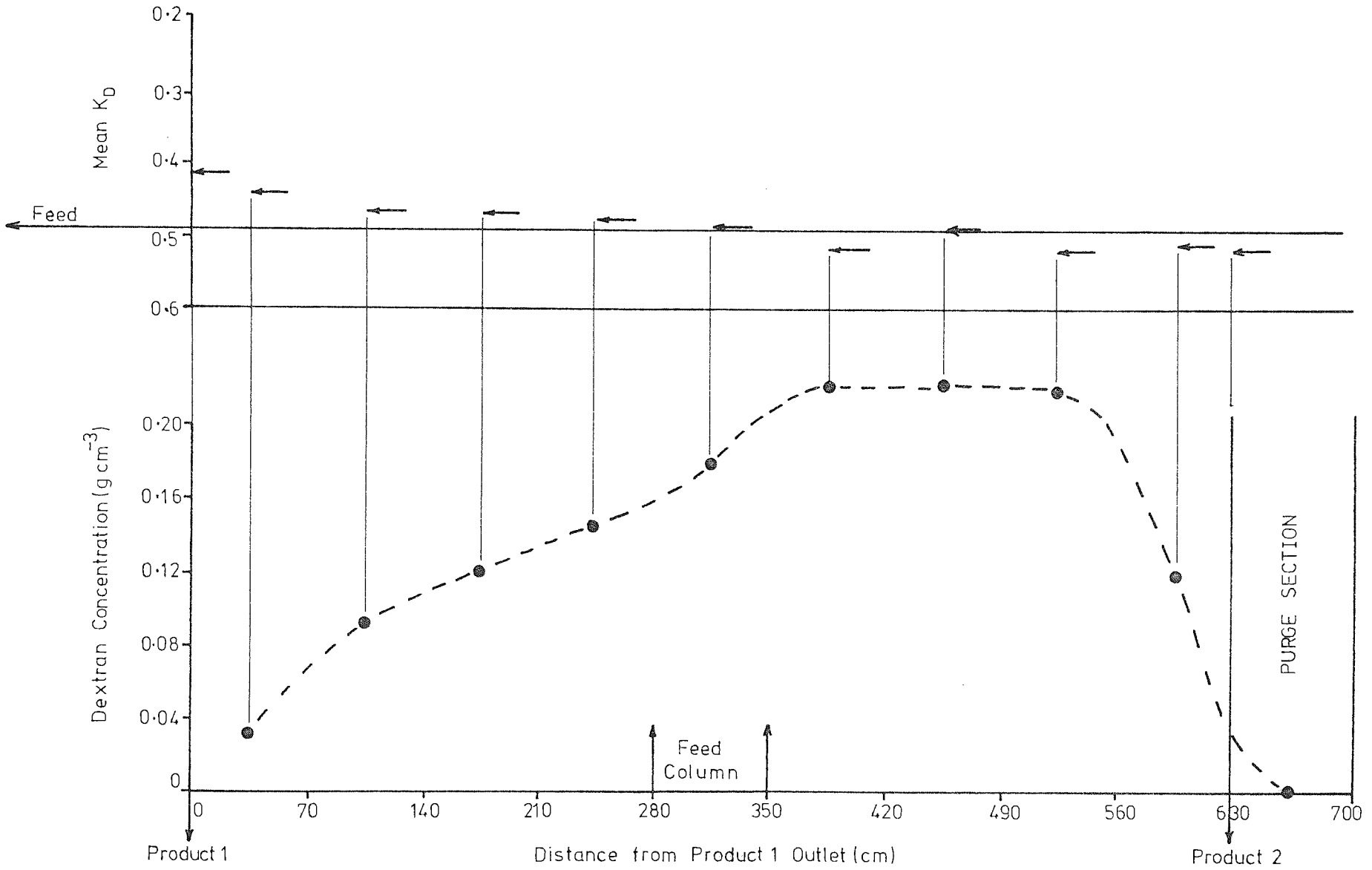

Figure 7.25 The Variation of Concentration and K_D around the SCCR3 Unit at the End of Run 20-400-1·1

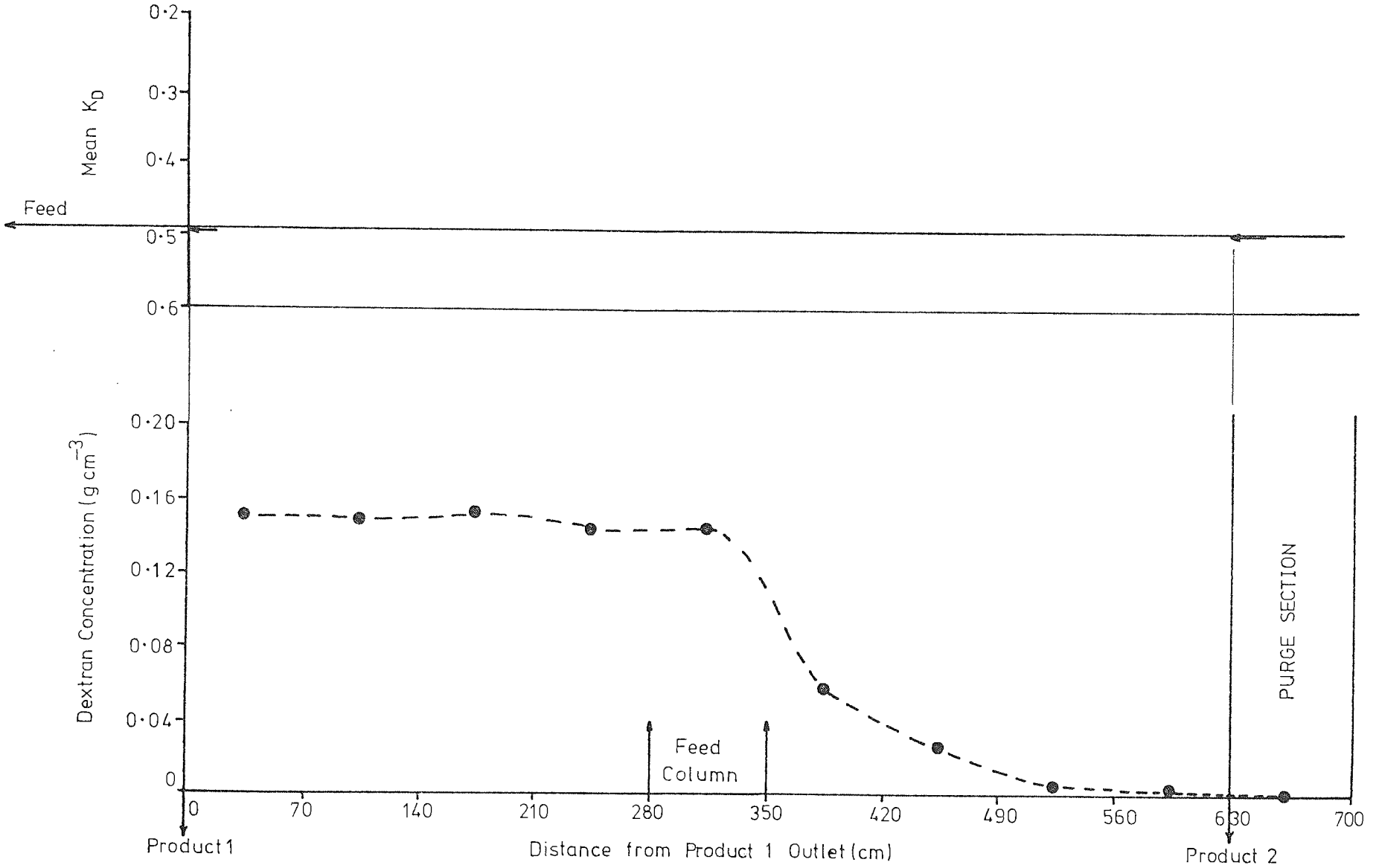

Figure 7.26 The Variation of Concentration and K_D around the SCCR3 Unit at the End of Run 01-600-0·7

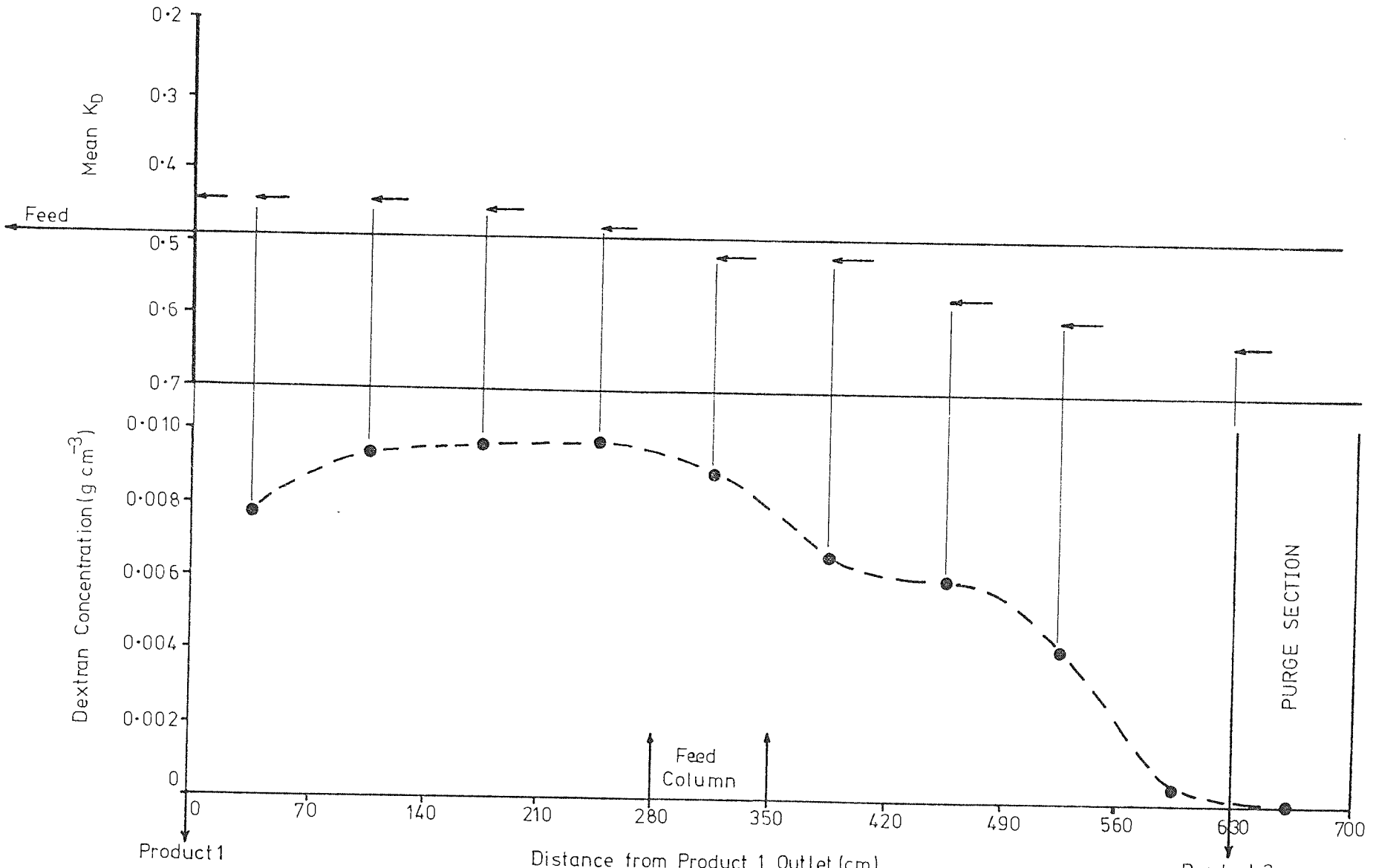

travelling with the mobile phase for the experimental conditions used in these cases. For FIG. 7.25 virtually all of the feed is seen to be travelling with the mobile phase, and pure feed to be emerging from the product 1 port, due to the extreme L'/P setting used. Although pure feed is also emerging from the product 2 port, which may be due to the difference in operating L'/P ratio in each half of the unit, or slight leakage of feed into the pre-feed section, this represents <2% of the total feed input. This run has therefore exceeded the limiting L'/P ratio for fractionation of the dextran feed at ~20% feed concentration and a mobile phase/feed flowrate ratio of ~5.2. It is apparent from FIGS. 7.19-7.26 that very little fractionation is achieved over the plateau region of each concentration profile, e.g. A-B in FIG. 7.19, and the major fractionation is being achieved in less than two-thirds of the total separating length. In part this is due to the discontinuous nature of operation of the SCCR3 unit, and the step-change in the mobile phase flowrate at the feed inlet point. Movement of the feed inlet position in the direction of the plateau region would be expected to increase the effective separating length. However, this restricts the flexibility of the SCCR3 machine as an experimental unit, because it would then only be suitable for removing the end of the feed distribution away from which the feed point had been moved.

The mean K_D values of column samples, given in FIGS. 7.19-7.26, generally provide a useful indication of the degree of fractionation being achieved in a particular part of the separating section, and can be compared with the mean K_D values of products and feed for the run.

Perhaps the most striking feature of the concentration profiles is the high concentrations (>20% w/v dextran), by batch g.p.c. standards, that the SCCR3 unit can tolerate. Conventionally, batch g.p.c. columns are operated at on-column sample concentrations <1% w/v,

to maintain sample resolution, and 20% w/v dextran represents severe overloading by these standards, indicating a particular advantage of the counter-current operational mode.

Generally, the build-up of dextran on the high concentration side of the feed point continued until a value 0.7-1.1 times greater than the feed inlet concentration was reached. Within this range, the particular value of concentration that was reached was dependent on the operating concentration, the mobile phase/feed flowrate ratio, and the L'/P ratio. The build-up of dextran on the low concentration side of the feed point generally reflected the fraction of feed material travelling preferentially with the mobile phase. For example, a larger fraction of material travelled preferentially with the mobile phase in RUN 20-500-0.8 than in RUN 20-600-0.7, and this is reflected in the higher concentration level of the former, compared with the latter, on the left-hand side of the feed point.

Initial on-column feed concentrations and maximum recorded on-column concentrations are summarized in FIG. 7.27. Initial on-column feed concentration is defined as:

$$\text{INITIAL ON-COLUMN FEED CONCENTRATION} = \text{FEED CONCENTRATION} \times \left(\frac{\text{MOBILE PHASE FLOWRATE} + \text{FEED FLOWRATE}}{\text{FEED FLOWRATE}} \right)$$

As such it gives a measure of the initial concentration at the start of the feed column, and, comparison of this figure with the final on-column concentrations, provides an indication of the extent of dextran build-up during each experimental run.

7.4.3.2 Product Molecular Weight Distributions

FIGS. 7.28 to 7.35 compare the distributions of average products, from each dextran fractionation run, with that of the

Figure 7.27 Summary of Results of Dextran Fractionations with the SCCR3 Unit

Run No.	Total Time of Run	Total No. of Cycles of SCCR3 Unit	PRODUCT ANALYSIS								CONC. PROFILE ANALYSIS			
			Time of Collection of Products	Product 1 (High M.W.)			Product 2 (Low M.W.)			$\frac{\sigma_1^2+\sigma_2^2}{\sigma_{feed}^2}$	Time to Analysis	Initial on-Col. Conc.	Maximum on-Col. Conc.	
				Mean K_D	Mean M.W.	$\frac{\sigma_1^2}{\sigma_{feed}^2}$	Mean K_D	Mean M.W.	$\frac{\sigma_2^2}{\sigma_{feed}^2}$				Pre-Feed Point	Post-Feed Point
	hrs		hrs								hrs	$g\,cm^{-3}$	$g\,cm^{-3}$	$g\,cm^{-3}$
10-500-0·5	94·3	16·0	53·5 – 94·3	0·274	77 000	0·73	0·515	26 000	0·74	1·47	83·0	0·0155	0·0779	0·0357
20-500-0·5	43·9	15·0	8·8 – 35·2	0·235	95 000	0·69	0·505	27 000	0·98	1·67	43·9	0·0320	0·152	0·0315
20-1000-0·4	38·3	13·3	11·6 – 38·3	0·300	68 000	1·11	0·490	28 500	0·92	2·03	38·3	0·0658	0·200	0·0424
20-1700-0·3	38·4	13·5	5·6 – 38·4	0·310	63 000	1·22	0·485	29 000	0·92	2·14	38·4	0·104	0·205	0·0593
20-600-0·7	28·4	10·0	17·0 – 28·4	0·390	44 000	1·38	0·515	26 000	0·91	2·29	28·4	0·0351	0·195	0·158
20-500-0·8	38·3	10·0	15·3 – 38·3	0·418	39 000	1·03	0·520	25 000	0·71	1·74	38·3	0·0334	0·226	0·179
20-400-1·1	40·0	8·0	15·0 – 40·0	0·494	29 000	1·0	0·490	28 500	1·0	2·0	40·0	0·0353	0·0577	0·151
01-600-0·7	34·0	12·0	14·1 – 34·0	0·445	35 000	0·87	0·630	16 000	0·60	1·46	34·0	0·00167	0·00662	0·00970

Figure 7.28 Comparison of Feed and Product Distributions for Run 10-500-0·5

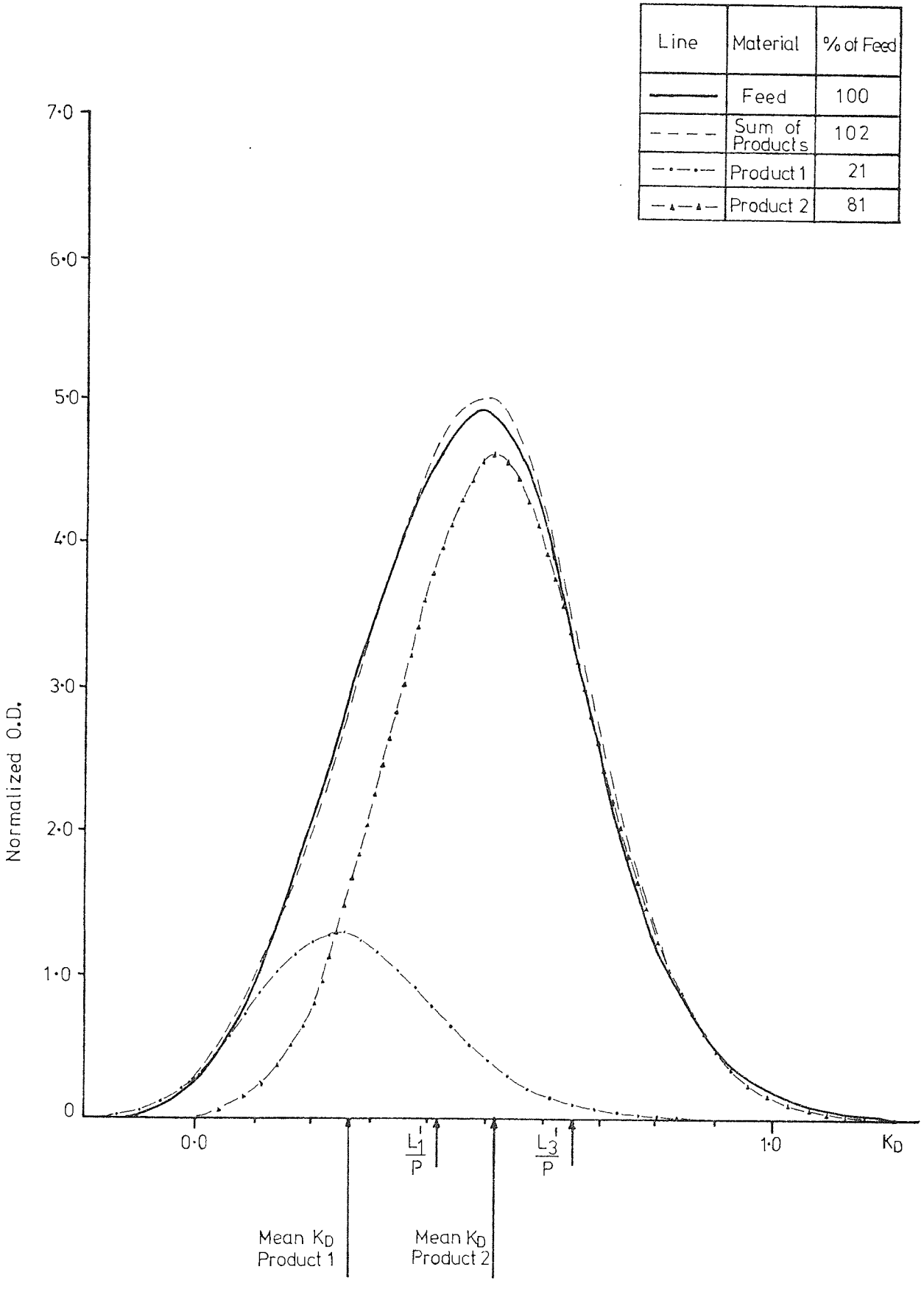

Figure 7.29 Comparison of Feed and Product Distributions for Run 20-500-0·5

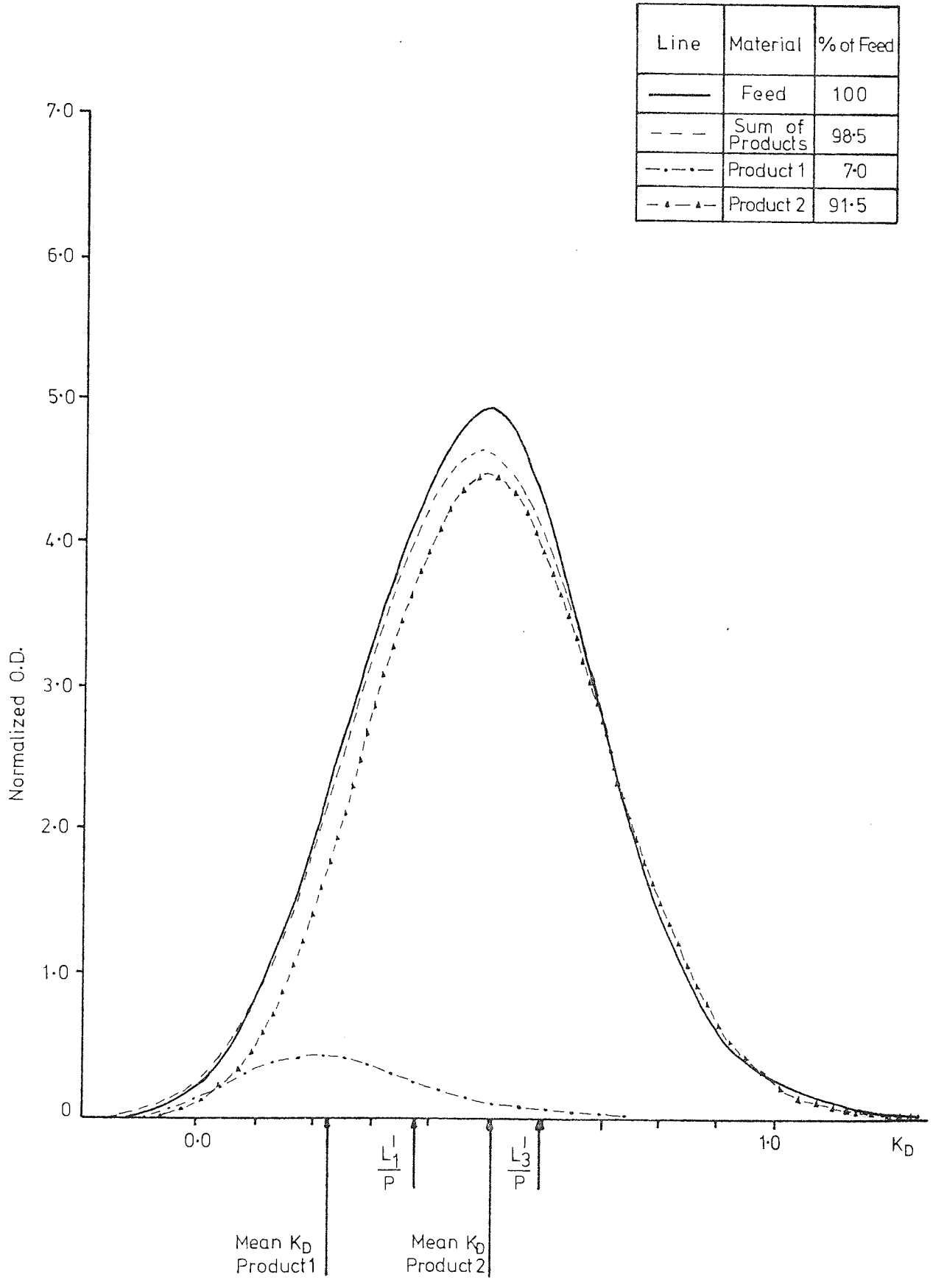

Figure 7.30 Comparison of Feed and Product Distributions for Run 20-1000-0·4

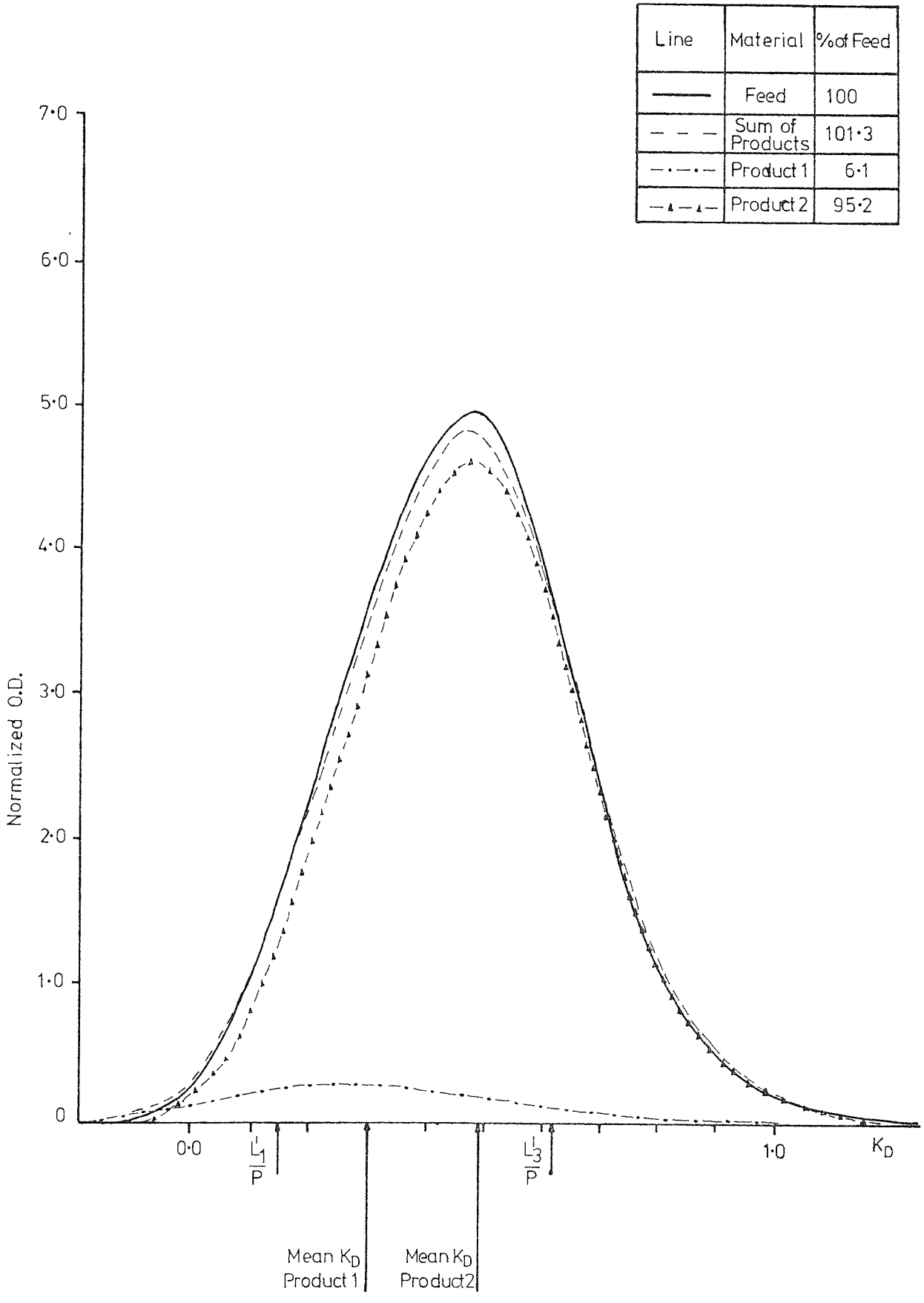

Figure 7.31 Comparison of Feed and Product Distributions for Run 20-1700-0·3

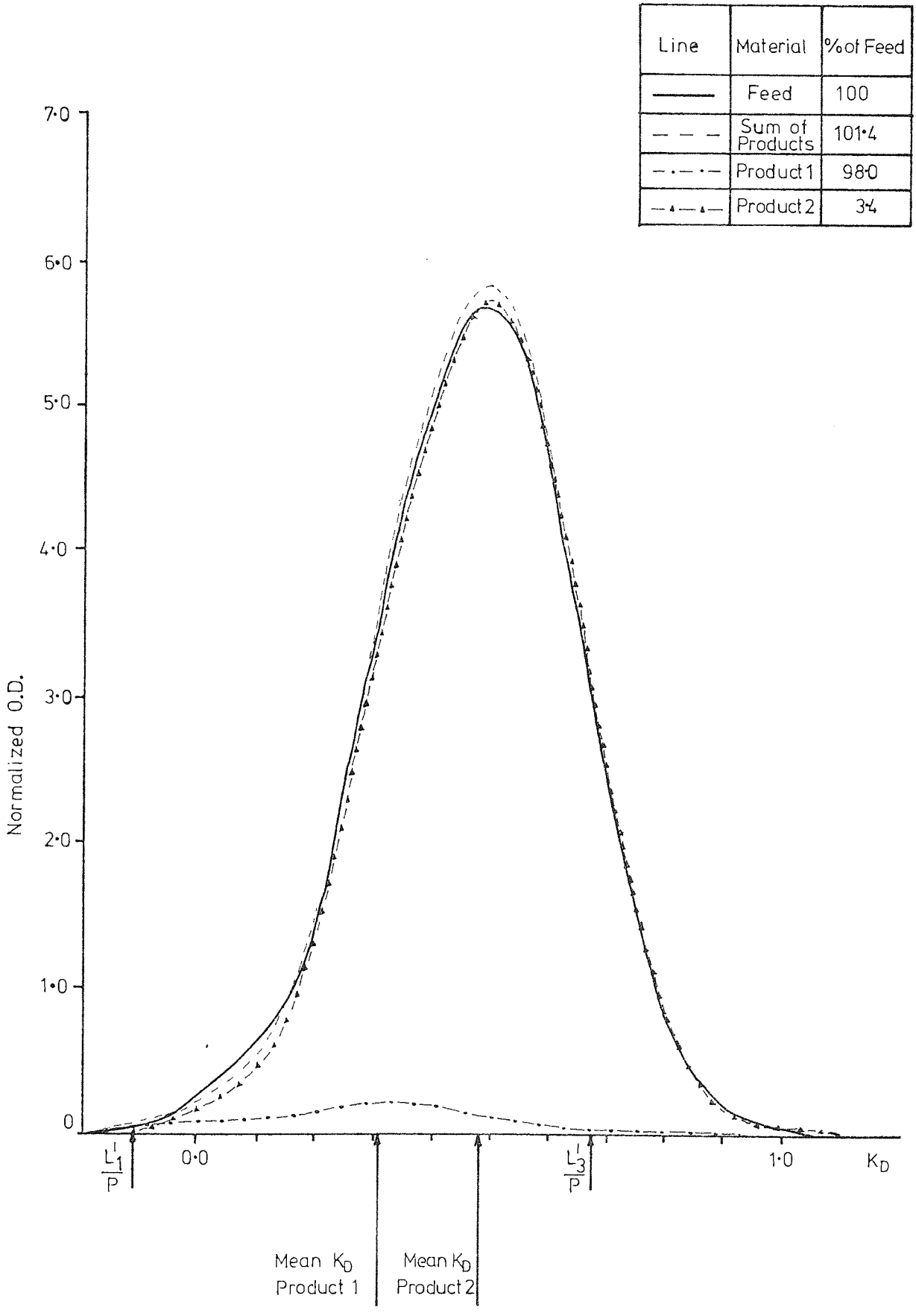

Figure 7.32 Comparison of Feed and Product Distributions for Run 20-600-0·7

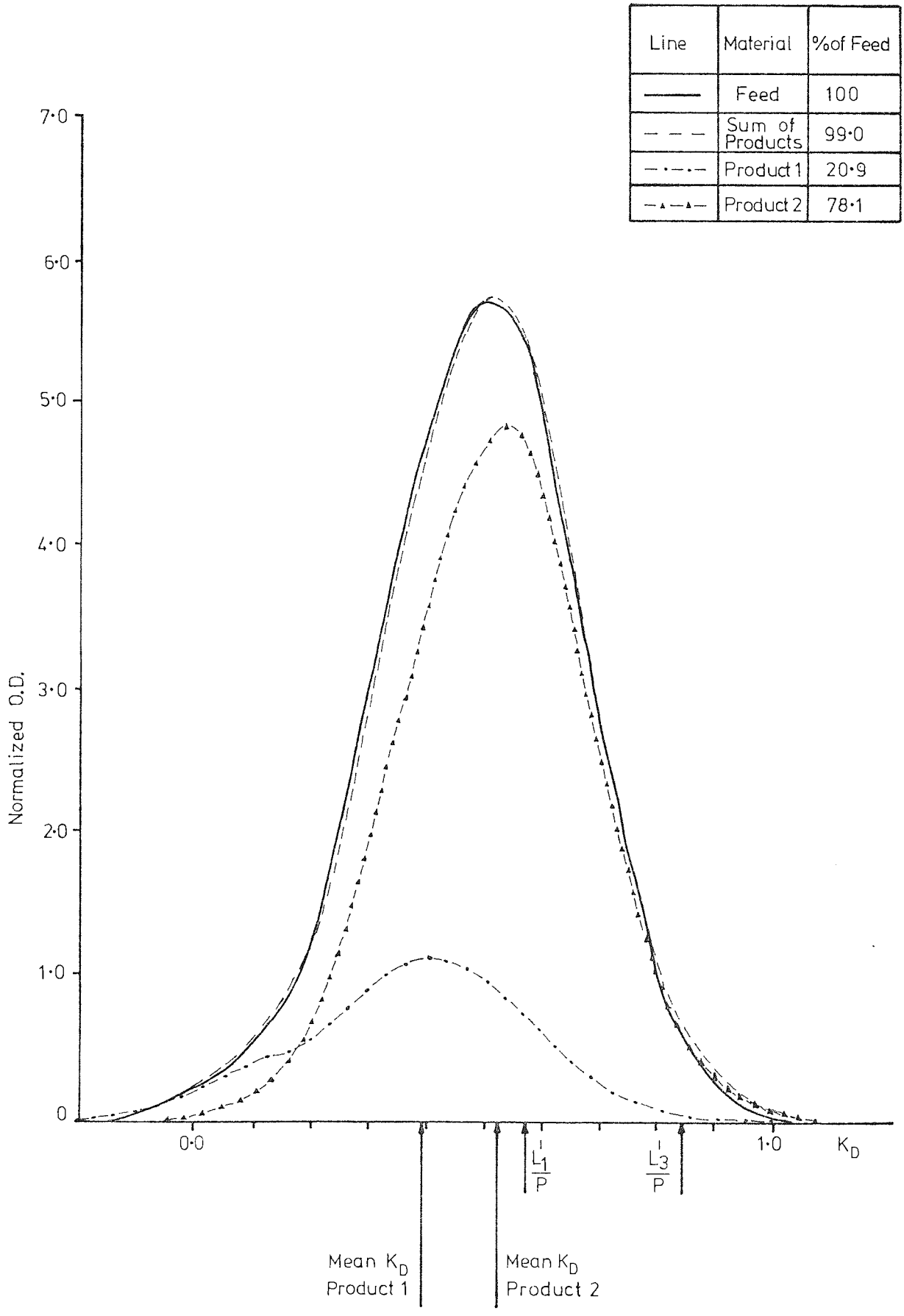

Figure 7.33 Comparison of Feed and Product Distributions for Run 20-500-0·8

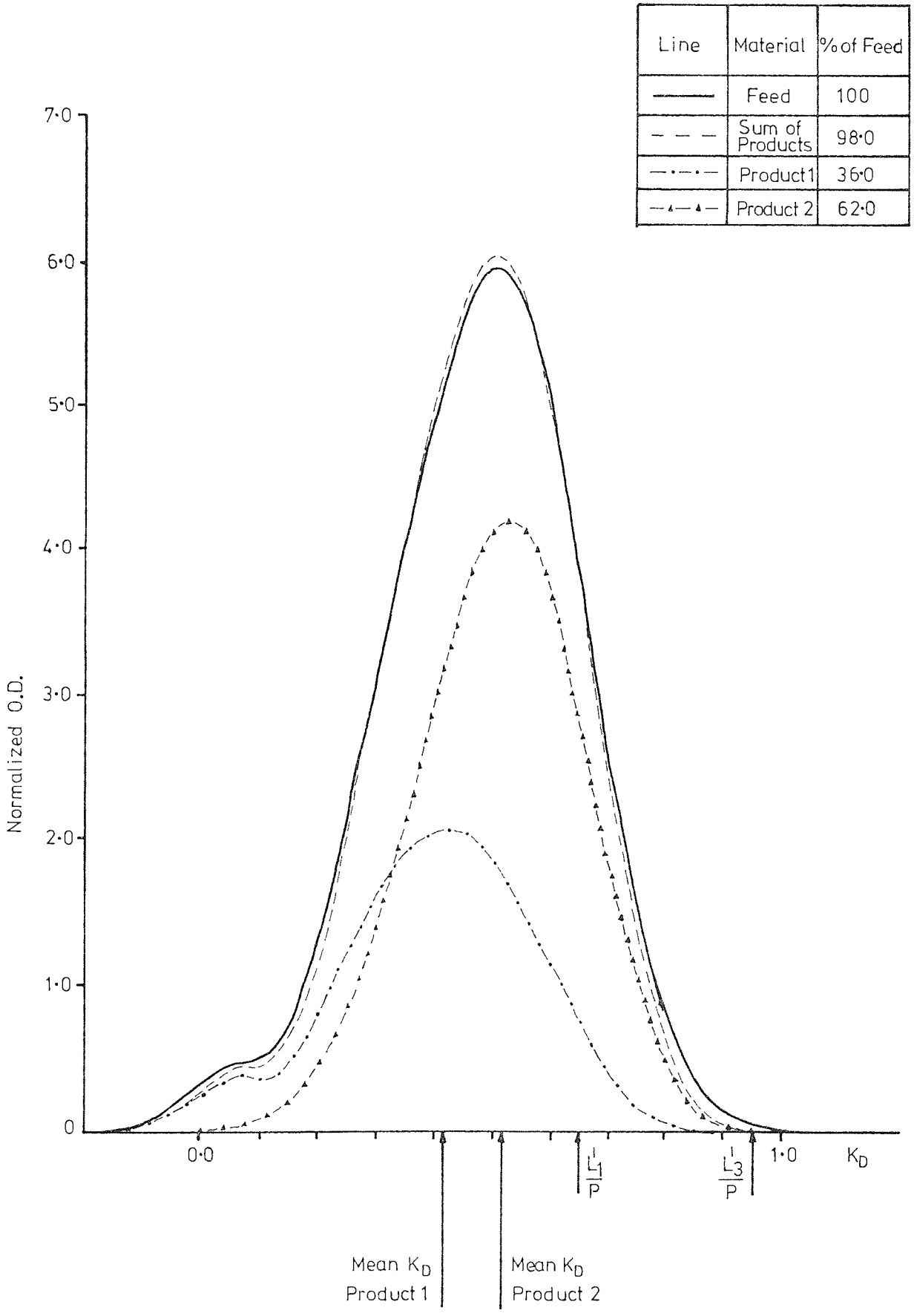

Figure 7.34 Comparison of Feed and Product Distributions for Run 20-400-1·1

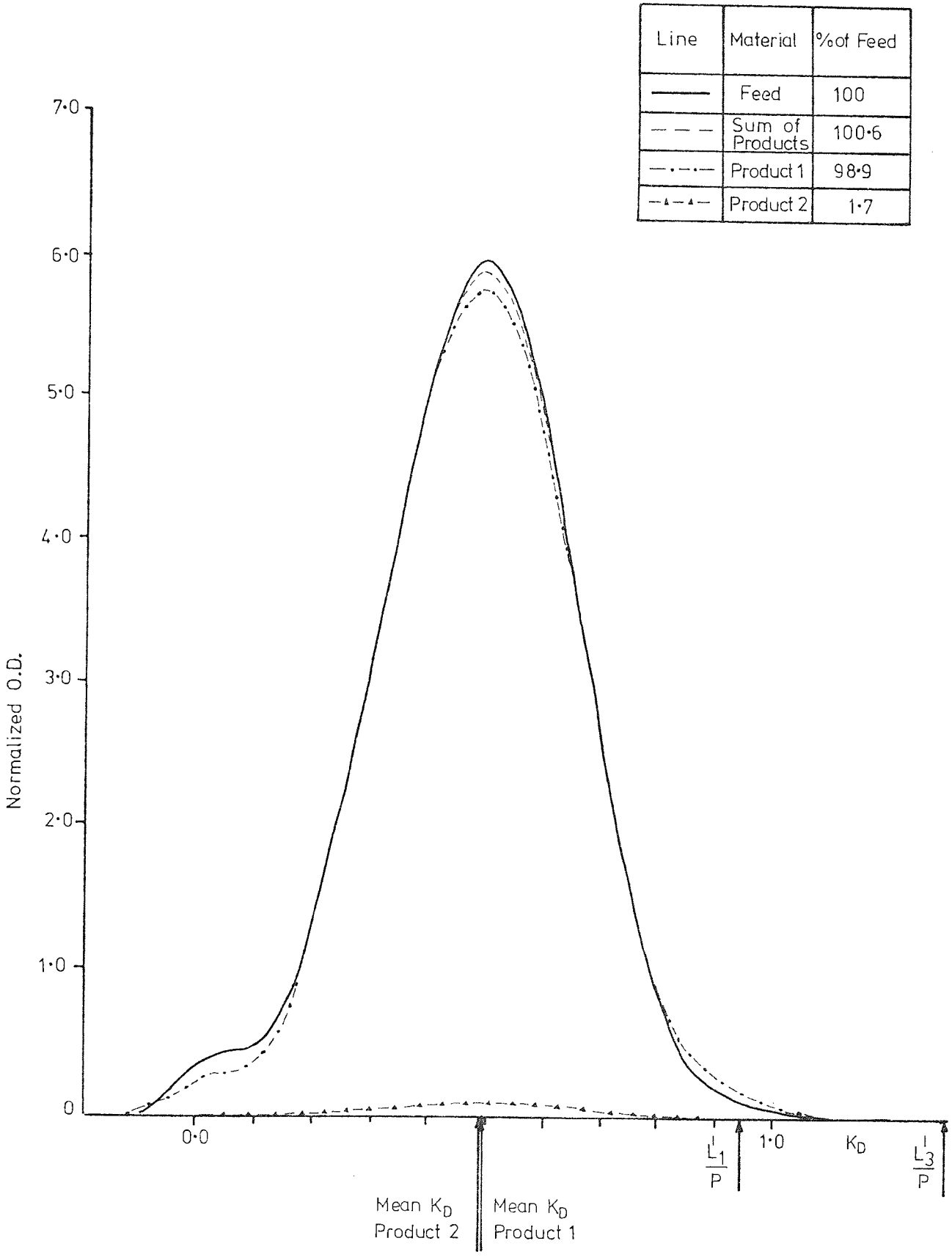

Figure 7.35 Comparison of Feed and Product Distributions for Run 01-600-0·7

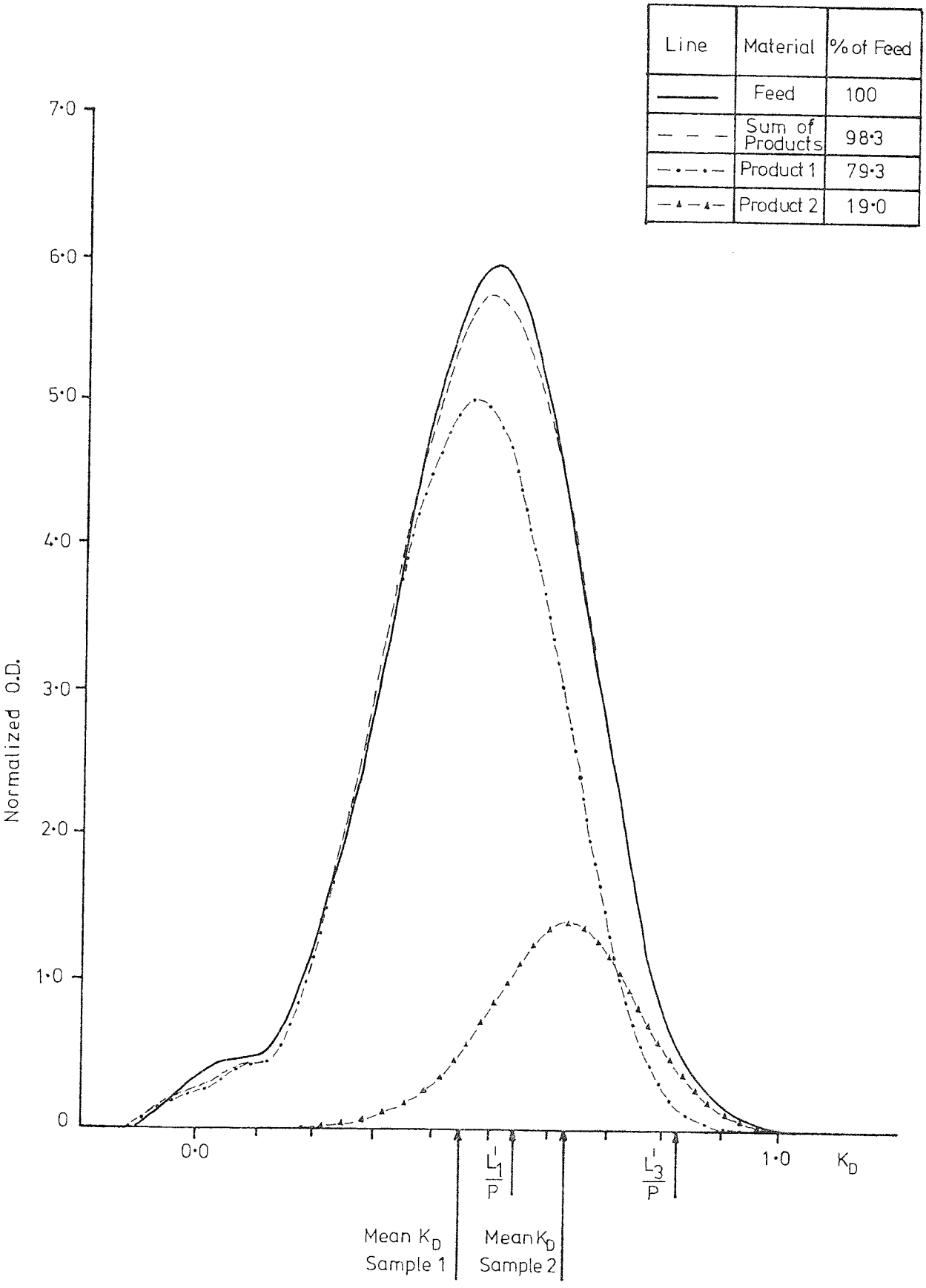

corresponding feed distribution for each run. Each average product analysis corresponds to all of the product obtained, from the time of attainment of approximate steady output concentration values, to the end of the run. The vertical line drawn for each product distribution represents the 50% cumulative weight point, or mean K_D, of the sample. All analyses were performed by g.p.c. using the techniques described in CHAPTER 4. Each product chromatogram has been scaled to an area proportional to the particular product dextran rate from the SCCR3 machine, using the method discussed in SECTION 7.2.3. Points corresponding to the values of the theoretical pre-feed cut position, L_1'/P, and post-feed cut position, L_3'/P, (SECTION 7.3.4), for each experimental run are indicated. Summation of the two product distributions for each run produced a total distribution in good agreement with the original feed distribution, which is apparent from FIGS. 7.28-7.35. Thus the total recorded dextran input rate, and M.W. distribution, balanced with the total recorded dextran output rate, and M.W. distribution, for each run.

FIGS. 7.29, 7.30 and 7.31, illustrate the effect of the flowrate step-change in the middle of the SCCR3 unit. The post-feed mobile phase/stationary phase rate, L_3'/P, is 0.594, 0.620, and 0.673 for each run respectively, and, if the feed flowrate was only a small part of the overall mobile phase flowrate, more dextran should travel with the mobile phase at a higher L_3'/P ratio. However, because the feed flowrate contributes a successively greater amount, to the overall mobile phase flowrate from FIG. 7.29 to FIG. 7.31, which more than counteracts the successive increase in L_3'/P, the reverse effect occurs, and less dextran travels with the mobile phase at a higher L_3'/P ratio. Qualitatively, an increase in the average L/P ratio, $(L/P)_{MEAN}$, is reflected by an increase in the amount of dextran travelling with the

mobile phase, at a given operating concentration. This is illustrated by FIGS. 7.32, 7.33 and 7.34, wherein the fraction of the feed travelling with the mobile phase increases from 20.9% to 98.9%.

Comparison of FIGS. 7.32 and 7.35 illustrates the concentration dependence of the migration rate of dextran through the SCCR3 unit. These runs were carried out at a feed concentration of 22.0% and 1.02% dextran respectively, with all other operating conditions approximately constant. For RUN 20-600-0.7, 20.9% of the product emerged from the high M.W. outlet port, while for RUN 01-600-0.7 this was found to increase to 79.3%. The positions of the theoretical cuts for RUN 01-600-0.7, based on the assumption of dilute operating conditions (SECTION 7.3.4), and the observed separation position of the products are in approximate agreement. However, the concentration dependence of the distribution coefficient, K_D, means that the theoretical cut positions, calculated for dilute operating conditions, disagree markedly from the observed separation position for conditions of higher concentration. Generally, the concentration dependence of K_D observed here is in qualitative agreement with the results discussed in SECTION 4.4. Since a dextran component's migration rate is reduced as the overall dextran concentration is increased (SECTION 4.4.4), this results in a greater portion of feed travelling in the direction of movement of the packing in the SCCR3 unit as the on-column dextran concentration is increased. Therefore the separation position or 'cut' position obtained moves towards the high molecular weight end of the dextran feed distribution.

As experience was gained with the SCCR3 unit, operating conditions for runs using high on-column concentrations were estimated from the observed separating positions of earlier runs. The range of settings covered with the SCCR3 unit during this research will allow

adjustment of operating conditions to produce an approximate separating position, up to on-column concentrations of 20% w/v dextran, during any future work.

FIG. 7.27 summarizes information concerning products for all experimental runs. The mean K_D, and corresponding molecular weight, for each sample is indicated, together with a measure of individual, and total, product variance for each run. The variance of each product distribution was computed using PROGRAM 1, listed in APPENDIX 5, and expressed as the ratio of product distribution variance to feed distribution variance. This was necessary as two different feed batches were used, with different molecular weight distributions (APPENDIX 2), and hence different variance values. The total product/feed variance ratio provides a measure of the effectiveness of each fractionation, and allows comparison of SCCR3 experimental runs. Values are given in FIG. 7.27. Use of the second moment gives each product distribution equal weighting, and measures the spread of each about its mean. This extent of product overlap is more apparent if all products are plotted to equal area, and this is done in FIGS. 7.36-7.42.

It is apparent from FIG. 7.27 that the order of experimental runs, in terms of best-worst fractionation, based on the second moment, is:

1-600-0.7, 10-500-0.5, 20-500-0.5, 20-500-0.8, 20-1000-0.4, 20-1700-0.3, 20-600-0.7.

A number of general conclusions are indicated from this fractionation order:

(i) Operating at high on-column concentrations produces some loss of fractionation, although direct comparison of two runs is

Figure 7·36 Product Distributions for Run 10-500-0·5 : Scaled to Equal Area

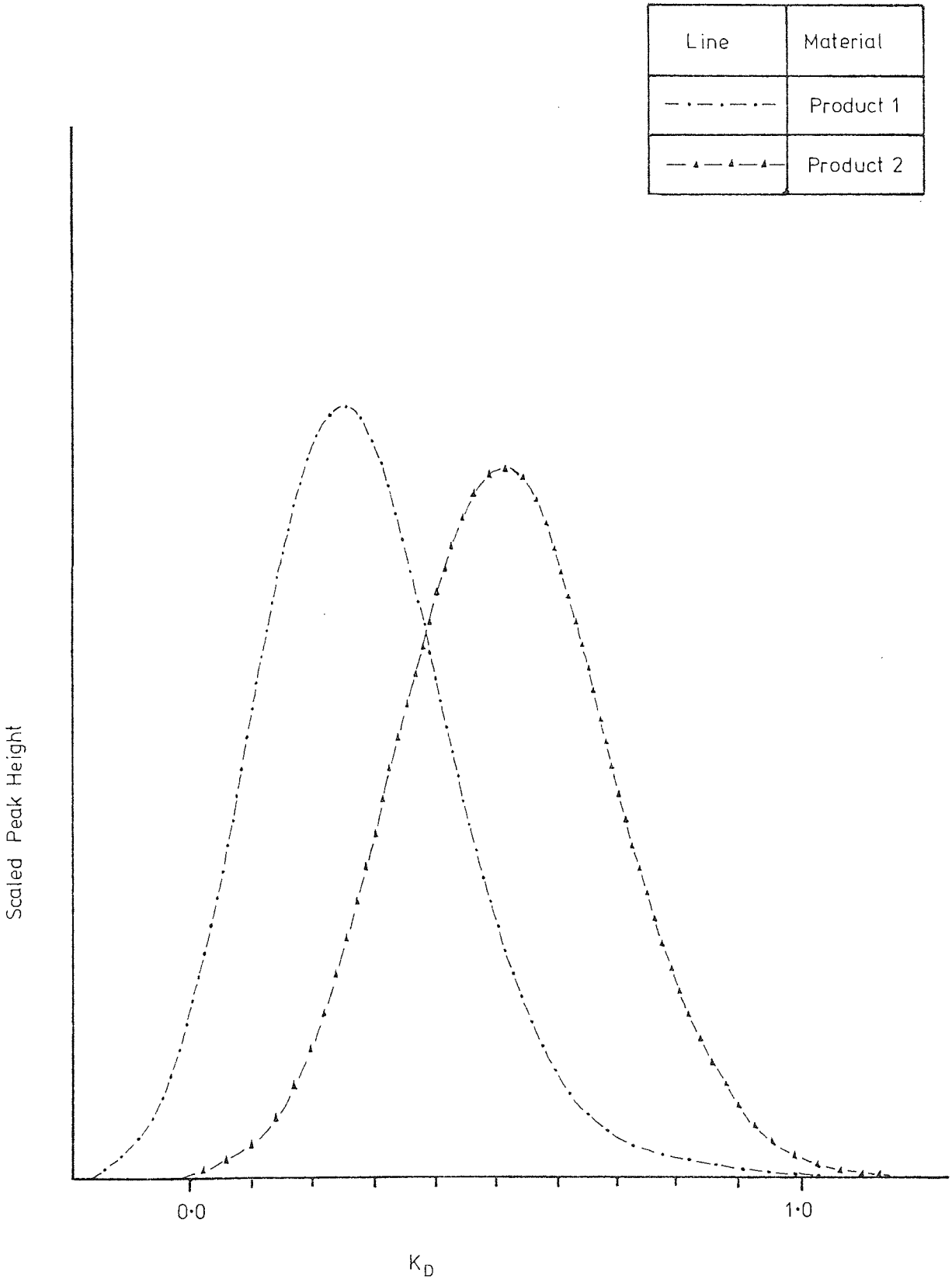

Figure 7.37 Product Distributions for Run 20-500-0·5 : Scaled to Equal Area

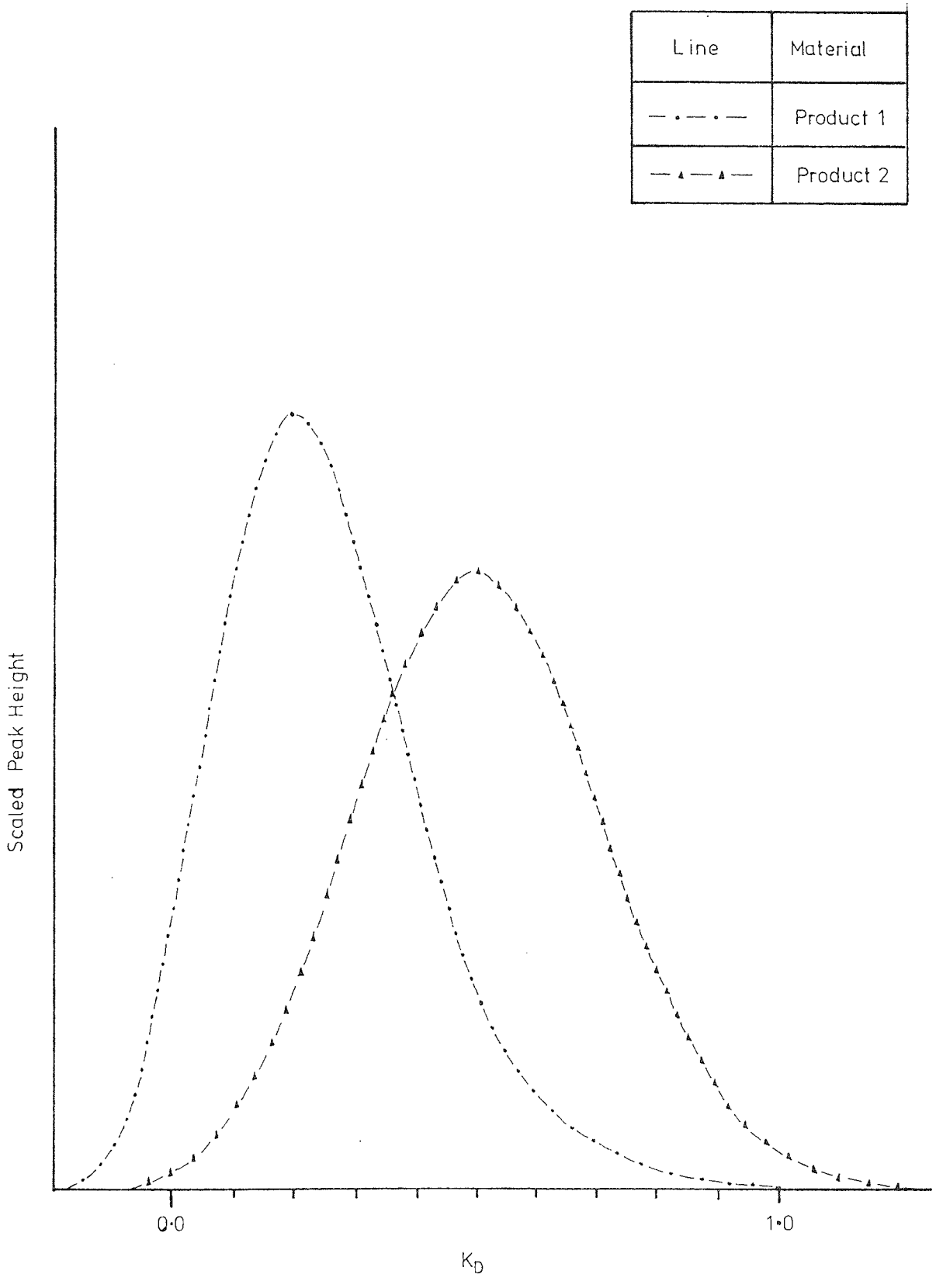

Figure 7·38 Product Distributions for Run 20-1000-0·4: Scaled to Equal Area

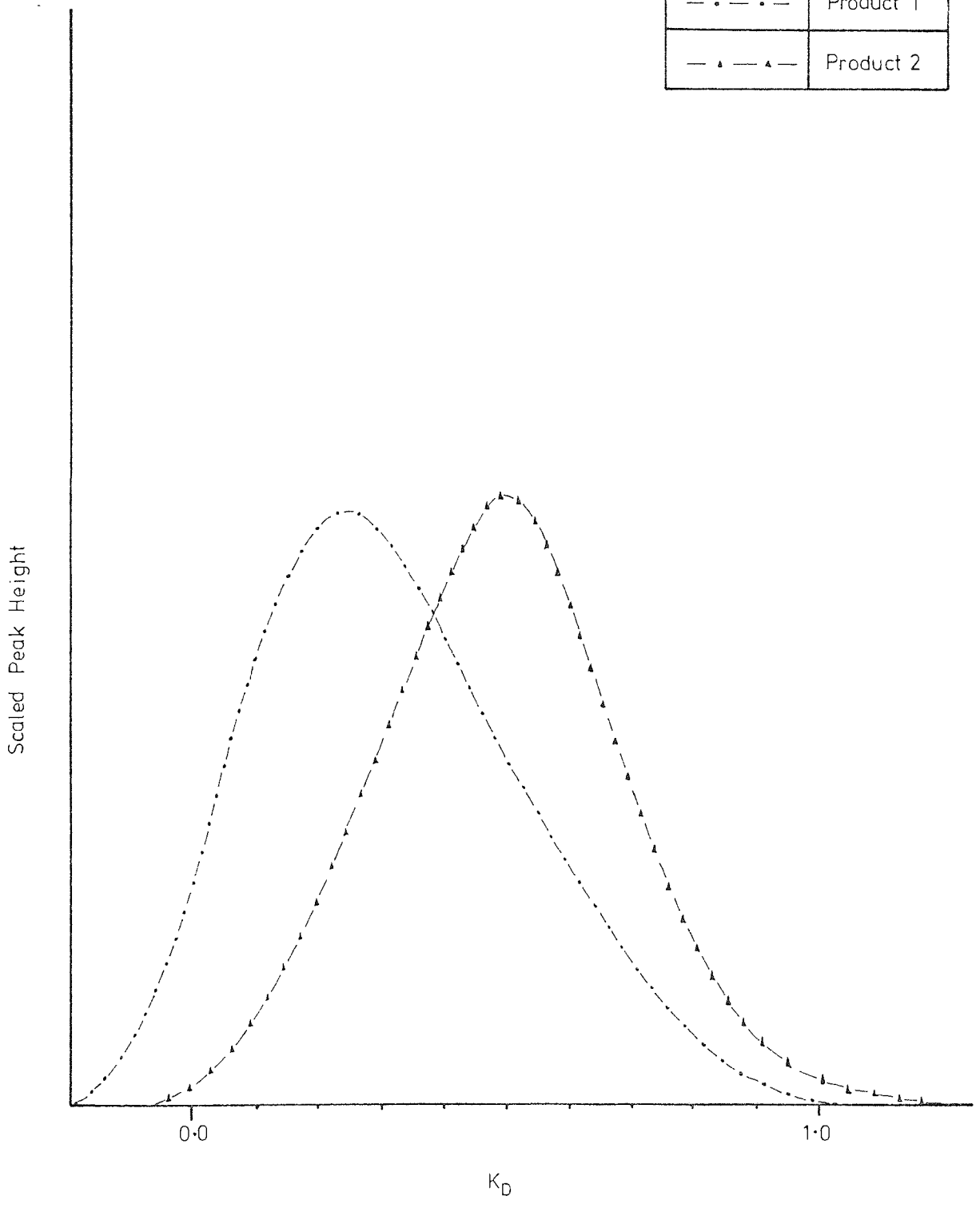

Figure 7.39 Product Distributions for Run 20-1700-0·3: Scaled to Equal Area

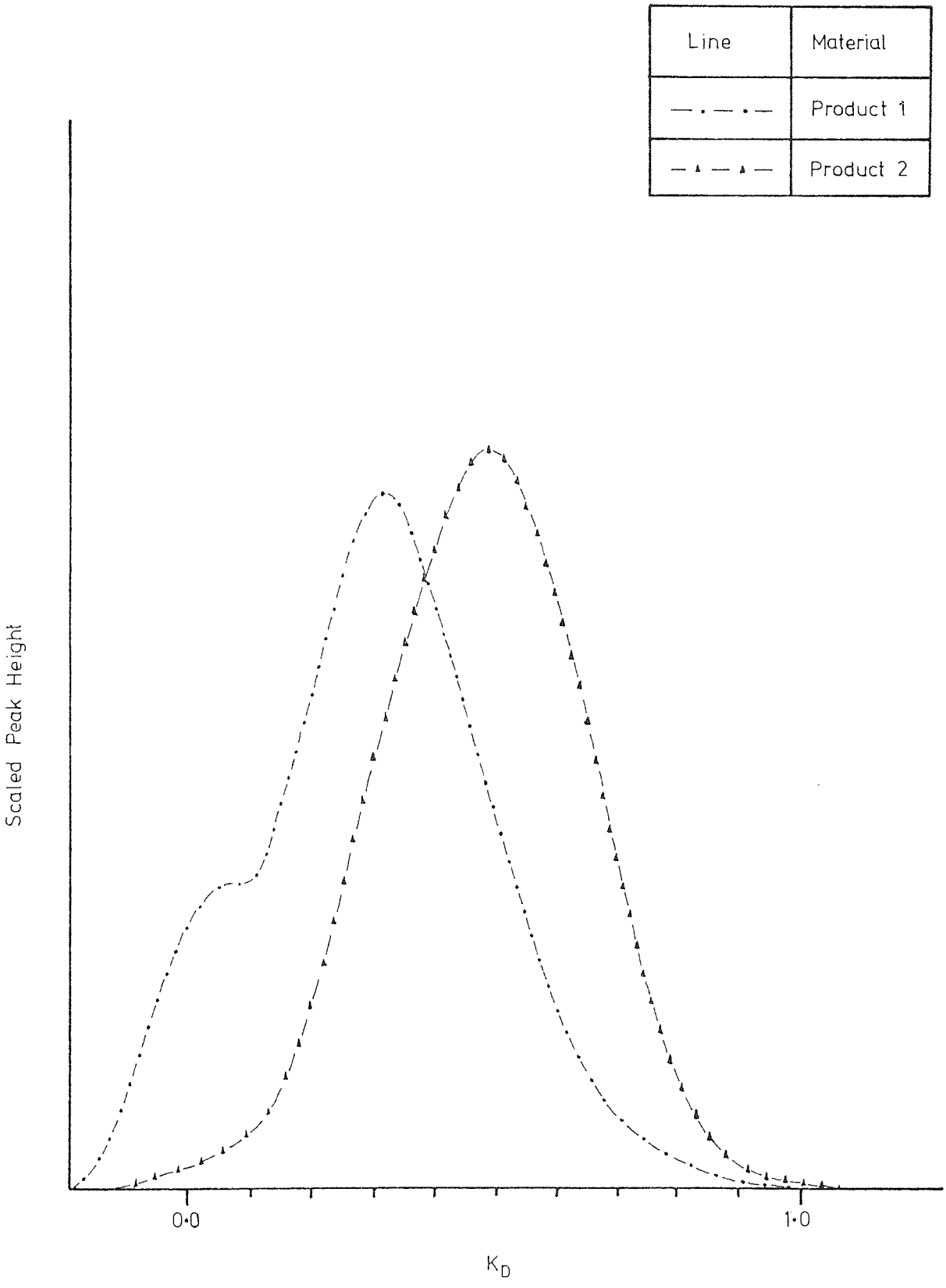

Figure 7.40 Product Distributions for Run 20-600-0·7: Scaled to Equal Area

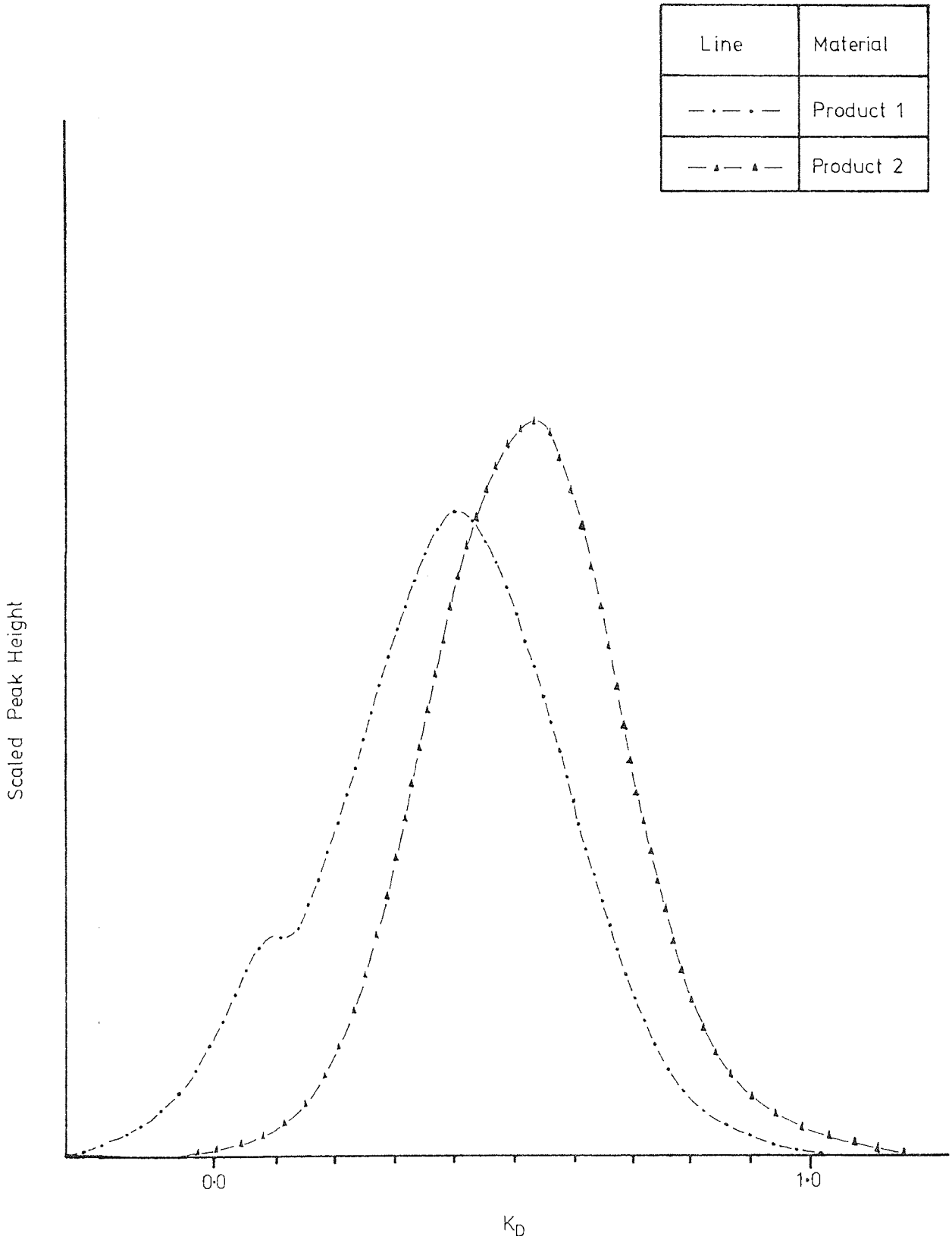

Figure 7.41 Product Distributions for Run 20-500-0·8 : Scaled to Equal Area

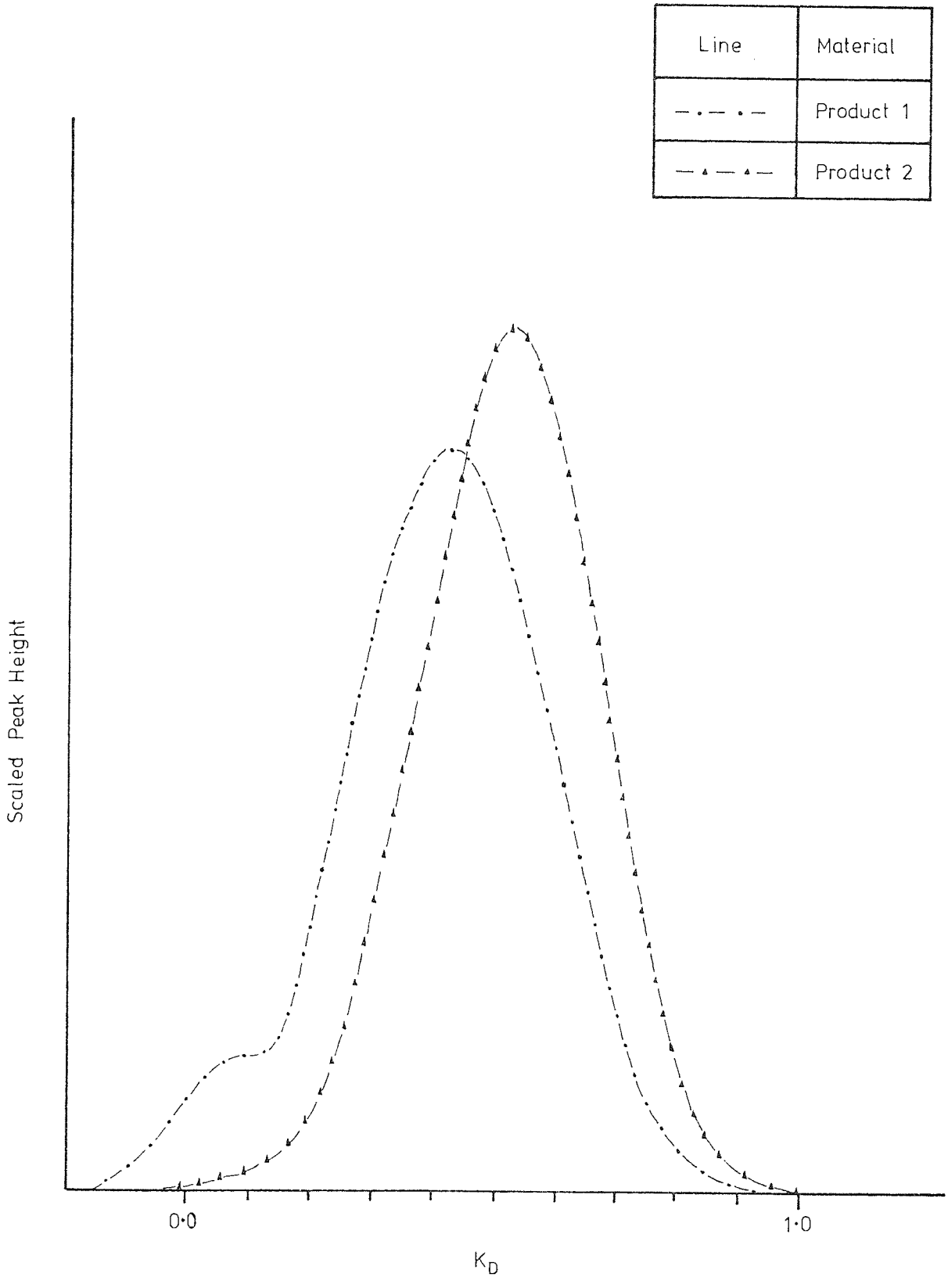

Figure 7.4.2 Product Distributions for Run 01-600-0·7: Scaled to Equal Area

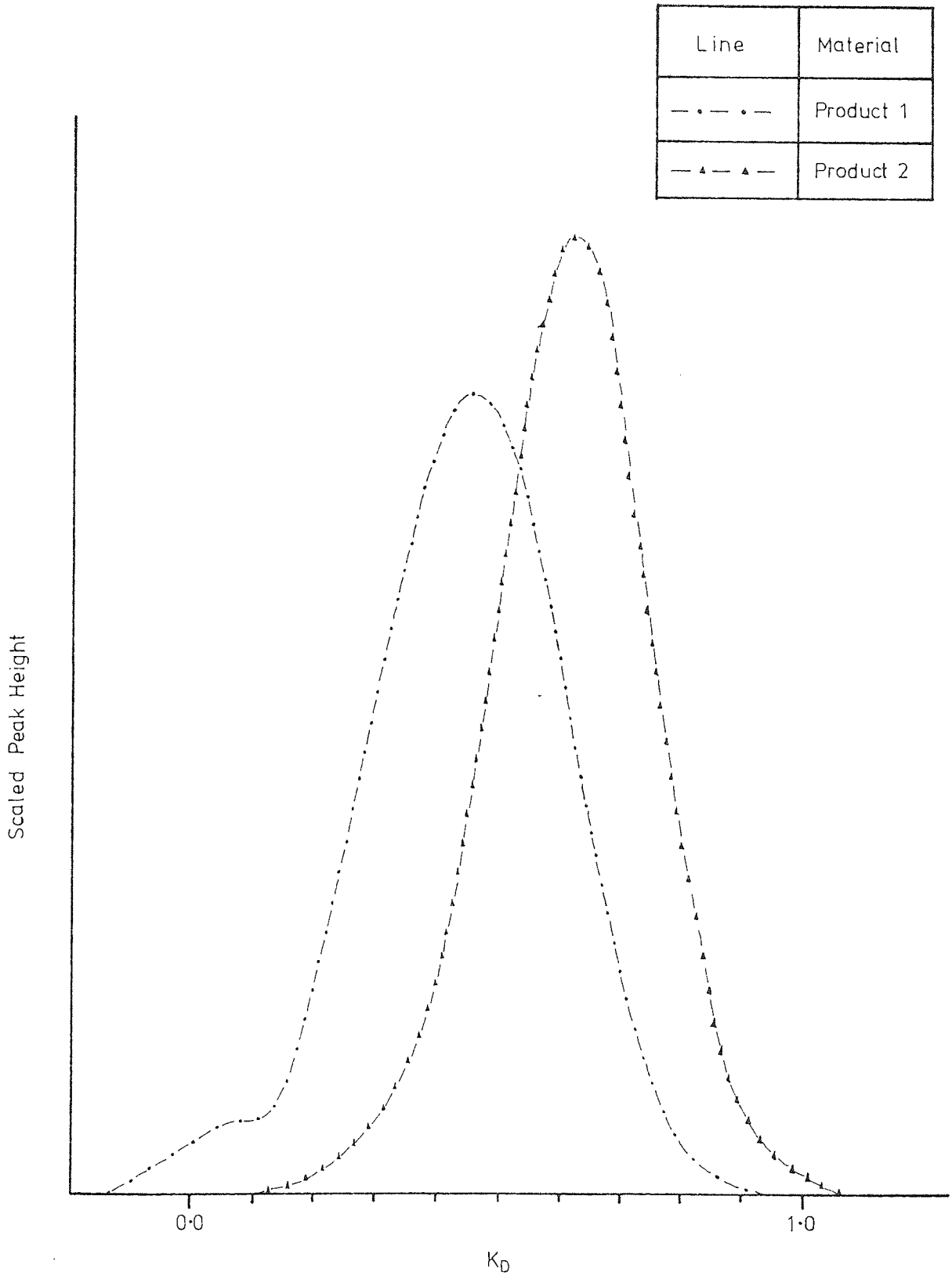

not possible because of variations in the operating conditions. Generally, a degree of fractionation loss may be expected from chromatographic theory at finite concentration discussed in SECTIONS 2.3.1.2 and 3.4.1.

(ii) A reduction in the mobile phase/feed flowrate ratio while maintaing an approximately constant overall mobile phase flowrate and feed concentration, produces a poorer fractionation. This is apparent from RUNS 20-500-0.5, 20-1000-0.4, and 20-1700-0.3, when the mobile phase/feed flowrate ratios were 5.56, 2.13, and 0.95 respectively. This effect is expected as a lower mobile phase/feed ratio signifies a greater departure from the idealized case of a negligible feed input volume (SECTION 7.3.3.4).

(iii) Increasing the feed concentration from 10.1% to 21.0% w/v dextran, and reducing the number of columns from twenty to ten, while maintaining the mobile phase/feed flowrate ratio, L'/P ratios, and overall mobile phase flowrate approximately constant, is shown, by comparison of the variance values of RUNS 10-500-0.5, and 20-500-0.5, to result in only a 14% increase in the total product/feed variance ratio, indicating the ability of the SCCR3 unit to maintain fractionation performance under arduous operating conditions.

7.4.3.3 Concluding Discussion of Fractionation Studies

Prediction of operating conditions for the SCCR3 unit at high on-column concentrations is complicated by a concentration dependence of the distribution coefficient, K_D. The results presented in this thesis will enable experimental conditions to be estimated in future work, until a detailed quantitative treatment of this non-linearity of the distribution isotherm is established.

A considerable increase in throughput has been achieved

Figure 7.43 Estimated Dextran Throughputs for Larger Diameter Sequential Units based on SCCR3 Results

Note Annual Throughputs Calculated Assuming Continuous Operation for 8000 hrs.

Run No.	Total Column Length (m)	Overall Pressure Drop (kNm^{-2})	Dextran Throughput (Tonnes/Annum)	Estimated Throughputs (Tonnes/Annum) for Larger Diameter Columns Based on Scale-up of SCCR3 Throughputs in Proportion to Cross-Sectional Column Area				
				10·2 cm dia. (4 ins)	15·3 cm dia. (6 ins)	20·3 cm dia. (8 ins)	25·4 cm dia. (10 ins)	30·5 cm dia. (12 ins)
10-500-0·5	14·0	325	0·40	1·60	3·60	6·40	10·0	14·4
20-500-0·5	7·0	220	0·82	3·28	7·38	13·1	20·5	29·5
20-1000-0·4	7·0	280	1·69	6·76	15·2	27·0	42·3	60·8
20-1700-0·3	7·0	300	2·78	11·1	25·0	44·5	69·5	100
20-600-0·7	7·0	400	1·04	4·16	9·36	16·7	26·0	37·4
20-500-0·8	7·0	440	0·80	3·20	7·20	12·8	20·0	28·8
20-400-1·1	7·0	225	0·77	3·08	6·93	12·3	19·2	27·7
01-600-0·7	7·0	90	0·05	0·20	0·45	0·80	1·25	1·80

with the use of concentrated feed solutions, up to 22% w/v dextran, with the SCCR3 unit. The recorded throughputs in this study, converted to annual quantities, based on continuous operation for 8000 hours per annum, are detailed in FIG. 7.43. Other figures given are the production rates for a series of larger diameter columns, based on scaling the results of the present study in proportion to column cross-sectional area. The increase in throughput gained by the use of high dextran feed concentrations has been offset by only a modest loss of fractionation performance. The use of higher feed flowrates, for a given overall mobile phase flowrate, has, however, produced a more serious loss of fractionation, and may restrict future successful operation of the unit to mobile phase/feed flowrate ratios above a value of about 2-3.

CHAPTER 8

Theoretical Treatment of the Continuous Counter-Current Chromatographic Process

8.1 INTRODUCTION

Sciance and Crosser (242) used a probabilistic model approach, for the moving-bed form of continuous chromatography, to relate the operating flowrates, feed-point location, degree of separation, and required column length for a binary feed mixture. For the case when the feed is introduced into the mid-point of the column, they obtain the equations:

$$\ell n\ (u_z)_A = \frac{\ell k''_A}{2u}\ (K_A - \psi) \tag{8.1}$$

$$\ell n\ [1 - (u_z)_B] = \frac{-\ell k''_B}{2u_G}\ (K_B - \psi) \tag{8.2}$$

A refers to the faster moving component

B refers to the slower moving component

$(u_z)_A$ = Bottoms/feed mass flowrate ratio of component A

$(u_z)_B$ = Tops/feed mass flowrate ratio of component B

k'' = rate constant of desorption

u = Average mobile phase velocity

ψ = Operating mobile phase/stationary phase velocity ratio

ℓ = required column length

A disadvantage of this method is the fact that k''_A and k''_B must be determined experimentally as published values are scarce.

Al-Madfai (21) applied the random walk approach, discussed in SECTION 2.2.4.3, to describe solute zone broadening in continuous counter-current g.l.c., and obtained an expression:

$$H = d_p + \frac{2D_m}{u} + \frac{2r_1 r_2}{u\, r_2 - u_L r_1}\ \left(\frac{u + u_L}{r_1 + r_2}\right)^2 \tag{8.3}$$

r_1 = Rate of transfer of molecules from gas to liquid

r_2 = Rate of transfer of molecules from liquid to gas

u_L = Stationary (liquid) phase velocity

This was compared to the static column case:

$$H = d_p + \frac{2D_m}{u} + \frac{2r_1 u}{(r_1 + r_2)^2} \qquad (8.4)$$

The difference between EQUATIONS 8.3 and 8.4 lies in the inclusion of a term in u_L for the continuous chromatography case which accounts for increased zone broadening caused by movement of the stationary phase.

Quoting the work of Gluekauf, Al-Madfai (21) also relates the number of theoretical plates required to separate two components using a static column, N, to the required number, N_{cc}, for the continuous chromatographic column, discussed in SECTION 2.4.3.2.2, which he used:

$$\frac{N_{cc}}{N} = 3(\alpha-1) \qquad (8.5)$$

N_{cc} = Number of counter-current theoretical plates or stages.

N = Number of co-current theoretical plates (elution chromatography).

This equation indicates that, for separation factors below 1.33, less theoretical plates would be required for the continuous case than for the static column, and the ratio N_{cc}/N becomes smaller as α approaches unity, suggesting that continuous counter-current operation might be particularly useful for difficult separations.

Rony (243) derived the relationship between the number of stages in a counter-current multistage system (operated at total reflux),

N_{cc}, that are required to obtain a separation identical to that achieved in a co-current chromatographic system with N theoretical plates:

$$\frac{N_{cc}}{N} = \frac{(1 + K_1)^2}{\sqrt{2\pi}\ (u_m{}^t/\sigma)} \qquad (8.6)$$

K_1 = Partition coefficient of component 1

u_m = Molar velocity of mobile phase

σ = Peak standard deviation (units of length)

t = Time

The equivalent expression for the case of a counter-current multi-stage system with no reflux is:

$$\frac{N_{cc}}{N} = \frac{2(1+K_1)^2}{\sqrt{2\pi}\ \ (u_m{}^t/\sigma)} \qquad (8.7)$$

Tiley and co-workers (107) treated the continuous moving bed process, in a manner analogous to the theoretical treatment of stagewise liquid-liquid extraction given by Alders (244), for the separation, to an equal degree of purity, of a two component equimolar feed mixture. A more general relationship for binary separations was developed, using the same concept, by Huntington (16):

$$\log \frac{\psi_{MAX}}{\psi_{MIN}} = \log \frac{K_B}{K_A} + \frac{2}{N_{cc}} \left[\log \left(1 - \frac{A_c}{W'_A}\right) + \log \frac{B_c}{W'_B} \right] \qquad (8.8)$$

ψ_{MAX}, ψ_{MIN} are the maximum and minimum allowable values of $\left(\frac{u}{u_L}\right)$ to produce products of the required purity.

A_c, B_c are the collection rates of components A and B at the top of the column.

N_{cc} is the number of counter-current theoretical plates, or stages, in the column.

W'_A, W'_B are the feed rates of components A and B.

This relationship has been employed to evaluate the overall efficiency of two-component continuous chromatographic separations, by Barker and Huntington (16,17) and Al-Madfai (21). One major disadvantage of EQUATIONS 8.6-8.8 is the inherent assumption of a constant partition coefficient, which is not usually obtained in practice. Tiley (245) overcame this problem by developing a digital computer program to perform stage-to-stage calculations and allow introduction of a non-linear absorption isotherm.

Another approach to the theoretical treatment of continuous mass transfer operations is the use of the transfer unit concept, in which the height of a transfer unit (H.T.U.) is used to express the efficiency of continuous mass transfer processes carried out in packed columns. For practical reasons, as it is usually necessary to deal with overall mass transfer coefficients, the number of overall transfer units is used. Barker and Lloyd (12,22) used this approach in their treatment of the counter-current gas/liquid chromatographic process and derived the following equations:

$$(N_{OG})_R = \frac{1}{Q_G/(KQ_L - 1)} \ln \left[\frac{M_A/KQ_L - y_1(Q_G/KQ_L - 1)}{M_A/KQ_L - y_2(Q_G/KQ_L - 1)} \right] \qquad (8.9)$$

$$(N_{OG})_S = \frac{1}{(1 - Q_G/KQ_L)} \ln \left[\frac{M_B/KQ_L - y_1 (1 - Q_G/KQ_L)}{M_B/KQ_L - y_2 (1 - Q_G/KQ_L)} \right] \qquad (8.10)$$

Q_G = Gas volumetric flowrate

Q_L = Liquid volumetric flowrate

M_A, M_B = Mass flowrate of solute leaving the column in the product A and product B streams, respectively

$(N_{OG})_R, (N_{OG})_S$ = Number of overall gas phase transfer units in the 'rectifying' and 'stripping' sections respectively

y_1, y_2 = Gas phase solute concentrations at points 1 and 2 in the column

This method has been applied, by Barker and Lloyd (12,22), to the vertical moving-bed column shown in FIG. 2.17. Sunal (25) developed a computer model of the continuous chromatographic process, using the H.T.U. approach, based on the 'two film theory' of mass transfer and compared it with the results of Huntington (16), concluding that the effect of axial mixing on separation efficiency was negligible.

These methods of treatment of the counter-current chromatographic process are based on true steady-state operation, and as such they should, strictly, only be applied to the original moving bed, or moving stationary phase, systems discussed in SECTIONS 2.4.2 and 2.4.3. In later process schemes, the packing and stationary phase is maintained in a fixed position within a series of packed columns. The relative movement of the mobile and stationary phases is achieved by moving the columns, or simulating their movement, in the opposite direction to the carrier flow. The operating principle of these units is similar to the frontal elution technique, discussed in SECTION 2.3.1, with an imposed column sequencing action. Sunal (25) developed a

digital computer program for gas/liquid chromatography based on plate-to-plate calculations for the type of continuous counter-current chromatograph shown in FIG. 2.19(b). This approach was also used by Deeble (29) to simulate operation of the SCCR1 gas-liquid chromatographic unit. In the present work, the concept of the plate model, used by Sunal (25) and Deeble (29) for gas/liquid chromatography, has been used to simulate operation of the SCCR3 liquid-liquid chromatographic unit.

8.2 THE PROGRAM

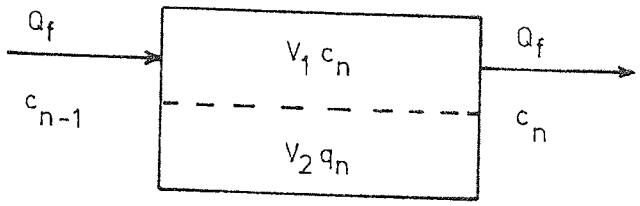

Plate n

The chromatographic column is considered to consist of a series of idealized mixing stages or theoretical plates, and a mass balance over plate n gives:

$$Q_f c_{n-1} = Q_f c_n + V_1 \frac{dc_n}{dt} + V_2 \frac{dq_n}{dt} \qquad (8.11)$$

Q_f = Mobile phase volumetric flowrate

c = Solute concentration in mobile phase

q = Solute concentration in stationary phase

V_1 = Volume of mobile phase on a plate

V_2 = Volume of stationary phase on a plate

Substituting $K = q_n/c_n$:

$$Q_f c_{n-1} = Q_f c_n + (V_1 + K V_2) \frac{dc_n}{dt} \qquad (8.12)$$

Assuming that the time increment, Δt, over which EQUATION 8.12 is integrated, is sufficiently small so that c_{n-1} may be considered constant, integration of EQUATION 8.12 gives:

$$c_n = c_{n-1}\left(1 - e^{-\left(\frac{Q_f \Delta t}{V_1 + V_2 K}\right)}\right) + c_n(o)\, e^{-\left(\frac{Q_f \Delta t}{V_1 + V_2 K}\right)} \qquad (8.13)$$

The first term on the right-hand side of EQUATION 8.13 represents the contribution to c_n from the inlet stream to the n^{th} plate, which may be output from the $(n-1)^{th}$ plate and/or an external feed, while the second term represents the contribution from material present on the n^{th} plate at the beginning of the time increment. The feed input is assumed to be introduced into the SCCR3 unit, on the first plate in the feed column, at the relevant on-column concentration (SECTION 7.4.3.1). The sequencing action occurring in the SCCR3 unit is imposed on the plate-to-plate calculations by stepping the concentration profile backwards, by one column, at the end of a sequencing interval.

The inclusion of a second component, or several other components, is achieved by repeating the plate-to-plate calculations for another, or several other, variable names, and it is assumed that the components do not interact. Allowance is made for the finite feed flowrate by incorporating a pre feed-point mobile phase flowrate into the plate-to-plate calculations. A flow sheet for the program used in this research is given in FIG. 8.1, and a listing of the program, the program variables, and a sample of the print-out, for a nine-component feed mixture, is given in APPENDIX 5.

Figure 8.1 Flow Chart for the Computer Simulation of the SCCR3 Unit

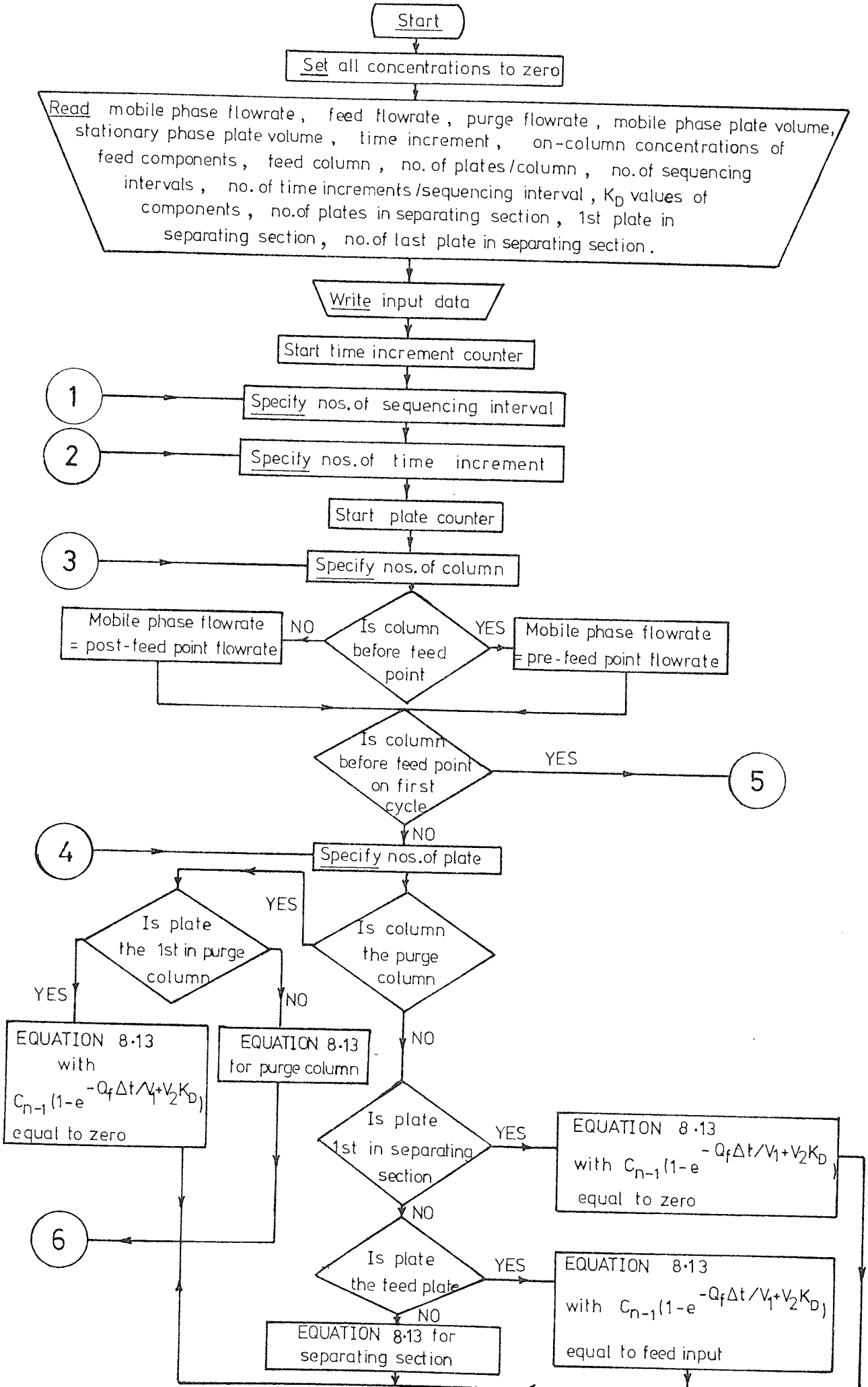

Figure 8.1 (contd.)

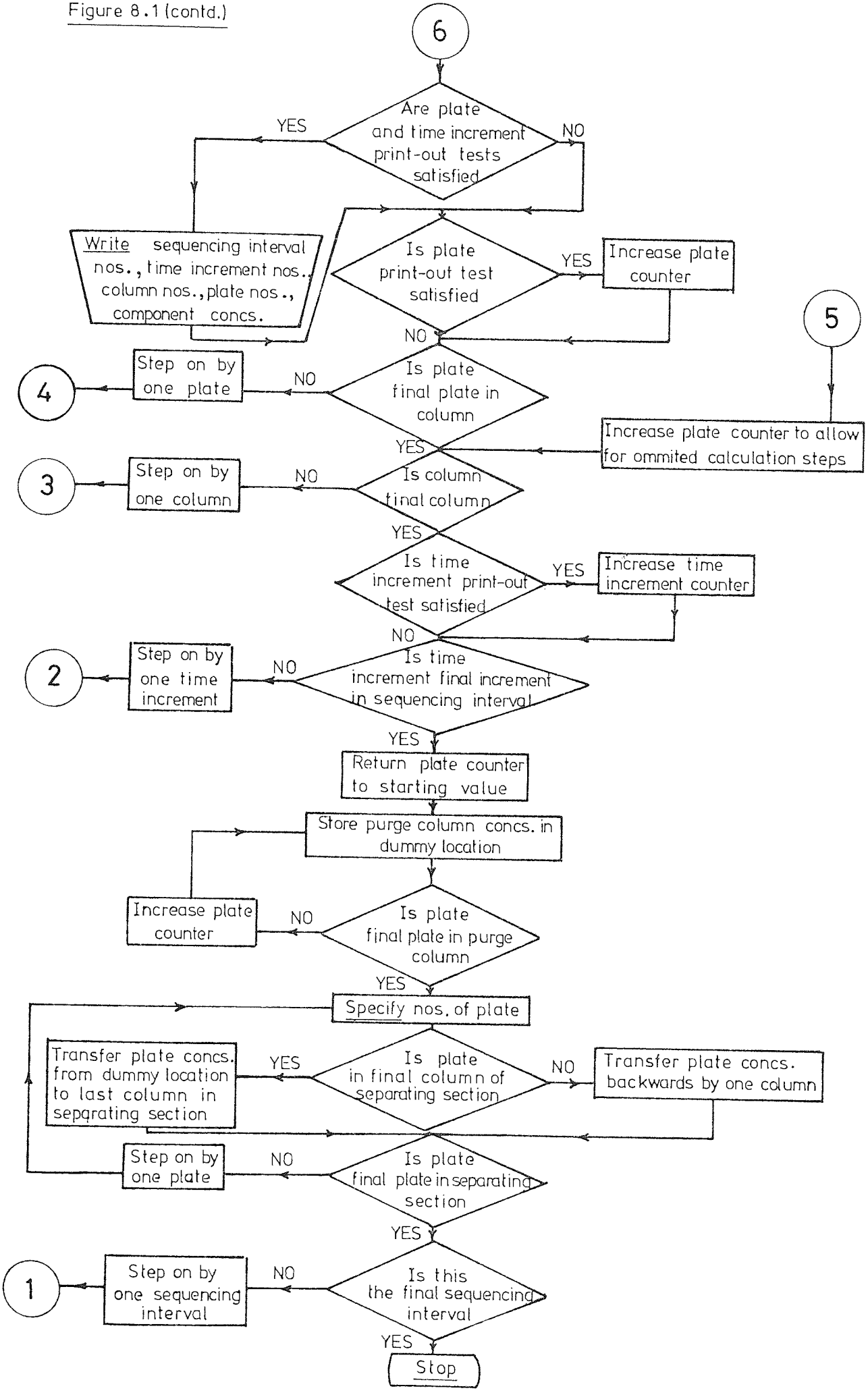

8.3 RESULTS

Sixteen computer runs are given for a two-component feed mixture, and two runs for a nine-component feed mixture, which was an attempt to simulate polymer fractionation with the SCCR3 unit. Details of the runs are summarized in FIG. 8.2. Attention was focused on the following parameters.

(i) The length of the time increment, Δt. Five runs are shown in FIGS. 8.3-8.7, with time increments of 20.0s, 8.0s, 4.0s, 2.0s and 1.0s, and other operating conditions constant.

(ii) The number of theoretical plates per column, N. For $K_{D_1} = 0.1$, $K_{D_2} = 0.9$, five runs are shown with 20, 80, 40, 10, 5, theoretical plates respectively (FIGS. 8.7-8.11) and other operating conditions similar.

(iii) The separation factor, $\alpha = K_{D_2}/K_{D_1}$. Four runs are given with separation factors of 9.0, 2.33, 1.50, and 1.22 respectively (FIGS. 8.7, 8.12, 8.13, 8.14) and other operating conditions constant. Separation factors of 2.33 and 1.50 are also treated in (iv).

(iv) The finite feed flowrate. Three runs are shown at mobile phase/feed flowrate ratios of 7.21, 3.11, and 3.41 respectively, and a separation factor of 2.33 (FIGS. 8.15-8.17). One further run is given for a separation factor of 1.5, and a value of the mobile phase/feed flowrate ratio of 7.21 (FIG. 8.18).

(v) The accuracy of simulation of the SCCR3 unit. A nine-component feed (FIG. 8.19) was used to approximate the M.W. distribution of the dextran 40 polymer used for SCCR3 runs, and simulation of experimental run 1-600-0.7 was attempted. The result is shown in FIG. 8.20. FIG. 8.21 shows another nine-component run, under similar conditions, but with a constant mobile phase flowrate throughout the separating section.

A table of values for the variables used in the computer runs is given in FIG. 8.2. Separation conditions were set such that the theoretical separation position, or cut-point, usually corresponded to a K_D of about 0.5. The concentration profiles given in FIGS. 8.3-8.18, 8.20, and 8.21 are profiles corresponding to the end of a sequencing interval, with the exception of FIG. 8.7, which compares the concentration profiles obtained at the beginning, middle, and end of a sequencing interval. The computer runs were performed on a CDC 7600 digital computer, at the University of Manchester Regional Computer Centre.

Figure 8.2 Summary of Conditions for Computer Simulation Runs

Standard Conditions

Sequencing interval = 1020 s , Purge flowrate = 3·17 $cm^3 s^{-1}$, Total mobile phase volume/column = 538 cm^3, Total stationary phase volume/column = 599 cm^3, Total no.of columns = 10 , Feed column = 6 (feed introduced on 1st plate).

(a) Two-Component Runs

On-column feed concentration of components = 0·01 $g\,cm^{-3}$

No.	No.of Figure	KTOTAL	NNBED	KKINK	ΔT (s)	CFLOW ($cm^3 s^{-1}$)	FFLOW ($cm^3 s^{-1}$)	KD1	KD2	Approx no.of sequences to pseudo-eqm.	
										comp.1	comp.2
1	8·3	80	20	51	20	0·836	0·0	0·1	0·9	10	> 80
2	8·4	60	"	128	8	"	"	"	"	14	58
3	8·5	"	"	255	4	"	"	"	"	17	45
4	8·6	50	"	1020	1	"	"	"	"	20	40
5	8·7	"	"	510	2	"	"	"	"	20	40
6	8·8	"	80	"	"	"	"	"	"	11	38
7	8·9	"	40	"	"	"	"	"	"	15	40
8	8·10	60	10	"	"	"	"	"	"	24	50
9	8·11	80	5	"	"	"	"	"	"	30	60
10	8·12	60	20	"	"	0·821	"	0·3	0·7	45	>60
11	8·13	120	"	"	"	"	"	0·4	0·6	100	>120
12	8·14	150	"	"	"	"	"	0·45	0·55	>150	>150
13	8·15	80	"	"	"	0·721	0·1	0·3	0·7	>80	65
14	8·16	100	"	"	"	0·621	0·2	"	"	>100	60
15	8·17	80	"	"	"	0·681	0·2	"	"	>80	>80
16	8·18	120	"	"	"	0·721	0·1	0·4	0·6	>120	>120

(b) Nine-Component Runs

KTOTAL = 57 , NNBED = 40 , KKINK = 508 , ΔT = 2s , KD and conc.values in FIG 8.19

No.	No.of Figure	CFLOW ($cm^3 s^{-1}$)	FFLOW ($cm^3 s^{-1}$)	Approx no.of sequences to pseudo-eqm. for each component								
				1	2	3	4	5	6	7	8	9
17	8·20	0·862	0·168	7	9	12	16	35	>57	>57	>57	>57
18	8·21	0·946	0·0	8	9	13	19	32	>57	>57	>57	52

Figure 8.3 Computer Simulation No. 1 The Effect of Δt

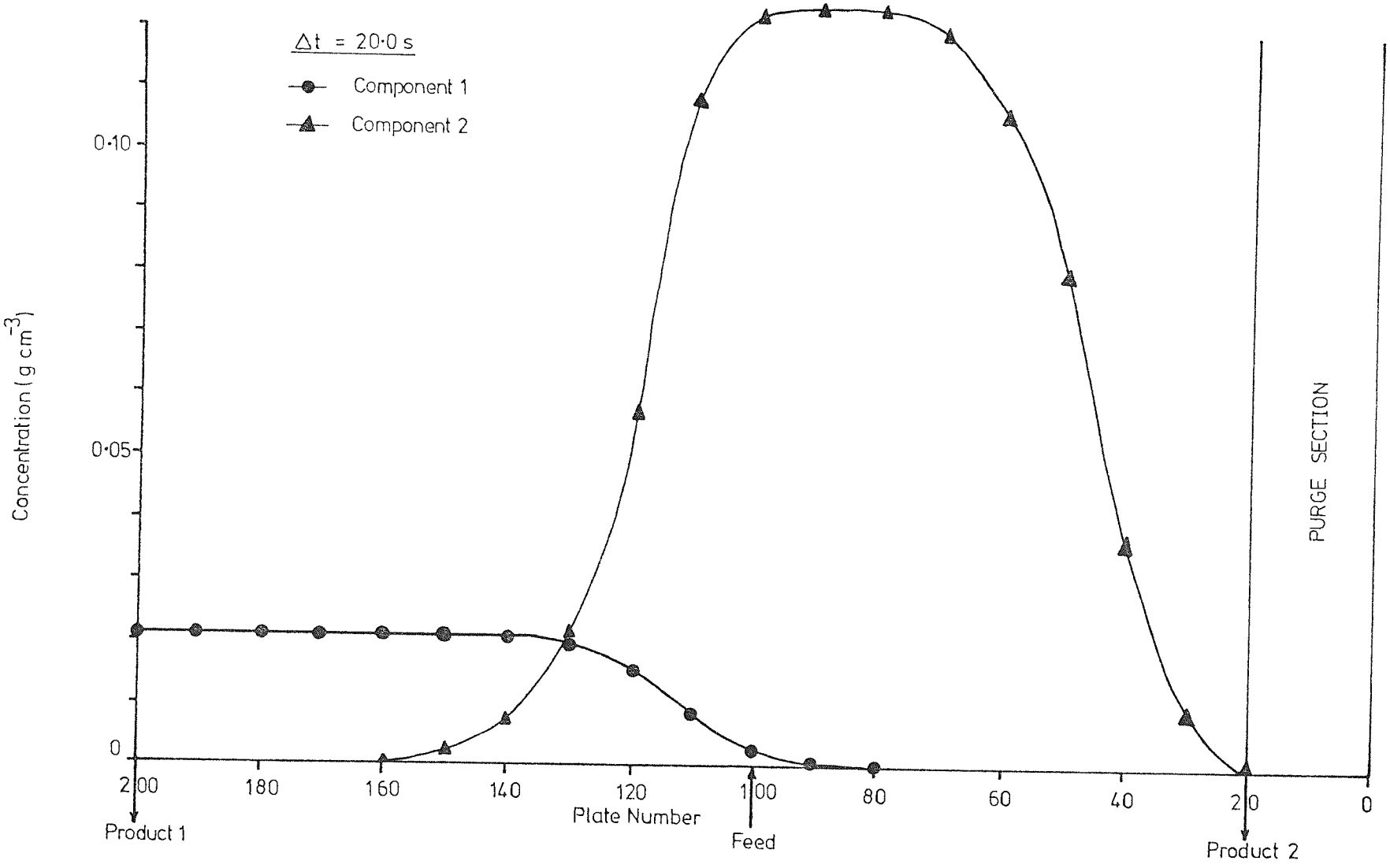

Figure 8.4 Computer Simulation No. 2 The Effect of Δt

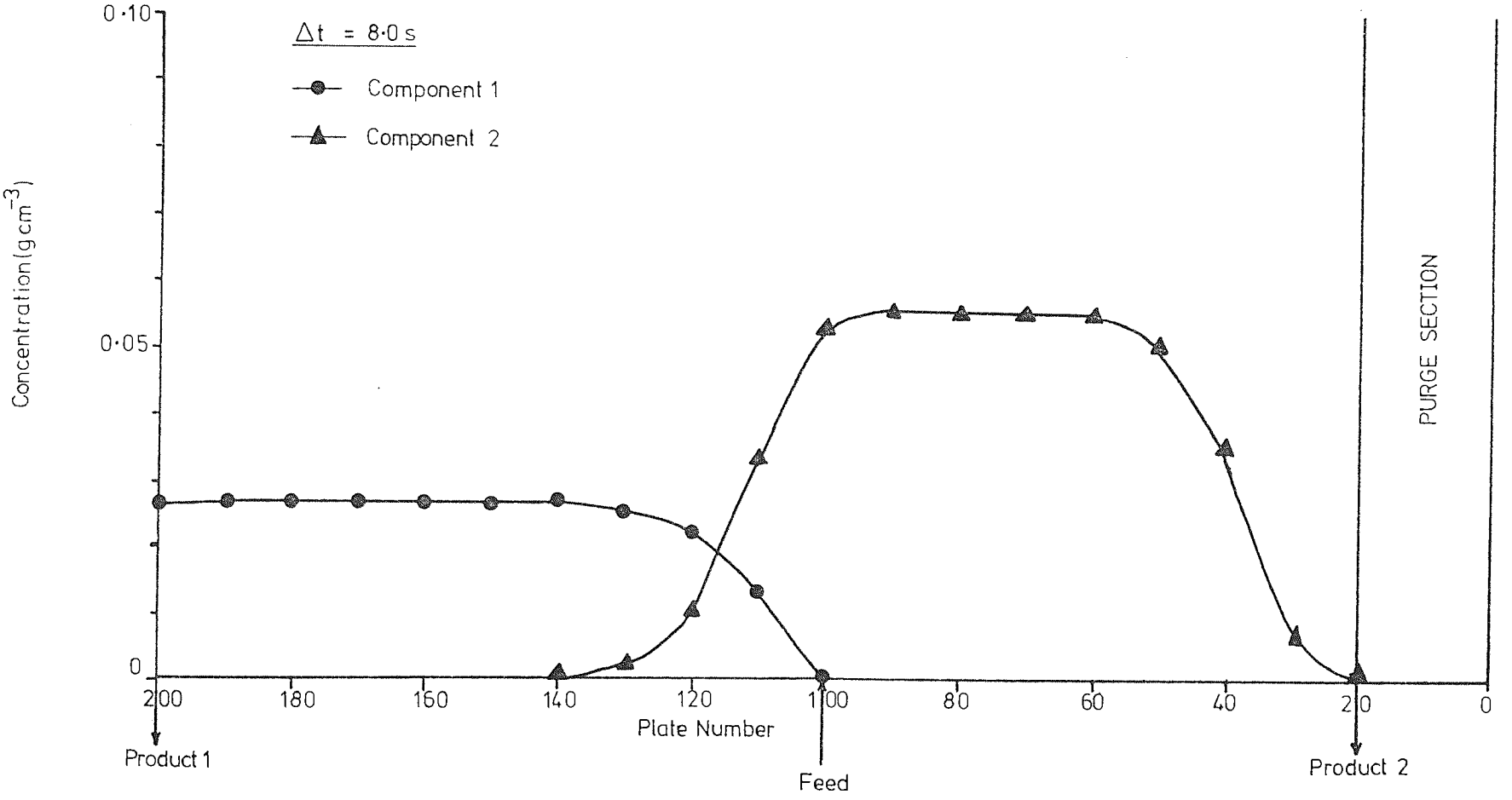

Figure 8.5 Computer Simulation No. 3 The Effect of Δt

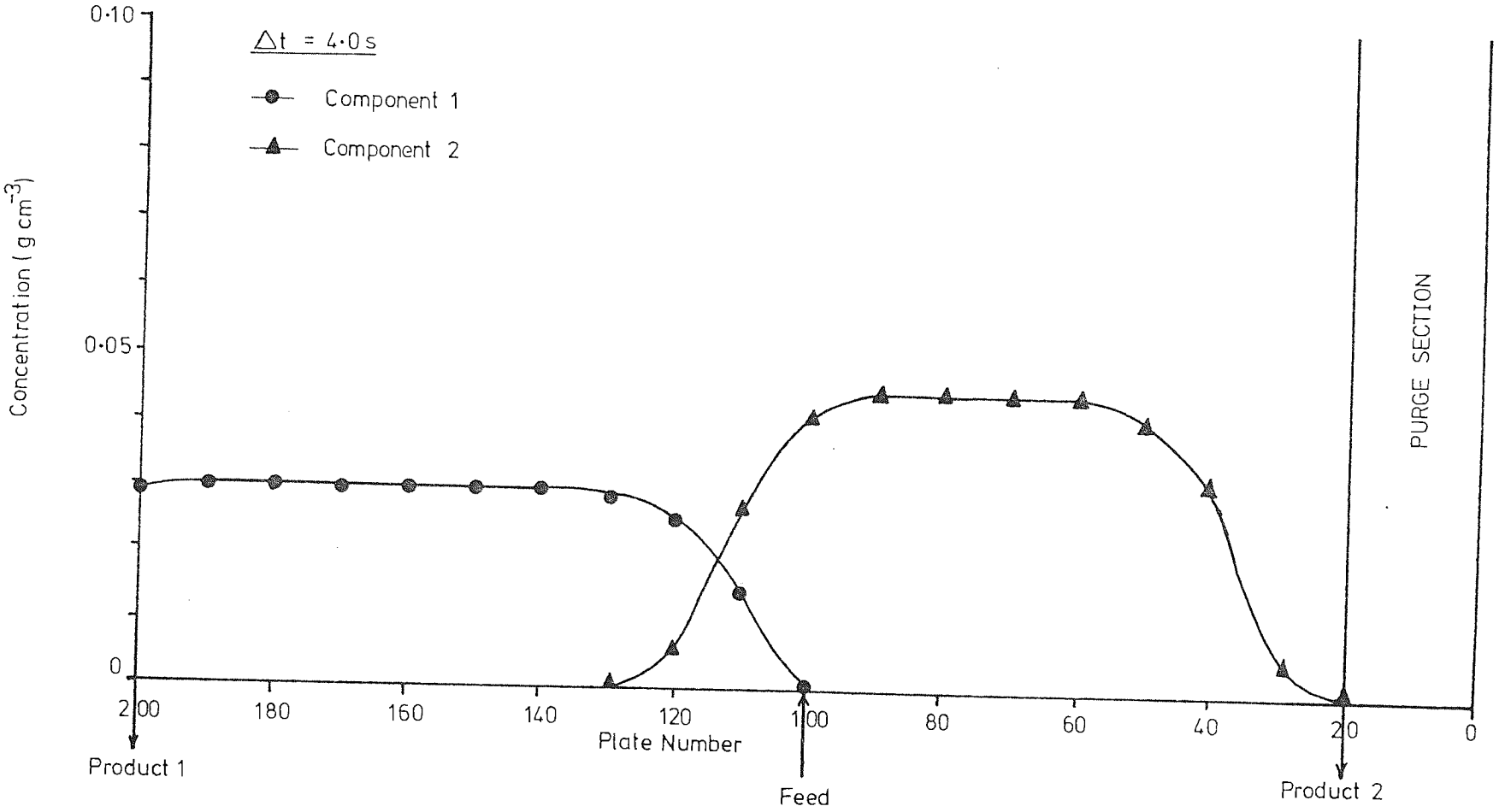

Figure 8.6 Computer Simulation No. 4 The Effect of Δt

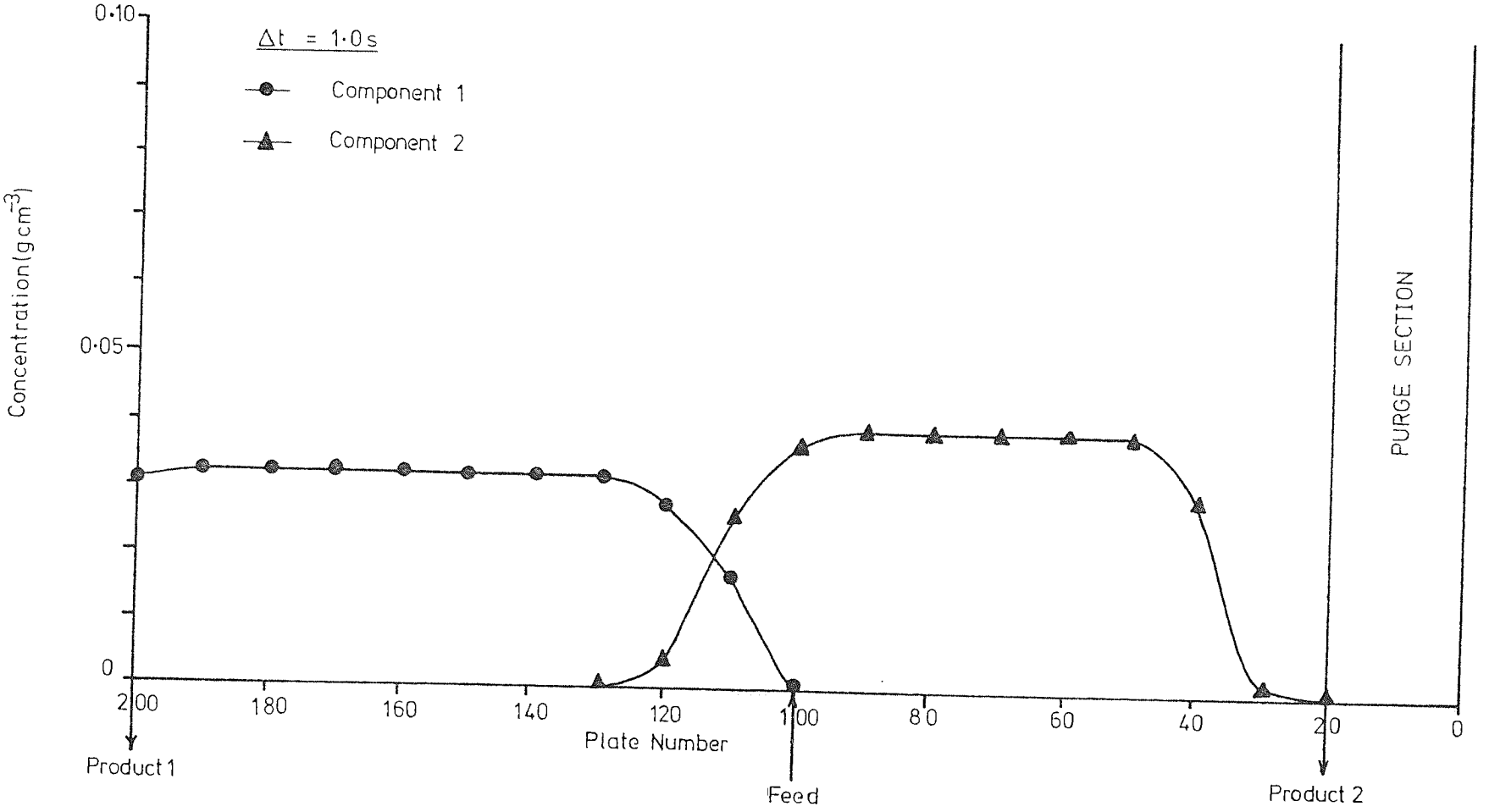

Figure 8.7 Computer Simulation No. 5 The Effect of Δt

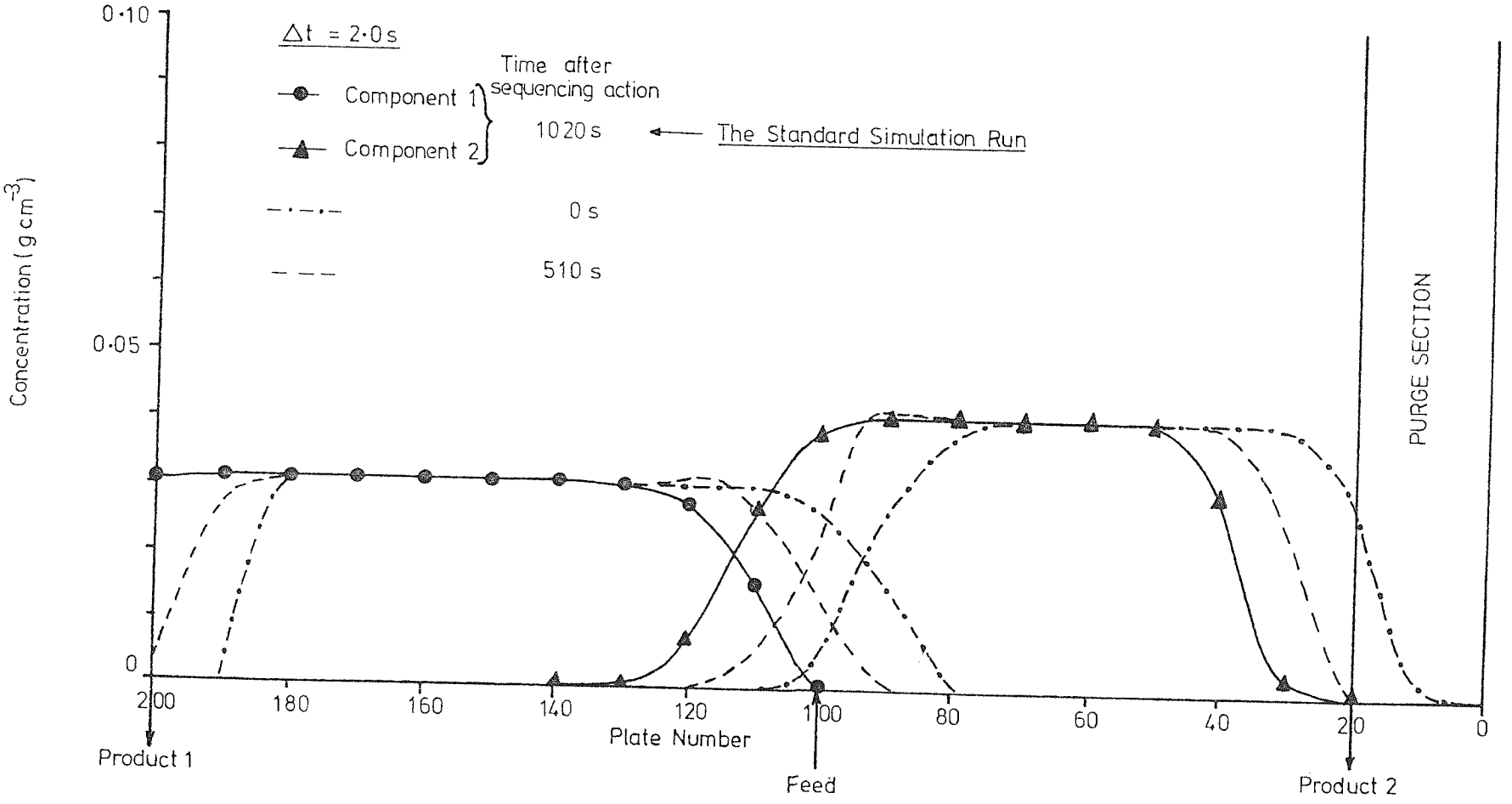

Figure 8.8 Computer Simulation No.6 The Effect of N

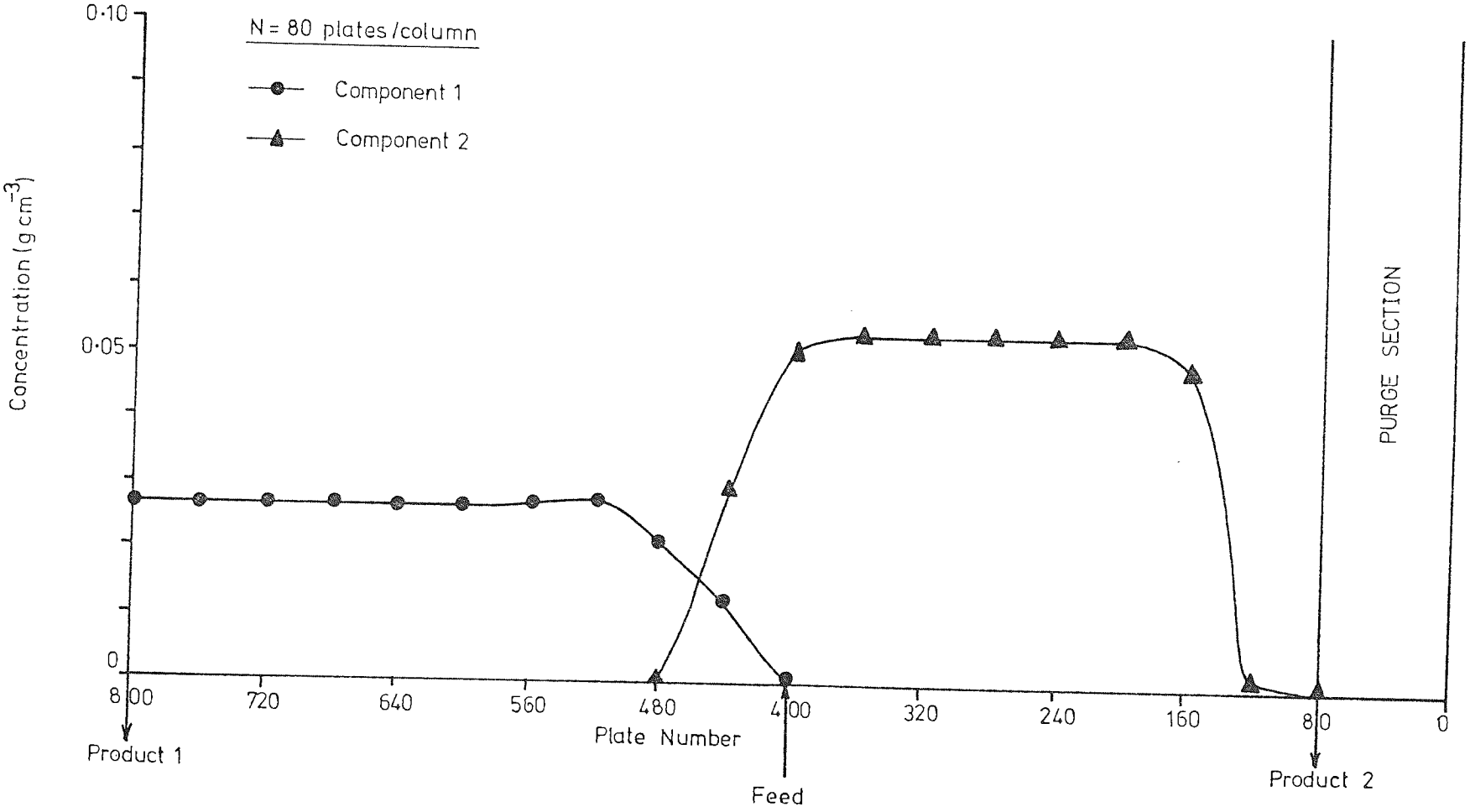

Figure 8.9 Computer Simulation No.7 The Effect of N

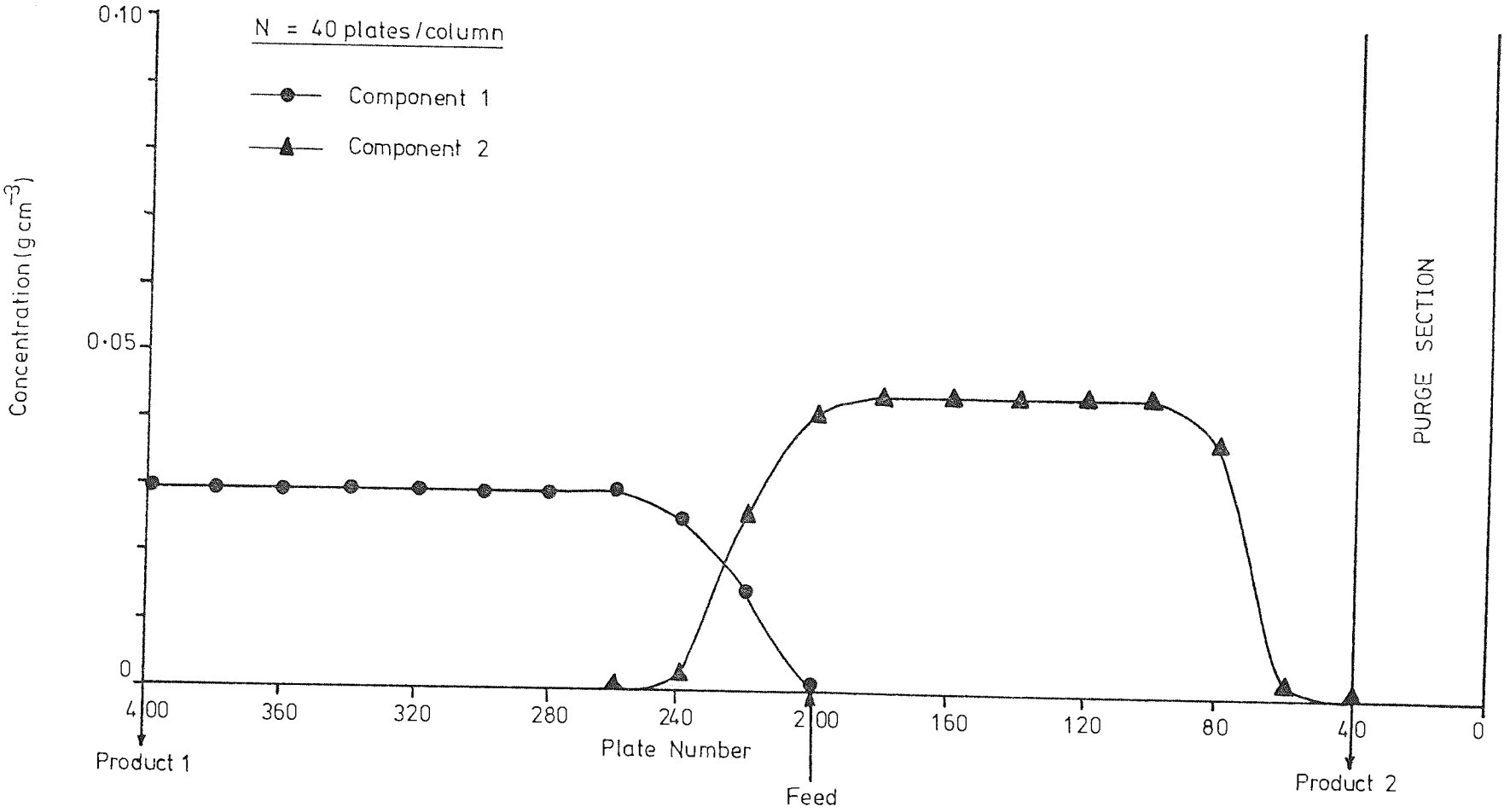

Figure 8.10 Computer Simulation No.8 The Effect of N

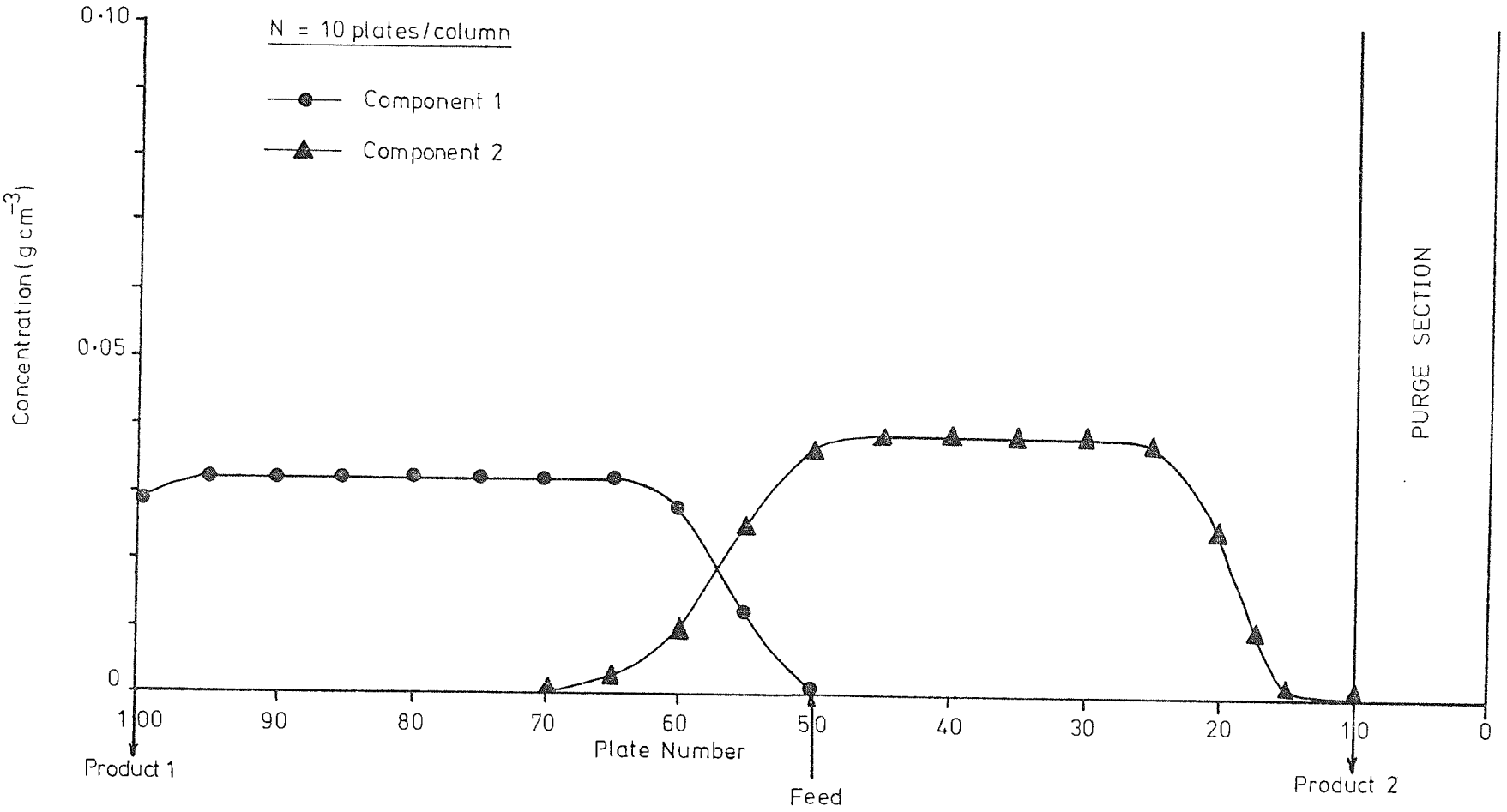

Figure 8.11 Computer Simulation No. 9 The Effect of N

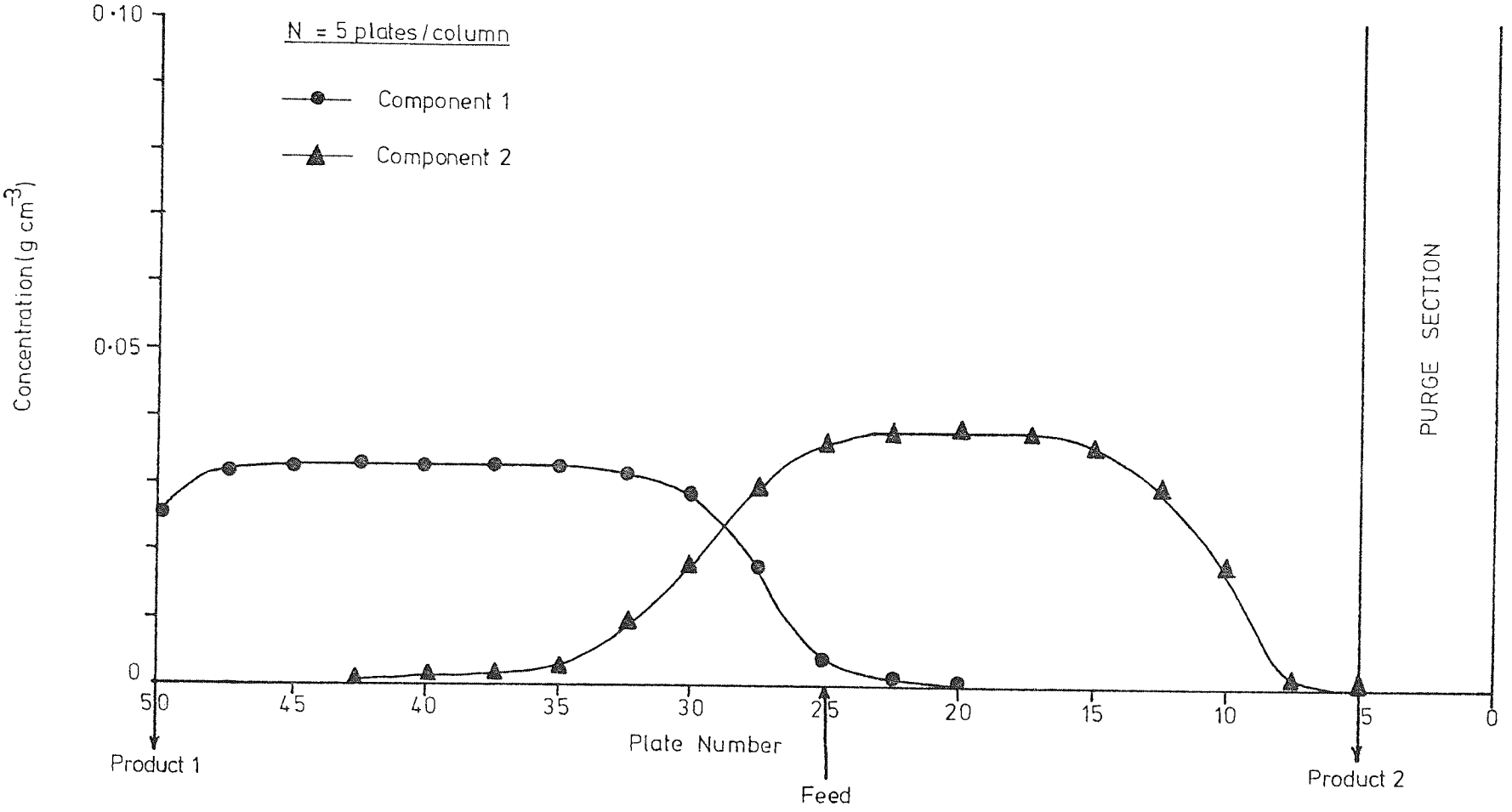

Figure 8.12 Computer Simulation No.10 The Effect of α

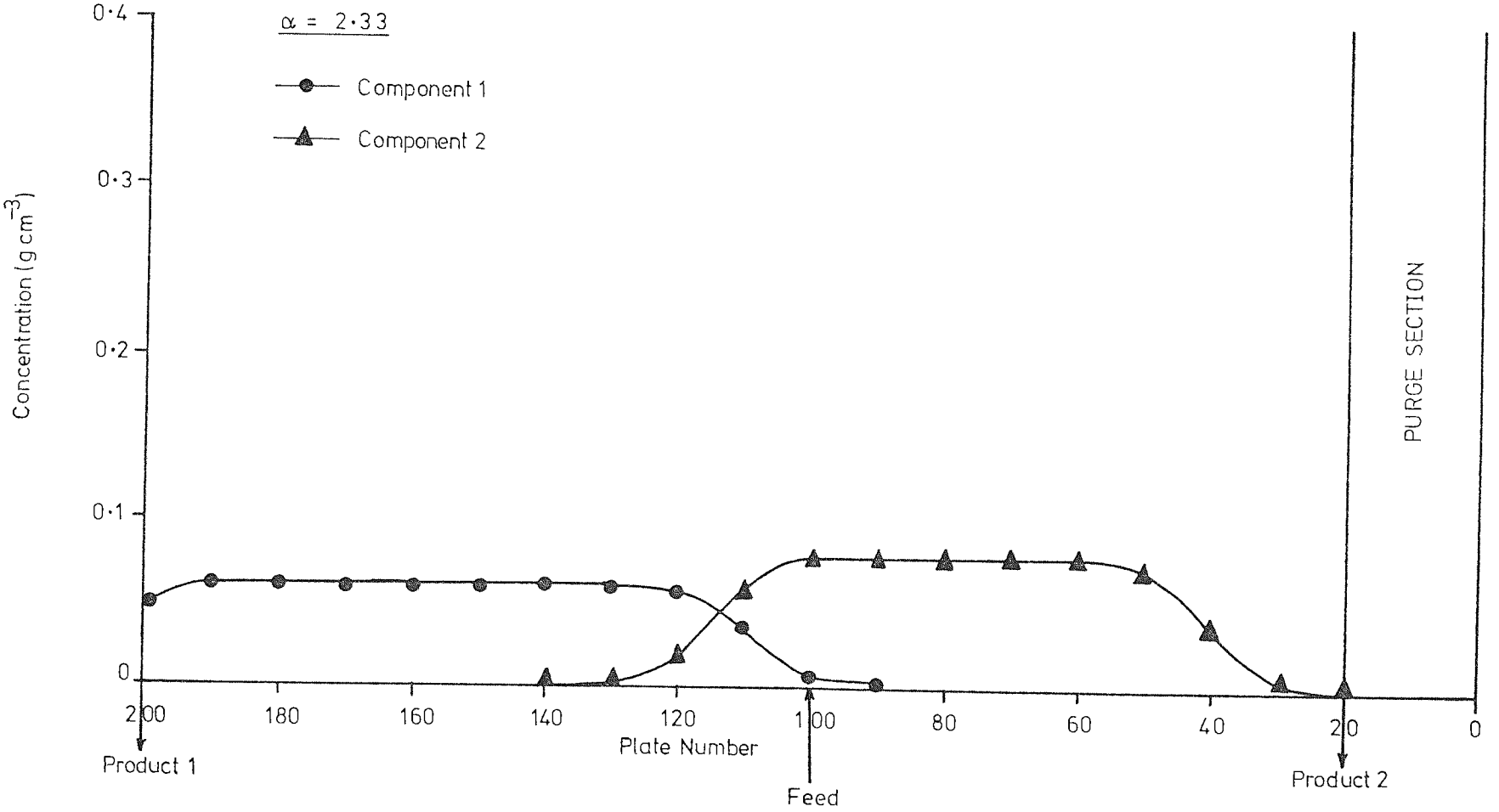

Figure 8.13 Computer Simulation No.11 The Effect of α

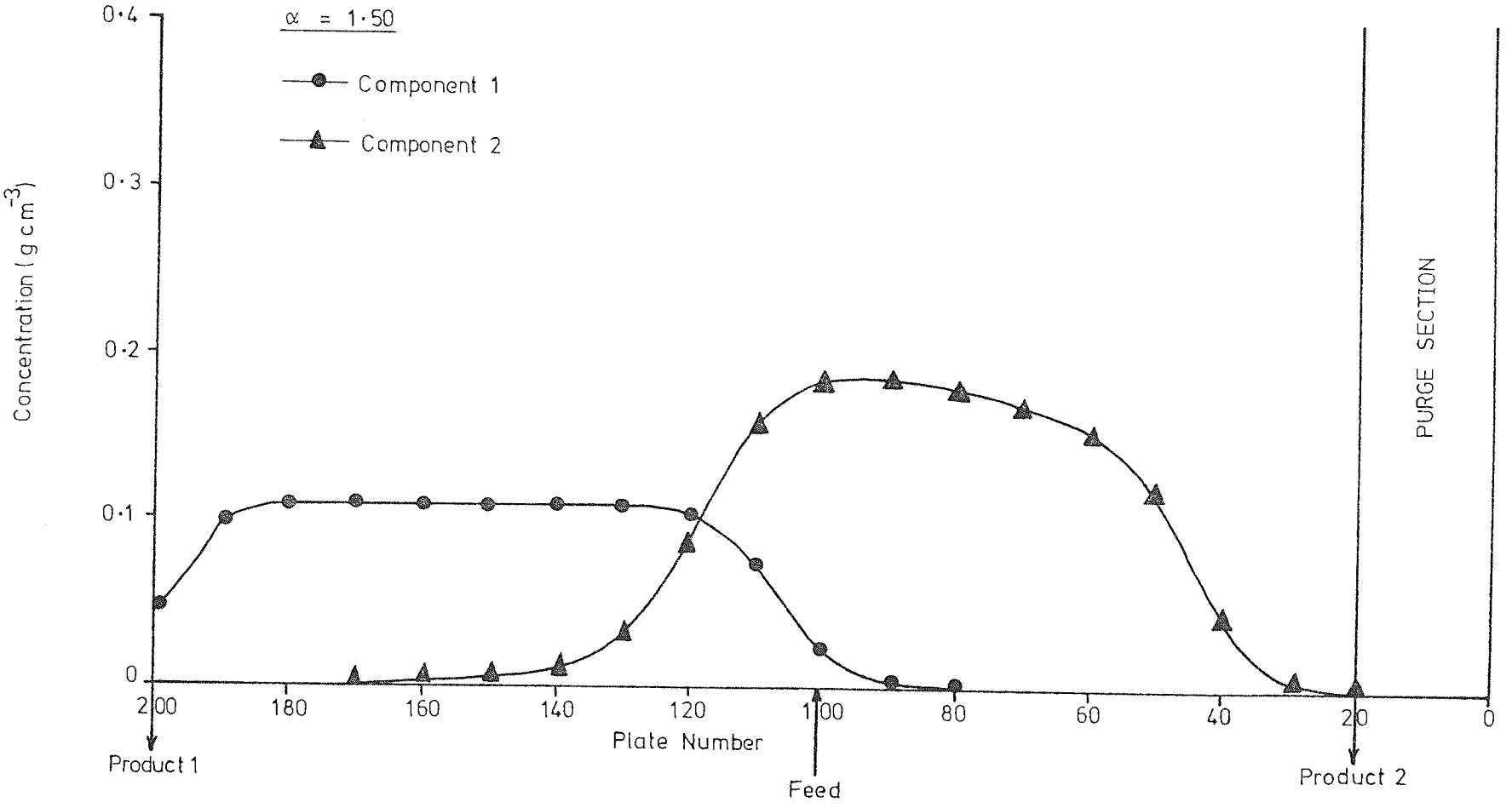

Figure 8.14 Computer Simulation No. 12 The Effect of α

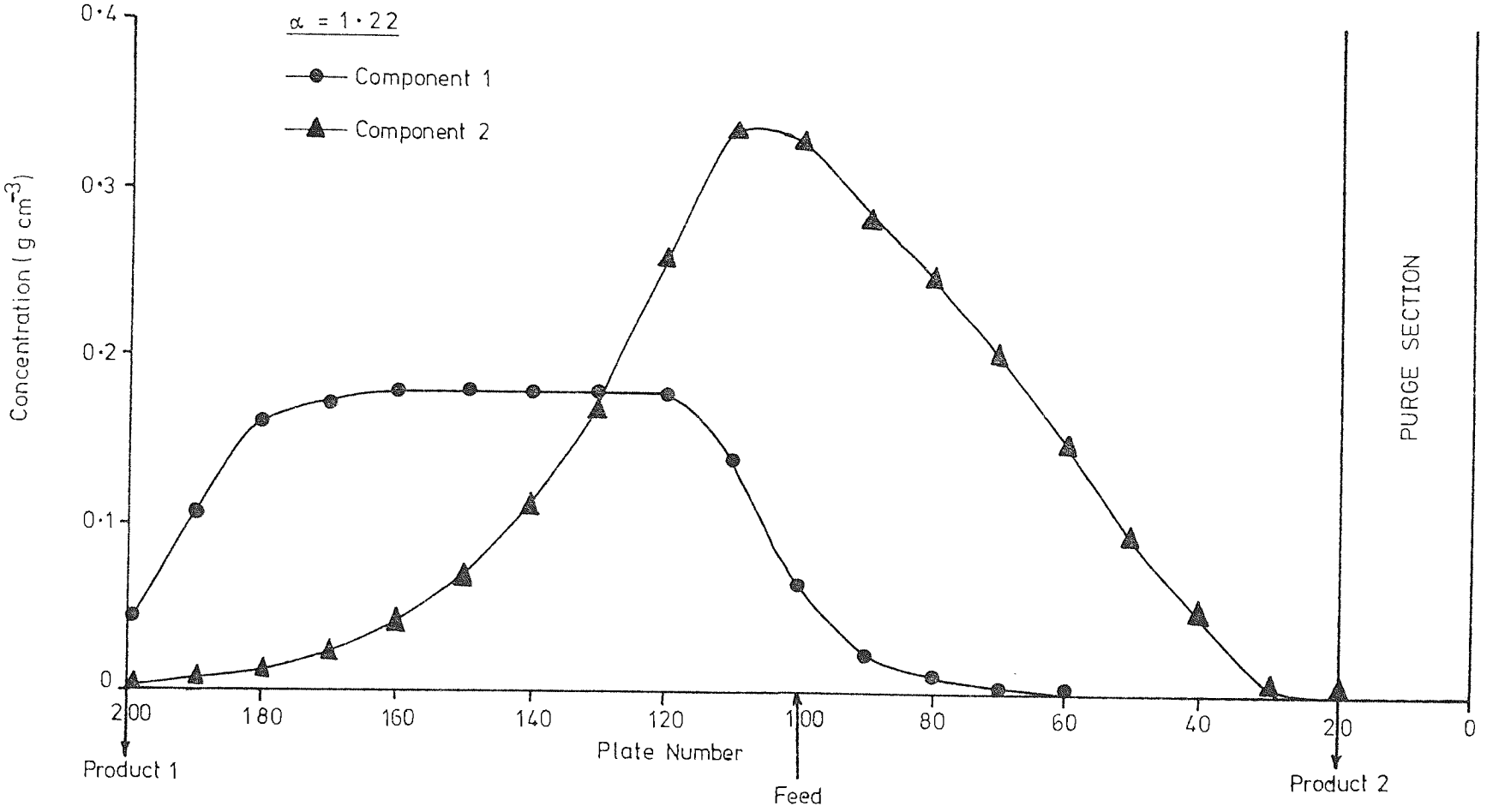

Figure 8.15 Computer Simulation No. 13 The Effect of CFLOW / FFLOW

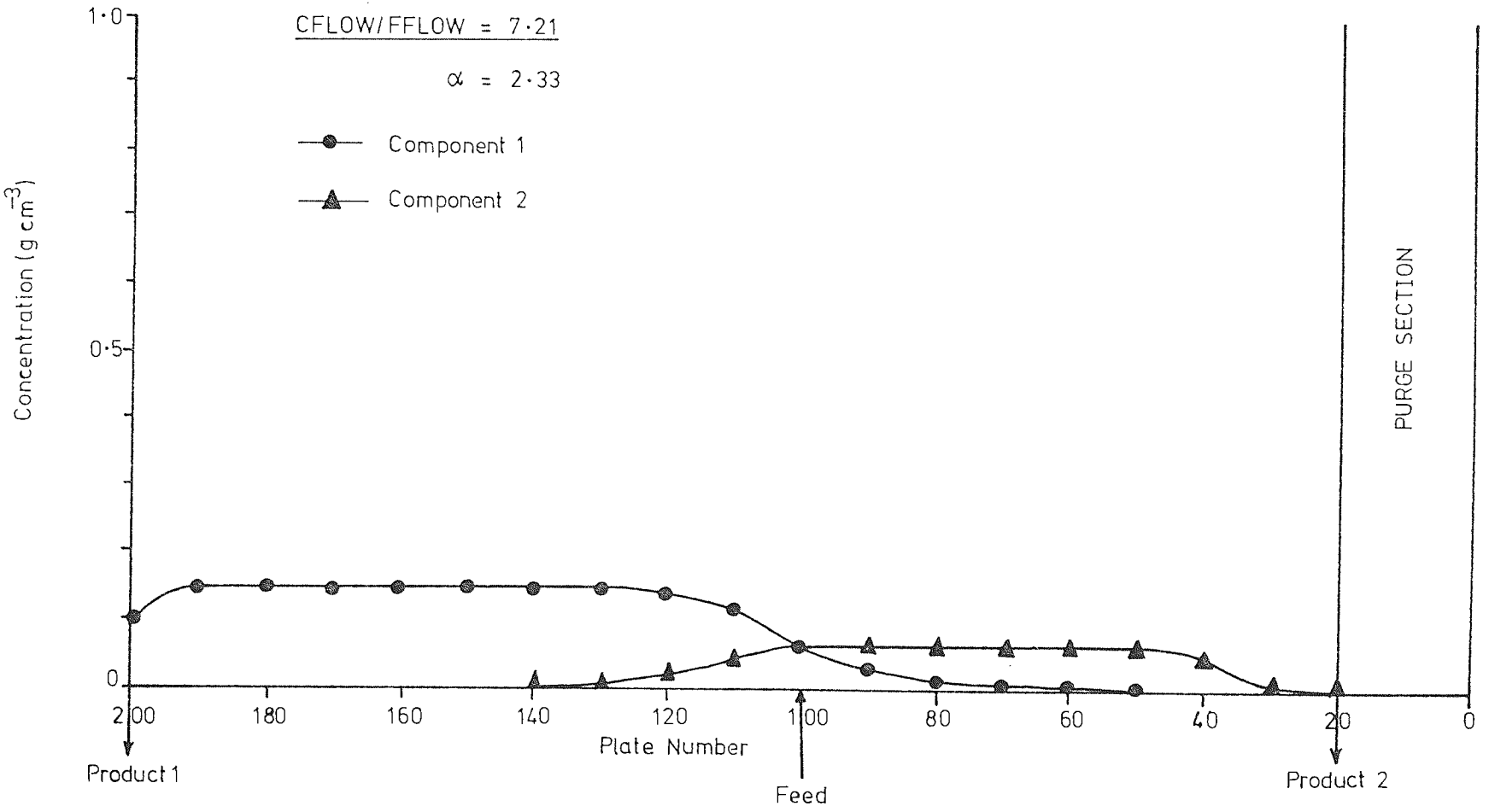

Figure 8.16 Computer Simulation No. 14 The Effect of CFLOW/FFLOW

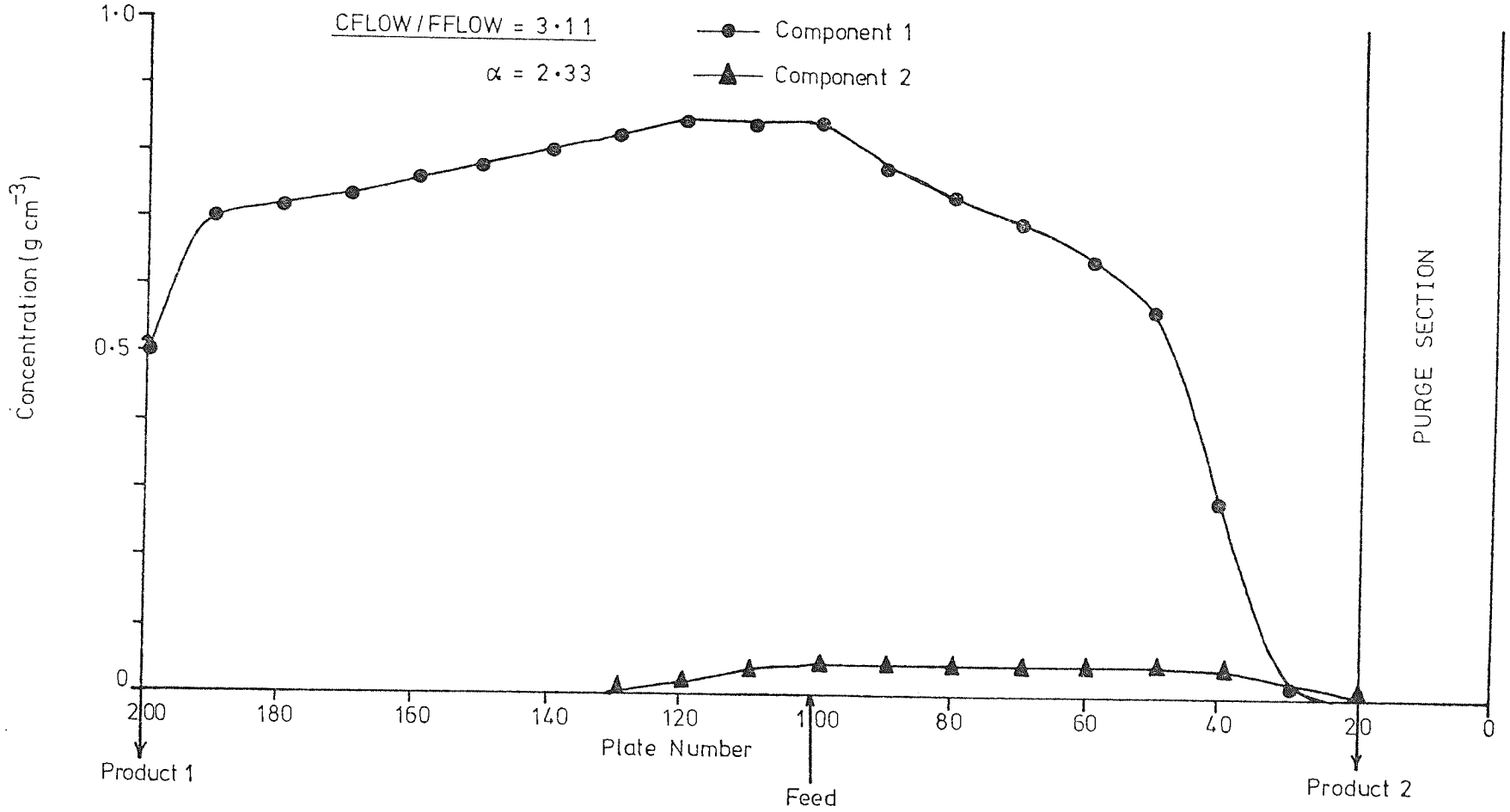

Figure 8.17 Computer Simulation No. 15 The Effect of CFLOW/FFLOW

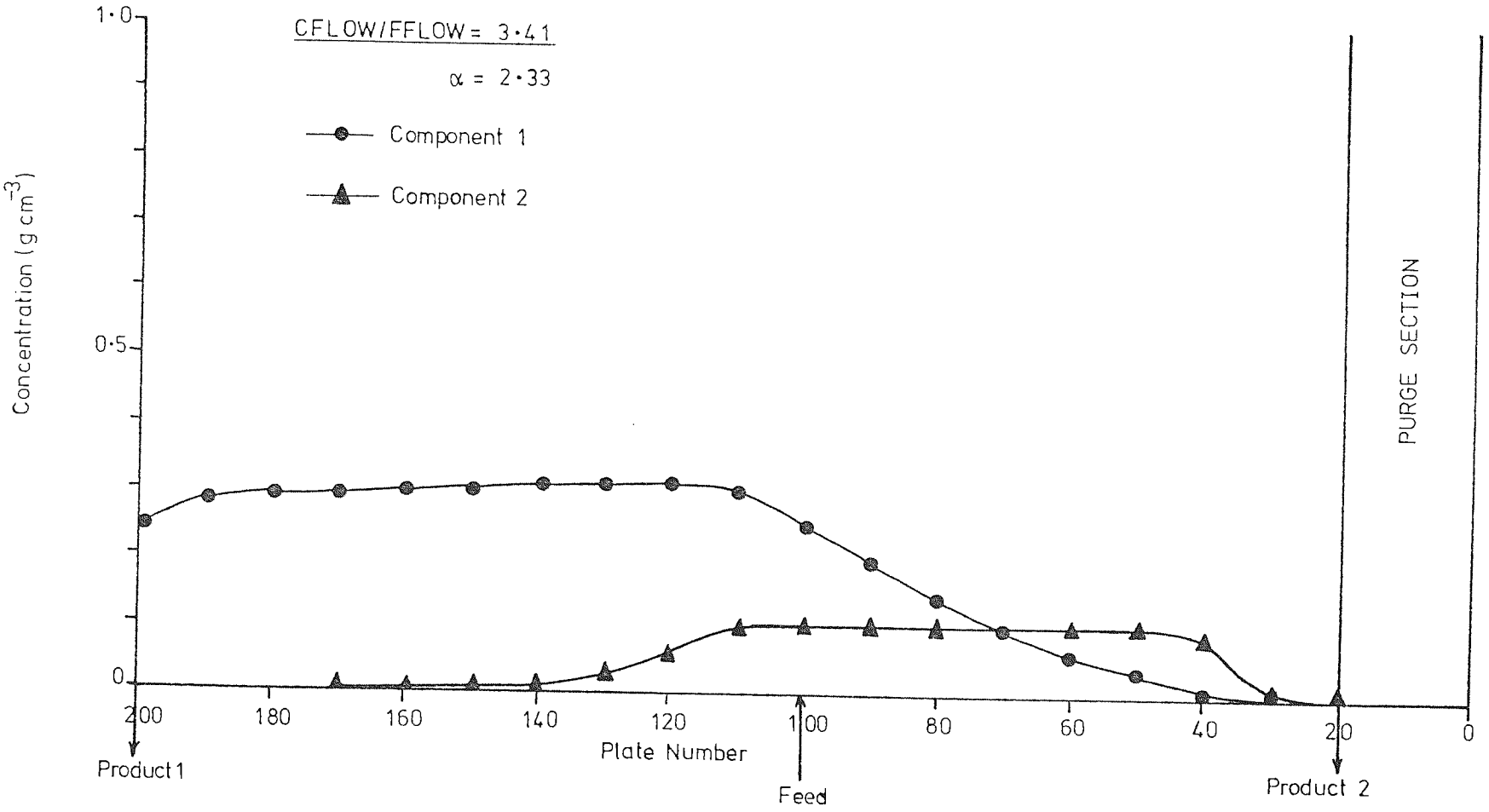

Figure 8.18 Computer Simulation No.16 The Effect of CFLOW/FFLOW

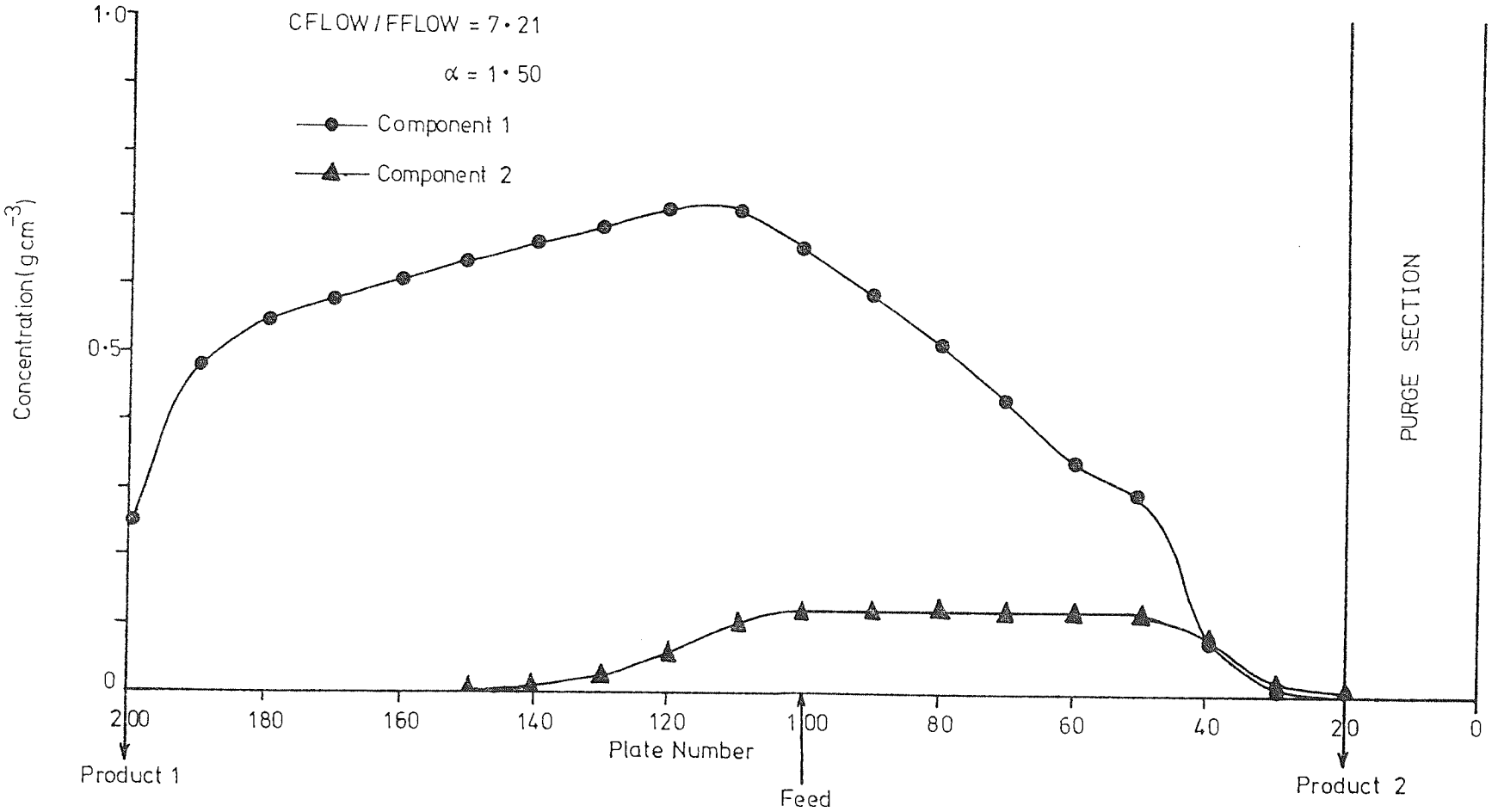

Figure 8.19 Representation of a Dextran 40 Polymer Distribution by a Nine-Component Mixture

Component No.	1	2	3	4	5	6	7	8	9
K_D	0·0	0·08	0·208	0·338	0·466	0·595	0·725	0·853	0·995
% of Mixture	0·96	3·13	9·40	21·73	28·80	23·45	10·21	2·12	0·20
C_i FEED, i = 1 → 9 (10^{-4} g cm^{-3})	0·16	0·52	1·56	3·62	4·79	3·90	1·70	0·35	0·03

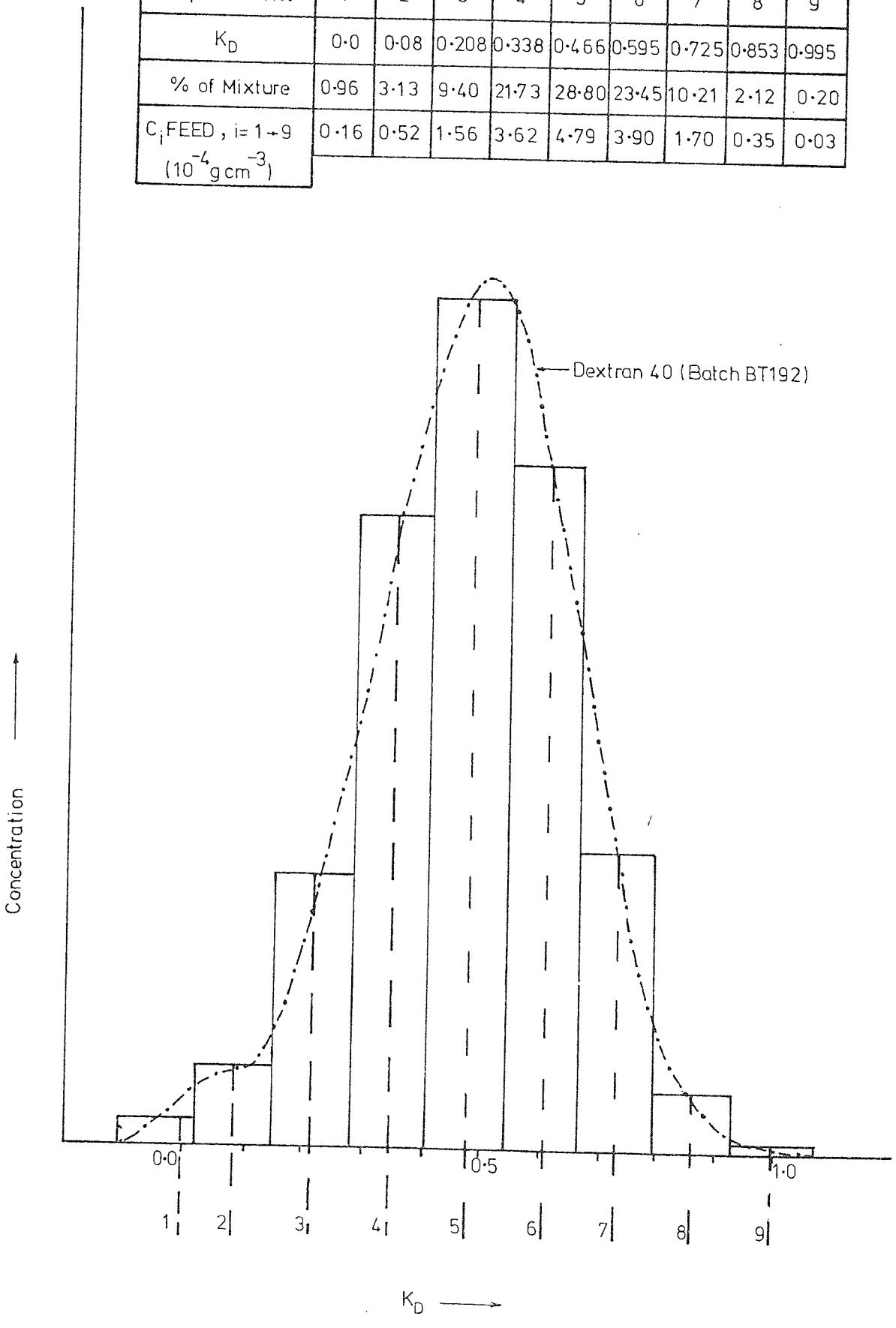

Figure 8.20 Computer Simulation No.17 Nine Components - CFLOW/FFLOW = 5·13

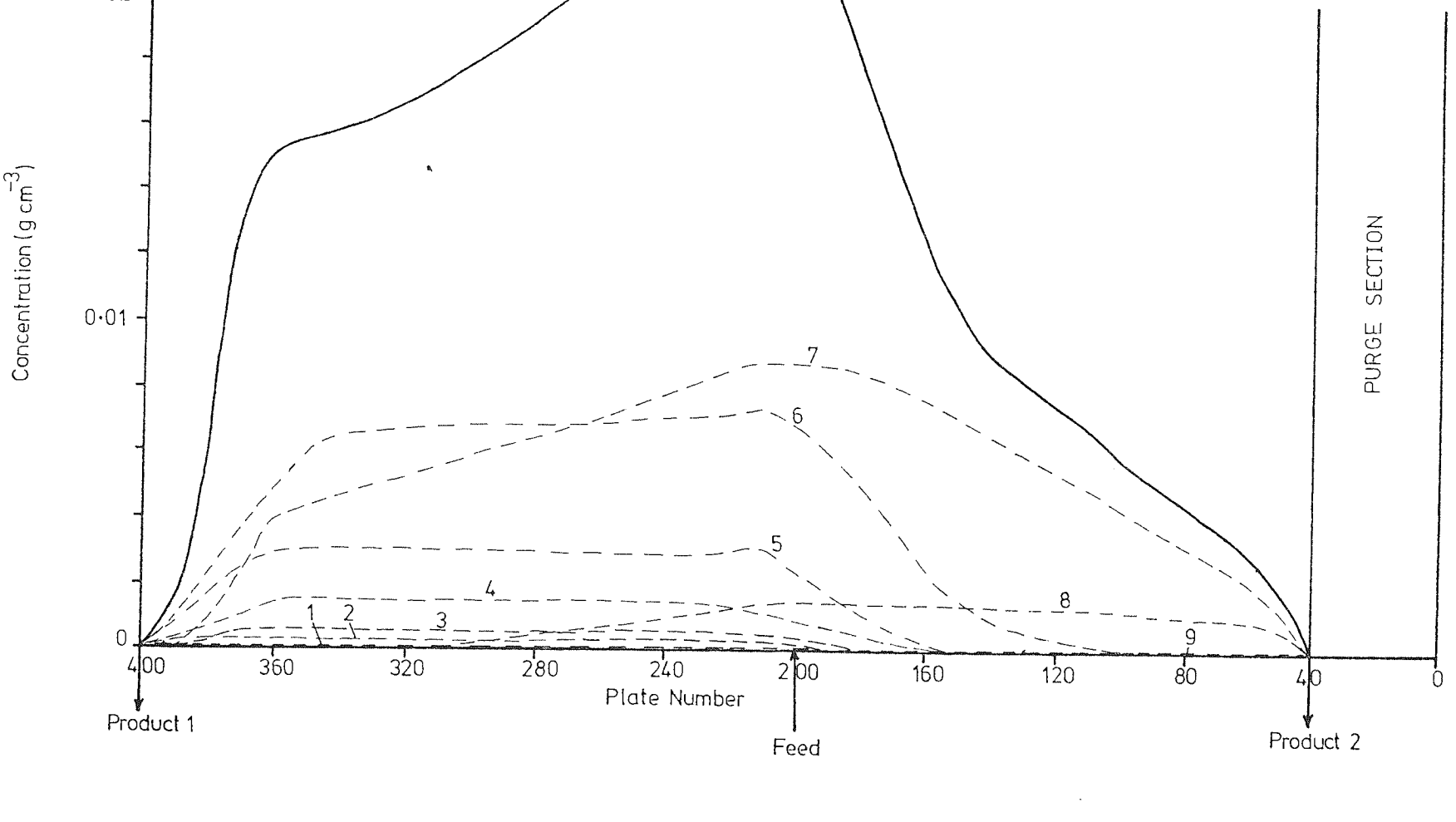

Figure 8.21 Computer Simulation No. 18 Nine Components - FFLOW = 0·0

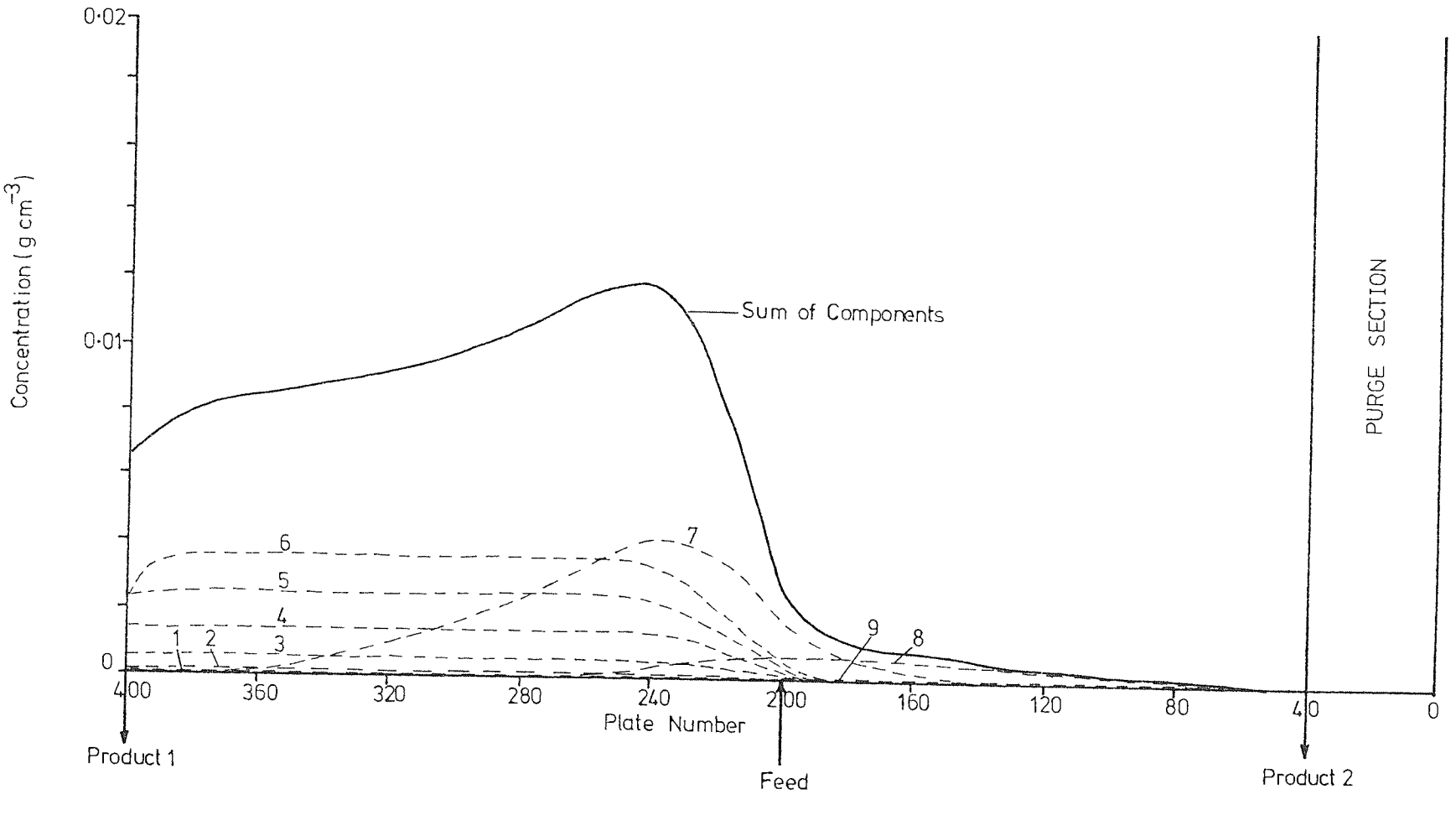

8.4 DISCUSSION

A major factor in the computer runs reported in this thesis was found to be the large amount of computing time necessary for each run. This is illustrated if we consider typical values for the number of plates per column, number of time increments/sequencing interval, and number of sequencing intervals, of 40, 500, and 80 respectively. These values necessitate performing the calculation steps of the inner program loop a total of 16,000,000 times for a ten column series. Because of the long execution time of the program, it was necessary to study the program parameters using a two-component feed, to restrict the cost, and simulation of a multi-component, or polymer, feed was only attempted in a limited manner.

8.4.1 The Effect of the Length of the Time Increment, Δt

The assumption in the derivation of EQUATION 8.13 that c_{n-1} is constant is only valid if Δt is small, and ideally, therefore, Δt should be as small as possible. FIGS. 8.3-8.7 show the effect of reducing Δt, in the range 20.0s-1.0s. A significant difference is obtained between the concentration profiles for 20.0s, 8.0s, 4.0s and 2.0s, while the concentration profiles for 2.0s and 1.0s are in good agreement. Consequently, any improvement in accuracy with the use of a time increment less than 2.0s was thought to be minimal, and 2.0s was adopted as the standard time increment for the remaining computer runs.

8.4.2 The Effect of the Number of Theoretical Plates/Column, N

FIGS. 8.7-8.11 show the effect of reducing the number of plates/column from 80 to 5 for a separation factor of 9.0. The extent of overlap of the concentration profiles for the two components increases as the number of plates is reduced. This is because a

reduction in the number of plates/column reduces the degree of separation achieved in a given number of columns. Consequently a greater number of columns are necessary to maintain the same degree of separation as the number of plates/column is reduced. A value of 20 plates/column was used for the remaining two-component runs, to maintain reasonable computing times, and Run 8.7 was adopted as the standard run.

It is interesting to note the differences in the concentration profiles of the two components. At the beginning of each simulation run the mobile phase concentration of component 1, the component with least affinity for the stationary phase, builds up faster than component 2, even though they are both introduced at the same concentration. This is because component 2 has a larger liquid volume accessible to it in the column, and its concentration in the mobile phase is consequently reduced to a greater degree than component 1. The final concentration level of each component, and the time taken to establish this level, is dependent on:

(i) The component input concentration.

(ii) The component migration rate relative to the feed point.

(ii) in turn is dependent on the component K_D and the operating conditions in the separating section of the sequential unit. A component zone migrates at some fraction R of the mobile phase velocity, during a sequencing interval, where R is given by:

$$R = \frac{V_M}{V_M + K_D V_S} \qquad (8.14)$$

If we consider the case of $V_M \simeq V_S$ (true for g.p.c. on Porasils):

$$R \simeq \frac{1}{1 + K_D} \qquad (8.15)$$

Thus the relative migration rates of components with K_D values ranging between 0 and 1 are:

K_D	0.0	0.1	0.2	0.3	0.4	0.5	0.6	0.7	0.8	0.9	1.0
R	1.0	0.91	0.83	0.77	0.71	0.67	0.64	0.59	0.56	0.53	0.5

These figures show that, for the SCCR3 unit, if the sequencing interval was set to give a separation position corresponding to a $K_D \simeq 0.5$, as in the simulation runs, components travelling with the mobile phase ($K_D < 0.5$) travel away from the feed point at a faster rate than components travelling with the stationary phase ($K_D > 0.5$). This explains the greater concentration build-up of material travelling with the mobile phase recorded in the simulation runs, and selection of a separating position corresponding to the average migration rate of the two components may prove useful in future simulation runs. It is interesting to note that, during operation of the SCCR3 unit, material travelling with the stationary phase generally required a longer time to reach its pseudo-equilibrium condition than material travelling with the mobile phase.

8.4.3 The Effect of the Separation Factor, α

FIGS. 8.7, 8.12-8.14 show the effect of reducing the separation factor from 9.0 to 1.22, for a given number of plates. The component 1 concentration profile extends further towards the isolated column as its K_D is reduced, until at $K_D = 0.45$, it has extended into the second column of the separating section. Similarly, the concentration profile of component 2 extends further towards the product 1 outlet as K_D is reduced, until, at $K_D = 0.55$, it is contaminating product 1. This observation is valid, even though the condition of reproducible

concentrations for successive sequencing intervals had not yet been attained, since the contamination of product 1 would increase as the concentration profile of component 2 built up to higher concentration values. The time required to establish pseudo-equilibrium operation increases as the separation factor is reduced, because of the reduction in the component migration rates. This also results in an increase in the pseudo-equilibrium concentration values.

8.4.4 The Effect of the Finite Feed Flowrate

FIGS. 8.15 and 8.16 show the effect of the finite feed flowrate on separation performance, for a separation factor of 2.33. For a mobile phase/feed flowrate ratio of 7.21, obtained by reducing the pre-feed point mobile phase flowrate and keeping the post-feed point mobile phase flowrate constant, the overlap of the component concentration profiles is increased although complete separation is still achieved. However, a reduction of the mobile phase/feed flowrate ratio to 3.11, again maintaining a constant post-feed point mobile phase flowrate, results in the component 1 profile extending over the whole separating section, even though it has not reached its maximum concentration values, showing separation of the two components to be impossible under these conditions. A more judicious selection of the mobile phase flowrate improves the separation (FIG. 8.17) although it is apparent that the limiting mobile phase/feed flowrate ratio has been reached. FIGS. 8.15 and 8.18 show that the limiting mobile phase/feed flowrate ratio is increased as the difficulty of separation is increased (α reduced). The observation of a reduction in separation performance with a reduction in the mobile phase/feed flowrate ratio is in agreement with the results obtained for dextran fractionations with the SCCR3 unit

(RUNS 20-500-0.5, 20-1000-0.4, 20-1700-0.3). FIGS. 8.15 and 8.16 also illustrate the reduction in the migration rate of component 1 and increase in migration rate of component 2, corresponding to an increase and decrease in the respective pseudo-equilibrium concentration levels, produced by a reduction in $(L'/P)_{MEAN}$.

8.4.5 Multi-Component, or Polymer, Feed

FIG. 8.20 shows the concentration profiles for a nine-component feed mixture (8.19) after 57 sequencing intervals, equivalent to 5.7 cycles of the SCCR3 unit, for the attempted simulation of experimental RUN 01-600-0.7. Although pseudo-equilibrium values have not been attained for components 6-9 it is apparent that the concentration levels of the components, which have K_D values near to the separation positions (Pre-feed K_D = 0.568, Post-feed K_D = 0.852), are greatly in excess of those obtained for the experimental run. Although the concentration levels of components 6-9 were greatly reduced when the effect of the finite feed flowrate was excluded from the simulation (FIG. 8.21), it is apparent that the agreement between computer and experimental results is poor. Reasons for the poor agreement may be identified as:

(i) The assumption of constant partition coefficients for the nine components. The variation of K_D with concentration, observed for elution of dextran 40 on Porasil C (SECTION 4.4), would have a marked effect on the migration rates of components in the SCCR3 unit, and would need to be included in a realistic computer simulation.

(ii) The assumption that the elution characteristics of the components are independent of each other. The mutual interaction of dextrans of different molecular weights, at finite concentrations, was discussed in SECTION 4.4.4, and this interaction would affect the relative

migration rates of molecules in the SCCR3 unit. This effect is interrelated with (i).

(iii) The assumption of constant characteristics (V_o, V_i, N) for each column. This is inconsistent with the experimental observations given in SECTION 6.2. The column-to-column variations in these values would result in a variation of component migration rates through each column. Inclusion of these variations in the computer model would, however, have the disadvantage of increasing considerably its complexity.

(iv) Representation of a polymer as a nine-component mixture. Although this method gives an approximate representation of a polymer distribution, there are obviously inaccuracies involved, since an accurate representation of a dextran polymer M.W. distribution would require one component for each M.W. difference of 162.

(v) The assumption of a value for the number of theoretical plates/column, N. Ideally a value for N should be calculated theoretically, although the variation of N with packing type, column and packing geometry, component M.W. and concentration, and mobile phase composition and flowrate would make this extremely complex.

Although these factors would need to be considered for a more detailed simulation of the SCCR3 unit, the present model has served to highlight some of the essential operating features, and should be useful for directing future models of the process. Particularly, the following factors have been observed from results obtained with the model:

(i) Reproducible component concentration values are obtained for successive cycles, after the attainment of pseudo-equilibrium operation, and the time required to reach these values increases as the component's K_D approaches the separation position.

(ii) The length of column required to achieve complete separation of a two-component mixture increases as the number of plates/column is reduced.

(iii) The number of plates required to achieve complete separation of a two-component mixture increases as the separation factor is reduced.

(iv) For the separation of a two-component mixture, the minimum separation factor that may be used, for successful operation of the SCCR3 unit, is increased as the mobile phase/feed flowrate is reduced.

Summarizing, the effect of the number of theoretical plates/column, separation factor, and mobile phase/feed flowrate ratio have been investigated, and improvements to the present model suggested. A final factor that should be considered for future computer models is to use a short-cut mathematical method to produce pseudo-equilibrium concentration values with less computer time, as computing times of 30 minutes were reached during the work reported in this section, using a CDC 7600 digital computer.

CHAPTER 9

Conclusions and Recommendations for Future Work

The ability to fractionate dextrans continuously, using gel permeation chromatography in a counter-current operating mode, has been demonstrated successfully using columns 5.1 cm in diameter. Dextran throughputs up to 350 g hr^{-1} have been achieved, at operating pressures below 550 kN m^{-2} (80 p.s.i.a.), by using feed solutions containing dextran in concentrations of up to 22% w/v, and maintaining operation at mobile phase flowrates below 3.3 cm^3 min^{-1} cm^{-2}. The modest loss of performance incurred by operation under conditions of high dextran concentration is contrasted by the significant loss of performance obtained by increasing the feed flowrate relative to the mobile phase flowrate, and a limiting mobile phase/feed flowrate ratio exists for a given fractionation problem.

A significant dependence of the distribution coefficients of dextrans on operating concentration has been recorded during operation of the SCCR3 unit. This effect has also been demonstrated on a small scale, using batch operation, and the suggested cause is the phenomenon of 'secondary exclusion', wherein dextran solutions are reported to show similar exclusion properties to dextran gel g.p.c. packings. Further investigation of this phenomenon is necessary to establish, in detail, the theory of continuous g.p.c. at finite concentrations.

A simple chromatographic plate model has been used as a preliminary attempt to establish the individual effect of key parameters on the overall separation performance of the SCCR3 unit. Although the model does not reproduce concentration profiles recorded with the SCCR3 unit accurately, improvements which should lead to a more accurate simulation are suggested, notably the inclusion of a concentration dependence of the distribution coefficient. Qualitatively, the model in its present form has shown:

(i) A pseudo-steady state operating condition is established, which is consistent with experimental results, and the number of sequencing intervals necessary to establish pseudo-equilibrium increases as the difficulty of the separation increases ($\alpha \rightarrow 1$).

(ii) The pseudo-equilibrium concentration level of a component increases as its K_D approaches the K_D equivalent to the separation or 'cut' position, because of its longer residence time in the SCCR3 unit.

(iii) The number of theoretical plates necessary to produce a certain degree of separation of two components increases as the separation becomes more difficult.

(iv) The step-change in the mobile phase flowrate, caused by the introduction of the feed in a finite volume, reduces the degree of separation obtained for a given number of theoretical plates, and a limiting mobile phase/feed flowrate ratio exists for complete separation of a two component mixture, which increases as the separation becomes more difficult. A reduction in separation performance with a decrease in the mobile phase/feed flowrate ratio is consistent with experimental results with the SCCR3 unit.

Future areas of investigation, which have been indicated by the present research, are:

(i) Investigation of the effect of changing the feed input position within the separating section of the SCCR3 unit. This should enable more efficient use of the available separating length.

(ii) Investigation of the effect of the degree of discontinuity of the SCCR3 unit on the separating length required for

a given product purity. This would enable the optimum combination of column length and number of columns to be determined.

(iii) Use of a two-component feed mixture to allow characterization of the SCCR3 unit. A thorough experimental and theoretical treatment of the counter-current g.p.c. process would be greatly simplified by the use of monodisperse materials such as proteins and enzymes. This would also have the added advantage of extending the range of applications of continuous g.p.c.

For production operation higher dextran throughputs should be attainable in one or more of the following ways:

(i) Increasing the mobile phase flowrate, and proportionally increasing the feed flowrate, while reducing the sequencing interval to retain the desired operating value of $(L'/P)_{MEAN}$. However, this would result in a higher pressure drop/unit column length, and therefore necessitate the use of equipment suitable for operation at pressures above 550 kN m^{-2}.

(ii) Increasing the concentration of dextran in the feed. This too would result in a higher pressure drop/unit length, due to the increase in viscosity of the feed solution, and this viscosity increase would also make pumping more difficult. Operation at elevated temperature may overcome these problems, by reducing viscosity, and the preliminary results shown in APPENDIX 2 indicate, for example, that operation at a temperature of approximately 50°C would allow a 30% w/v dextran 40 solution to be used while maintaining the feed viscosity at the same value obtained for a 20% w/v dextran 40 solution at 20°C. Another advantage expected with the use of elevated temperature is the improvement in resolution discussed in SECTION 3.3.2.2.

(iii) Using larger diameter columns. Methods for improving column efficiency for large diameter columns were reviewed in SECTION 2.3.2.3. Generally the decrease in column efficiency expected with increasing column diameter may be largely offset by careful packing, the use of grids and/or inert spheres in the column end fittings, and the use of baffles within the columns.

The required commercial dextran production rate is approximately 100 tonnes per annum, and it can be seen from FIG. 7.43 in SECTION 7.4.3.3 that throughputs of this order would be achieved with columns of about 30 cm. diameter, based on scale-up of present results, and the major portion of the feed input would emerge from the unit as salable product. Any gain in throughput/cross-sectional area that could be achieved by (i) and/or (ii) would reduce the expected column diameter required for a commercial unit, and therefore make the process more attractive by reducing capital equipment costs. Otocka (246) suggests that g.p.c. is ready for the advent of "second generation" techniques, due to the rapid advances made in the field of High Speed Liquid Chromatography (H.S.L.C.) over the last ten years, which have been reviewed recently by Knox (247). New packing materials such as Hydrogel (248), Ultragel (249), and Spheron (250), details of which are given in FIG. 3.2 in SECTION 3.1.2.1, may offer improvements in column efficiency, and generally it is expected that future advances in the area of High Speed Gel Permeation Chromatography should result in significant benefits at the production level.

APPENDIX 1

Calibration Charts

Figure A.1.1 Responce of AutoAnalyser to Glucose Concentration L-cysteine hydrochloride/sulphuric acid assay

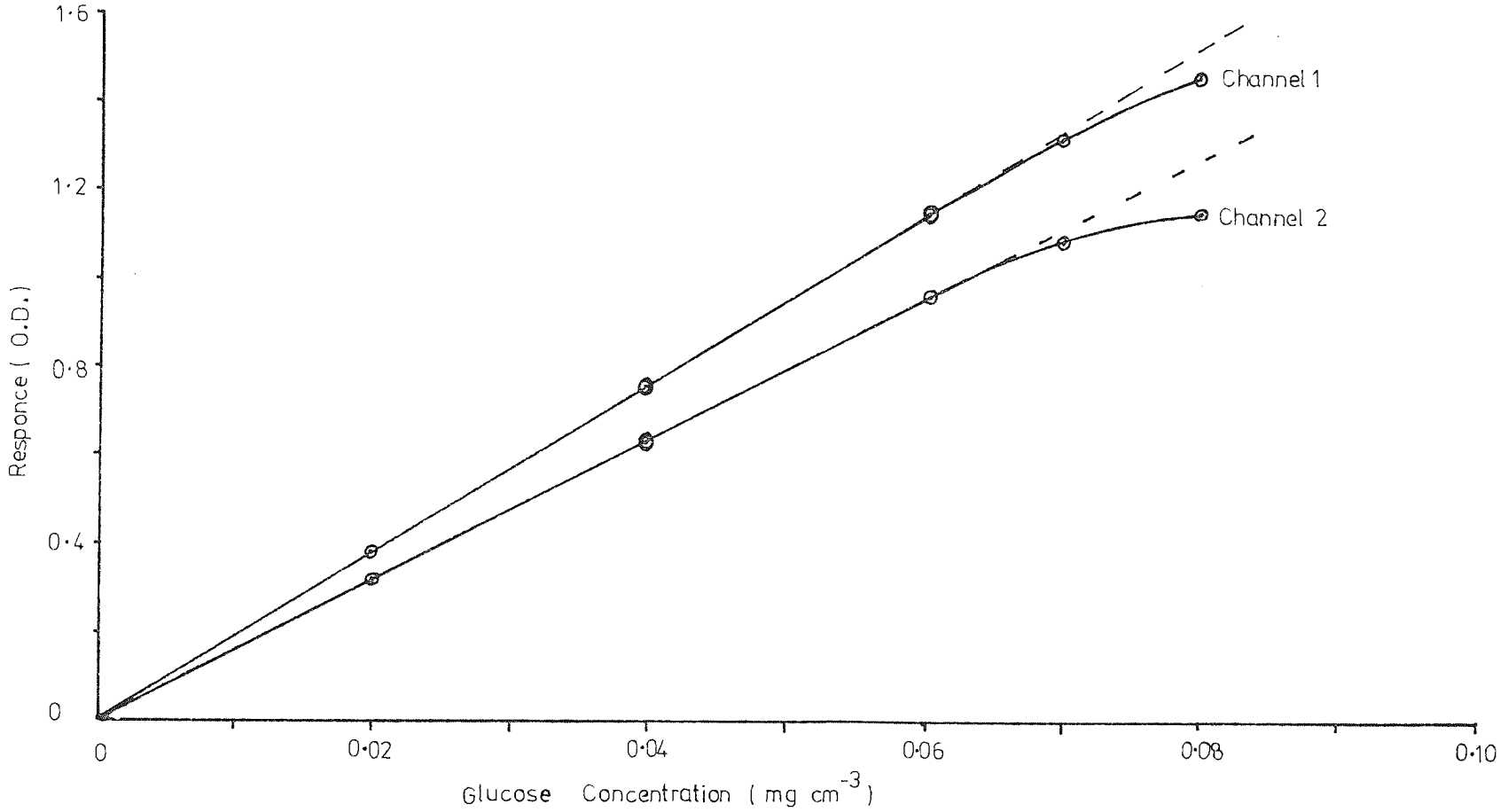

Figure A.1.2 Calibration of SCCR3 Automatic Sequencing Unit

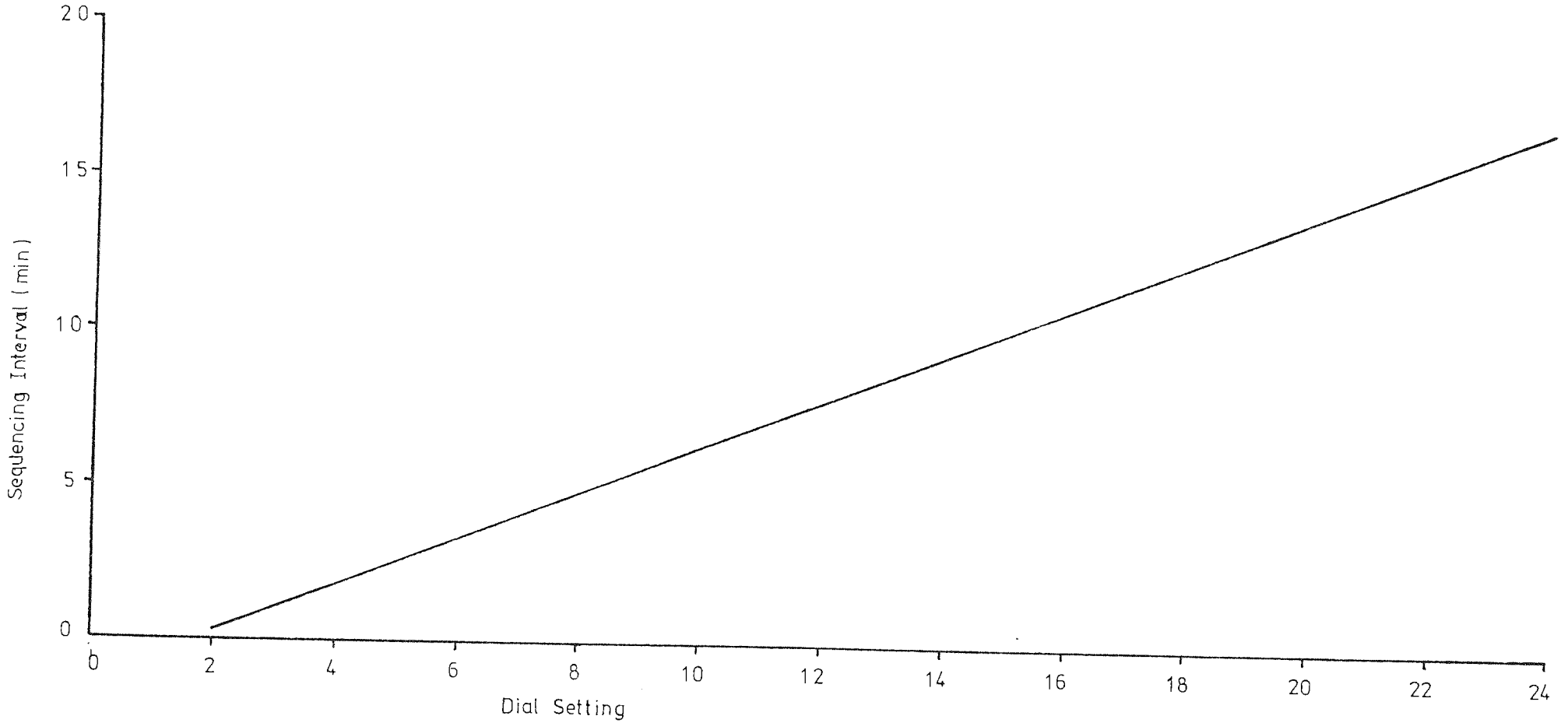

Figure A.1.3 Nominal Throughputs of SCCR3 Pumps

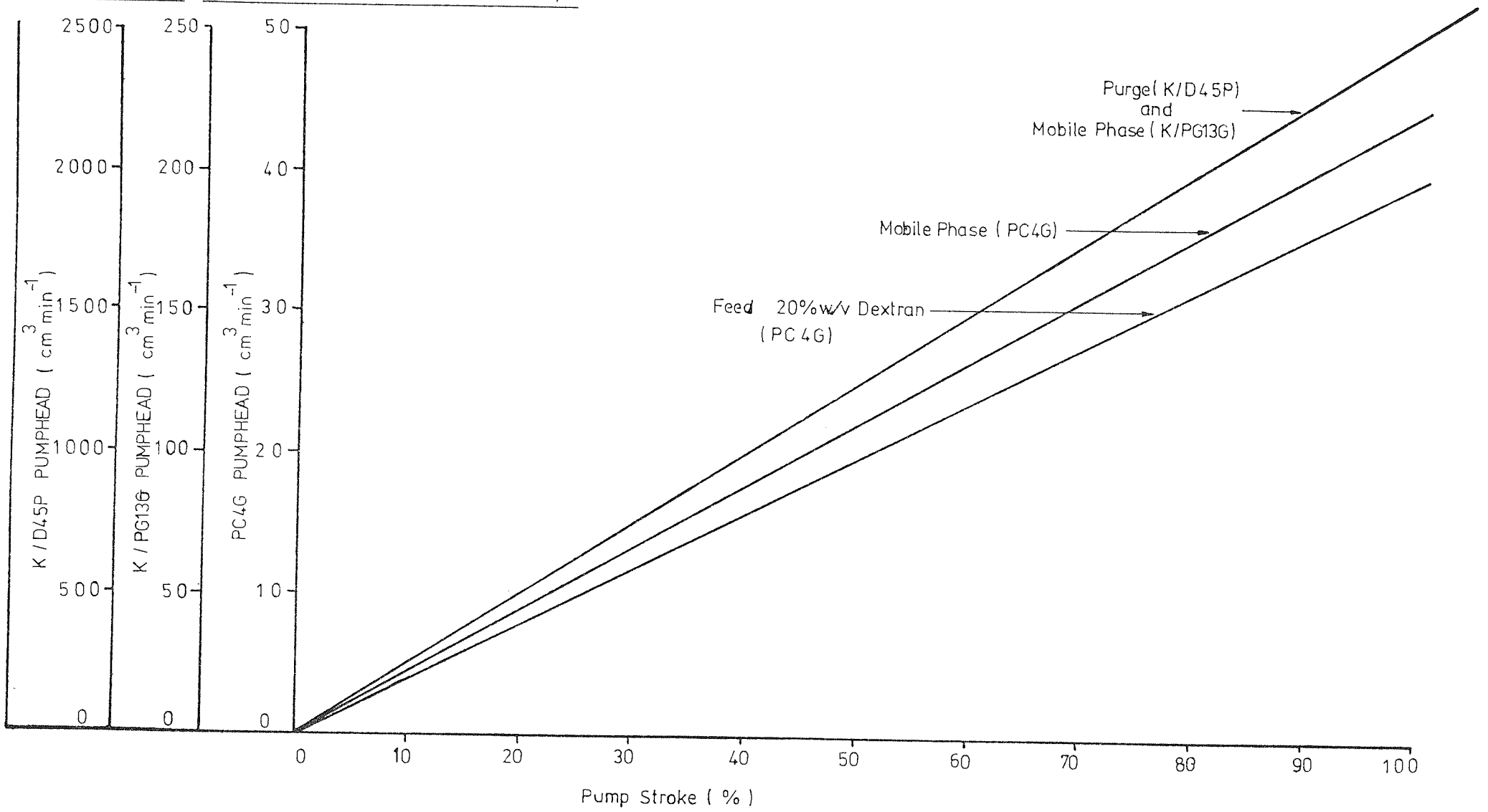

Figure A.1.4 Calibration of Mobile Phase / Purge Flowrate Measurement Cylinder

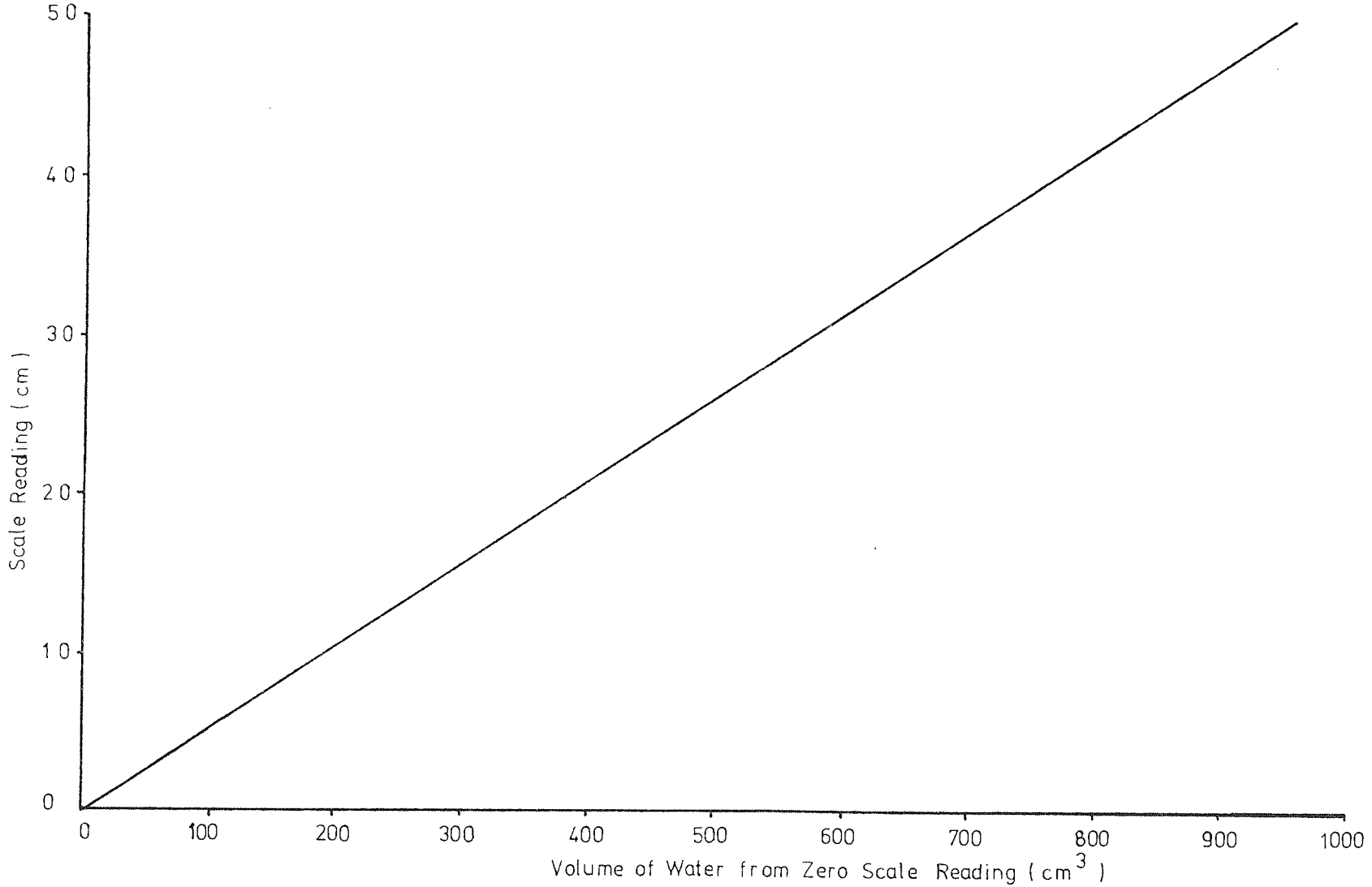

APPENDIX 2

Physical and Chemical Properties of Dextran Fractions

Figure A.2.1

(a) Partial Structure of Dextran Synthesized from Sucrose using Leuconostoc Mesenteroides B512

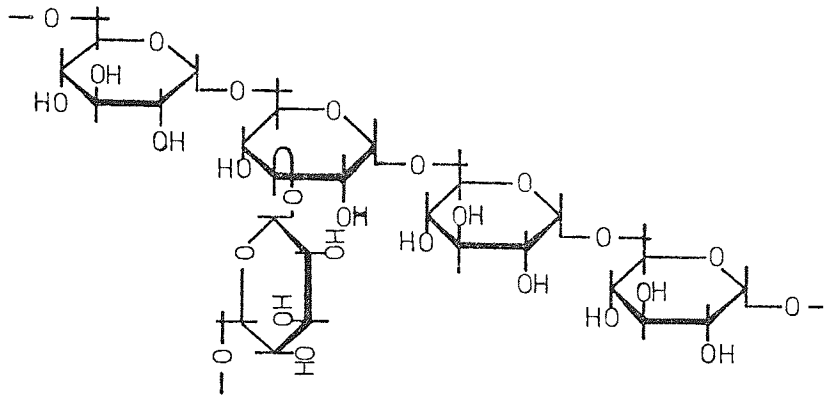

(b) M.W. Details of Dextran T-Fractions (Pharmacia Ltd.)

Fraction	Lot No.	$\overline{M}_w$	$\overline{M}_n$	$M_{0.5}$
T-10	9846	10 500	6400	10 800
T-20	7968	22 300	15 000	17 700
T-40	2540	44 400	28 900	32 300
T-70	1730	70 000	42 500	59 600
T-110	5404	101 000	62 000	96 000
T-150	921	154 000	86 000	116 000
T-250	1343	231 000	113 000	167 000
T-500	1342	450 000	194 000	300 000
2000	4033			~ 2 000 000
BLUE DEXTRAN	2536			~ 2 000 000
FITC-DEXTRAN40	3567	39 000	32000	33 000

Figure A.2.2 Molecular Weight Distributions of Dextran Feeds used in Fractionation Studies, Determined by G.P.C

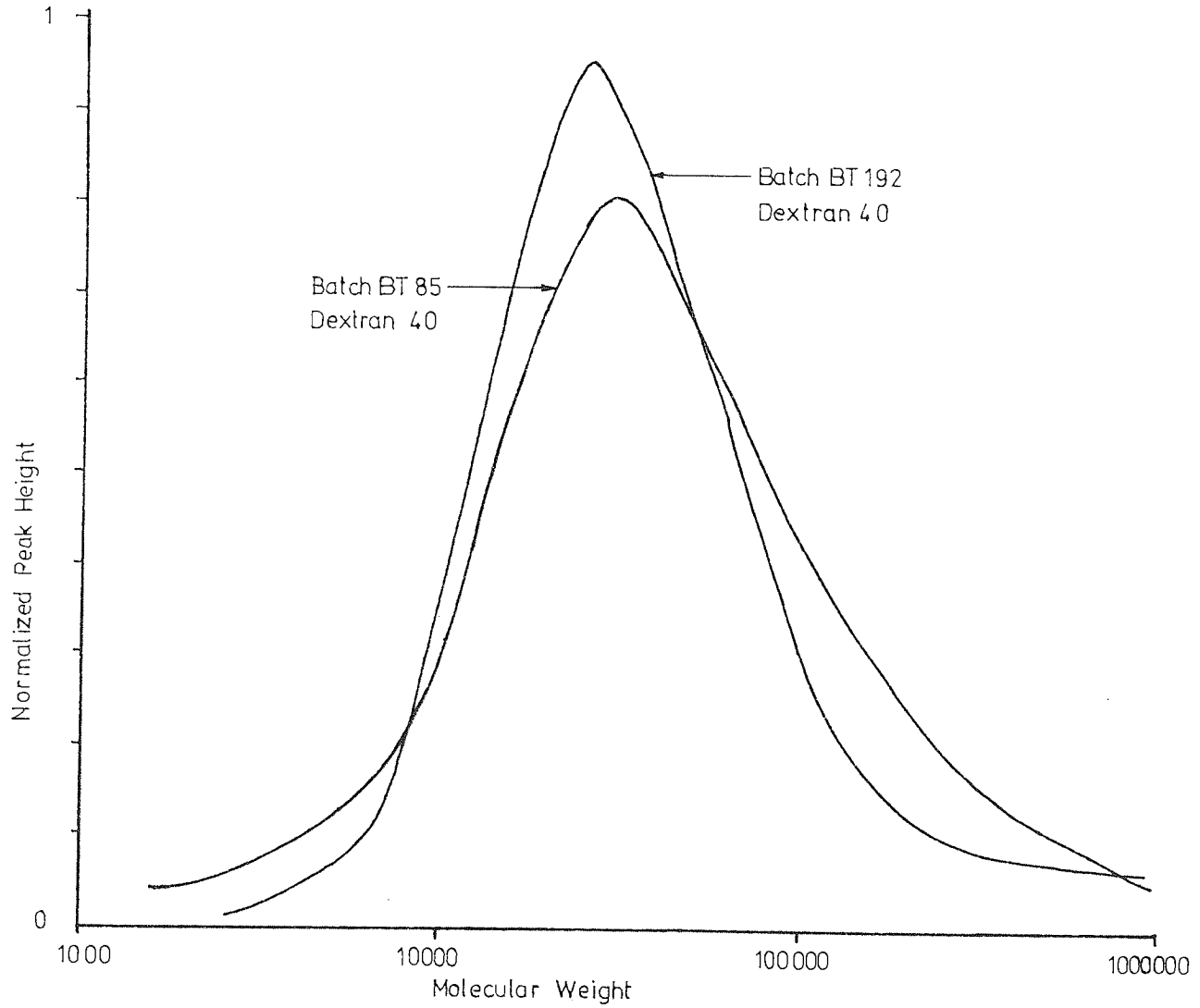

Figure A.2.3 Density of Dextran 40 Solutions at 20°C

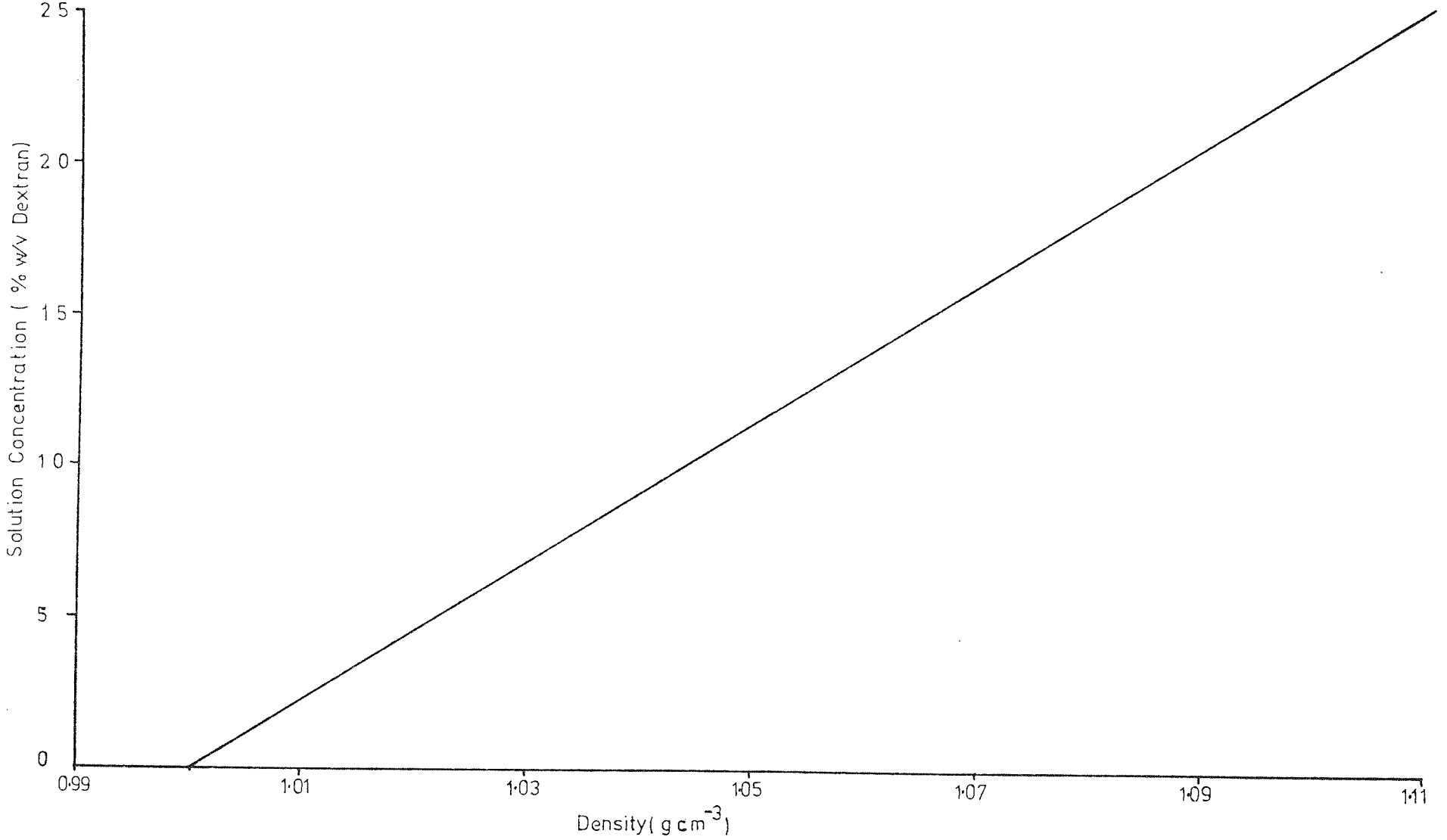

Viscosity of Dextran 40 Solutions

FIG.A.2.4 shows the variation of viscosity of Dextran 40 solutions with concentration and temperature. Readings obtained with a Cannon Fenske viscometer are also compared with readings obtained with a Ferranti viscometer for various dextran concentrations at 20°C. The size of the measured viscosity increase with increasing concentration is supported by the recorded increase in pressure drop readings obtained during operation of the SCCR3 unit. Approximate agreement was obtained between the recorded SCCR3 pressure drops, and the increase in pressure drop, relative to the pressure drops recorded with water (FIG. 6.9), expected from the viscosity readings in FIG. A.2.4, assuming $\Delta P \propto \mu$. This suggests that, although polymer solutions often exhibit non-Newtonian behaviour, Dextran 40 solutions approximate to Newtonian fluids for the range of conditions used in this study. This approximation may not hold for future work at higher operating flowrates and dextran concentrations, however, and a more detailed study in this area may be necessary. A general review of non-Newtonian flow through porous media is given by Savins (251), and another area of interest may be the elasticity sometimes exhibited by polymer solutions (252) which can lead to pressure drops being obtained which are higher than those expected from viscosity considerations alone.

Figure A.2.4 Viscosity of Dextran 40 Solutions

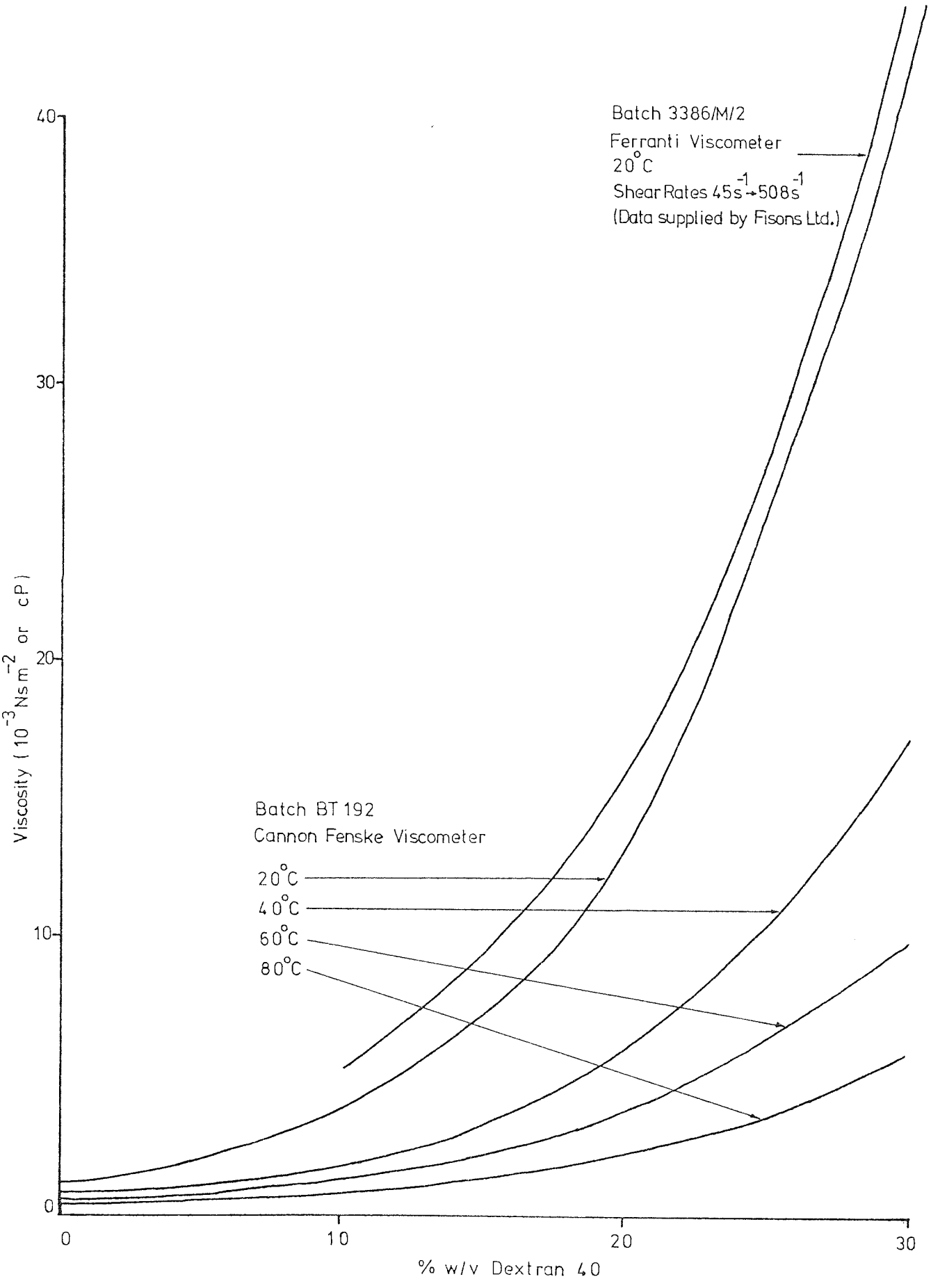

APPENDIX 3

Example of Calculation of Chromatogram Normalization Scaling Factor, and SCCR3 On-Column Dextran Concentrations

FIG. A.3.1 Calculation of the Chromatogram Normalization Scaling Factor for a Typical SCCR3 Product

Analysis performed by g.p.c. on Column 5 (SECTION 4.3.3.2) at 0.0836 $cm^3\ min^{-1}$ mobile phase flowrate.

Number of equal time intervals into which the chromatogram is divided = 38.

Width of each time interval = 2.5 min.

Width of each time interval (R.F. units) = $\frac{2.5 \times 0.0836}{14.67}$ = 0.0142 R.F. units where 14.67 cm^3 is the total volume (V_t) of Column 5.

Sum of the mean heights of the chromatogram intervals Σh_i = 8.21 O.D. units.

Total area of product chromatogram = 8.21 x 0.0142 = 0.117 R.F.-O.D. units.

Total dextran rate of product from the SCCR3 unit = 1.711 g min^{-1}.

Total dextran feed input rate to the SCCR3 unit = 2.192 g min^{-1}.

Product fraction of dextran input rate = $\frac{1.711}{2.192}$ = 0.780.

Scaling factor for product chromatogram = $\frac{0.780}{0.117}$ = 6.67.

Normalized height of each product chromatogram time interval = 6.67 x h_i where i = 1→38.

FIG. A.3.2 Calculation of On-column Dextran Concentration of a Typical Sample Purged from the SCCR3 unit at the End of an Experimental Run

Total weight of sample purged from the SCCR3 unit = 4163 g.

Concentration of dextran in sample = 40.0 mg cm^{-3}.

Density of sample (see APPENDIX 2) = 1.013 g cm^{-3}.

Volume of Sample = $\frac{4163}{1.013}$ = 4120 cm^3.

Weight of dextran in sample = 4120 x 0.040 = 165 g.

Average K_D of sample (determined by g.p.c.) = 0.497.

Interstitial volume, V_o, for the SCCR3 column from which the sample was obtained = 527 cm^3.

Pore volume, V_i, for the SCCR3 column from which the sample was obtained = 621 cm^3.

Volume of liquid within the SCCR3 column which is accessible to the sample, $V_o + V_i K_D$, = 836 cm^3.

On-column dextran concentration = $\frac{165}{836}$ = 19.8% w/v.

APPENDIX 4

Details of SCCR3 Operating Conditions, and Concentration/Molecular Weight Distribution Profiles

Figure A.4.1 Variation of Operating Conditions During Run 10-500-0·5

Cycle No.	Period of Operation	Average Inlet Operating Pressures			Average S	Average Feed Flowrate	Average Product Data							Feed Dextran Input Rate
		Purge	Mobile Phase	Feed			Product 1 Flowrate	Product 2 Flowrate	Product 1 Conc.	Product 2 Conc.	Product 1 Dextran Rate	Product 2 Dextran Rate	Total Dextran Rate	
	hrs	kNm^{-2}	kNm^{-2}	kNm^{-2}	min	cm^3min^{-1}	cm^3min^{-1}	cm^3min^{-1}	$mg\ cm^{-3}$	$mg\ cm^{-3}$	$g\ min^{-1}$	$g\ min^{-1}$	$g\ min^{-1}$	$g\ min^{-1}$
1, 2	0 – 12·0	147	285	252	18·0	—	—	—	—	—	—	—	—	—
3, 4	12·0 – 23·9	146	399	335	17·9	—	—	—	—	—	—	—	—	—
5	23·9 – 29·9	149	423	319	18·0	8·33	54·7	194	3·77	0·037	0·206	0·072	0·278	0·841
6, 7	29·9 – 41·8	149	422	292	17·9	8·33	57·0	194	5·07	3·23	0·289	0·627	0·916	0·840
8, 9	41·8 – 53·6	149	425	292	17·7	8·27	56·0	192	3·41	2·47	0·191	0·473	0·664	0·834
10, 11	53·6 – 65·4	146	424	277	17·8	8·15	53·9	187	3·86	3·44	0·208	0·644	0·852	0·822
12, 13	65·4 – 77·0	147	428	274	17·7	8·30	53·3	192	2·76	3·62	0·147	0·696	0·843	0·837
14, 15, 16	77·0 – 94·3	149	421	264	17·7	8·24	53·4	192	2·68	3·67	0·143	0·706	0·849	0·831

Figure A.4.2 Variation of Operating Conditions During Run 20-500-0·5

Cycle No.	Period of Operation	Average Inlet Operating Pressures			Average S	Average Feed Flowrate	Average Product Data							Feed Dextran Input Rate
		Purge	Mobile Phase	Feed			Product 1 Flowrate	Product 2 Flowrate	Product 1 Conc.	Product 2 Conc.	Product 1 Dextran Rate	Product 2 Dextran Rate	Total Dextran Rate	
	hrs	kNm^{-2}	kNm^{-2}	kNm^{-2}	min	cm^3min^{-1}	cm^3min^{-1}	cm^3min^{-1}	$mg\ cm^{-3}$	$mg\ cm^{-3}$	$g\ min^{-1}$	$g\ min^{-1}$	$g\ min^{-1}$	$g min^{-1}$
1,2	0 – 5·9	143	232	177	17·6	8·18	52·6	191	0·68	1·15	0·046	0·210	0·246	1·718
3,4	5·9–11·7	143	288	184	17·6	8·16	51·4	196	2·28	7·40	0·117	1·451	1·568	1·714
5,6	11·7–17·6	143	301	190	17·6	8·14	51·3	197	1·97	6·81	0·101	1·339	1·440	1·709
7,8	17·6–23·5	145	313	198	17·6	8·14	52·4	196	2·21	6·70	0·116	1·311	1·427	1·709
9,10	23·5–29·3	150	331	205	17·6	8·28	51·9	197	2·47	7·37	0·128	1·448	1·576	1·739
11,12	29·3–35·2	148	335	206	17·6	8·09	52·1	196	2·74	8·32	0·143	1·631	1·774	1·699
13,14	35·2–41·0	146	311	197	17·5	8·20	51·3	195	2·48	8·49	0·127	1·655	1·781	1·722
15	41·0–43·9	146	309	197	17·5	8·10	52·0	197	2·48	8·38	0·129	1·650	1·780	1·701

Figure A.4.3 Variation of Operating Conditions During Run 20-1000-0·4

Cycle No.	Period of Operation	Average Inlet Operating Pressures			Average S	Average Feed Flowrate	Average Product Data							Feed Dextran Input Rate
		Purge	Mobile Phase	Feed			Product 1 Flowrate	Product 2 Flowrate	Product 1 Conc.	Product 2 Conc.	Product 1 Dextran Rate	Product 2 Dextran Rate	Total Dextran Rate	
	hrs	$kN m^{-2}$	$kN m^{-2}$	$kN m^{-2}$	min	$cm^3 min^{-1}$	$cm^3 min^{-1}$	$cm^3 min^{-1}$	$mg\ cm^{-3}$	$mg\ cm^{-3}$	$g\ min^{-1}$	$g\ min^{-1}$	$g\ min^{-1}$	$g\ min^{-1}$
1,2	0 – 5·8	151	303	217	17·4	17·2	52·1	181	1·450	7·200	0·075	1·302	1·377	3·540
3,4	5·8 – 11·6	148	369	220	17·4	16·6	51·9	180	3·218	16·20	0·167	2·921	3·088	3·420
5,6	11·6 – 17·5	148	365	221	17·4	17·0	52·9	190	2·968	16·80	0·157	3·185	3·342	3·500
7,8	17·5 – 23·2	145	358	219	17·3	17·5	50·6	179	2·964	19·60	0·150	3·501	3·651	3·610
9,10	23·2 – 28·9	148	378	226	17·2	17·1	55·9	188	6·959	17·29	0·389	3·251	3·640	3·520
11,12	28·9 – 34·6	147	383	231	17·1	17·0	55·3	190	3·363	16·67	0·186	3·161	3·347	3·500
13,14	34·6 – 38·3	147	379	228	17·1	17·1	56·5	189	3·487	19·29	0·197	3·654	3·851	3·520

Figure A.4.4 Variation of Operating Conditions During Run 20-1700-0·3

Cycle No.	Period of Operation	Average Inlet Operating Pressures			Average S	Average Feed Flowrate	Average Product Data							Feed Dextran Input Rate
		Purge	Mobile Phase	Feed			Product 1 Flowrate	Product 2 Flowrate	Product 1 Conc.	Product 2 Conc.	Product 1 Dextran Rate	Product 2 Dextran Rate	Total Dextran Rate	
	hrs	kNm^{-2}	kNm^{-2}	kNm^{-2}	min	$cm^3 min^{-1}$	$cm^3 min^{-1}$	$cm^3 min^{-1}$	$mg\ cm^{-3}$	$mg\ cm^{-3}$	$g\ min^{-1}$	$g\ min^{-1}$	$g\ min^{-1}$	$g\ min^{-1}$
1,2	0 – 5·6	150	308	234	17·0	30·4	56·4	193	1·220	13·33	0·069	2·569	2·638	6·141
3,4	5·6–11·3	150	383	259	17·0	29·4	56·4	187	3·030	30·50	0·171	5·692	5·836	5·939
5,6	11·3-17·0	148	385	261	17·0	28·9	55·7	186	3·040	30·50	0·169	5·684	5·853	5·838
7,8	17·0-22·6	148	401	266	17·1	29·2	56·6	185	3·570	31·90	0·202	5·907	6·109	5·898
9,10	22·6–28·4	148	410	272	17·2	29·3	56·6	185	3·810	31·40	0·216	5·793	6·009	5·919
11,12	28·4–34·1	149	400	268	17·1	28·3	56·2	184	3·850	30·90	0·216	5·679	5·895	5·717
13,14	34·1–38·4	148	389	253	17·1	27·0	55·5	177	3·480	30·80	0·193	5·452	5·645	5·454

Figure A.4.5 Variation of Operating Conditions During Run 20-600-0·7

Cycle No.	Period of Operation	Average Inlet Operating Pressures			Average S	Average Feed Flowrate	Average Product Data							Feed Dextran Input Rate
		Purge	Mobile Phase	Feed			Product 1 Flowrate	Product 2 Flowrate	Product 1 Conc.	Product 2 Conc.	Product 1 Dextran Rate	Product 2 Dextran Rate	Total Dextran Rate	
	hrs	kNm^{-2}	kNm^{-2}	kNm^{-2}	min	$cm^3 min^{-1}$	$cm^3 min^{-1}$	$cm^3 min^{-1}$	$mg\ cm^{-3}$	$mg\ cm^{-3}$	$g\ min^{-1}$	$g\ min^{-1}$	$g\ min^{-1}$	$g\ min^{-1}$
1,2	0 – 5·7	148	301	250	17·0	10·0	65·0	190	2·650	0·395	0·172	0·075	0·247	2·200
3,4	5·7–11·4	144	454	288	17·0	10·1	59·6	192	5·150	6·060	0·307	1·165	1·472	2·222
5,6	11·4–17·0	145	494	312	17·0	10·0	63·4	189	7·730	7·860	0·490	1·485	1·975	2·200
7,8	17·0–22·7	146	504	314	17·0	9·8	62·4	190	7·310	8·990	0·456	1·709	2·165	2·156
9,10	22·7–28·4	145	501	314	17·0	9·9	62·5	190	7·360	9·020	0·460	1·713	2·173	2·178

Figure A.4.6 Variation of Operating Conditions During Run 20-500-0·8

Cycle No.	Period of Operation	Average Inlet Operating Pressures			Average S	Average Feed Flowrate	Average Product Data							Feed Dextran Input Rate
		Purge	Mobile Phase	Feed			Product 1 Flowrate	Product 2 Flowrate	Product 1 Conc.	Product 2 Conc.	Product 1 Dextran Rate	Product 2 Dextran Rate	Total Dextran Rate	
	hrs	$kN\,m^{-2}$	$kN\,m^{-2}$	$kN\,m^{-2}$	min	$cm^3\,min^{-1}$	$cm^3\,min^{-1}$	$cm^3\,min^{-1}$	$mg\,cm^{-3}$	$mg\,cm^{-3}$	$g\,min^{-1}$	$g\,min^{-1}$	$g\,min^{-1}$	$g\,min^{-1}$
1, 2	0 – 7·7	145	249	224	23·0	8·05	52·0	194	4·16	0·127	0·216	0·025	0·241	1·626
3, 4	7·7 – 15·3	143	413	324	23·0	8·10	49·8	194	11·52	0·684	0·574	0·133	0·707	1·636
5, 6	15·3 – 23·0	137	470	337	23·0	8·30	49·9	177	13·66	5·84	0·682	1·031	1·713	1·677
7, 8	23·0 – 30·7	138	529	359	23·0	8·06	47·9	171	11·74	5·62	0·562	0·958	1·520	1·628
9, 10	30·7 – 38·3	139	551	376	23·0	8·35	47·4	179	11·40	6·04	0·540	1·083	1·623	1·687

Figure A.4.7 Variation of Operating Conditions During Run 20-400-1-1

Cycle No.	Period of Operation	Average Inlet Operating Pressures			Average S	Average Feed Flowrate	Average Product Data							Feed Dextran Input Rate
		Purge	Mobile Phase	Feed			Product 1 Flowrate	Product 2 Flowrate	Product 1 Conc.	Product 2 Conc.	Product 1 Dextran Rate	Product 2 Dextran Rate	Total Dextran Rate	
	hrs	kNm^{-2}	kNm^{-2}	kNm^{-2}	min	$cm^3 min^{-1}$	$cm^3 min^{-1}$	$cm^3 min^{-1}$	$mg cm^{-3}$	$mg cm^{-3}$	$g min^{-1}$	$g min^{-1}$	$g min^{-1}$	$g min^{-1}$
1, 2	0 - 10·0	136	252	238	30·0	7·18	44·6	160	8·100	0·092	0·361	0·015	0·376	1·580
3	10·0-15·0	136	356	345	30·0	6·85	44·3	157	25·40	0·084	1·125	0·013	1·138	1·507
4	15·0-20·0	136	343	330	30·0	7·22	45·4	163	35·49	0·156	1·611	0·026	1·637	1·588
5	20·0-25·0	136	342	331	30·0	7·33	45·2	154	33·37	0·186	1·508	0·028	1·536	1·613
6	25·0-30·0	136	328	316	30·0	7·31	44·6	160	35·43	0·181	1·580	0·029	1·609	1·603
7	30·0-35·0	136	323	312	30·0	7·33	45·3	153	33·96	0·229	1·538	0·025	1·563	1·613
8	35·0-40·0	136	323	312	30·0	7·33	45·4	157	35·63	0·261	1·618	0·031	1·649	1·613

Figure A.4.8 Variation of Operating Conditions During Run 01-600-0·7

Cycle No.	Period of Operation	Average Inlet Operating Pressures			Average S	Average Feed Flowrate	Average Product Data							Feed Dextran Input Rate
		Purge	Mobile Phase	Feed			Product 1 Flowrate	Product 2 Flowrate	Product 1 Conc.	Product 2 Conc.	Product 1 Dextran Rate	Product 2 Dextran Rate	Total Dextran Rate	
	hrs	$kN\,m^{-2}$	$kN\,m^{-2}$	$kN\,m^{-2}$	min	$cm^3\,min^{-1}$	$cm^3\,min^{-1}$	$cm^3\,min^{-1}$	$mg\,cm^{-3}$	$mg\,cm^{-3}$	$g\,min^{-1}$	$g\,min^{-1}$	$g\,min^{-1}$	$g\,min^{-1}$
1	0 – 2·8	147	187	163	17·0	11·20	64·5	186	0·386	0·0102	0·0249	0·0019	0·0268	0·1144
2	2·8 – 5·7	143	186	168	16·9	10·10	62·7	192	0·611	0·0209	0·0383	0·0040	0·0423	0·1031
3	5·7 – 8·5	143	182	166	17·0	10·14	61·0	192	0·938	0·0242	0·0572	0·0046	0·0618	0·1034
4	8·5 – 11·3	143	183	167	17·0	10·10	61·1	190	1·076	0·0364	0·0657	0·0069	0·0726	0·1031
5	11·3 – 14·1	143	185	168	16·9	10·24	61·0	188	1·220	0·0561	0·0744	0·0106	0·0850	0·1046
6	14·1 – 16·9	143	185	166	16·8	10·10	61·8	187	1·298	0·0796	0·0802	0·0149	0·0951	0·1031
7	16·9 – 19·7	143	188	169	16·8	10·10	62·6	190	1·448	0·0764	0·0907	0·0145	0·1052	0·1031
8	19·7 – 22·5	143	188	169	16·8	10·00	62·2	189	1·421	0·0883	0·0884	0·0167	0·1051	0·1021
9	22·5 – 25·3	145	188	168	16·8	10·00	60·7	191	1·212	0·1123	0·0736	0·0214	0·0950	0·1021
10	25·3 – 28·1	143	188	170	16·9	10·20	61·0	191	1·238	0·1189	0·0755	0·0227	0·0982	0·1041
11	28·1 – 30·9	143	190	170	16·8	10·00	61·7	190	1·357	0·1193	0·0837	0·0227	0·1064	0·1021
12	30·9 – 33·8	145	193	170	17·0	9·30	60·8	191	1·349	0·1289	0·0820	0·0246	0·1066	0·0950

Figure A.4.9 Details of Concentration and M.W. Profile for Run 10-500-0·5

Note Analysis of point samples after 83·0 hrs of operation

No. of Sample Point	Distance of Sample Point from Product 1 Outlet	Sample Dextran Concentration	Sample Mean K_D (Analysis on Porasil C)	Sample Mean M.W.
	cm	g cm^{-3}		
17	0	0·0079	0·274	77 000
16	70	0·0179	——	——
14	210	0·0253	0·330	58 000
12	350	0·0301	——	——
11	420	0·0303	0·350	53 000
10	490	0·0341	——	——
9	560	0·0357	0·365	49 000
8	630	0·0545	0·450	33 000
7	700	0·0779	0·500	28 000
6	770	0·0771	——	——
4	910	0·0759	——	——
3	980	0·0779	0·505	27 000
2	1050	0·0759	——	——
20	1190	0·0779	0·505	27 000
18	1330	0·0014	0·515	26 000

Figure A.4.10 Details of Concentration and M.W. Profile for Run 20-500-0·5

Column No.	Distance of Column Mid-point from Product 1 Outlet	Weight of Dextran in Column (W)	Mean K_D of Dextran (Analysis on Porasil C)	Volume of Water Accessible to Dextran in Column $(V_o + V_i K_D)$	Concentration of Dextran $\left(\frac{W}{(V_o + V_i K_D)}\right)$	Mean M.W. of Dextran
	cm	g		cm^3	$g\,cm^{-3}$	
14	35	8·1	0·255	685	0·0120	87 000
13	105	14·1	0·295	705	0·0200	70 000
12	175	15·7	0·340	745	0·0211	56 000
17	245	24·1	0·390	766	0·0315	44 000
1	315	95·2	0·453	811	0·117	33 000
15	385	128·7	0·507	842	0·152	27 000
8	455	119·3	0·500	859	0·138	28 000
7	525	107·4	0·495	837	0·128	28 000
6	595	29·5	0·505	835	0·0353	27 000
19	665	0·0	—	—	0·0	—

Figure A.4.11 Details of Concentration and M.W. Profile for Run 20-1000-0·4

Column No.	Distance of Column Mid-point from Product 1 Outlet	Weight of Dextran in Column (W)	Mean K_D of Dextran (Analysis on Porasil C)	Volume of Water Accessible to Dextran in Column ($V_o + V_i K_D$)	Concentration of Dextran ($\frac{W}{V_o + V_i K_D}$)	Mean M.W. of Dextran
	cm	g		cm^3	$g\,cm^{-3}$	
7	35	13·4	0·315	735	0·0182	63 000
6	105	18·3	0·330	731	0·0250	58 000
19	175	23·0	0·350	742	0·0310	53 000
14	245	32·5	0·385	766	0·0424	45 000
13	315	121·2	0·450	795	0·153	34 000
12	385	157·2	0·465	820	0·192	32 000
17	455	164·2	0·485	823	0·200	29 000
1	525	146·5	0·480	832	0·176	30 000
15	595	50·3	0·495	829	0·0607	28 000
8	665	1·2	——	——	~ 0·0014	——

Figure A.4.12 Details of Concentration and M.W. Profile for Run 20-1700-0·3

Column No.	Distance of Column Mid-point from Product 1 Outlet	Weight of Dextran in Column (W)	Mean K_D of Dextran (Analysis on Porasil C)	Volume of Water Accessible to Dextran in Column ($V_o + V_i K_D$)	Concentration of Dextran ($\frac{W}{V_o + V_i K_D}$)	Mean M.W. of Dextran
	cm	g		cm^3	$g\ cm^{-3}$	
15	35	14·1	0·360	749	0·0188	51 000
8	105	25·9	0·390	791	0·0327	44 000
7	175	27·3	0·423	796	0·0343	37 000
6	245	47·8	0·454	806	0·0593	33 000
19	315	139·3	0·505	834	0·167	27 000
14	385	165·1	0·497	836	0·198	28 000
13	455	167·9	0·492	819	0·205	28 000
12	525	155·2	0·495	838	0·185	28 000
17	595	77·2	0·495	839	0·0920	28 000
1	665	1·7	——	——	~ 0·0020	——

Figure A.4.13 Details of Concentration and M.W. Profile for Run 20-600-0·7

Column No.	Distance of Column Mid-point from Product 1 Outlet	Weight of Dextran in Column (W)	Mean K_D of Dextran (Analysis on Porasil C)	Volume of Water Accessible to Dextran in Column ($V_o + V_i K_D$)	Concentration of Dextran $\left(\frac{W}{V_o + V_i K_D} \right)$	Mean M.W. of Dextran
	cm	g		cm^3	$g\ cm^{-3}$	
6	35	28·0	0·420	785	0·0356	38 000
19	105	53·8	0·450	801	0·0672	34 000
14	175	70·2	0·457	811	0·0866	33 000
13	245	89·5	0·472	807	0·111	31 000
12	315	132·2	0·490	835	0·158	28 000
17	385	162·2	0·500	833	0·195	28 000
1	455	164·5	0·500	844	0·195	28 000
15	525	152·7	0·507	836	0·183	27 000
8	595	47·1	0·528	876	0·0538	24 000
7	665	1·7	—	—	~ 0·0020	—

Figure A.4.14 Details of Concentration and M.W. Profile for Run 20-500-0·8

Column No.	Distance of Column Mid-point from Product1 Outlet	Weight of Dextran in Column (W)	Mean K_D of Dextran(Analysis on Porasil C)	Volume of Water Accessible to Dextran in Column ($V_o + V_i K_D$)	Concentration of Dextran ($\frac{W}{V_o + V_i K_D}$)	Mean M.W. of Dextran
	cm	g		cm^3	$g\ cm^{-3}$	
14	35	24·9	0·440	810	0·0307	35 000
13	105	73·1	0·464	817	0·0895	32 000
12	175	101·3	0·467	837	0·121	32 000
17	245	120·4	0·472	829	0·145	31 000
1	315	148·3	0·482	844	0·176	29 000
15	385	191·1	0·513	852	0·224	26 000
8	455	192·8	0·485	862	0·224	29 000
7	525	189·8	0·513	862	0·220	26 000
6	595	102·4	0·503	862	0·119	27 000
19	665	0·6	—	—	~ 0·0007	—

Figure A.4.15 Details of Concentration and M.W. Profile for Run 20-400-1·1

Column No.	Distance of Column Mid-point from Product 1 Outlet	Weight of Dextran in Column (W)	Mean K_D of Dextran (Analysis on Porasil C)	Volume of Water Accessible to Dextran in Column ($V_o + V_i K_D$)	Concentration of Dextran ($\frac{W}{V_o + V_i K_D}$)	Mean M.W. of Dextran
	cm	g		cm^3	$g\,cm^{-3}$	
14	35	123·0	0·494 (Assumed from K_D of Products)	834	0·148	29 000 (Assumed from M.W. of Products)
13	105	119·4	"	820	0·146	"
12	175	126·2	"	837	0·151	"
17	245	117·9	"	829	0·142	"
1	315	118·2	"	840	0·141	"
15	385	47·8	"	828	0·0577	"
8	455	23·5	"	855	0·0275	"
7	525	4·9	"	836	0·0059	"
6	595	1·9	"	830	0·0023	"
19	665	0·8	"	827	0·0010	"

Figure A.4.16 Details of Concentration and M.W. Profile for Run 01-600-0·7

Column No.	Distance of Column Mid-point from Product 1 Outlet	Weight of Dextran in Column (W)	Mean K_D of Dextran(Analysis on Porasil C)	Volume of Water Accessible to Dextran in Column ($V_o + V_i K_D$)	Concentration of Dextran ($\frac{W}{V_o + V_i K_D}$)	Mean M.W. of Dextran
	cm	g		cm^3	$g\ cm^{-3}$	
14	35	6·29	0·445	810	0·00776	34 000
13	105	7·38	0·443	790	0·00934	35 000
12	175	7·79	0·450	811	0·00960	33 000
17	245	7·90	0·470	814	0·00970	31 000
1	315	7·63	0·515	853	0·00894	25 500
15	385	5·53	0·510	835	0·00662	26 000
8	455	5·47	0·570	902	0·00606	20 000
7	525	3·67	0·595	893	0·00412	18 000
6	595	0·428	0·610	900	0·00048	17 000
19	665	0·0	——	——	0·0	——

APPENDIX 5

Listing of Computer Programs

Figure A.5.1 Listing of PROGRAM 1 — Calculation of 2nd, 3rd, and 4th Moments

Language-BASIC

```
10  DIM H(100)
20  INPUT N,I1,I,M
30  FOR J=1 TO N
40  INPUT H(J)
50  NEXT J
60  S=0
70  S1=0
80  S2=0
90  S3=0
100 S4=0
110 FOR J=1 TO N
120 S=S+H(J)
130 S1=S1+(H(J)*I*J)
140 NEXT J
150 M1=S1/S
160 FOR J=1 TO N
170 S2=S2+H(J)*(((I*J)-M1)↑2)
180 S3=S3+H(J)*(((I*J)-M1)↑3)
190 S4=S4+H(J)*(((I*J)-M1)↑4)
200 NEXT J
210 V3=S2/S
220 D3=SQR(V3)
250 M3=(S3/S)/(D3↑3)
260 M4=((S4/S)/(D3↑4))-3
270 PRINT TAB(8),"SAMPLE NO.=",M
280 PRINT TAB(8),"MEAN TIME=",M1,"MIN"
290 PRINT TAB(8),"2ND MOMENT (VARIANCE)=",V3,"MIN↑2"
300 PRINT TAB(8),"S.D.=",D3,"MIN"
310 PRINT TAB(8),"3RD MOMENT(SKEW)=",M3
320 PRINT TAB(8),"4TH MOMENT(KURTOSIS)=",M4
330 STOP
340 END
```

Figure A.5.2 Listing of PROGRAM 2 — Calculation of H.E.T.P.

Language – BASIC

```
10  DIM A(100)
20  INPUT M,C,F,I1,I,V1,V2,M1,L,N
30  FOR J=1 TO N
40  INPUT A(J)
50  NEXT J
60  S=0
70  S1=0
80  S2=0
90  S3=0
100 S4=0
110 FOR J=1 TO N
120 S=S+A(J)
130 S1=S1+(A(J)*I*J)
140 NEXT J
150 M1=S1/S
160 FOR J=1 TO N
170 S2=S2+A(J)*(((I*J)-M1)↑2)
180 S3=S3+A(J)*((I*J-M1)↑3)
190 S4=S4+A(J)*((I*J-M1)↑4)
200 NEXT J
210 V3=S2/S
220 D3=SQR(V3)
230 V=V3-V2-V1
240 D=SQR(V)
250 M3=(S3/S)/(D3↑3)
260 M4=((S4/S)/(D3↑4))-3
270 I2=I1+M1
280 E2=I2*F
290 N1=8*((I2/W1)↑2)
300 N2=((I2↑2)/V3)
310 N3=((I2↑2)/V)
320 H1=L/N1
330 H2=L/N2
340 H3=L/N3
350 PRINT TAB(8),"SAMPLE NO.=",M
360 PRINT TAB(8),"COLUMN NO.=",C
370 PRINT TAB(8),"FLOW=",F,"CM↑3/MIN."
380 PRINT TAB(8),"V2=",V2,"MIN↑2"
390 PRINT TAB(8),"V1=",V1,"MIN↑2"
400 PRINT TAB(8),"M1=",M1,"MIN"
410 PRINT TAB(8),"I2=",I2,"MIN"
420 PRINT TAB(8),"E2=",E2,"CM↑3"
430 PRINT TAB(8),"V3=",V3,"MIN↑2"
440 PRINT TAB(8),"V=",V,"MIN↑2"
450 PRINT TAB(8),"D3=",D3,"MIN"
460 PRINT TAB(8),"D=",D,"MIN"
470 PRINT TAB(8),"M3(SKEW)=",M3
480 PRINT TAB(8),"M4(KURTOSIS)=",M4
490 PRINT TAB(8),"N.T.P.1=",N1
500 PRINT TAB(8),"N.T.P.2=",N2
510 PRINT TAB(8),"N.T.P.3=",N3
520 PRINT TAB(8),"HETP1=",H1,"CM"
530 PRINT TAB(8),"HETP2=",H2,"CM"
540 PRINT TAB(8),"HETP3=",H3,"CM"
550 STOP
560 END
```

FIG. A.5.3 List of Symbols for PROGRAMS 1 and 2

C	Column number
D	Corrected sample standard deviation
D_3	Total measured standard deviation
E_2	Average elution volume of sample
F	Mobile phase flowrate
H(J)	Height of data points
J=1-N	
H_1	H.E.T.P. calculated from N_1
H_2	H.E.T.P. calculated from N_2
H_3	H.E.T.P. calculated from N_3
L	Column length
M	Sample number
M_1	Mean time of sample
M_3	3rd moment (skew)
M_4	4th moment (kurtosis)
N	Number of data points
N_1	N.T.P. based on the assumption of a Gaussian peak shape
N_2	N.T.P. based on the total measured sample variance
N_3	N.T.P. based on the sample variance produced by the column alone
S and $S_1 \rightarrow S_4$	Summation terms used in calculations
T	Time interval between data points
T_1	Time to first data point
T_2	Average elution time of sample
V	Sample variance produced by column alone
V_1	Sample variance produced by detection system
V_2	Variance of injected sample at column inlet
V_3	Total measured sample variance

Figure A.5.4 Listing of PROGRAM 3 — SCCR3 Computer Simulation (9 Components)

Language – FORTRAN 4

```
      PRØGRAM PLATES2(INPUT,ØUTPUT,TAPE1=INPUT,TAPE2=ØUTPUT)
      DIMENSIØN CR(1500),CS(1500),CT(1500),CU(1500),CV(1500),CW(1500),CX
     1(1500),CY(1500),CZ(1500),AR(150),AS(150),AT(150),AU(150),AV(150),A
     2W(150),AX(150),AY(150),AZ(150)
      REAL KD1,KD2,KD3,KD4,KD5,KD6,KD7,KD8,KD9
      DØ 1 NN=1,1500
      CR(NN)=0.0
      CS(NN)=0.0
      CT(NN)=0.0
      CU(NN)=0.0
      CV(NN)=0.0
      CW(NN)=0.0
      CX(NN)=0.0
      CY(NN)=0.0
      CZ(NN)=0.0
    1 CØNTINUE
      DØ 2 NN=1,150
      AR(NN)=0.0
      AS(NN)=0.0
      AT(NN)=0.0
      AU(NN)=0.0
      AV(NN)=0.0
      AW(NN)=0.0
      AX(NN)=0.0
      AY(NN)=0.0
      AZ(NN)=0.0
    2 CØNTINUE
      READ(1,3)CFLØW,FFLØW,SFLØW,V1,V2,DT
      READ(1,111)CRFEED,CSFEED,CTFEED,CUFEED,CVFEED,CWFEED,CXFEED,CYFEED
     1,CZFEED
      READ(1,4) NFEED,NNBED,KTØTAL,KKINK,KKTYPE,NNTYPE
      READ(1,5)KD1,KD2,KD3,KD4,KD5,KD6,KD7,KD8,KD9
      WRITE(2,7)CFLØW,SFLØW,FFLØW,V1,V2
      WRITE(2,8)CRFEED,CSFEED,CTFEED,CUFEED,CVFEED
      WRITE(2,81)CWFEED,CXFEED,CYFEED,CZFEED,DT
      WRITE(2,9)NFEED,NNBED,KTØTAL,KKINK,KKTYPE,NNTYPE
      WRITE(2,11)KD1,KD2,KD3,KD4,KD5
      WRITE(2,110)KD6,KD7,KD8,KD9
      NNTØT=NNBED*10
      NNNINE=NNBED*9+1
      NNFEED=(NFEED-1)*NNBED+1
      WRITE(2,12)
      KKSUM=1
      DØ 100 K=1,KTØTAL
      ISTKK=KKINK*(K-1)+1
      LSTKK=KKINK*K
      DØ 200 KK=ISTKK,LSTKK
      NNSUM=1
      DØ 300 N=1,10
      IF(N.LE.5)CFLØWC=CFLØW
      IF(N.GE.6)CFLØWC=CFLØW+FFLØW
      IF(N.LE.(NFEED-K))GØ TØ 500
      NNFST=NNBED*(N-1)+1
      NNLST=NNBED*N
      DØ 400 NN=NNFST,NNLST
      IF(N.EQ.1)GØ TØ 80
      IF((N.EQ.2).AND.(NN.EQ.NNFST)) GØ TØ 40
```

Figure A.5.4 (contd.)

```
      IF(NN.EQ.NNFEED)GO TO 50
      CRINPUT=0.0
      CSINPUT=0.0
      CTINPUT=0.0
      CUINPUT=0.0
      CVINPUT=0.0
      CWINPUT=0.0
      CXINPUT=0.0
      CYINPUT=0.0
      CZINPUT=0.0
      GO TO 60
   40 CR(NN-1)=0.0
      CS(NN-1)=0.0
      CT(NN-1)=0.0
      CU(NN-1)=0.0
      CV(NN-1)=0.0
      CW(NN-1)=0.0
      CX(NN-1)=0.0
      CY(NN-1)=0.0
      CZ(NN-1)=0.0
      GO TO 70
   50 CRINPUT=CRFEED
      CSINPUT=CSFEED
      CTINPUT=CTFEED
      CUINPUT=CUFEED
      CVINPUT=CVFEED
      CWINPUT=CWFEED
      CXINPUT=CXFEED
      CYINPUT=CYFEED
      CZINPUT=CZFEED
   60 IF(CR(NN-1).LT.0.1E-10)CR(NN-1)=0.0
      IF(CS(NN-1).LT.0.1E-10)CS(NN-1)=0.0
      IF(CT(NN-1).LT.0.1E-10)CT(NN-1)=0.0
      IF(CU(NN-1).LT.0.1E-10)CU(NN-1)=0.0
      IF(CV(NN-1).LT.0.1E-10)CV(NN-1)=0.0
      IF(CW(NN-1).LT.0.1E-10)CW(NN-1)=0.0
      IF(CX(NN-1).LT.0.1E-10)CX(NN-1)=0.0
      IF(CY(NN-1).LT.0.1E-10)CY(NN-1)=0.0
      IF(CZ(NN-1).LT.0.1E-10)CZ(NN-1)=0.0
   70 A=CFLOWC*DT
      RR=EXP(-A/(V1+V2*KD1))
      SS=EXP(-A/(V1+V2*KD2))
      TT=EXP(-A/(V1+V2*KD3))
      UU=EXP(-A/(V1+V2*KD4))
      VV=EXP(-A/(V1+V2*KD5))
      WW=EXP(-A/(V1+V2*KD6))
      XX=EXP(-A/(V1+V2*KD7))
      YY=EXP(-A/(V1+V2*KD8))
      ZZ=EXP(-A/(V1+V2*KD9))
      CR(NN)=(1.-RR)*(CR(NN-1)+CRINPUT)+RR*CR(NN)
      CS(NN)=(1.-SS)*(CS(NN-1)+CSINPUT)+SS*CS(NN)
      CT(NN)=(1.-TT)*(CT(NN-1)+CTINPUT)+TT*CT(NN)
      CU(NN)=(1.-UU)*(CU(NN-1)+CUINPUT)+UU*CU(NN)
      CV(NN)=(1.-VV)*(CV(NN-1)+CVINPUT)+VV*CV(NN)
      CW(NN)=(1.-WW)*(CW(NN-1)+CWINPUT)+WW*CW(NN)
      CX(NN)=(1.-XX)*(CX(NN-1)+CXINPUT)+XX*CX(NN)
      CY(NN)=(1.-YY)*(CY(NN-1)+CYINPUT)+YY*CY(NN)
```

Figure A.5.4 (contd.)

```
      CZ(NN)=(1.-ZZ)*(CZ(NN-1)+CZINPUT)+ZZ*CZ(NN)
      GØ TØ 150
   80 IF(NN.EQ.NNFST)GØ TØ 90
      IF(CR(NN-1).LT.0.1E-10)CR(NN-1)=0.0
      IF(CS(NN-1).LT.0.1E-10)CS(NN-1)=0.0
      IF(CT(NN-1).LT.0.1E-10)CT(NN-1)=0.0
      IF(CU(NN-1).LT.0.1E-10)CU(NN-1)=0.0
      IF(CV(NN-1).LT.0.1E-10)CV(NN-1)=0.0
      IF(CW(NN-1).LT.0.1E-10)CW(NN-1)=0.0
      IF(CX(NN-1).LT.0.1E-10)CX(NN-1)=0.0
      IF(CY(NN-1).LT.0.1E-10)CY(NN-1)=0.0
      IF(CZ(NN-1).LT.0.1E-10)CZ(NN-1)=0.0
      GØ TØ 95
   90 CR(NN-1)=0.0
      CS(NN-1)=0.0
      CT(NN-1)=0.0
      CU(NN-1)=0.0
      CV(NN-1)=0.0
      CW(NN-1)=0.0
      CX(NN-1)=0.0
      CY(NN-1)=0.0
      CZ(NN-1)=0.0
   95 A=SFLØW*DT
      RR=EXP(-A/(V1+V2*KD1))
      SS=EXP(-A/(V1+V2*KD2))
      TT=EXP(-A/(V1+V2*KD3))
      UU=EXP(-A/(V1+V2*KD4))
      VV=EXP(-A/(V1+V2*KD5))
      WW=EXP(-A/(V1+V2*KD6))
      XX=EXP(-A/(V1+V2*KD7))
      YY=EXP(-A/(V1+V2*KD8))
      ZZ=EXP(-A/(V1+V2*KD9))
      CR(NN)=(1.-RR)*(CR(NN-1)+CRINPUT)+RR*CR(NN)
      CS(NN)=(1.-SS)*(CS(NN-1)+CSINPUT)+SS*CS(NN)
      CT(NN)=(1.-TT)*(CT(NN-1)+CTINPUT)+TT*CT(NN)
      CU(NN)=(1.-UU)*(CU(NN-1)+CUINPUT)+UU*CU(NN)
      CV(NN)=(1.-VV)*(CV(NN-1)+CVINPUT)+VV*CV(NN)
      CW(NN)=(1.-WW)*(CW(NN-1)+CWINPUT)+WW*CW(NN)
      CX(NN)=(1.-XX)*(CX(NN-1)+CXINPUT)+XX*CX(NN)
      CY(NN)=(1.-YY)*(CY(NN-1)+CYINPUT)+YY*CY(NN)
      CZ(NN)=(1.-ZZ)*(CZ(NN-1)+CZINPUT)+ZZ*CZ(NN)
  150 IF((NN.EQ.(NNTYPE*NNSUM)).AND.(KK.EQ.(KKTYPE*KKSUM)))GØ TØ 160
      GØ TØ 170
  160 WRITE(2,161)K,KK,N,NN,CR(NN),CS(NN),CT(NN),CU(NN),CV(NN),CW(NN),CX
     1(NN),CY(NN),CZ(NN)
  170 IF(NN.EQ.(NNTYPE*NNSUM))NNSUM=NNSUM+1
  400 CØNTINUE
      GØ TØ 300
  500 NNSUM=NNSUM+NNBED/NNTYPE
  300 CØNTINUE
      IF(KK.EQ.(KKTYPE*KKSUM)) GØ TØ 180
      GØ TØ 200
  180 KKSUM=KKSUM+1
      WRITE(2,185)
  200 CØNTINUE
      WRITE(2,190)
      WRITE(2,12)
```

Figure A.5.4 (contd.)

```
      DØ 1500 NN=1,NNBED
      AR(NN)=CR(NN)
      AS(NN)=CS(NN)
      AT(NN)=CT(NN)
      AU(NN)=CU(NN)
      AV(NN)=CV(NN)
      AW(NN)=CW(NN)
      AX(NN)=CX(NN)
      AY(NN)=CY(NN)
      AZ(NN)=CZ(NN)
 1500 CØNTINUE
      DØ 2000 NN=1,NNTØT
      IF(NN.GE.NNNINE)GØ TØ 2010
      NNADJ=NN+NNBED
      CR(NN)=CR(NNADJ)
      CS(NN)=CS(NNADJ)
      CT(NN)=CT(NNADJ)
      CU(NN)=CU(NNADJ)
      CV(NN)=CV(NNADJ)
      CW(NN)=CW(NNADJ)
      CX(NN)=CX(NNADJ)
      CY(NN)=CY(NNADJ)
      CZ(NN)=CZ(NNADJ)
      GØ TØ 2000
 2010 NNADJ=NN+1-NNNINE
      CR(NN)=AR(NNADJ)
      CS(NN)=AS(NNADJ)
      CT(NN)=AT(NNADJ)
      CU(NN)=AU(NNADJ)
      CV(NN)=AV(NNADJ)
      CW(NN)=AW(NNADJ)
      CX(NN)=AX(NNADJ)
      CY(NN)=AY(NNADJ)
      CZ(NN)=AZ(NNADJ)
 2000 CØNTINUE
  100 CØNTINUE
    3 FØRMAT(6F10.5)
    4 FØRMAT(6I4)
    5 FØRMAT(9F8.4)
    7 FØRMAT(1H ,7HCFLØW= ,F8.3,4X,7HSFLØW= ,F8.3,4X,7HFFLØW= ,F8.3,4X,4
     1HV1= ,F10.5,4X,4HV2= ,F10.5)
    8 FØRMAT(1H ,8HCRFEED= ,E13.6,4X,8HCSFEED= ,E13.6,4X,8HCTFEED= ,E13.
     16,4X,8HCUFFED= ,E13.6,4X,8HCVFEED= ,E13.6)
   81 FØRMAT(1H ,8HCWFEED= ,E13.6,4X,8HCXFEED= ,E13.6,4X,8HCYFEED= ,E13.
     16,4X,8HCZFEED= ,E13.6,4X,4HDT= ,F10.5)
    9 FØRMAT(1H ,7HNFEED= ,I2,1X,7HNNBED= ,I3,1X,8HKTØTAL= ,I3,1X,7HKKIN
     1K= ,I4,1X,8HKKTYPE= ,I3,1X,8HNNTYPE= ,I3)
   11 FØRMAT(1H ,5HKD1= ,E13.6,4X,5HKD2= ,F13.6,4X,5HKD3= ,E13.6,4X,5HKD
     14= ,F13.6,4X,5HKD5= ,E13.6)
  110 FØRMAT(1H ,5HKD6= ,E13.6,4X,5HKD7= ,E13.6,4X,5HKD8= ,E13.6,4X,5HKD
     19= ,E13.6)
  111 FØRMAT(9F8.6)
   12 FØRMAT(1H ,2H K,2X,4H  KK,2X,2H N,2X,4H  NN,2X,9H  CR(NN) ,2X,9H
     1CS(NN) ,2X,9H  CT(NN) ,2X,9H  CU(NN) ,2X,9H  CV(NN) ,2X,9H  CW(NN)
     2 ,2X,9H  CX(NN) ,2X,9H  CY(NN) ,2X,9H  CZ(NN) )
  161 FØRMAT(1H ,I2,2X,I5,2X,I2,2X,I4,2X,E9.3,2X,E9.3,2X,E9.3,2X,E9.3,2X
     1,E9.3,2X,E9.3,2X,E9.3,2X,E9.3,2X,E9.3)
  185 FØRMAT(1H ,32HNEXT TIME INTERVAL FØR PRINT ØUT)
  190 FØRMAT(1H ,23HNEXT SWITCHING INTERVAL)
      END
```

Figure A.5.5 Example of Print-Out for PROGRAM 3

K	KK	N	NN	CR(NN)	CS(NN)	CT(NN)	CU(NN)	CV(NN)	CW(NN)	CX(NN)	CY(NN)	CZ(NN)
56	28067	1	10	0.	0.	0.	0.	0.	0.	0.	0.	0.
56	28067	1	20	0.	0.	0.	0.	0.	0.	0.	0.	0.
56	28067	1	30	0.	0.	0.	0.	0.	0.	0.	0.	0.
56	28067	1	40	0.	0.	0.	0.	0.	0.	0.	0.	0.
56	28067	2	50	0.	0.	0.	0.	0.	0.	0.	.373E-09	.729E-09
56	28067	2	60	0.	0.	0.	0.	0.	0.	.746E-07	.518E-04	.107E-04
56	28067	2	70	0.	0.	0.	0.	0.	0.	.466E-06	.160E-03	.203E-04
56	28067	2	80	0.	0.	0.	0.	0.	0.	.129E-05	.224E-03	.211E-04
56	28067	3	90	0.	0.	0.	0.	0.	0.	.313E-05	.280E-03	.211E-04
56	28067	3	100	0.	0.	0.	0.	0.	0.	.718E-05	.333E-03	.212E-04
56	28067	3	110	0.	0.	0.	0.	0.	.257E-10	.159E-04	.386E-03	.212E-04
56	28067	3	120	0.	0.	0.	0.	0.	.873E-09	.340E-04	.436E-03	.212E-04
56	28067	4	130	0.	0.	0.	0.	0.	.809E-08	.706E-04	.481E-03	.212E-04
56	28067	4	140	0.	0.	0.	0.	0.	.696E-07	.142E-03	.521E-03	.212E-04
56	28067	4	150	0.	0.	0.	.183E-09	.766E-09	.594E-06	.280E-03	.555E-03	.212E-04
56	28067	4	160	0.	0.	.665E-09	.729E-07	.432E-07	.506E-05	.536E-03	.583E-03	.212E-04
56	28067	5	170	.191E-06	.139E-05	.111E-04	.555E-04	.225E-05	.431E-04	.100E-02	.605E-03	.212E-04
56	28067	5	180	.876E-05	.358E-04	.136E-03	.400E-03	.160E-03	.406E-03	.186E-02	.626E-03	.216E-04
56	28067	5	190	.158E-04	.533E-04	.191E-03	.620E-03	.778E-03	.128E-02	.290E-02	.582E-03	.182E-04
56	28067	5	200	.169E-04	.633E-04	.264E-03	.873E-03	.128E-02	.208E-02	.369E-02	.461E-03	.124E-04
56	28067	6	210	.363E-04	.134E-03	.485E-03	.143E-02	.180E-02	.285E-02	.414E-02	.310E-03	.637E-05
56	28067	6	220	.337E-04	.119E-03	.431E-03	.133E-02	.264E-02	.369E-02	.421E-02	.178E-03	.287E-05
56	28067	6	230	.315E-04	.117E-03	.449E-03	.136E-02	.254E-02	.362E-02	.374E-02	.655E-04	.226E-06
56	28067	6	240	.338E-04	.124E-03	.450E-03	.135E-02	.255E-02	.363E-02	.327E-02	.246E-04	.200E-07
56	28067	7	250	.344E-04	.122E-03	.446E-03	.135E-02	.255E-02	.363E-02	.280E-02	.918E-05	.130E-08
56	28067	7	260	.333E-04	.120E-03	.448E-03	.135E-02	.255E-02	.363E-02	.234E-02	.338E-05	0.
56	28067	7	270	.330E-04	.122E-03	.448E-03	.135E-02	.255E-02	.363E-02	.191E-02	.123E-05	0.
56	28067	7	280	.336E-04	.122E-03	.448E-03	.135E-02	.255E-02	.363E-02	.152E-02	.441E-06	0.
56	28067	8	290	.337E-04	.121E-03	.448E-03	.135E-02	.255E-02	.363E-02	.117E-02	.155E-06	0.
56	28067	8	300	.334E-04	.121E-03	.448E-03	.135E-02	.255E-02	.363E-02	.884E-03	.530E-07	0.
56	28067	8	310	.333E-04	.122E-03	.448E-03	.135E-02	.255E-02	.362E-02	.647E-03	.173E-07	0.
56	28067	8	320	.335E-04	.121E-03	.448E-03	.135E-02	.255E-02	.362E-02	.459E-03	.501E-08	0.
56	28067	9	330	.335E-04	.121E-03	.448E-03	.135E-02	.255E-02	.361E-02	.316E-03	.876E-09	0.
56	28067	9	340	.334E-04	.121E-03	.448E-03	.135E-02	.255E-02	.359E-02	.211E-03	0.	0.
56	28067	9	350	.334E-04	.121E-03	.448E-03	.135E-02	.255E-02	.356E-02	.137E-03	0.	0.
56	28067	9	360	.335E-04	.121E-03	.448E-03	.135E-02	.255E-02	.351E-02	.845E-04	0.	0.
56	28067	10	370	.331E-04	.118E-03	.416E-03	.116E-02	.254E-02	.332E-02	.473E-04	0.	0.
56	28067	10	380	.151E-04	.379E-04	.705E-04	.975E-04	.187E-02	.183E-02	.137E-04	0.	0.
56	28067	10	390	.657E-06	.835E-06	.554E-06	.291E-06	.777E-04	.365E-04	.126E-06	0.	0.
56	28067	10	400	.288E-08	.170E-08	.337E-09	.353E-10	0.	0.	0.	0.	0.

FIG. A.5.6 List of Symbols for Program 3

C_i FEED, i = R-Z	On-column feed inlet concentration of component ($g\ cm^{-3}$)
C_i(NN), i = R-Z	Component concentration on n^{th} plate ($g\ cm^{-3}$)
CFLOW	Mobile phase flowrate ($cm^3\ s^{-1}$)
CFLOWC	(Mobile phase + feed) flowrate ($cm^3\ s^{-1}$)
DT	Length of time increment (s)
FFLOW	Feed flowrate ($cm^3\ s^{-1}$)
IST KK	First time increment in sequencing interval
LST KK	Last time increment in sequencing interval
K	Counter for number of sequencing intervals
KK	Counter for number of time increments
KD_i, i = 1-9	Distribution coefficient of component
KKINK	Number of time increments within a sequencing interval
KKTYPE	Number of time increments between print-outs
KKSUM	Time increment counter used for print-out condition
N	Counter for number of columns
NN	Counter for number of plates
NFEED	Number of feed column
NNFEED	Number of feed plate
NNBED	Total number of plates per column
NNBED1	First plate in separating section
NNFST	First plate in a column
NNLST	Last plate in a column
NNSUM	Counter used for plate print-out condition
NNTOT	Number of final plate in separating section, or total number of plates

NNTYPE	Number of plates between print-outs
NNNINE	First plate in last column of separating section
SFLOW	Purge flowrate ($cm^3\ s^{-1}$)
V_1	Mobile phase volume per plate (cm^3)
V_2	Stationary phase volume per plate (cm^3)

NOMENCLATURE

A	Term accounting for eddy diffusion in chromatographic theoretical plate height equation
A_c	Collection rate of component A at the top of a continuous moving-bed chromatographic column
A_1	Surface area of a molecule in theoretical treatment of g.p.c. process
A'	Column cross-sectional area
a_1-a_5	Constants in chromatographic theoretical plate height equation
a_r	Stokes radius of a molecule
B	Term accounting for longitudinal diffusion in chromatographic theoretical plate height equation
B_c	Collection rate of component B at the top of a continuous moving-bed chromatographic column
b	Used to represent several constant powers in models of g.p.c. process
C_s	Term accounting for stationary phase resistance to mass transfer in chromatographic theoretical plate height equation
C_m	Term accounting for mobile phase resistance to mass transfer in chromatographic theoretical plate height equation
C_p	Permeation constant in theoretical g.p.c. plate height equation
c	Solute concentration in the mobile phase
D	Diffusion coefficient
D'	Constant in semi-empirical plate height equation

D_m	Mobile phase molecular diffusivity
D_r	Radial diffusion coefficient
D_S	Stationary phase molecular diffusivity
d	Thickness of stationary phase liquid film
d_c	Column internal diameter
d_p	Mean particle diameter
E	Eddy diffusivity
E_p	Production rate of a component in theoretical equation for co-current operation of a chromatographic column
F_m	Mobile phase volumetric flowrate
F'_M	Fractional volume of mobile phase in chromatographic column
F'_S	Fractional volume of stationary phase in chromatographic column
g	Constant in theoretical model of g.p.c. process
G_o	Mass velocity of a fluid
G_2	Constant in chromatographic theoretical plate height equation for large diameter columns
H	Height equivalent to a (chromatographic) theoretical plate (H.E.T.P.)
H_c	Contribution to H in large diameter columns caused by non-uniformity of the velocity profile
H'	Intrinsic plate height for packing, i.e. value obtained for small diameter columns
H'_C	Plate height for a large diameter column without mixing devices
H'_{CN}	Plate height for a large diameter column with mixing devices
H.E.T.P.1	H.E.T.P. calculated assuming a Gaussian peak
H.E.T.P.2	H.E.T.P. calculated from the total measured peak variance

H.E.T.P.3 — H.E.T.P. calculated from peak variance caused by chromatographic column alone

h — Reduced plate height = H/d_p

h' — Velocity profile constant in chromatographic theoretical plate height equation

K — Partition coefficient of solute between mobile and stationary phases

K_D — Equilibrium distribution coefficient of solute between mobile and stationary phases, used for g.p.c.

K_{GPC} — Distribution coefficient of solute between mobile and stationary phases measured by g.p.c. analysis

$K_{D\infty}$ — Distribution coefficient at infinite dilution

ΔK_D — Change in value of $K_{D\infty}$ with increasing solute concentration

K_{AV} — Alternative distribution coefficient used in g.p.c. $= K_D \dfrac{V_i}{V_i + V_{GM}}$

$(K_{AV})_M$ — Available volume for solute molecule in mobile phase

$(K_{AV})_G$ — Available volume for solute molecule in gel phase

K' — Dimensionless flow profile factor in chromatographic plate height equation incorporating column diameter

K'' — Kozeny's constant

k — Average K value of two components $= \dfrac{{}^1/_2(V_{R_1} + V_{R_2}) - V_M}{V_M}$

k_f — Solute exchange rate between mobile and stationary phases in chromatographic theoretical plate height equation

k' — Capacity ratio = $K F_S'/F_M'$

k'' — Rate constant of desorption in probabilistic model of moving-bed chromatographic column

k_1 — Constant factor in relationship between intrinsic viscosity and M.W.

L	SCCR3 mobile phase volumetric flowrate
L_M	Distance migrated by the centre of a component zone
L_1	SCCR3 mobile phase volumetric flowrate in pre-feed section
L_2	SCCR3 feed volumetric flowrate
L_3	SCCR3 mobile phase volumetric flowrate in post-feed section
L_4	SCCR3 purge volumetric flowrate through isolated section
L'	Effective SCCR3 mobile phase flowrate
L'_1	SCCR3 effective mobile phase volumetric flowrate in pre-feed section
L'_3	SCCR3 effective mobile phase volumetric flowrate in post-feed section
L_d	Transition length, or minimum theoretical length of column required for attainment of lateral equilibrium $= d_c^2 u/8D_m$
$\overline{L}$	Mean external length of a molecule
L''	Concentration of dextran chains forming gel matrix in g.p.c., expressed as cm. rod cm^{-3}
ℓ	Column length
ℓ'	Root mean square step length in random walk model
ℓ_t	Length of tube section in separation by flow model of g.p.c. process
M_A	Mass flowrate of solute leaving the column in the product A stream, in H.T.U. model of the counter-current g.l.c. process
M_B	Mass flowrate of solute leaving the column in the product B stream, in H.T.U. model of the counter-current g.l.c. process

M_f	Average, or component, M.W. of feed in chromatographic production rate equation
m	Total mass of component in sample
Δ_m	Mass of component discarded during fraction cutting
$\overline{M_n}$	Number average M.W.
$\overline{M_w}$	Weight average M.W.
$\overline{M_z}$	Z average M.W.
$\overline{M_v}$	Viscosity average M.W.
$M_{0.5}$	M.W. corresponding to half-area point of sample distribution
$(N_{OG})_R$	Number of overall gas phase transfer units in the rectifying section, in H.T.U. model of the counter-current g.l.c. process
$(N_{OG})_S$	Number of overall gas phase transfer units in the stripping section, in H.T.U. model of the counter-current g.l.c. process
N	Number of theoretical co-current chromatographic plates, or stages, within a column (N.T.P.)
N_{CC}	Number of theoretical counter-current plates or stages within a column
N_f	Number of theoretical co-current chromatographic plates occupied by feed inlet solute band
N_{EFF}	Effective number of co-current chromatographic theoretical plates within a column = $(\frac{k'}{1 + k'})^2 N$
N_{REQ}	Number of co-current chromatographic theoretical plates required to exactly separate two peak centres by 6σ
N_{REQ}^*	Apparent number of co-current chromatographic theoretical plates required to exactly separate two peak centres by 6σ

N_{MIN}	Minimum number of co-current chromatographic theoretical plates required to achieve a separation
N_1	Number of co-current chromatographic theoretical plates corresponding to H.E.T.P.1
N_2	Number of co-current chromatographic theoretical plates corresponding to H.E.T.P.2
N_3	Number of co-current chromatographic theoretical plates corresponding to H.E.T.P.3
n	Reduced value of N, $= \frac{N \left(\frac{\alpha-1}{\alpha+1}\right)^2 \left(\frac{k}{1+k}\right)^2}{9}$, used in equations describing chromatographic operational modes
n_f	Reduced value of N_f
n_t	Number of tube sections in separation by flow model of g.p.c. process
n'	Number of steps in random walk model
n_1	No. of mixing devices in theoretical plate ht. equation for gain in efficiency by using mixing devices
P	Effective SCCR3 stationary phase flowrate
ΔP	Pressure drop
p	Used to represent various constants in models of g.p.c. process
p_f	Total, or component, partial pressure of feed input before column inlet
P_L, P_S	Probability that a molecule will travel through a large or small tube in separation by flow model of g.p.c. process
p'	Peak elution position of a component
Q	Production rate of a component by chromatography
Q_f	Mobile phase volumetric flowrate

Q_G Gas phase volumetric flowrate in g.l.c.

Q_L Liquid phase volumetric flowrate in g.l.c.

Q_f Total mobile phase volumetric flowrate

Q' Packing geometry factor

q Solute concentration in stationary phase

q' Configuration factor dependent on shape of stationary phase layer

R Relative solute band migration rate

Re Reynolds No. for packed column = $(d_p u\rho/\mu)\left(\frac{\varepsilon}{1-\varepsilon}\right)$

R_s Resolution = $\frac{(t_{R_2} - t_{R_1})}{1/2(W_1 + W_2)}$

R.F. Retention factor = Elution volume/Total bed volume

R' Gas constant

R'_s Radius of solid micro-spheres in model of Porasil structure

r Internal radius of column

r_c Radius of cylinder in separation by flow model of g.p.c.

r_g Radius of gyration of molecule

r_p Pore radius in model of g.p.c. packing

$\bar{r}$ Effective molecular radius

$\psi(\bar{r})$ Void fraction of packing available to molecule of radius $\bar{r}$

r' Effective radius of dextran chains in model of dextran gels

r_{mi} Rate of movement of component with mobile phase in SCCR3 machine

r_{si} Rate of movement of component with stationary phase in SCCR3 machine

r_l Rate of transfer of molecules from gas to liquid in random walk model of continuous counter-current g.l.c.

r_2	Rate of transfer of molecules from liquid to gas in random walk model of continuous counter-current g.l.c.
S	Sequencing interval of the SCCR3 unit
S_p	Specific surface area of a particle
S'	Slope of log M.W. vs peak elution volume g.p.c. calibration curve
T	Temperature
t	Time
t_d	Diffusion time
t_d'	Mean desorption time
t_o	Elution, or retention, time of unretained component
t_R	Elution, or retention, time of component
u	Average interstitial mobile phase velocity
u_L	Stationary phase velocity in continuous chromatography
u_m	Molar velocity of mobile phase
$(u_z)_A$	Bottoms/feed mass flowrate ratio of component A in probabilistic model of moving-bed chromatographic column
$(u_z)_B$	Tops/feed mass flowrate ratio of component B in probabilistic model of moving-bed chromatographic column
$\bar{u}$	Compressibility-corrected mobile phase velocity
$\langle u_p \rangle$	Mean particle velocity in separation by flow model of g.p.c. process
$\langle u \rangle$	Mean solvent velocity in separation by flow model of g.p.c. process
V_{GM}	Volume of gel matrix in a g.p.c. column
V_i	Gel internal, or pore, volume in a g.p.c. column
$V_{i_{ACC}}$	Gel internal, or pore volume, accessible to a solute in a g.p.c. column

$(V_{i_{ACC\ M}})$	Volume of mobile phase accessible to a solute in a g.p.c. column
$(V_{i_{ACC\ S}})$	Volume of stationary phase (pores) accessible to a solute in a g.p.c. column
$(V_i)_M$	Volume of mobile phase in a g.p.c. column
$(V_i)_S$	Volume of stationary phase (pores) in a g.p.c. column
V'_L, V'_S	Volume of large and small tubes in separation by flow model of g.p.c. process
V_M	Volume of mobile phase in column
$V_{m_{AV}}$	Effective average velocity of SCCR3 mobile phase = L'/A_o
V_o	Interstitial volume of packed column
V_R	Elution, or retention, volume of component
$\overline{V_R}$	Average elution volume used in separation by flow model of g.p.c. process
V_S	Volume of stationary phase in column
$V_{S_{AV}}$	Effective average velocity of SCCR3 stationary phase = P/A_i
V_t	Total column volume
V_1	Volume of mobile phase on a plate in the plate model of a chromatographic column
V_2	Volume of stationary phase on a plate in the plate model of a chromatographic column
W	Characteristic baseline width of a single solute chromatographic peak
W'_A	Feed rate of component A to a continuous moving-bed chromatographic column
W'_B	Feed rate of component B to a continuous moving-bed chromatographic column

$w, w_\alpha, w_\beta, w_\lambda$	Factors used in chromatographic theoretical plate height equation to allow for non-uniformity of velocity profile and packing structure
$w_{h'/e}$	Peak width at 1/e of peak height, used to calculate N_1
w_{to}	Total chromatogram width/sample at column outlet in production equation for co-current chromatographic operation
x	Concentration of feed in mobile phase during injection for co-current chromatographic production equation
x_i	Weight fraction
y_1	Gas phase solute concentration at point 1 in H.T.U. model of the counter-current g.l.c. process
y_2	Gas phase solute concentration at point 2 in H.T.U. model of the counter-current g.l.c. process
α	Separation factor = K_2/K_1.
α'	Packing geometry constant in chromatographic plate height equation for large diameter columns
γ	Coefficient to allow for polymer M.W. distribution
γ'	Labyrinth factor
$\delta_i, \delta_i', \delta_i''$	Series of factors to correct theoretical operating L'/P limits of the SCCR3 unit
Δt	Small time increment in plate model of a chromatographic column
ε	Column void fraction
ε_L	Column utilization = $\frac{\text{Feedrate}}{\text{Column volume}}$
η_L	Mobile phase utilization = $\frac{\text{Feedrate}}{\text{Mobile phase rate}}$
θ	$N_f/\sqrt{N}$

λ	Eddy diffusion factor
μ	Dynamic viscosity
ν	Reduced velocity = ud_p/D_m
ρ	Density
σ	Standard deviation
σ_f	Standard deviation of feed inlet profile
σ_p	Standard deviation of product outlet profile
σ^2	Variance
σ_t^2	Time based variance
σ_1^2	Variance of Product 1 from SCCR3 unit
σ_2^2	Variance of Product 2 from SCCR3 unit
ϕ	Porosity
ψ	Operating mobile phase/stationary phase velocity ratio in probabilistic model of moving-bed chromatographic column

REFERENCES

1. J.C. Moore, J. Polym. Sci., A2, 835, (1964).

2. M.S. Tsvet, Proc. Warsaw Soc. Nat. Sci. Biol. Sec., 14, No.6 (1903).

3. M.S. Tsvet, Ber. deut. botan. Ges., 24, 316,384 (1906).

4. A.J.P. Martin and R.L.M. Synge, Biochem. J., 35, 1358 (1941).

5. A.T. James and A.J.P. Martin, Biochem. J., 50, 679 (1952).

6. J. Porath and P. Flodin, Nature, 183, 1657 (1959).

7. D.B. Broughton, Chem. Eng. Prog., 64 (8), 60 (1968).

8. D.B. Broughton, R.W. Neuzil, J.M. Pharis and C.S. Brearley, Chem. Eng. Prog., 66 (9), 70 (1970).

9. P.E. Barker and D. Critcher, Chem. Eng. Sci., 13, 82 (1960).

10. D. Critcher, PhD Thesis, Univ. of Birmingham, 1963.

11. P.E. Barker and D. Lloyd, Symposium on the Less Common Means of Separation, 1963, Inst. Chem. Eng., London, 1964, p.68.

12. D. Lloyd, PhD Thesis, Univ. of Birmingham, 1963.

13. P.E. Barker and D. Lloyd, U.S. Patent 3,338,031.

14. P.E. Barker and D.H. Huntington, J. Gas Chromatog., 4, 59 (1966).

15. P.E. Barker and D.H. Huntington, "Gas Chromatography 1966", A.B. Littlewood, Ed., Inst. of Petroleum, 1967, p.135.

16. D.H. Huntington, PhD Thesis, Univ. of Birmingham, 1967.

17. P.E. Barker and D.H. Huntington, Dechema Monograph, 62, 153 (1969).

18. P.E. Barker and Universal Fisher Engineering Co.Ltd., British Patent Applications 33630/65; 43629/65; 5764/68; 44375/68.

19. P.E. Barker and S. Al-Madfai, J. Chromatog. Sci., 7, 425 (1969).

20. P.E. Barker and S. Al-Madfai, Proc. 5th International Symposium on Advances in Chromatography, Las Vegas, 1969, Preston Technical Abstracts Co., Evanston, Illinois, 1969, p.123.

21. S. Al-Madfai, PhD Thesis, Univ. of Birmingham, 1969.

22. P.E. Barker, "Preparative Gas Chromatography", A. Zlatkis, Ed., Wiley-Interscience, London, 1971, p.325.

23. B.W. Hatt, PhD Thesis, Univ. of Birmingham, 1970.

24. P.E. Barker, S.A. Barker, B.W. Hatt and P.J. Somers, Chem. and Proc. Eng., 52 (1), 64 (1971).

25. A.B. Sunal, PhD Thesis, Univ. of Aston in Birmingham, 1973.

26. P.E. Barker and R.E. Deeble, paper presented at Symposium on Less Common Means of Separation, Inst. of Chem. Eng., London, 1972.

27. P.E. Barker and R.E. Deeble, Anal. Chem., 45, 1121 (1973).

28. P.E. Barker and R.E. Deeble, British Patent Appl. 27786/72, and U.S. Patent Appl. 368,584.

29. R.E. Deeble, PhD Thesis, Univ. of Aston in Birmingham, 1974.

30. P.E. Barker and R.E. Deeble, Chromatographia, 8 (2), 67 (1975).

31. A.N. Williams, PhD Thesis, Univ. of Aston in Birmingham, submitted 1976.

32. S. Ergun, Chem. Eng. Prog., 48 (2), 89 (1952).

33. J.C. Giddings, "Dynamics of Chromatography, Pt.1 Principles and Theory", Edward Arnold Ltd., London, 1965.

34. P.B. Hamilton, D.C. Bogue and R.A. Anderson, Anal. Chem., 32, 1782 (1960).

35. J.C. Giddings, W.A. Manwaring and M.N. Myers, Science, 154, 146 (1966).

36. S.W. Mayer and E.R. Tompkins, J. Am. Chem. Soc., 69, 2866 (1947).

37. E. Glueckauf, Trans. Faraday Soc., 51, 34 (1955).

38. L. Lapidus and N.R. Amundson, J. Phys. Chem., 56, 984 (1952).

39. J.J. Van Deemter, F.J. Zuiderweg and A. Klinkenberg, Chem. Eng. Sci., 5, 271 (1956).

40. J.J. Van Deemter, 2nd Informal Symp., Gas Chromatography Discussion Group, Cambridge, 1957.

41. E. Kucera, J. Chromatog., 19, 237 (1965).

42. O. Grubner, "Advances in Chromatography Vol.6", R.A. Keller and J.C. Giddings, Eds., Marcel Dekker Inc., New York, 1968, p.173.

43. E. Grushka, J. Phys. Chem., 76, 2586 (1972).

44. J.C. Giddings, J. Chem. Ed., 35, 588 (1958).

45. J.C. Giddings and H. Eyring, J. Phys. Chem., 59, 416 (1955).

46. D.A. McQuarrie, J. Chem. Phys., 38, 437 (1963).

47. A. Einstein, Ann. der Physik, 17, 549 (1905).

48. J.M. Haper and E.G. Hammond, Anal. Chem., 37, 486 (1965).

49. L.R. Snyder, J. Chromatog. Sci., 7, 352 (1969).

50. J.L. Waters, J.N. Little and D.F. Horgan, J. Chromatog. Sci., 7, 293 (1969).

51. G.J. Kennedy and J.H. Knox, J. Chromatog. Sci., 10, 549 (1972).

52. J.F.K. Huber, J. Chromatog. Sci., 7, 86 (1969).

53. J.R. Conder and J.H. Purnell, Chem. Eng. Prog. Symp. Ser., 91 (65), 1 (1969).

54. J.R. Conder and J.H. Purnell, Chem. Eng. Sci., 25, 353 (1970).

55. V. Pretorius and K. de Clerk, "Preparative Gas Chromatography", A. Zlatkis and V. Pretorius, Eds., Wiley - Interscience, London, 1971, p.1.

56. G.J. Krige and V. Pretorius, J. Gas Chromatog., 2, 115 (1964).

57. S.M. Gordon and V. Pretorius, J. Gas Chromatog., 2, 196 (1964).

58. S.M. Gordon, G.J. Krige and V. Pretorius, J. Gas Chromatog., 2, 241 (1964).

59. S.M. Gordon, G.J. Krige and V. Pretorius, J. Gas Chromatog., 2, 246 (1964).

60. S.M. Gordon, G.J. Krige and V. Pretorius, J. Gas Chromatog., 2, 285 (1964).

61. S.M. Gordon, G.J. Krige and V. Pretorius, J. Gas Chromatog., 3, 87 (1965).

62. C.N. Reilly, G.P. Hildebrand and J.W. Ashley Jr., Anal. Chem. 34, 1198 (1962).

63. F. Helfferich, J. Chem. Educ., 41, 410 (1964).

64. J.R. Conder, "Advances in Analytical Chemistry and Instrumentation, Vol.6 Progress in Gas Chromatography", J.H. Purnell, Ed., Wiley - Interscience, London, 1968, p.209.

65. J. C. Giddings, J. Gas Chromatog., 1 (1), 12 (1963).

66. F.H. Huyten, W. Van Beersum and G.W.A. Rijinders, "Gas Chromatography 1960", R.P.W. Scott, Ed., Butterworths, London, 1960, p.224.

67. G.J. Friscone, J. Chromatog., 6, 97 (1961).

68. K.-P. Hupe, U. Busch and K. Winde, J. Chromatog. Sci., 7, 1 (1969).

69. S.A. Volkov, J. Chromatog., 77, 97 (1973).

70. J.C. Giddings, J. Gas. Chromatog., 1 (4), 38 (1963).

71. J.C. Giddings and G.E. Jensen, J. Gas Chromatog., 2 (9), 290 (1964).

72. G.M.C. Higgins and J.F. Smith, "Gas Chromatography 1964", A. Goldup, Ed., Inst. of Petroleum, London, 1965, p.94.

73. G.W.A. Rijinders, "Advances in Chromatography Vol.3", Marcel Dekker, New York, 1966, p.215.

74. E. Bayer, K.-P. Hupe and H. Mack, Anal. Chem., 35, 492 (1963).

75. A.B. Littlewood, Anal. Chem., 38, 2 (1966).

76. S.T. Sie and G.W.A. Rijinders, Anal. Chem. Acta, 38, 3 (1967).

77. S.F. Spencer and P. Kucharski, Facts and Methods, 7 (4), 8 (1966).

78. J.H. Knox, "Advances in Gas Chromatography", A. Zlatkis and L. Ettre, Eds., Preston Technical Abstracts Co., Illinois, 1966.

79. S.E. Charm, C.C. Matteo and R.A. Carlson, Chem. Eng. Prog. Symp. Ser., 64 (80), 9 (1968).

80. J.H. Knox and J.F. Parcher, Anal. Chem., 41, 1599 (1969).

81. J.J. De Stefano and H.C. Beachell, J. Chromatog. Sci., 8, 434 (1970).

82. J.P. Wolf III, "Advances in Chromatography 1973", A. Zlatkis, Ed., pub'd by Chromatography Symposium, Dept. of Chemistry, Houston Univ, Texas.

83. L.R. Snyder, Anal. Chem., 39, 698 (1967).

84. H.N.M. Stewart, R. Amos and S.G.J. Perry, J. Chromatog., 38, 209 (1968).

85. J.J. Kirkland, J. Chromatog. Sci., 7, 7 (1969).

86. J.J. Kirkland, J. Chromatog. Sci., 7, 361 (1969).

87. J.J. Kirkland and J.J. De Stefano, J. Chromatog. Sci., 8, 309 (1970).

88. H.R. Felton, J. Chromatog. Sci., 7, 13 (1969).

89. W.N. Musser and R.E. Sparks, J. Chromatog. Sci., 9, 116 (1971).

90. J. Albrecht and M. Verzele, J. Chromatog. Sci., 9, 745 (1971).

91. J.M. Ryan, R.S. Timmins and J.F. O'Donnell, Chem. Eng. Prog., 64, 53 (1968).

92. R.S. Timmins, L. Mir and J.M. Ryan, Chem. Eng., 76, 170 (1969).

93. A.B. Carel and G. Perkins Jr., J. Anal. Chim. Acta, 34, 83 (1966).

94. A.B. Carel, R.E. Clement and G. Perkins Jr., J. Chromatog. Sci., 7, 218 (1969).

95. M.J. Golay, "Gas Chromatography", H.J. Noebels, R.F. Wall, N. Brenner, Eds., Academic Press, New York, 1961.

96. L. Mir, J. Chromatog. Sci., 9, 436 (1971).

97. J.R. Conder, paper presented at Symposium on Less Common Means of Separation, Inst. Chem. Eng., London, 1972.

98. E.g. Pharmacia Fine Chemicals, Uppsala, Sweden.

99. L. Ek, Process Biochem., p.25, September 1968.

100. J.-C. Janson, J. Agr. Food Chem., 19 (4), 581 (1971).

101. Australian Patent No. 362/66.

102. J.H. Purnell, J. Chem. Soc., 1268 (1960).

103. E. Glueckauf, Trans. Faraday Soc., 60, 729 (1964).

104. T. Johns, M.R. Burnett and D.W. Clarke, "Gas Chromatography", H.J. Noebels, R.F. Wall and N. Brenner, Eds., Academic Press, New York, 1961, p.207.

105. R.W. Reiser, J. Gas Chromatog., 4, 390 (1966).

106. B.J. Bradley and P.F. Tiley, Chem. Ind. (London), 18, 743 (1963).

107. G.R. Fitch, M.E. Probert and P.F. Tiley, J. Chem. Soc., 4875 (1962).

108. D.W. Pritchard, M.E. Probert and P.F. Tiley, Chem. Eng. Sci., 26, 2063 (1971).

109. W. Kuhn, E. Narten and M. Thurkauf, 5th World Petroleum Congress, 1958, Section 5, paper 5, p.45.

110. W. Kuhn, E. Narten and M. Thurkauf, Helv. Chim. Acta, 41, 2135 (1958).

111. D.W. Thompson, Trans. Inst. Chem. Engrs., 39, 19 (1961).

112. U.S. Patent 3,136,616.

113. R.H. Wilhelm, R.W. Rice and A.R. Bendelius, Ind. Eng. Chem. Fundamentals, 5, 141 (1966).

114. R.H. Wilhelm and N.M. Sweed, Science, 159, 522 (1968).

115. R.H. Wilhelm, A.W. Rice, R.W. Wolke and N.M. Sweed, Ind. Eng. Chem. Fundamentals, 7, 337 (1968).

116. R.L. Pigford, B. Baker III and D.E. Blum, Ind. Eng. Chem. Fundamentals, 8, 144 (1969).

117. R.L. Pigford, B. Baker III and D.E. Blum, Ind. Eng. Chem. Fundamentals, 8, 848 (1969).

118. P.C. Wankat, Separat. Sci., 9, 85 (1974).

119. P.C. Wankat, Ind. Eng. Chem. Fundamentals, 14 (2), 102 (1975).

120. S. Turina, V. Krajovan and T. Kostomaj, Z. Anal. Chem., 189, 100 (1962).

121. E.J. Tuthill, J. Chromatog. Sci., 8, 285 (1970).

122. Z. Pucar, Chromatog. Rev., 3, 38 (1961).

123. R. Hybarger, C.W. Tobias and T. Vermeulen, Ind. Eng. Chem., Proc. Design and Developments, 2, 65 (1963).

124. A.J.P. Martin, Discussions Faraday Soc., 7, 332 (1949).

125. J.C. Giddings, Anal. Chem., 34, 37 (1962).

126. J.B. Fox Jr., R.C. Calhoun and W.J. Eglinton, J. Chromatog., 43, 48 (1969).

127. J.B. Fox Jr., J. Chromatog., 43, 55 (1969).

128. R.A. Nicholas and J.B. Fox Jr., J. Chromatog., 43, 61 (1969).

129. H. Svensson, Swedish Patent 133,851 (1951).

130. H. Svensson, C.E. Agrell, S.O. Dehlen and L. Hagdahl, Sci. Tools, 2, 17 (1955).

131. D. Dinelli, S. Polezzo and M. Taramasso, J. Chromatog., 7, 447 (1962).

132. D. Dinelli, M. Taramasso and S. Polezzo, U.S. Patent 3,187,486 (1965).

133. M. Taramasso and D. Dinelli, J. Gas Chromatog., 2, 150 (1962).

134. M. Taramasso, F. Sallusto and A. Guerra, J. Chromatog. 20, 226 (1965).

135. M. Taramasso, J. Chromatog., 49, 27 (1970).

136. U.S. Patent 3,078, 647 (1963).

137. U.S. Patent 3,503,712 (1970).

138. M.V. Sussman, K.N. Astill, R. Bombach, A. Cerrulo and S.S. Chen, Ind. Eng. Chem. Fundamentals, 11, 181 (1972).

139. M.V. Sussman, K.N. Astill and R.N.S. Rathore, J. Chromatog. Sci., 12, 91 (1974).

140. R.P.W. Scott, "Gas Chromatography 1958", D.H. Desty, Ed., Butterworths, London, 1958, p.189.

141. H. Schultz, "Gas Chromatography 1962", M. Van Swaay, Ed., Butterworths, London, 1963, p.225.

142. W.L. Nelson, "Petroleum Refinery Engineering", McGraw-Hill, New York, 1958.

143. U.S. Patent 2,869,672.

144. H. Pichler and H. Schultz, Brennstoff Chem., 39, 48 (1958).

145. U.S. Patent 2,893,955 (1959).

146. U.S. Patent 3,016,107 (1962).

147. D. Glasser, "Gas Chromatography 1966", R.B. Littlewood, Ed., Inst. of Petroleum, London, 1967, p.119.

148. Unidev leaflet on Sequential Separation, Unidev Ltd., Crawley, Sussex.

149. P. Carr, Unilever Ltd., paper presented at 8th International Symposium on Advances in Chromatography, Toronto, 1973.

150. L. Szepesy, Zs. Sebestyén, I. Fehér and Z.Nagy, J. Chromatog., 108, 285 (1975).

151. S. Hjertén and R. Mosbach, Anal. Biochem., 3, 109 (1962).

152. K.O. Pedersen, Arch. Biochem. Biophys. Suppl., 1, 157 (1962).

153. R.L. Steere and G.K. Ackers, Nature, 196, 475 (1962).

154. F.H. Verhoff and N.D. Sylvester, J. Macromol. Sci.-Chem., A4 (4), 979 (1970).

155. C.M. Guttman and E.A. Dimarzio, Macromolecules, 3, 681 (1970).

156. H. Determann, Angew. Chem. Intern. Ed., 3 (9), 608 (1964).

157. J.C. Moore and J.G. Hendrickson, J. Polym. Sci., C(8), 233 (1965).

158. G.K. Ackers, Biochemistry, 3, 723 (1964).

159. H. Benoitz, Z. Grubisic, P. Rempp, D. Decker and J.G. Zilliox, J. Chim. Phys., 63, 1507 (1966).

160. W.V. Smith and G.A. Feldman, J. Polym. Sci., A-2(7), 163 (1969).

161. H.E. Picket, M.J.R. Cantow and J.F. Johnson, J. Polym. Sci., 21, 67 (1968).

162. L.H. Tung, J. Appl. Polym. Sci., 10, 375 (1966).

163. W.N. Smith, J. Appl. Polym. Sci., 11, 639 (1967).

164. J.H. Duerksen and A.E. Hamielec, J. Polym. Sci., C(21), 83 (1968).

165. K.S. Chang and R.Y. Huang, J. Appl. Polym. Sci., 16, 329 (1972).

166. J.C. Giddings, E. Kucera, C.P. Russell and M.N. Myers, J. Phys. Chem., 72(13), 4397 (1968).

167. J. Porath, J. Pure Appl. Chem., 6, 233 (1963).

168. P. Andrews, Biochem. J., 91, 222 (1964).

169. P.G. Squire, Arch. Biochem. Biophys., 107, 471 (1964).

170. T.C. Laurent and J. Killander, J. Chromatog., 14, 317 (1964).

171. A.G. Ogston, Trans. Faraday Soc., 54, 1754 (1958).

172. J.S. Fawcett and C.J.O.R. Morris, Separat. Sci., 1, 9 (1966).

173. M. Partridge, Biochim. Biophys. Acta, 140, 132 (1967).

174. L. Fischer, "Introduction to Gel Chromatography", North-Holland Publishers, Amsterdam, 1968.

175. E.F. Casassa, J. Polym. Sci., B(5), 773 (1967).

176. E.F. Casassa and Y. Tagami, Macromolecules, 2(1), 14 (1969).

177. J.C. Moore and M.C. Arrington, Int. Symp. Macromol. Chem., Tokyo, Kyoto, Preprints 6-107, 1966.

178. M.E. Van Kreveld and N. Van den Hoed, J. Chromatog., 83, 111 (1973).

179. C.K. Colton, C.N. Satterfield and C.-J. Lai, A. I. Chem. E. Journal, 21(2), 289 (1975).

180. W.W. Yau and C.P. Malone, J. Polym. Sci., B(5), 663 (1967).

181. W.W. Yau, C.P. Malone and S.W. Fleming, J. Polym. Sci., B(6), 803 (1968).

182. M.J.R. Cantow, R.S. Porter and J.F. Johnson, J. Polym. Sci., A-1(5), 987 (1967).

183. J.N. Little, J.L. Waters, K.J. Bombaugh and W.J. Pauplis, J. Polym. Sci., A-2(7), 1775 (1969).

184. J.N. Little, J.L. Waters, K.J. Bombaugh and W.J. Pauplis, J. Chromatog. Sci., 9, 341 (1971).

185. A.R. Cooper, Br. Polym. J., 5, 109 (1973).

186. W.B. Smith and A. Kollmansberger, J. Phys. Chem., 69, 4157 (1965).

187. J.C. Moore and M.C. Arrington, 3rd International Seminar on G.P.C., Geneva, 1966.

188. G. Meyerhoff and S. Jovanovic, J. Polym. Sci., B(5), 495 (1967).

189. K.A. Boni, F.A. Sliemers and P.B. Stickney, 4th International Seminar on G.P.C., Miami Beach, 1967.

190. B.J. Gudzinowicz and K. Alden, J. Chromatog. Sci., 9, 65 (1971).

191. R. Beau, M. Le Page and A.J. de Vries, Appl. Polym. Symposia, 8, 137 (1969).

192. W.J. Haller, J. Chromatog., 32, 676 (1968).

193. W.W. Yau, H.L. Suchan and C.P. Malone, J. Polym. Sci., A-2(6), 1349 (1968).

194. E.F. Casassa, J. Phys. Chem., 75, 3929 (1971).

195. K.H. Altgelt, "Advances in Chromatography Vol. 7", J.C. Giddings and R.A. Keller, Eds., Dekker, New York, 1968, p.3.

196. M. Kubín, J. Chromatog., 108, 1 (1975).

197. W.W. Yau, J. Polym. Sci., A-2(7), 483 (1969).

198. J.J. Hermans, J. Polym. Sci., A-2(6), 1217 (1968).

199. A.C. Burton, "Medical Physiology and Biophysics", T.C. Ruch and J.F. Fulton, Eds., W.B. Saunders, Philadelphia, 1966, Ch.29.

200. E.A. Dimarzio and C.M. Guttman, J. Polym. Sci., B(7), 267 (1969).

201. E.A. Dimarzio and C.M. Guttman, Macromolecules, 3, 131 (1970).

202. E.A. Dimarzio and C.M. Guttman, J. Chromatog., 55, 83 (1971).

203. J.D. Ferry, J. Gen. Physiol., 20, 95 (1936).

204. D.M.W. Anderson and J.F. Stoddart, Lab. Practice, 16 (7), 841 (1967).

205. J.C. Giddings and K.L. Mallik, Anal. Chem., 38, 997 (1966).

206. S.B. Horowitz and I.R. Fenichel, J. Phys. Chem., 68, 3378 (1964).

207. W. Heitz and J. Čoupek, Macromol. Chem., 105, 280 (1967).

208. M. Le Page, R. Beau and A.J. de Vries, J. Polym. Sci., C(21), 119 (1968).

209. F.W. Billmeyer Jr., G.W. Johnson and R.N. Kelley, J. Chromatog., 34, 316 (1968).

210. R.N. Kelley and F.W. Billmeyer Jr., Anal. Chem., 41, 874 (1969).

211. R.N. Kelley and F.W. Billmeyer Jr., Anal. Chem., 42, 399 (1970).

212. J.V. Dawkins and G. Taylor, Polymer, 15, 687 (1974).

213. D.S. Horne, J.H. Knox and L. McLaren, Separat. Sci., 1(5), 531 (1966).

214. A.J. de Vries, M. Le Page, R. Beau and C.L. Guillemin, Anal. Chem., 39, 935 (1967).

215. R.N. Kelly and F.W. Billmeyer Jr., Separat. Sci., 5 (3), 291 (1970).

216. A.R. Cooper and I. Kiss Jr., Br. Polym. J., 5, 433 (1973).

217. K.J. Bombaugh, W.A. Dark and R.F. Levangie, Separat Sci., 3 (4), 375 (1968).

218. K.J. Bombaugh, "Modern Practice of Liquid Chromatography", J.J. Kirkland, Ed., Wiley-Interscience, New York, 1971.

219. K.J. Bombaugh and R.F. Levangie, Anal. Chem., 41, 1357 (1969).

220. A.R. Cooper, A.R. Bruzzone, J.H. Cain, and E.M. Barrall II, J. Appl. Polym. Sci., 15, 571 (1971).

221. K.H. Altgelt and J.C. Moore, "Polymer Fractionation", M.J.R. Cantow, Ed., Academic Press, New York, 1967, p.164.

222. M.J.R. Cantow, R.S. Porter and J.F. Johnson, J. Polym. Sci., B(4), 707 (1966).

223. F. Rodriguez, R.A. Kulakowski and O.K. Clark, Ind. Eng. Chem. Prod. Res. Develop., 5, 121 (1966).

224. T.C. Laurent and K.A. Granath, Biochim. Biophys. Acta, 136, 191 (1967).

225. K.P. Goetze, R.S. Porter and J.F. Johnson, J. Polym. Sci., A-2(9), 2255 (1971).

226. K. Berger, Symposium on G.P.C., Mainz, 1967.

227. T.C. Laurent, Acta Chem. Scand., 17, 2664 (1963).

228. T.C. Laurent, Biochem. J., 89, 253 (1963).

229. K. Hellsing, J. Chromatog., 36, 170 (1968).

230. S.A. Barker, B.W. Hatt and P.J. Somers, Carbohyd. Res., 11, 355 (1969).

231. Z. Dische, L.B. Shettles and M. Osmos, Arch. Biochem., 22, 169 (1949).

232. E. Glueckauf, "Ion-Exchange and its Applications", Soc. Chem. Ind., London, 1955, p.34

233. J.C. Sternberg, "Advances in Chromatography Vol. 2", J.C. Giddings and R.A. Keller, Eds., Edward Arnold, New York, 1966, p.205.

234. M.R. Spiegel, "Theory and Problems of Statistics", Schaum Publishing Co., New York, 1961.

235. S. Holding, Unpublished work, University of Aston.

236. W.F. Dudman and C.T. Bishop, Can. J. Chem., 46, 3079 (1968).

237. As supplied by A.J. de Vries, Rhone Progil, France.

238. A.R. Cooper and E.M. Barrall II, J. Appl. Polym. Sci., 17, 1253 (1973).

239. J.M. Coulson and J.F. Richardson, "Chemical Engineering Vol.2 - Unit Operations", Pergamon Press, Oxford, 1968, p.6.

240. Recommended by Fisons Ltd. (Pharmaceuticals Division), Holmes Chapel.

241. Private communication, Dr. R. Gibbs, Fisons Ltd. (Pharmaceuticals Division), Holmes Chapel, 1975.

242. C.T. Sciance and O.K. Crosser, A. I. Chem. E. Journal, 12 (1), 100, 1966.

243. P.R. Rony, Separation Science, 5 (2), 121 (1970).

244. L. Alders, "Liquid-Liquid Extraction", Elsevier, Amsterdam, 1959.

245. P.F. Tiley, J. Appl. Chem., 17 (5), 131 (1967).

246. E.P. Otocka, J. Chromatog., 76, 149 (1973).

247. J.H. Knox, Chem. Ind. (London), January 1975, p.29.

248. Waters Associates, Technical publication DS013, 1975.

249. L.K.B., Data Sheet 5210, 1975.

250. J. Čoupek, M. Křiváková and S. Pokorný, Knauer Information paper on Spheron, 1975.

251. J.G. Savins, Ind. Eng. Chem., 16 (10), 18 (1969).

252. G. Laufer, C. Gutfinger and N. Abuaf, Ind. Eng. Chem. Fundam., 15 (1), 74 (1976).

PROVISIONAL BRITISH PATENT APPLICATION

NO. BA 45858/75

TITLE: DEVICE

APPLICANTS: FISONS LIMITED - PHARMACEUTICAL DIVISION

INVENTORS: P. E. BARKER

B. W. HATT

F. J. ELLISON

Aston University

Content has been removed for copyright reasons